Cambridge Environmental Research Consultants

Air Quality Studies for Heathrow: Base Case, Segregated Mode, Mixed Mode and Third Runway Scenarios modelled using ADMS-Airport

Final report

Prepared for
Department for Transport

15 November 2007

CERC

Report Information

CERC Job Number:	699
Job Title:	Air Quality Studies for Heathrow: Base Case, Segregated Mode, Mixed Mode and Third Runway Scenarios modelled using ADMS-Airport
Prepared for:	Department for Transport
Report Status:	Final
Report Reference:	FM699/R23_Final/07
Issue Date:	15 November 2007
Author(s):	C. McHugh, M. Williams, C. Price & C. Lad
Reviewer(s):	D. J. Carruthers

To order further copies contact:
DfT Publications
Tel: 0845 600 4170
Fax: 0870 1226 237
Textphone: 0870 1207 405
E-mail: heathrowconsultation@dft.gsi.gov.uk
or online via www.dft.gov.uk/heathrowconsultation

Printed in Great Britain November 2007 on paper containing at least 75% recycled fibre.

Product Code 78APD02904CERC

CONTENTS

Summary

This report presents modelling using ADMS-Airport of air quality around Heathrow airport for the 2002 Base Case and nine future scenarios. The work has been undertaken for the Department for Transport's Project for the Sustainable Development of Heathrow. The pollutants modelled are NO_X, NO_2 and PM_{10} with most attention directed to predicted NO_2 concentrations and whether they are likely to exceed the EU air quality Limit Value of 40μg/m^3 as an annual average, to be achieved by 1 January 2010[1]. Modelled concentrations for the 2002 Base Case are compared with monitored data to demonstrate the performance of the model.

The future scenarios considered are:

- 2010 Segregated Mode (2010SM)
- 2015 Segregated Mode (2015SM)
- 2015 Segregated Mode with Easterly Preference (2015EP)
- 2015 Segregated Mode with No Cranford Agreement (2015NoC)
- 2015 Mixed Mode (2015MM)
- 2015 Mixed Mode with traffic mitigation (2015MMRd)
- 2030 Mixed Mode (2030MM)
- 2020 Third Runway (2020R3)
- 2030 Third Runway (2030R3)

In segregated mode take-offs and landings take place on parallel runways (this is the current mode of operation). In mixed mode both take-offs and landings occur on both runways. The results for the third runway scenarios presented in this report are hybrid results of MDL (mixed mode on the northern runway, departures on the central runway and landings on the southern runway) and MLD (mixed mode on the northern runway, landings on the central runway and departures on the southern runway) scenarios. The hybrid results have been constructed assuming the airport operates with equal alternation between MDL and MLD modes of operation.

Two variations on the 2015 Segregated Mode scenario have been modelled. In one variation an easterly preference is assumed instead of a westerly preference (2015EP) and in the second variation there is no Cranford Agreement in place (2015NoC). One variation on the 2015 Mixed Mode scenario was modelled: a scenario with traffic mitigation measures (2015MMRd).

Scenario 2030MM is included for comparative purposes. Mixed mode operation would be superseded by third runway operation from around 2020.

Emissions

Airport data from which the airport emissions inventories were compiled were supplied by AEA and traffic data for the major roads, from which road traffic emissions were calculated, were supplied by Hyder Consulting. The emissions inventory data have been compiled based on the

[1] www.defra.gov.uk/environment/airquality/strategy/pdf/air-qualitystrategy-vol1.pdf

recommendations of the Project for the Sustainable Development of Heathrow Panel Report (PSDH)[2]. The report presents the emissions of NO_X, NO_2 and PM_{10} supplied as input to the air quality modelling.

Between 2002 and 2030 there is a 51% decrease in total NO_X emissions modelled and this is mostly because of the predicted 80% reduction in NO_X due to road traffic due to improved vehicle technology. Over the same period NO_2 from road traffic is also predicted to decrease significantly although by less, by approximately 60%.

Between 2002 and 2030 PM_{10} emissions from the inventory are predicted to decrease by 24% and this is again due mostly to predicted reductions in emissions from road traffic. In all the scenarios background PM_{10} is the main contributor to total PM_{10} concentrations. The airport contribution to total PM_{10} concentrations is in all cases small.

Emissions due to airport sources change in magnitude and spatial distribution according to the scenario modelled. In all the future scenarios airport emissions increase, in some cases significantly, with respect to 2002, due to the increased number of take-offs and landings (air traffic movements or ATM). After 2020 predicted improvements in aircraft technology lead to a decrease in emissions per plane that partly offsets the increase in ATM. There are five main changes in spatial distribution:

(i) The operation of Terminal 5 and reconfiguration of stands (for all cases except the Base Case) causes a redistribution of airport emissions from east to west.

(ii) The introduction of mixed mode compared with segregated mode significantly increases the take-offs from runway 09L and reduces the take-offs from 09R, thereby causing a shift in emissions from the southern to the northern runway.

(iii) The creation of a third runway increases emissions to the north of the current airport boundary.

(iv) Operation of an easterly rather than a westerly preference shifts take-off emissions from the north-eastern end of runway 27R to the south-western end of runway 09R. There are associated changes in taxiing and hold emissions.

(v) The effect of the No Cranford option is to increase the use of runway 09L (and hence reduce the use of 09R) shifting take-off emissions from the south-west of the airport to the north-west.

Predicted concentrations of NO_X and NO_2

The 2002 Base Case predicted concentrations are compared with automatic monitoring data and are presented using a range of diagnostic tools including BOOT statistics[3], box and whisker plots, analysis according to runway use dependence and polar plots. Taken as a whole the diagnostic tools show that the model has good performance.

[2] www.dft.gov.uk/pgr/aviation/environmentalissues/secheatrowsustain/

[3] Hanna S. R., Strimaitis D. G. And Chang J. C. (1991) Hazard response Modeling Uncertainty (A quantitative method) Sigma Research Corporation report.

For the Base Case and the future scenarios the report presents long term average concentrations at specified receptors and contour plots of annual average NO_X in an area 9.7km x 9.1km for all the sources together and for groups of sources: the aircraft and other airport sources; road traffic sources; other background sources (Base Case only). Concentrations of NO_2 have been calculated for all the sources together for each scenario. For the 2015SM, 2015MM and 2015MMRd, NO_2 concentrations have also been predicted at receptor locations representing residential properties used for population exposure studies. These results have been presented in the PSDH population exposure report.[4]

In 2002 the annual average Limit Value for NO_2 is predicted by the modelling to be exceeded on the airport, along the motorways and some main roads, along the main railway line and in areas of Harlington. In the future cases the areas of exceedence are reduced compared with 2002 and are confined mainly to the airport and along the motorways. This reduction is largely due to the reduction in NO_X emissions from road traffic. Rail emissions are predicted to decrease in 2010 and further in 2015 due to re-engining of high speed trains so the air quality impact of the railway emissions is predicted to decrease in future years.

In the 2030 mixed mode (2030MM) scenario there are no exceedences of the Limit Value at the receptors considered.

In the scenarios considered the predicted concentrations show the following features:

- ***Mixed Mode (2015MM):*** In the absence of any other changes the effect of mixed mode compared to segregated mode is to increase concentrations to the north-west of the airport (Longford) and to decrease concentrations to the south-west (Stanwell).

- ***Third Runway, MDL and MLD (2020R3, 2030R3):*** The model results for 2020R3 and 2030R3 are hybrid results that have been constructed assuming the airport operates with equal alternation between the MDL and MLD modes of operation. The take-off emissions are the most significant ground level emissions and therefore in the MDL mode of operation higher concentrations are predicted to the north-east of the airport when 27C is used for take-offs than under MLD operation when 27C is used for landings.

- ***Easterly Preference (2015EP):*** Compared with the westerly preference scenario (2015SM), NO_x concentrations are predicted to increase at some receptors to the west of the airport, due to the increase in emissions on the 09L and 09R runways, and to decrease at receptors to the east of the airport. The greatest predicted increase in annual average NO_2 concentrations compared with segregated mode operation is an increase of 5% at LHR15 near the 09L runway and the greatest decrease is 5% at X11 near to 27R.

- ***No Cranford Agreement (2015NoC):*** For the "No Cranford Agreement" scenario the estimated annual average concentrations of NO_2 were 95%-113% of the corresponding "with Cranford Agreement" (2015SM) predicted concentrations. The largest increases in NO_2 concentrations are predicted at receptors to the north-west of the airport (BAA14, BAA15, BAA16) and the greatest decreases in concentration are

[4] PSDH "Population Exposure to Air Pollution", Atkins Limited, November 2007.

at receptors to the south-west of the airport (BAA49, BAA50, BAA51) near to 09R where there is decreased activity.

- ***Roads mitigation scenario (2015MMRd):*** Decreases in predicted NO_2 annual average concentration of up to 2μg/m^3 were predicted with the largest decreases in concentration along the M4 and smaller decreases near to the airport around Harlington.

Predicted concentrations of PM_{10}

The EU Limit Value for PM_{10} is 40μg/m^3 as an annual average. In 2002 the highest predicted annual average concentration of PM_{10} is 28.63μg/m^3 at receptor LHR10 that is beside the M25. In all future scenarios the predicted annual average PM_{10} concentration does not exceed 25μg/m^3. Therefore, at the receptors considered in this modelling study there are no predicted exceedences of the annual average Limit Value for PM_{10}. Annual average contour plots of PM_{10} are presented for the Base Case.

The EU is currently negotiating the introduction of a target value of 25μg/m^3 of $PM_{2.5}$ as an annual average, to be achieved by 2010, whilst the same value has recently been adopted as an objective in the Air Quality Strategy[1] to be achieved by 2020. As $PM_{2.5}$ is a component of PM_{10} there are no predicted exceedences of 25μg/m^3 by the annual mean $PM_{2.5}$ in the future scenarios.

1 Introduction

ADMS-Airport has been used to model the 2002 Base Case for air quality around Heathrow Airport and nine future scenarios. Airport data were supplied by AEA and traffic data were supplied by Hyder Consulting for the major roads. Other inventory data were taken from the London Atmospheric Emissions Inventory (LAEI) for London and the National Atmospheric Emissions Inventory (NAEI) for the area to the west of Heathrow.

ADMS-Airport was used in the PSDH Modelling Inter-comparison (MIC) exercise that used an earlier airport emissions inventory and roads data from the LAEI. ADMS-Airport[5] is an advanced dispersion model (based on ADMS-Urban) that models the important take-off ground roll sources as moving, high momentum, buoyant jet sources and hence the near field dispersion of pollutants emitted from the aircraft jet engines.

Section 2 of this report describes the meteorological data used and Section 3 the rural background concentrations used in the modelling. The overall inventory, airport emissions inventory and major road emissions inventory are described in Sections 4-6 respectively. Section 7 details the output receptors and Section 8 the model set up. Section 9 analyses the 2002 Base Case model results and includes comparisons of modelled concentrations with ambient monitored values in order to assess the model performance. Section 10 presents the results of the 2002 Base Case dispersion modelling and the results of the future scenarios. The results are annual average concentrations at specified receptors and contour plots of annual average NO_X and NO_2 in a domain 9.7km x 9.1km. Contours of predicted PM_{10} concentrations are presented for the Base Case only. Concentrations at the specified receptors and for the contour domain are also presented for the following source groups: aircraft, other non-aircraft airport sources and roads. Section 11 presents the conclusions.

[5] Project for the Sustainable Development of Heathrow. Airport Dispersion Model Evaluation – Scientific Assessment, Inter-comparison and Validation. Calculations with ADMS-Airport. CERC report to DfT. December 2005. Available from CERC, 3 Kings Parade, Cambridge, CB2 1 SJ.

2 Meteorological data

Modelling was carried out using hourly sequential meteorological data obtained for the Heathrow Airport station for the year 2002. The data set used was the same as that used in the PSDH Model Inter-comparison (MIC). The meteorological station is situated within the modelling area, and these data are therefore considered to be the most appropriate for this study.

The hours of meteorological data used in the analysis exclude hours of calm, hours of variable wind direction and unavailable data.

A summary of the data provided is given below in Table 2.1.

Table 2.1 Summary of meteorological data

Parameter	**Heathrow 2002**		
Data capture	99.2%		
Height	10m		
Roughness length at met site	0.2m		
Location	(507700, 176700)		
Statistics	**Mean**	**Minimum**	**Maximum**
Temperature (°C)	11.9	-4.7	31.6
Wind speed (m/s)	4.4	0.4	19.5
Cloud cover (oktas)	6	0	8

The ADMS meteorological pre-processor, written by the UK Met Office, uses these data to calculate the parameters required by the programme. Figure 2.1 shows the wind rose for the station giving the frequency of occurrence of wind from different directions for a number of wind speed ranges, for the year 2002.

Figure 2.1: Heathrow Airport wind rose for 2002, the angle of an element represents wind direction and the radial distance from the centre represents the frequency of occurrence.

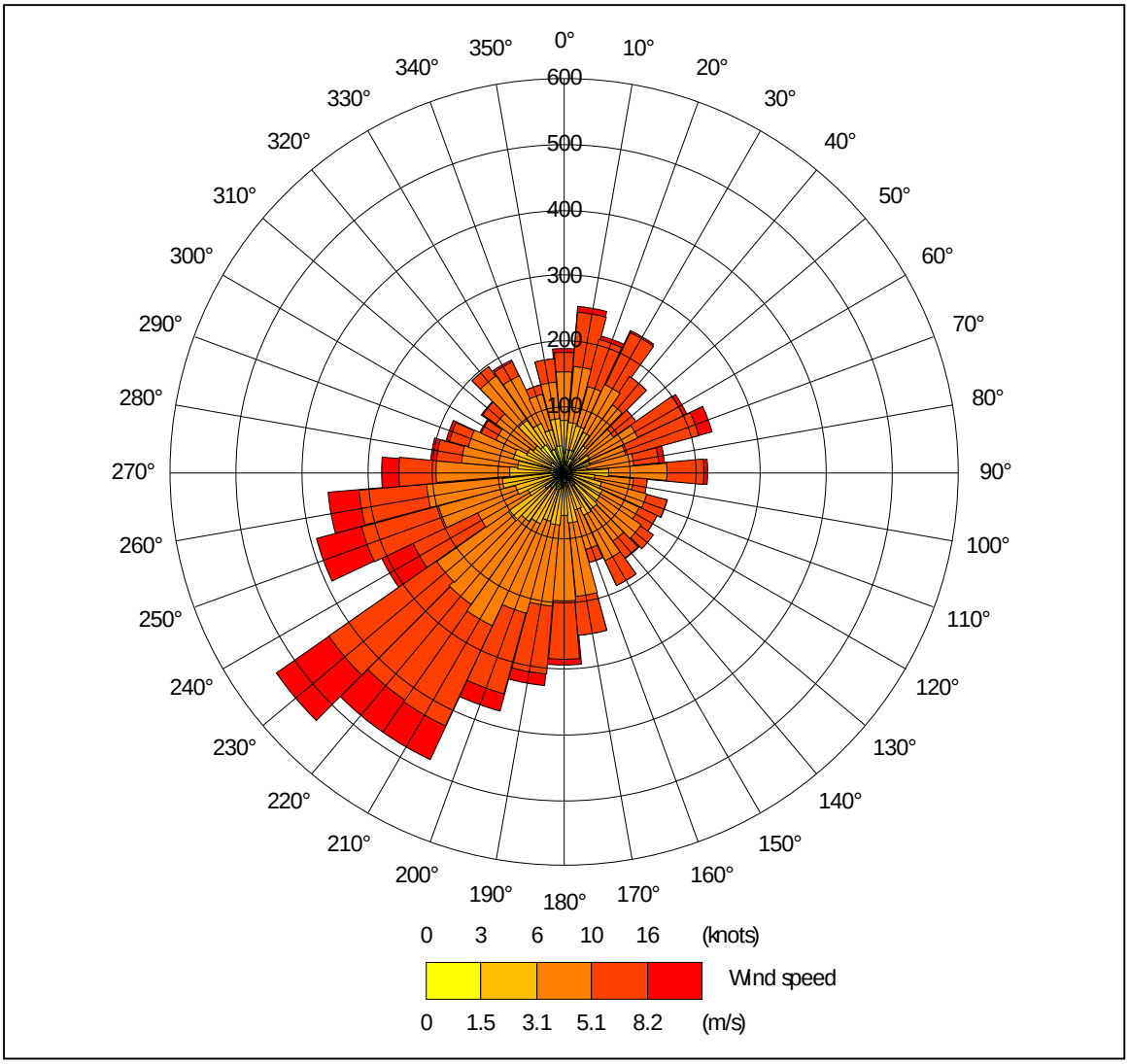

3 Rural background concentration

3.1 Rural background concentration for 2002

ADMS-Airport requires rural background concentration as input to the system. In the case of NO_x, NO_2 and O_3, monitored concentrations from 2002 from Rochester, Harwell, Lullington Heath and Wicken Fen were used, the monitored concentration used for a particular hour depending upon the wind direction for that hour. The wind direction used was taken from the supplied meteorological data. Figure 3.1 shows the wind direction segments used for each background site. It shows that, for example, if the wind during a particular hour is blowing from between 60° and 135° then the background NO_x, NO_2 and O_3 concentrations are taken to be the monitored values for that hour at Rochester.

In the case of PM_{10}, monitored TEOM PM_{10} data from Rochester and Harwell were used. PM_{10} is not monitored at Lullington Heath or Wicken Fen. For each hour of the year either the Rochester or Harwell observation was chosen depending upon the wind direction for that hour. The Rochester data were used for hours when the wind direction was between 4° and 184°, otherwise the Harwell observation was chosen. The TEOM values were then converted to gravimetric units by multiplying by a factor of 1.3[6].

An additional coarse contribution due to resuspension, construction dust etc was added to the measured background based on the work CERC is undertaking for DEFRA on "Dispersion Modelling of Air Pollutants in Urban Areas in the UK". The coarse contribution to background PM_{10} concentration used is 4μg/m^3. Thus for each hour:

$$\text{Total 2002 } PM_{10} \text{ background } (\mu g/m^3) = (\text{2002 observed TEOM value} \times 1.3) + 4.0$$

Figure 3.1 Wind direction segments used to calculate background concentrations

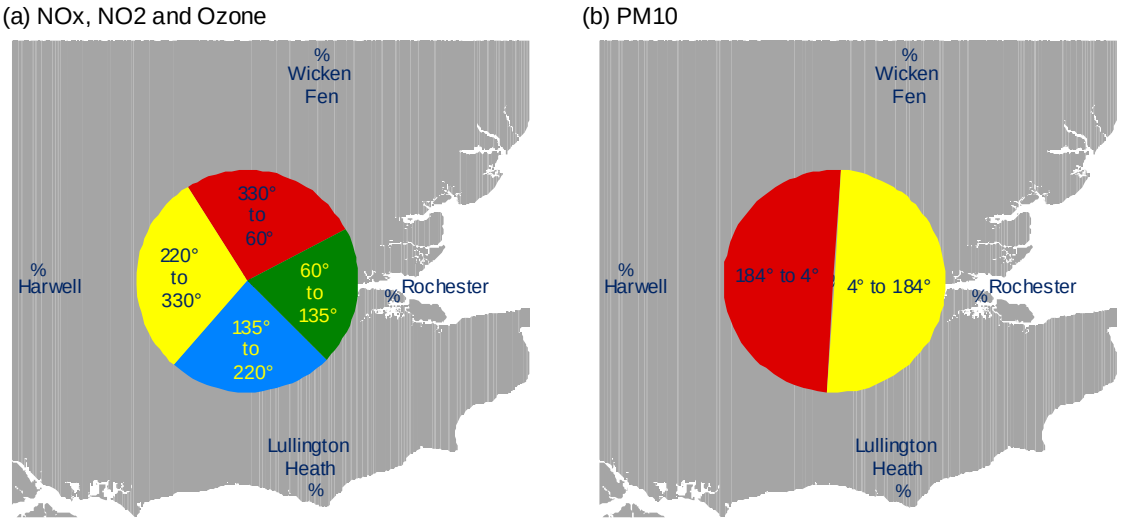

[6] DEFRA Technical Guidance TG(03), Section 8.08
www.defra.gov.uk/environment/airquality/local/guidance/pdf/laqm-tg03.pdf

3.2 Rural background concentration for future years

Table 3.1 summarises the background concentration data statistics for all of the modelled years.

3.2.1 NO_X, NO_2 and ozone

The annual average concentrations of NO_X, NO_2 and ozone for future years were calculated by averaging the predictions of future hourly concentrations. The future hourly concentrations were calculated as follows:

Step 1. Future hourly NO_X concentrations were obtained by multiplying the 2002 hourly monitored values by the background factors supplied by DEFRA[7] and shown in Table 3.2. Factors for 2030 were calculated by linear extrapolation of the 2015 – 2020 factors.

Step 2. Future hourly NO_2 concentrations were calculated using a correlation polynomial derived from the 2002 hourly background NO_X and NO_2 concentrations:

$$[NO_2] = 3x10^{-6}[NO_X]^3 - 4.7x10^{-3}[NO_x]^2 + 0.97[NO_x]$$

$[NO_X]$ and $[NO_2]$ are the concentrations in $\mu g/m^3$ of NO_X and NO_2 respectively.

Step 3. Future hourly ozone (O_3) concentrations were calculated from one of three expressions according to the concentration in ppb (parts per billion) of available oxidant in 2002 for that hour ($[OX_{(2002)}]$). $[OX_{(2002)}]$ was calculated for each hour from the 2002 hourly NO_2 and NO_X concentrations in ppb, $[NO_{2(2002)}]$ and $[NO_{X(2002)}]$ respectively.

$$[OX_{(2002)}] = [O_{3\,(2002)}] + [NO_{2(2002)}] - (0.1 \times [NO_{x(2002)}])$$

For the future years hourly ozone was calculated as follows:

If $[OX_{(2002)}] < 30ppb$

$$[O_{3(future)}] = O_{3L} = [OX_{(2002)}] - [NO_{2(future)}] + (0.1 \times [NO_{x(future)}])$$

If $[OX_{(2002)}] > 40ppb$

$$[O_{3(future)}] = O_{3H} = [O_{3(2002)}]$$

If $30ppb =< [OX_{(2002)}] =< 40ppb$

$$[O_{3(future)}] = O_{3L} + (([OX_{(2002)}] - 30)/10) \times (O_{3H} - O_{3L})$$

3.2.2 PM_{10}

The 2002 annual average PM_{10} background concentration was assumed to be composed of a primary, secondary and coarse component. The coarse component was $4\mu g/m^3$ (Section 3.1) and this was assumed not to change in future years. The split between the primary and

[7] www.airquality.co.uk/archive/laqm/tools/yearfactorsdd2004.xls

secondary components in 2002 was determined on the basis of work carried out for DEFRA[8]. The 2002 primary and secondary components were each projected forwards using the factors shown in Table 3.2.

Table 3.1 Background concentrations for NO_x, NO_2, O_3 and PM_{10} in $\mu g/m^3$. (The PM_{10} values include the estimated coarse contribution.) The number of exceedences is

		2002	2010	2015	2020	2030
NO_x as NO_2	Annual average	15	11	10	9	9
	Maximum hourly average	215	157	140	134	131
	99.79th percentile (18 exceedences)*	127	93	83	79	77
NO_2	Annual average	12	9	9	8	8
	Maximum hourly average	84	53	53	53	53
	99.79th percentile (18 exceedences)*	62	51	49	48	48
O_3	Annual average	53	56	57	56	56
	Maximum hourly average	188	188	188	188	188
	99.79th percentile (18 exceedences)*	135	135	135	133	133
PM_{10}	Annual average	21	19	18	18	17
	Maximum hourly average	126	111	107	100	103
	90.41st percentile of 24 hour averages (35 exceedences)*	35	28	27	25	26
	98.08th percentile of 24 hour averages (7 exceedences)*	50	39	37	35	36

*Some concentrations are expressed as a percentile value and a number of exceedences e.g. if the 99.79th percentile hourly average concentration is 127$\mu g/m^3$, the hourly concentration exceeds 127$\mu g/m^3$ 18 times (during 18 hours) per year.

Table 3.2 Background concentration factors for NO_x and PM_{10}

Ratio of years	NO_x	Primary PM_{10}	Secondary PM_{10}
2010/2002	0.73	0.88	0.81
2015/2002	0.65	0.85	0.75
2020/2002	0.62	0.86	0.69
2030/2002	0.57	0.88	0.67

[8] www.airquality.co.uk/archive/reports/cat16/0605181650_TR04_R1_ModellingforLondon_01Mar06h.pdf *"Modelling of Current and Future Concentrations of PM, NOx and O_3 in London using ADMS-Urban"*

4 Emissions Inventory

The airport data, from which the airport emissions inventories were compiled, were supplied by AEA and are described in more detail in Section 5. The roads data were supplied by Hyder Consulting with emissions due to the road traffic being calculated using CERC's EMIT[9] model (Emissions Inventory Toolkit). The road traffic data and the calculated emissions are described

in more detail in Section 6. Other emissions data were obtained from the London Atmospheric Emission Inventory for 2002 (LAEI)[10] for the area within the M25 and the National Atmospheric Emission Inventory (NAEI) for the area to the west of Heathrow outside the M25. These are described in Section 4.1. The projections of LAEI and NAEI emissions data for future years are described in Section 4.2.

In Section 4.3 the emissions modelled for each scenario: aircraft, road traffic and all other emission sources are presented. Tables 4.5-4.15 list the source groups modelled with their annual emission of NO_X, NO_2 and PM_{10} in tonnes/year for the Base Case and the future scenarios. (For legibility the NO_X and NO_2 data in the body of each table are shown rounded to the nearest integer or two significant figures for smaller values for legibility. The totals shown at the bottom of each table are the "true total" of the un-rounded figures.) These data are also presented in Figures 4.1-4.4, as bar charts showing percentage change from the Base Case. Figure 4.5 presents bar charts showing the percentage change of aircraft emissions for scenarios 2015EP and 2015NoC from scenario 2015SM, the scenario of which they are variants.

Airport data were supplied by AEA for all the scenarios except the "no Cranford Agreement" scenario (2015NoC) for which emissions were estimated from other inventories. Emissions for 2015NoC have been estimated by assuming that all non-airport emissions are the same as 2015SM, aircraft emissions are the same as those for 2015MM and by applying a scaling factor of 0.885 to other airport sources of 2015MM, with the exception of fire training ground and heating plant groups, which are assumed to be unchanged. Concentrations of NO_x and NO_2 at receptor locations were estimated for 2015NoC from 2015SM and 2015MM predicted concentrations using the same methodology.

Hyder supplied road traffic data for the different roads scenarios. The 2015MM roads mitigation scenario (2015MMRd) differs from scenario 2015MM only in the major road emissions around Heathrow. The 2015MMRd major road emissions are given following Table 4.10.

For the two third runway scenarios (2020R3 and 2030R3) two airport emissions inventories were supplied, corresponding to two different modes of operation that are termed MDL and MLD. MDL refers to the mode of operation with mixed mode (landings and departures) on the northern runway, departures on the central runway and landings on the southern runway. In MLD the northern runway continues to operate in mixed mode (landings and departures), but landings are now on the central runway and departures on the southern runway. Modelling has been carried out for both MDL and MLD for 2002R3 and 2030R3. The

[9] www.cerc.co.uk/software/emit.htm
[10] London Atmospheric Emissions Inventory 2002 (LAEI 2002), Greater London Authority, February 2005, julius.mattai@london.gov.uk

concentration results presented in Section 10 are hybrid results from MDL and MLD modes of operation, calculated by assuming equal alternation between the MDL and MLD modes of operation.

From 2002 to 2030 (2030MM) the overall inventory emissions decrease, for NO_X from 96673t/yr to 47578t/yr and for NO_2 from 9734t/yr to 6082t/yr; PM_{10} emissions decrease from 4454t/yr in 2002 to 3383t/yr (2030MM). Comparing like for like scenarios i.e. segregated mode with segregated mode, mixed mode with mixed mode, and third runway with third runway, emissions of NO_X and NO_2 also decrease with time.

The major cause of the decrease in NO_X emissions is the predicted 80% reduction in NO_X due to road traffic due to improved vehicle technology. Over the same period NO_2 from road traffic is also predicted to decrease significantly, by approximately 60%. The decrease in NO_2 is not as great as the decrease in NO_X, which reflects the increase in primary NO_2 (the percentage of emitted NO_X that is NO_2) from road traffic with time[11].

Emissions due to airport sources change in magnitude and spatial distribution according to the scenario modelled. In all the future scenarios airport emissions increase, in some cases significantly, with respect to 2002 due to the increased number of take-offs and landings (air traffic movements or ATM). After 2020 predicted improvements in aircraft technology lead to a decrease in emissions per plane that partly offsets the increase in ATM. There are five main changes in spatial distribution:

(i) The operation of Terminal 5 and reconfiguration of stands (for all cases except the Base Case) causes a redistribution of airport emissions from east to west.

(ii) The introduction of mixed mode compared with segregated mode significantly increases the take-offs from runway 09L and reduces the take-offs from 09R, thereby causing a shift in emissions from the southern to the northern runway.

(iii) The creation of a third runway increases emissions to the north of the current airport boundary.

(iv) Operation of an easterly rather than a westerly preference shifts take-off emissions from the north-eastern end of runway 27R to the south-western end of runway 09R. There are associated changes in taxiing and hold emissions.

(v) The effect of the No Cranford option is to increase the use of runway 09L (and hence reduce the use of 09R) shifting take-off emissions from the south-west of the airport to the north-west.

[11] DEFRA's Air Quality Expert Group. Annex 2: Interim Guidance on UK Fleet-Average Projections in Values of f-NO_2 for Use in Models

4.1 LAEI and NAEI emissions data

LAEI and NAEI contain emissions data for the following pollutants:

- Nitrogen Oxides (NO_x);
- Sulphur Dioxide (SO_2);
- Carbon Monoxide (CO);
- Non-Methane Volatile Organic Compounds (NMVOC);
- Carbon Dioxide (CO_2);
- Benzene;
- 1,3-Butadiene; and,
- Particulate matter less than 10micrometres aerodynamic diameter (PM_{10}).

Table 4.4 lists the source categories for which emissions data were obtained from the LAEI and used in this modelling.

From NAEI total emissions were obtained, from which the major road emissions calculated from traffic data supplied by Hyder Consulting were subtracted to give the residual emissions.

4.2 LAEI and NAEI future years emissions data

The LAEI includes emissions data for all source groups for 2010. The following source groups have been assumed to remain constant between 2010, and 2030:

- Agriculture;
- City Airport;
- Domestic Coal;
- Domestic Oil;
- Nature;
- Sewage;
- Shipping;
- Solvents.

Boilers, Part A and Part B

Emissions from industrial sources (Part A and Part B) and Boilers are assumed constant in the LAEI between 2002 and 2010. For third runway scenarios, sources that fall inside the expanded airport site have been removed. In 2015MM and 2030R3 (that were the last two scenarios modelled) the old Colnbrook incinerator data have been replaced with data for the new Waste to Energy and clinical waste incineration facilities. Emissions from the new Colnbrook facility are significantly higher than those from the old facility but are emitted from a higher stack and therefore the impact on ground level concentrations is small. Annual average NO_X concentrations at Longford are predicted to increase by less than $0.1\mu g/m^3$ and annual average PM_{10} concentrations around Longford are predicted to decrease slightly due to the new facility.

Non-airport, non-road emissions

For the remaining non-airport, non-road sources, emissions have been projected from 2010 to 2030 using the LAEI predictions for 2010, together with national emissions projection data

from the DTI[12,13] (now the Department for Business, Enterprise and Regulatory Reform). Table 4.1 shows the growth in NO_x emissions assumed for each of the source groups for each modelled year.

Table 4.1 Non-airport, non-road emissions projections

	% Growth 2010 to 2015	% Growth 2010 to 2020	% Growth 2010 to 2030
Commercial Gas	7.2	13.1	15.6
Domestic Gas*	3.3	5.5	8.0
Gas Leak	4.0	7.9	12.8
Industrial Coal	-	-	17.6

*For 2015 and 2020 the average of the "with Climate Change Programme measures" and "without measures" has been used.

Rail

For rail emissions, an annual growth rate in activity (train movements) of 2.7% has been assumed between 2002 and 2006. Activity has been assumed to grow by 19% between 2006 and 2010, corresponding to an annual growth rate of 4.4%, with no growth after 2010. The re-engining of high speed trains (HSTs) is predicted to reduce emission factors in 2010 and 2015 compared with 2002. Emission factors for 2020 and 2030 are assumed to be the same as 2015. The predicted reduction in emissions is given in Table 4.2.

Table 4.2 Reduction in rail emission factors due to re-engining of high speed trains

	% Reduction 2002 to 2010	% Reduction 2002 to 2015
NO_x	30.8	62.6
PM_{10}	50.0	50.0

NAEI non-road

The NAEI non-road emissions used to the west of the M25 were projected from 2002 to 2015, 2020 and 2030 using the projected change in emissions from the equivalent source groups within London. The emissions for 2010 were projected on the basis of the growth in gas usage only in LAEI which is a conservative assumption. These factors are given in Table 4.3.

Table 4.3 NAEI non-road emissions growth

	% Growth 2002 to 2010	% Growth 2002 to 2015	% Growth 2002 to 2020	% Growth 2002 to 2030
NO_x	+5	-2	+1	-1
PM_{10}	+5	-20	-17	-18

[12] DTI "UK Energy and CO_2 Emissions projections, Updated projections to 2020 February 2006" 2006 http://www.dti.gov.uk/files/file26363.pdf

[13] DTI "UK Energy and CO_2 Emissions Projections, July 2006" http://www.dti.gov.uk/files/file31861.pdf

Table 4.4 Data groups for which emissions were obtained from the LAEI

Name	Description	Pollutants included
Point sources		
Part A processes	These are 'prescribed processes' that are most likely to cause serious pollution and they require authorisation from the Environment Agency under the Environmental Protection Act 1990	SO_2, NO_x, CO, CO_2, NMVOC, benzene, TSP, PM_{10}, methane
Part B processes	These are 'prescribed processes' designated for local authority control and must not operate without an authorisation from the local authority	SO_2, NO_x, CO, CO_2, NMVOC, Benzene, TSP, PM_{10}
Boilers	Emissions from boiler plants with a capacity greater than 2 megawatt hours	SO_2, NO_x, CO, CO_2, NMVOC, TSP, PM_{10}, methane
Area sources		
Agricultural	Emissions from soils, livestock, agricultural power units and stationary sources, domestic gardens, animal incineration and wood impregnation	SO_2, NO_x, CO, CO_2, NMVOC, benzene, 1,3-butadiene, PM_{10}
Nature	Emissions from forests and landfill activities	SO_2, NO_x, CO, CO_2, NMVOC, benzene, 1,3-butadiene, PM_{10}
Domestic coal	Emissions from combustion of domestic coal	SO_2, NO_x, CO, CO_2, NMVOC, benzene, TSP, PM_{10}, methane, smoke
Industrial coal	Emissions from combustion of industrial coal	SO_2, NO_x, CO, CO_2, NMVOC, benzene, TSP, PM_{10}, methane, smoke
Domestic gas	Emissions from domestic gas usage	NO_x, CO, CO_2, NMVOC, Benzene, PM_{10}, methane
Industrial-Commercial gas	Emissions from industrial and commercial gas usage excluding that already accounted for under point source emissions	NO_x, CO, CO_2, NMVOC, benzene, PM_{10}, methane
Gas leakage	Emissions from leakage on the gas distribution system	NMVOC, benzene, methane
Domestic Oil	Emissions from domestic oil combustion	SO_2, NO_x, CO, CO_2, NMVOC, TSP, PM_{10}, methane, smoke
Sewage treatment	Emissions from biogas production from sewage works	NO_x, CO, CO_2, NMVOC, methane
Solvents - building	Emissions from domestic and industrial solvent use (excluding that already accounted for under point sources), such as brewing and industrial painting, and emissions from building construction	NMVOC, $_{PM10}$

Table 4.4 (cont) Data groups for which emissions were obtained from the LAEI

Name	Description	Pollutants included
Mobile sources		
Minor roads	Emissions due to all traffic movements on minor roads	SO_2, NO_x, CO, CO_2, NMVOC, Benzene, 1,3-butadiene, PM_{10}
Cold start emissions	An additional emission from cars and LGVs due to the effect of cold starts	CO, NMVOC, NO_x, PM_{10}
Evaporative emissions	Emissions due to evaporation occurring from the fuel delivery system of cars and LGVs when a vehicle is stationary but with a hot engine.	NMVOC, benzene, 1,3-butadiene
Rail	Emissions from rail sources	SO_2, NO_x, CO, CO_2, NMVOC, Benzene, 1,3-butadiene, TSP, PM_{10}, smoke
Ships	Emissions from ships	SO_2, NO_x, CO, CO_2, NMVOC, TSP
London City airport	Emissions from London City airport	SO_2, NO_x, CO, CO_2, NMVOC, benzene, 1,3-butadiene, PM_{10}, methane

4.3 Emissions inventory totals

Table 4.5 2002 Base Case source groups modelled, comparison of annual NO_X, NO_2 and PM_{10} emissions. Domain: Easting=496000-559000, Northing=152000-204000. *For approach, climb out and initial climb all the emissions are included (Easting=485000-559000, Northing=152000-204000).

Group	NO_X (t/yr)	NO_2 (t/yr)	NO_2/NO_X (%)	PM_{10} (t/yr)
Agriculture	288	29	10%	118.8
* Aircraft approach	507	76	15%	3.9
Aircraft APUs	385	39	10%	8.7
* Aircraft climb out	1318	70	5.3%	4.7
* Aircraft initial climb	659	36	5.4%	2.2
Aircraft Hold	149	56	37.7%	3.1
Aircraft Landing Roll	39	9	24.4%	13.4
Aircraft Pushback + Taxi-out	273	101	37.1%	5.7
Aircraft Taxi-in	148	55	37.0%	3.2
Aircraft Take-off	653	38	5.8%	2.5
Airport Roads	38	4	10%	2.0
Airside vehicles	237	24	10%	18.5
Boilers	186	19	10%	14.9
Car Parks Etc	24	2	10%	1.4
City Airport	19	2	10%	0
Cold Start	430	43	10%	89.8
Commercial Gas	9112	911	10%	311.7
Domestic Coal	2.2E-05	2.2E-06	10%	4.7E-05
Domestic Gas	8808	881	10%	590.2
Domestic Oil	83	8	10%	6.9
Engine testing	16	2	10%	0.4
Evaporative	0	0	-	0
Fire training ground	1.4E-01	1.4E-02	10%	4.8E-03
Gas Leak	0	0	-	0
Heating Plant	179	18	10%	22.8
Helipad	5.1E-02	5.1E-03	10%	4.8E-04
Industrial Coal	1.8E-04	1.8E-05	10%	1.2E-04
Minor Roads	3763	376	10%	324.5
Nature	0	0	-	0
Paint shop	0	0	-	1.3E-02
Part A & B	4604	460	10%	693.4
Rail Line	3873	387	10%	144.8
Major roads around Heathrow	3571	357	10%	130.1
Major roads in rest of Greater London	55072	5507	10%	1800.9
NAEI Non-Road Sources	2017	202	10%	94.4
Sewage	28	3	10%	0
Shipping	196	20	10%	2.5
Solvents	0	0	-	38.3
Taxi ranks/queue	2.25	0.23	10%	0.2
Total	**96673**	**9734**	**10.1%**	**4454**

Table 4.6 2010SM source groups modelled, comparison of annual NO_X, NO_2 and PM_{10} emissions. Domain: Easting=496000-559000, Northing=152000-204000.
****For approach, climb out and initial climb all the emissions are included (Easting=485000-559000, Northing=152000-204000).***

Group	NO_X (t/yr)	NO_2 (t/yr)	NO_2/NO_X (%)	PM_{10} (t/yr)
Agriculture	288	29	10%	118.8
* Aircraft approach	669	100	15%	3.8
Aircraft APUs	384	38	10%	5.8
* Aircraft climb out	1895	100	5.3%	4.8
* Aircraft initial climb	999	53	5.3%	2.4
Aircraft Hold	174	65	37.5%	2.6
Aircraft Landing Roll	50	12	24.7%	18.2
Aircraft Pushback + Taxi-out	359	135	37.5%	5.3
Aircraft Taxi-in	191	72	37.5%	2.8
Aircraft Take-off	947	50	5.3%	2.6
Airport Roads	18	3	16.5%	0.6
Airside vehicles	169	17	10%	11.9
Boilers	186	19	10%	14.9
Car Parks Etc	13	2	16.5%	1.3
City Airport	19	2	10%	0
Cold Start	219	42	19.1%	52.7
Commercial Gas	9634	963	10%	329.5
Domestic Coal	2.2E-05	2.2E-06	10%	4.7E-05
Domestic Gas	9171	917	10%	614.5
Domestic Oil	83	8	10%	6.9
Engine testing	22	2	10%	0.4
Evaporative	0	0	-	0
Fire training ground	1.4E-01	1.4E-02	10%	4.8E-03
Gas Leak	0	0	-	0
Heating Plant	191	19	10%	25.0
Helipad	0	0	-	0
Industrial Coal	1.8E-04	1.8E-05	10%	1.2E-04
Minor Roads	1916	366	19.1%	190.2
Nature	0	0	-	0
Paint shop	0	0	-	1.3E-02
Part A & B	4604	460	10%	693.4
Rail Line	3543	354	10%	95.7
Major roads around Heathrow	1921	317	16.5%	72.5
Major roads in rest of Greater London	27926	5334	19.1%	1059.2
NAEI Non-Road Sources	2118	212	10%	98.9
Sewage	28	3	10%	0
Shipping	178	18	10%	1.6
Solvents	0	0	-	38.3
Taxi ranks/queue	2.23	0.37	16.5%	0.1
Total	**67915**	**9714**	**14.3%**	**3475**

Table 4.7 2015SM source groups modelled, comparison of annual NO_X, NO_2 and PM_{10} emissions. Domain: Easting=496000-559000, Northing=152000-204000.
****For approach, climb out and initial climb all the emissions are included (Easting=485000-559000, Northing=152000-204000).***

Group	NO_X (t/yr)	NO_2 (t/yr)	NO_2/NO_X (%)	PM_{10} (t/yr)
Agriculture	288	29	10%	118.8
* Aircraft approach	690	103	15%	3.6
Aircraft APUs	306	31	10%	4.3
* Aircraft climb out	2174	115	5.3%	4.4
* Aircraft initial climb	1115	59	5.3%	2.1
Aircraft Hold	187	70	37.5%	2.5
Aircraft Landing Roll	56	14	24.2%	20.4
Aircraft Pushback + Taxi-out	377	142	37.5%	5.0
Aircraft Taxi-in	203	76	37.5%	2.7
Aircraft Take-off	1071	57	5.3%	2.4
Airport Roads	15	3	18.5%	0.5
Airside vehicles	126	13	10%	9.9
Boilers	186	19	10%	14.9
Car Parks Etc	10	2	18.5%	1.3
City Airport	19	2	10%	0
Cold Start	172	36	21.1%	45.4
Commercial Gas	10330	1033	10%	353.2
Domestic Coal	2.2E-05	2.2E-06	10%	4.7E-05
Domestic Gas	9473	947	10%	634.8
Domestic Oil	83	8	10%	6.9
Engine testing	24	2	10%	0.3
Evaporative	0	0	-	0
Fire training ground	1.4E-01	1.4E-02	10%	4.8E-03
Gas Leak	0	0	-	0
Heating Plant	191	19	10%	25.0
Helipad	0	0	-	0
Industrial Coal	1.8E-04	1.8E-05	10%	1.2E-04
Minor Roads	1505	318	21.1%	163.9
Nature	0	0	-	0
Paint shop	0	0	-	1.3E-02
Part A & B	4604	460	10%	693.4
Rail Line	1917	192	10%	95.7
Major roads around Heathrow	1474	273	18.5%	59.6
Major roads in rest of Greater London	21964	4635	21.1%	914.8
NAEI Non-Road Sources	1977	198	10%	75.6
Sewage	28	3	10%	0
Shipping	178	18	10%	1.6
Solvents	0	0	-	38.3
Taxi ranks/queue	2.11	0.39	18.5%	0.1
Total	**60743**	**8875**	**14.6%**	**3301**

Table 4.8 2015EP source groups modelled, comparison of annual NO_X, NO_2 and PM_{10} emissions. Domain: Easting=496000-559000, Northing=152000-204000.
****For approach, climb out and initial climb all the emissions are included (Easting=485000-559000, Northing=152000-204000).***

Group	NO_X (t/yr)	NO_2 (t/yr)	NO_2/NO_X (%)	PM_{10} (t/yr)
Agriculture	288	29	10%	118.8
* Aircraft approach	690	103	15%	3.6
Aircraft APUs	306	31	10%	4.3
* Aircraft climb out	2174	115	5.3%	4.4
* Aircraft initial climb	1115	59	5.3%	2.1
Aircraft Hold	190	71	37.5%	2.5
Aircraft Landing Roll	56	14	24.2%	20.4
Aircraft Pushback + Taxi-out	381	143	37.5%	5.0
Aircraft Taxi-in	208	78	37.5%	2.8
Aircraft Take-off	1071	57	5.3%	2.4
Airport Roads	15	3	18.5%	0.5
Airside vehicles	126	13	10%	9.9
Boilers	186	19	10%	14.9
Car Parks Etc	10	2	18.5%	1.3
City Airport	19	2	10%	0
Cold Start	172	36	21.1%	45.4
Commercial Gas	10330	1033	10%	353.2
Domestic Coal	2.2E-05	2.2E-06	10%	4.7E-05
Domestic Gas	9473	947	10%	634.8
Domestic Oil	83	8	10%	6.9
Engine testing	24	2	10%	0.3
Evaporative	0	0	-	0
Fire training ground	1.4E-01	1.4E-02	10%	4.8E-03
Gas Leak	0	0	-	0
Heating Plant	191	19	10%	25.0
Helipad	0	0	-	0
Industrial Coal	1.8E-04	1.8E-05	10%	1.2E-04
Minor Roads	1505	318	21.1%	163.9
Nature	0	0	-	0
Paint shop	0	0	-	1.3E-02
Part A & B	4604	460	10%	693.4
Rail Line	1917	192	10%	95.7
Major roads around Heathrow	1474	273	18.5%	59.6
Major roads in rest of Greater London	21964	4635	21.1%	914.8
NAEI Non-Road Sources	1977	198	10%	75.6
Sewage	28	3	10%	0
Shipping	178	18	10%	1.6
Solvents	0	0	-	38.3
Taxi ranks/queue	2.11	0.39	18.5%	0.1
Total	**60755**	**8879**	**14.6%**	**3301**

Table 4.9 2015NoC source groups, comparison of estimated annual NO_X, NO_2 and PM_{10} emissions. Domain: Easting=496000-559000, Northing=152000-204000.
****For approach, climb out and initial climb all the emissions are included (Easting=485000-559000, Northing=152000-204000).***

Group	NO_X (t/yr)	NO_2 (t/yr)	NO_2/NO_X (%)	PM_{10} (t/yr)
Agriculture	288	29	10%	118.8
* Aircraft approach	705	106	15%	3.8
Aircraft APUs	279	28	10%	4.2
* Aircraft climb out	2151	114	5.3%	4.6
* Aircraft initial climb	1109	59	5.3%	2.2
Aircraft Hold	169	63	37.5%	2.3
Aircraft Landing Roll	55	14	24.8%	20.6
Aircraft Pushback + Taxi-out	377	141	37.5%	5.2
Aircraft Taxi-in	199	75	37.5%	2.7
Aircraft Take-off	1065	56	5.3%	2.5
Airport Roads	13	2	18.5%	0.5
Airside vehicles	117	12	10%	9.2
Boilers	186	19	10%	14.9
Car Parks Etc	10	2	18.5%	1.5
City Airport	19	2	10%	0
Cold Start	172	36	21.1%	45.4
Commercial Gas	10330	1033	10%	353.2
Domestic Coal	2.2E-05	2.2E-06	10%	4.7E-05
Domestic Gas	9473	947	10%	634.8
Domestic Oil	83	8	10%	6.9
Engine testing	24	2	10%	0.3
Evaporative	0	0	-	0
Fire training ground	1.4E-01	1.4E-02	10%	4.8E-03
Gas Leak	0	0	-	0
Heating Plant	191	19	10%	25.0
Helipad	0	0	-	0
Industrial Coal	1.8E-04	1.8E-05	10%	1.2E-04
Minor Roads	1505	318	21.1%	163.9
Nature	0	0	-	0
Paint shop	0	0	-	1.3E-02
Part A & B	4604	460	10%	693.4
Rail Line	1917	192	10%	95.7
Major roads around Heathrow	1474	273	18.5%	59.6
Major roads in rest of Greater London	21964	4635	21.1%	914.8
NAEI Non-Road Sources	1977	198	10%	75.6
Sewage	28	3	10%	0
Shipping	178	18	10%	1.6
Solvents	0	0	-	38.3
Taxi ranks/queue	1.84	0.34	18.5%	0.1
Total	**60653**	**8861**	**14.6%**	**3301**

Table 4.10 2015MM source groups modelled, comparison of annual NO_X, NO_2 and PM_{10} emissions. Domain: Easting=496000-559000, Northing=152000-204000.
****For approach, climb out and initial climb all the emissions are included (Easting=485000-559000, Northing=152000-204000).***

Group	NO_X (t/yr)	NO_2 (t/yr)	NO_2/NO_X (%)	PM_{10} (t/yr)
Agriculture	288	29	10%	118.8
* Aircraft approach	705	106	15%	3.8
Aircraft APUs	279	28	10%	4.2
* Aircraft climb out	2151	114	5.3%	4.6
* Aircraft initial climb	1109	59	5.3%	2.2
Aircraft Hold	169	63	37.5%	2.3
Aircraft Landing Roll	55	14	24.8%	20.6
Aircraft Pushback + Taxi-out	377	141	37.5%	5.2
Aircraft Taxi-in	199	75	37.5%	2.7
Aircraft Take-off	1065	56	5.3%	2.5
Airport Roads	15	3	18.5%	0.5
Airside vehicles	132	13	10%	10.4
Boilers	186	19	10%	14.9
Car Parks Etc	11	2	18%	1.7
City Airport	19	2	10%	0
Cold Start	172	36	21.1%	45.4
Commercial Gas	10330	1033	10%	353.2
Domestic Coal	2.2E-05	2.2E-06	10%	4.7E-05
Domestic Gas	9473	947	10%	634.8
Domestic Oil	83	8	10%	6.9
Engine testing	24	2	10%	0.3
Evaporative	0	0	-	0
Fire training ground	1.4E-01	1.4E-02	10%	4.8E-03
Gas Leak	0	0	-	0
Heating Plant	191	19	10%	25.0
Helipad	0	0	-	0
Industrial Coal	1.8E-04	1.8E-05	10%	1.2E-04
Minor Roads	1505	318	21.1%	163.9
Nature	0	0	-	0
Paint shop	0	0	-	1.3E-02
Part A & B	5123	512	10%	712.7
Rail Line	1917	192	10%	95.7
Major roads around Heathrow	1474	273	18.5%	59.8
Major roads in rest of Greater London	21970	4635	21.1%	914.9
NAEI Non-Road Sources	1977	198	10%	75.6
Sewage	28	3	10%	0
Shipping	178	18	10%	1.6
Solvents	0	0	-	38.3
Taxi ranks/queue	2.08	0.38	18.5%	0.1
Total	**61195**	**8915**	**14.6%**	**3323**

The ***2015MMRd*** scenario has identical emission except for the major roads around Heathrow where the emissions are 1424t/yr NO_X, 263t/yr NO_2, 59.5t/yr PM_{10}.

Table 4.11 2030MM source groups modelled, comparison of annual NO_X, NO_2 and PM_{10} emissions. Domain: Easting=496000-559000, Northing=152000-204000.
****For approach, climb out and initial climb all the emissions are included (Easting=485000-559000, Northing=152000-204000).***

Group	NO_X (t/yr)	NO_2 (t/yr)	NO_2/NO_X (%)	PM_{10} (t/yr)
Agriculture	288	29	10%	118.8
* Aircraft approach	617	93	15%	3.6
Aircraft APUs	242	24	10%	3.8
* Aircraft climb out	2147	114	5.3%	4.4
* Aircraft initial climb	1085	57	5.3%	2.1
Aircraft Hold	123	46	37.5%	1.6
Aircraft Landing Roll	51	13	25.2%	22.8
Aircraft Pushback + Taxi-out	372	139	37.5%	4.7
Aircraft Taxi-in	193	73	37.5%	2.4
Aircraft Take-off	1034	55	5.3%	2.3
Airport Roads	5	1	19.1%	0.4
Airside vehicles	93	9	10%	9.7
Boilers	186	19	10%	14.9
Car Parks Etc	11	2	19.1%	1.7
City Airport	19	2	10%	0
Cold Start	76	17	21.8%	46.2
Commercial Gas	11140	1114	10%	380.9
Domestic Coal	2.2E-05	2.2E-06	10%	4.7E-05
Domestic Gas	9907	991	10%	663.9
Domestic Oil	83	8	10%	6.9
Engine testing	23	2	10%	0.3
Evaporative	0	0	-	0
Fire training ground	1.4E-01	1.4E-02	10%	4.8E-03
Gas Leak	0	0	-	0
Heating Plant	191	19	10%	25.0
Helipad	0	0	-	0
Industrial Coal	2.1E-04	2.1E-05	10%	1.4E-04
Minor Roads	667	145	21.8%	167.0
Nature	0	0	-	0
Paint shop	0	0	-	1.3E-02
Part A & B	4604	460	10%	693.4
Rail Line	1917	192	10%	95.7
Major roads around Heathrow	661	126	19.1%	61.2
Major roads in rest of Greater London	9727	2120	21.8%	931.9
NAEI Non-Road Sources	1997	200	10%	77.3
Sewage	28	3	10%	0
Shipping	178	18	10%	1.6
Solvents	0	0	-	38.3
Taxi ranks/queue	2.37	0.45	19.1%	0.1
Total	**47666**	**6091**	**12.8%**	**3383**

Table 4.12 2020R3 MDL source groups modelled, comparison of annual NO_X, NO_2 and PM_{10} emissions. Domain: Easting=496000-559000, Northing=152000-204000.
****For approach, climb out and initial climb all the emissions are included (Easting=485000-559000, Northing=152000-204000).***

Group	NO_X (t/yr)	NO_2 (t/yr)	NO_2/NO_X (%)	PM_{10} (t/yr)
Agriculture	288	29	10%	118.8
* Aircraft approach	839	126	15%	4.6
Aircraft APUs	292	29	10%	4.6
* Aircraft climb out	2829	150	5.3%	5.6
* Aircraft initial climb	1450	77	5.3%	2.6
Aircraft Hold	187	70	37.5%	2.2
Aircraft Landing Roll	68	17	25.5%	27.3
Aircraft Pushback + Taxi-out	446	167	37.5%	5.4
Aircraft Taxi-in	207	77	37.5%	2.6
Aircraft Take-off	1378	73	5.3%	3.0
Airport Roads	7	1	19.2%	0.4
Airside vehicles	127	13	10%	11.9
Boilers	171	17	10%	14.1
Car Parks Etc	12	2	19.2%	1.7
City Airport	19	2	10%	0
Cold Start	91	20	21.9%	44.0
Commercial Gas	10900	1090	10%	372.7
Domestic Coal	2.2E-05	2.2E-06	10%	4.7E-05
Domestic Gas	9675	968	10%	648.3
Domestic Oil	83	8	10%	6.9
Engine testing	31	3	10%	0.4
Evaporative	0	0	-	0
Fire training ground	1.4E-01	1.4E-02	10%	4.8E-03
Gas Leak	0	0	-	0
Heating Plant	197	20	10%	25.7
Helipad	0	0	-	0
Industrial Coal	1.8E-04	1.8E-05	10%	1.2E-04
Minor Roads	799	175	21.9%	159.1
Nature	0	0	-	0
Paint shop	0	0	-	1.3E-02
Part A & B	4580	458	10%	686.2
Rail Line	1917	192	10%	95.7
Major roads around Heathrow	789	151	19.2%	58.6
Major roads in rest of Greater London	11659	2553	21.9%	887.7
NAEI Non-Road Sources	2037	204	10%	78.4
Sewage	28	3	10%	0
Shipping	178	18	10%	1.6
Solvents	0	0	-	38.3
Taxi ranks/queue	2.57	0.49	19.2%	0.1
Total	**51284**	**6713**	**13.1%**	**3309**

Table 4.13 2020R3 MLD source groups modelled, comparison of annual NO_X, NO_2 and PM_{10} emissions. Domain: Easting=496000-559000, Northing=152000-204000.
****For approach, climb out and initial climb all the emissions are included (Easting=485000-559000, Northing=152000-204000).***

Group	NO_X (t/yr)	NO_2 (t/yr)	NO_2/NO_X (%)	PM_{10} (t/yr)
Agriculture	288	29	10%	118.8
* Aircraft approach	839	126	15%	4.6
Aircraft APUs	297	30	10%	4.7
* Aircraft climb out	2831	150	5.3%	5.6
* Aircraft initial climb	1451	77	5.3%	2.6
Aircraft Hold	193	72	37.5%	2.3
Aircraft Landing Roll	68	18	25.6%	27.3
Aircraft Pushback + Taxi-out	520	195	37.5%	6.2
Aircraft Taxi-in	217	81	37.5%	2.7
Aircraft Take-off	1380	73	5.3%	3.0
Airport Roads	7	1	19.2%	0.4
Airside vehicles	127	13	10%	11.9
Boilers	171	17	10%	14.1
Car Parks Etc	12	2	19.2%	1.7
City Airport	19	2	10%	0
Cold Start	91	20	21.9%	44.0
Commercial Gas	10900	1090	10%	372.7
Domestic Coal	2.2E-05	2.2E-06	10%	4.7E-05
Domestic Gas	9675	968	10%	648.3
Domestic Oil	83	8	10%	6.9
Engine testing	31	3	10%	0.4
Evaporative	0	0	-	0
Fire training ground	1.4E-01	1.4E-02	10%	4.8E-03
Gas Leak	0	0	-	0
Heating Plant	197	20	10%	25.7
Helipad	0	0	-	0
Industrial Coal	1.8E-04	1.8E-05	10%	1.2E-04
Minor Roads	799	175	21.9%	159.1
Nature	0	0	-	0
Paint shop	0	0	-	1.3E-02
Part A & B	4580	458	10%	696.2
Rail Line	1917	192	10%	95.7
Major roads around Heathrow	789	151	19.2%	58.6
Major roads in rest of Greater London	11659	2553	21.9%	887.7
NAEI Non-Road Sources	2037	204	10%	78.4
Sewage	28	3	10%	0
Shipping	178	18	10%	1.6
Solvents	0	0	-	38.3
Taxi ranks/queue	2.57	0.49	19.2%	0.1
Total	**51384**	**6748**	**13.1%**	**3310**

Table 4.14 2030R3 MDL source groups modelled, comparison of annual NO_X, NO_2 and PM_{10} emissions. Domain: Easting=496000-559000, Northing=152000-204000.
****For approach, climb out and initial climb all the emissions are included (Easting=485000-559000, Northing=152000-204000).***

Group	NO_X (t/yr)	NO_2 (t/yr)	NO_2/NO_X (%)	PM_{10} (t/yr)
Agriculture	288	29	10%	118.8
* Aircraft approach	719	108	15%	4.5
Aircraft APUs	271	27	10%	4.6
* Aircraft climb out	2523	134	5.3%	5.7
* Aircraft initial climb	1261	67	5.3%	2.7
Aircraft Hold	145	54	37.5%	2.0
Aircraft Landing Roll	57	14	24.7%	25.0
Aircraft Pushback + Taxi-out	364	137	37.5%	5.1
Aircraft Taxi-in	170	64	37.5%	2.5
Aircraft Take-off	1205	64	5.3%	3.0
Airport Roads	5	1	19.1%	0.4
Airside vehicles	108	11	10%	11.3
Boilers	171	17	10%	14.1
Car Parks Etc	12	2	19.1%	1.7
City Airport	19	2	10%	0
Cold Start	76	17	21.8%	46.2
Commercial Gas	11140	1114	10%	380.9
Domestic Coal	2.2E-05	2.2E-06	10%	4.7E-05
Domestic Gas	9907	991	10%	663.9
Domestic Oil	83	8	10%	6.9
Engine testing	27	3	10%	0.4
Evaporative	0	0	-	0
Fire training ground	1.4E-01	1.4E-02	10%	4.8E-03
Gas Leak	0	0	-	0
Heating Plant	197	20	10%	25.7
Helipad	0	0	-	0
Industrial Coal	2.1E-04	2.1E-05	10%	1.4E-04
Minor Roads	667	145	21.8%	167.0
Nature	0	0	-	0
Paint shop	0	0	-	1.3E-02
Part A & B	5099	510	10%	705.5
Rail Line	1917	192	10%	95.7
Major roads around Heathrow	665	127	19.1%	61.8
Major roads in rest of Greater London	9728	2120	21.8%	932.3
NAEI Non-Road Sources	1997	200	10%	77.3
Sewage	28	3	10%	0
Shipping	178	18	10%	1.6
Solvents	0	0	-	38.3
Taxi ranks/queue	2.67	0.51	19.1%	0.1
Total	**49026**	**6197**	**12.6%**	**3405**

Table 4.15 2030R3 MLD source groups modelled, comparison of annual NO_X, NO_2 and PM_{10} emissions. Domain: Easting=496000-559000, Northing=152000-204000.
****For approach, climb out and initial climb all the emissions are included (Easting=485000-559000, Northing=152000-204000).***

Group	NO_X (t/yr)	NO_2 (t/yr)	NO_2/NO_X (%)	PM_{10} (t/yr)
Agriculture	288	29	10%	118.8
* Aircraft approach	719	108	15%	4.5
Aircraft APUs	271	27	10%	4.6
* Aircraft climb out	2523	134	5.3%	5.7
* Aircraft initial climb	1261	67	5.3%	2.7
Aircraft Hold	153	57	37.5%	2.1
Aircraft Landing Roll	58	14	24.8%	25.0
Aircraft Pushback + Taxi-out	441	165	37.5%	6.1
Aircraft Taxi-in	177	66	37.5%	2.5
Aircraft Take-off	1206	64	5.3%	3.0
Airport Roads	5	1	19.1%	0.4
Airside vehicles	108	11	10%	11.3
Boilers	171	17	10%	14.1
Car Parks Etc	12	2	19.1%	1.7
City Airport	19	2	10%	0
Cold Start	76	17	21.8%	46.2
Commercial Gas	11140	1114	10%	380.9
Domestic Coal	2.2E-05	2.2E-06	10%	4.7E-05
Domestic Gas	9907	991	10%	663.9
Domestic Oil	83	8	10%	6.9
Engine testing	27	3	10%	0.4
Evaporative	0	0	-	0
Fire training ground	1.4E-01	1.4E-02	10%	4.8E-03
Gas Leak	0	0	-	0
Heating Plant	197	20	10%	25.7
Helipad	0	0	-	0
Industrial Coal	2.1E-04	2.1E-05	10%	1.4E-04
Minor Roads	667	145	21.8%	167.0
Nature	0	0	-	0
Paint shop	0	0	-	1.3E-02
Part A & B	5099	510	10%	705.5
Rail Line	1917	192	10%	95.7
Major roads around Heathrow	665	127	19.1%	61.8
Major roads in rest of Greater London	9728	2120	21.8%	932.3
NAEI Non-Road Sources	1997	200	10%	77.3
Sewage	28	3	10%	0
Shipping	178	18	10%	1.6
Solvents	0	0	-	38.3
Taxi ranks/queue	2.67	0.51	19.1%	0.1
Total	**49119**	**6231**	**12.7%**	**3406**

Figure 4.1 NO_x emissions of modelled source groups for 2002 Base case, 2010SM and 2015SM, as a percentage of 2002 Base case emissions.

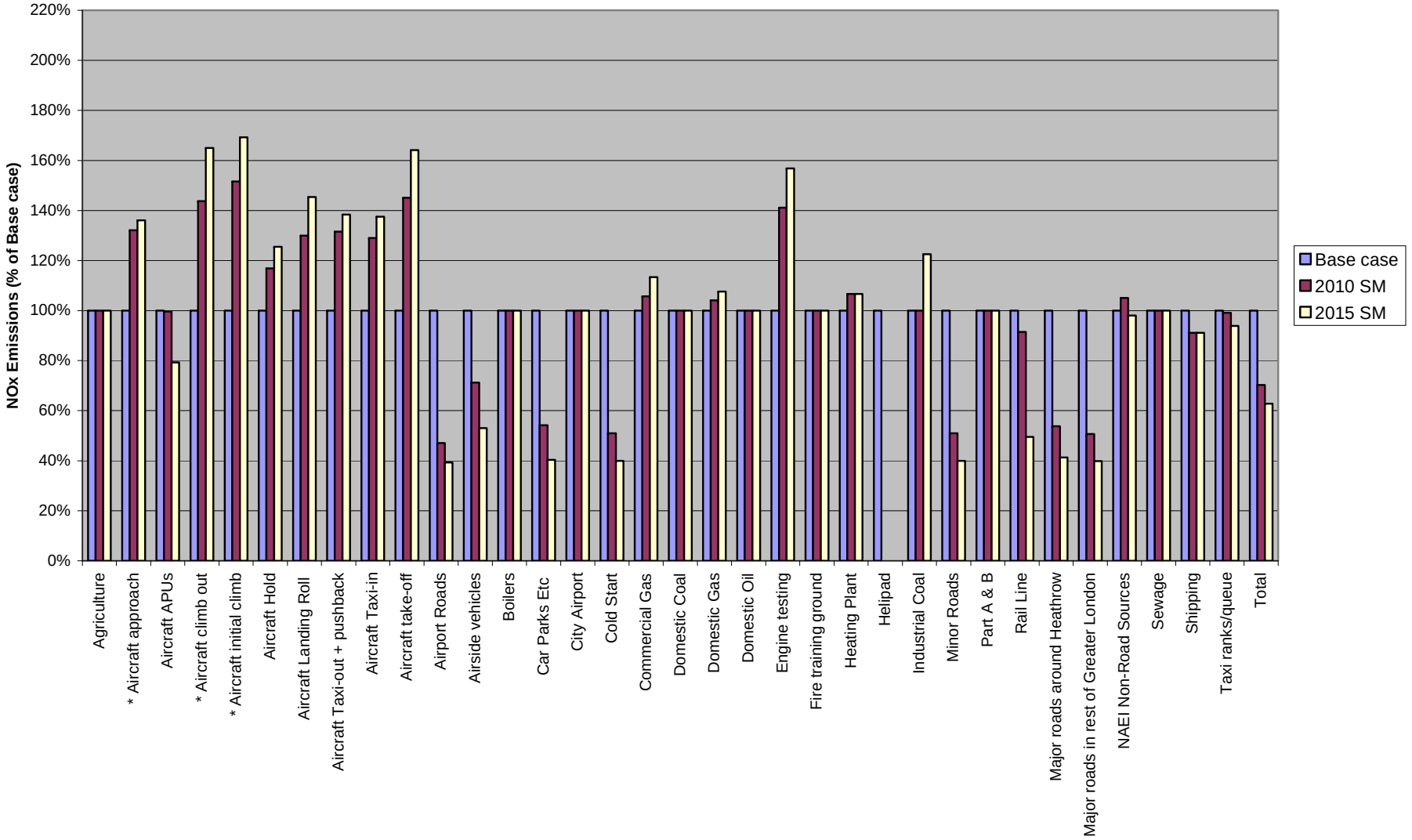

Figure 4.2 NO_x emissions of modelled source groups for 2002 Base case, 2015MM and 2030MM, as a percentage of 2002 Base case emissions.

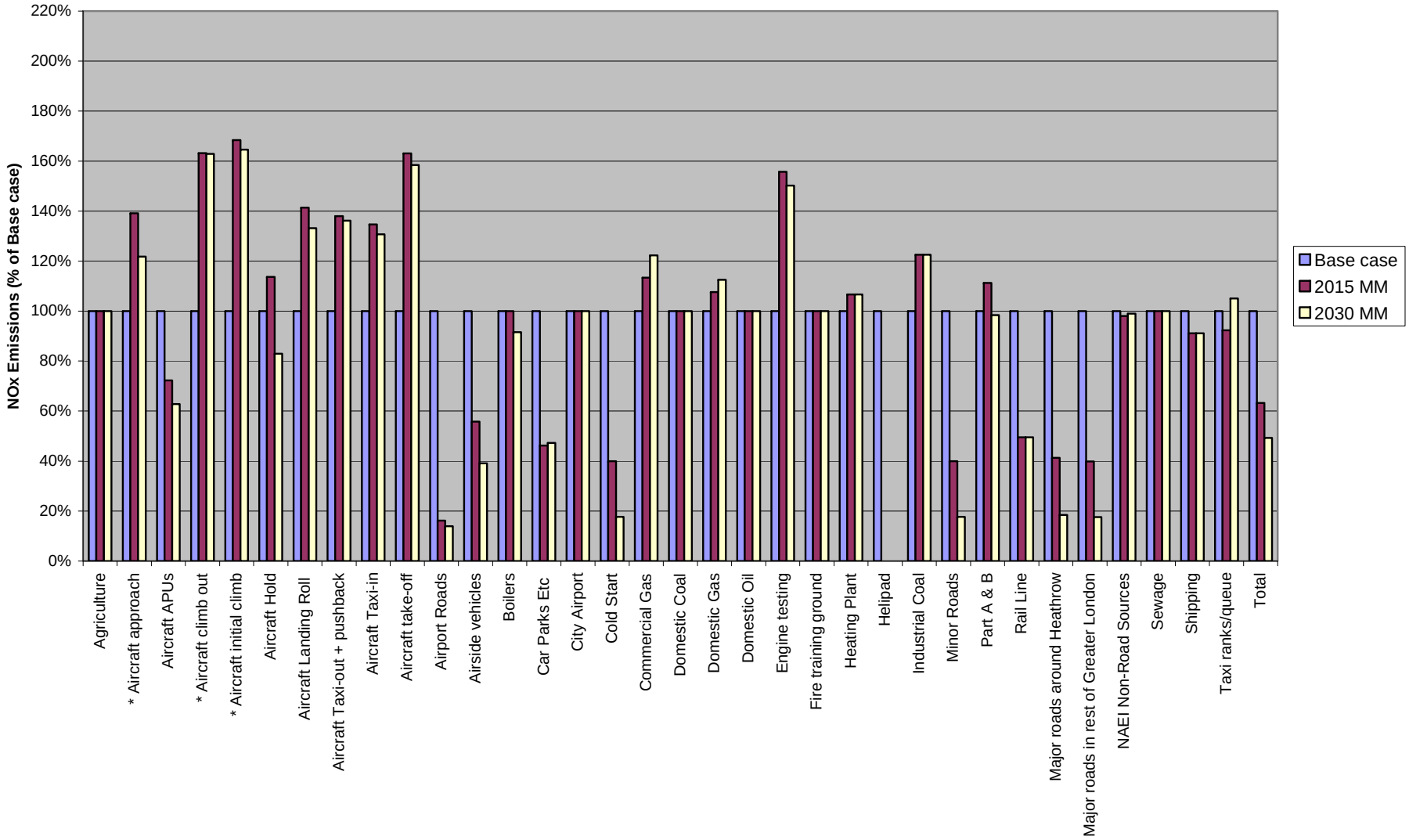

Figure 4.3 NO_x emissions of modelled source groups for 2002 Base case, 2020 MDL and 2020 MLD, as a percentage of 2002 Base case emissions

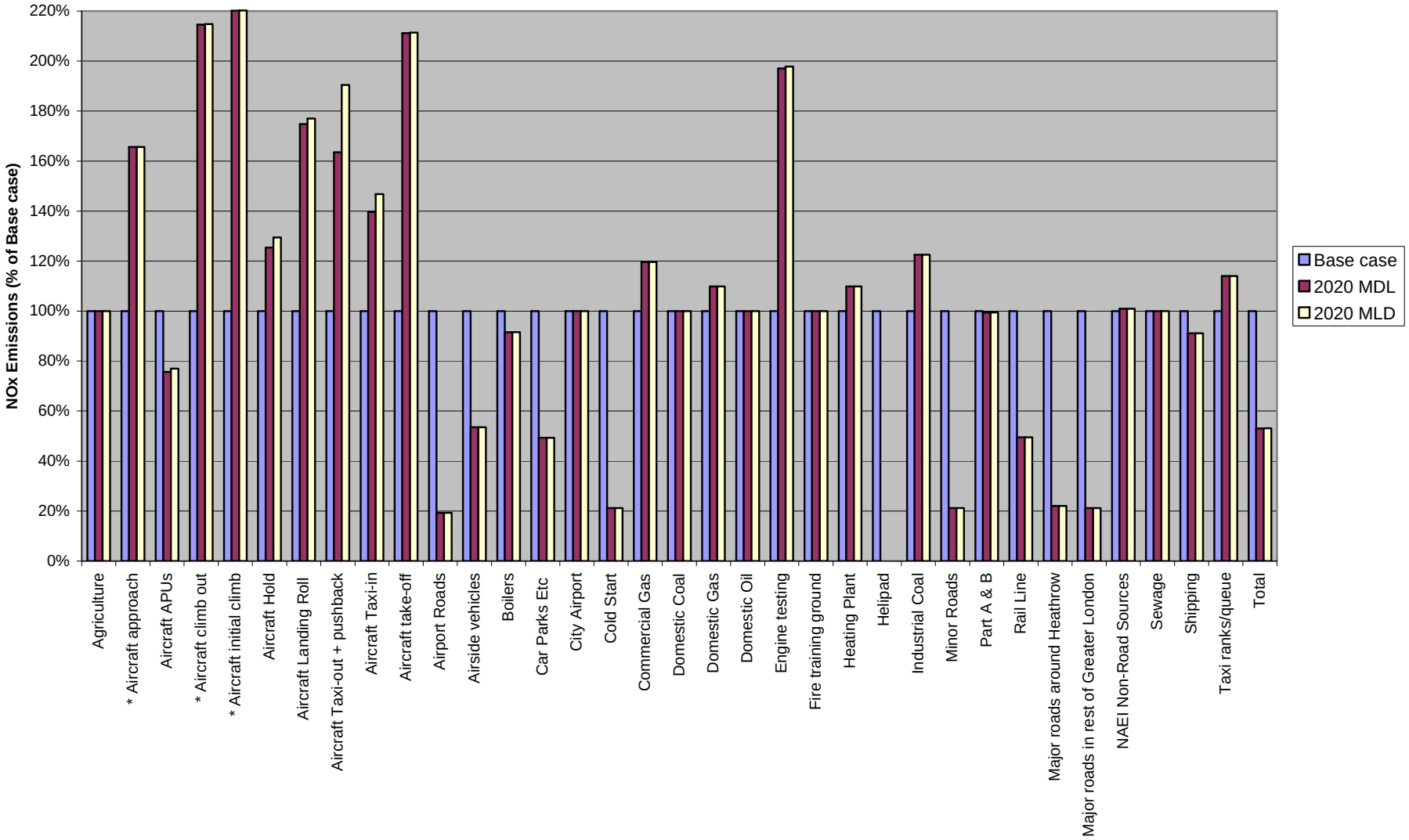

Figure 4.4 NO_x emissions of modelled source groups for 2002 Base case, 2030 MDL and 2030 MLD, as a percentage of 2002 Base case emissions

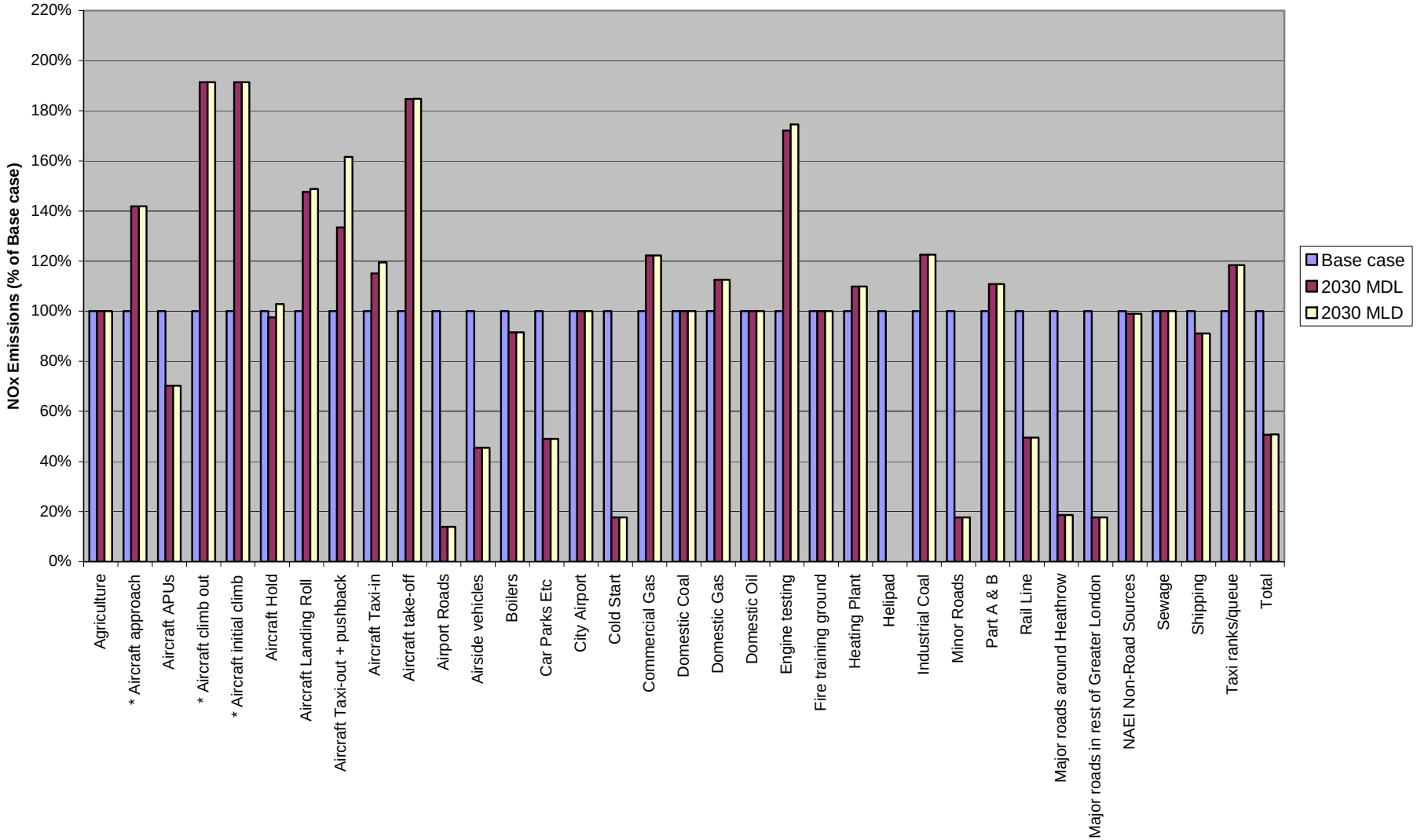

Figure 4.5 NO_x emissions of aircraft source groups for 2015SM, 2015EP and 2015NoC, as a percentage of 2015SM emissions. Emissions from other source groups are the same for all three scenarios.

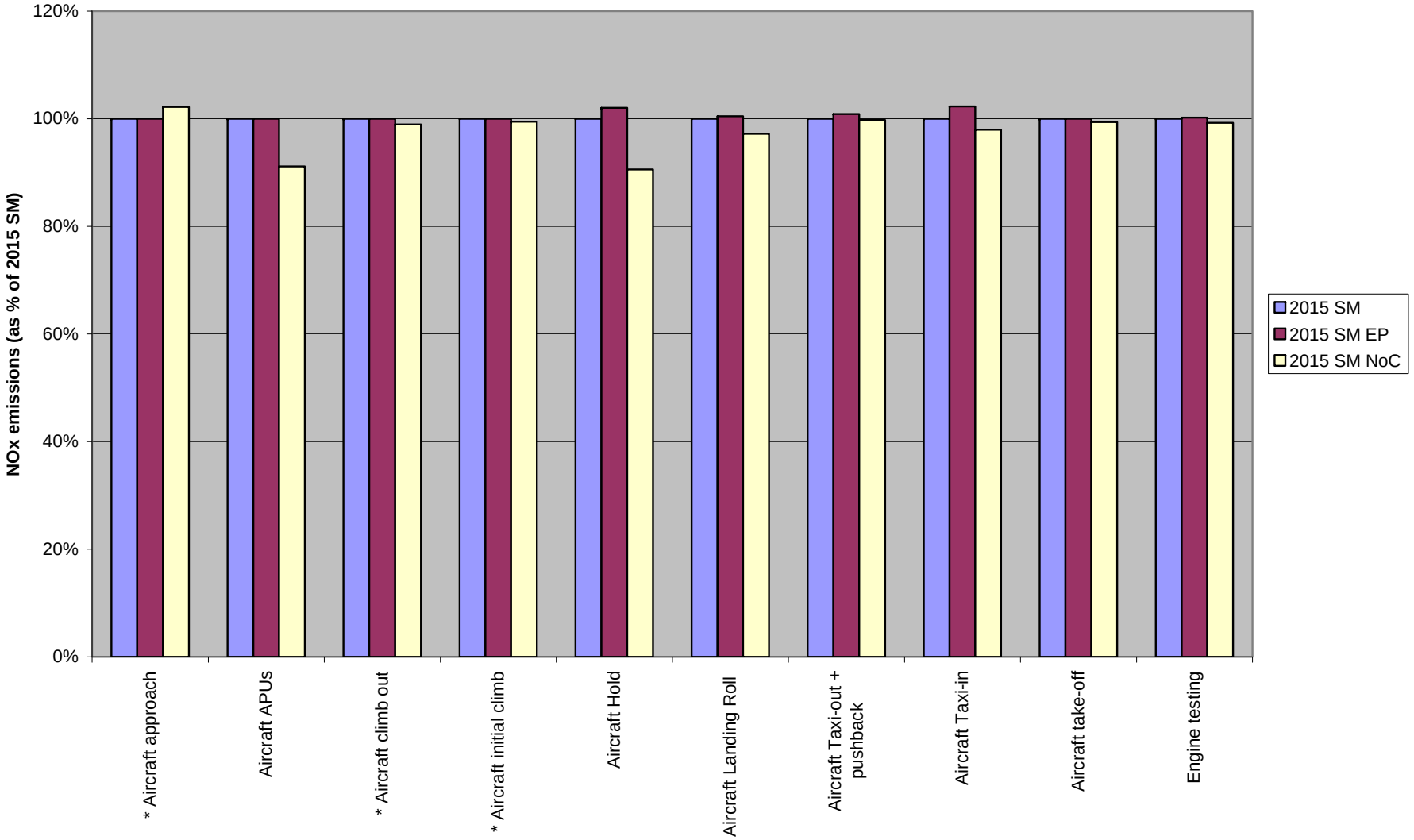

5 Airport Emissions Inventory

The airport emissions inventories were compiled from data supplied by AEA.

5.1 Time varying nature of the aircraft sources

Time varying emissions data were provided for most sources on an 8760-hour-of-the-year basis or a 24-hour diurnal basis (assuming all days of the week are the same).

For 2002 Base case, no data on the time varying operation of the heating plant were supplied and so they were assumed to operate at a constant rate. This is a commonly used approach for industrial sources and should not significantly affect the calculation of annual average concentrations. For the future scenarios monthly profiles were supplied and used for the heating plant.

Take-off, initial climb, landing roll without reverse thrust and hold sources were modelled in ADMS-Airport as jet sources using hourly profiles with 8760 elements (corresponding to the 8760 hours in a year) that were source-specific for the take-off roll i.e. varied with aircraft group, speed at wheels off and take-off time. For initial climb, landing roll without reverse thrust and hold the hourly profiles were averaged over the aircraft groups.

Taxiing sources were modelled as moving jet sources with the exception of light aircraft and Concorde in the Base case, which were modelled as volume sources. In all other scenarios the lowest-emitting sources were modelled as volume sources. All taxiing sources were modelled with diurnal profiles.

Approach was modelled as volume sources using time varying profiles with 8760 elements that were runway (and mode) specific. The diurnal profiles for the airside vehicles, APU, Taxi-in, Taxi-out and Push back were derived from 8760-hour data.

5.2 Primary NO_2

The percentage of primary NO_2 used for each of the aircraft sources was as given by the University of Sheffield report[14] and recommended by the PSDH Panel report. The 85% thrust value was used for take-off roll as this reflected the aircraft operation at Heathrow. The percentages of primary NO_2 are given in Table 5.1. Emissions of NO_X from Concorde were assumed to be 50% NO_2 for all modes.

Table 5.1 Data groups for which emissions were obtained from the LAEI

Thrust (%)	Mode	Primary NO_2 (%)
100%	Take-off roll (not used)	4.5%
85%	Take-off roll, Initial climb, Climb out	5.3%
30%	Approach, Reverse thrust	15.0%
7%	Idle i.e. Hold, Taxiing, part of Landing	37.5%

[14] Garcia-Naranjo A and Wilson CW. 2005. Primary NO2 from Aircraft Engines operating over the LTO cycle. RC110187//05/01.

6 Road Emissions Inventory

Major road data were supplied by Hyder Consulting for eight different modelling scenarios, the 2002 Base case and seven future scenarios. Future scenarios 2015EP and 2015NoC were assumed to have the same road traffic data as scenario 2015SM as they differed from 2015SM only in the airport operation. In the third runway cases (2020R3, 2030R3) the same traffic data was used for the two modes of airport operation, MDL and MLD. The data supplied were the output from the RRTM2[15] model and were of two types:

- UK-wide roads AADT, speed, straight line geometry and actual length for all the roads in the UK. These were divided into motorways and non-motorways. A subset of these data, covering approximately Greater London except the area around Heathrow, were used in the modelling. The road emissions were calculated on a $1km^2$ gridded basis. These are described in more detail in Section 6.2.
- Heathrow major roads Hourly flows for cars and heavy vehicles separately and hourly speeds on approximately 500 road links in the area around Heathrow. The links are defined as "Heathrow" or "Strategic" and, within each of those categories, as motorway or non-motorway. The diurnal profiles (weekday, Saturday, Sunday) of AADT and of speed were used to calculate diurnal and hence annual emissions. These are described in more detail in Section 6.3.

The data for 2002 are illustrated in Figure 6.1. Treatment of primary NO_2 is described in Section 6.1.

6.1 Primary NO_2

For 2002 it was assumed that 10% of the NO_X emitted from road traffic was emitted as NO_2 (referred to as primary NO_2). Data for the primary NO_2 percentage for future years was obtained from the Air Quality Expert Group[11] for LDV (light duty vehicles), HGV (heavy duty vehicles) and buses with DPF (diesel particulate filter) and are shown in Table 6.1. These factors have been applied to the emissions from major roads, minor roads and cold start emissions.

Table 6.1 Primary NO_2 percentages for roads in the Heathrow area and the rest of London

	2002	2010	2015	2020	2030
Heathrow area	10%	16.5%	18.5%	19.2	19.1%
Rest of London	10%	19.1%	21.1%	21.9	21.8%

6.2 UK-wide roads

The AADT, average speed and motorway/non-motorway designation were used to calculate the annual emissions that were then aggregated onto a $1km^2$ grid. Figure 6.2 shows the aggregated major road emissions modelled for the Base Case. Emissions for other scenarios are shown in Figure 6.3. The extent modelled is a "Greater London plus" domain i.e. the M25 and roads within it plus roads outside the M25 to the west of Heathrow.

[15] PSDH "Surface Access Report", D. Coombe, November 2007.

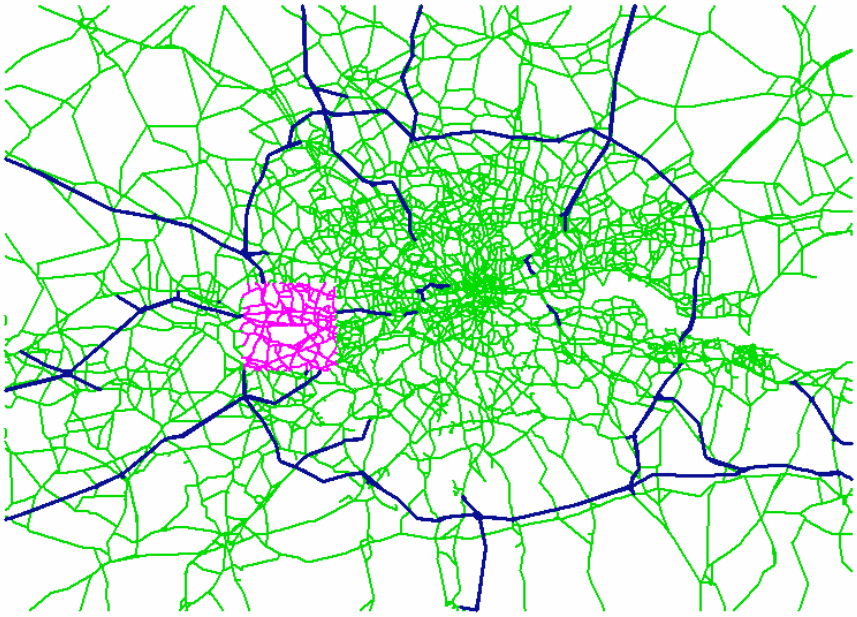

Figure 6.1 Major roads around Great London supplied by Hyder Consulting for 2002. The roads in pink are those around Heathrow in the detailed modelling area. The roads in blue are motorways outside the Heathrow detailed modelling area and the roads in green are non-motorways outside the Heathrow detailed modelling area.

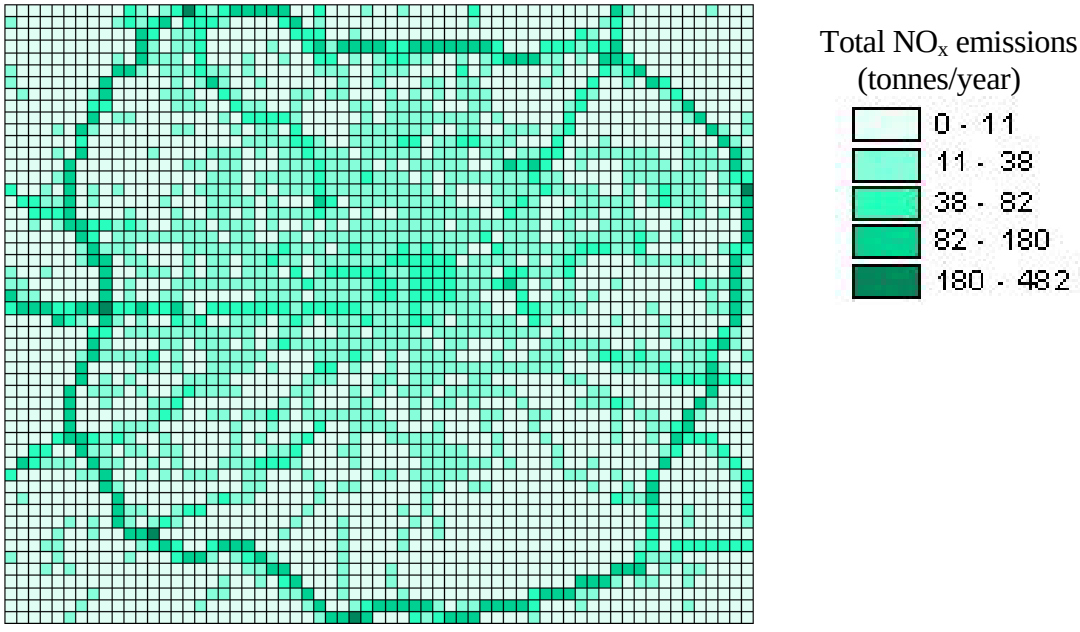

Figure 6.2 2002 Base Case, aggregated NO_X (tonnes/year) due to major roads in a "Greater London plus" area. Total annual emission = 58,010 tonnes/year.

2010SM
Total annual NO_x emission = 29,527 tonnes/year

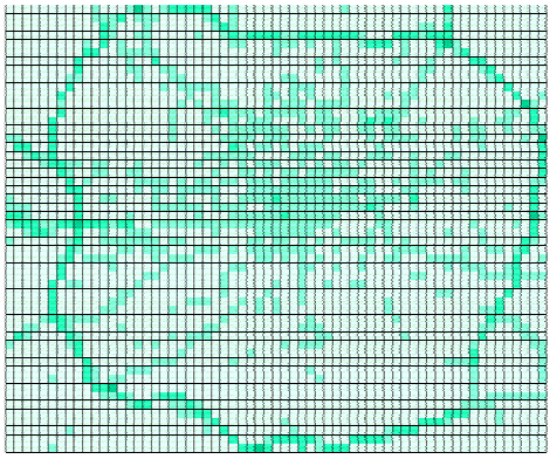

2015SM / EP / NoC
Total annual NO_x emission = 23,187 tonnes/year

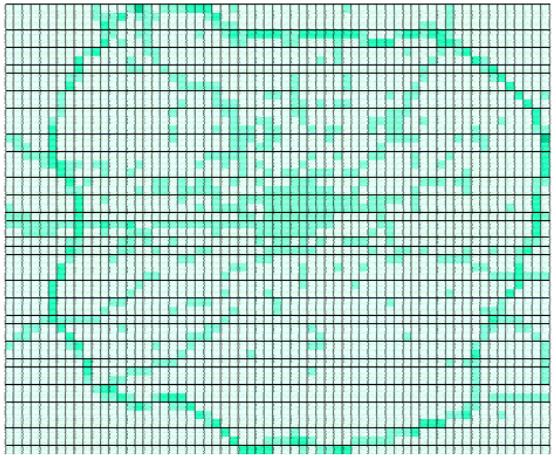

2015MM
Total annual NO_x emission = 23,192 tonnes/year

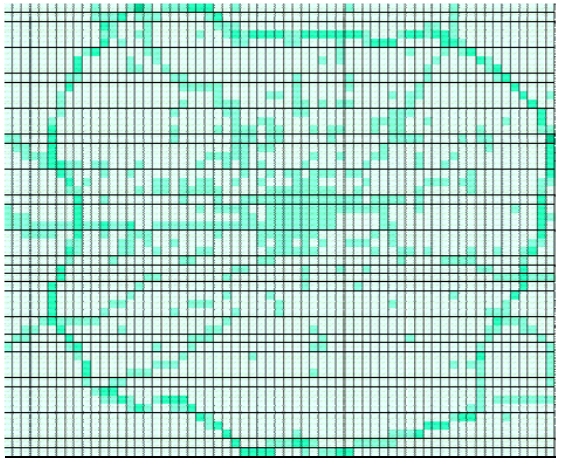

Total NO_x emissions (tonnes/year)

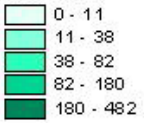

2020 MDL / MLD
Total annual NO_x emission = 12,315 tonnes/year

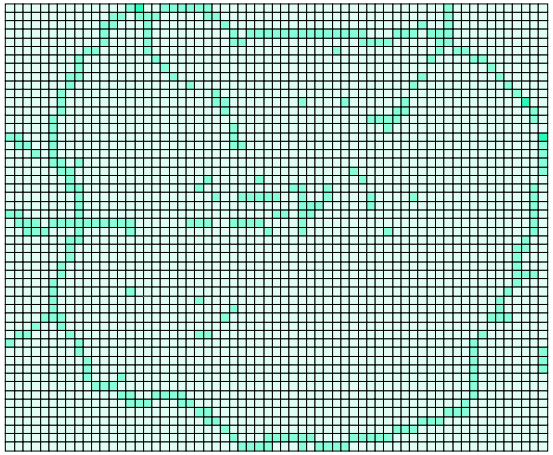

2030MM
Total annual NO_x emission = 10,277 tonnes/year

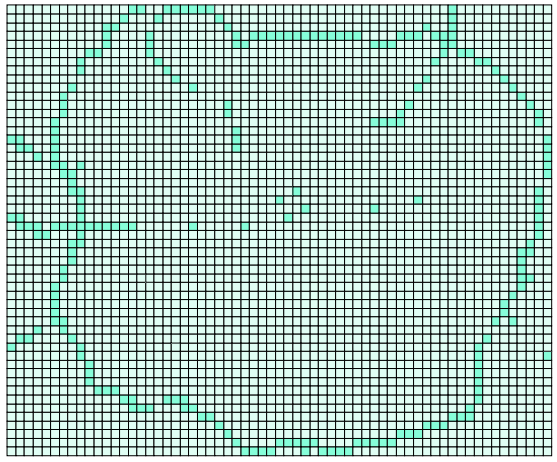

2030 MDL / MLD
Total annual NO_x emission = 10,282 tonnes/year

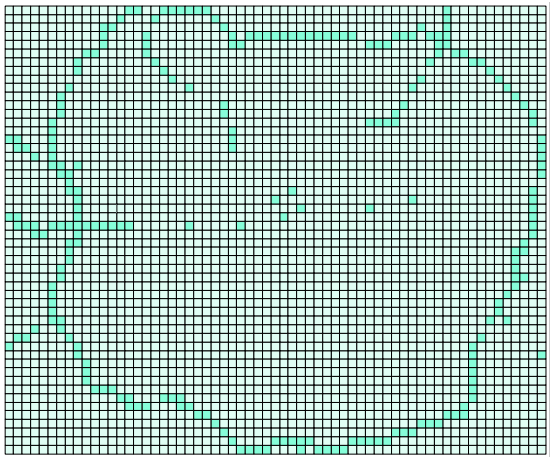

Figure 6.3 Future years, aggregated NO_x (tonnes/year) due to major roads in a "Greater London plus" area.

6.3 Heathrow major roads

The diurnal profiles (weekday, Saturday, Sunday) of flow and diurnal profiles of speed for heavy and light vehicles were used with the motorway/non-motorway designation for each link to calculate diurnal and hence annual emissions.

Figures 6.4 and 6.5 show the roads modelled in around Heathrow and their aggregated annual emissions of NO_X. These were modelled explicitly i.e. as road sources not as aggregated sources. Note that although the roads are colour shaded according to the emission rate in g/(km.s) care should be taken interpreting the figure as some roads are modelled by two 1-way links that overlap.

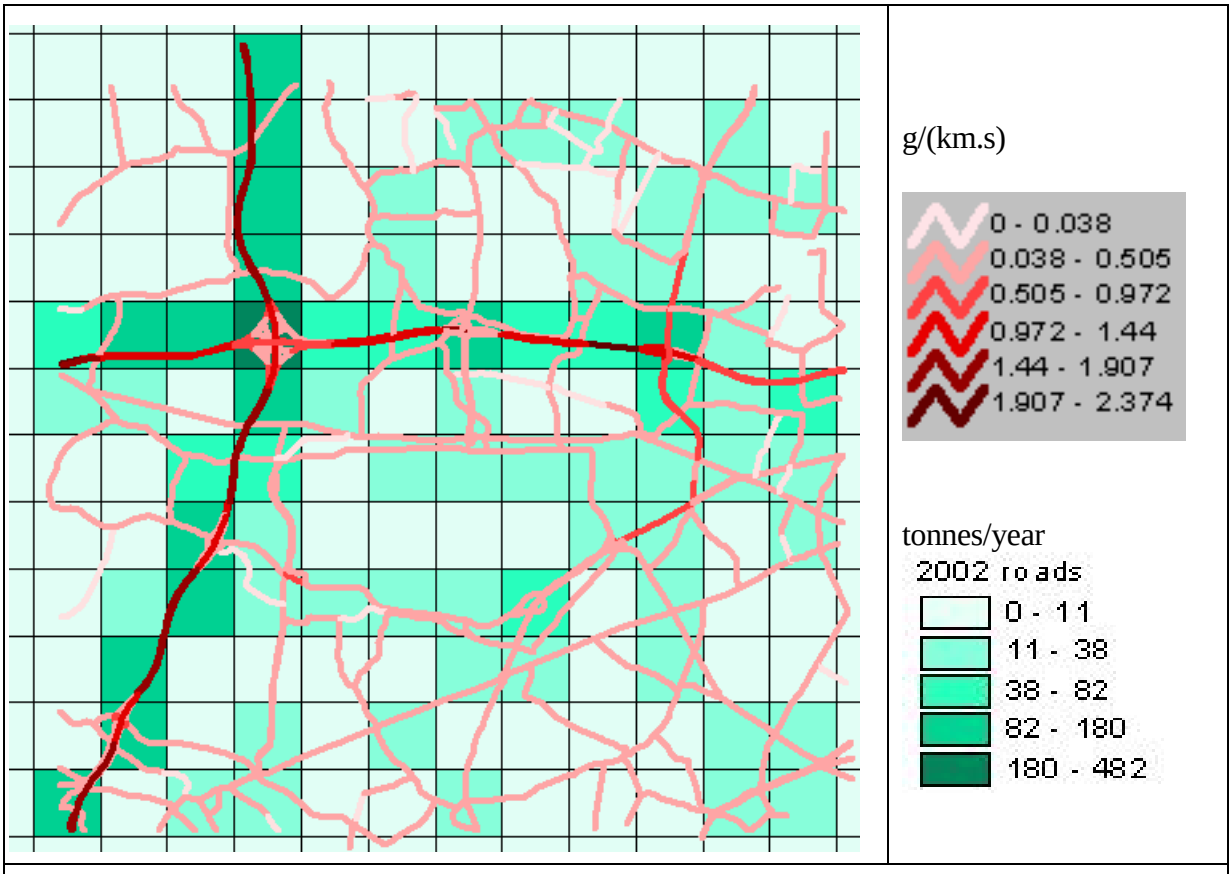

Figure 6.4 2002 Base Case, Heathrow major roads (g/(km.s)) and aggregated NO_X (tonnes/year). Total annual emission of NO_X in the domain* = 3544 tonnes/year. **excludes airport tunnel emissions*

2010SM
Annual NO_x emission = 1907 tonnes/year

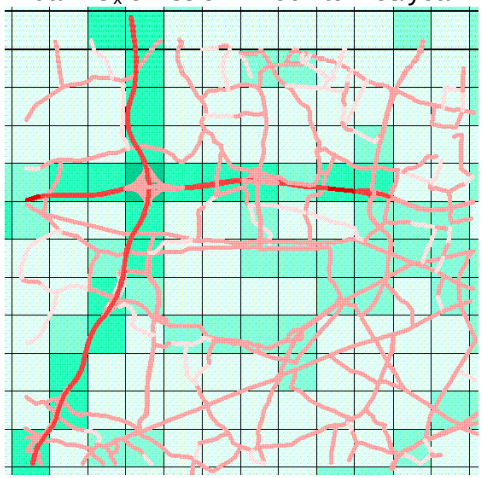

2015SM / EP / NoC
Annual NO_x emission = 1464 tonnes/year

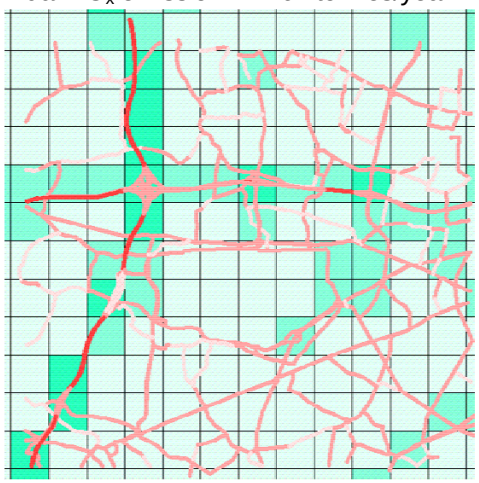

2015MM
Annual NO_x emission = 1463 tonnes/year

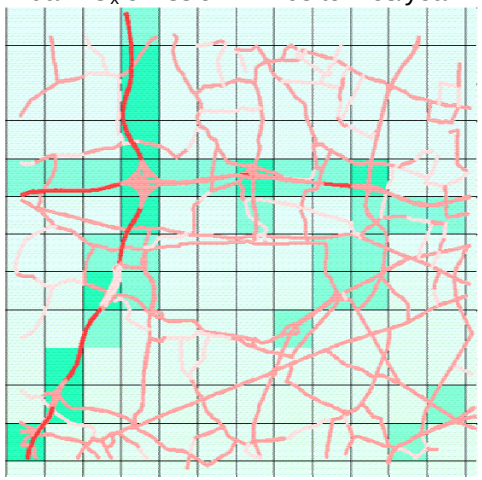

NO_x emissions tonnes/year

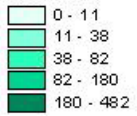

2020 MDL / MLD
Annual NO_x emission = 784 tonnes/year

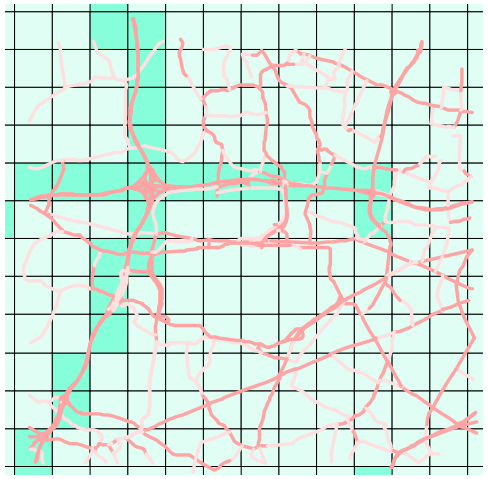

2030MM
Annual NO_x emission = 657 tonnes/year

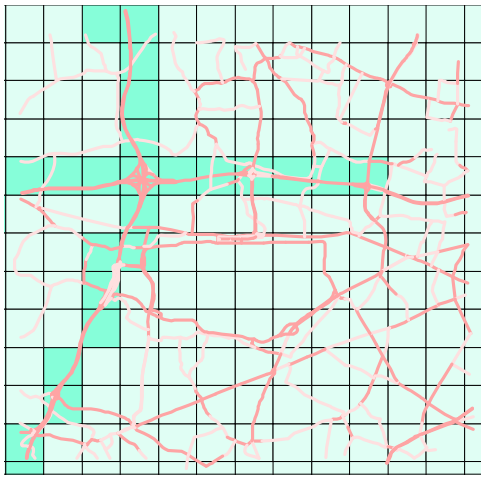

2030 MDL / MLD
Annual NO_x emission = 661 tonnes/year

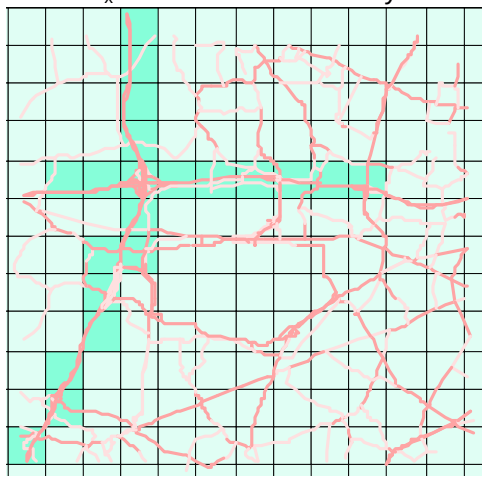

g/(km.s)

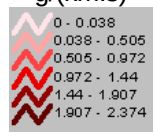

Note: Annual emissions figures exclude airport tunnel emissions

Figure 6.5 Future years Heathrow major roads (g/(km.s)) and aggregated NO_X (tonnes/year).

6.4 Minor Roads and Cold Starts

Data on minor roads and cold start emissions were obtained from the LAEI (London Atmospheric Emissions Inventory) on a 1km^2 aggregated basis. Minor road and cold start emissions for future years were calculated assuming the change would be the same as the change in major road emissions between 2002 and the future year.

6.5 Airport roads

The 2002 emissions data for the airport roads i.e. on-airport roads and roads leading to airport car parks and warehouses, were those supplied by AEA for the PSDH Model Inter-comparison exercise. The tunnel from the M4 spur onto the airport is included in the airport roads source group (Section 10.1) although traffic data for the tunnel were supplied by Hyder Consulting. The tunnel is naturally ventilated so the emissions from traffic passing through the tunnel were modelled as volume sources at the ends of the tunnel. Figure 6.6 shows the 2002 airport roads.

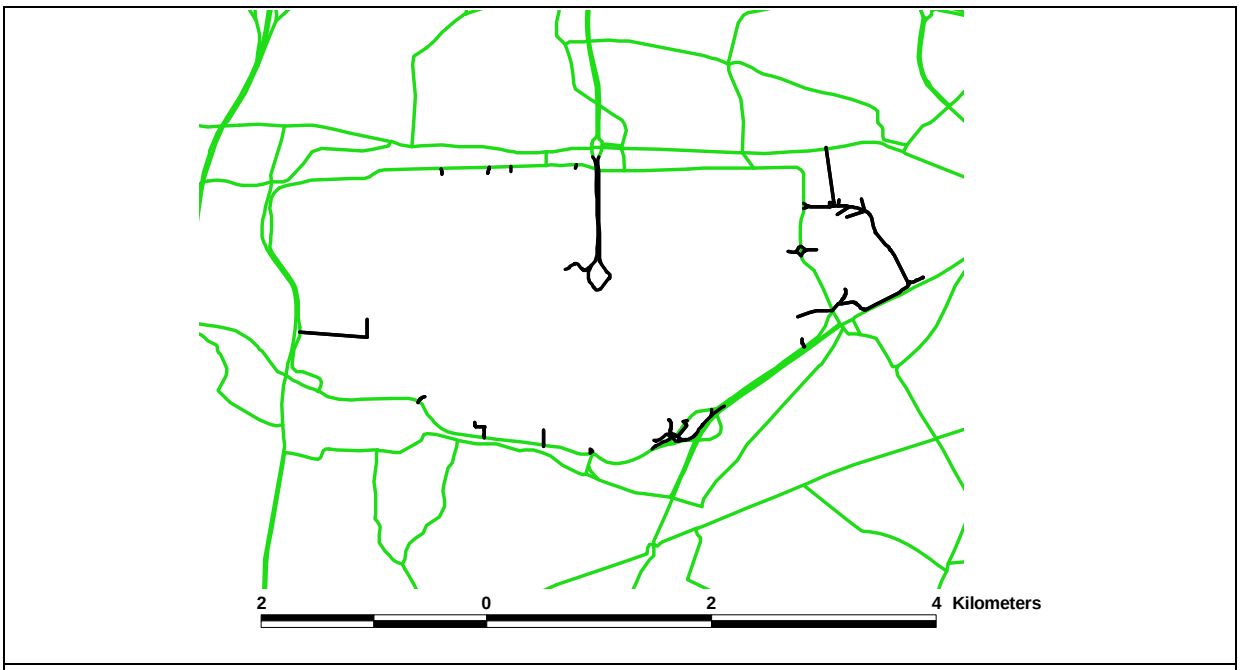

Figure 6.6 2002 Base Case, airport roads (black) other major roads (green).

6.6 Time varying nature of the major road sources

The major roads around Heathrow were divided into Heathrow and non-Heathrow, the latter termed "Strategic" roads. Within each of those groups the road links were designated motorway or non-motorway. Figures 6.7 and 6.8 show the assignment of the roads.

Diurnal profiles of emissions (weekday, Saturday, Sunday) were calculated for each link. The average profiles were calculated for four groups:

- Heathrow motorway
- Heathrow non-motorway
- Strategic motorway
- Strategic non-motorway

Figure 6.9 shows the four diurnal profiles used for the 2002 Base case. Figures 6.10-6.13 show each profile compared to the future case profiles for the same group. For the minor roads and major roads in the rest of Greater London the diurnal profile shown in Figure 6.14 was used for all scenarios. This profile has been used in studies of London carried out for DEFRA[8]. All the profiles have been normalised so that the average over one week (5 weekdays, Saturday and Sunday) is 1.

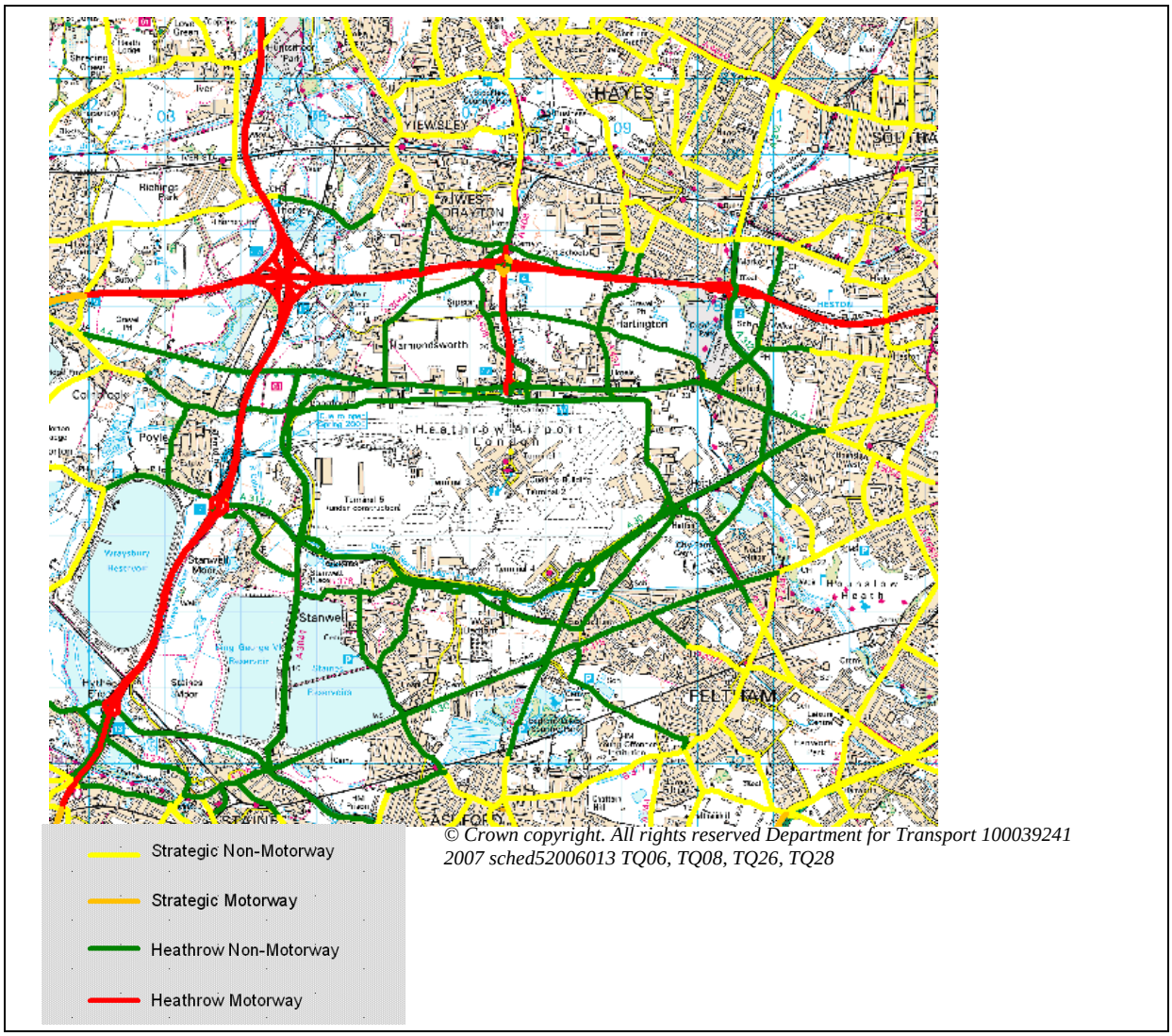

Figure 6.7 Base case, assignment of road links to Heathrow/Strategic and motorway/non-motorway groups.

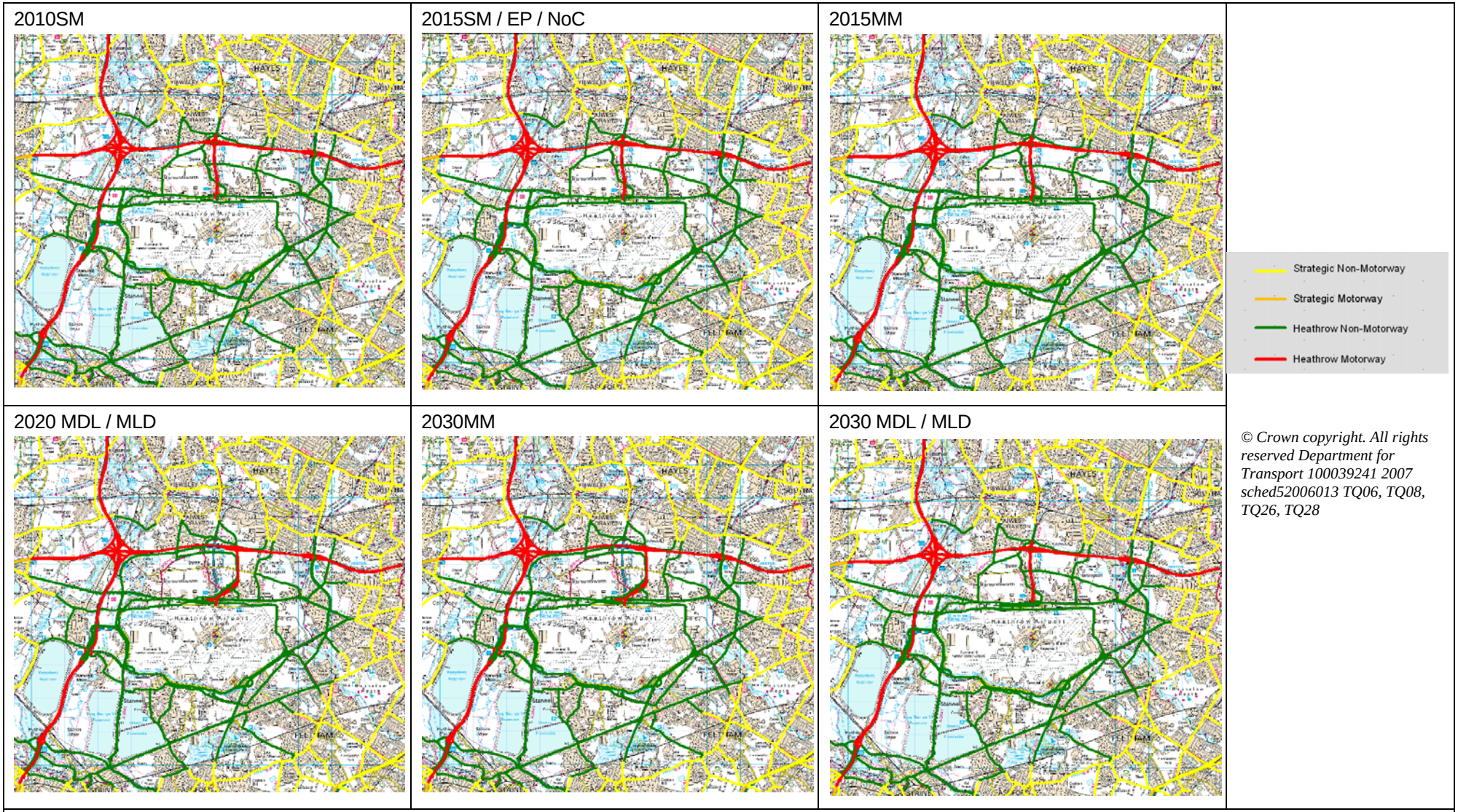

Figure 6.8 Future years, assignment of road links to Heathrow/Strategic and motorway/non-motorway groups.

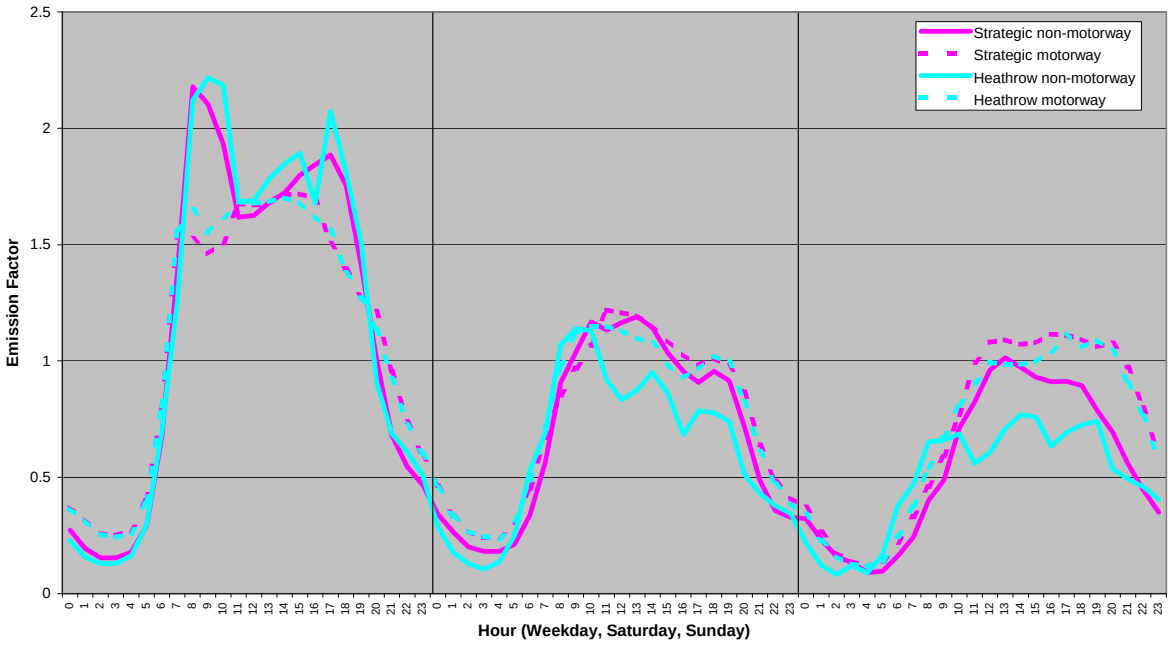

Figure 6.9 Base case, diurnal profiles of normalised emissions. (Average over 7 days =1)

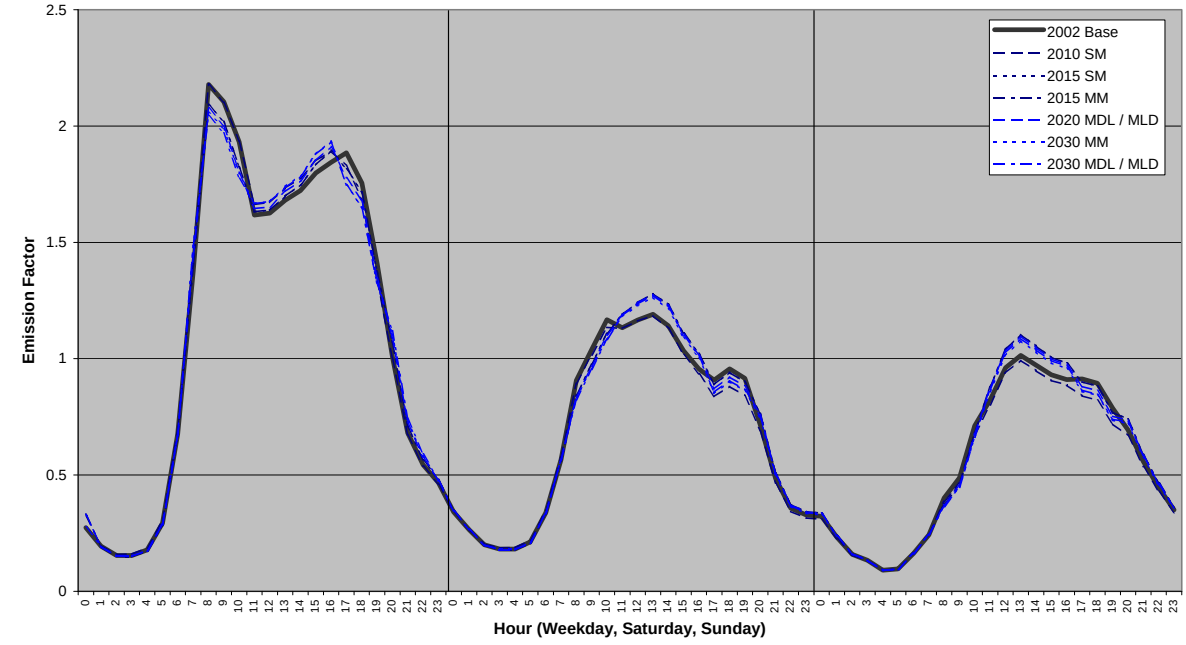

Figure 6.10 Diurnal profile of normalised emissions for strategic non-motorway roads. (Average over 7 days =1)

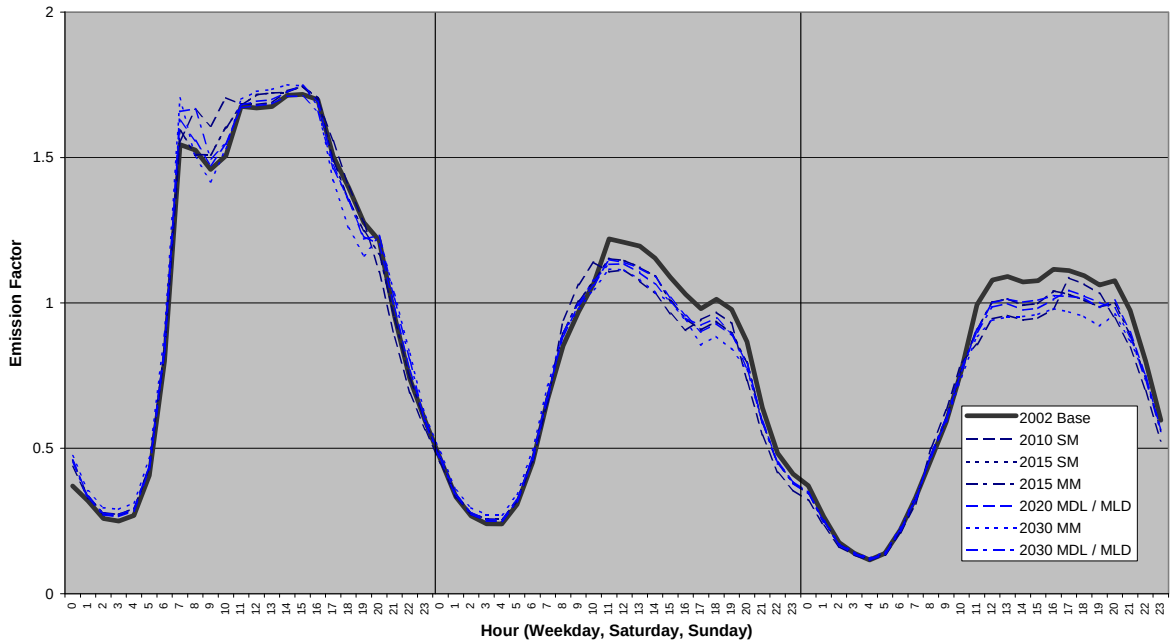

Figure 6.11 Diurnal profiles of normalised emissions for strategic motorway roads. (Average over 7 days =1)

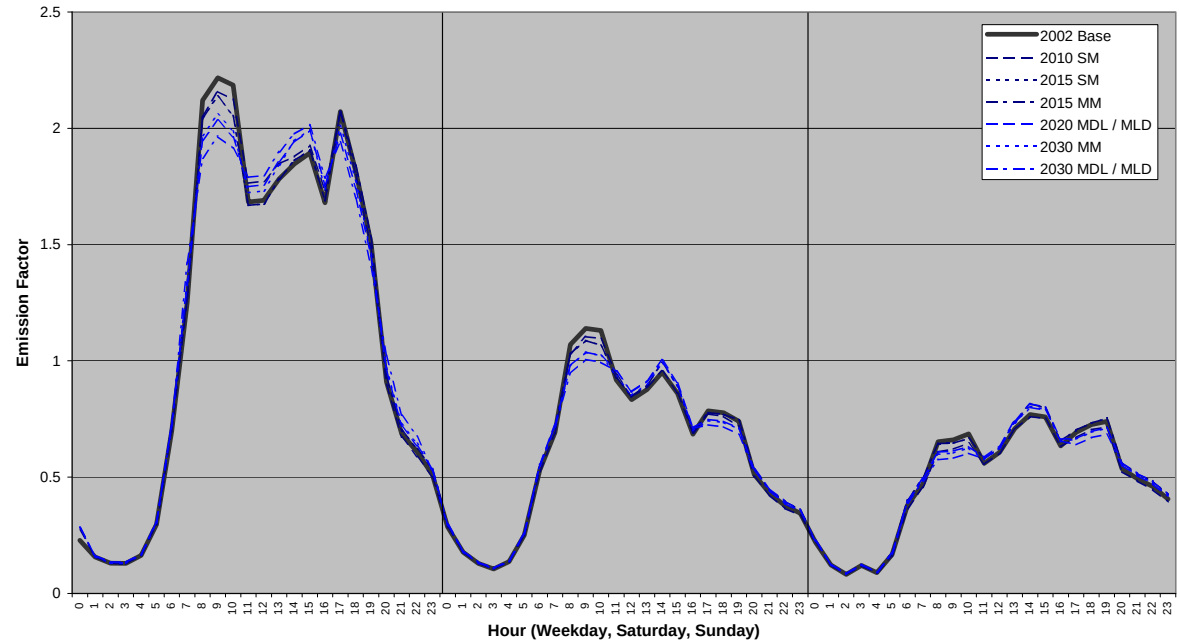

Figure 6.12 Diurnal profile of normalised emissions for heathrow non-motorway roads. (Average over 7 days =1)

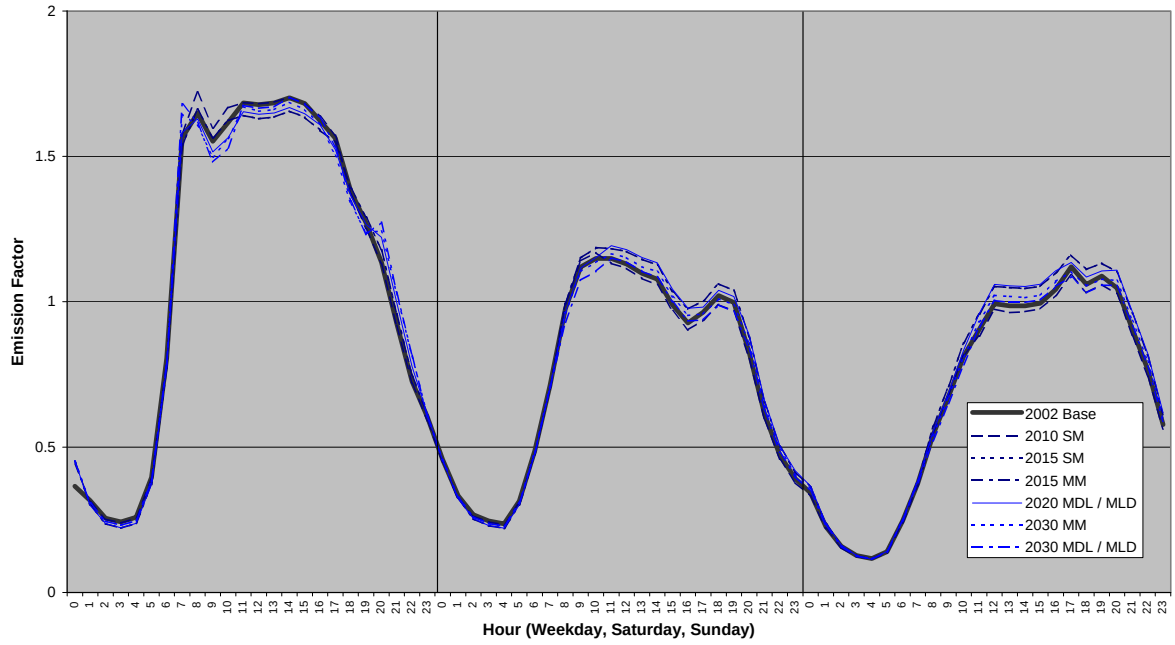

Figure 6.13 Diurnal profiles of normalised emissions for heathrow motorway roads. (Average over 7 days =1)

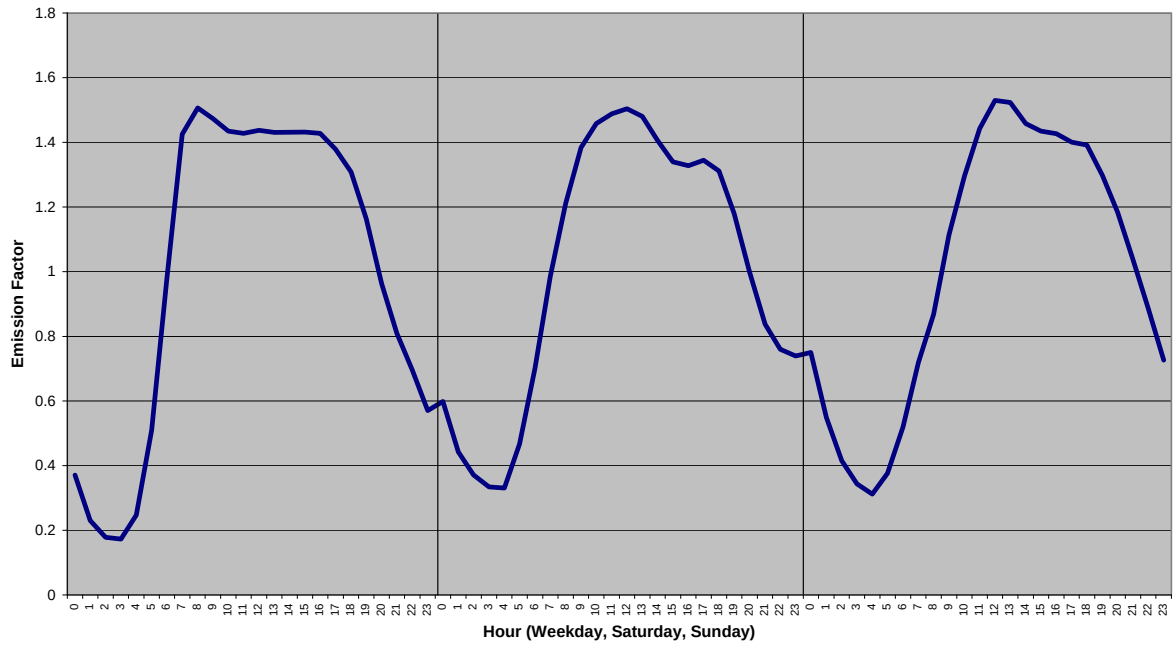

Figure 6.14 Diurnal profile of normalised emissions for minor and Greater London roads. Profile used for all scenarios. (Average over 7 days =1)

7 Output Receptors

The receptor locations used for the modelling comprised automatic monitor locations (labelled LHR, HD and HS), a range of receptors around the airport and major roads (labelled BAA) chosen to assess impacts across the study area and 13 extra receptors in the Harlington area (labelled X) chosen to assess the impact of the third runway scenarios on areas where the public may be.

The locations of receptors X1 to X13 are shown in Figure 7.1. The receptor locations corresponding to LHR automatic monitoring sites are shown in Figure 7.2 and the locations of the other receptors are shown in Figure 7.3. The easting and northing of each these receptors are given in the results tables, Table 10.2-10.8.

In addition to the receptor locations described above, for scenarios 2015SM, 2015MM and 2015MMRd pollutant concentrations were also predicted at 2900 locations that represent residential property locations, shown in Figure 7.4. Predicted concentrations at these receptors are presented in the PSDH population exposure report.[4]

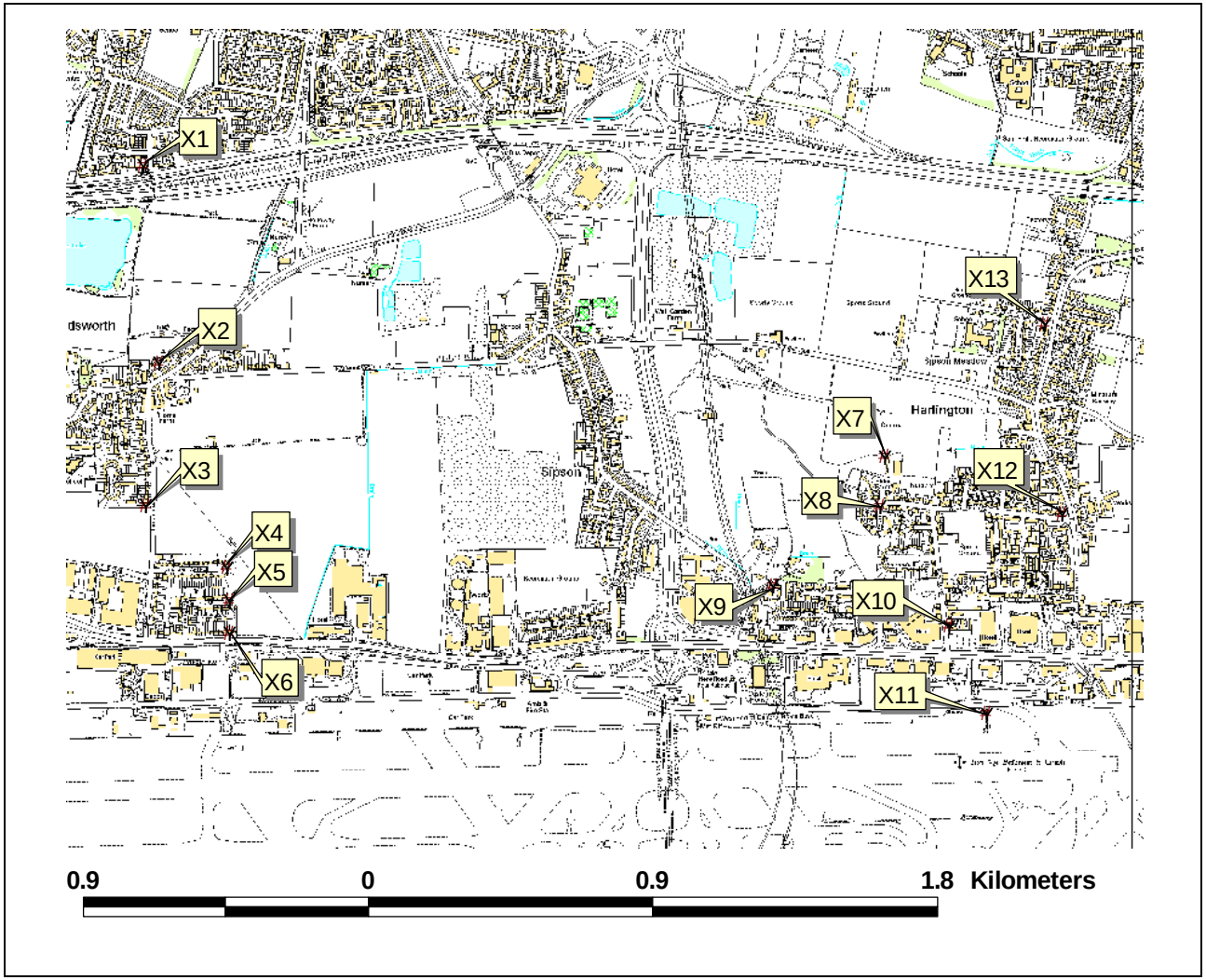

Figure 7.1 Locations of receptors X1 to X13, around Harlington (north of the airport). Heathrow's northern runway can be seen at the bottom of the figure and the M4 junction 4 in the top-centre of the figure

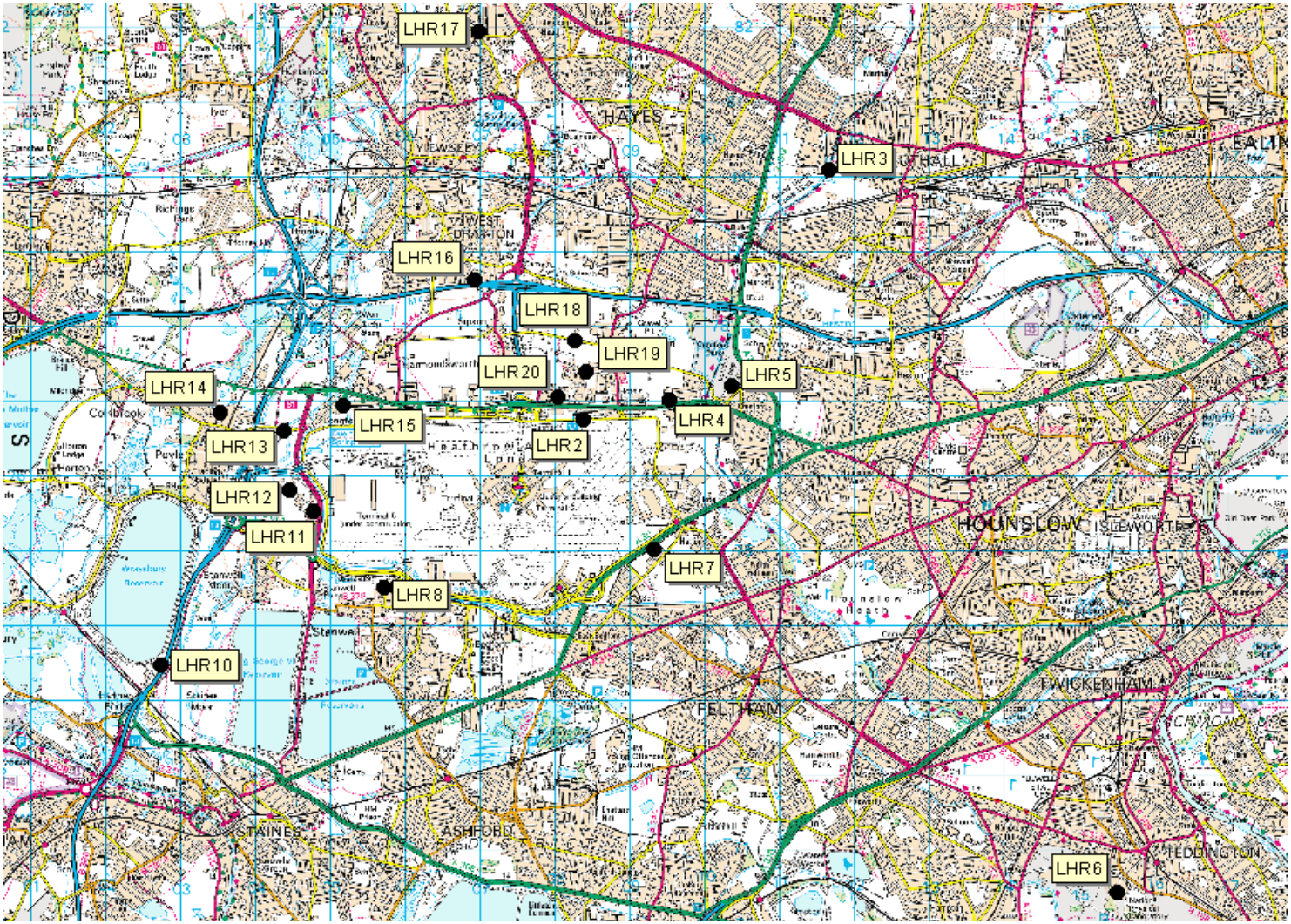

Figure 7.2 Locations of LHR automatic monitoring site receptors

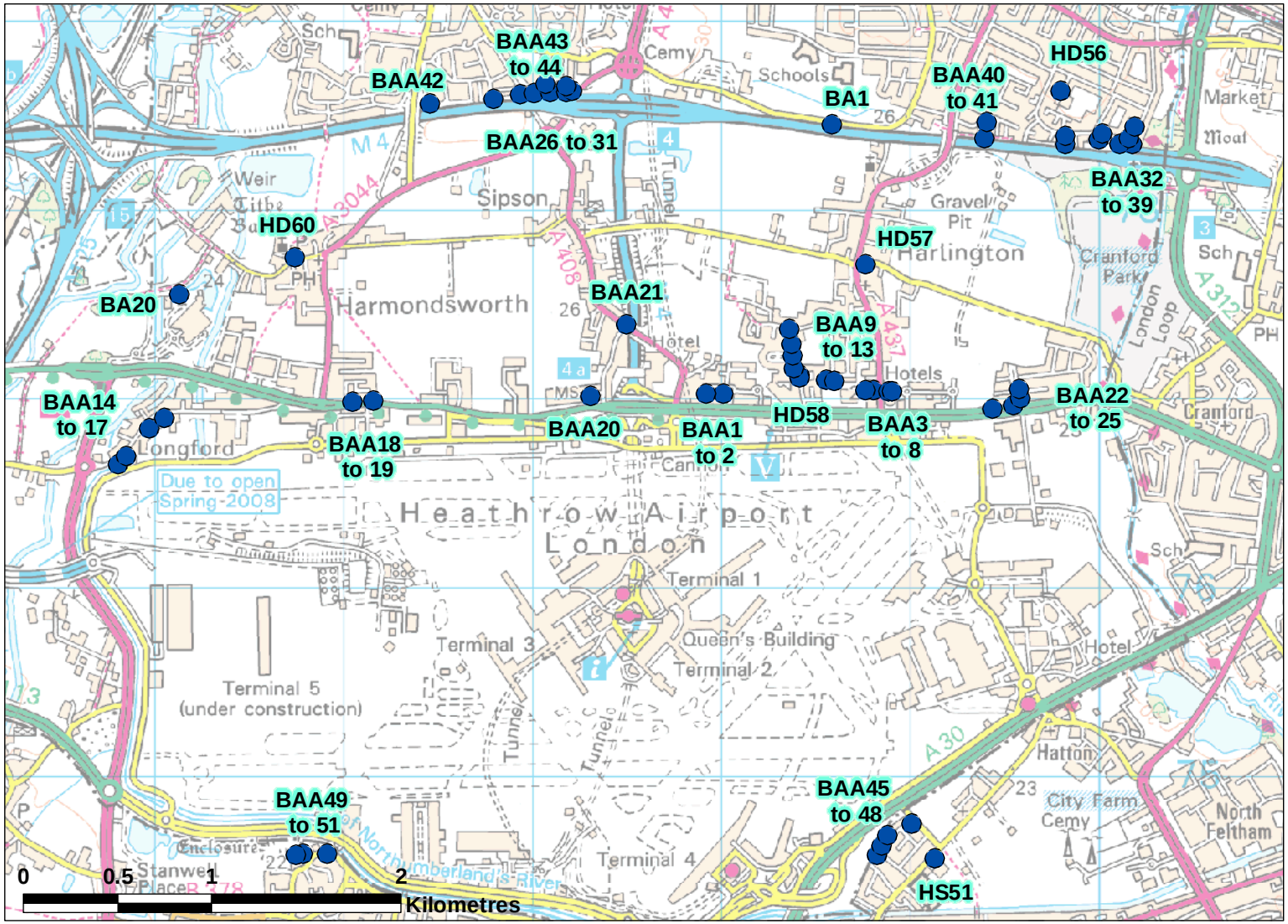

Figure 7.3 Location of the BAA, HD and HS receptor locations

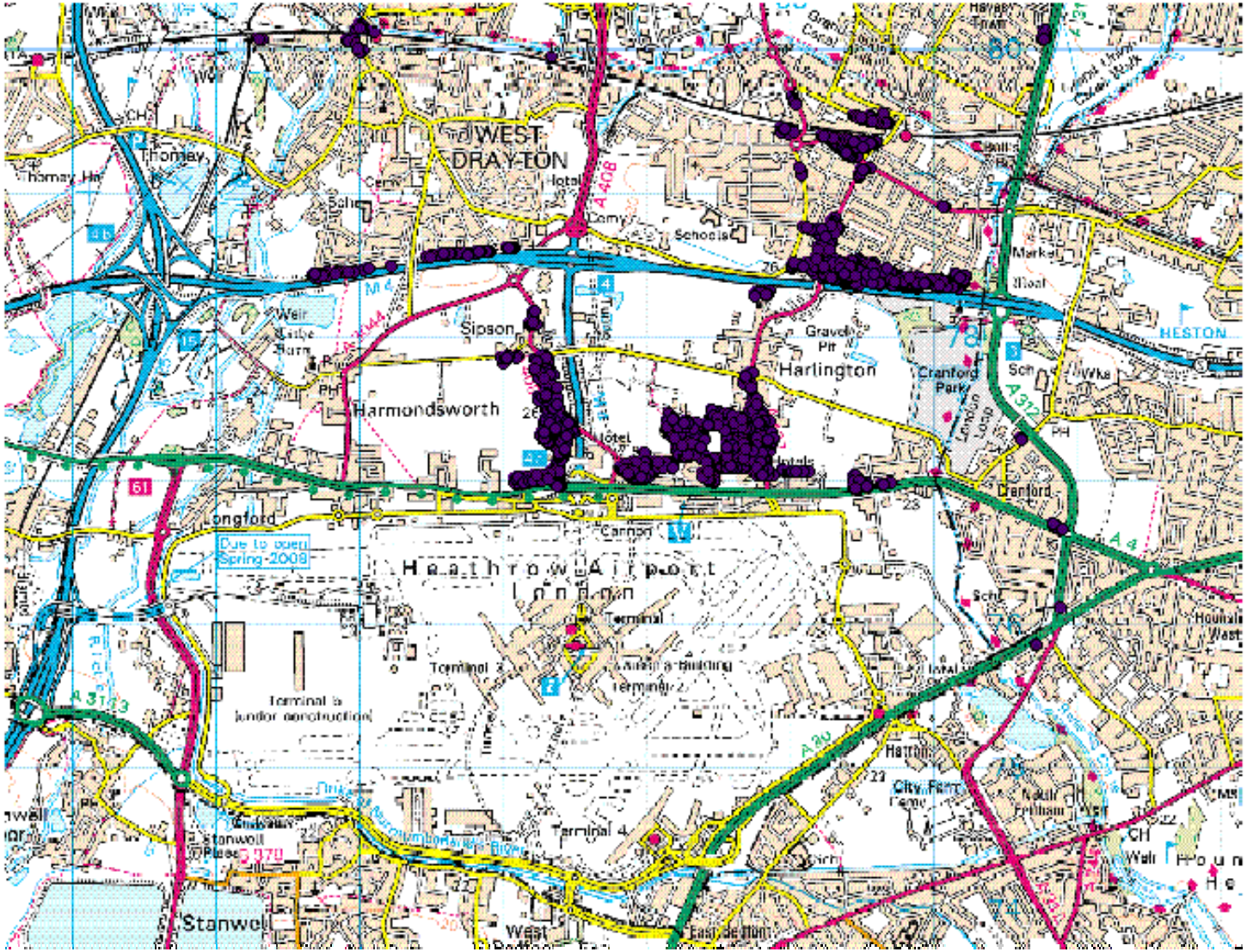

Figure 7.4 Location of the residential property receptors used scenarios 2015SM, 2015MM and 2015MMRd

8 ADMS-Airport

8.1 ADMS-Airport Summary

ADMS-Airport is an extension to the ADMS-Urban air quality model that enables airports to be modelled in a physically realistic manner by modelling emissions from the important sources of the landing and take-off cycle as moving jet sources. The acceleration of the aircraft along the runway is modelled not only to determine the distribution of emissions but also to represent the different behaviour of the aircraft exhaust plume. LIDAR measurements (Light Detection and Ranging remote sensing technique) confirm the significant plume rise of the aircraft exhaust at the beginning of the take-off roll (low aircraft speed) and that the plume rise reduces as the aircraft accelerates.

The versions of ADMS-Airport used to generate the results presented in this report were versions 2.2.3.4-2.2.3.9. These versions differ from each only in the emissions rate and speed data described in (i) below which varied from scenario to scenario. As the emissions data for each scenario were received the emissions rate and speed data were incorporated into successive versions of the model.

Versions 2.2.3.4-2.2.3.9 used to generate the results that are presented in this report differ from version 2.1.3, the version used for the MIC, in two major respects:

(i) In the MIC constant acceleration and a constant rate of emission was assumed during take-off roll. In this modelling constant rates were not assumed. The take-off roll emission rates of NO_X and NO_2 and aircraft speed were defined as functions of time from the start of take-off roll. The functions were supplied by AEA as part of the airport data for each scenario.

(ii) For road sources, the height of the centre of the road source has been reduced from 2m to 1m above the given source height and the initial σ_z of the plume, a measure of vertical plume spread, has also been decreased from 2m to 1m.

In addition, in running the model a change has been made since the MIC reflecting the increased information available in the emissions inventory:

(a) Engine efflux parameters have been categorised into MCATs (modelling categories) and efflux parameters determined for each MCAT, on the basis of data supplied for airframe-engine combinations by QinetiQ. The determination of the MCATs is described in Section 12.

An action arising from the MIC was for CERC to carry out a study into the sensitivity of predicted concentrations to changes in efflux parameters, the exhaust plume buoyancy and the effect of combining engine exhausts. The sensitivity study can be found in Section 13.

8.2 Model set up

Table 8.1 shows the model parameters used in modelling the Base Case and all future scenarios.

Table 8.1 Model set up parameters

Minimum Monin-Obukhov length (m)	20
Grid depth (m)	10
Surface roughness (m)	0.5
Meteorology	Heathrow 2002
Surface roughness at met site (m)	0.2

9 Analysis of model predictions and comparison with monitoring data

A key requirement of the Project for the Sustainable Development of Heathrow is to compare annual average NO_2 concentrations with the air quality objective value of 40μg/m^3 i.e. it is the calculation of the annual average concentration that is important. Section 9.1 compares the annual average predictions from ADMS-Airport with monitored data and shows ADMS-Airport in close agreement with monitored data for annual averages. Sections 9.1-9.3 then look at the performance of the model in calculating hourly concentrations and analyse the results in terms of wind speed, hour of the day, wind direction and runway operation to test the response of the model and gain confidence that the model is really capturing the essential physics of the modelling scenario and is therefore predicting "the right answer for the right reason". Section 9.4 plots the predicted NO_X and NO_2 annual average concentrations on a transect through receptor location LHR2 crossing the Perimeter Road, A4 and M4. It shows the gradient in concentration due to each source group and is for comparison with the previous Model Inter-comparison output. For completeness Section 9.5 compares predicted and monitored annual average PM_{10} concentrations. Less analysis has been carried out on PM_{10} as the EU objectives for PM_{10} are not likely to be approached around Heathrow.

Deterministic models that calculate long term averages such as annual averages from the component hourly averages may have a poorer performance in predicting hourly concentrations (or concentrations over any shorter period) than annual averages as the averaging of the short term components will tend to smooth out over-predictions and under-predictions on the short timescale. The over-predictions and under-predictions may arise, for example, because the actual hourly variation in emissions is not being accurately represented by a diurnal profile or because the met data do not fully reflect average conditions over the hour being considered. In addition, the stochastic nature of small scale atmospheric turbulence results in there being a difference between the concentration measured by a monitor and the ensemble average predicted even for a perfect model.

In comparing the ADMS-Airport model predictions against ambient monitoring data it is not just the ADMS-Airport model performance that determines the comparison but the accuracy of the model inputs (spatial, quantitative and temporal source data, emissions factors used to calculate traffic emissions from traffic data, meteorological data and ambient background data). It is also usually assumed that the ambient monitoring data are a "gold standard" although in examining monitoring data, for instance the year to year trends, or the ratio of NO_2 to NO_X, some features appear which can seem anomalous.

The series of Workshops on Harmonisation Within Dispersion Modelling for Regulatory Purposes that started in 1992[16] has devoted a lot of its efforts to assessing model performance. In those studies a correlation between hourly averages of 0.6 and a fraction of modelled values within a factor of 2 of the monitored values of over 0.6 would be considered good performance by the model. The series of workshops has often discussed the importance of looking not just at one overall statistic to measure model performance but looking at a range of measures.

[16] www.harmo.org

9.1 Statistical analysis of NO_X and NO_2 model predictions

Tables 9.1 and 9.2 compare annual averages of NO_X and NO_2 calculated from the hourly time series of concentrations, excluding those hours for which either modelled (162 hours) or monitored concentrations (up to 1195 hours) are missing. It is, therefore, a like-for-like comparison. The Tables also show the BOOT statistics[3]: standard deviation, correlation, fraction of modelled values within a factor of two of monitored values and the fractional bias of the hourly averages. If, for each hour, the model predicted concentrations that were identical to those monitored, the correlation and fraction of values within a factor of 2 would take their maximum values of 1, whilst the fractional bias would be 0.

Across the sites the mean correlation for hourly NO_X is 0.61, there is an average of 0.77 of modelled values within a factor of 2 of monitored values and the average fractional bias is +0.013 corresponding to a very small mean over-estimate by the model. For NO_2 the mean correlation is 0.68 and the fraction of values within a factor of 2 is 0.84; the mean fractional bias for NO_2 is +0.018.

Figure 9.1 shows the comparison of monitored and modelled annual averages of NO_X and NO_2 (calculated from hourly time series output) as scatter plots. The dotted lines show where the annual average is a factor of 2 of the monitored value.

Figure 9.2 shows "box and whisker" plots for each receptor for NO_X and NO_2. In the "box and whisker" plots percentiles of the ratio (modelled/monitored) are plotted. The percentiles are 95^{th} (top) 75^{th}, 50^{th} (middle), 25^{th} and 5^{th} (bottom). Remembering that the model is predicting an ensemble average (the average of a large number of repetitions of the same event) whilst the monitor records one particular event (which may be different from the ensemble mean because of concentration fluctuations due to local atmospheric turbulence), a good model would not have all the values equal to one. Assuming the small scale turbulence results in a Gaussian distribution of concentrations with the mean equal to the ensemble average, the 50^{th} percentile would be expected to be equal to one with the other percentiles symmetrically distributed above and below 1.

Tables 9.1-9.2 and Figures 9.1-9.2 show that there is no significant trend to over or under-prediction by ADMS-Airport and that most hourly predictions are within a factor of 2 of the monitored (0.77 for NO_X and 0.84 for NO_2).

Table 9.1 Comparison of mean ($\mu g/m^3$), standard deviation ($\mu g/m^3$), correlation, fraction within a factor of 2 (FA2) and fractional bias for monitored and modelled NO_X at automatic monitoring sites. Values are calculated from hourly time series output, excluding those hours for which either monitored and modelled values are not present.

	Annual average		Standard deviation		Correlation (Monitored = 1)	FA2 (Monitored = 1)	Fractional bias (Monitored = 0)
	Monitored	Calculated	Monitored	Calculated			
LHR2	119.49	110.27	98.97	107.53	0.63	0.76	0.08
LHR5	73.74	68.39	79.16	87.77	0.58	0.76	0.08
LHR6	38.92	51.30	42.51	76.09	0.55	0.73	-0.27
LHR8	63.53	59.10	76.13	84.89	0.60	0.75	0.07
LHR10	198.04	225.56	173.61	251.61	0.61	0.68	-0.13
LHR11	74.13	68.32	82.69	90.39	0.60	0.75	0.08
LHR14	71.18	64.32	88.31	89.19	0.65	0.77	0.10
LHR15	66.34	63.15	75.01	84.31	0.61	0.79	0.05
LHR16	113.26	124.44	97.60	139.59	0.62	0.81	-0.09
Average*	**90.96**	**92.76**	**90.44**	**112.37**	**0.61**	**0.76**	**-0.003**
Average	77.57	76.16	80.05	94.97	0.61	0.77	0.013

*Excluding LHR10 that was acknowledged in the MIC to be an outlier.

Table 9.2 Comparison of mean ($\mu g/m^3$), standard deviation ($\mu g/m^3$), correlation, fraction within a factor of 2 (FA2) and fractional bias for monitored and modelled NO_2 at automatic monitoring sites. Values are calculated from hourly time series output, excluding those hours for which either monitored and modelled values are not present.

	Annual average		Standard deviation		Correlation (Monitored = 1)	FA2 (Monitored = 1)	Fractional bias (Monitored = 0)
	Monitored	Calculated	Monitored	Calculated			
LHR2	52.09	48.04	23.39	26.21	0.62	0.86	0.08
LHR5	43.41	36.31	20.99	23.34	0.63	0.80	0.18
LHR6	25.47	28.40	18.42	22.91	0.64	0.78	-0.11
LHR8	32.07	31.67	21.88	24.59	0.72	0.82	0.01
LHR10	39.28	58.65	24.04	40.56	0.57	0.71	-0.40
LHR11	35.93	35.16	21.05	25.75	0.71	0.85	0.02
LHR14	36.30	34.57	24.44	24.4	0.75	0.85	0.05
LHR15	32.43	34.15	18.58	23.63	0.66	0.85	-0.05
LHR16	45.26	47.18	22.47	29.44	0.67	0.87	-0.04
Average*	**38.03**	**39.35**	**21.70**	**26.76**	**0.66**	**0.82**	**-0.029**
Average	37.87	36.94	21.40	25.03	0.68	0.84	0.018

*Excluding LHR10 that was acknowledged in the MIC to be an outlier.

Figure 9.1 Comparison of monitored and modelled annual average NO_X (top) and NO_2 (bottom) concentration ($\mu g/m^3$) at the automatic monitoring sites. Dotted lines show where modelled values are a factor of 2 of monitored values.

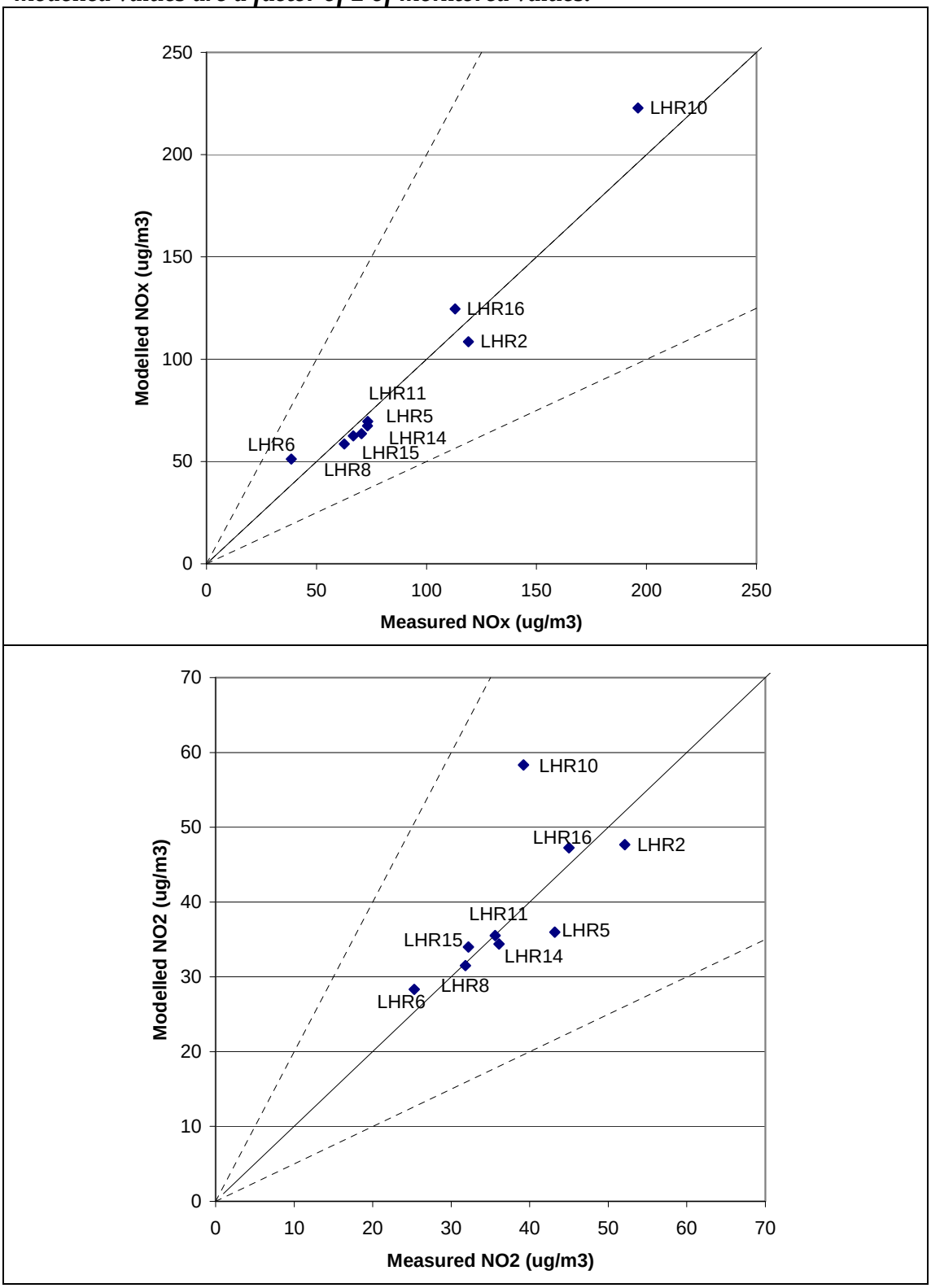

Figure 9.2 "Box and whisker" plots for the ratio of (modelled/monitored) hourly concentrations of NO_X (top) and NO_2 (bottom). The plots indicate the 95th percentile ratio (top), 75th, 50th (middle bold), 25th and 5th (bottom).

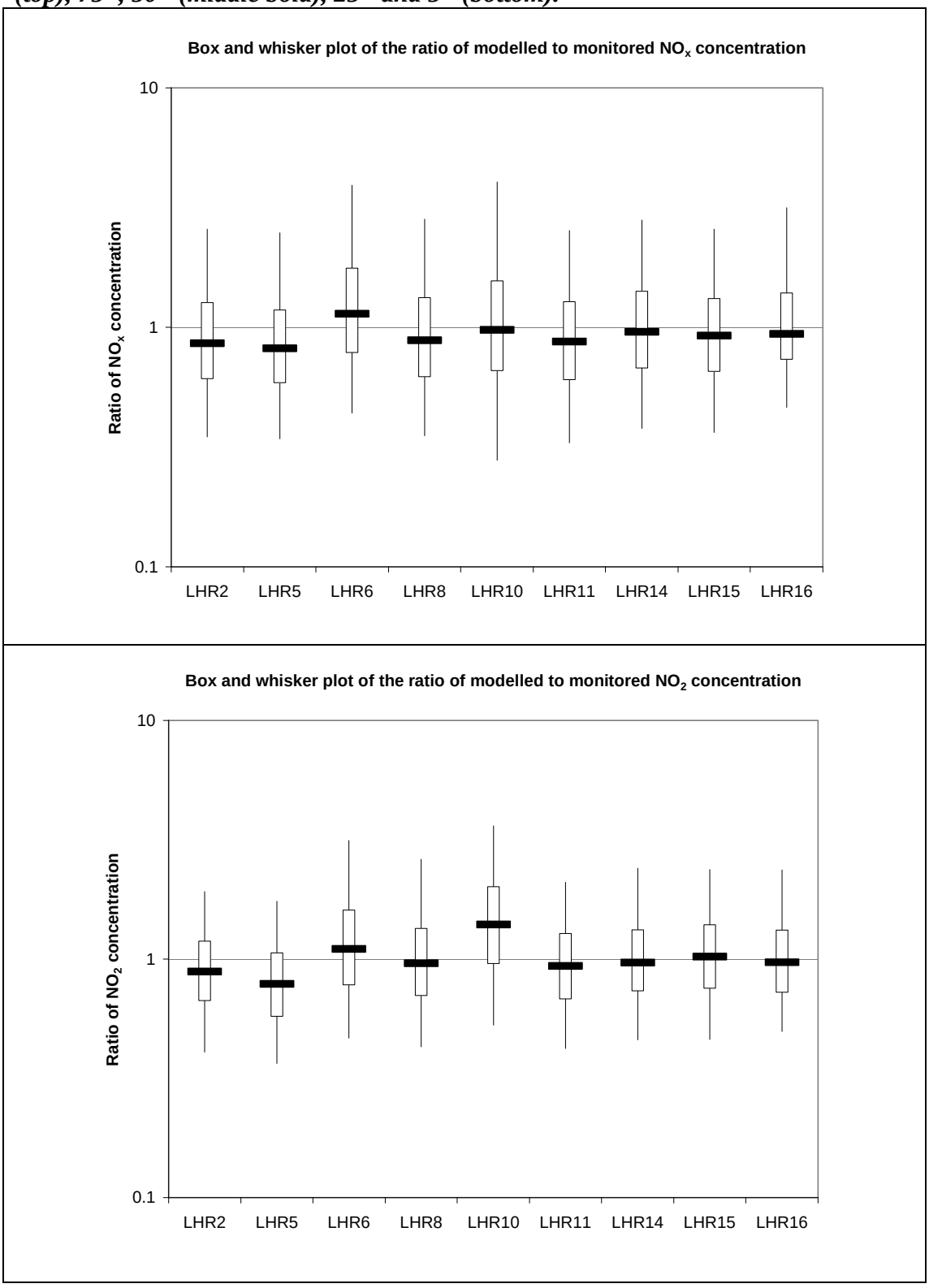

9.2 Analysis as a function of operation of runway 27R

At Heathrow airport there is a northern and a southern runway both of which have close to an east-west alignment. Allowing for take-offs to the east or the west there are four modes of runway operation referred to as 27R, 27L, 09R and 09L which describe,

- 27R take-off to the west from the northern runway.
- 27L take-off to the west from the southern runway.
- 09R take-off to the east from the southern runway.
- 09L take-off to the east from the northern runway.

The LHR2 monitoring site is just north of the eastern end of the northern runway, close to the starting position of aircraft taking off on 27R. LHR2 monitoring site records a strong signature from aircraft take-off when runway 27R is operational. When 27R is operational the wind is mostly, but not exclusively, from the south-west, west or north-west. In this analysis concentrations at monitoring site LHR8, Oaks Road in Stanwell, south-west of the airport have been used as a "background" site and the difference between concentrations at LHR2 and LHR8 taken as a measure of the airport contribution to concentration at LHR2. Hours when monitored concentrations at LHR8 are greater than monitored concentrations at LHR2 (or when modelled concentrations at LHR8 are greater than modelled concentrations at LHR2) are excluded.

Table 9.3 compares average monitored and modelled concentrations for (LHR2-LHR8) during the hours when 27R is operational for departures, when 27R is operational for arrivals (and departures are on 27L) and when 27R is not operational for departures or arrivals. Hours when it is operational for departures are defined as those hours when the number of departures on 27R is greater than or equal to the number of arrivals on 27R. Similarly, the hours when it is operational for arrivals are defined as those hours when the number of arrivals on 27R is greater than or equal to the number of departures on 27R.

There is a difference of approximately 60$\mu g/m^3$ of NO_X in the average concentration for (LHR2-LHR8) when there are departures on 27R and when there are arrivals on 27R. The good agreement between the modelled and monitored average concentrations when there are departures on 27R and when there are arrivals on 27R (and departures on 27L) suggests that ADMS-Airport is modelling the activity from the airport sources well. The take-off roll sources are the most significant ground level airport emissions. That the model predicts the average well when there are departures on 27R (less than 250m from 27R) and when there are take-offs on 27L that is about 1.5km from 27R (and arrivals on 27R) suggest that the model is capturing well the variation in concentration due to the important take-off roll sources with distance.

Table 9.3 Comparison of modelled and monitored average NO_X concentration ($\mu g/m^3$) for (LHR2-LHR8) for those hours when there departures on 27R, arrivals on 27R, neither departures nor arrivals on 27R and all hours. The number of hourly concentrations averaged in each case is given.

	Departures on 27R	Arrivals on 27R	No departures or arrivals on 27R	All hours
Modelled ($\mu g/m^3$)	**153.3**	**96.8**	92.2	110.8
Monitored ($\mu g/m^3$)	**154.0**	**92.9**	118.4	120.1
Number of hours	2214	2750	3283	8199

Figure 9.3 shows the comparison of hours when there are departures on 27R and hours when there are arrivals on 27R as a function of hour of the day. The diurnal variation as well as the difference between departures and arrivals on 27R is well-captured.

Figure 9.3 Comparison of modelled and monitored average NO_X concentration ($\mu g/m^3$), as a function of hour of the day, for (LHR2-LHR8) for those hours when there are departures on 27R (blue) or arrivals on 27R (red). Monitored concentrations are shown by dashed lines and modelled concentrations by solid lines.

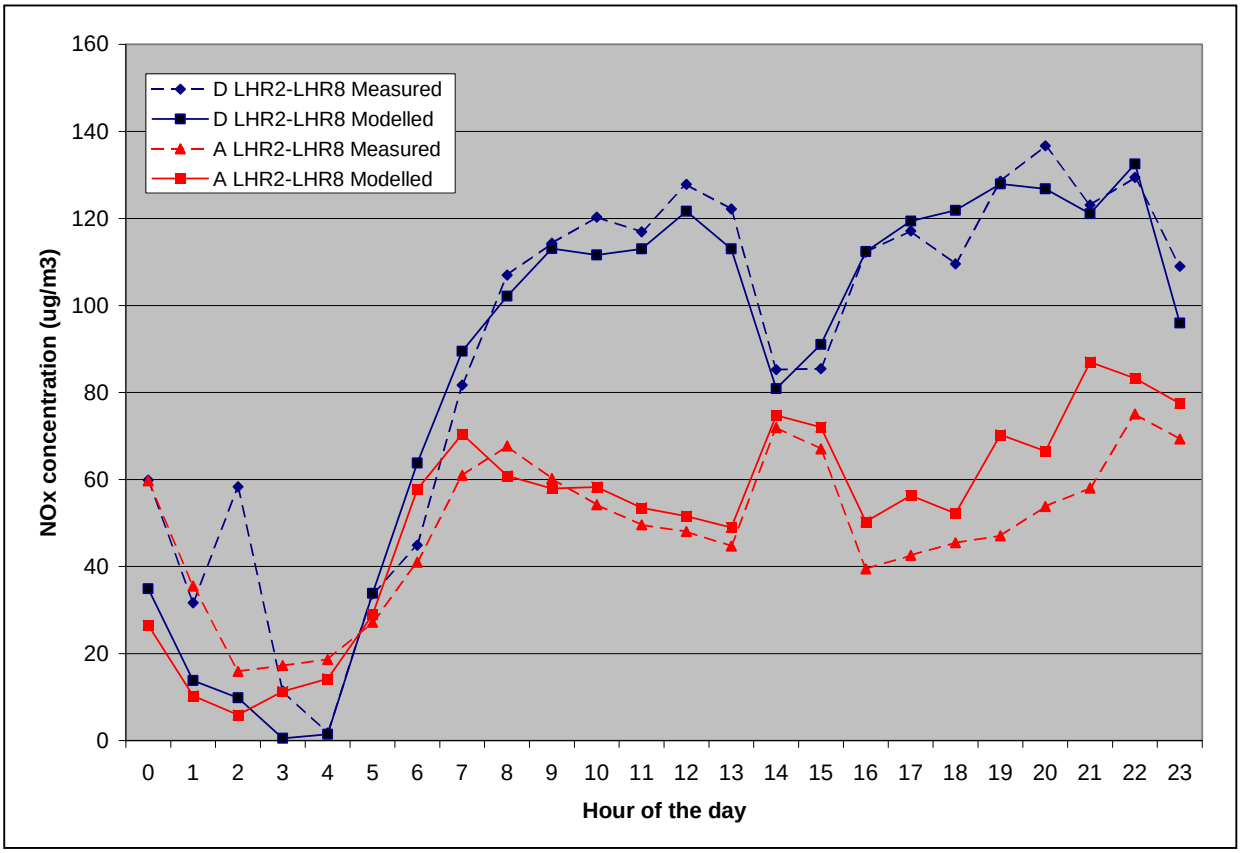

Figure 9.4 shows the same data as Figure 9.3 but averaged and plotted as a function of wind speed. The number of hours averaged for each pair of data points (modelled and monitored) is given on the plot. The variation with departures and arrivals on 27R is well-captured. At the very lowest wind speeds there is a tendency for the model to over-estimate.

Figure 9.4 Comparison of modelled and monitored average NO_X concentration ($\mu g/m^3$), as a function of wind speed, for (LHR2-LHR8) for those hours when there are departures on 27R (blue) or arrivals on 27R (red). Monitored concentrations are shown by dashed lines and modelled concentrations by solid lines.

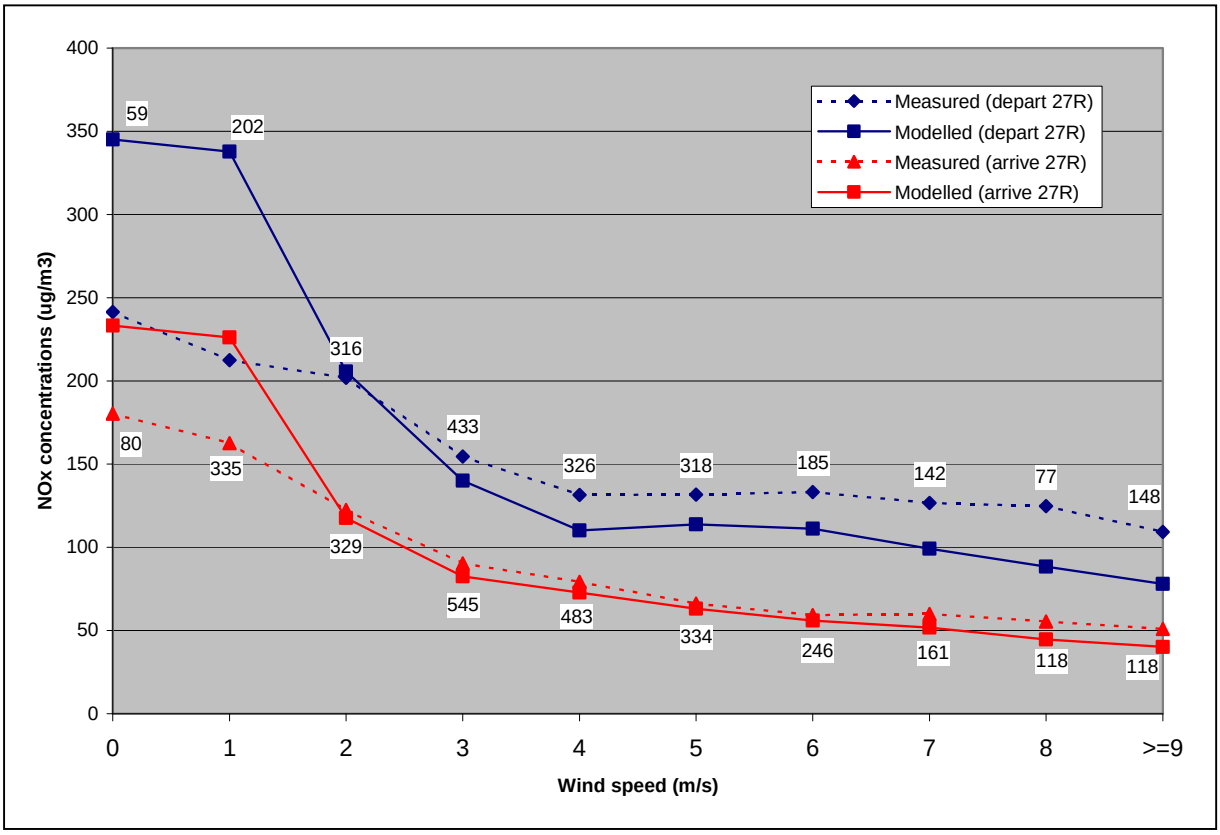

9.3 Polar Plots

Polar plots, in which average concentrations are plotted as a function of wind speed and wind direction, have been used to gain insight into the behaviour of sources by indicating the location and nature of the important sources. They have proved particularly useful at LHR2 since monitored concentrations for airport sources (from the south west) tend to show large concentrations for large wind speeds, indicating that the aircraft sources are buoyant, in contrast to other ground level sources such as road traffic emissions that are less buoyant and show the highest concentrations for the lower wind speeds.

Figures 9.5-9.7 show polar plots for monitored and modelled NO_X and NO_2 concentrations at LHR2, LHR8 and LHR5 the Hounslow 2 monitor in Cranford. Combinations of wind speed and wind direction for which there are fewer than 4 hourly averages have been excluded from the plots, so that the plots will not be skewed by a few hours that may be atypical.

The monitored and modelled plots compare well, the modelled plots capturing the main features. At LHR2 the maximum NO_X concentrations are due to north-easterly, low wind speed conditions that would indicate the influence of non-airport sources including the airport Perimeter Road. The NO_2 plots at LHR2 reveal the impact of airport sources under south-westerly conditions with the monitored data plot in particular showing high concentrations at LHR2 at medium to high south-westerly wind speeds.

Figure 9.5 Monitored and modelled NO_X and NO_2 concentrations at LHR2 ($\mu g/m^3$), averaged per wind direction-wind speed category. Categories with fewer than 4 hourly concentrations are excluded.

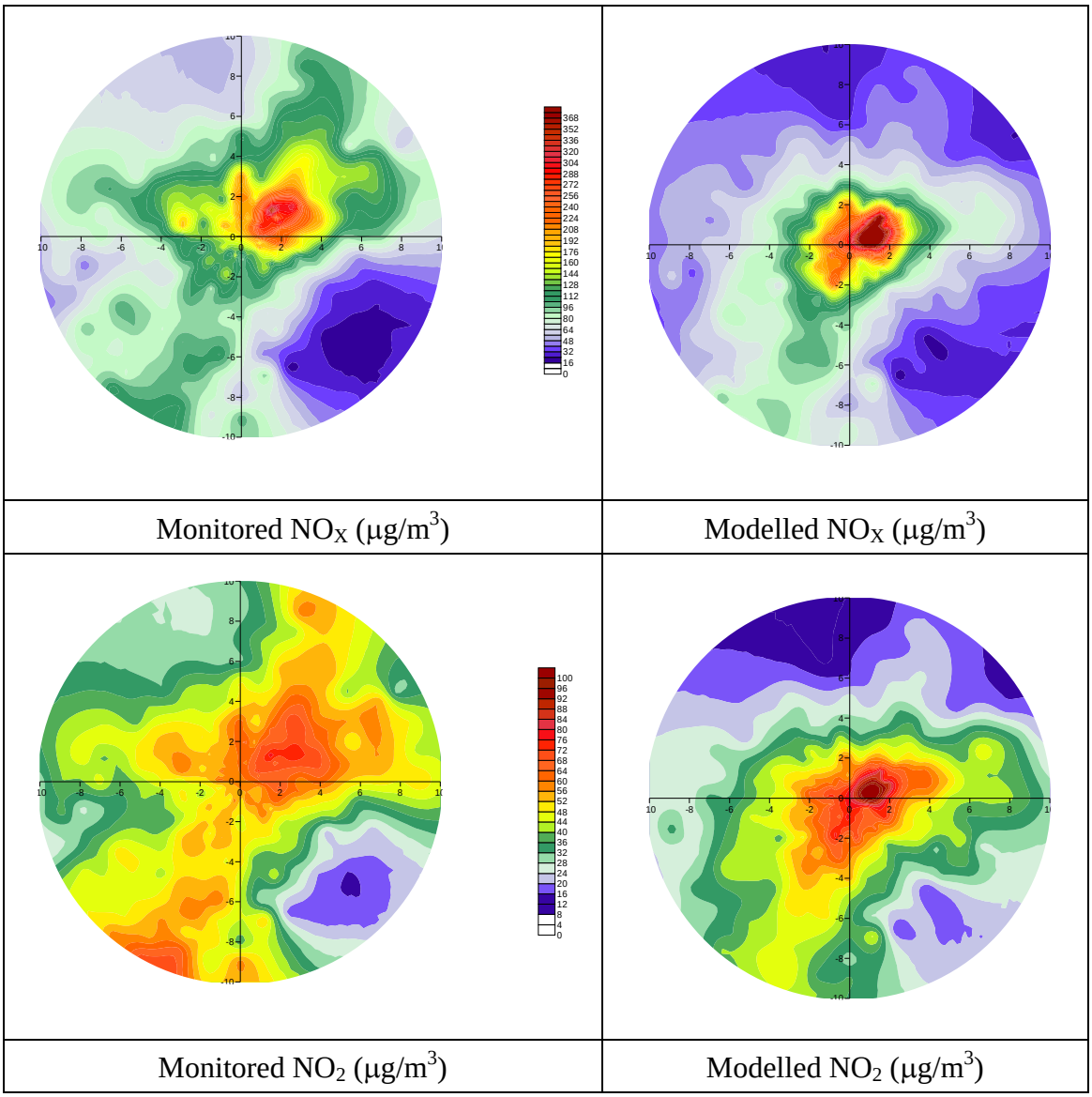

Figure 9.6 shows the polar plots for receptor LHR8, the Oaks Road monitor, located in Stanwell to the south-west of the airport. The monitor is to the south of the A30 dual carriageway and south of runway 09R. The impact of the road and airport on concentrations at LHR8 can clearly be seen in all the plots.

Figure 9.6 Monitored and modelled NO_X and NO_2 concentrations at LHR8 ($\mu g/m^3$), averaged per wind direction-wind speed category. Categories with fewer than 4 hourly concentrations are excluded.

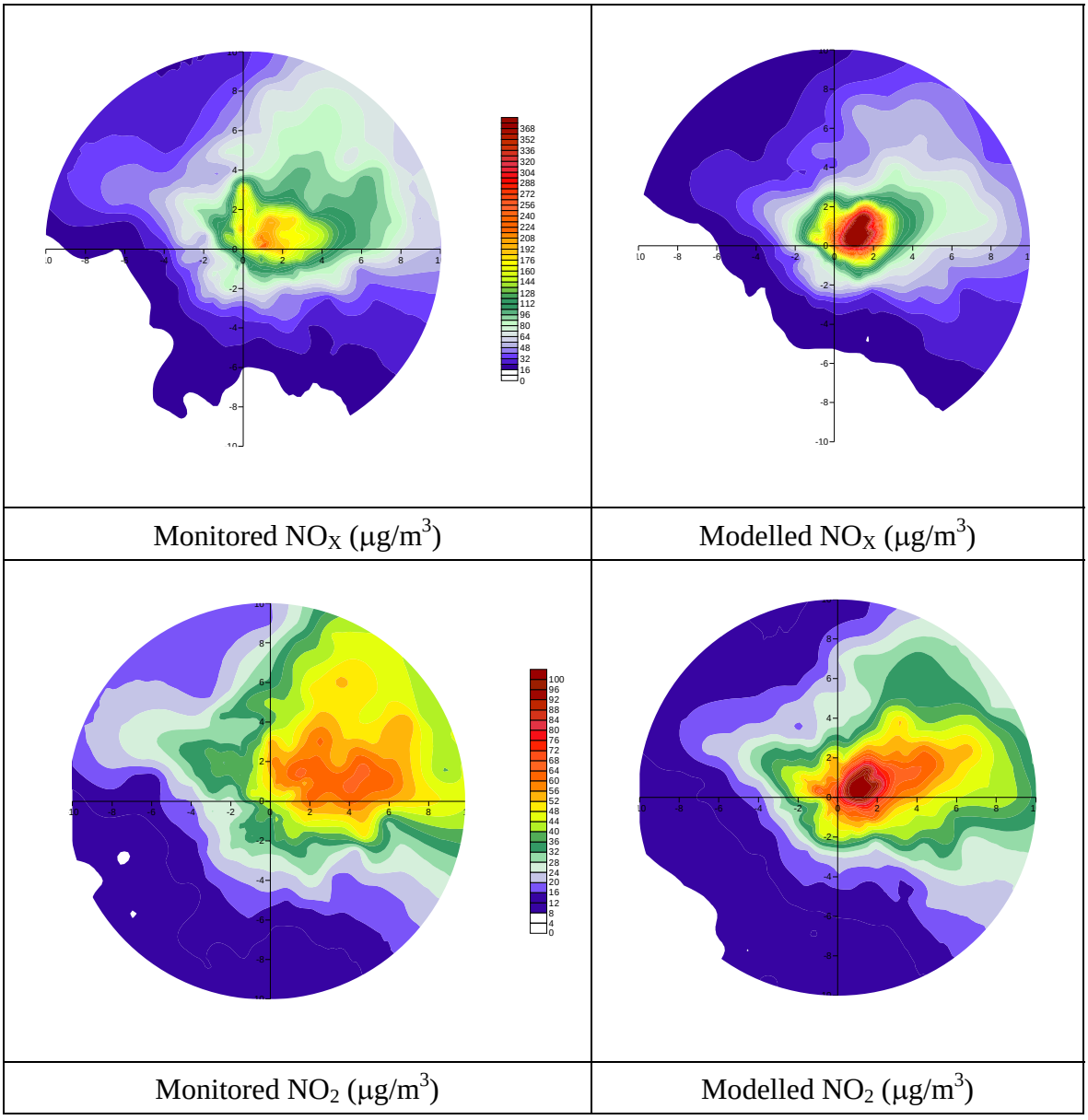

Figure 9.7 shows the polar plots for receptor LHR5, the Hounslow 2 monitor located in Cranford, to the north-east of the airport and to the west of the A321(T). Monitored and modelled plots show the highest concentrations occurring under low to medium easterly and north-easterly winds and some influence of the airport sources to the south-west of the monitor.

Figure 9.7 Monitored and modelled NO_X and NO_2 concentrations at LHR5 ($\mu g/m^3$), averaged per wind direction-wind speed category. Categories with fewer than 4 hourly concentrations are excluded.

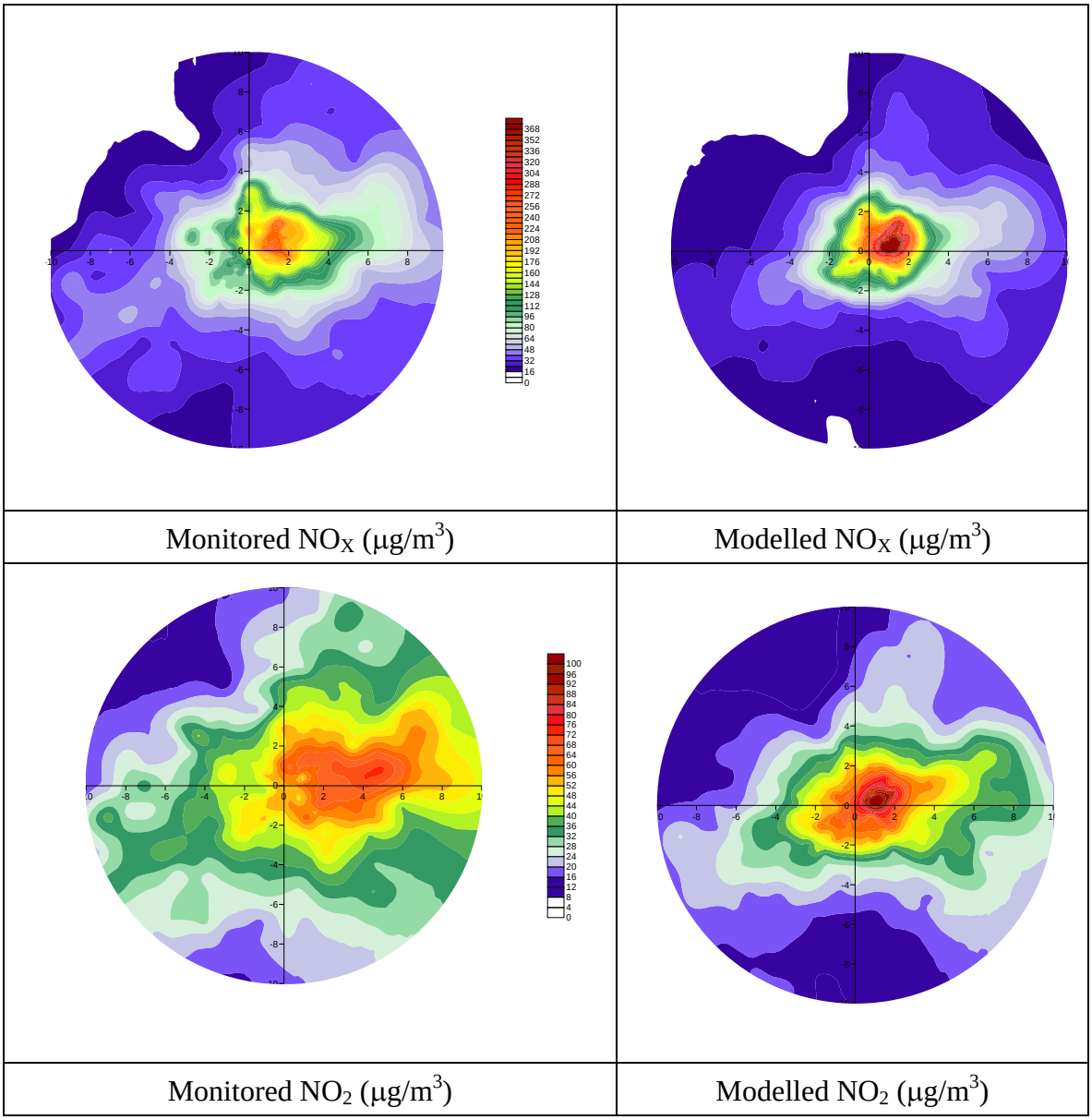

9.4 Transects of long term average concentrations of NO_X and NO_2

Figure 9.8 shows modelled concentrations of NO_X (top) and NO_2 (bottom) on a transect running south-north through LHR2, crossing the airport Perimeter Road, the A4 and the M4. The transects of NO_X show the contribution of each source group to show the gradient in concentration due to each source group. The steepest gradients in NO_X and NO_2 concentration are due to the major roads (the Perimeter Road, A4 and M4). Compared with the transect plots for ADMS-Airport shown in the MIC these plots do not show a jump in NO_X due to background sources at large distances as the railway emissions contributing to the jump are now modelled as

a line source rather than on an aggregated basis. The impact of the railway emissions is therefore seen in the contour plots (see Section 11) as more localised peaks in concentration.

Figure 9.8 (Top) Transect of NO_X modelled concentrations ($\mu g/m^3$) due to all sources(dark blue) and the various source groups. (Bottom) Transect of NO_2 modelled concentration ($\mu g/m^3$)

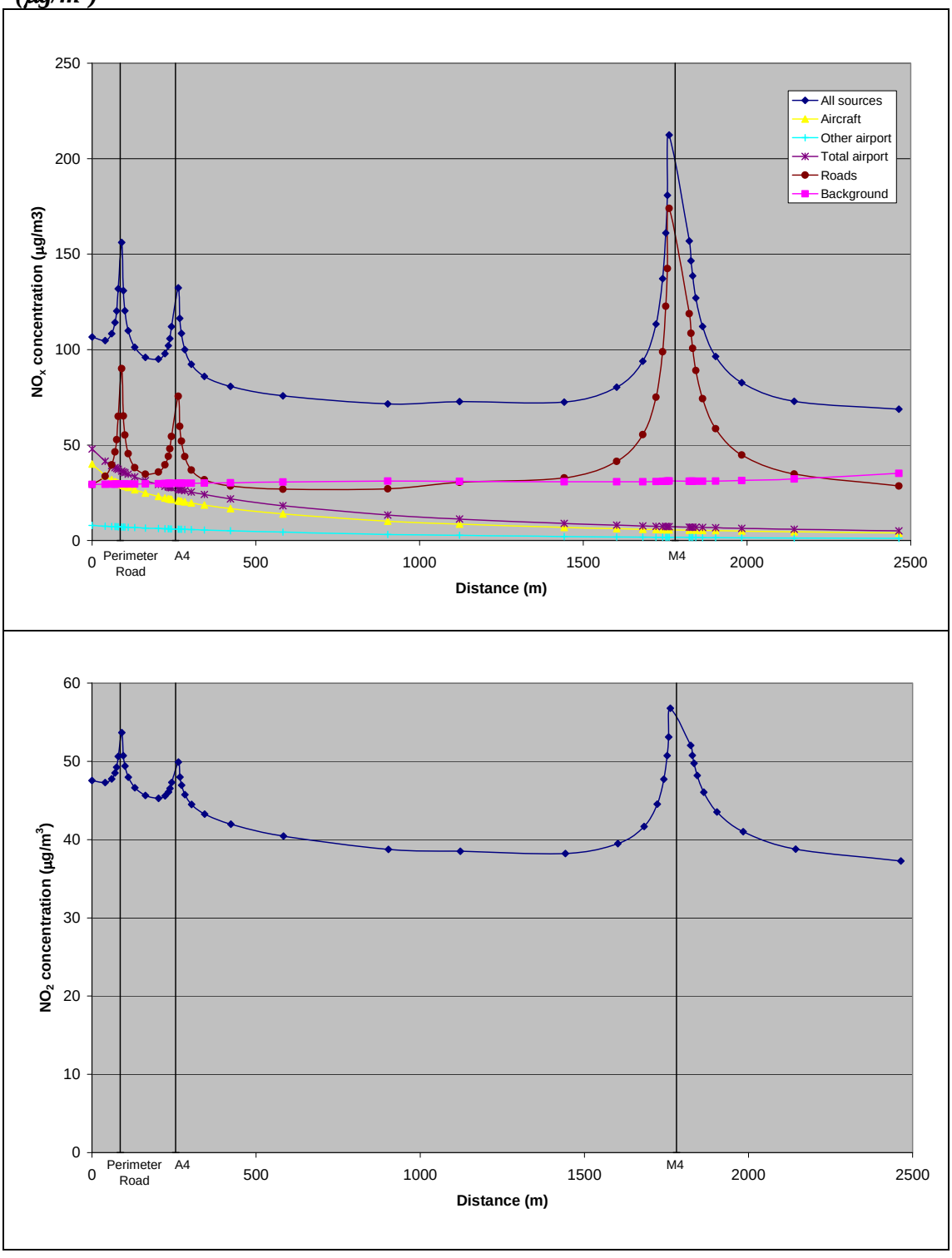

9.5 Comparison of annual average PM_{10} concentrations

Table 9.4 and Figure 9.9 show the comparison of modelled and monitored annual average concentrations at the automatic monitoring locations. It is a like-for-like comparison with hours for which either modelled or monitored concentrations are missing excluded.

Table 9.4 Comparison of predicted annual average concentrations of PM_{10} ($\mu g/m^3$) from the 2002 Base Case and automatic monitoring data.

Receptor name	Modelled concentration ($\mu g/m^3$)	Monitored concentration ($\mu g/m^3$)
LHR2	28.52	27.74
LHR5	24.26	23.01
LHR8	23.57	19.23
LHR10	29.44	30.00
LHR11	24.42	27.65
LHR12	24.09	22.71
LHR13	24.48	25.91
LHR14	23.64	24.38
LHR15	23.88	19.10
LHR16	26.31	24.72

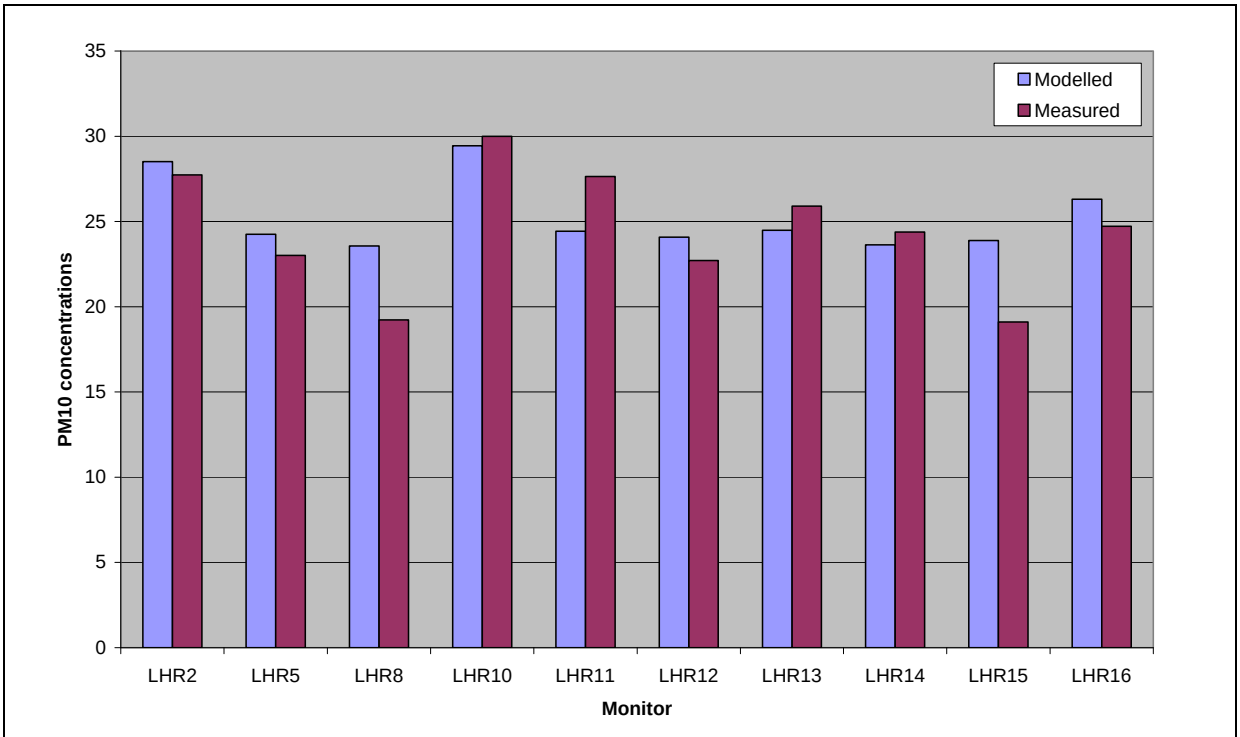

Figure 9.9 Predicted total PM_{10} concentrations in $\mu g/m^3$ from the 2002 Base Case (blue) and automatic monitors (red).

10 Results of Base Case and Future Scenario Modelling

This section presents the results of the 2002 Base Case modelling (Section 10.2) and the future scenarios (Sections 10.3-10.11). Concentrations for 2015NoC (Section 10.6) have been estimated from 2015SM and 2015MM modelling results.

Section 10.1 defines the source groups for which concentrations have been calculated. Tables
10.2-10.11 and Figures 10.1-10.37 show the results for NO_X, NO_2 and PM_{10}. The relevant EU air quality objectives for annual averages are 40μg/m^3 for NO_2 and 40μg/m^3 for PM_{10}.

For the main scenarios (i.e. all except 2015NoC and 2015MMRd) the tabulated results are the predicted annual concentrations of NO_X, NO_2 and PM_{10} due to all sources and predicted annual concentrations of NO_X and PM_{10} due to aircraft sources, non-aircraft airport sources and background sources at the receptors shown in Figures 7.1 and 7.2. Contour plots of NO_X and NO_2 due to all sources, NO_X due to aircraft and other airport sources and NO_X due to roads are presented for all the main scenarios. For the Base case there are additional contour plots of PM_{10} due to all sources, PM_{10} due to aircraft and other airport sources, PM_{10} due to roads and PM_{10} and NO_X due to background sources.

For the "No Cranford Agreement" variant case 2015NoC (Section10.6) the results are tabulated values of predicted annual average concentrations of NO_X and NO_2 due to all sources, NO_X due to aircraft and NO_X due to other airport sources with the percentage difference in predicted annual average NO_2 concentrations between 2015NoC and Case 2015SM at the receptor points.

For the variant case 2015MMRd, a road mitigation scenario, results are given as predicted annual average concentration of NO_X, NO_2 and PM_{10} due to all sources and the percentage difference in predicted annual average NO_2 concentrations between 2015MMRd and 2015MM at the receptor points. Figure 10.25 shows the difference in predicted NO_2 concentration at receptor locations.

2002-2030

In 2002 the annual average Limit Value for NO_2 is predicted by the modelling to be exceeded on the airport, along the motorways and some main roads, along the main railway line and in areas of Harlington. In the future scenarios the areas of exceedence are reduced compared with 2002 and are confined mainly to the airport and along the motorways. This reduction is largely due to the reduction in NO_X emissions from road traffic. In the 2030 mixed mode (2030MM) scenario there are no exceedences of the Limit Value at the receptors considered.

The greatest changes in concentration over the period considered are due to the predicted change in emissions from road traffic. In the Base case NO_2 concentrations at receptor LHR10, alongside the M25 where traffic emissions dominate, were modelled to be 58.3μg/m^3. In 2030 (2030R3) they are predicted to be 30.0 μg/m^3, a decrease of 48.5%.

Rail emissions are predicted to decrease in 2010 and further in 2015 due to re-engining of high speed trains. Whereas the air quality impact of the railway emissions is clearly seen in 2002 (Figure 10.5), its importance is predicted to decrease in future years.

Mixed Mode

Mixed mode operation compared with segregated mode operation significantly increases the take-offs from runway 09L and reduces the take-offs from 09R, thereby causing a shift in emissions from the southern to the northern runway. In the absence of any other changes the effect of mixed mode is to increase concentrations to the north-west of the airport (Longford) and to decrease concentrations to the south-west (Stanwell).

Third Runway, MDL and MLD

The third runway introduces emissions to the north of the current airport site. The results for the third runway cases shown, 2020R3 and 2030R3, are hybrid results of two modes of operation: MDL (mixed mode on the northern runway, departures on the central runway and landings on the southern runway) and MLD (mixed mode on the northern runway, landings on the central runway and departures on the southern runway) scenarios. The hybrid results have been constructed assuming the airport operates with equal alternation between MDL and MLD modes of operation. The take-off emissions are the highest emissions at ground level and therefore in the MDL mode of operation, when 27C is used for take-offs, higher concentrations are predicted to the north-east of the airport than under MLD operation when 27C is used for landings.

Easterly Preference (2015EP)

The change from a westerly preference operation to an easterly preference operation results in a change in the spatial pattern of emissions, with the significant take-off emissions moving from the north-eastern end of runway 27R to the south-western end of runway 09R. There are associated changes in taxiing and hold emissions. NO_x concentrations are predicted to increase at some receptors to the west of the airport, due to the increase in emissions on the 09L and 09R runways, and to decrease at receptors to the east of the airport. The greatest predicted increase in NO_2 concentrations compared with the westerly preference scenario (2015SM) is an increase of 5% at LHR15 near the 09L runway and the greatest decrease is 5% at X11, near to 27R.

No Cranford Agreement (2015NoC)

For the "No Cranford Agreement" scenario the estimated annual average concentrations of NO_2 were 95%-113% of the corresponding "with Cranford Agreement" (2015SM) predicted concentrations. The largest increases in NO_2 concentrations are predicted at receptors to the north-west of the airport (BAA14, BAA15, BAA16) near to 09L where there are increased movements. The greatest decreases in concentration are at receptors to the south-west of the airport (BAA49, BAA50, BAA51) near to 09R where there is decreased activity.

Roads mitigation scenario (2015MMRd)

Table 10.8 shows that the effect of the roads mitigation scenario is to reduce predicted NO_2 concentrations at most of the receptors considered. The biggest percentage decrease in predicted NO_2 concentration was 5.7% at receptor BAA34 and the biggest absolute decrease was 1.9μg/m^3 at receptor BAA32. Both these receptors are near to the M4. There is a small increase predicted at some receptors, the largest increase is 0.1μg/m^3 predicted at receptor LHR10 near to the M25. Figure 10.22 shows the predicted change in annual average concentrations of NO_2 at 2,900 additional near road receptors. The largest decreases in concentration are seen along the M4 with smaller decreases near to the airport around Harlington.

Particulates

The EU Limit Value for PM_{10} is 40μg/m^3 as an annual average. In 2002 the highest modelled annual average concentration of PM_{10} is 28.63μg/m^3 at receptor LHR10 that is beside the M25. In all future scenarios the predicted annual average PM_{10} concentration does not exceed 25μg/m^3. Therefore, at the receptors considered in this modelling study there are no predicted exceedences of the annual average Limit Value for PM_{10}.

The EU is currently negotiating the introduction of a target value of 25μg/m^3 of $PM_{2.5}$ as an annual average, to be achieved by 2010, whilst the same value has recently been adopted as an objective in the Air Quality Strategy[1] to be achieved by 2020. As $PM_{2.5}$ is a component of PM_{10} there are no predicted exceedences of 25μg/m^3 by the annual mean $PM_{2.5}$ in the future scenarios.

10.1 Source groups

The sources included in each sub-group of sources are listed in Table 10.1.

Table 10.1 Source groups

Category	Sources included
Aircraft	Approach, APU, Brake & tyre, Hold, Initial climb, Landing roll with and without reverse thrust, Push back, Take-off roll, Taxi in, Taxi out, Engine testing, Helipad.
Other airport	Airport roads, Airside vehicles, Car parks etc, Fire training, Heating plant, Paint shop, Taxi queues.
Roads	Major roads for Greater London area, Minor roads for Greater London area, Cold starts, Evaporative emissions (hot soak).
Other background	Agriculture, Boilers, City airport, Commercial gas, Domestic gas, Domestic coal, Domestic oil, Gas leak, Industrial coal, Natural sources, Part A industrial sources, Part B industrial sources, Rail lines, Sewage, Shipping, Solvents.
Background	Rural background plus Other background sources (listed above)

10.2 2002 Base Case

Modelled concentrations of NO_x, NO_2 and PM_{10} for 2002 Base Case at receptor locations are presented in Table 10.2.

Contour plots of modelled NO_x and NO_2 concentrations due to all sources are presented in Figure 10.1 and Figure 10.2 respectively. Contour plots of modelled NO_x concentrations due to aircraft and other airport sources, road sources and other background sources are presented in Figures 10.3-10.5 respectively.

Contour plot of modelled PM_{10} concentrations due to all sources is presented Figure 10.6. Contour plots of modelled PM_{10} concentrations due to aircraft and other airport sources, road sources and other background sources are presented in Figures 10.7-10.9.

Table 10.2 Modelled concentrations of NO_X, NO_2 and PM_{10} for 2002 Base Case ($\mu g/m^3$)

Receptor name	X(m)	Y(m)	Total NO_X	Total NO_2	Aircraft NO_X	Other airport NO_X	Road NO_X	Background NO_X	Total PM_{10}	Aircraft PM_{10}	Other airport PM_{10}	Road PM_{10}	Background PM_{10}
LHR2	508399	176744	108.6	47.7	31.2	6.5	41.6	29.3	25.69	1.22	0.46	1.66	22.35
LHR3	511679	180072	68.0	36.7	2.6	0.7	24.2	40.5	24.15	0.06	0.05	1.00	23.04
LHR4	509550	176997	77.9	39.8	12.5	3.0	32.9	29.5	24.06	0.26	0.20	1.28	22.32
LHR5	510370	177195	67.4	36.0	6.3	1.9	31.1	28.2	23.84	0.14	0.12	1.27	22.31
LHR6	515540	170420	51.2	28.3	0.7	0.2	22.8	27.5	23.22	0.02	0.01	0.92	22.28
LHR7	509333	175002	76.0	36.7	10.7	3.4	35.4	26.6	24.07	0.24	0.23	1.41	22.19
LHR8	505739	174497	58.6	31.5	7.5	1.8	24.4	25.0	23.37	0.16	0.13	0.96	22.11
LHR10	502741	173460	222.9	58.3	1.7	0.3	196.7	24.2	28.63	0.03	0.03	6.63	21.95
LHR11	504780	175510	69.6	35.5	7.4	0.9	34.8	26.5	24.02	0.13	0.07	1.32	22.51
LHR12	504466	175794	65.4	35.0	4.6	0.7	33.3	26.7	23.90	0.09	0.05	1.25	22.51
LHR13	504393	176591	85.2	39.5	3.2	0.7	55.0	26.3	24.29	0.07	0.05	2.01	22.15
LHR14	503535	176829	63.7	34.4	2.1	0.5	32.9	28.2	23.52	0.05	0.03	1.26	22.18
LHR15	505185	176922	62.6	34.0	3.6	1.2	31.2	26.5	23.56	0.11	0.08	1.19	22.17
LHR16	506945	178609	124.7	47.3	3.7	1.2	91.1	28.8	26.08	0.11	0.08	3.43	22.46
LHR17	506990	181919	57.2	32.1	1.4	0.4	26.0	29.4	23.52	0.04	0.03	1.05	22.40
LHR18	508279	177792	71.4	38.3	8.5	2.7	29.6	30.6	24.20	0.25	0.18	1.20	22.57
LHR19	508434	177376	73.7	39.7	12.4	3.6	26.6	31.1	24.19	0.36	0.24	1.07	22.51
LHR20	508058	177040	84.7	42.9	17.6	6.5	31.3	29.3	24.83	0.65	0.40	1.25	22.53
BA20	505127	177559	63.8	34.8	2.7	0.9	33.9	26.3	23.60	0.08	0.06	1.28	22.17
HD60	505736	177752	62.7	34.1	3.2	1.1	30.9	27.4	23.76	0.11	0.08	1.19	22.37
HD58	508414	177125	79.1	41.5	16.3	4.5	27.9	30.3	24.39	0.50	0.31	1.12	22.45
HD57	508758	177718	79.8	39.9	9.3	2.5	36.3	31.6	24.42	0.24	0.17	1.52	22.48
BA1	508582	178453	158.2	52.3	5.7	1.6	119.5	31.4	27.09	0.15	0.11	4.38	22.45
HD56	509798	178634	82.3	41.2	5.0	1.3	36.1	39.9	24.42	0.12	0.09	1.42	22.79
HS51	509127	174568	72.0	35.0	9.2	3.4	33.8	25.6	24.06	0.22	0.24	1.44	22.16
X1	505883	178463	114.5	45.3	2.7	0.9	83.5	27.4	25.53	0.08	0.07	3.12	22.27
X2	505932	177842	67.8	35.4	3.4	1.2	35.2	27.9	24.06	0.12	0.08	1.37	22.49
X3	505890	177393	73.7	36.0	4.1	1.5	40.2	27.9	24.44	0.16	0.10	1.66	22.52
X4	506146	177197	64.2	34.6	5.4	2.0	28.1	28.7	24.11	0.24	0.14	1.10	22.64

Table 10.2 (cont) Modelled concentrations of NO_X, NO_2 and PM_{10} for 2002 Base Case ($\mu g/m^3$)

Receptor name	X(m)	Y(m)	Total NO_X	Total NO_2	Aircraft NO_X	Other airport NO_X	Road NO_X	Background NO_X	Total PM_{10}	Aircraft PM_{10}	Other airport PM_{10}	Road PM_{10}	Background PM_{10}
X5	506156	177092	66.0	35.1	5.8	2.2	29.4	28.5	24.16	0.28	0.15	1.15	22.58
X6	506154	176991	84.0	37.9	6.2	2.4	47.0	28.3	24.85	0.33	0.16	1.83	22.52
X7	508228	177545	71.2	38.7	10.3	3.4	26.9	30.7	24.25	0.31	0.22	1.08	22.65
X8	508212	177390	73.0	39.5	11.9	4.0	26.7	30.4	24.32	0.38	0.26	1.07	22.62
X9	507873	177139	81.9	42.1	15.0	7.3	30.6	29.1	24.83	0.55	0.41	1.22	22.65
X10	508429	177012	85.6	43.2	18.8	5.0	31.7	30.1	24.63	0.60	0.35	1.27	22.41
X11	508549	176736	106.6	47.4	32.8	5.7	38.6	29.5	25.28	0.98	0.42	1.54	22.33
X12	508789	177365	82.2	41.0	12.6	3.2	35.5	30.9	24.44	0.33	0.22	1.46	22.44
X13	508735	177965	79.7	39.6	7.8	2.2	37.7	31.9	24.36	0.20	0.15	1.52	22.48
BAA1	508009	177028	86.3	43.3	17.7	7.0	32.3	29.2	24.92	0.66	0.42	1.29	22.54
BAA2	507914	177030	87.6	43.5	17.4	7.9	33.3	29.0	25.02	0.67	0.45	1.33	22.57
BAA3	508802	177048	91.1	43.8	18.3	3.9	38.7	30.1	24.69	0.44	0.28	1.59	22.38
BAA4	508762	177049	85.0	42.8	18.3	4.0	32.6	30.1	24.44	0.46	0.29	1.32	22.38
BAA5	508885	177042	85.9	43.0	18.4	3.8	33.6	30.1	24.42	0.42	0.27	1.36	22.37
BAA6	508902	177045	84.8	42.7	18.3	3.7	32.7	30.1	24.36	0.41	0.26	1.32	22.37
BAA7	508552	177102	80.0	41.8	16.9	4.3	28.5	30.4	24.34	0.49	0.30	1.14	22.41
BAA8	508598	177100	80.2	41.8	17.0	4.2	28.6	30.4	24.33	0.48	0.30	1.15	22.41
BAA9	508412	177117	79.4	41.6	16.4	4.6	28.0	30.3	24.40	0.51	0.31	1.13	22.45
BAA10	508380	177164	77.8	41.1	15.5	4.5	27.4	30.4	24.36	0.48	0.30	1.10	22.47
BAA11	508373	177231	76.0	40.6	14.4	4.2	26.9	30.5	24.30	0.44	0.29	1.08	22.50
BAA12	508366	177292	74.8	40.1	13.4	4.0	26.7	30.7	24.27	0.41	0.27	1.07	22.52
BAA13	508356	177373	73.5	39.6	12.3	3.7	26.6	30.9	24.23	0.37	0.25	1.07	22.55
BAA14	504799	176658	70.2	36.2	3.7	1.0	39.3	26.2	23.79	0.09	0.07	1.47	22.16
BAA15	504842	176702	67.1	35.5	3.6	1.0	36.2	26.3	23.69	0.09	0.07	1.36	22.16
BAA16	504966	176844	63.9	34.6	3.5	1.1	33.0	26.3	23.59	0.10	0.07	1.25	22.16
BAA17	505043	176904	63.3	34.4	3.5	1.1	32.4	26.4	23.58	0.10	0.08	1.23	22.17
BAA18	506046	176986	85.5	38.0	5.8	2.2	49.4	28.1	24.84	0.30	0.15	1.93	22.46
BAA19	506153	176991	84.0	37.9	6.2	2.4	47.1	28.3	24.85	0.33	0.16	1.83	22.52
BAA20	507307	177018	85.3	41.7	13.9	8.9	34.1	28.4	25.14	0.62	0.47	1.36	22.70
BAA21	507496	177400	97.0	42.4	9.7	4.5	54.8	27.9	25.75	0.36	0.26	2.16	22.97

Table 10.2 (cont) Modelled concentrations of NO_X, NO_2 and PM_{10} for 2002 Base Case ($\mu g/m^3$)

Receptor name	X(m)	Y(m)	Total NO_X	Total NO_2	Aircraft NO_X	Other airport NO_X	Road NO_X	Background NO_X	Total PM_{10}	Aircraft PM_{10}	Other airport PM_{10}	Road PM_{10}	Background PM_{10}
BAA22	509431	176952	89.0	42.1	14.4	3.2	41.9	29.6	24.43	0.29	0.21	1.61	22.32
BAA23	509544	176967	85.4	41.0	12.8	3.1	40.1	29.4	24.31	0.27	0.20	1.53	22.31
BAA24	509582	177007	76.6	39.5	12.1	3.0	32.1	29.4	24.02	0.25	0.19	1.26	22.32
BAA25	509574	177054	73.5	38.9	11.9	2.9	29.2	29.5	23.92	0.25	0.19	1.16	22.32
BAA26	506791	178593	131.4	48.1	3.5	1.2	98.1	28.6	26.28	0.11	0.08	3.68	22.42
BAA27	506928	178615	122.0	46.9	3.6	1.2	88.4	28.8	25.98	0.11	0.08	3.33	22.46
BAA28	507004	178623	118.8	46.5	3.7	1.2	85.0	28.9	25.89	0.11	0.08	3.21	22.48
BAA29	507089	178626	120.8	46.9	3.8	1.2	86.8	29.0	25.98	0.12	0.08	3.28	22.50
BAA30	507176	178628	125.9	47.8	3.9	1.2	91.7	29.1	26.22	0.12	0.09	3.49	22.52
BAA31	507207	178632	127.6	48.1	3.9	1.2	93.3	29.1	26.35	0.12	0.09	3.61	22.53
BAA32	510172	178352	133.0	50.1	5.2	1.3	91.1	35.4	26.39	0.12	0.09	3.54	22.64
BAA33	510109	178351	131.1	49.6	5.3	1.3	88.8	35.7	26.27	0.12	0.09	3.41	22.65
BAA34	509999	178376	111.4	46.5	5.4	1.4	68.0	36.6	25.46	0.12	0.09	2.57	22.67
BAA35	510016	178407	101.9	44.9	5.3	1.3	58.4	36.9	25.14	0.12	0.09	2.23	22.69
BAA36	510157	178384	113.2	47.0	5.2	1.3	70.9	35.9	25.63	0.12	0.09	2.76	22.66
BAA37	510188	178445	97.1	44.3	5.0	1.3	54.5	36.4	25.04	0.11	0.09	2.14	22.69
BAA38	509820	178355	132.4	49.5	5.6	1.4	88.1	37.2	26.15	0.13	0.10	3.25	22.67
BAA39	509822	178396	107.9	45.9	5.5	1.4	63.2	37.7	25.30	0.13	0.10	2.37	22.70
BAA40	509392	178382	149.1	52.0	5.9	1.6	103.5	38.1	26.71	0.14	0.11	3.78	22.67
BAA41	509403	178468	101.2	45.0	5.6	1.5	54.8	39.2	25.04	0.14	0.10	2.08	22.72
BAA42	506456	178564	111.1	45.0	3.2	1.1	78.6	28.3	25.49	0.10	0.08	2.96	22.35
BAA43	507178	178659	106.2	44.7	3.8	1.2	72.0	29.1	25.51	0.12	0.08	2.77	22.54
BAA44	507066	178668	98.3	43.3	3.7	1.2	64.4	29.1	25.17	0.11	0.08	2.47	22.51
BAA45	508822	174587	75.0	36.6	12.3	5.1	32.0	25.6	24.11	0.31	0.37	1.28	22.16
BAA46	508849	174638	77.1	37.2	12.9	5.0	33.4	25.7	24.17	0.32	0.36	1.33	22.16
BAA47	508877	174691	80.4	37.9	13.5	4.9	36.1	25.8	24.27	0.32	0.36	1.43	22.16
BAA48	509007	174755	76.1	36.9	12.7	4.2	33.3	25.9	24.08	0.29	0.30	1.32	22.17
BAA49	505777	174594	61.9	32.3	8.5	1.9	26.4	25.1	23.45	0.18	0.14	1.02	22.11
BAA50	505744	174588	61.4	32.2	8.4	1.8	26.1	25.1	23.44	0.18	0.13	1.01	22.11
BAA51	505909	174592	64.4	32.8	8.8	2.3	28.2	25.1	23.56	0.20	0.16	1.08	22.11

Figure 10.1 2002 Base Case, modelled total NO_X concentrations in $\mu g/m^3$ around Heathrow.

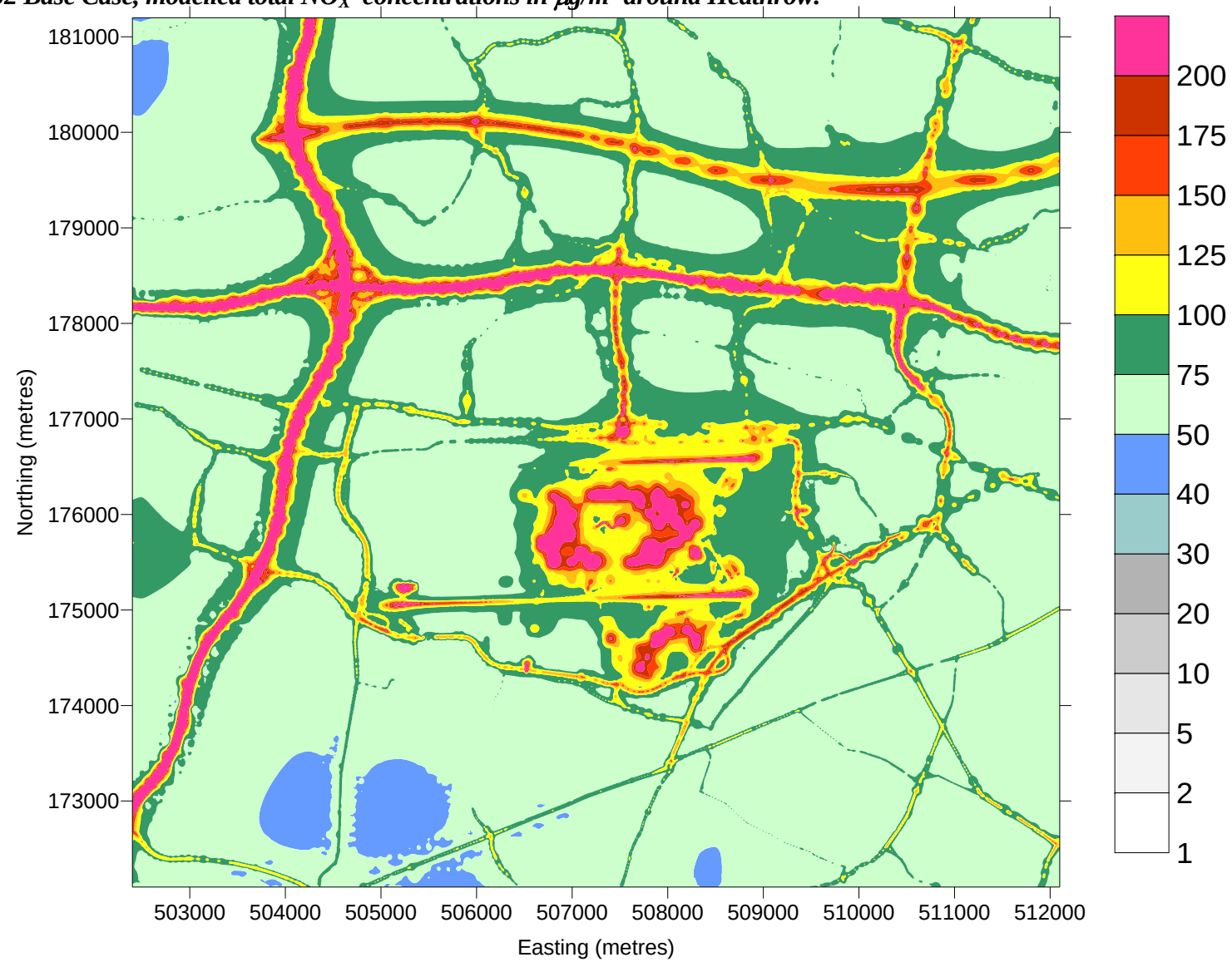

Figure 10.2 2002 Base Case, modelled total NO_2 concentrations in $\mu g/m^3$ around Heathrow.

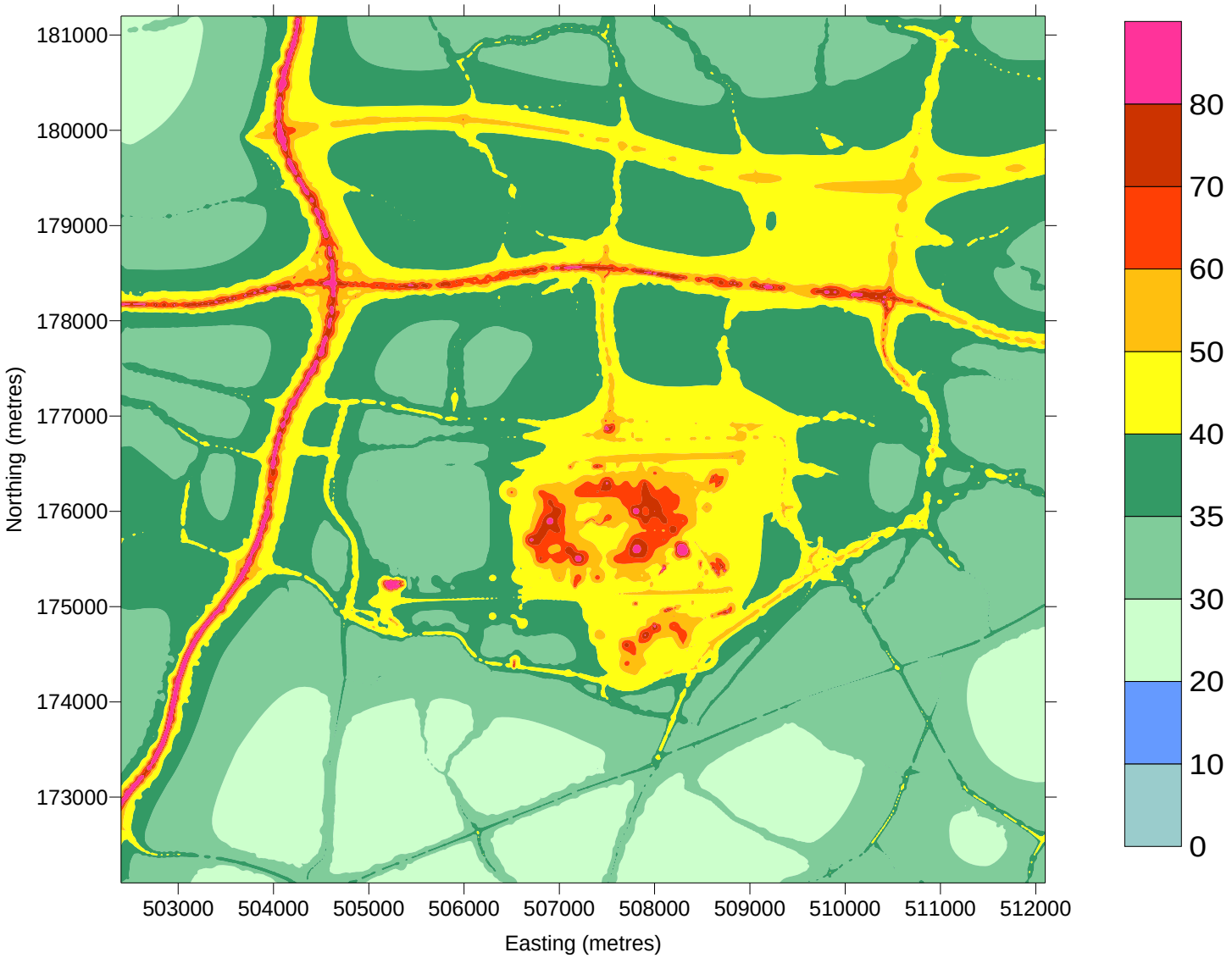

Figure 10.3 2002 Base Case, modelled NO_X concentration in $\mu g/m^3$ around Heathrow due to aircraft and other airport sources.

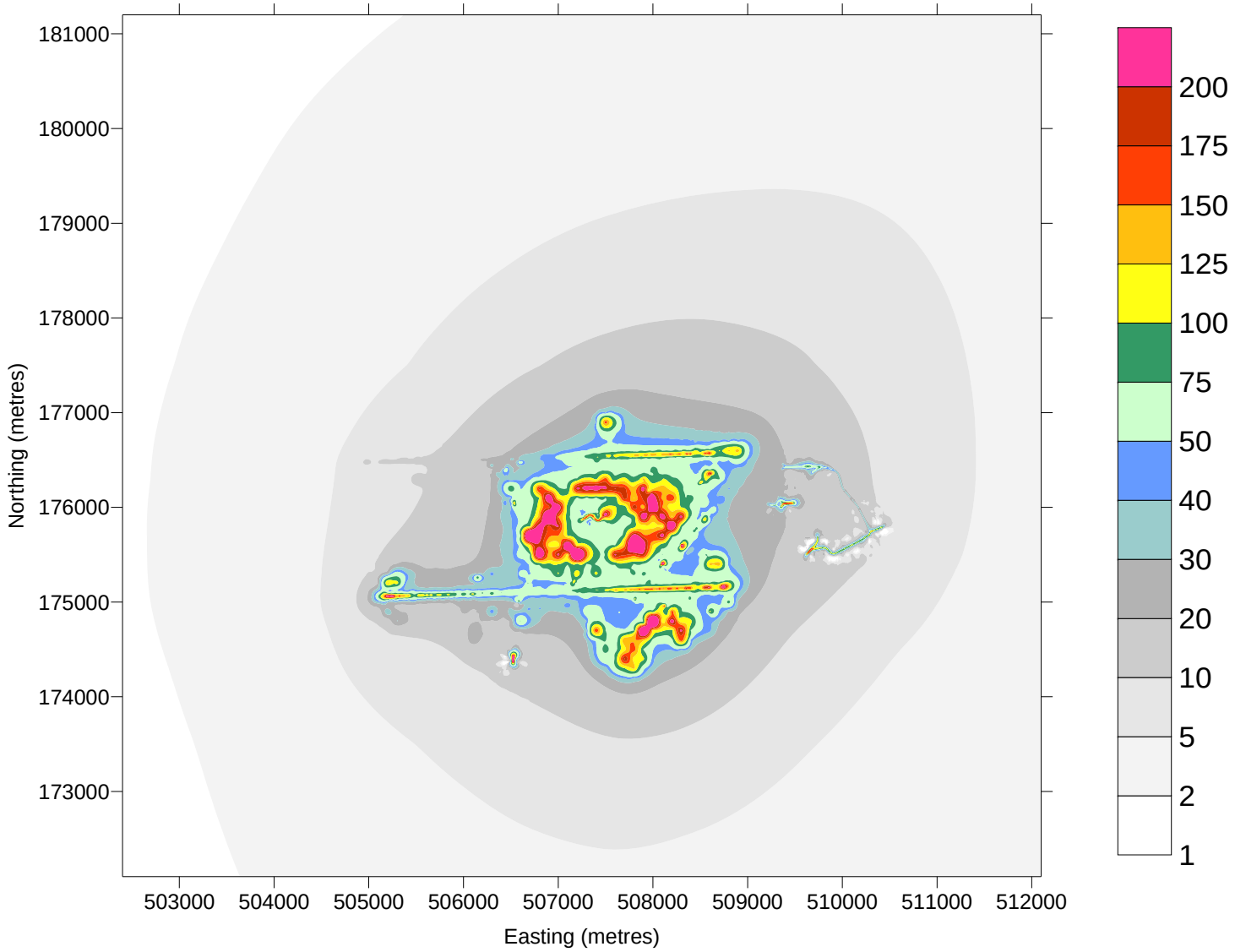

Figure 10.4 2002 Base Case, modelled NO_X concentration in $\mu g/m^3$ around Heathrow due to road sources.

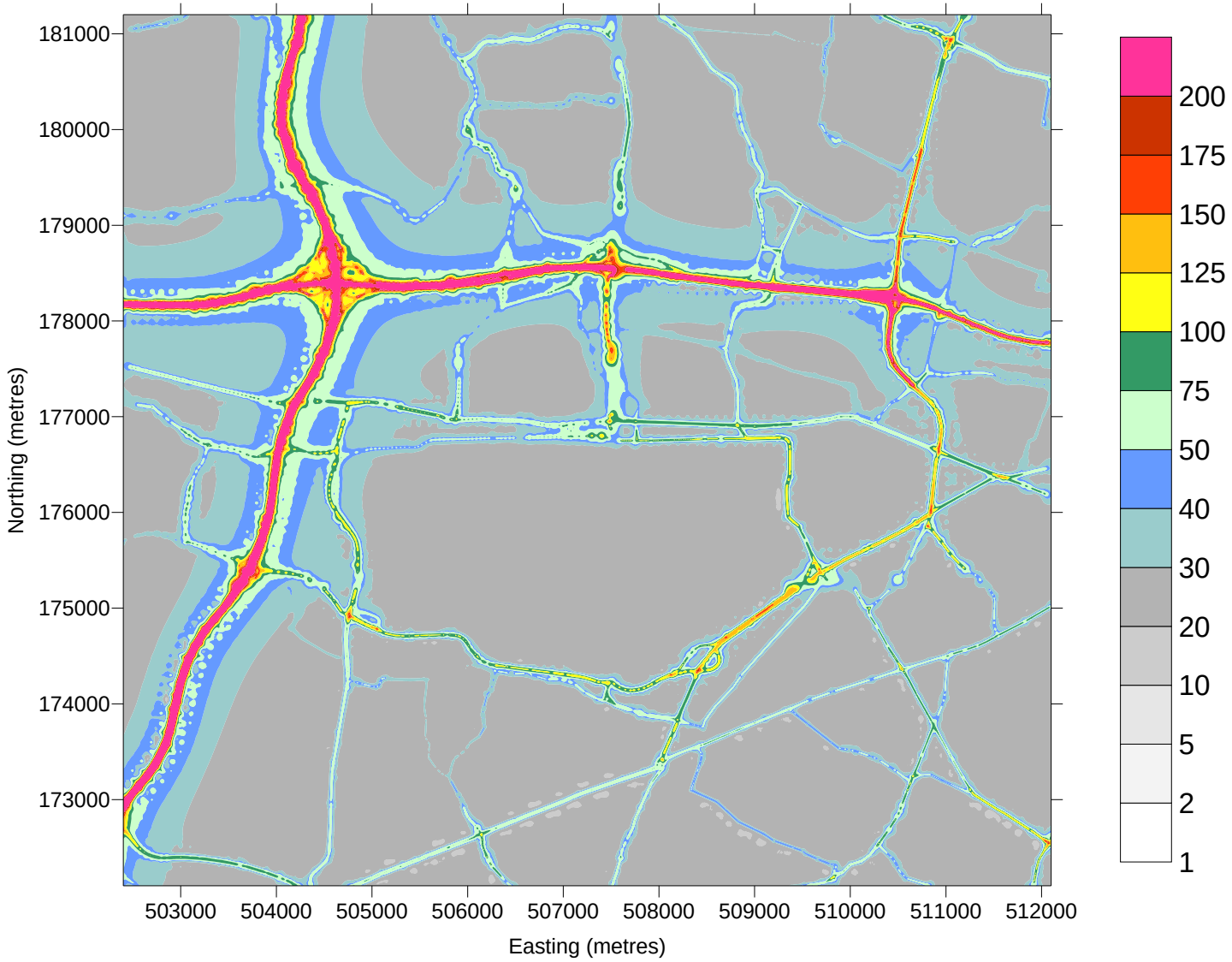

Figure 10.5 2002 Base Case, modelled NO_X concentration in $\mu g/m^3$ around Heathrow due to other background sources.

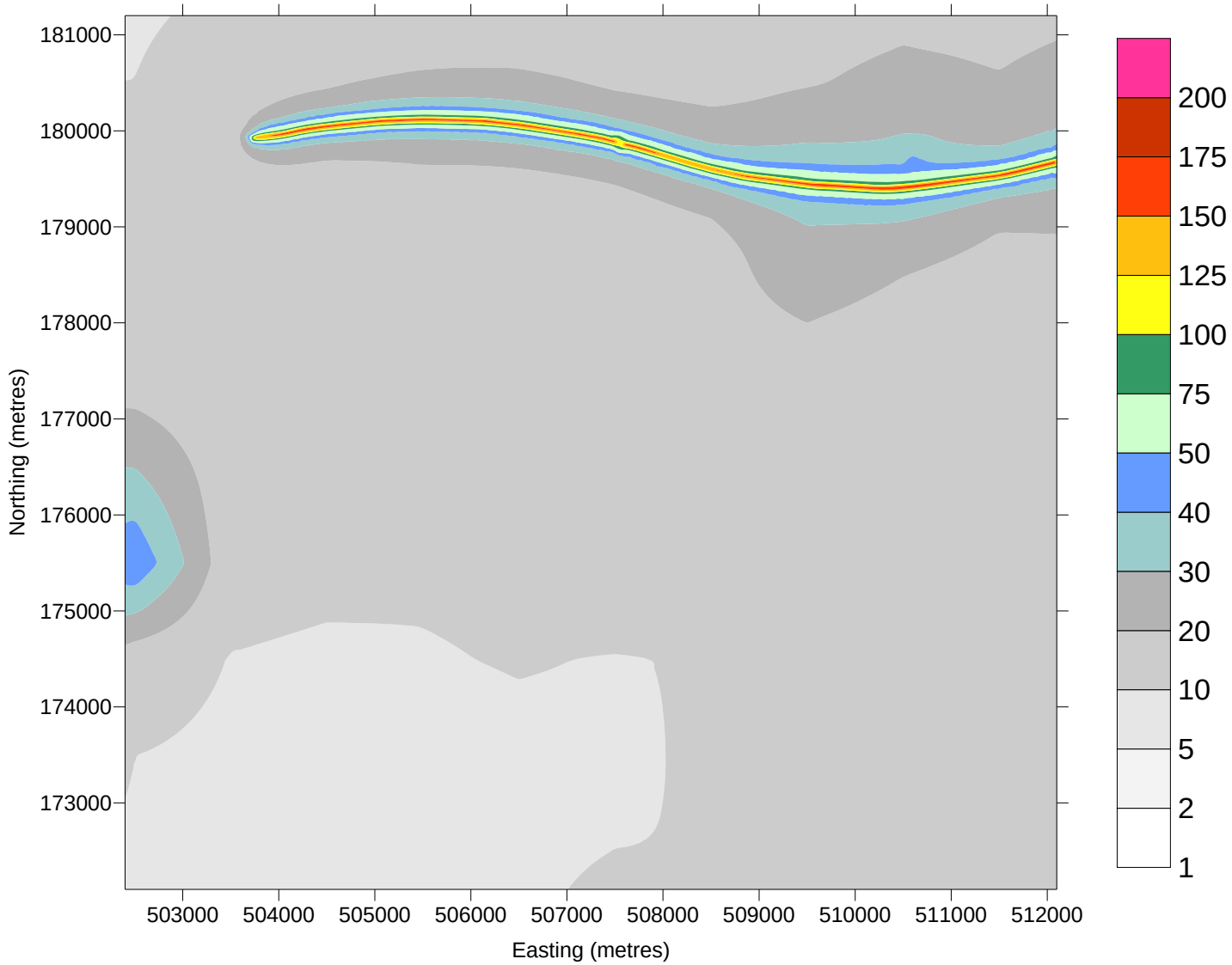

Figure 10.6 2002 Base Case, modelled total PM_{10} concentrations in $\mu g/m^3$ around Heathrow.

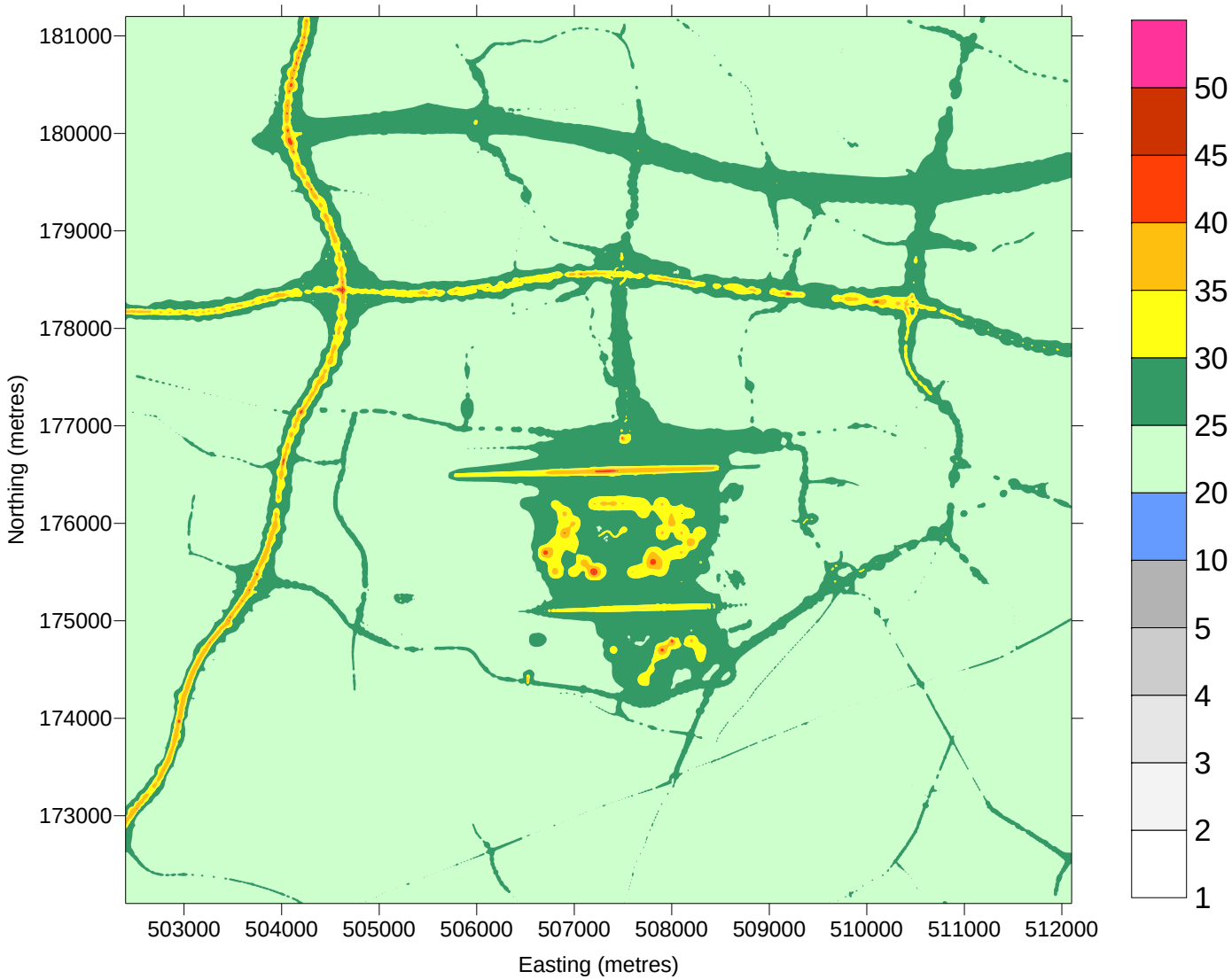

Figure 10.7 2002 Base Case, modelled PM_{10} concentration in $\mu g/m^3$ around Heathrow due to aircraft and other airport sources.

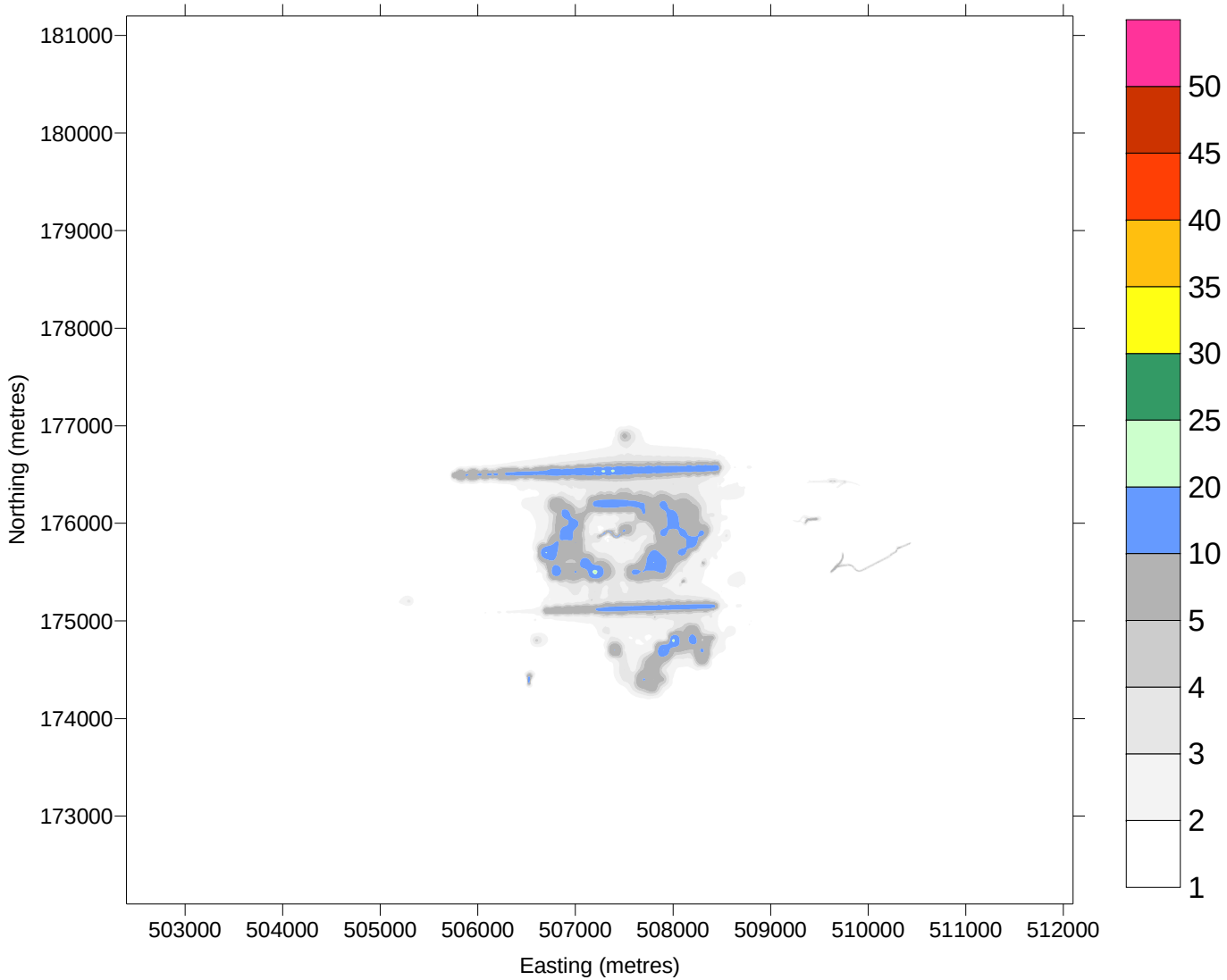

Figure 10.8 2002 Base Case, modelled PM_{10} concentration in $\mu g/m^3$ around Heathrow due to road sources.

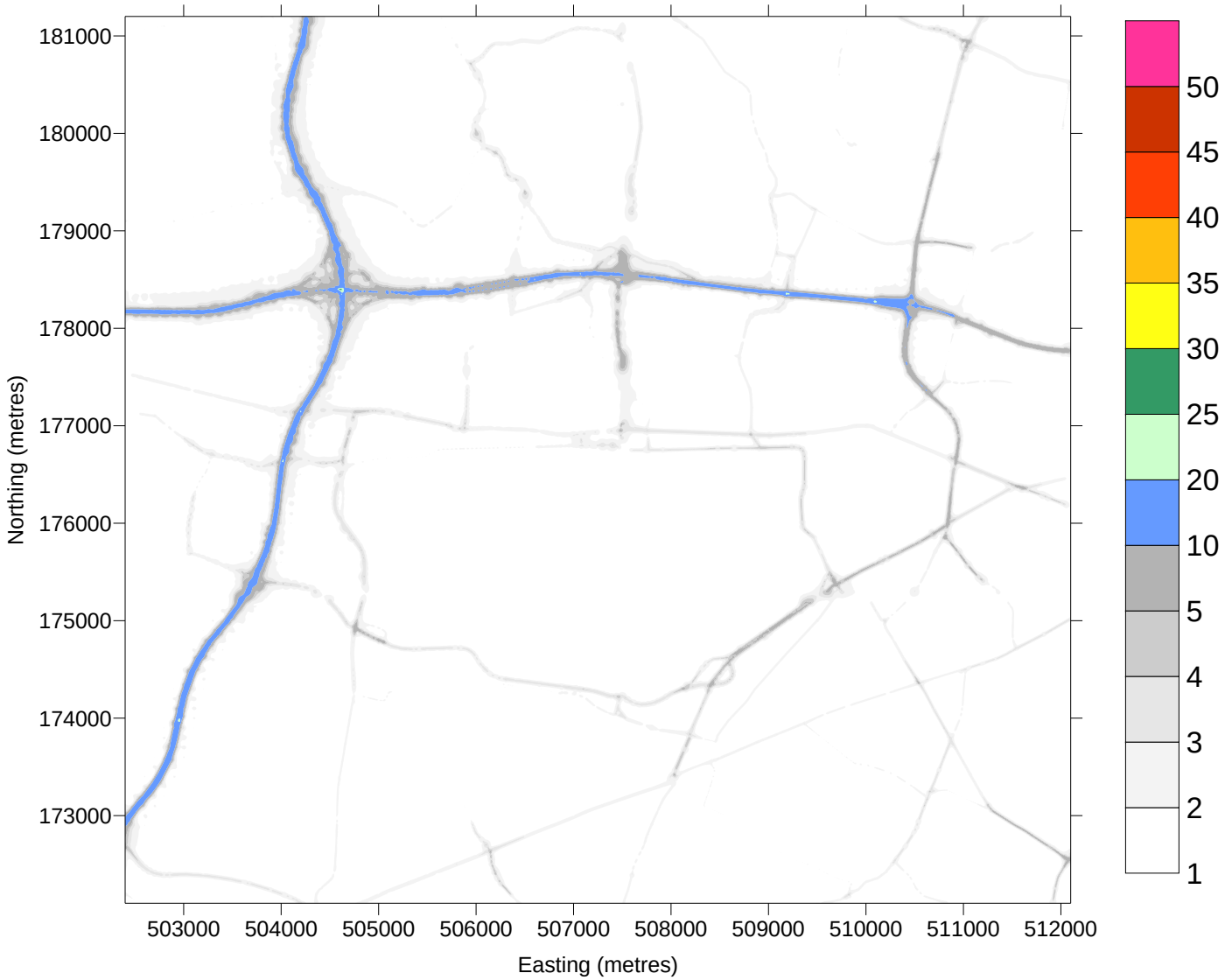

Figure 10.9 2002 Base Case, modelled PM_{10} concentration in $\mu g/m^3$ around Heathrow due to other background sources.

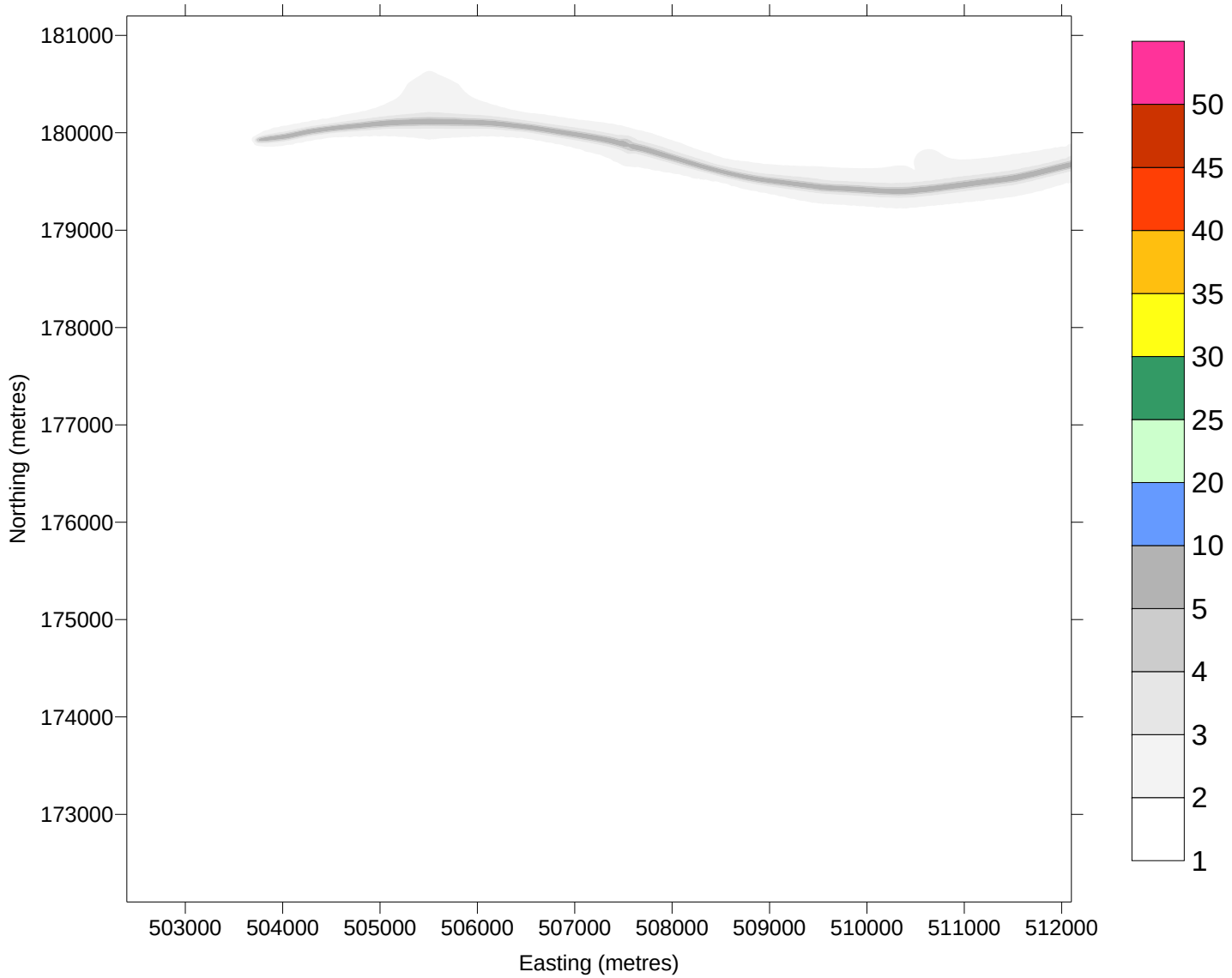

10.3 2010SM

Predicted concentrations of NO_x, NO_2 and PM_{10} for 2010SM at receptor locations are presented in Table 10.3.

Contour plots of predicted NO_x and NO_2 concentrations due to all sources are presented in Figure 10.10 and Figure 10.11 respectively. Contour plots of predicted NO_x concentrations due to aircraft and other airport sources and road sources are presented in Figure 10.12 and Figure 10.13 respectively

Table 10.3 Predicted concentrations of NO_X, NO_2 and PM_{10} for 2010SM ($\mu g/m^3$)

Receptor name	X(m)	Y(m)	Total NO_X	Total NO_2	Aircraft NO_X	Other airport NO_X	Road NO_X	Background NO_X	Total PM_{10}	Aircraft PM_{10}	Other airport PM_{10}	Road PM_{10}	Background PM_{10}
LHR2	508399	176744	90.9	45.7	37.1	3.6	24.8	25.5	22.45	1.32	0.25	0.94	19.94
LHR3	511679	180072	52.3	33.7	3.2	0.4	12.6	36.1	21.17	0.06	0.03	0.58	20.50
LHR4	509550	176997	59.5	36.9	14.1	2.3	17.4	25.7	20.99	0.22	0.13	0.73	19.90
LHR5	510370	177195	49.4	32.5	7.4	1.2	16.6	24.2	20.80	0.12	0.07	0.72	19.88
LHR6	515540	170420	36.3	24.2	0.8	0.1	11.6	23.7	20.43	0.02	0.01	0.54	19.87
LHR7	509333	175002	57.0	32.9	13.3	1.7	19.3	22.7	20.91	0.23	0.11	0.79	19.78
LHR8	505739	174497	46.1	28.9	10.4	1.6	12.9	21.1	20.57	0.17	0.12	0.56	19.71
LHR10	502741	173460	131.7	49.9	2.2	0.3	108.5	20.7	23.93	0.04	0.02	4.29	19.57
LHR11	504780	175510	55.9	33.0	10.9	3.0	19.4	22.7	21.30	0.16	0.25	0.78	20.11
LHR12	504466	175794	49.4	31.4	6.5	2.1	17.9	22.9	21.15	0.11	0.18	0.75	20.11
LHR13	504393	176591	56.6	34.1	4.3	1.1	28.7	22.5	21.04	0.09	0.09	1.13	19.74
LHR14	503535	176829	44.7	30.0	2.7	0.5	16.9	24.6	20.57	0.05	0.04	0.73	19.75
LHR15	505185	176922	46.5	31.0	5.7	1.8	16.4	22.6	20.75	0.15	0.14	0.70	19.76
LHR16	506945	178609	77.6	40.5	4.8	0.9	47.1	24.8	22.23	0.13	0.06	2.01	20.02
LHR17	506990	181919	41.1	27.9	1.8	0.3	13.4	25.5	20.65	0.04	0.02	0.61	19.97
LHR18	508279	177792	54.0	35.3	10.5	1.5	15.2	26.8	21.20	0.26	0.10	0.69	20.15
LHR19	508434	177376	57.8	37.2	14.7	2.0	13.8	27.3	21.21	0.37	0.13	0.62	20.10
LHR20	508058	177040	65.6	40.1	20.7	3.1	16.3	25.5	21.71	0.69	0.20	0.70	20.12
BA20	505127	177559	44.7	30.5	3.9	0.9	17.4	22.4	20.67	0.11	0.07	0.75	19.74
HD60	505736	177752	45.1	30.5	4.6	1.1	16.0	23.5	20.86	0.14	0.08	0.70	19.95
HD58	508414	177125	62.6	39.1	19.0	2.4	14.6	26.6	21.35	0.51	0.17	0.64	20.04
HD57	508758	177718	60.0	36.9	11.2	1.5	19.5	27.9	21.27	0.24	0.10	0.88	20.06
BA1	508582	178453	99.1	45.9	7.1	1.0	63.5	27.5	22.80	0.15	0.07	2.56	20.01
HD56	509798	178634	61.9	37.5	6.1	0.8	18.7	36.2	21.32	0.11	0.06	0.81	20.34
HS51	509127	174568	50.9	30.5	10.4	1.7	17.1	21.7	20.80	0.19	0.11	0.75	19.76
X1	505883	178463	70.6	38.3	3.6	0.8	42.8	23.5	21.82	0.10	0.06	1.82	19.84
X2	505932	177842	48.7	31.6	4.8	1.1	18.8	24.0	21.10	0.14	0.08	0.81	20.07
X3	505890	177393	53.5	32.7	6.0	1.5	21.9	24.1	21.34	0.20	0.11	0.93	20.11
X4	506146	177197	49.4	32.5	8.1	1.9	14.6	24.8	21.30	0.31	0.14	0.63	20.22

Table 10.3 (cont) Predicted concentrations of NO_X, NO_2 and PM_{10} for 2010SM ($\mu g/m^3$)

Receptor name	X(m)	Y(m)	Total NO_X	Total NO_2	Aircraft NO_X	Other airport NO_X	Road NO_X	Background NO_X	Total PM_{10}	Aircraft PM_{10}	Other airport PM_{10}	Road PM_{10}	Background PM_{10}
X5	506156	177092	50.9	33.1	8.9	2.1	15.2	24.7	21.35	0.37	0.15	0.65	20.17
X6	506154	176991	60.3	35.5	9.7	2.3	23.7	24.5	21.68	0.44	0.17	0.96	20.12
X7	508228	177545	55.0	36.0	12.4	1.8	13.9	26.9	21.30	0.33	0.12	0.62	20.23
X8	508212	177390	56.8	36.9	14.3	2.1	13.8	26.6	21.35	0.39	0.14	0.62	20.20
X9	507873	177139	62.3	39.0	18.0	3.3	15.8	25.2	21.72	0.60	0.19	0.69	20.23
X10	508429	177012	67.5	40.6	21.9	2.7	16.7	26.3	21.51	0.60	0.19	0.72	20.00
X11	508549	176736	90.7	45.4	39.1	3.3	22.6	25.7	22.03	1.00	0.24	0.88	19.92
X12	508789	177365	63.5	38.5	14.8	1.8	19.7	27.2	21.32	0.31	0.12	0.86	20.02
X13	508735	177965	59.3	36.5	9.5	1.3	20.4	28.1	21.24	0.21	0.09	0.88	20.06
BAA1	508009	177028	66.5	40.4	21.0	3.2	16.9	25.4	21.78	0.71	0.20	0.73	20.13
BAA2	507914	177030	66.8	40.5	20.7	3.5	17.3	25.2	21.85	0.73	0.21	0.74	20.16
BAA3	508802	177048	71.5	41.3	21.3	2.2	21.7	26.3	21.43	0.41	0.16	0.90	19.96
BAA4	508762	177049	67.4	40.4	21.2	2.2	17.6	26.4	21.30	0.43	0.16	0.75	19.97
BAA5	508885	177042	68.2	40.5	21.5	2.1	18.3	26.3	21.26	0.39	0.15	0.77	19.95
BAA6	508902	177045	67.4	40.3	21.4	2.1	17.6	26.3	21.23	0.38	0.15	0.75	19.95
BAA7	508552	177102	63.6	39.4	19.6	2.3	15.0	26.7	21.30	0.48	0.17	0.65	20.00
BAA8	508598	177100	63.8	39.4	19.7	2.3	15.1	26.6	21.28	0.47	0.16	0.66	19.99
BAA9	508412	177117	62.8	39.2	19.2	2.4	14.7	26.5	21.36	0.51	0.17	0.64	20.04
BAA10	508380	177164	61.4	38.7	18.1	2.4	14.3	26.6	21.34	0.49	0.16	0.63	20.06
BAA11	508373	177231	59.9	38.1	16.9	2.3	14.0	26.7	21.30	0.45	0.16	0.62	20.08
BAA12	508366	177292	58.7	37.6	15.9	2.1	13.9	26.9	21.28	0.42	0.15	0.62	20.10
BAA13	508356	177373	57.5	37.1	14.7	2.0	13.8	27.1	21.26	0.38	0.14	0.61	20.13
BAA14	504799	176658	51.7	32.7	5.4	1.7	22.3	22.4	20.90	0.12	0.13	0.90	19.75
BAA15	504842	176702	49.3	32.0	5.4	1.7	19.8	22.4	20.82	0.12	0.13	0.82	19.75
BAA16	504966	176844	46.8	31.2	5.2	1.6	17.4	22.5	20.75	0.13	0.13	0.74	19.75
BAA17	505043	176904	46.5	31.1	5.3	1.6	17.0	22.6	20.74	0.14	0.13	0.72	19.76
BAA18	506046	176986	60.7	35.4	9.1	2.3	25.0	24.3	21.64	0.40	0.17	1.01	20.06
BAA19	506153	176991	60.3	35.5	9.7	2.3	23.7	24.5	21.68	0.44	0.17	0.96	20.12
BAA20	507307	177018	64.0	39.1	17.9	4.0	17.6	24.6	22.02	0.75	0.22	0.75	20.29
BAA21	507496	177400	65.9	38.4	12.4	2.3	27.0	24.1	22.39	0.41	0.14	1.28	20.55

Table 10.3 (cont) Predicted concentrations of NO_X, NO_2 and PM_{10} for 2010SM ($\mu g/m^3$)

Receptor name	X(m)	Y(m)	Total NO_X	Total NO_2	Aircraft NO_X	Other airport NO_X	Road NO_X	Background NO_X	Total PM_{10}	Aircraft PM_{10}	Other airport PM_{10}	Road PM_{10}	Background PM_{10}
BAA22	509431	176952	66.6	38.9	16.4	2.1	22.3	25.8	21.20	0.25	0.13	0.92	19.90
BAA23	509544	176967	64.0	37.9	14.4	2.7	21.2	25.6	21.14	0.23	0.15	0.87	19.89
BAA24	509582	177007	58.5	36.6	13.6	2.3	16.9	25.6	20.96	0.22	0.13	0.72	19.90
BAA25	509574	177054	56.6	36.1	13.5	2.0	15.4	25.7	20.90	0.22	0.12	0.66	19.90
BAA26	506791	178593	80.7	41.1	4.6	0.9	50.6	24.6	22.33	0.13	0.06	2.16	19.99
BAA27	506928	178615	76.0	40.2	4.8	0.9	45.6	24.8	22.16	0.13	0.06	1.95	20.02
BAA28	507004	178623	74.5	39.9	4.8	0.9	43.9	24.9	22.11	0.13	0.06	1.88	20.05
BAA29	507089	178626	75.7	40.3	5.0	0.9	44.9	25.0	22.17	0.13	0.06	1.91	20.07
BAA30	507176	178628	78.7	41.1	5.1	0.9	47.7	25.1	22.31	0.13	0.06	2.02	20.09
BAA31	507207	178632	80.0	41.4	5.1	0.9	48.9	25.1	22.37	0.13	0.06	2.08	20.10
BAA32	510172	178352	89.9	45.0	6.3	0.8	51.1	31.7	22.38	0.11	0.06	2.00	20.20
BAA33	510109	178351	88.3	44.4	6.4	0.8	49.1	32.0	22.32	0.11	0.06	1.94	20.21
BAA34	509999	178376	76.3	41.5	6.5	0.8	36.0	32.9	21.87	0.12	0.06	1.46	20.23
BAA35	510016	178407	71.4	40.3	6.4	0.8	31.0	33.2	21.69	0.12	0.06	1.27	20.25
BAA36	510157	178384	78.4	42.3	6.2	0.8	39.2	32.1	21.96	0.11	0.06	1.57	20.22
BAA37	510188	178445	69.1	40.0	6.1	0.8	29.7	32.6	21.62	0.11	0.06	1.21	20.25
BAA38	509820	178355	87.3	43.9	6.8	0.9	46.0	33.6	22.27	0.12	0.06	1.84	20.24
BAA39	509822	178396	74.5	41.1	6.7	0.9	32.9	34.1	21.79	0.12	0.06	1.35	20.26
BAA40	509392	178382	96.7	46.0	7.2	1.0	54.0	34.5	22.61	0.14	0.07	2.16	20.25
BAA41	509403	178468	71.8	40.5	6.9	0.9	28.4	35.6	21.67	0.13	0.06	1.18	20.29
BAA42	506456	178564	69.6	38.4	4.2	0.8	40.2	24.3	21.82	0.12	0.06	1.72	19.92
BAA43	507178	178659	68.3	38.6	5.0	0.9	37.3	25.1	21.89	0.13	0.06	1.60	20.10
BAA44	507066	178668	63.9	37.4	4.8	0.9	33.1	25.1	21.69	0.13	0.06	1.43	20.08
BAA45	508822	174587	54.4	32.2	12.9	2.5	17.4	21.7	20.88	0.25	0.16	0.72	19.75
BAA46	508849	174638	56.0	32.8	13.6	2.4	18.2	21.7	20.92	0.25	0.16	0.75	19.75
BAA47	508877	174691	58.6	33.5	14.4	2.4	19.9	21.8	20.99	0.26	0.16	0.81	19.76
BAA48	509007	174755	56.6	32.8	14.4	2.1	18.2	22.0	20.90	0.25	0.14	0.75	19.76
BAA49	505777	174594	49.2	29.9	11.9	1.8	14.3	21.2	20.64	0.18	0.13	0.60	19.72
BAA50	505744	174588	48.9	29.7	11.7	1.8	14.1	21.2	20.62	0.18	0.13	0.60	19.72
BAA51	505909	174592	50.9	30.3	12.0	2.0	15.6	21.3	20.70	0.20	0.14	0.64	19.71

Figure 10.10 2010SM predicted total NO_X concentrations in $\mu g/m^3$ around Heathrow.

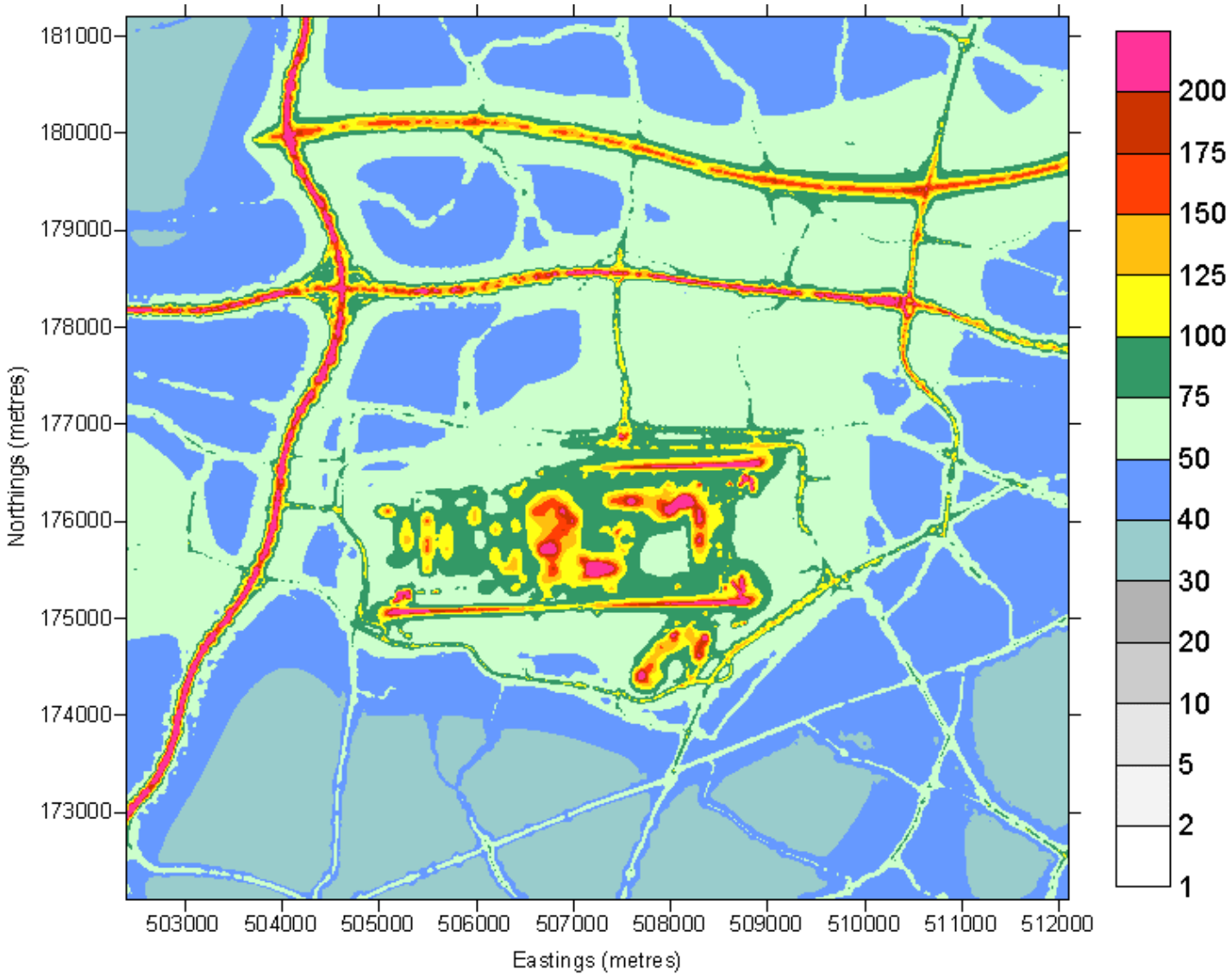

Figure 10.11 2010SM predicted total NO_2 concentrations in µg/m^3 around Heathrow.

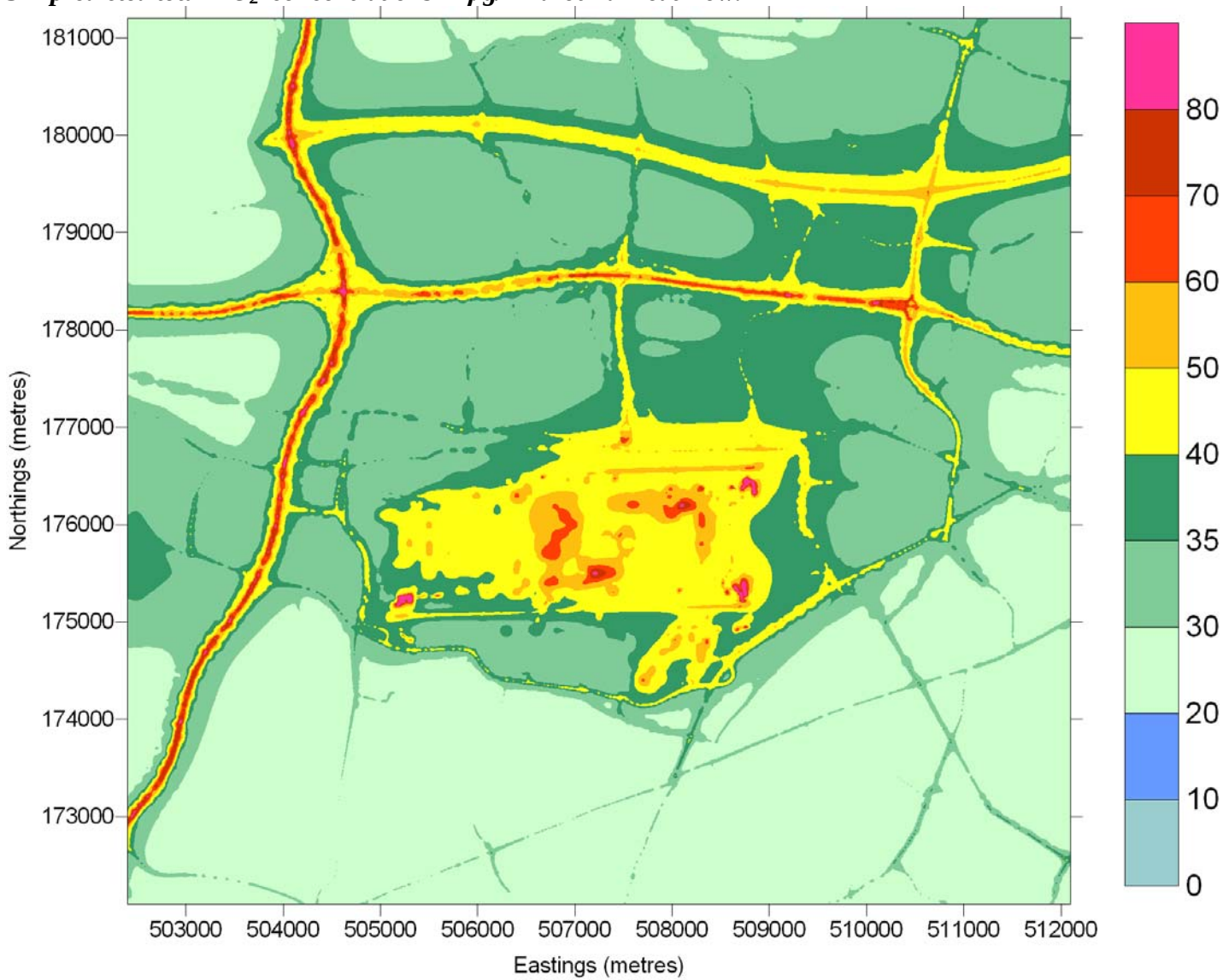

Figure 10.12 2010SM predicted NO_X concentration in $\mu g/m^3$ around Heathrow due to aircraft and other airport sources.

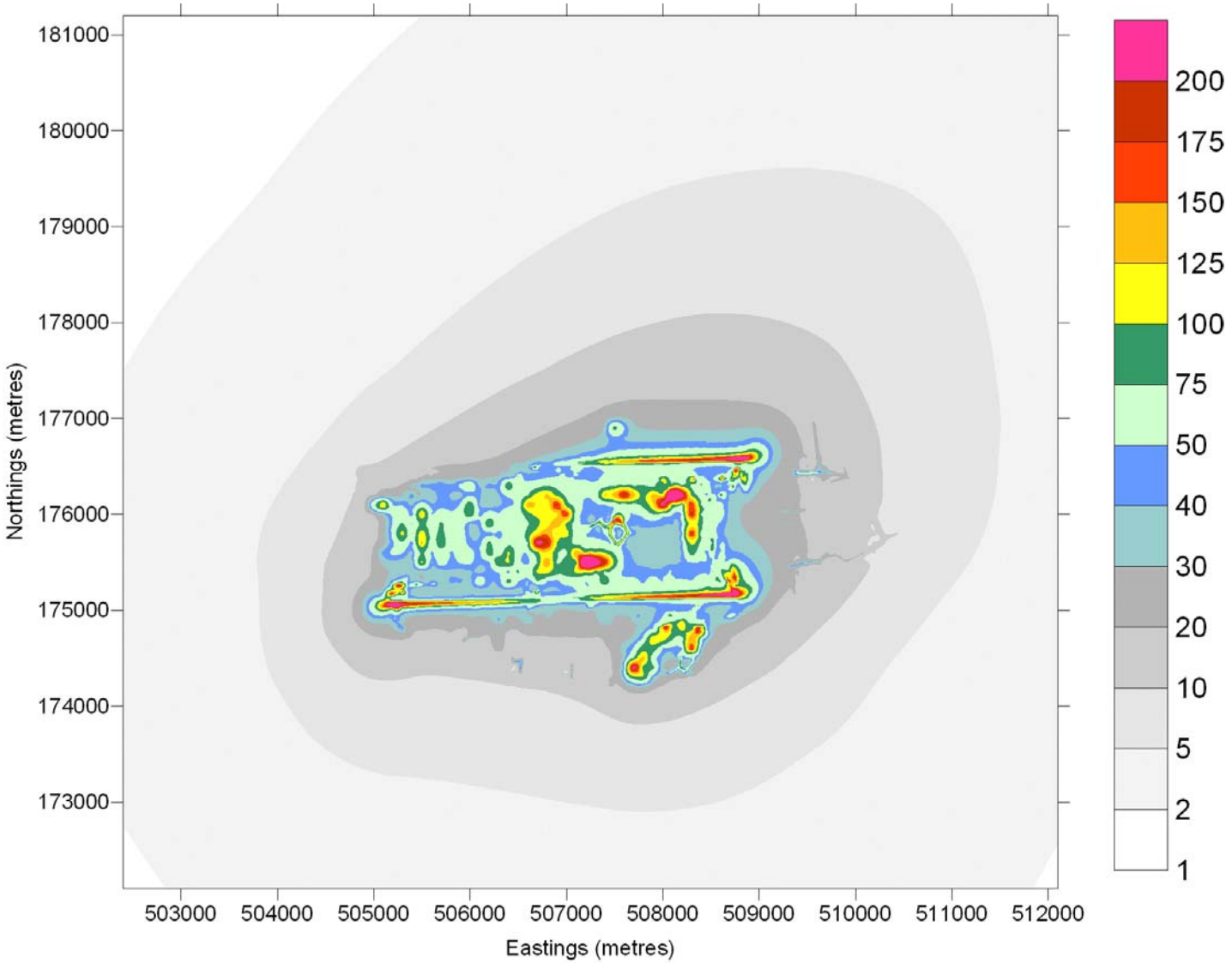

Figure 10.13 2010SM predicted NO_X concentration in $\mu g/m^3$ around Heathrow due to road sources.

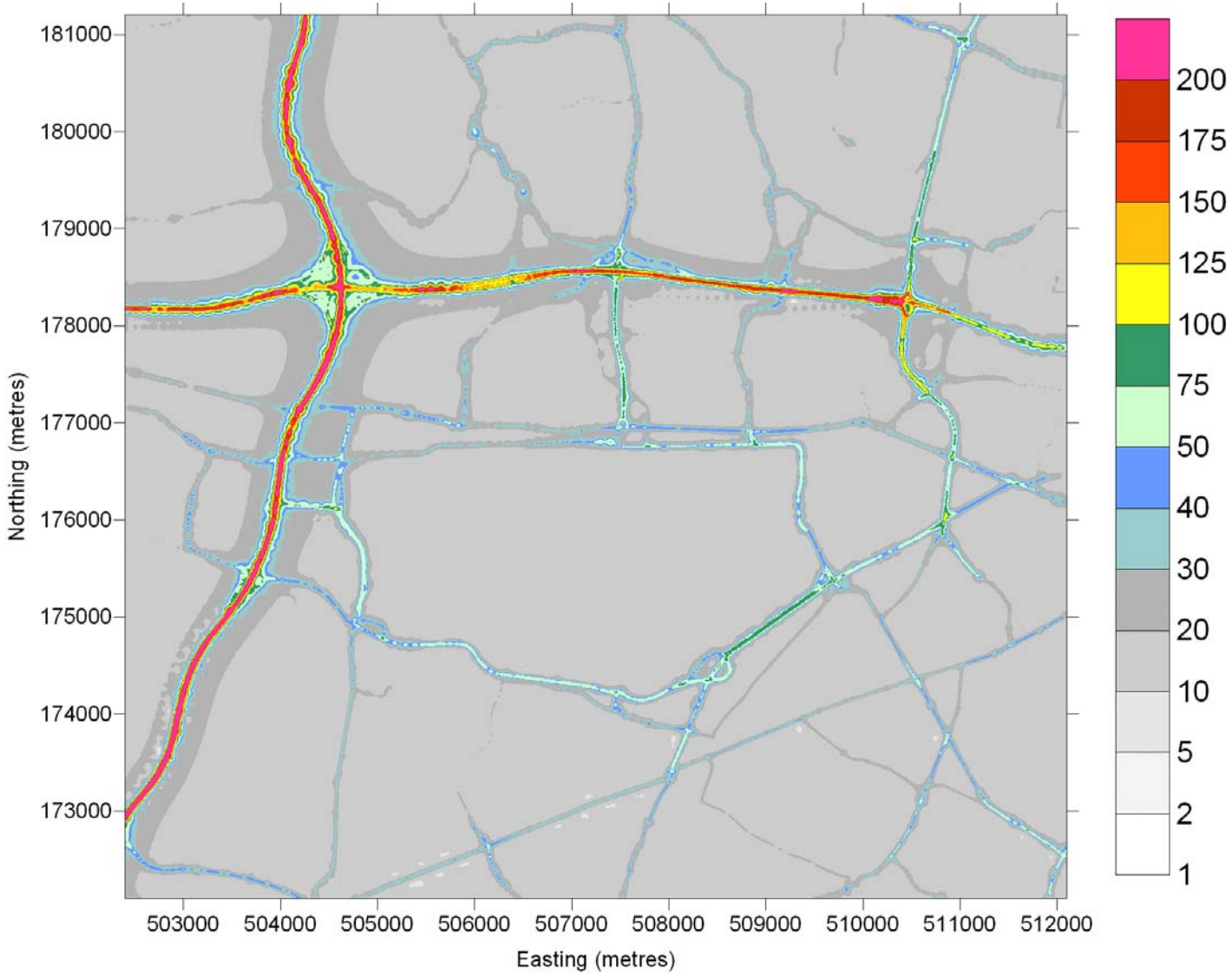

10.4 2015SM

Predicted concentrations of NO_x, NO_2 and PM_{10} for 2015SM at receptor locations are presented in Table 10.4.

Contour plots of predicted NO_x and NO_2 concentrations due to all sources are presented in Figure 10.14 and Figure 10.15 respectively. Contour plots of predicted NO_x concentrations due to aircraft and other airport sources and road sources are presented in Figure 10.16 and Figure 10.17 respectively

Table 10.4 Predicted concentrations of NO_X, NO_2 and PM_{10} for 2015SM ($\mu g/m^3$)

Receptor name	X(m)	Y(m)	Total NO_X	Total NO_2	Aircraft NO_X	Other airport NO_X	Road NO_X	Background NO_X	Total PM_{10}	Aircraft PM_{10}	Other airport PM_{10}	Road PM_{10}	Background PM_{10}
LHR2	508399	176744	82.7	42.6	38.1	2.6	18.3	23.8	21.61	1.37	0.20	0.75	19.29
LHR3	511679	180072	44.3	29.9	3.4	0.4	9.9	30.7	20.44	0.06	0.03	0.50	19.86
LHR4	509550	176997	54.5	34.6	15.0	1.8	13.8	23.9	20.22	0.22	0.11	0.64	19.25
LHR5	510370	177195	44.1	30.1	7.8	1.0	13.0	22.3	20.03	0.12	0.06	0.61	19.23
LHR6	515540	170420	32.4	22.2	0.9	0.1	9.1	22.3	19.71	0.02	0.01	0.46	19.22
LHR7	509333	175002	51.8	30.5	14.3	1.4	15.1	21.0	20.13	0.23	0.10	0.67	19.13
LHR8	505739	174497	41.8	26.9	10.9	1.3	10.1	19.5	19.81	0.17	0.11	0.48	19.05
LHR10	502741	173460	103.8	43.6	2.3	0.2	82.3	19.0	22.41	0.03	0.02	3.46	18.90
LHR11	504780	175510	49.5	30.1	11.1	2.1	15.3	21.0	20.47	0.15	0.22	0.67	19.44
LHR12	504466	175794	43.5	28.5	6.7	1.5	14.3	21.1	20.35	0.10	0.17	0.64	19.43
LHR13	504393	176591	48.7	30.8	4.4	0.8	22.9	20.6	20.18	0.09	0.08	0.96	19.06
LHR14	503535	176829	39.0	27.1	2.8	0.4	13.2	22.6	19.76	0.05	0.03	0.61	19.06
LHR15	505185	176922	40.8	28.2	5.7	1.3	13.1	20.8	19.96	0.15	0.11	0.60	19.10
LHR16	506945	178609	64.2	36.0	4.9	0.7	36.4	22.2	21.23	0.13	0.05	1.68	19.36
LHR17	506990	181919	36.0	25.2	1.9	0.2	10.6	23.2	19.91	0.04	0.02	0.53	19.32
LHR18	508279	177792	48.7	32.9	10.8	1.2	12.0	24.7	20.44	0.26	0.09	0.59	19.50
LHR19	508434	177376	53.0	34.9	15.1	1.5	10.8	25.5	20.46	0.37	0.11	0.52	19.45
LHR20	508058	177040	60.1	37.6	21.2	2.3	12.8	23.8	20.95	0.71	0.16	0.60	19.47
BA20	505127	177559	38.6	27.4	3.9	0.7	13.6	20.5	19.87	0.10	0.06	0.63	19.07
HD60	505736	177752	39.3	27.6	4.6	0.8	12.4	21.5	20.08	0.14	0.07	0.59	19.29
HD58	508414	177125	57.6	36.8	19.5	1.8	11.4	24.8	20.59	0.52	0.14	0.54	19.39
HD57	508758	177718	54.3	34.5	11.6	1.1	15.7	25.9	20.50	0.24	0.09	0.76	19.41
BA1	508582	178453	81.8	41.1	7.4	0.8	48.7	24.9	21.70	0.16	0.06	2.12	19.37
HD56	509798	178634	55.0	34.5	6.4	0.7	14.5	33.5	20.55	0.11	0.05	0.68	19.71
HS51	509127	174568	46.0	28.3	11.0	1.3	13.6	20.0	20.04	0.19	0.10	0.64	19.10
X1	505883	178463	58.4	33.9	3.7	0.6	32.9	21.2	20.84	0.10	0.05	1.52	19.18
X2	505932	177842	42.3	28.6	4.8	0.8	14.7	22.0	20.30	0.15	0.07	0.69	19.40
X3	505890	177393	46.7	29.8	6.0	1.1	17.4	22.2	20.54	0.21	0.09	0.79	19.44
X4	506146	177197	44.0	29.9	8.1	1.5	11.5	23.0	20.54	0.32	0.12	0.54	19.56
X5	506156	177092	45.5	30.5	9.0	1.6	12.0	22.9	20.58	0.38	0.14	0.56	19.51

Table 10.4 (cont) Predicted concentrations of NO_X, NO_2 and PM_{10} for 2015SM ($\mu g/m^3$)

Receptor name	X(m)	Y(m)	Total NO_X	Total NO_2	Aircraft NO_X	Other airport NO_X	Road NO_X	Background NO_X	Total PM_{10}	Aircraft PM_{10}	Other airport PM_{10}	Road PM_{10}	Background PM_{10}
X6	506154	176991	53.4	32.7	9.8	1.8	19.0	22.7	20.90	0.46	0.15	0.83	19.45
X7	508228	177545	50.0	33.7	12.8	1.4	10.8	25.0	20.55	0.33	0.10	0.53	19.58
X8	508212	177390	51.8	34.5	14.7	1.6	10.8	24.7	20.60	0.40	0.12	0.53	19.55
X9	507873	177139	56.8	36.5	18.5	2.5	12.4	23.4	20.96	0.63	0.16	0.60	19.58
X10	508429	177012	62.1	38.2	22.5	2.0	13.1	24.5	20.74	0.62	0.16	0.61	19.35
X11	508549	176736	83.8	42.6	40.7	2.4	16.8	24.0	21.19	1.03	0.19	0.70	19.27
X12	508789	177365	57.9	36.1	15.4	1.4	15.8	25.3	20.54	0.32	0.11	0.75	19.37
X13	508735	177965	53.0	33.9	9.9	1.0	16.1	26.0	20.45	0.21	0.08	0.76	19.41
BAA1	508009	177028	60.8	37.8	21.5	2.4	13.3	23.6	21.01	0.74	0.17	0.62	19.48
BAA2	507914	177030	61.0	37.9	21.3	2.6	13.6	23.4	21.08	0.76	0.18	0.64	19.51
BAA3	508802	177048	65.6	38.9	22.2	1.7	17.2	24.6	20.64	0.42	0.13	0.77	19.31
BAA4	508762	177049	62.2	38.1	22.1	1.7	13.8	24.6	20.52	0.43	0.13	0.64	19.32
BAA5	508885	177042	63.1	38.2	22.6	1.7	14.4	24.5	20.48	0.39	0.13	0.66	19.31
BAA6	508902	177045	62.5	38.1	22.5	1.6	13.9	24.5	20.45	0.38	0.13	0.64	19.31
BAA7	508552	177102	58.6	37.1	20.2	1.8	11.7	24.9	20.53	0.49	0.14	0.56	19.35
BAA8	508598	177100	58.8	37.1	20.4	1.8	11.8	24.9	20.51	0.47	0.14	0.56	19.34
BAA9	508412	177117	57.8	36.8	19.7	1.9	11.5	24.8	20.60	0.52	0.14	0.55	19.39
BAA10	508380	177164	56.5	36.4	18.7	1.8	11.2	24.8	20.58	0.50	0.14	0.54	19.41
BAA11	508373	177231	55.0	35.8	17.4	1.7	10.9	24.9	20.55	0.46	0.13	0.53	19.43
BAA12	508366	177292	53.9	35.3	16.3	1.6	10.8	25.1	20.53	0.42	0.12	0.52	19.45
BAA13	508356	177373	52.7	34.8	15.1	1.6	10.8	25.2	20.51	0.39	0.12	0.52	19.48
BAA14	504799	176658	45.9	29.9	5.4	1.2	18.7	20.6	20.09	0.12	0.11	0.79	19.08
BAA15	504842	176702	43.4	29.2	5.4	1.2	16.3	20.6	20.01	0.12	0.11	0.71	19.08
BAA16	504966	176844	41.0	28.3	5.2	1.2	14.0	20.7	19.94	0.13	0.10	0.63	19.08
BAA17	505043	176904	40.7	28.2	5.3	1.2	13.5	20.7	19.94	0.13	0.10	0.62	19.09
BAA18	506046	176986	53.5	32.5	9.2	1.8	20.1	22.5	20.84	0.42	0.15	0.88	19.40
BAA19	506153	176991	53.4	32.7	9.8	1.8	19.0	22.7	20.90	0.46	0.15	0.83	19.45
BAA20	507307	177018	58.2	36.6	18.6	3.0	13.8	22.8	21.26	0.80	0.19	0.65	19.63
BAA21	507496	177400	58.2	35.6	12.7	1.8	21.4	22.2	21.57	0.43	0.12	1.12	19.90
BAA22	509431	176952	61.1	36.5	17.5	1.6	18.0	24.0	20.42	0.25	0.11	0.80	19.25

Table 10.4 (cont) Predicted concentrations of NO_X, NO_2 and PM_{10} for 2015SM ($\mu g/m^3$)

Receptor name	X(m)	Y(m)	Total NO_X	Total NO_2	Aircraft NO_X	Other airport NO_X	Road NO_X	Background NO_X	Total PM_{10}	Aircraft PM_{10}	Other airport PM_{10}	Road PM_{10}	Background PM_{10}
BAA23	509544	176967	58.3	35.5	15.3	2.0	17.1	23.9	20.36	0.23	0.12	0.77	19.25
BAA24	509582	177007	53.5	34.3	14.5	1.7	13.5	23.8	20.20	0.22	0.11	0.62	19.25
BAA25	509574	177054	51.9	33.9	14.3	1.5	12.1	23.9	20.14	0.21	0.10	0.57	19.25
BAA26	506791	178593	66.5	36.5	4.7	0.7	39.0	22.1	21.31	0.13	0.05	1.80	19.33
BAA27	506928	178615	63.0	35.7	4.8	0.7	35.2	22.3	21.17	0.13	0.05	1.63	19.36
BAA28	507004	178623	61.9	35.5	4.9	0.7	33.9	22.3	21.14	0.13	0.05	1.57	19.39
BAA29	507089	178626	62.9	35.9	5.1	0.7	34.8	22.4	21.20	0.13	0.06	1.60	19.41
BAA30	507176	178628	65.4	36.7	5.2	0.7	37.1	22.5	21.32	0.14	0.06	1.70	19.43
BAA31	507207	178632	66.5	36.9	5.2	0.7	38.1	22.5	21.38	0.14	0.06	1.75	19.44
BAA32	510172	178352	75.3	40.4	6.6	0.7	38.7	29.3	21.31	0.11	0.05	1.58	19.57
BAA33	510109	178351	74.2	40.0	6.7	0.7	37.2	29.7	21.27	0.11	0.05	1.54	19.57
BAA34	509999	178376	65.5	37.7	6.8	0.7	27.4	30.6	20.96	0.12	0.05	1.19	19.60
BAA35	510016	178407	61.8	36.7	6.7	0.7	23.6	30.8	20.81	0.11	0.05	1.03	19.61
BAA36	510157	178384	66.7	38.2	6.6	0.7	29.8	29.7	21.00	0.11	0.05	1.25	19.59
BAA37	510188	178445	59.8	36.3	6.4	0.6	22.6	30.1	20.75	0.11	0.05	0.98	19.61
BAA38	509820	178355	74.2	39.8	7.1	0.7	35.0	31.4	21.29	0.12	0.06	1.50	19.61
BAA39	509822	178396	64.6	37.4	7.0	0.7	25.1	31.8	20.91	0.12	0.05	1.10	19.63
BAA40	509392	178382	81.7	41.6	7.5	0.8	41.1	32.4	21.58	0.14	0.06	1.76	19.61
BAA41	509403	178468	63.0	37.1	7.2	0.7	21.8	33.4	20.83	0.13	0.06	0.98	19.66
BAA42	506456	178564	58.0	34.1	4.3	0.6	31.1	21.9	20.87	0.12	0.05	1.44	19.26
BAA43	507178	178659	57.3	34.5	5.1	0.7	29.0	22.5	20.97	0.13	0.05	1.34	19.44
BAA44	507066	178668	53.7	33.3	4.9	0.7	25.7	22.4	20.80	0.13	0.05	1.20	19.42
BAA45	508822	174587	48.9	29.7	13.4	1.9	13.5	20.0	20.10	0.25	0.14	0.61	19.10
BAA46	508849	174638	50.5	30.3	14.3	1.9	14.2	20.1	20.14	0.26	0.14	0.64	19.10
BAA47	508877	174691	52.7	31.0	15.2	1.9	15.5	20.2	20.19	0.27	0.14	0.68	19.10
BAA48	509007	174755	51.4	30.5	15.3	1.6	14.2	20.3	20.12	0.25	0.12	0.64	19.11
BAA49	505777	174594	44.7	27.7	12.4	1.5	11.2	19.6	19.87	0.18	0.12	0.51	19.05
BAA50	505744	174588	44.4	27.6	12.3	1.4	11.0	19.6	19.86	0.18	0.12	0.51	19.05
BAA51	505909	174592	45.9	28.1	12.5	1.6	12.1	19.7	19.92	0.20	0.13	0.54	19.05

Figure 10.14 2015SM predicted total NO_X concentrations in $\mu g/m^3$ around Heathrow.

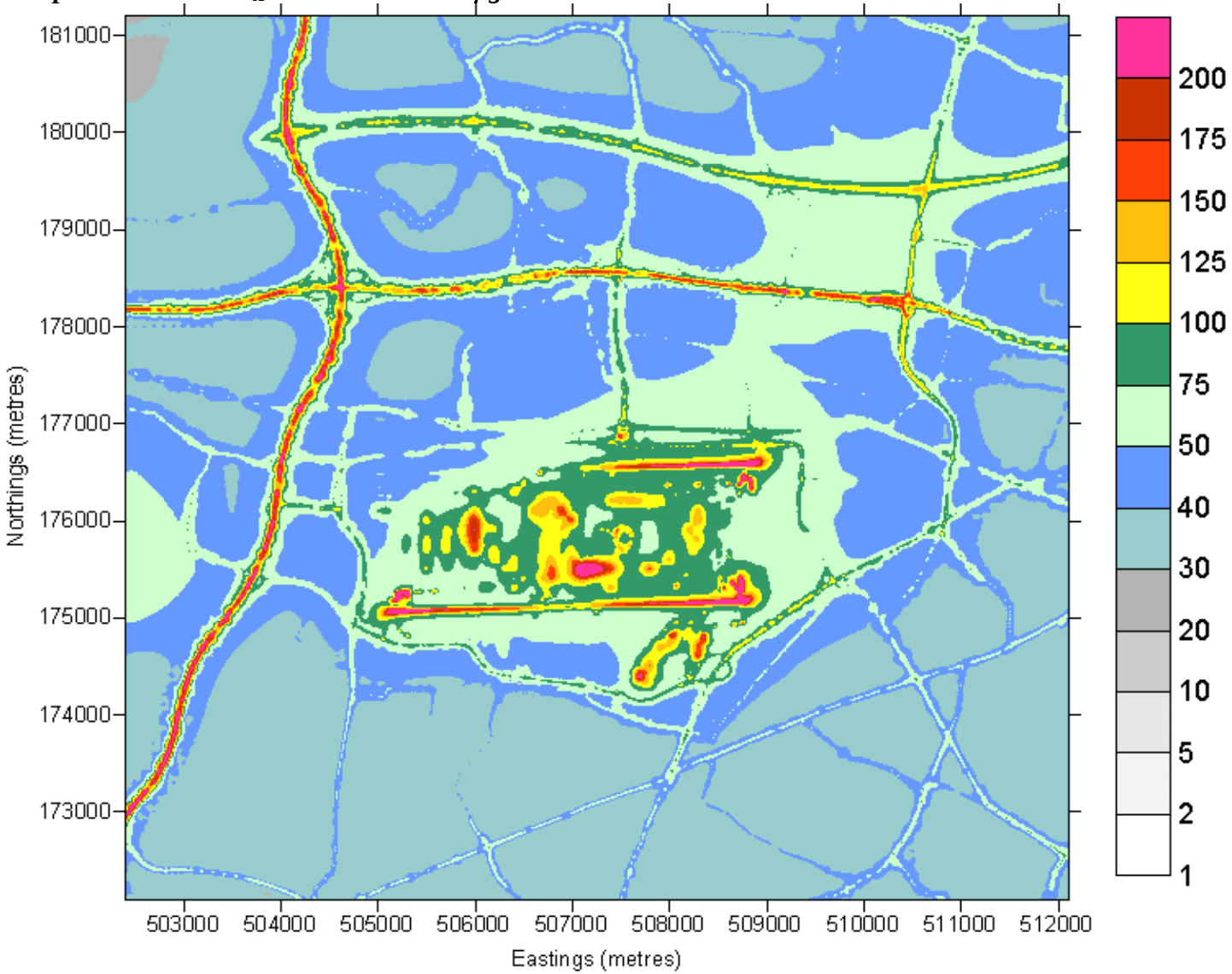

Figure 10.15 2015SM predicted total NO_2 concentrations in $\mu g/m^3$ around Heathrow.

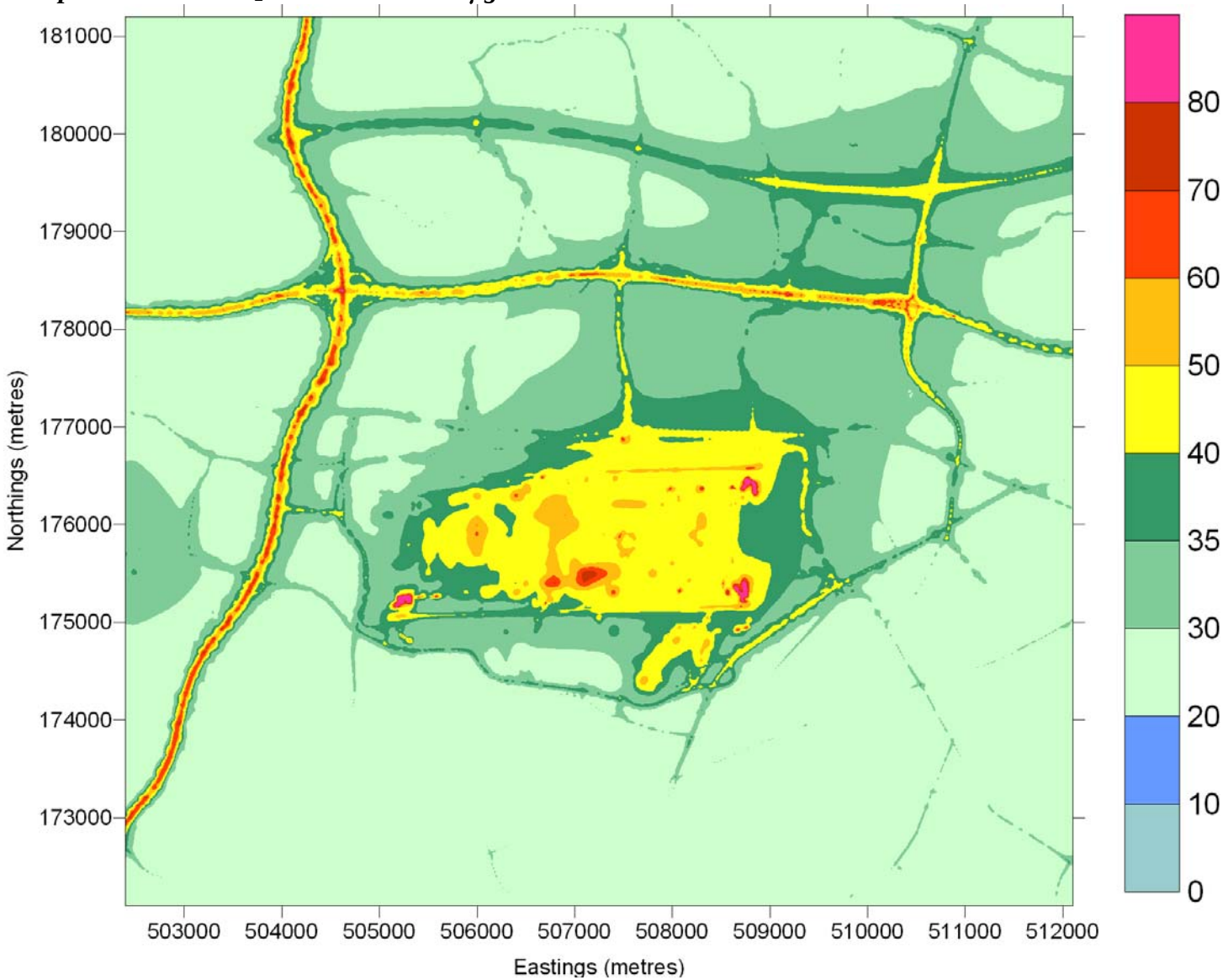

Figure 10.16 2015SM, predicted NO_X concentration in $\mu g/m^3$ around Heathrow due to aircraft and other airport sources.

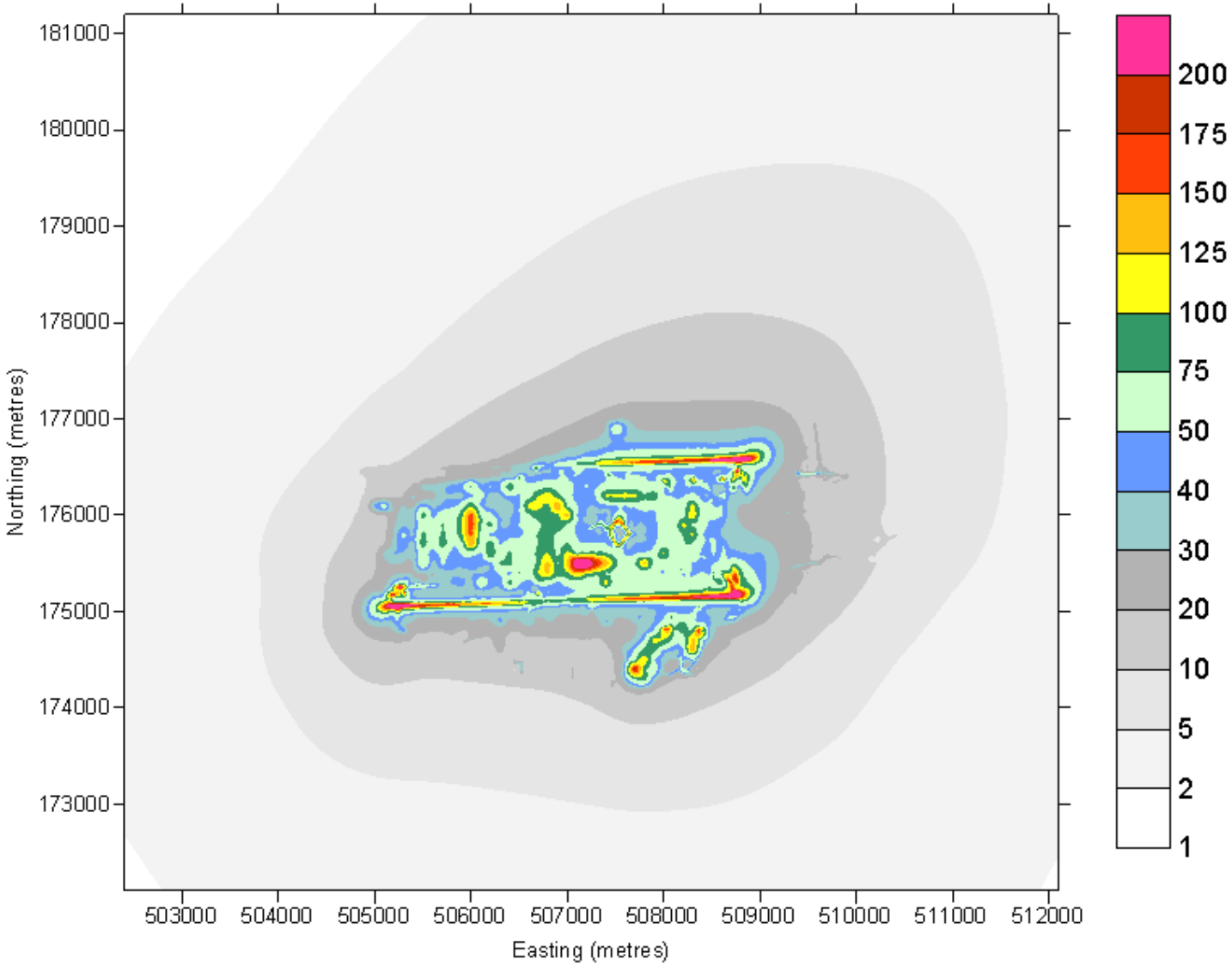

Figure 10.17 2015SM predicted NO_X concentration in $\mu g/m^3$ around Heathrow due to road sources.

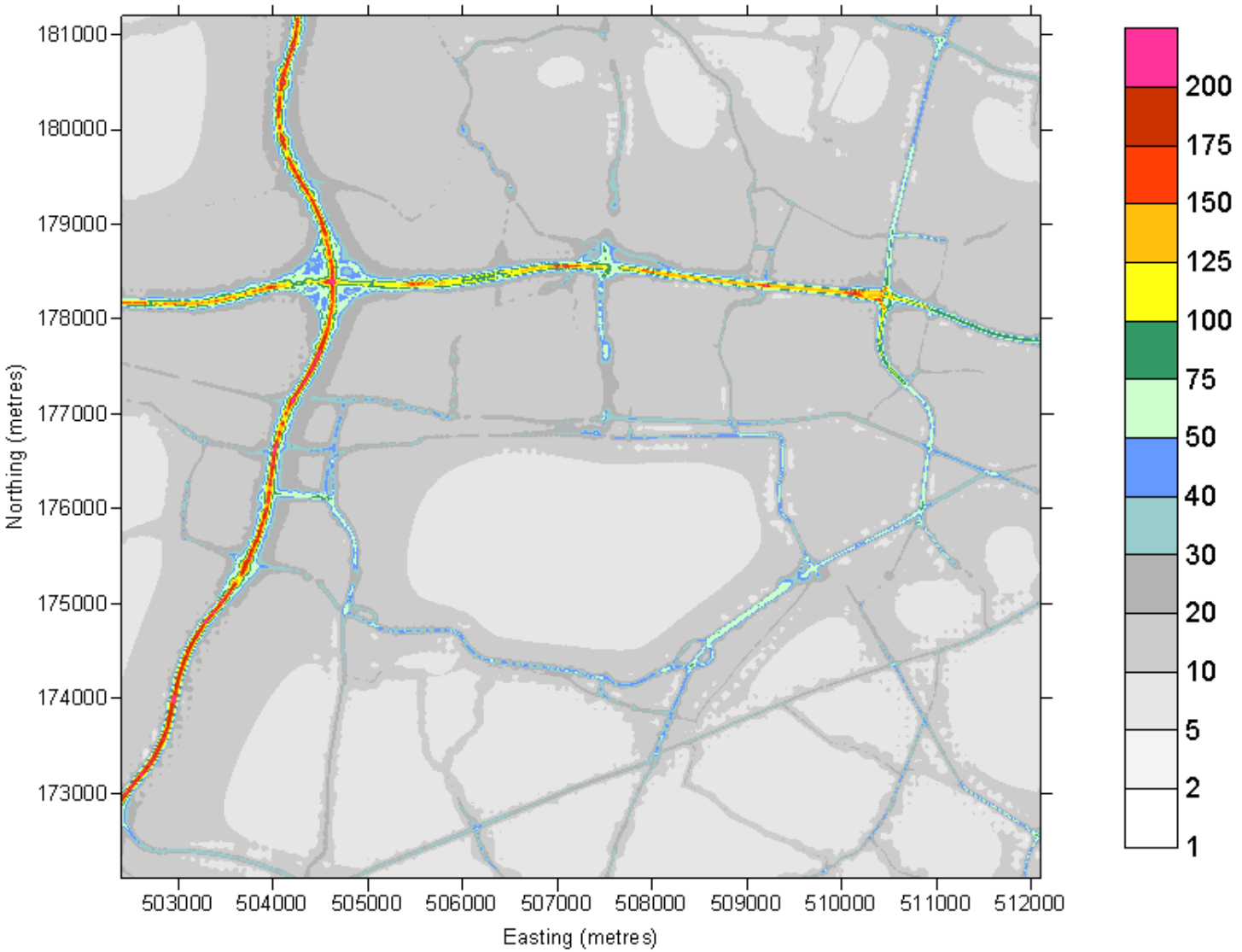

10.5 2015EP

Predicted concentrations of NO_x, NO_2 and PM_{10} for 2015EP at receptor locations are presented in Table 10.5.

Contour plots of predicted NO_x and NO_2 concentrations due to all sources are presented in Figure 10.18 and Figure 10.19 respectively. Contour plot of predicted NO_x concentrations due to aircraft and other airport sources is presented in Figure 10.20.

Table 10.5 Predicted concentrations of NO_X, NO_2 and PM_{10} for 2015EP ($\mu g/m^3$)

Receptor name	X(m)	Y(m)	Total NO_X	Total NO_2	Aircraft NO_X	Other airport NO_X	Road NO_X	Background NO_X	Total PM_{10}	Aircraft PM_{10}	Other airport PM_{10}	Road PM_{10}	Background PM_{10}
LHR2	508399	176744	75.8	40.6	31.1	2.6	18.3	23.8	21.4	1.16	0.20	0.75	19.3
LHR3	511679	180072	44.1	29.8	3.2	0.4	9.9	30.7	20.4	0.05	0.03	0.50	19.9
LHR4	509550	176997	53.9	34.4	14.4	1.8	13.8	23.9	20.2	0.21	0.11	0.64	19.2
LHR5	510370	177195	43.9	30.0	7.6	1.0	13.0	22.3	20.0	0.12	0.06	0.61	19.2
LHR6	515540	170420	32.3	22.2	0.8	0.1	9.1	22.3	19.7	0.02	0.01	0.46	19.2
LHR7	509333	175002	51.1	30.3	13.6	1.4	15.1	21.0	20.1	0.21	0.10	0.67	19.1
LHR8	505739	174497	44.4	27.7	13.4	1.3	10.1	19.5	19.8	0.18	0.11	0.48	19.0
LHR10	502741	173460	103.9	43.6	2.4	0.2	82.3	19.0	22.4	0.04	0.02	3.46	18.9
LHR11	504780	175510	53.1	31.4	14.7	2.1	15.3	21.0	20.5	0.17	0.22	0.67	19.4
LHR12	504466	175794	45.1	29.2	8.2	1.5	14.3	21.1	20.4	0.12	0.17	0.64	19.4
LHR13	504393	176591	50.1	31.6	5.8	0.8	22.9	20.6	20.2	0.10	0.08	0.96	19.1
LHR14	503535	176829	39.6	27.4	3.4	0.4	13.2	22.6	19.8	0.06	0.03	0.61	19.1
LHR15	505185	176922	43.3	29.5	8.1	1.3	13.1	20.8	20.0	0.18	0.11	0.60	19.1
LHR16	506945	178609	63.8	35.8	4.5	0.7	36.4	22.2	21.2	0.14	0.05	1.68	19.4
LHR17	506990	181919	35.8	25.1	1.8	0.2	10.6	23.2	19.9	0.04	0.02	0.53	19.3
LHR18	508279	177792	46.6	31.8	8.7	1.2	12.0	24.7	20.4	0.25	0.09	0.59	19.5
LHR19	508434	177376	50.0	33.5	12.2	1.5	10.8	25.5	20.4	0.34	0.11	0.52	19.4
LHR20	508058	177040	56.5	36.3	17.7	2.3	12.8	23.8	20.9	0.66	0.16	0.60	19.5
BA20	505127	177559	40.2	28.4	5.4	0.7	13.6	20.5	19.9	0.12	0.06	0.63	19.1
HD60	505736	177752	40.4	28.2	5.7	0.8	12.4	21.5	20.1	0.16	0.07	0.59	19.3
HD58	508414	177125	53.8	35.2	15.8	1.8	11.4	24.8	20.5	0.46	0.14	0.54	19.4
HD57	508758	177718	52.2	33.5	9.6	1.1	15.7	25.9	20.5	0.23	0.09	0.76	19.4
BA1	508582	178453	80.5	40.5	6.1	0.8	48.7	24.9	21.7	0.15	0.06	2.12	19.4
HD56	509798	178634	54.5	34.3	5.9	0.7	14.5	33.5	20.5	0.11	0.05	0.68	19.7
HS51	509127	174568	44.7	27.8	9.6	1.3	13.6	20.0	20.0	0.17	0.10	0.64	19.1
X1	505883	178463	58.9	34.2	4.2	0.6	32.9	21.2	20.8	0.11	0.05	1.52	19.2
X2	505932	177842	43.2	29.1	5.7	0.8	14.7	22.0	20.3	0.17	0.07	0.69	19.4
X3	505890	177393	48.0	30.5	7.3	1.1	17.4	22.2	20.6	0.25	0.09	0.79	19.4
X4	506146	177197	45.2	30.4	9.3	1.5	11.5	23.0	20.6	0.39	0.12	0.54	19.6

Table 10.5 (cont) Predicted concentrations of NO_X, NO_2 and PM_{10} for 2015EP ($\mu g/m^3$)

Receptor name	X(m)	Y(m)	Total NO_X	Total NO_2	Aircraft NO_X	Other airport NO_X	Road NO_X	Background NO_X	Total PM_{10}	Aircraft PM_{10}	Other airport PM_{10}	Road PM_{10}	Background PM_{10}
X5	506156	177092	46.7	31.1	10.2	1.6	12.0	22.9	20.7	0.47	0.14	0.56	19.5
X6	506154	176991	54.8	33.4	11.2	1.8	19.0	22.7	21.0	0.58	0.15	0.83	19.5
X7	508228	177545	47.6	32.5	10.4	1.4	10.8	24.9	20.5	0.32	0.10	0.53	19.6
X8	508212	177390	49.1	33.2	12.0	1.6	10.8	24.7	20.6	0.38	0.12	0.53	19.6
X9	507873	177139	53.8	35.3	15.5	2.5	12.4	23.4	20.9	0.60	0.16	0.60	19.6
X10	508429	177012	57.8	36.5	18.2	2.0	13.1	24.5	20.7	0.54	0.15	0.61	19.4
X11	508549	176736	76.1	40.3	32.9	2.4	16.8	24.0	21.0	0.87	0.19	0.70	19.3
X12	508789	177365	55.1	34.8	12.6	1.4	15.8	25.3	20.5	0.29	0.11	0.75	19.4
X13	508735	177965	51.3	33.0	8.2	1.0	16.1	26.0	20.4	0.20	0.08	0.76	19.4
BAA1	508009	177028	57.3	36.5	18.0	2.4	13.3	23.6	21.0	0.69	0.17	0.62	19.5
BAA2	507914	177030	57.6	36.7	17.9	2.6	13.6	23.4	21.0	0.71	0.18	0.64	19.5
BAA3	508802	177048	61.5	37.3	18.1	1.7	17.2	24.5	20.6	0.37	0.13	0.77	19.3
BAA4	508762	177049	58.0	36.4	17.9	1.7	13.8	24.6	20.5	0.38	0.13	0.64	19.3
BAA5	508885	177042	59.3	36.8	18.8	1.7	14.4	24.5	20.4	0.34	0.13	0.66	19.3
BAA6	508902	177045	58.8	36.6	18.8	1.6	13.9	24.5	20.4	0.34	0.13	0.64	19.3
BAA7	508552	177102	54.7	35.4	16.3	1.8	11.7	24.9	20.5	0.43	0.14	0.56	19.3
BAA8	508598	177100	54.8	35.4	16.4	1.8	11.8	24.9	20.5	0.42	0.14	0.56	19.3
BAA9	508412	177117	54.0	35.2	15.9	1.9	11.5	24.8	20.5	0.47	0.14	0.55	19.4
BAA10	508380	177164	52.9	34.8	15.1	1.8	11.2	24.8	20.5	0.45	0.14	0.54	19.4
BAA11	508373	177231	51.7	34.3	14.1	1.7	10.9	24.9	20.5	0.42	0.13	0.53	19.4
BAA12	508366	177292	50.8	33.9	13.2	1.6	10.8	25.1	20.5	0.39	0.12	0.52	19.5
BAA13	508356	177373	49.8	33.4	12.2	1.6	10.8	25.2	20.5	0.36	0.12	0.52	19.5
BAA14	504799	176658	48.3	31.1	7.8	1.1	18.7	20.6	20.1	0.14	0.11	0.79	19.1
BAA15	504842	176702	45.8	30.4	7.8	1.2	16.3	20.6	20.0	0.14	0.11	0.71	19.1
BAA16	504966	176844	43.5	29.7	7.7	1.2	14.0	20.7	20.0	0.15	0.10	0.63	19.1
BAA17	505043	176904	43.1	29.5	7.7	1.2	13.5	20.7	20.0	0.16	0.10	0.62	19.1
BAA18	506046	176986	55.1	33.3	10.8	1.8	20.1	22.5	20.9	0.53	0.15	0.88	19.4
BAA19	506153	176991	54.8	33.4	11.2	1.8	19.0	22.7	21.0	0.58	0.15	0.83	19.5
BAA20	507307	177018	56.0	35.9	16.4	3.0	13.8	22.8	21.3	0.84	0.19	0.65	19.6
BAA21	507496	177400	56.4	34.9	11.0	1.8	21.4	22.2	21.6	0.44	0.12	1.12	19.9

Table 10.5 (cont) Predicted concentrations of NO_X, NO_2 and PM_{10} for 2015EP ($\mu g/m^3$)

Receptor name	X(m)	Y(m)	Total NO_X	Total NO_2	Aircraft NO_X	Other airport NO_X	Road NO_X	Background NO_X	Total PM_{10}	Aircraft PM_{10}	Other airport PM_{10}	Road PM_{10}	Background PM_{10}
BAA22	509431	176952	60.3	36.3	16.7	1.6	18.0	24.0	20.4	0.23	0.11	0.80	19.3
BAA23	509544	176967	57.7	35.3	14.7	2.0	17.1	23.9	20.3	0.21	0.12	0.77	19.2
BAA24	509582	177007	52.9	34.1	13.9	1.7	13.5	23.8	20.2	0.20	0.11	0.62	19.2
BAA25	509574	177054	51.3	33.7	13.7	1.5	12.1	23.9	20.1	0.20	0.10	0.57	19.3
BAA26	506791	178593	66.3	36.3	4.4	0.7	39.0	22.1	21.3	0.14	0.05	1.80	19.3
BAA27	506928	178615	62.6	35.5	4.5	0.7	35.2	22.3	21.2	0.14	0.05	1.63	19.4
BAA28	507004	178623	61.4	35.3	4.5	0.7	33.9	22.3	21.1	0.14	0.05	1.57	19.4
BAA29	507089	178626	62.4	35.6	4.5	0.7	34.8	22.4	21.2	0.14	0.06	1.60	19.4
BAA30	507176	178628	64.8	36.3	4.6	0.7	37.1	22.5	21.3	0.14	0.06	1.70	19.4
BAA31	507207	178632	65.9	36.6	4.6	0.7	38.1	22.5	21.4	0.14	0.06	1.75	19.4
BAA32	510172	178352	74.9	40.3	6.2	0.7	38.7	29.3	21.3	0.11	0.05	1.58	19.6
BAA33	510109	178351	73.8	39.9	6.3	0.7	37.2	29.7	21.3	0.11	0.05	1.54	19.6
BAA34	509999	178376	65.1	37.5	6.4	0.7	27.4	30.6	21.0	0.11	0.05	1.19	19.6
BAA35	510016	178407	61.3	36.6	6.3	0.7	23.6	30.8	20.8	0.11	0.05	1.03	19.6
BAA36	510157	178384	66.3	38.1	6.1	0.7	29.8	29.7	21.0	0.11	0.05	1.25	19.6
BAA37	510188	178445	59.4	36.2	6.0	0.6	22.6	30.1	20.7	0.10	0.05	0.98	19.6
BAA38	509820	178355	73.7	39.6	6.6	0.7	35.0	31.4	21.3	0.12	0.06	1.50	19.6
BAA39	509822	178396	64.1	37.2	6.5	0.7	25.1	31.8	20.9	0.12	0.05	1.10	19.6
BAA40	509392	178382	80.9	41.3	6.7	0.8	41.1	32.4	21.6	0.13	0.06	1.76	19.6
BAA41	509403	178468	62.3	36.8	6.5	0.7	21.8	33.3	20.8	0.13	0.06	0.98	19.7
BAA42	506456	178564	58.0	34.1	4.3	0.6	31.1	21.9	20.9	0.13	0.05	1.44	19.3
BAA43	507178	178659	56.7	34.2	4.5	0.7	29.0	22.5	21.0	0.14	0.05	1.34	19.4
BAA44	507066	178668	53.2	33.1	4.4	0.7	25.7	22.4	20.8	0.13	0.05	1.20	19.4
BAA45	508822	174587	46.7	29.0	11.2	1.9	13.5	20.0	20.1	0.22	0.14	0.61	19.1
BAA46	508849	174638	48.1	29.5	12.0	1.9	14.2	20.1	20.1	0.23	0.14	0.64	19.1
BAA47	508877	174691	50.3	30.2	12.8	1.9	15.5	20.2	20.2	0.24	0.14	0.68	19.1
BAA48	509007	174755	49.4	29.8	13.3	1.6	14.2	20.3	20.1	0.22	0.12	0.64	19.1
BAA49	505777	174594	47.4	28.6	15.2	1.5	11.2	19.6	19.9	0.20	0.12	0.51	19.1
BAA50	505744	174588	47.2	28.5	15.1	1.4	11.0	19.6	19.9	0.19	0.12	0.51	19.1
BAA51	505909	174592	48.4	28.9	15.0	1.6	12.1	19.7	19.9	0.21	0.13	0.54	19.1

Figure 10.18 2015EP predicted total NO_X concentrations in $\mu g/m^3$ around Heathrow.

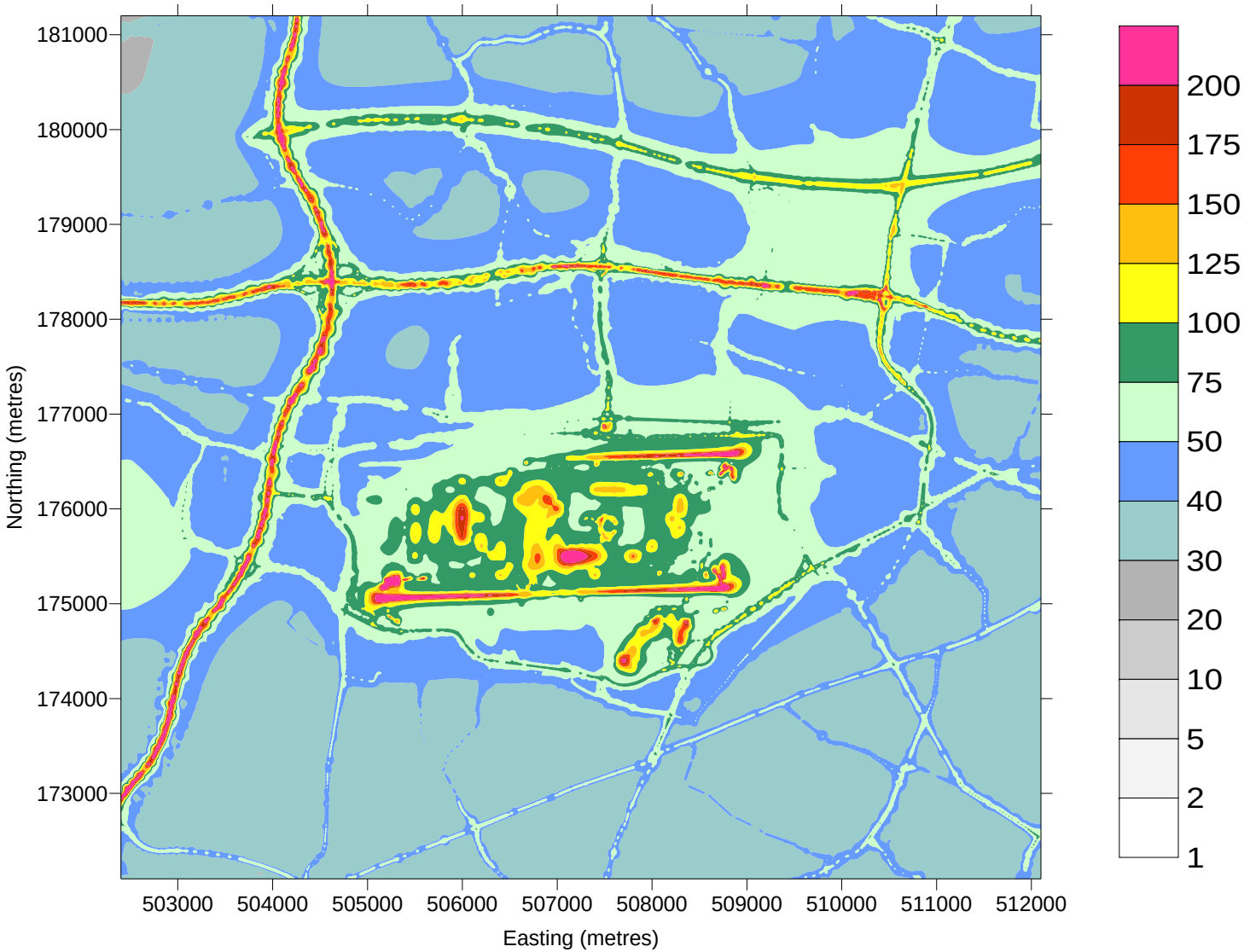

Figure 10.19 2015EP predicted total NO_2 concentrations in $\mu g/m^3$ around Heathrow.

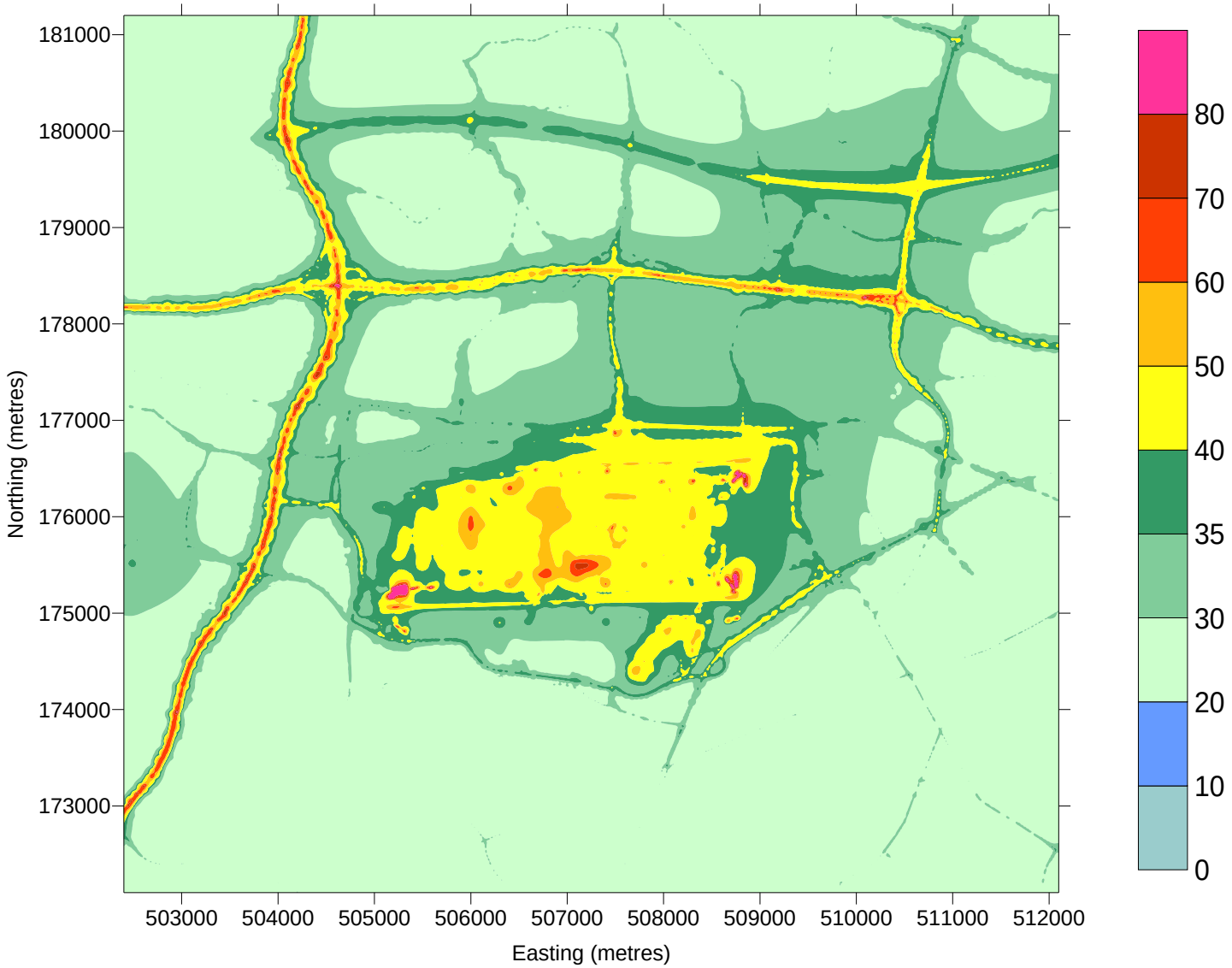

Figure 10.20 2015EP, predicted NO_X concentration in $\mu g/m^3$ around Heathrow due to aircraft and other airport sources.

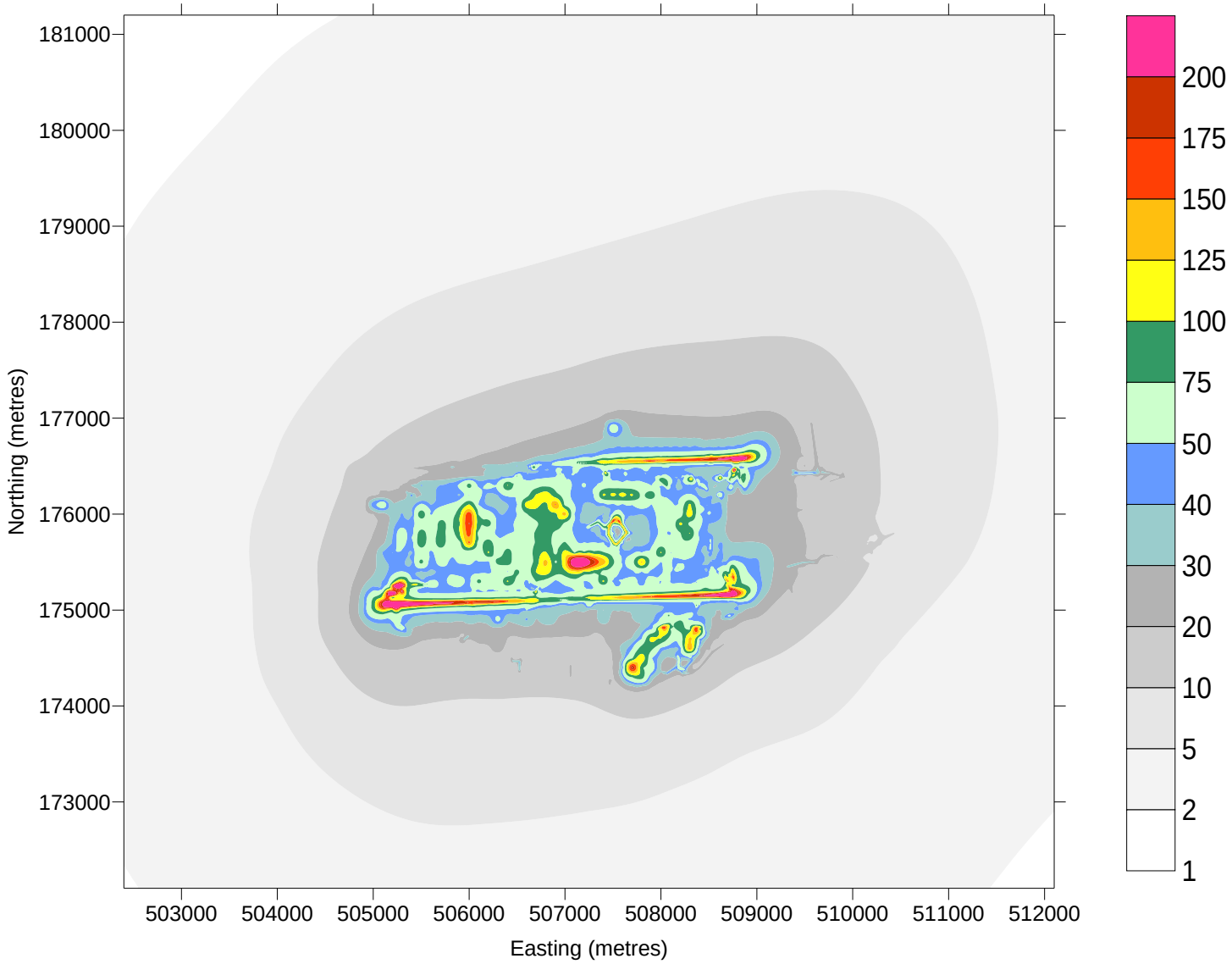

10.6 2015NoC

Estimated concentrations of NO_x and NO_2 for 2015NoC at receptor locations are presented in Table 10.6

Table 10.6 Estimated concentrations of NO_X, NO_2 and PM_{10} for 2015NoC ($\mu g/m^3$)

Receptor name	X(m)	Y(m)	Total NO_X	Total NO_2	Aircraft NO_X	Other airport NO_X	2015NoC/2015SM NO_2
LHR2	508399	176744	87.0	44.6	42.0	2.9	105%
LHR3	511679	180072	44.4	30.0	3.5	0.4	100%
LHR4	509550	176997	56.2	35.6	16.3	2.1	103%
LHR5	510370	177195	44.7	30.6	8.4	1.1	102%
LHR6	515540	170420	32.4	22.2	0.9	0.1	100%
LHR7	509333	175002	53.7	31.6	15.9	1.7	103%
LHR8	505739	174497	39.4	25.7	8.4	1.4	96%
LHR10	502741	173460	103.7	43.5	2.2	0.2	100%
LHR11	504780	175510	48.1	29.8	10.4	1.4	99%
LHR12	504466	175794	44.3	29.1	8.1	0.8	102%
LHR13	504393	176591	51.8	32.1	7.7	0.6	104%
LHR14	503535	176829	39.4	27.4	3.3	0.3	101%
LHR15	505185	176922	43.2	29.5	8.2	1.2	105%
LHR16	506945	178609	64.2	36.1	4.9	0.6	100%
LHR17	506990	181919	36.0	25.2	1.9	0.2	100%
LHR18	508279	177792	48.8	33.0	10.9	1.2	100%
LHR19	508434	177376	53.5	35.3	15.6	1.6	101%
LHR20	508058	177040	60.5	37.9	21.6	2.4	101%
BA20	505127	177559	39.3	27.9	4.6	0.6	102%
HD60	505736	177752	39.6	27.8	4.9	0.7	101%
HD58	508414	177125	58.6	37.4	20.5	1.9	102%
HD57	508758	177718	54.8	34.8	12.0	1.2	101%
BA1	508582	178453	81.9	41.3	7.5	0.8	100%
HD56	509798	178634	55.3	34.6	6.6	0.7	101%
HS51	509127	174568	46.1	28.4	10.9	1.5	100%
X1	505883	178463	58.4	34.0	3.8	0.5	100%
X2	505932	177842	42.4	28.8	5.0	0.8	100%
X3	505890	177393	47.1	30.1	6.4	1.0	101%
X4	506146	177197	44.2	30.0	8.4	1.4	100%

Table 10.6 (cont) Estimated concentrations of NO_X, NO_2 and PM_{10} for 2015NoC ($\mu g/m^3$)

Receptor name	X(m)	Y(m)	Total NO_X	Total NO_2	Aircraft NO_X	Other airport NO_X	2015NoC/2015SM NO_2
X5	506156	177092	45.7	30.7	9.3	1.5	101%
X6	506154	176991	53.7	33.0	10.3	1.7	101%
X7	508228	177545	50.2	33.9	13.0	1.4	101%
X8	508212	177390	52.1	34.8	14.9	1.6	101%
X9	507873	177139	56.7	36.6	18.3	2.6	100%
X10	508429	177012	63.6	39.1	23.8	2.1	102%
X11	508549	176736	89.2	45.0	45.6	2.9	106%
X12	508789	177365	59.0	36.8	16.3	1.5	102%
X13	508735	177965	53.3	34.1	10.2	1.0	101%
BAA1	508009	177028	61.1	38.1	21.7	2.5	101%
BAA2	507914	177030	61.1	38.1	21.3	2.8	100%
BAA3	508802	177048	68.0	40.2	24.2	2.1	103%
BAA4	508762	177049	64.5	39.4	24.0	2.1	103%
BAA5	508885	177042	65.7	39.7	24.7	2.1	104%
BAA6	508902	177045	65.0	39.5	24.6	2.1	104%
BAA7	508552	177102	60.1	38.0	21.5	1.9	102%
BAA8	508598	177100	60.4	38.1	21.8	2.0	103%
BAA9	508412	177117	58.8	37.5	20.6	2.0	102%
BAA10	508380	177164	57.3	36.9	19.4	1.9	102%
BAA11	508373	177231	55.7	36.3	18.0	1.8	101%
BAA12	508366	177292	54.4	35.8	16.9	1.7	101%
BAA13	508356	177373	53.1	35.1	15.5	1.6	101%
BAA14	504799	176658	54.7	33.8	14.4	1.0	113%
BAA15	504842	176702	50.2	32.4	12.3	1.0	111%
BAA16	504966	176844	44.6	30.2	8.9	1.0	107%
BAA17	505043	176904	43.5	29.7	8.2	1.1	105%
BAA18	506046	176986	54.2	32.9	10.0	1.7	101%
BAA19	506153	176991	53.7	32.9	10.3	1.7	101%
BAA20	507307	177018	56.9	35.8	17.3	3.0	98%
BAA21	507496	177400	57.7	35.2	12.3	1.7	99%

Table 10.6 (cont) Estimated concentrations of NO_X, NO_2 and PM_{10} for 2015NoC ($\mu g/m^3$)

Receptor name	X(m)	Y(m)	Total NO_X	Total NO_2	Aircraft NO_X	Other airport NO_X	2015NoC/2015SM NO_2
BAA22	509431	176952	63.3	37.8	19.1	2.3	103%
BAA23	509544	176967	59.8	36.5	16.6	2.2	103%
BAA24	509582	177007	55.1	35.3	15.7	2.1	103%
BAA25	509574	177054	53.5	34.9	15.5	2.0	103%
BAA26	506791	178593	66.5	36.5	4.7	0.6	100%
BAA27	506928	178615	63.0	35.8	4.9	0.6	100%
BAA28	507004	178623	61.9	35.6	5.0	0.6	100%
BAA29	507089	178626	62.9	35.9	5.1	0.7	100%
BAA30	507176	178628	65.4	36.7	5.2	0.7	100%
BAA31	507207	178632	66.5	37.0	5.2	0.7	100%
BAA32	510172	178352	75.6	40.7	6.9	0.7	101%
BAA33	510109	178351	74.5	40.3	7.0	0.7	101%
BAA34	509999	178376	65.8	37.9	7.1	0.7	101%
BAA35	510016	178407	62.1	36.9	7.0	0.7	101%
BAA36	510157	178384	67.0	38.5	6.8	0.7	101%
BAA37	510188	178445	60.1	36.5	6.7	0.7	101%
BAA38	509820	178355	74.5	40.0	7.4	0.8	101%
BAA39	509822	178396	64.9	37.6	7.3	0.7	101%
BAA40	509392	178382	82.0	41.8	7.7	0.8	100%
BAA41	509403	178468	63.3	37.3	7.4	0.8	101%
BAA42	506456	178564	58.0	34.2	4.3	0.6	100%
BAA43	507178	178659	57.3	34.5	5.1	0.7	100%
BAA44	507066	178668	53.7	33.4	5.0	0.6	100%
BAA45	508822	174587	48.8	29.7	13.2	2.0	100%
BAA46	508849	174638	50.3	30.3	14.0	2.0	100%
BAA47	508877	174691	52.5	31.0	14.9	2.0	100%
BAA48	509007	174755	51.4	30.6	15.1	1.8	100%
BAA49	505777	174594	41.7	26.4	9.4	1.4	95%
BAA50	505744	174588	41.4	26.3	9.3	1.4	95%
BAA51	505909	174592	42.9	26.7	9.6	1.5	95%

10.7 2015MM

Predicted concentrations of NO_x, NO_2 and PM_{10} for 2015MM at receptor locations are presented in Table 10.7.

Contour plots of predicted NO_x and NO_2 concentrations due to all sources are presented in Figure 10.26 and Figure 10.27 respectively. Contour plots of predicted NO_x concentrations due to aircraft and other airport sources and road sources are presented in Figure 10.28 and Figure 10.29 respectively.

Table 10.7 Predicted concentrations of NO_X, NO_2 and PM_{10} for 2015MM ($\mu g/m^3$)

Receptor name	X(m)	Y(m)	Total NO_X	Total NO_2	Aircraft NO_X	Other airport NO_X	Road NO_X	Background NO_X	Total PM_{10}	Aircraft PM_{10}	Other airport PM_{10}	Road PM_{10}	Background PM_{10}
LHR2	508399	176744	83.7	43.7	38.3	3.0	18.5	23.9	21.63	1.33	0.25	0.66	19.38
LHR3	511679	180072	44.4	30.0	3.4	0.4	9.8	30.8	20.45	0.06	0.03	0.45	19.90
LHR4	509550	176997	55.6	35.5	15.6	2.2	13.7	24.0	20.34	0.23	0.22	0.59	19.30
LHR5	510370	177195	44.7	30.6	8.3	1.2	12.9	22.3	20.07	0.13	0.09	0.54	19.30
LHR6	515540	170420	32.4	22.2	0.9	0.1	9.1	22.3	19.71	0.02	0.01	0.41	19.27
LHR7	509333	175002	53.9	31.5	16.3	1.7	14.8	21.1	20.19	0.26	0.14	0.60	19.19
LHR8	505739	174497	39.3	26.0	8.3	1.4	10.0	19.6	19.84	0.19	0.12	0.42	19.11
LHR10	502741	173460	103.9	43.6	2.1	0.2	82.5	19.1	22.44	0.03	0.02	3.14	19.25
LHR11	504780	175510	47.6	30.1	10.0	1.5	15.0	21.1	20.37	0.14	0.13	0.58	19.52
LHR12	504466	175794	44.0	29.2	7.7	0.9	14.1	21.3	20.27	0.11	0.08	0.58	19.50
LHR13	504393	176591	51.0	31.3	7.1	0.7	22.4	20.8	20.17	0.09	0.06	0.86	19.16
LHR14	503535	176829	39.3	27.2	3.2	0.3	13.1	22.6	19.76	0.05	0.03	0.53	19.15
LHR15	505185	176922	42.7	29.0	7.7	1.2	12.9	21.0	19.95	0.14	0.11	0.54	19.16
LHR16	506945	178609	64.1	36.1	4.7	0.7	36.3	22.5	21.23	0.12	0.06	1.65	19.40
LHR17	506990	181919	36.1	25.3	1.9	0.2	10.6	23.4	19.92	0.04	0.02	0.48	19.38
LHR18	508279	177792	48.4	32.8	10.4	1.2	12.0	24.8	20.44	0.24	0.10	0.53	19.57
LHR19	508434	177376	52.7	35.0	14.7	1.6	10.8	25.6	20.46	0.35	0.13	0.47	19.51
LHR20	508058	177040	59.1	37.4	20.1	2.4	12.7	23.9	20.92	0.66	0.18	0.55	19.53
BA20	505127	177559	39.4	28.0	4.3	0.7	13.5	20.9	19.88	0.10	0.06	0.58	19.15
HD60	505736	177752	39.6	27.9	4.7	0.8	12.4	21.8	20.08	0.12	0.07	0.53	19.36
HD58	508414	177125	57.4	36.9	19.1	2.0	11.4	24.9	20.60	0.50	0.16	0.49	19.45
HD57	508758	177718	54.2	34.6	11.4	1.2	15.6	26.0	20.52	0.24	0.10	0.71	19.47
BA1	508582	178453	81.5	41.1	7.2	0.8	48.5	25.0	21.71	0.15	0.07	2.11	19.38
HD56	509798	178634	55.1	34.6	6.4	0.7	14.4	33.6	20.57	0.12	0.06	0.63	19.76
HS51	509127	174568	46.1	28.4	11.2	1.4	13.4	20.1	20.06	0.21	0.11	0.58	19.16
X1	505883	178463	58.6	34.2	3.6	0.6	32.8	21.5	20.85	0.09	0.05	1.49	19.22
X2	505932	177842	42.5	28.9	4.8	0.8	14.6	22.3	20.30	0.13	0.07	0.62	19.48
X3	505890	177393	46.8	30.1	6.1	1.1	17.3	22.4	20.51	0.17	0.09	0.70	19.55
X4	506146	177197	43.9	30.0	8.0	1.4	11.4	23.1	20.48	0.25	0.13	0.49	19.62

Table 10.7 (cont) Predicted concentrations of NO_X, NO_2 and PM_{10} for 2015MM ($\mu g/m^3$)

Receptor name	X(m)	Y(m)	Total NO_X	Total NO_2	Aircraft NO_X	Other airport NO_X	Road NO_X	Background NO_X	Total PM_{10}	Aircraft PM_{10}	Other airport PM_{10}	Road PM_{10}	Background PM_{10}
X5	506156	177092	45.3	30.6	8.8	1.6	11.9	23.0	20.51	0.29	0.14	0.51	19.57
X6	506154	176991	53.2	32.7	9.7	1.8	18.8	22.9	20.78	0.34	0.16	0.78	19.51
X7	508228	177545	49.6	33.6	12.3	1.4	10.8	25.1	20.54	0.31	0.11	0.48	19.64
X8	508212	177390	51.3	34.4	14.0	1.6	10.8	24.9	20.59	0.37	0.13	0.47	19.61
X9	507873	177139	55.6	36.1	17.2	2.5	12.4	23.5	20.92	0.56	0.17	0.55	19.64
X10	508429	177012	62.0	38.4	22.2	2.2	13.0	24.6	20.74	0.59	0.18	0.56	19.41
X11	508549	176736	85.4	44.0	41.4	3.0	16.9	24.1	21.25	1.01	0.25	0.62	19.36
X12	508789	177365	58.0	36.4	15.3	1.6	15.7	25.4	20.57	0.31	0.14	0.65	19.47
X13	508735	177965	52.9	33.9	9.6	1.1	16.1	26.1	20.47	0.20	0.09	0.67	19.51
BAA1	508009	177028	59.6	37.6	20.3	2.5	13.1	23.7	20.97	0.68	0.19	0.57	19.54
BAA2	507914	177030	59.6	37.5	19.9	2.7	13.5	23.5	21.03	0.69	0.19	0.59	19.57
BAA3	508802	177048	66.3	39.5	22.5	2.1	17.1	24.6	20.70	0.41	0.19	0.69	19.40
BAA4	508762	177049	62.9	38.7	22.3	2.1	13.7	24.7	20.58	0.43	0.19	0.57	19.39
BAA5	508885	177042	63.9	39.0	22.9	2.2	14.3	24.6	20.55	0.39	0.20	0.61	19.36
BAA6	508902	177045	63.3	38.8	22.8	2.1	13.8	24.6	20.53	0.38	0.20	0.59	19.36
BAA7	508552	177102	58.7	37.4	20.1	2.0	11.7	25.0	20.55	0.47	0.17	0.50	19.41
BAA8	508598	177100	59.0	37.5	20.3	2.0	11.7	25.0	20.54	0.46	0.17	0.50	19.40
BAA9	508412	177117	57.6	37.0	19.3	2.0	11.4	24.9	20.60	0.50	0.16	0.49	19.44
BAA10	508380	177164	56.1	36.5	18.2	1.9	11.1	24.9	20.58	0.47	0.16	0.48	19.47
BAA11	508373	177231	54.6	35.9	16.9	1.8	10.9	25.0	20.55	0.43	0.15	0.47	19.49
BAA12	508366	177292	53.5	35.4	15.8	1.7	10.8	25.2	20.53	0.40	0.14	0.47	19.51
BAA13	508356	177373	52.3	34.8	14.6	1.6	10.8	25.3	20.51	0.37	0.13	0.47	19.54
BAA14	504799	176658	53.1	31.5	13.2	1.0	18.1	20.8	20.09	0.14	0.09	0.72	19.13
BAA15	504842	176702	49.0	30.7	11.3	1.1	15.8	20.8	20.01	0.13	0.10	0.65	19.14
BAA16	504966	176844	43.9	29.4	8.3	1.1	13.7	20.8	19.94	0.13	0.10	0.57	19.14
BAA17	505043	176904	43.0	29.1	7.6	1.1	13.4	20.9	19.94	0.13	0.10	0.56	19.15
BAA18	506046	176986	53.6	32.7	9.4	1.7	19.8	22.6	20.74	0.31	0.16	0.82	19.45
BAA19	506153	176991	53.2	32.7	9.7	1.8	18.8	22.9	20.78	0.34	0.16	0.78	19.51
BAA20	507307	177018	55.9	35.5	16.3	2.9	13.8	22.9	21.14	0.66	0.19	0.59	19.70
BAA21	507496	177400	58.1	35.3	11.7	1.7	22.3	22.3	21.58	0.37	0.13	1.02	20.06

Table 10.7 (cont) Predicted concentrations of NO_X, NO_2 and PM_{10} for 2015MM ($\mu g/m^3$)

Receptor name	X(m)	Y(m)	Total NO_X	Total NO_2	Aircraft NO_X	Other airport NO_X	Road NO_X	Background NO_X	Total PM_{10}	Aircraft PM_{10}	Other airport PM_{10}	Road PM_{10}	Background PM_{10}
BAA22	509431	176952	62.3	37.5	18.1	2.3	17.8	24.1	20.55	0.26	0.24	0.76	19.30
BAA23	509544	176967	59.2	36.3	15.9	2.3	16.9	24.0	20.48	0.24	0.23	0.71	19.30
BAA24	509582	177007	54.5	35.1	15.1	2.1	13.4	23.9	20.31	0.23	0.21	0.57	19.30
BAA25	509574	177054	53.0	34.7	14.9	2.0	12.1	24.0	20.25	0.22	0.20	0.52	19.31
BAA26	506791	178593	66.4	36.6	4.5	0.7	38.9	22.4	21.31	0.12	0.05	1.76	19.37
BAA27	506928	178615	62.9	35.8	4.7	0.7	35.1	22.5	21.18	0.12	0.06	1.60	19.40
BAA28	507004	178623	61.8	35.6	4.8	0.7	33.8	22.6	21.14	0.12	0.06	1.54	19.43
BAA29	507089	178626	62.9	36.0	4.9	0.7	34.7	22.6	21.21	0.12	0.06	1.57	19.45
BAA30	507176	178628	65.4	36.7	5.0	0.7	37.0	22.7	21.33	0.13	0.06	1.67	19.48
BAA31	507207	178632	66.4	37.0	5.0	0.7	38.0	22.7	21.39	0.13	0.06	1.71	19.50
BAA32	510172	178352	75.0	40.5	6.7	0.7	38.2	29.4	21.32	0.11	0.06	1.52	19.62
BAA33	510109	178351	74.1	40.1	6.8	0.8	36.8	29.8	21.29	0.12	0.06	1.47	19.63
BAA34	509999	178376	65.6	37.8	6.9	0.8	27.3	30.7	20.98	0.12	0.06	1.14	19.65
BAA35	510016	178407	61.8	36.8	6.8	0.7	23.5	30.9	20.83	0.12	0.06	0.98	19.67
BAA36	510157	178384	66.6	38.3	6.6	0.7	29.5	29.8	21.01	0.11	0.06	1.19	19.64
BAA37	510188	178445	59.7	36.4	6.4	0.7	22.4	30.2	20.76	0.11	0.06	0.92	19.67
BAA38	509820	178355	74.3	39.9	7.2	0.8	34.9	31.5	21.32	0.13	0.07	1.48	19.64
BAA39	509822	178396	64.7	37.6	7.0	0.8	25.0	31.9	20.93	0.12	0.07	1.07	19.67
BAA40	509392	178382	81.7	41.8	7.4	0.8	41.0	32.5	21.60	0.14	0.07	1.76	19.64
BAA41	509403	178468	63.1	37.2	7.1	0.8	21.7	33.5	20.84	0.13	0.07	0.95	19.69
BAA42	506456	178564	58.0	34.3	4.2	0.6	31.0	22.2	20.87	0.11	0.05	1.41	19.31
BAA43	507178	178659	57.3	34.6	4.9	0.7	28.9	22.7	20.98	0.12	0.06	1.30	19.50
BAA44	507066	178668	53.7	33.4	4.8	0.7	25.6	22.7	20.80	0.12	0.06	1.16	19.47
BAA45	508822	174587	49.0	29.9	13.6	2.0	13.3	20.1	20.13	0.27	0.16	0.55	19.15
BAA46	508849	174638	50.5	30.5	14.4	2.0	14.0	20.1	20.17	0.28	0.16	0.57	19.16
BAA47	508877	174691	52.8	31.3	15.4	2.0	15.3	20.2	20.22	0.29	0.16	0.61	19.17
BAA48	509007	174755	51.8	30.8	15.7	1.8	14.0	20.4	20.15	0.27	0.14	0.57	19.17
BAA49	505777	174594	41.7	26.8	9.4	1.6	11.0	19.7	19.91	0.22	0.13	0.45	19.11
BAA50	505744	174588	41.3	26.6	9.3	1.5	10.8	19.7	19.89	0.21	0.12	0.44	19.11
BAA51	505909	174592	43.6	27.3	9.7	2.3	11.9	19.7	20.00	0.25	0.16	0.47	19.12

Figure 10.21 2015MM predicted total NO_X concentrations in $\mu g/m^3$ around Heathrow.

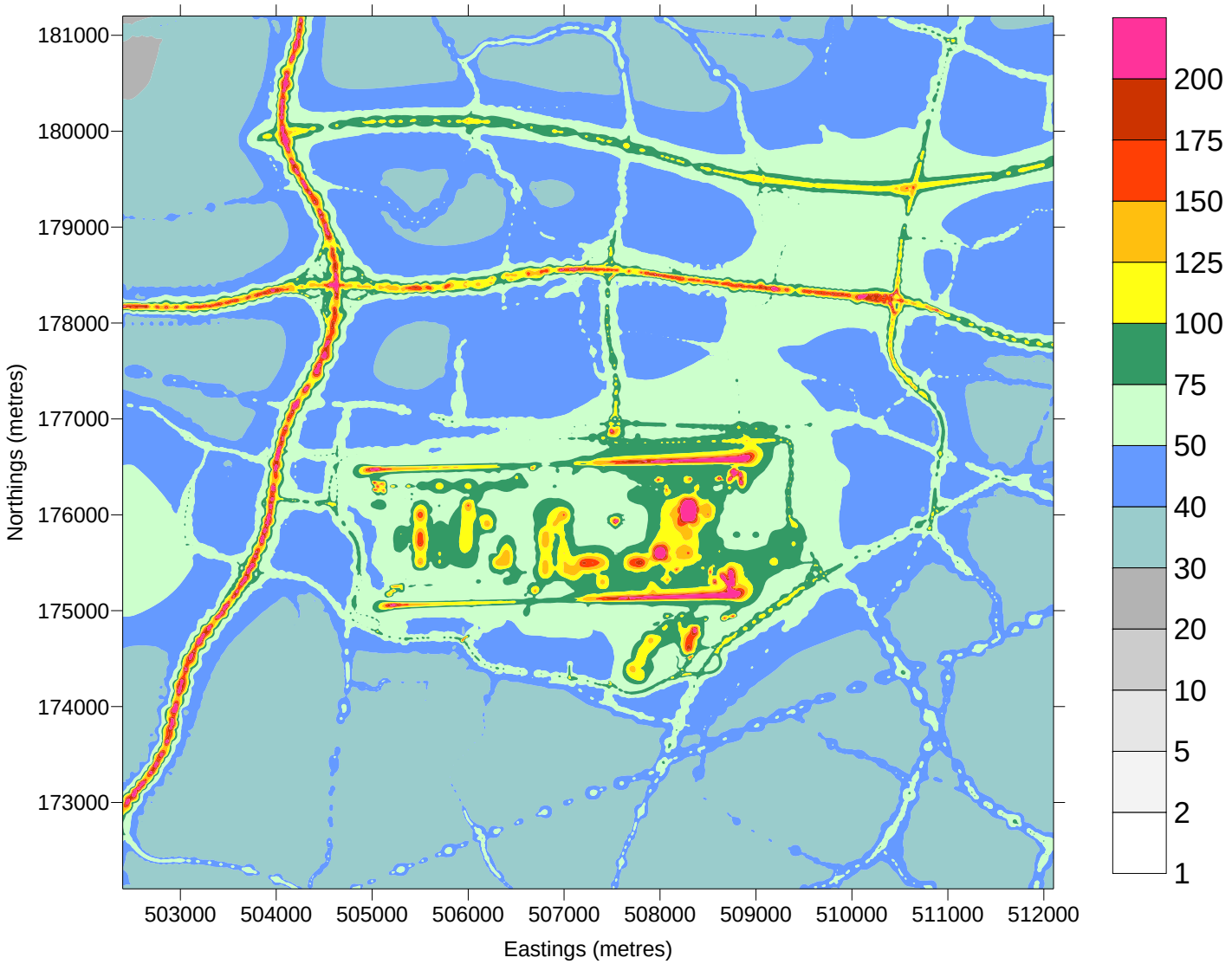

Figure 10.22 2015MM predicted total NO_2 concentrations in $\mu g/m^3$ around Heathrow.

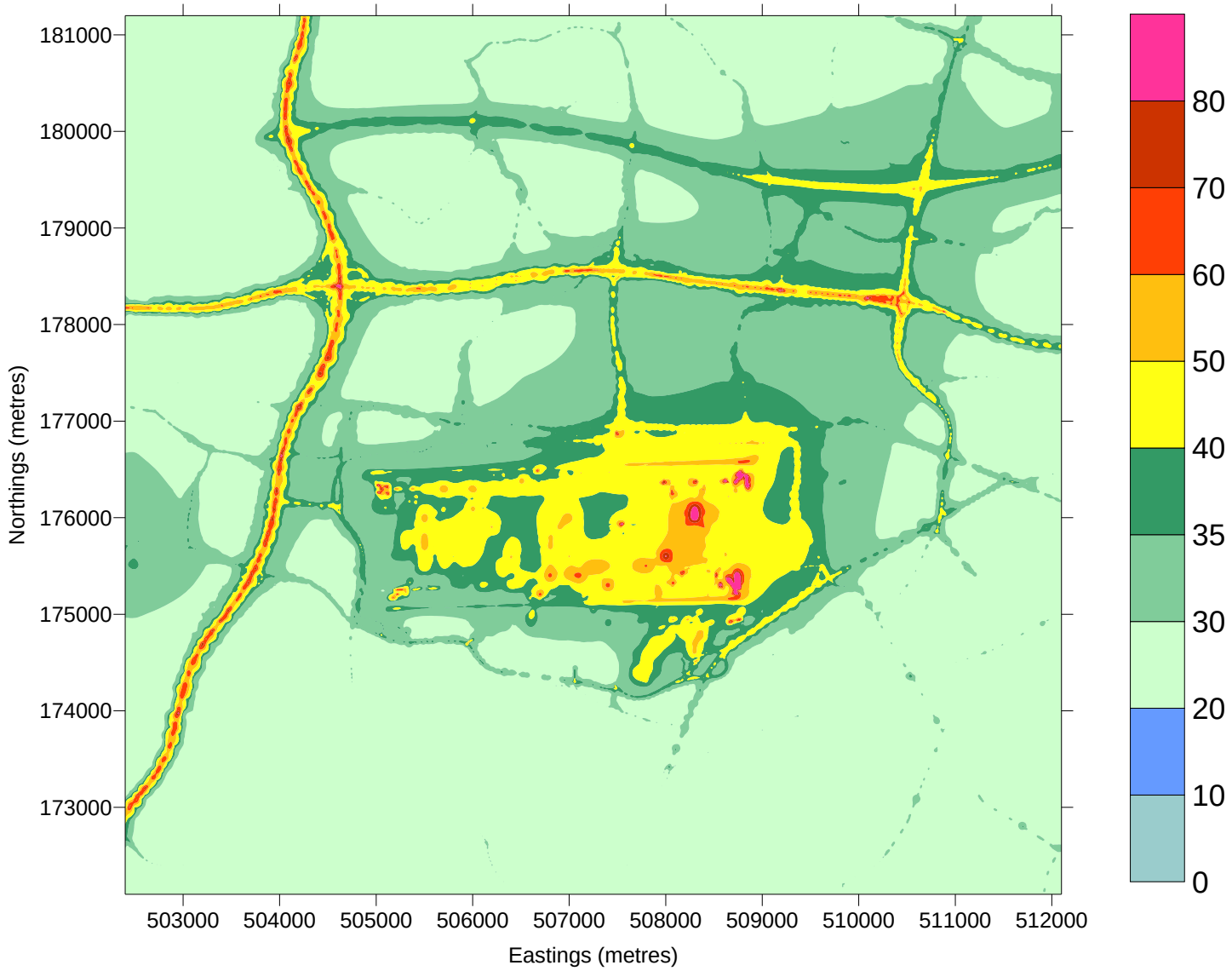

Figure 10.23 2015MM predicted NO_X concentration in $\mu g/m^3$ around Heathrow due to aircraft and other airport sources.

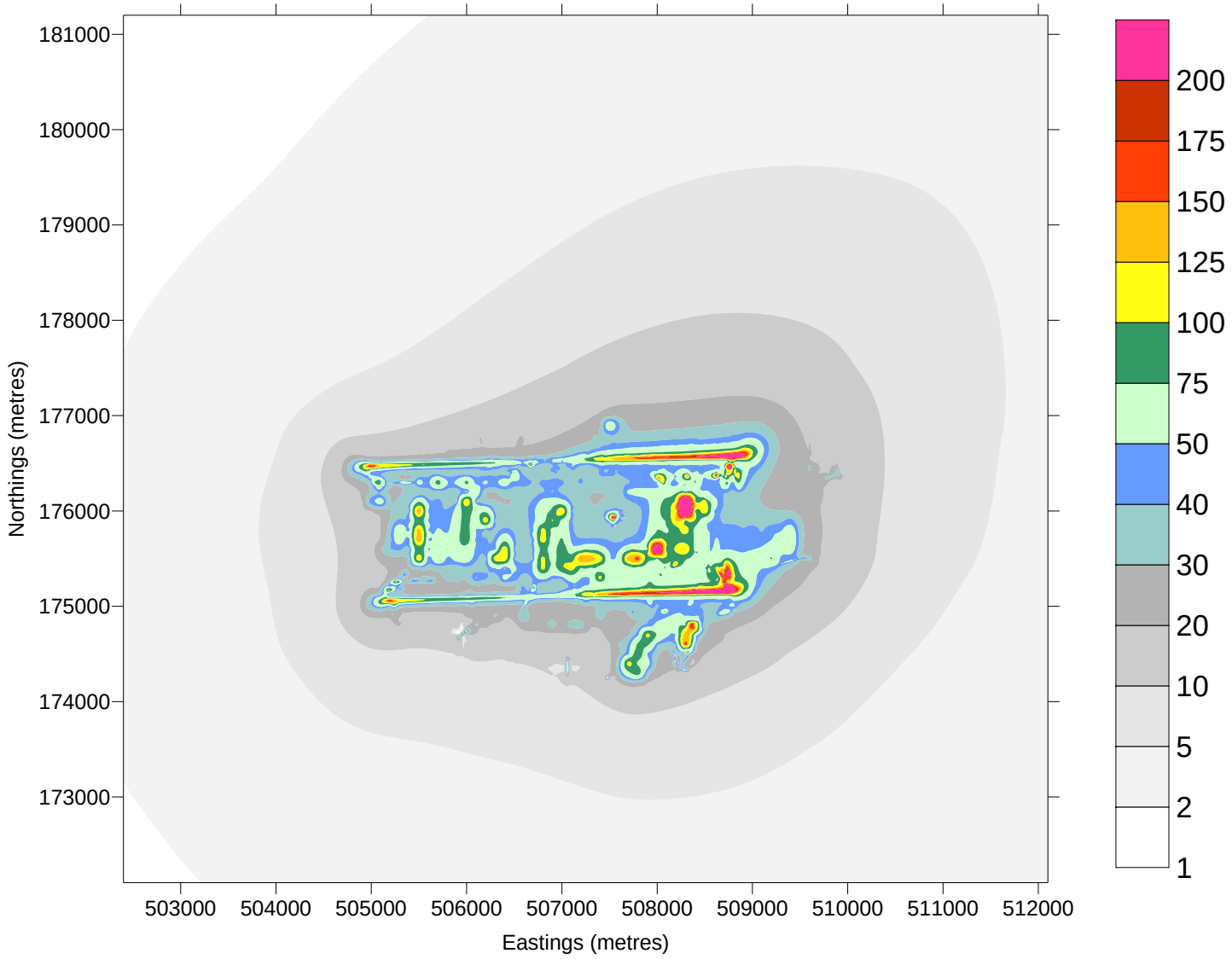

Figure 10.24 2015MM predicted NO_X concentration in $\mu g/m^3$ around Heathrow due to road sources.

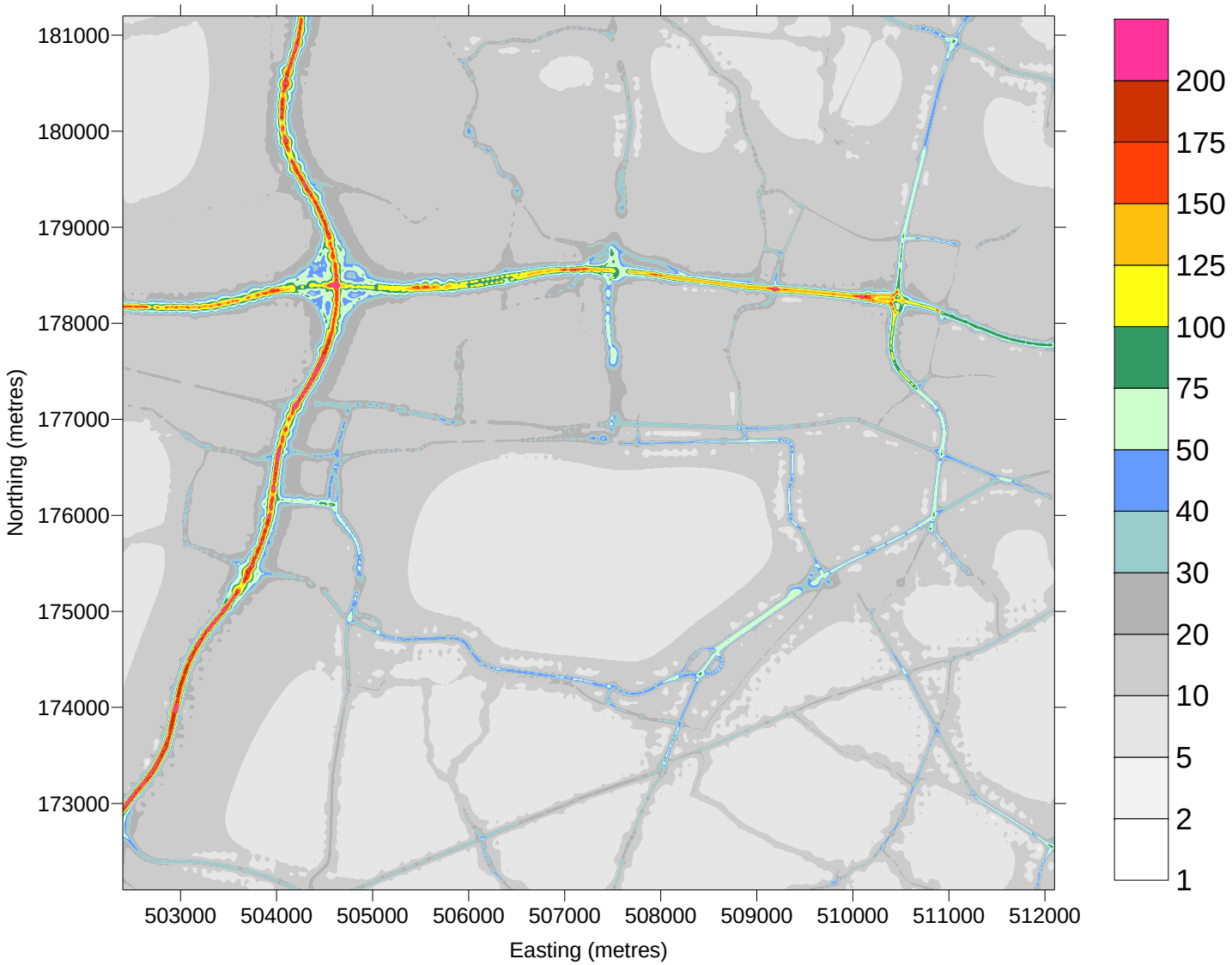

10.8 2015MMRd

Predicted concentrations of NO_x, NO_2 and PM_{10} for 2015MMRd at receptor locations are presented in Table 10.8.

A difference plot between predicted NO_2 concentrations of 2015MM and 2015MMRd at receptor locations is presented in Figure 10.25

Table 10.8 Predicted concentrations of NO_X, NO_2 and PM_{10} for 2015MMRd ($\mu g/m^3$)

Receptor name	X(m)	Y(m)	Total NO_X	Total NO_2	Total PM_{10}	2015MMRd/2015MM NO_2
LHR2	508399	176744	83.6	43.6	21.63	99.8%
LHR3	511679	180072	44.3	29.9	20.45	99.7%
LHR4	509550	176997	55.2	35.3	20.34	99.4%
LHR5	510370	177195	44.5	30.5	20.07	99.7%
LHR6	515540	170420	32.4	22.2	19.71	100.0%
LHR7	509333	175002	53.3	31.3	20.19	99.4%
LHR8	505739	174497	39.1	25.9	19.84	99.6%
LHR10	502741	173460	104.3	43.7	22.44	100.2%
LHR11	504780	175510	47.0	29.9	20.37	99.3%
LHR12	504466	175794	43.7	29.1	20.27	99.7%
LHR13	504393	176591	50.4	31.0	20.17	99.0%
LHR14	503535	176829	39.1	27.1	19.76	99.6%
LHR15	505185	176922	42.5	28.9	19.95	99.7%
LHR16	506945	178609	59.4	34.6	21.23	95.8%
LHR17	506990	181919	36.1	25.3	19.92	100.0%
LHR18	508279	177792	48.0	32.6	20.44	99.4%
LHR19	508434	177376	52.4	34.8	20.46	99.4%
LHR20	508058	177040	58.9	37.3	20.92	99.7%
BA20	505127	177559	39.1	27.8	19.88	99.3%
HD60	505736	177752	39.2	27.7	20.08	99.3%
HD58	508414	177125	57.1	36.8	20.60	99.7%
HD57	508758	177718	53.5	34.3	20.52	99.1%
BA1	508582	178453	75.1	39.3	21.71	95.6%
HD56	509798	178634	54.1	34.1	20.57	98.6%
HS51	509127	174568	46.0	28.4	20.06	100.0%
X1	505883	178463	54.4	32.8	20.85	95.9%
X2	505932	177842	42.1	28.7	20.30	99.3%
X3	505890	177393	46.7	30.0	20.51	99.7%
X4	506146	177197	43.7	29.9	20.48	99.7%

Table 10.8 (cont) Predicted concentrations of NO_X, NO_2 and PM_{10} for 2015MMRd ($\mu g/m^3$)

Receptor name	X(m)	Y(m)	Total NO_X	Total NO_2	Total PM_{10}	2015MMRd/2015MM NO_2
X5	506156	177092	45.1	30.5	20.51	99.7%
X6	506154	176991	53.0	32.6	20.78	99.7%
X7	508228	177545	49.4	33.5	20.54	99.7%
X8	508212	177390	51.1	34.3	20.59	99.7%
X9	507873	177139	55.5	36.1	20.92	100.0%
X10	508429	177012	61.8	38.3	20.74	99.7%
X11	508549	176736	85.3	43.9	21.25	99.8%
X12	508789	177365	57.2	36.2	20.57	99.5%
X13	508735	177965	51.9	33.5	20.47	98.8%
BAA1	508009	177028	59.5	37.5	20.97	99.7%
BAA2	507914	177030	59.4	37.4	21.03	99.7%
BAA3	508802	177048	65.5	39.2	20.70	99.2%
BAA4	508762	177049	62.5	38.5	20.58	99.5%
BAA5	508885	177042	63.5	38.8	20.55	99.5%
BAA6	508902	177045	62.9	38.6	20.53	99.5%
BAA7	508552	177102	58.5	37.3	20.55	99.7%
BAA8	508598	177100	58.7	37.4	20.54	99.7%
BAA9	508412	177117	57.4	36.9	20.60	99.7%
BAA10	508380	177164	55.9	36.4	20.58	99.7%
BAA11	508373	177231	54.4	35.8	20.55	99.7%
BAA12	508366	177292	53.3	35.3	20.53	99.7%
BAA13	508356	177373	52.0	34.7	20.51	99.7%
BAA14	504799	176658	52.9	31.4	20.09	99.7%
BAA15	504842	176702	48.8	30.5	20.01	99.3%
BAA16	504966	176844	43.7	29.3	19.94	99.7%
BAA17	505043	176904	42.7	29.0	19.94	99.7%
BAA18	506046	176986	53.4	32.6	20.74	99.7%
BAA19	506153	176991	53.0	32.6	20.78	99.7%
BAA20	507307	177018	55.8	35.5	21.14	100.0%
BAA21	507496	177400	58.2	35.3	21.58	100.0%

Table 10.8 (cont) Predicted concentrations of NO_X, NO_2 and PM_{10} for 2015MMRd ($\mu g/m^3$)

Receptor name	X(m)	Y(m)	Total NO_X	Total NO_2	Total PM_{10}	2015MMRd/2015MM NO_2
BAA22	509431	176952	61.8	37.3	20.55	99.5%
BAA23	509544	176967	58.6	36.2	20.48	99.7%
BAA24	509582	177007	54.2	35.0	20.31	99.7%
BAA25	509574	177054	52.7	34.6	20.25	99.7%
BAA26	506791	178593	61.2	34.9	21.31	95.4%
BAA27	506928	178615	58.4	34.3	21.18	95.8%
BAA28	507004	178623	57.5	34.2	21.14	96.1%
BAA29	507089	178626	58.4	34.5	21.21	95.8%
BAA30	507176	178628	60.8	35.2	21.34	95.9%
BAA31	507207	178632	62.0	35.6	21.39	96.2%
BAA32	510172	178352	68.8	38.6	21.32	95.3%
BAA33	510109	178351	68.2	38.3	21.29	95.5%
BAA34	509999	178376	62.0	36.6	20.98	96.8%
BAA35	510016	178407	59.0	35.8	20.83	97.3%
BAA36	510157	178384	62.4	36.9	21.01	96.3%
BAA37	510188	178445	57.1	35.4	20.76	97.3%
BAA38	509820	178355	69.3	38.4	21.32	96.2%
BAA39	509822	178396	61.6	36.5	20.93	97.1%
BAA40	509392	178382	75.6	40.0	21.61	95.7%
BAA41	509403	178468	60.6	36.3	20.84	97.6%
BAA42	506456	178564	54.1	32.9	20.87	95.9%
BAA43	507178	178659	54.0	33.4	20.98	96.5%
BAA44	507066	178668	50.8	32.4	20.80	97.0%
BAA45	508822	174587	48.6	29.8	20.13	99.7%
BAA46	508849	174638	50.0	30.3	20.17	99.3%
BAA47	508877	174691	52.1	31.0	20.22	99.0%
BAA48	509007	174755	51.2	30.7	20.15	99.7%
BAA49	505777	174594	41.2	26.6	19.91	99.3%
BAA50	505744	174588	40.9	26.5	19.89	99.6%
BAA51	505909	174592	43.0	27.1	20.00	99.3%

Figure 10.25 Difference between 2015MM and 2015MMRd, predicted NO_2 concentrations in $\mu g/m^3$ at receptor locations around Heathrow .

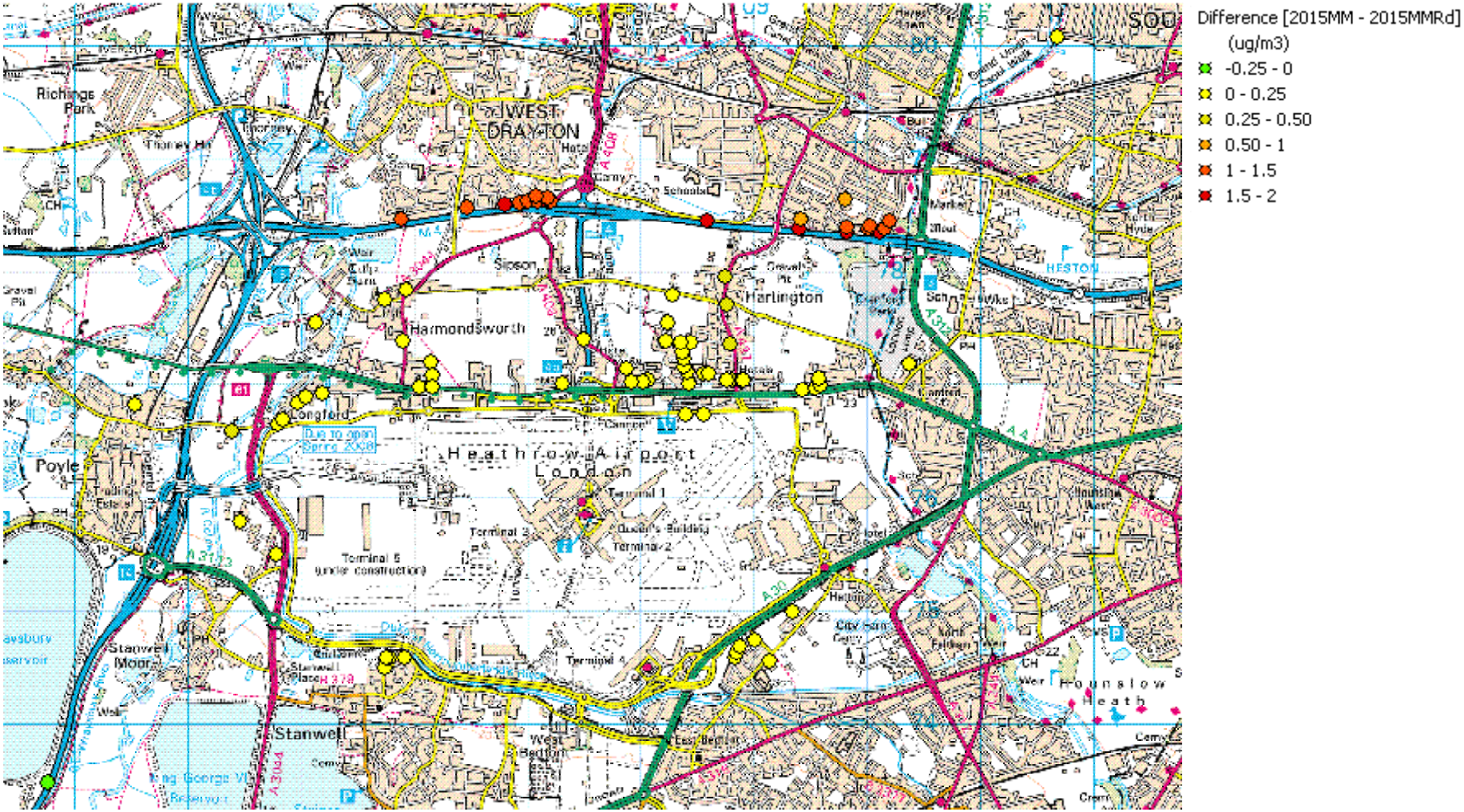

10.9 2030MM

Predicted concentrations of NO_x, NO_2 and PM_{10} for 2030MM at receptor locations are presented in Table 10.9.

Contour plots of predicted NO_x and NO_2 concentrations due to all sources are presented in Figure 10.26 and Figure 10.27 respectively. Contour plots of predicted NO_x concentrations due to aircraft and other airport sources and road sources are presented in Figure 10.28 and Figure 10.29 respectively.

Table 10.9 Predicted concentrations of NO_X, NO_2 and PM_{10} for 2030MM ($\mu g/m^3$)

Receptor name	X(m)	Y(m)	Total NO_X	Total NO_2	Aircraft NO_X	Other airport NO_X	Road NO_X	Background NO_X	Total PM_{10}	Aircraft PM_{10}	Other airport PM_{10}	Road PM_{10}	Background PM_{10}
LHR2	508399	176744	72.7	39.3	38.8	2.3	8.1	23.6	25.05	1.39	0.24	0.73	18.33
LHR3	511679	180072	37.8	26.5	3.1	0.3	4.3	30.7	19.70	0.06	0.03	0.51	19.00
LHR4	509550	176997	46.0	31.0	14.8	1.5	6.0	23.8	19.84	0.23	0.14	0.65	18.35
LHR5	510370	177195	35.8	26.1	7.4	0.9	5.6	22.0	19.42	0.13	0.07	0.62	18.34
LHR6	515540	170420	27.0	19.3	0.8	0.1	4.0	22.2	18.89	0.02	0.01	0.47	18.36
LHR7	509333	175002	42.4	26.7	14.0	1.2	6.5	20.7	19.74	0.25	0.12	0.67	18.23
LHR8	505739	174497	31.7	22.3	7.2	1.0	4.5	19.1	19.40	0.19	0.11	0.49	18.14
LHR10	502741	173460	58.0	29.9	1.9	0.2	37.3	18.6	21.46	0.03	0.02	3.34	17.99
LHR11	504780	175510	38.3	25.8	9.2	1.8	6.7	20.5	19.80	0.13	0.24	0.67	18.52
LHR12	504466	175794	35.6	24.9	7.3	1.4	6.3	20.7	19.65	0.10	0.19	0.65	18.53
LHR13	504393	176591	38.1	25.2	7.0	0.7	10.3	20.2	19.49	0.09	0.08	0.98	18.17
LHR14	503535	176829	30.9	22.9	2.9	0.3	5.9	22.2	18.99	0.05	0.03	0.63	18.20
LHR15	505185	176922	34.3	24.5	7.2	1.0	5.8	20.4	19.33	0.13	0.11	0.61	18.17
LHR16	506945	178609	42.9	27.7	4.2	0.5	16.9	21.3	20.62	0.12	0.05	1.79	18.34
LHR17	506990	181919	29.6	21.7	1.7	0.2	4.8	23.0	19.13	0.04	0.02	0.55	18.43
LHR18	508279	177792	40.1	28.6	9.8	0.9	5.3	24.2	20.02	0.25	0.09	0.61	18.41
LHR19	508434	177376	45.2	31.3	14.1	1.2	4.8	25.2	20.46	0.36	0.12	0.54	18.44
LHR20	508058	177040	50.3	33.5	19.7	1.7	5.7	23.3	21.87	0.68	0.17	0.63	18.33
BA20	505127	177559	30.4	23.0	4.0	0.5	6.1	19.9	19.18	0.09	0.06	0.64	18.15
HD60	505736	177752	30.4	23.0	4.2	0.6	5.6	20.1	19.27	0.11	0.07	0.60	18.17
HD58	508414	177125	49.7	33.3	18.7	1.5	5.1	24.5	21.07	0.51	0.16	0.56	18.40
HD57	508758	177718	44.1	30.2	10.8	0.9	6.8	25.7	20.19	0.24	0.09	0.78	18.46
BA1	508582	178453	52.8	31.7	6.7	0.6	21.2	24.5	21.11	0.15	0.06	2.12	18.40
HD56	509798	178634	45.7	29.9	5.9	0.6	6.3	33.9	19.92	0.11	0.05	0.68	18.84
HS51	509127	174568	36.1	24.0	9.5	1.1	5.9	19.7	19.59	0.20	0.11	0.65	18.20
X1	505883	178463	41.0	26.6	3.3	0.4	16.9	20.4	20.34	0.08	0.05	1.77	18.21
X2	505932	177842	31.5	23.4	4.3	0.6	6.6	20.1	19.41	0.12	0.07	0.71	18.18
X3	505890	177393	34.3	24.5	5.6	0.8	7.8	20.1	19.71	0.16	0.09	0.83	18.17
X4	506146	177197	34.1	25.1	7.4	1.1	5.3	20.4	19.81	0.24	0.12	0.56	18.18

Table 10.9 (cont) Predicted concentrations of NO_X, NO_2 and PM_{10} for 2030MM ($\mu g/m^3$)

Receptor name	X(m)	Y(m)	Total NO_X	Total NO_2	Aircraft NO_X	Other airport NO_X	Road NO_X	Background NO_X	Total PM_{10}	Aircraft PM_{10}	Other airport PM_{10}	Road PM_{10}	Background PM_{10}
X5	506156	177092	35.6	25.8	8.2	1.2	5.6	20.6	20.02	0.28	0.13	0.59	18.19
X6	506154	176991	39.1	27.0	9.2	1.3	7.9	20.8	20.46	0.33	0.14	0.81	18.19
X7	508228	177545	41.9	29.7	11.6	1.1	4.9	24.5	20.27	0.32	0.11	0.55	18.41
X8	508212	177390	43.7	30.7	13.5	1.2	4.8	24.3	20.53	0.38	0.12	0.54	18.40
X9	507873	177139	46.6	32.0	16.7	1.6	5.6	22.8	21.44	0.58	0.16	0.62	18.31
X10	508429	177012	53.5	34.7	21.8	1.7	5.8	24.3	21.56	0.61	0.17	0.63	18.38
X11	508549	176736	75.4	39.8	42.1	2.2	7.4	23.8	23.37	1.06	0.24	0.69	18.34
X12	508789	177365	47.9	32.1	14.8	1.2	6.9	25.1	20.45	0.32	0.12	0.77	18.43
X13	508735	177965	42.6	29.3	9.1	0.8	7.1	25.8	20.03	0.20	0.08	0.78	18.46
BAA1	508009	177028	50.6	33.5	19.9	1.7	5.9	23.2	22.00	0.70	0.18	0.65	18.33
BAA2	507914	177030	50.2	33.3	19.5	1.8	6.1	22.9	22.05	0.71	0.18	0.67	18.31
BAA3	508802	177048	55.4	35.1	22.2	1.5	7.4	24.4	20.82	0.43	0.16	0.78	18.38
BAA4	508762	177049	53.8	34.7	22.0	1.5	6.0	24.4	20.76	0.44	0.16	0.65	18.38
BAA5	508885	177042	54.5	34.9	22.6	1.5	6.2	24.3	20.54	0.40	0.16	0.66	18.38
BAA6	508902	177045	54.2	34.8	22.5	1.5	5.9	24.3	20.49	0.39	0.16	0.64	18.38
BAA7	508552	177102	50.9	33.8	19.7	1.5	5.2	24.7	20.96	0.49	0.16	0.57	18.40
BAA8	508598	177100	51.1	33.9	19.9	1.5	5.2	24.6	20.89	0.47	0.16	0.57	18.40
BAA9	508412	177117	49.9	33.4	18.9	1.5	5.1	24.5	21.10	0.52	0.16	0.56	18.39
BAA10	508380	177164	48.5	32.8	17.7	1.4	5.0	24.5	20.97	0.49	0.15	0.55	18.40
BAA11	508373	177231	47.1	32.2	16.4	1.4	4.9	24.6	20.79	0.44	0.14	0.54	18.41
BAA12	508366	177292	46.0	31.7	15.3	1.3	4.8	24.7	20.65	0.41	0.13	0.54	18.41
BAA13	508356	177373	44.8	31.1	14.0	1.2	4.8	24.9	20.50	0.37	0.12	0.54	18.42
BAA14	504799	176658	42.5	26.2	13.3	0.9	8.2	20.2	19.44	0.13	0.11	0.79	18.17
BAA15	504842	176702	39.4	25.7	11.2	0.9	7.2	20.2	19.36	0.12	0.11	0.72	18.17
BAA16	504966	176844	35.2	24.7	7.9	0.9	6.2	20.3	19.29	0.12	0.11	0.64	18.17
BAA17	505043	176904	34.4	24.5	7.3	0.9	6.0	20.3	19.29	0.12	0.11	0.63	18.17
BAA18	506046	176986	39.4	27.0	8.9	1.3	8.5	20.8	20.40	0.30	0.14	0.87	18.19
BAA19	506153	176991	39.1	27.0	9.2	1.3	7.9	20.8	20.46	0.33	0.14	0.81	18.19
BAA20	507307	177018	46.2	31.2	15.8	1.8	7.0	21.6	21.97	0.67	0.18	0.72	18.25
BAA21	507496	177400	43.2	29.5	11.0	1.2	9.9	21.2	21.12	0.38	0.12	1.23	18.25

Table 10.9 (cont) Predicted concentrations of NO_X, NO_2 and PM_{10} for 2030MM ($\mu g/m^3$)

Receptor name	X(m)	Y(m)	Total NO_X	Total NO_2	Aircraft NO_X	Other airport NO_X	Road NO_X	Background NO_X	Total PM_{10}	Aircraft PM_{10}	Other airport PM_{10}	Road PM_{10}	Background PM_{10}
BAA22	509431	176952	50.4	32.5	17.4	1.5	7.8	23.9	20.10	0.26	0.15	0.82	18.35
BAA23	509544	176967	47.8	31.5	15.1	1.7	7.5	23.7	20.00	0.23	0.15	0.79	18.35
BAA24	509582	177007	45.1	30.7	14.2	1.5	5.9	23.7	19.81	0.22	0.14	0.63	18.35
BAA25	509574	177054	44.3	30.5	14.0	1.4	5.3	23.8	19.74	0.22	0.13	0.58	18.36
BAA26	506791	178593	45.3	28.2	4.1	0.5	19.5	21.3	20.85	0.11	0.05	2.06	18.31
BAA27	506928	178615	42.4	27.6	4.2	0.5	16.4	21.4	20.57	0.11	0.05	1.74	18.35
BAA28	507004	178623	41.4	27.4	4.3	0.5	15.3	21.4	20.48	0.12	0.05	1.63	18.36
BAA29	507089	178626	41.6	27.5	4.4	0.5	15.3	21.5	20.51	0.12	0.05	1.63	18.38
BAA30	507176	178628	42.7	27.9	4.5	0.5	16.3	21.4	20.65	0.12	0.06	1.74	18.40
BAA31	507207	178632	43.2	28.1	4.5	0.5	16.7	21.5	20.71	0.12	0.06	1.79	18.40
BAA32	510172	178352	52.7	32.3	6.1	0.6	17.1	29.5	20.66	0.11	0.06	1.56	18.70
BAA33	510109	178351	52.5	32.2	6.2	0.6	16.4	29.9	20.63	0.12	0.06	1.52	18.70
BAA34	509999	178376	49.2	31.2	6.3	0.6	12.0	30.8	20.33	0.12	0.06	1.18	18.73
BAA35	510016	178407	47.6	30.7	6.2	0.6	10.3	31.0	20.18	0.12	0.06	1.03	18.73
BAA36	510157	178384	49.0	31.2	6.1	0.6	13.0	30.0	20.35	0.11	0.06	1.24	18.71
BAA37	510188	178445	46.0	30.3	5.9	0.6	9.9	30.3	20.10	0.11	0.05	0.97	18.74
BAA38	509820	178355	53.8	32.5	6.6	0.6	15.4	31.6	20.70	0.13	0.06	1.50	18.73
BAA39	509822	178396	49.7	31.4	6.5	0.6	11.0	32.1	20.31	0.12	0.06	1.10	18.75
BAA40	509392	178382	58.0	33.6	6.9	0.6	18.1	32.7	21.02	0.14	0.06	1.76	18.73
BAA41	509403	178468	50.1	31.5	6.6	0.6	9.5	33.7	20.26	0.13	0.06	0.98	18.77
BAA42	506456	178564	41.3	27.0	3.7	0.5	16.0	21.1	20.40	0.10	0.05	1.70	18.26
BAA43	507178	178659	39.1	26.9	4.5	0.5	12.7	21.5	20.29	0.12	0.05	1.37	18.41
BAA44	507066	178668	37.6	26.2	4.3	0.5	11.3	21.5	20.10	0.12	0.05	1.22	18.40
BAA45	508822	174587	38.3	25.1	11.4	1.5	5.9	19.6	19.81	0.26	0.15	0.62	18.19
BAA46	508849	174638	39.4	25.6	12.1	1.5	6.1	19.7	19.85	0.27	0.15	0.64	18.19
BAA47	508877	174691	40.8	26.1	12.9	1.5	6.7	19.8	19.92	0.28	0.15	0.69	18.20
BAA48	509007	174755	40.7	26.0	13.3	1.4	6.1	20.0	19.80	0.26	0.13	0.64	18.20
BAA49	505777	174594	33.3	22.9	8.2	1.0	4.9	19.2	19.53	0.21	0.11	0.52	18.14
BAA50	505744	174588	33.1	22.8	8.1	1.0	4.8	19.2	19.49	0.20	0.11	0.51	18.14
BAA51	505909	174592	33.9	23.1	8.3	1.1	5.3	19.2	19.70	0.24	0.12	0.55	18.14

Figure 10.26 2030MM predicted total NO_X concentrations in $\mu g/m^3$ around Heathrow

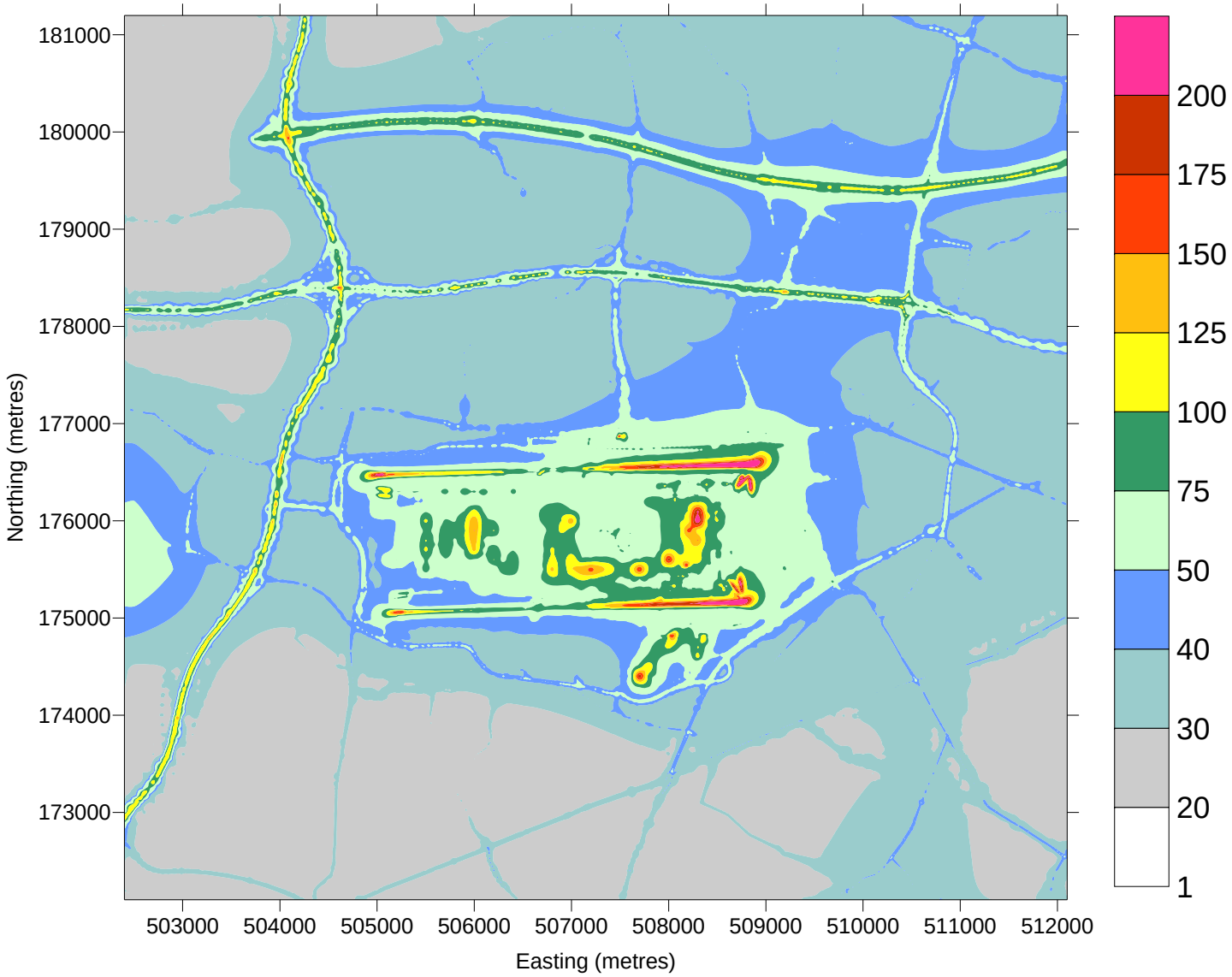

Figure 10.27 2030MM predicted total NO_2 concentrations in $\mu g/m^3$ around Heathrow

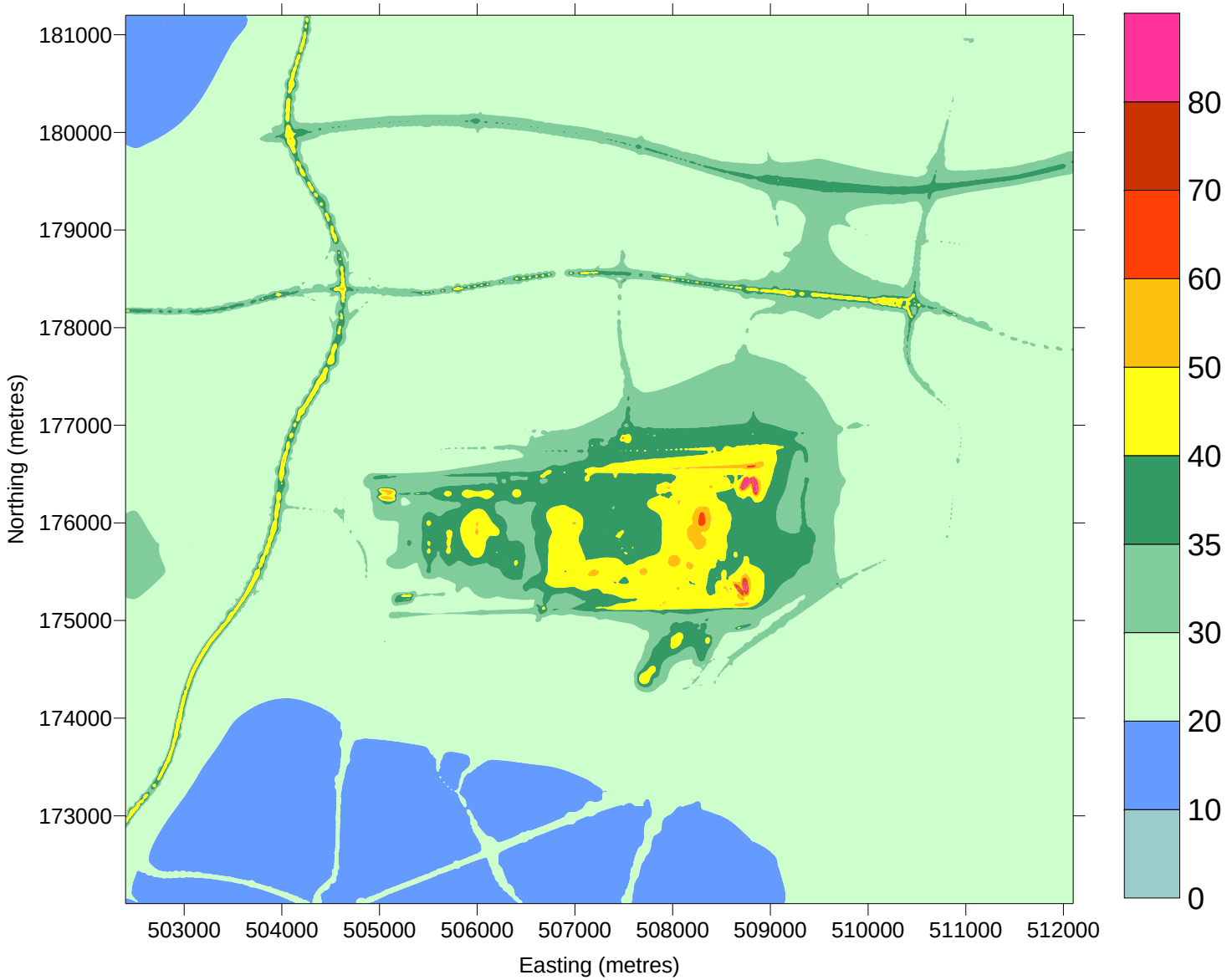

Figure 10.28 2030MM predicted NO_X concentration in $\mu g/m^3$ around Heathrow due to aircraft and other airport sources

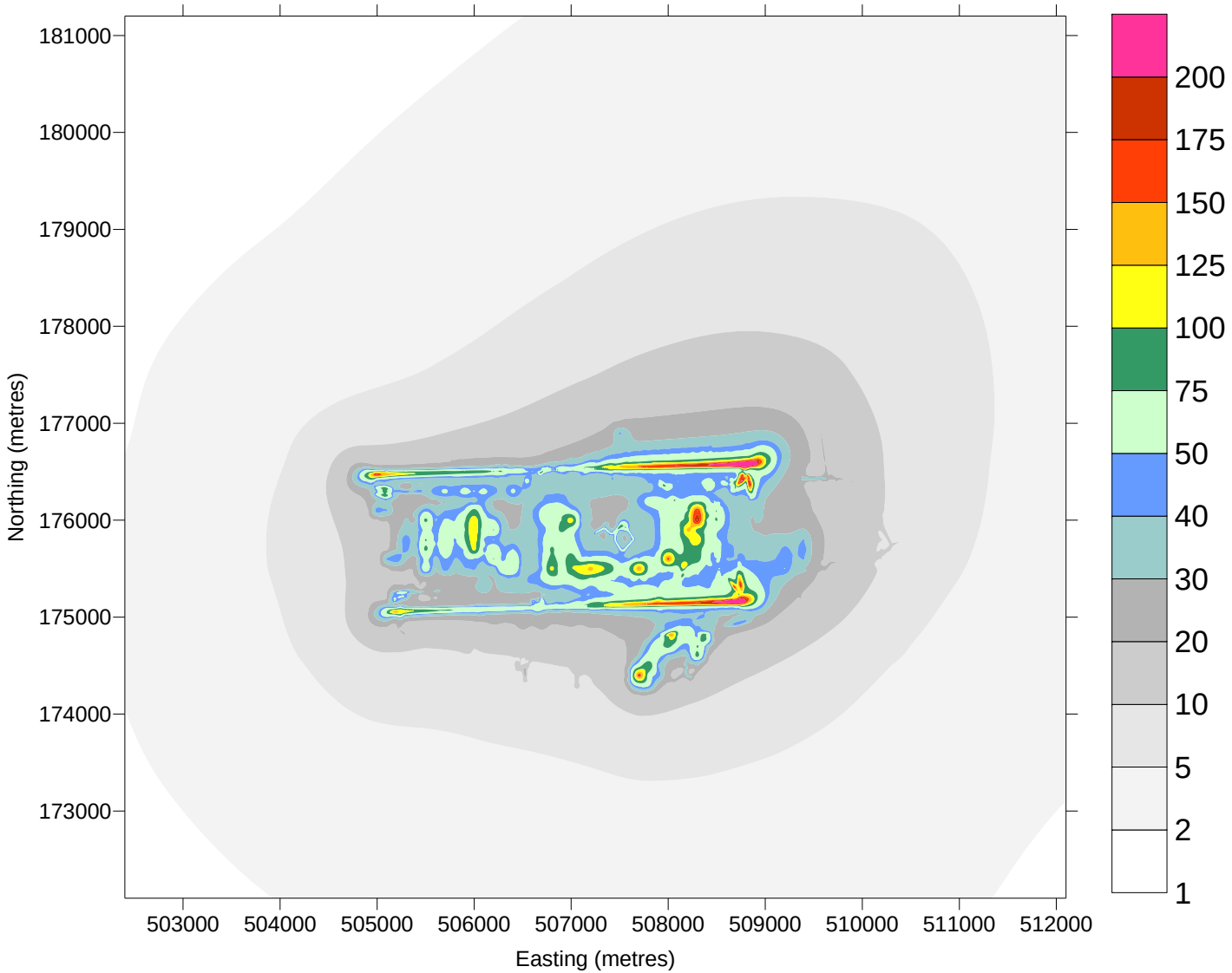

Figure 10.29 2030MM predicted NO_X concentration in $\mu g/m^3$ around Heathrow due to road sources

Predicted concentrations of NO_x, NO_2 and PM_{10} for 2020R3 at receptor locations are presented in Table 10.10.

Contour plots of predicted NO_x and NO_2 concentrations due to all sources are presented in Figure 10.30 and Figure 10.31 respectively. Contour plots of predicted NO_x concentrations due to aircraft and other airport sources and road sources are presented in Figure 10.32 and Figure 10.33 respectively.

Table 10.10 Predicted concentrations of NO_X, NO_2 and PM_{10} for 2020R3 ($\mu g/m^3$)

Receptor name	X(m)	Y(m)	Total NO_X	Total NO_2	Aircraft NO_X	Other airport NO_X	Road NO_X	Background NO_X	Total PM_{10}	Aircraft PM_{10}	Other airport PM_{10}	Road PM_{10}	Background PM_{10}
LHR2	508399	176744	79.9	41.0	47.2	2.4	6.6	23.7	20.56	1.45	0.23	0.54	18.33
LHR3	511679	180072	40.2	28.0	3.9	0.4	5.2	30.7	19.56	0.07	0.03	0.48	18.98
LHR4	509550	176997	48.7	32.1	16.1	1.5	7.1	23.9	19.33	0.25	0.13	0.59	18.36
LHR5	510370	177195	38.6	27.5	8.6	1.0	6.9	22.1	19.15	0.14	0.08	0.59	18.34
LHR6	515540	170420	28.1	19.9	1.0	0.1	4.9	22.2	18.83	0.02	0.01	0.45	18.35
LHR7	509333	175002	46.5	27.8	16.3	1.2	8.1	20.9	19.26	0.27	0.11	0.65	18.24
LHR8	505739	174497	34.9	23.6	9.0	1.2	5.5	19.2	18.95	0.21	0.12	0.47	18.15
LHR10	502741	173460	65.1	32.3	2.4	0.2	43.5	18.9	21.40	0.04	0.02	3.32	18.02
LHR11	504780	175510	42.5	27.1	11.9	2.0	7.9	20.8	19.57	0.17	0.22	0.63	18.54
LHR12	504466	175794	38.8	25.9	9.0	1.4	7.5	20.9	19.46	0.13	0.17	0.62	18.54
LHR13	504393	176591	41.7	26.9	8.4	0.8	12.1	20.4	19.30	0.12	0.09	0.93	18.17
LHR14	503535	176829	33.8	24.3	3.9	0.4	7.0	22.5	18.87	0.07	0.04	0.59	18.17
LHR15	505185	176922	38.8	26.9	10.2	1.3	6.7	20.5	19.08	0.20	0.14	0.57	18.18
LHR16	506945	178609	55.0	33.2	11.8	1.1	20.6	21.5	20.78	0.51	0.11	1.80	18.35
LHR17	506990	181919	31.6	22.9	2.5	0.3	5.7	23.1	19.03	0.06	0.03	0.52	18.43
LHR18	508279	177792	53.8	35.2	16.6	1.5	11.4	24.4	19.99	0.35	0.15	1.09	18.41
LHR19	508434	177376	52.0	34.7	18.2	1.6	6.9	25.3	19.63	0.42	0.15	0.61	18.44
LHR20	508058	177040	58.6	36.9	24.1	2.3	8.8	23.4	20.03	0.74	0.22	0.73	18.34
BA20	505127	177559	35.9	26.1	7.8	0.8	7.2	20.1	19.00	0.16	0.08	0.62	18.14
HD60	505736	177752	38.2	27.0	10.6	1.0	6.3	20.3	19.13	0.31	0.10	0.55	18.17
HD58	508414	177125	56.1	36.0	22.7	1.8	7.0	24.6	19.73	0.56	0.18	0.59	18.40
HD57	508758	177718	49.9	33.2	14.3	1.2	8.5	25.8	19.64	0.29	0.11	0.77	18.47
BA1	508582	178453	68.7	38.1	13.0	1.0	29.4	25.3	21.22	0.23	0.09	2.44	18.46
HD56	509798	178634	49.8	32.2	7.7	0.7	7.5	33.9	19.68	0.14	0.06	0.65	18.83
HS51	509127	174568	39.3	25.2	11.2	1.2	7.2	19.8	19.15	0.22	0.10	0.62	18.20
X1	505883	178463	48.9	30.3	7.9	0.7	19.6	20.7	20.31	0.31	0.07	1.72	18.21
X2	505932	177842	40.8	27.9	13.1	1.1	6.3	20.3	19.35	0.50	0.11	0.56	18.18
X3	505890	177393	37.6	27.1	10.1	1.3	5.9	20.3	19.14	0.32	0.13	0.51	18.17
X4	506146	177197	41.4	28.9	12.8	1.9	6.1	20.6	19.31	0.42	0.19	0.52	18.19

Table 10.10 (cont) Predicted concentrations of NO_X, NO_2 and PM_{10} for 2020R3 ($\mu g/m^3$)

Receptor name	X(m)	Y(m)	Total NO_X	Total NO_2	Aircraft NO_X	Other airport NO_X	Road NO_X	Background NO_X	Total PM_{10}	Aircraft PM_{10}	Other airport PM_{10}	Road PM_{10}	Background PM_{10}
X5	506156	177092	43.1	29.7	13.5	2.0	6.8	20.8	19.39	0.44	0.20	0.56	18.19
X6	506154	176991	51.4	32.1	14.2	2.0	14.2	21.0	19.92	0.48	0.20	1.04	18.20
X7	508228	177545	60.0	37.0	17.0	1.8	16.5	24.6	20.58	0.40	0.17	1.60	18.41
X8	508212	177390	56.3	36.1	18.2	1.9	11.7	24.4	20.12	0.46	0.18	1.09	18.40
X9	507873	177139	59.4	37.2	21.8	2.7	11.9	23.0	20.28	0.67	0.24	1.04	18.32
X10	508429	177012	60.5	37.3	26.1	2.0	8.0	24.4	19.89	0.66	0.19	0.66	18.38
X11	508549	176736	81.6	40.5	47.4	2.3	8.1	23.9	20.21	1.06	0.22	0.58	18.34
X12	508789	177365	53.0	34.5	17.8	1.4	8.5	25.2	19.65	0.36	0.13	0.73	18.43
X13	508735	177965	49.3	32.9	13.2	1.1	8.9	26.1	19.62	0.26	0.11	0.78	18.48
BAA1	508009	177028	59.1	37.0	24.3	2.4	9.0	23.3	20.07	0.77	0.23	0.75	18.33
BAA2	507914	177030	59.1	37.1	24.2	2.6	9.3	23.0	20.12	0.78	0.24	0.77	18.32
BAA3	508802	177048	60.8	36.9	24.9	1.7	9.8	24.5	19.78	0.45	0.16	0.78	18.38
BAA4	508762	177049	58.8	36.5	24.9	1.7	7.7	24.5	19.66	0.47	0.16	0.64	18.39
BAA5	508885	177042	58.8	36.3	25.0	1.6	7.8	24.4	19.61	0.42	0.16	0.65	18.38
BAA6	508902	177045	58.3	36.2	24.8	1.6	7.5	24.4	19.57	0.41	0.16	0.62	18.38
BAA7	508552	177102	56.7	36.1	23.3	1.8	6.8	24.8	19.68	0.53	0.17	0.58	18.40
BAA8	508598	177100	56.6	36.1	23.4	1.7	6.8	24.8	19.66	0.51	0.17	0.58	18.40
BAA9	508412	177117	56.3	36.1	22.9	1.9	7.0	24.6	19.74	0.57	0.18	0.60	18.40
BAA10	508380	177164	55.2	35.8	21.7	1.8	7.0	24.6	19.72	0.54	0.18	0.60	18.40
BAA11	508373	177231	53.9	35.4	20.4	1.8	7.0	24.7	19.69	0.50	0.17	0.61	18.41
BAA12	508366	177292	53.1	35.1	19.4	1.8	7.1	24.9	19.68	0.47	0.17	0.63	18.42
BAA13	508356	177373	52.4	34.9	18.3	1.7	7.4	25.0	19.69	0.44	0.16	0.66	18.43
BAA14	504799	176658	47.5	28.0	16.2	1.2	9.6	20.4	19.24	0.18	0.13	0.76	18.17
BAA15	504842	176702	44.0	27.6	13.9	1.2	8.4	20.4	19.16	0.17	0.13	0.68	18.17
BAA16	504966	176844	39.5	26.9	10.6	1.2	7.3	20.4	19.08	0.17	0.13	0.61	18.17
BAA17	505043	176904	38.7	26.7	10.0	1.2	7.0	20.5	19.07	0.18	0.13	0.59	18.17
BAA18	506046	176986	49.3	31.2	13.3	1.9	13.2	20.9	19.82	0.44	0.19	1.00	18.20
BAA19	506153	176991	51.4	32.1	14.2	2.0	14.2	21.0	19.92	0.48	0.20	1.04	18.20
BAA20	507307	177018	64.7	38.4	27.2	4.4	11.4	21.7	20.33	0.92	0.40	0.77	18.25
BAA21	507496	177400	56.1	36.0	23.4	5.2	6.2	21.4	19.92	0.64	0.48	0.53	18.26

Table 10.10 (cont) Predicted concentrations of NO_X, NO_2 and PM_{10} for 2020R3 ($\mu g/m^3$)

Receptor name	X(m)	Y(m)	Total NO_X	Total NO_2	Aircraft NO_X	Other airport NO_X	Road NO_X	Background NO_X	Total PM_{10}	Aircraft PM_{10}	Other airport PM_{10}	Road PM_{10}	Background PM_{10}
BAA22	509431	176952	53.3	33.5	18.6	1.6	9.1	24.0	19.51	0.28	0.14	0.74	18.35
BAA23	509544	176967	50.8	32.5	16.4	1.7	8.7	24.0	19.46	0.25	0.14	0.70	18.36
BAA24	509582	177007	48.0	31.8	15.6	1.5	7.0	23.9	19.31	0.24	0.13	0.58	18.36
BAA25	509574	177054	47.1	31.6	15.4	1.4	6.3	23.9	19.26	0.24	0.12	0.54	18.36
BAA26	506791	178593	56.2	33.3	11.1	1.1	22.6	21.4	20.93	0.52	0.11	1.99	18.32
BAA27	506928	178615	54.1	33.0	11.6	1.1	19.8	21.5	20.71	0.51	0.11	1.74	18.35
BAA28	507004	178623	53.5	33.0	11.9	1.1	18.9	21.6	20.64	0.50	0.11	1.66	18.36
BAA29	507089	178626	54.3	33.3	12.3	1.2	19.2	21.6	20.68	0.50	0.12	1.69	18.38
BAA30	507176	178628	55.7	33.9	12.7	1.2	20.2	21.6	20.78	0.49	0.12	1.77	18.40
BAA31	507207	178632	56.0	34.0	12.8	1.2	20.4	21.6	20.79	0.48	0.12	1.79	18.41
BAA32	510172	178352	57.2	34.5	7.6	0.7	19.4	29.5	20.37	0.13	0.06	1.49	18.68
BAA33	510109	178351	57.0	34.4	7.8	0.7	18.7	29.9	20.34	0.14	0.06	1.46	18.69
BAA34	509999	178376	53.5	33.4	8.0	0.7	14.0	30.8	20.06	0.14	0.06	1.13	18.71
BAA35	510016	178407	51.6	32.8	7.8	0.7	12.0	31.0	19.92	0.14	0.06	0.98	18.73
BAA36	510157	178384	53.1	33.3	7.6	0.7	14.9	29.9	20.07	0.13	0.06	1.18	18.70
BAA37	510188	178445	49.8	32.3	7.4	0.6	11.4	30.3	19.85	0.13	0.06	0.93	18.73
BAA38	509820	178355	58.8	34.8	8.4	0.7	17.9	31.7	20.39	0.15	0.07	1.45	18.72
BAA39	509822	178396	54.0	33.6	8.3	0.7	12.9	32.1	20.02	0.15	0.07	1.06	18.74
BAA40	509392	178382	63.8	36.4	9.3	0.8	20.6	33.1	20.66	0.18	0.07	1.66	18.75
BAA41	509403	178468	54.7	34.1	9.0	0.8	10.8	34.1	19.95	0.17	0.07	0.91	18.80
BAA42	506456	178564	50.6	31.4	9.6	1.0	18.8	21.3	20.51	0.50	0.10	1.66	18.26
BAA43	507178	178659	50.4	32.4	12.3	1.2	15.3	21.7	20.33	0.46	0.11	1.34	18.42
BAA44	507066	178668	48.1	31.5	11.6	1.1	13.7	21.7	20.17	0.46	0.11	1.20	18.40
BAA45	508822	174587	41.9	26.4	13.3	1.6	7.3	19.7	19.22	0.28	0.15	0.59	18.19
BAA46	508849	174638	43.1	26.9	14.1	1.6	7.6	19.8	19.25	0.29	0.15	0.62	18.20
BAA47	508877	174691	44.8	27.4	15.0	1.6	8.4	19.9	19.31	0.30	0.14	0.66	18.20
BAA48	509007	174755	44.7	27.2	15.6	1.4	7.6	20.1	19.24	0.28	0.13	0.62	18.21
BAA49	505777	174594	36.8	24.3	10.1	1.3	6.1	19.2	19.02	0.24	0.13	0.51	18.15
BAA50	505744	174588	36.6	24.2	10.0	1.3	6.0	19.3	19.01	0.23	0.12	0.50	18.15
BAA51	505909	174592	37.5	24.5	10.1	1.7	6.7	19.0	19.09	0.27	0.14	0.54	18.13

Figure 10.30 2020R3 predicted total NO_X concentrations in $\mu g/m^3$ around Heathrow.

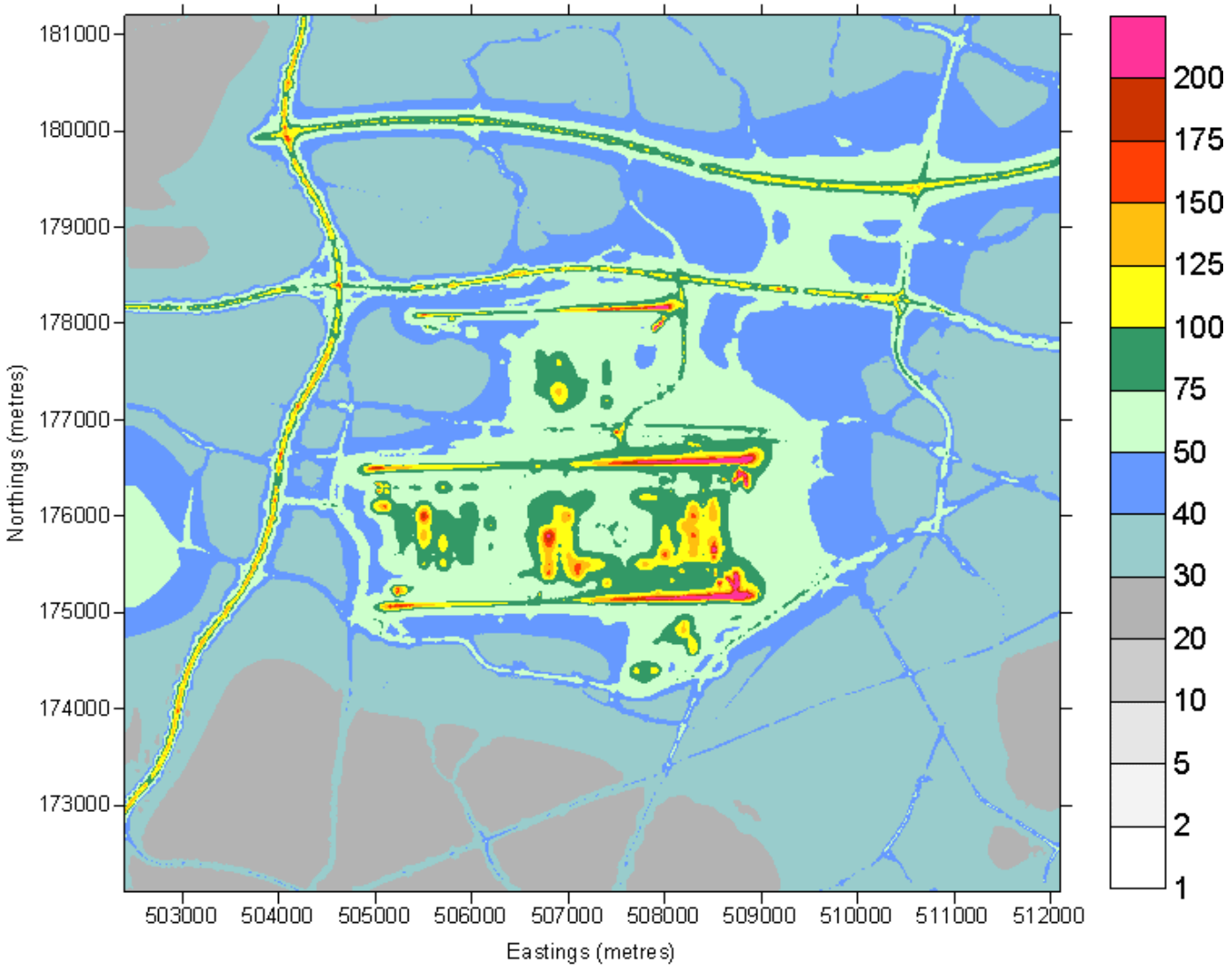

Figure 10.31 2020R3 predicted total NO_2 concentrations in $\mu g/m^3$ around Heathrow.

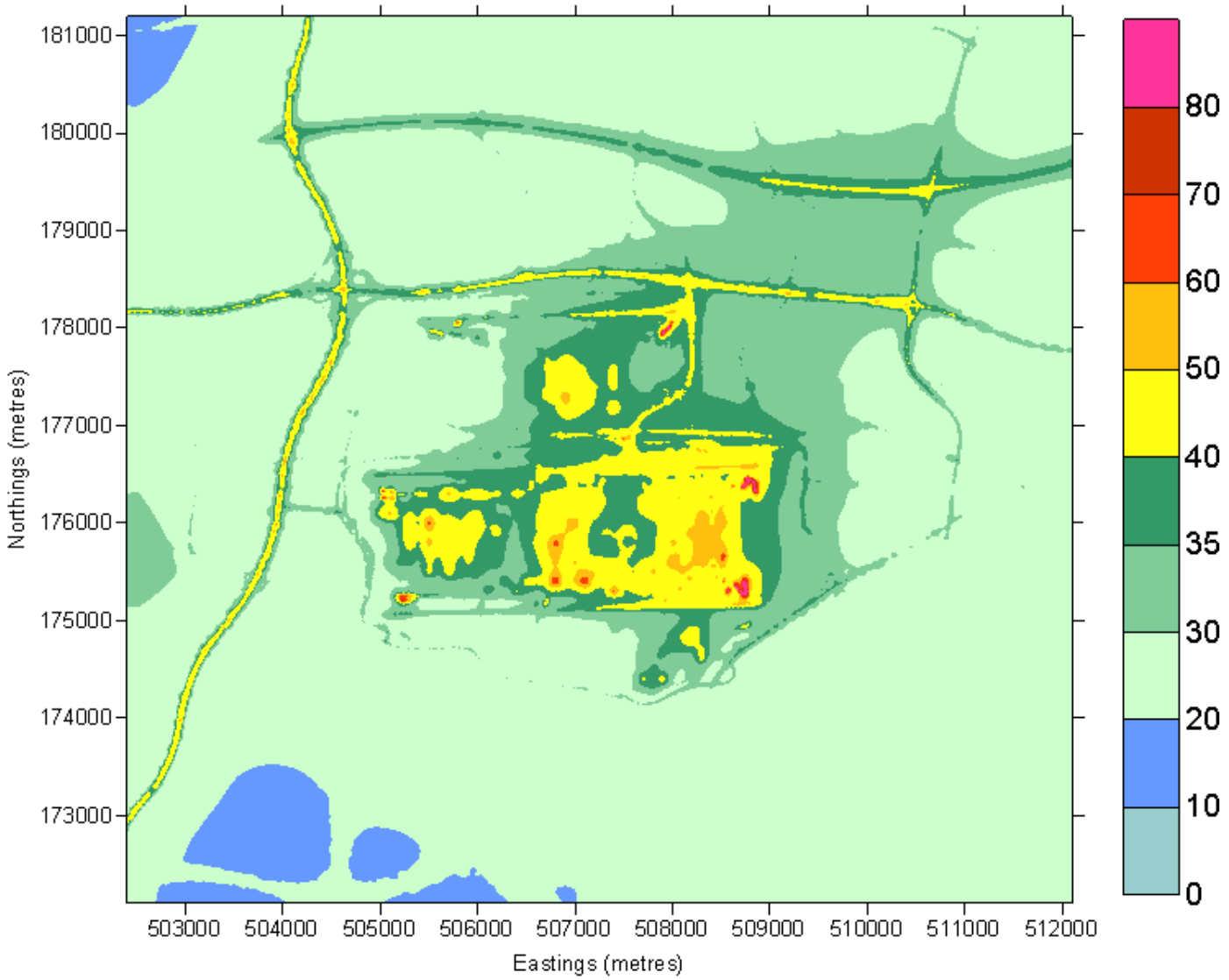

Figure 10.32 2020R3 predicted NO_X concentration in $\mu g/m^3$ around Heathrow due to aircraft and other airport sources

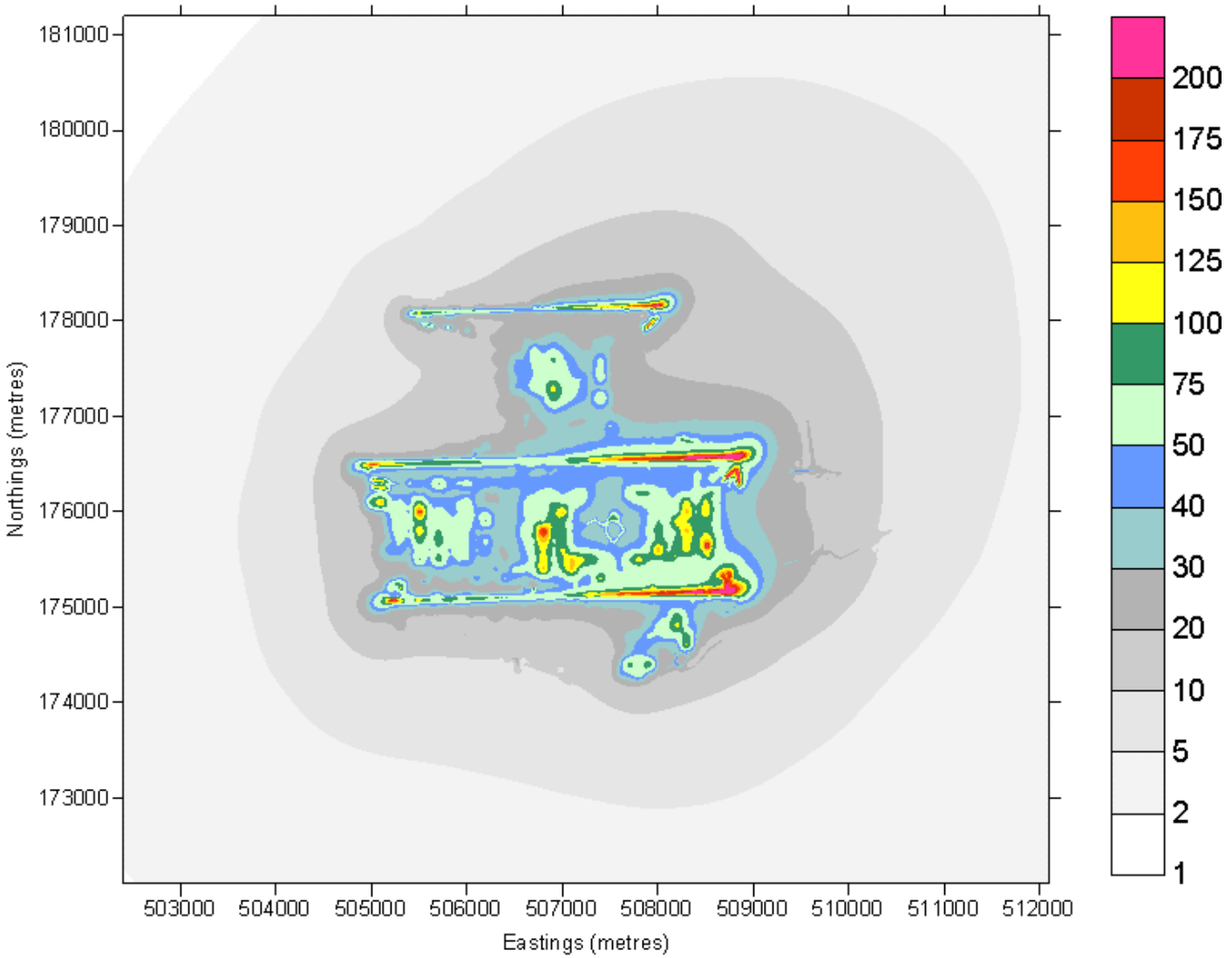

Figure 10.33 2020R3 predicted NO_X concentration in $\mu g/m^3$ around Heathrow due to road sources

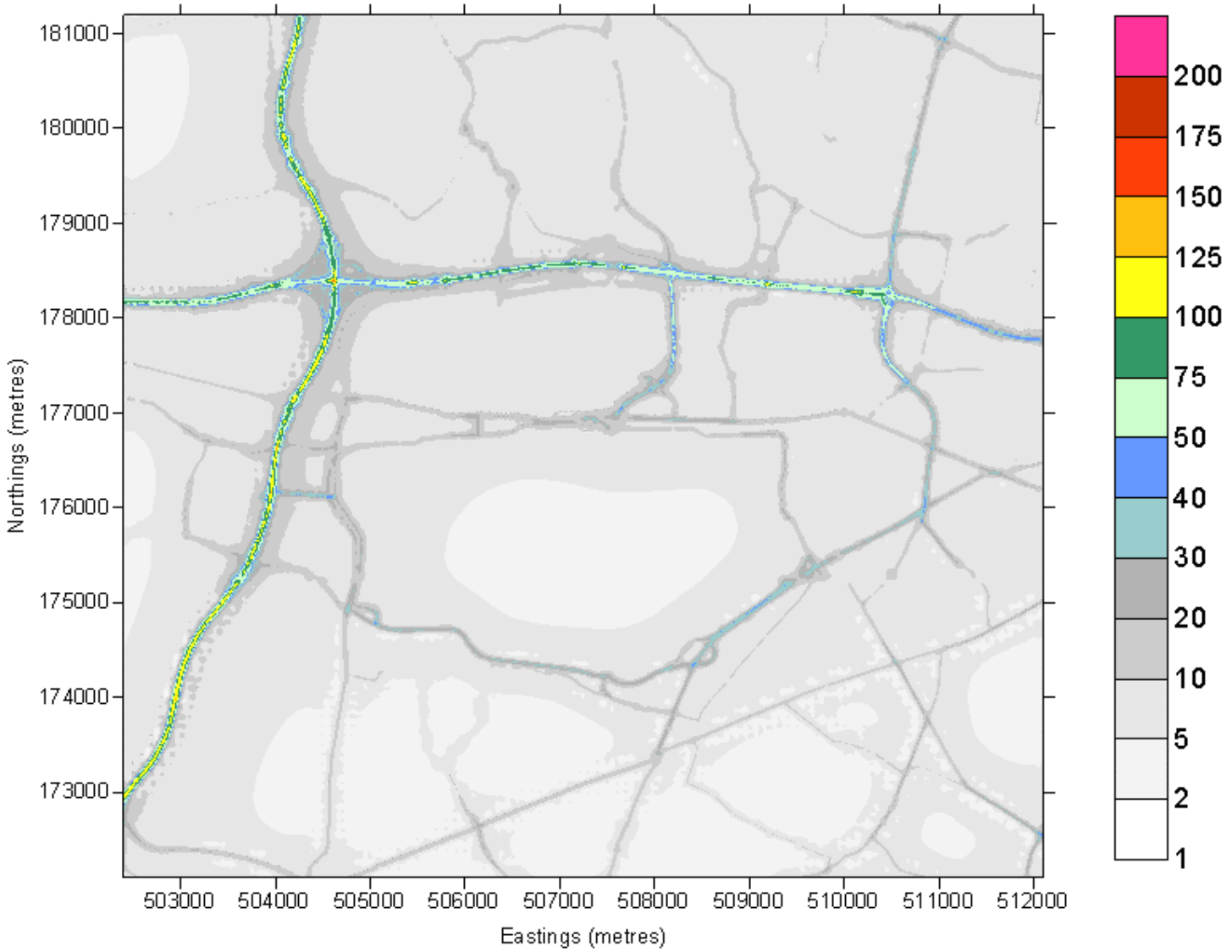

Predicted concentrations of NO_x, NO_2 and PM_{10} for 2030R3 at receptor locations are presented in Table 10.11.

Contour plots of predicted NO_x and NO_2 concentrations due to all sources are presented in Figure 10.34 and Figure 10.35 respectively. Contour plots of predicted NO_x concentrations due to aircraft and other airport sources and road sources are presented in Figure 10.36 and Figure 10.37 respectively.

Table 10.11 Predicted concentrations of NO_X, NO_2 and PM_{10} for 2030R3 ($\mu g/m^3$)

Receptor name	X(m)	Y(m)	Total NO_X	Total NO_2	Aircraft NO_X	Other airport NO_X	Road NO_X	Background NO_X	Total PM_{10}	Aircraft PM_{10}	Other airport PM_{10}	Road PM_{10}	Background PM_{10}
LHR2	508399	176744	80.2	41.3	48.8	2.3	5.4	23.7	20.63	1.49	0.24	0.56	18.33
LHR3	511679	180072	39.3	27.3	3.8	0.3	4.3	30.8	19.62	0.07	0.03	0.51	19.01
LHR4	509550	176997	46.6	31.0	15.3	1.5	5.9	23.9	19.37	0.25	0.14	0.63	18.35
LHR5	510370	177195	36.8	26.5	8.1	0.9	5.7	22.1	19.18	0.14	0.08	0.62	18.34
LHR6	515540	170420	27.3	19.4	1.0	0.1	4.0	22.2	18.86	0.02	0.01	0.47	18.36
LHR7	509333	175002	44.4	26.8	15.8	1.1	6.7	20.8	19.29	0.26	0.10	0.69	18.23
LHR8	505739	174497	33.5	22.9	8.7	1.1	4.6	19.2	18.96	0.21	0.12	0.49	18.14
LHR10	502741	173460	58.3	30.0	2.2	0.2	37.1	18.8	21.38	0.04	0.02	3.33	17.99
LHR11	504780	175510	41.3	26.5	12.0	2.0	6.6	20.7	19.61	0.18	0.24	0.66	18.52
LHR12	504466	175794	36.8	25.0	8.4	1.4	6.3	20.8	19.47	0.13	0.18	0.65	18.52
LHR13	504393	176591	39.2	25.8	7.9	0.7	10.2	20.4	19.33	0.11	0.08	0.97	18.16
LHR14	503535	176829	32.2	23.4	3.7	0.4	5.9	22.3	18.88	0.06	0.04	0.62	18.15
LHR15	505185	176922	37.2	26.1	9.9	1.2	5.6	20.5	19.08	0.19	0.13	0.60	18.16
LHR16	506945	178609	50.3	31.3	10.2	1.1	17.4	21.6	20.74	0.40	0.12	1.88	18.35
LHR17	506990	181919	30.6	22.3	2.4	0.2	4.8	23.2	19.06	0.05	0.03	0.55	18.43
LHR18	508279	177792	51.4	34.1	16.2	1.6	9.2	24.4	20.06	0.35	0.16	1.13	18.41
LHR19	508434	177376	50.6	33.9	18.0	1.6	5.6	25.4	19.67	0.42	0.16	0.64	18.44
LHR20	508058	177040	56.8	36.2	24.0	2.3	7.1	23.4	20.07	0.75	0.23	0.76	18.33
BA20	505127	177559	34.6	25.4	7.5	0.7	6.1	20.3	19.02	0.16	0.07	0.65	18.15
HD60	505736	177752	36.6	26.3	10.0	0.9	5.3	20.4	19.11	0.27	0.09	0.58	18.17
HD58	508414	177125	54.8	35.5	22.7	1.8	5.7	24.7	19.77	0.57	0.18	0.62	18.40
HD57	508758	177718	48.0	32.3	13.9	1.2	7.1	25.9	19.69	0.29	0.12	0.81	18.47
BA1	508582	178453	63.3	36.1	12.2	1.0	24.8	25.3	21.38	0.23	0.10	2.59	18.46
HD56	509798	178634	48.4	31.3	7.4	0.6	6.2	34.1	19.73	0.14	0.06	0.68	18.85
HS51	509127	174568	37.3	24.2	10.5	1.0	6.0	19.7	19.17	0.21	0.10	0.65	18.20
X1	505883	178463	45.1	28.8	6.9	0.7	16.6	20.9	20.31	0.25	0.07	1.78	18.21
X2	505932	177842	38.4	26.9	11.7	0.9	5.3	20.5	19.26	0.40	0.10	0.58	18.18
X3	505890	177393	36.7	26.6	10.3	1.2	5.0	20.3	19.12	0.30	0.13	0.54	18.17
X4	506146	177197	39.9	28.3	12.7	1.6	5.1	20.6	19.28	0.39	0.17	0.54	18.18

Table 10.11 (cont) Predicted concentrations of NO_X, NO_2 and PM_{10} for 2030R3 ($\mu g/m^3$)

Receptor name	X(m)	Y(m)	Total NO_X	Total NO_2	Aircraft NO_X	Other airport NO_X	Road NO_X	Background NO_X	Total PM_{10}	Aircraft PM_{10}	Other airport PM_{10}	Road PM_{10}	Background PM_{10}
X5	506156	177092	41.3	28.9	13.3	1.6	5.7	20.8	19.37	0.42	0.18	0.58	18.19
X6	506154	176991	48.2	31.0	13.9	1.7	11.7	21.0	19.93	0.46	0.19	1.09	18.19
X7	508228	177545	56.9	35.8	17.0	1.8	13.4	24.7	20.69	0.41	0.19	1.68	18.42
X8	508212	177390	54.1	35.2	18.3	1.9	9.5	24.5	20.20	0.46	0.19	1.14	18.40
X9	507873	177139	57.3	36.4	22.0	2.7	9.7	23.0	20.34	0.68	0.27	1.07	18.32
X10	508429	177012	59.1	36.7	26.3	1.9	6.5	24.4	19.94	0.67	0.20	0.69	18.38
X11	508549	176736	80.2	40.2	47.5	2.2	6.6	23.9	20.26	1.08	0.24	0.61	18.34
X12	508789	177365	51.1	33.7	17.4	1.4	7.1	25.3	19.71	0.36	0.14	0.77	18.44
X13	508735	177965	47.3	31.9	12.7	1.1	7.4	26.1	19.67	0.26	0.11	0.82	18.48
BAA1	508009	177028	57.2	36.3	24.2	2.3	7.3	23.3	20.12	0.77	0.24	0.78	18.33
BAA2	507914	177030	57.2	36.3	24.0	2.6	7.6	23.0	20.16	0.79	0.25	0.81	18.32
BAA3	508802	177048	58.3	36.0	24.3	1.6	7.9	24.5	19.83	0.46	0.17	0.82	18.38
BAA4	508762	177049	56.9	35.7	24.4	1.6	6.3	24.5	19.70	0.47	0.17	0.67	18.39
BAA5	508885	177042	56.6	35.5	24.2	1.6	6.4	24.5	19.65	0.42	0.17	0.68	18.38
BAA6	508902	177045	56.2	35.3	24.0	1.6	6.1	24.5	19.61	0.42	0.16	0.65	18.38
BAA7	508552	177102	55.3	35.5	23.2	1.7	5.6	24.8	19.72	0.54	0.18	0.61	18.40
BAA8	508598	177100	55.2	35.5	23.2	1.7	5.6	24.8	19.70	0.52	0.17	0.60	18.40
BAA9	508412	177117	55.0	35.5	22.9	1.8	5.7	24.6	19.78	0.57	0.19	0.62	18.40
BAA10	508380	177164	53.9	35.2	21.7	1.8	5.7	24.7	19.76	0.55	0.18	0.63	18.40
BAA11	508373	177231	52.6	34.7	20.4	1.7	5.7	24.8	19.73	0.51	0.18	0.64	18.41
BAA12	508366	177292	51.8	34.4	19.3	1.7	5.8	24.9	19.72	0.48	0.18	0.65	18.42
BAA13	508356	177373	51.0	34.1	18.2	1.7	6.1	25.1	19.73	0.44	0.17	0.69	18.43
BAA14	504799	176658	44.2	26.9	14.8	1.1	7.9	20.3	19.24	0.17	0.12	0.78	18.16
BAA15	504842	176702	41.3	26.5	12.8	1.1	7.0	20.4	19.16	0.16	0.12	0.71	18.16
BAA16	504966	176844	37.6	25.9	10.1	1.1	6.1	20.4	19.08	0.16	0.12	0.63	18.16
BAA17	505043	176904	37.0	25.9	9.6	1.1	5.9	20.4	19.07	0.17	0.12	0.62	18.16
BAA18	506046	176986	46.6	30.2	13.1	1.6	10.9	20.9	19.84	0.42	0.18	1.05	18.19
BAA19	506153	176991	48.3	31.0	13.9	1.7	11.7	21.0	19.93	0.46	0.19	1.09	18.19
BAA20	507307	177018	63.5	37.9	28.0	4.5	9.3	21.7	20.42	0.93	0.45	0.79	18.25
BAA21	507496	177400	64.4	38.3	30.0	7.9	5.1	21.4	20.40	0.78	0.81	0.56	18.25

Table 10.11 (cont) Predicted concentrations of NO_X, NO_2 and PM_{10} for 2030R3 ($\mu g/m^3$)

Receptor name	X(m)	Y(m)	Total NO_X	Total NO_2	Aircraft NO_X	Other airport NO_X	Road NO_X	Background NO_X	Total PM_{10}	Aircraft PM_{10}	Other airport PM_{10}	Road PM_{10}	Background PM_{10}
BAA22	509431	176952	50.7	32.4	17.6	1.5	7.6	24.0	19.56	0.28	0.14	0.79	18.35
BAA23	509544	176967	48.3	31.4	15.5	1.7	7.3	23.9	19.50	0.25	0.15	0.75	18.35
BAA24	509582	177007	45.9	30.7	14.8	1.5	5.8	23.8	19.35	0.24	0.14	0.62	18.36
BAA25	509574	177054	45.1	30.6	14.6	1.4	5.2	23.9	19.29	0.24	0.13	0.57	18.36
BAA26	506791	178593	51.1	31.3	9.4	1.0	19.1	21.6	20.90	0.40	0.11	2.07	18.32
BAA27	506928	178615	49.5	31.1	10.0	1.1	16.7	21.6	20.67	0.40	0.12	1.81	18.35
BAA28	507004	178623	49.2	31.2	10.4	1.1	16.0	21.7	20.61	0.39	0.12	1.73	18.37
BAA29	507089	178626	50.0	31.5	10.9	1.1	16.2	21.7	20.66	0.39	0.12	1.76	18.38
BAA30	507176	178628	51.3	32.1	11.4	1.2	17.0	21.7	20.76	0.39	0.13	1.85	18.40
BAA31	507207	178632	51.6	32.2	11.5	1.2	17.2	21.7	20.79	0.39	0.13	1.87	18.41
BAA32	510172	178352	54.2	33.1	7.2	0.6	16.7	29.7	20.45	0.13	0.06	1.56	18.70
BAA33	510109	178351	54.1	33.0	7.3	0.6	16.0	30.1	20.42	0.13	0.06	1.52	18.70
BAA34	509999	178376	51.0	32.1	7.5	0.7	11.8	31.0	20.11	0.14	0.07	1.18	18.73
BAA35	510016	178407	49.4	31.7	7.4	0.7	10.1	31.2	19.97	0.14	0.06	1.02	18.74
BAA36	510157	178384	50.7	32.1	7.2	0.6	12.8	30.1	20.14	0.13	0.06	1.23	18.72
BAA37	510188	178445	47.8	31.2	7.0	0.6	9.7	30.5	19.90	0.13	0.06	0.97	18.74
BAA38	509820	178355	55.7	33.5	8.0	0.7	15.1	31.9	20.45	0.15	0.07	1.50	18.74
BAA39	509822	178396	51.7	32.4	7.9	0.7	10.8	32.3	20.07	0.15	0.07	1.10	18.76
BAA40	509392	178382	60.3	34.9	8.9	0.8	17.4	33.3	20.73	0.17	0.08	1.72	18.77
BAA41	509403	178468	52.6	33.0	8.6	0.7	9.0	34.3	20.00	0.17	0.07	0.94	18.81
BAA42	506456	178564	46.1	29.6	8.0	0.9	15.9	21.4	20.46	0.38	0.09	1.73	18.26
BAA43	507178	178659	46.8	30.8	11.0	1.1	12.8	21.8	20.31	0.37	0.12	1.40	18.42
BAA44	507066	178668	44.6	29.9	10.3	1.1	11.5	21.8	20.13	0.37	0.12	1.25	18.40
BAA45	508822	174587	39.4	25.2	12.2	1.4	6.0	19.7	19.23	0.27	0.14	0.63	18.19
BAA46	508849	174638	40.6	25.7	13.1	1.4	6.4	19.8	19.27	0.28	0.14	0.65	18.20
BAA47	508877	174691	42.2	26.2	14.1	1.4	6.9	19.8	19.33	0.29	0.14	0.70	18.20
BAA48	509007	174755	42.4	26.1	14.8	1.2	6.3	20.0	19.26	0.28	0.12	0.65	18.20
BAA49	505777	174594	35.4	23.6	9.9	1.2	5.1	19.3	19.03	0.24	0.13	0.53	18.14
BAA50	505744	174588	35.2	23.5	9.8	1.1	5.0	19.3	19.02	0.23	0.12	0.53	18.14
BAA51	505909	174592	36.3	23.9	10.1	1.3	5.6	19.3	19.10	0.27	0.13	0.56	18.14

Figure 10.34 2030R3 predicted total NO_X concentrations in $\mu g/m^3$ around Heathrow.

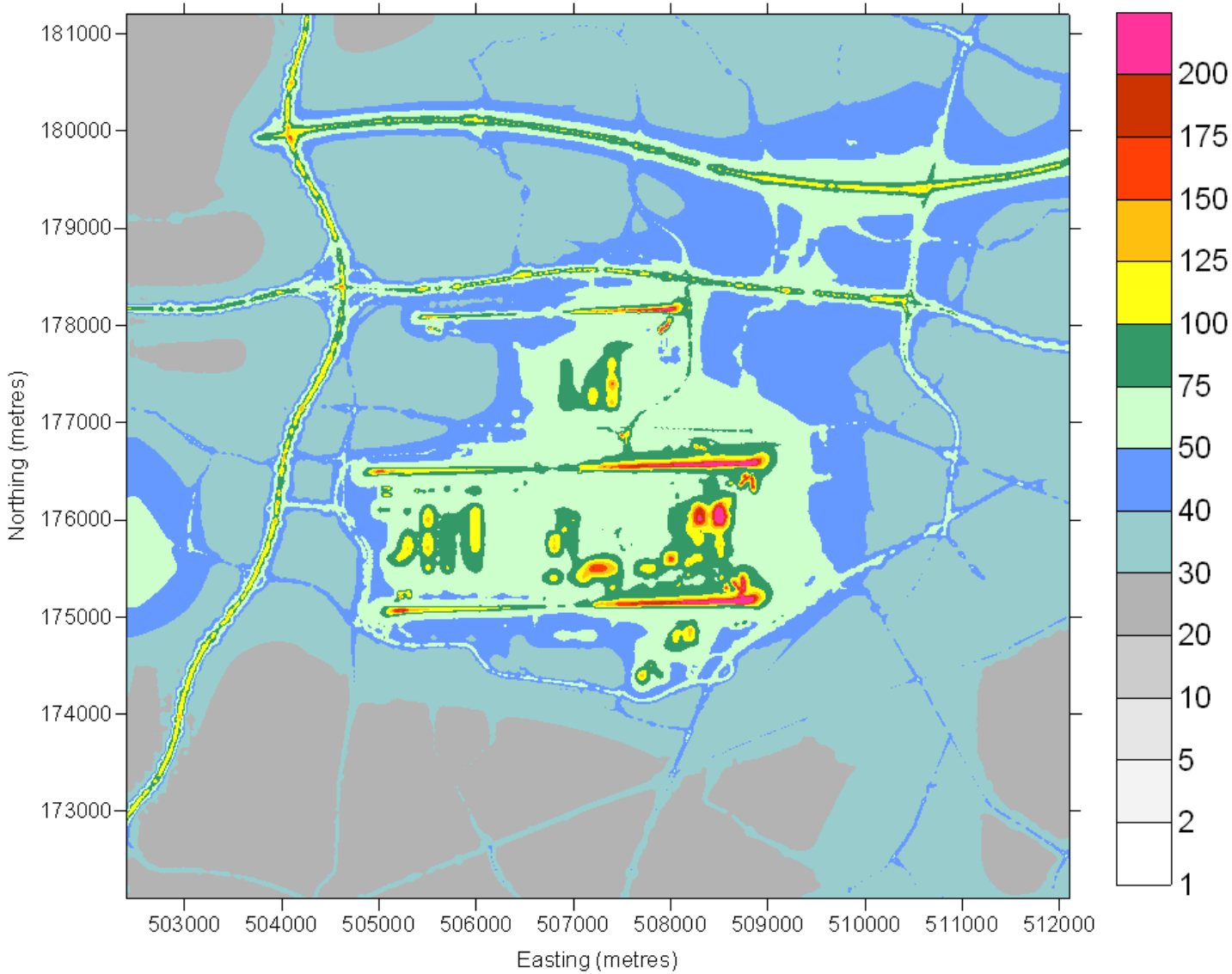

Figure 10.35 2030R3 predicted total NO_2 concentrations in $\mu g/m^3$ around Heathrow.

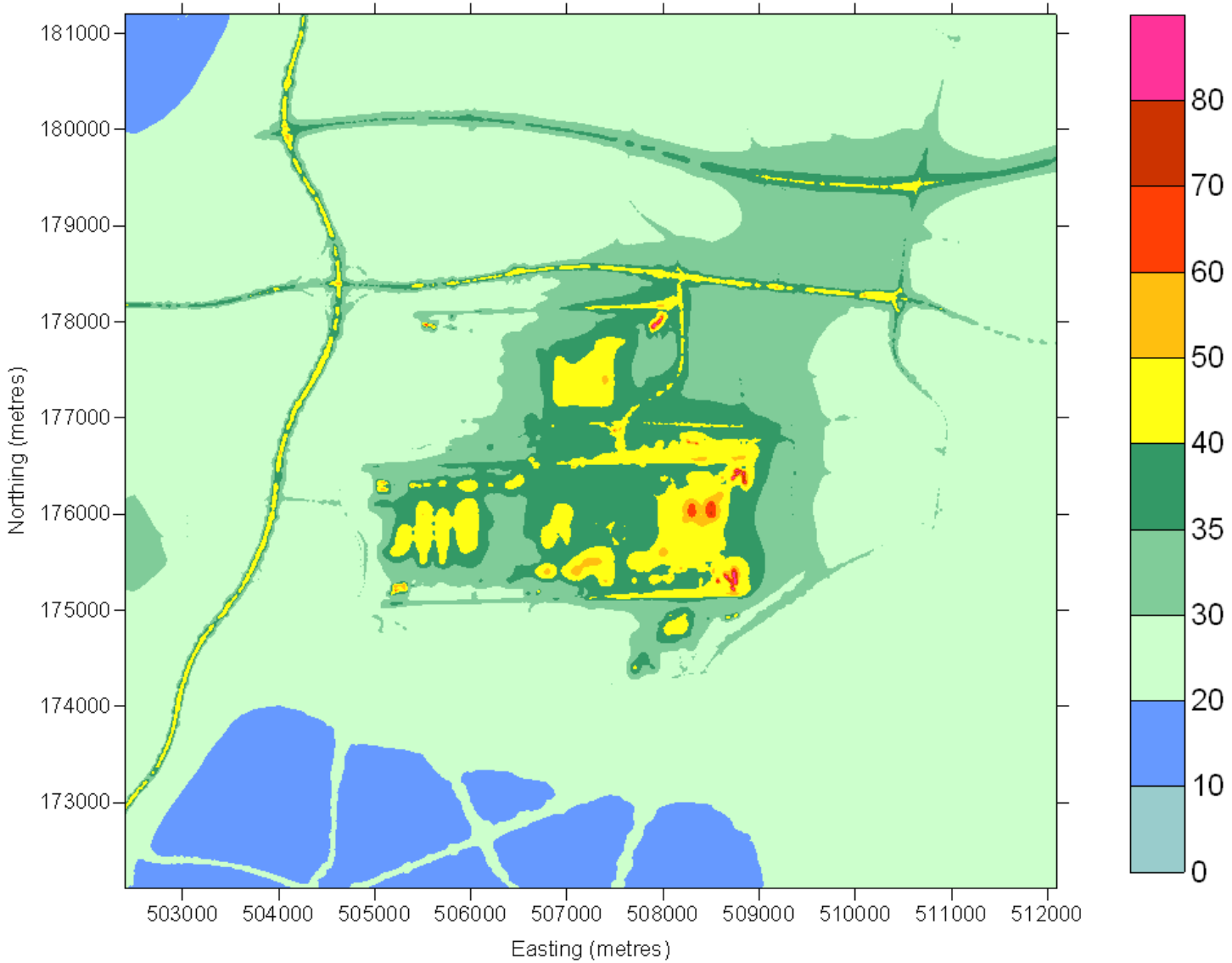

Figure 10.36 2030R3 predicted NO_X concentration in $\mu g/m^3$ around Heathrow due to aircraft and other airport sources

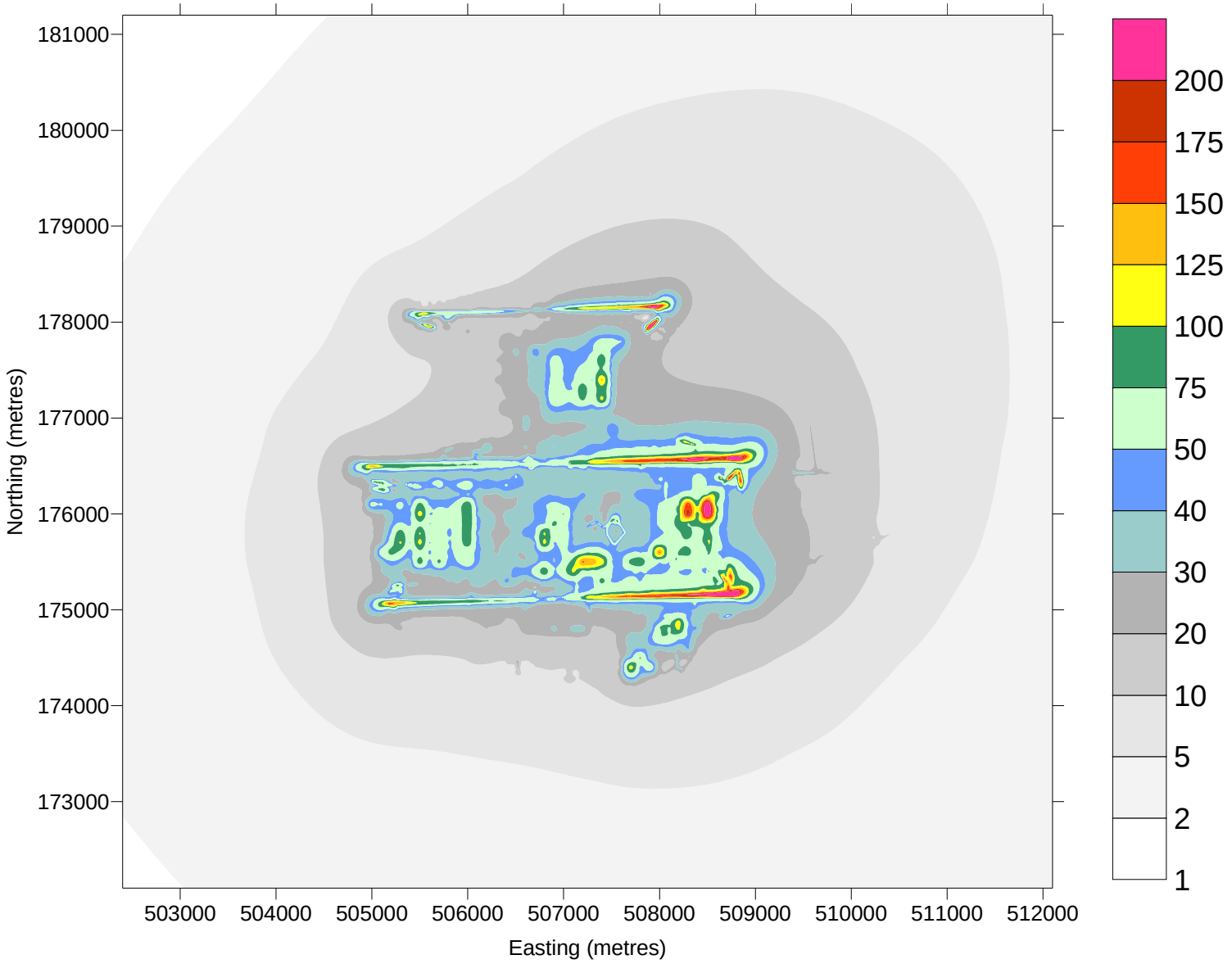

Figure 10.37 2030R3 predicted NO_X concentration in $\mu g/m^3$ around Heathrow due to road sources

11 Conclusions

Airport data from AEA and traffic data supplied by Hyder Consulting have been used to compile emissions data that were input to the ADMS-Airport air quality model to calculate annual average concentrations of NO_X, NO_2 and PM_{10} around Heathrow for the 2002 Base Case and nine future scenarios. The emissions inventory data have been compiled based on the recommendations of the Project for the Sustainable Development of Heathrow Panel Report (PSDH).[2]

The future scenarios considered are:

- 2010 Segregated Mode (2010SM)
- 2015 Segregated Mode (2015SM)
- 2015 Segregated Mode with Easterly Preference (2015EP)
- 2015 Segregated Mode with No Cranford Agreement (2015NoC)
- 2015 Mixed Mode (2015MM)
- 2015 Mixed Mode with traffic mitigation (2015MMRd)
- 2030 Mixed Mode (2030MM)
- 2020 Third Runway (2020R3)
- 2030 Third Runway (2030R3)

In Section 9 calculated concentrations for the Base case have been compared with concentrations measured by automatic monitors and are presented using a range of diagnostic tools including BOOT statistics[3], box and whisker plots, runway use dependence and polar plots. Taken as a whole the diagnostic tools show that the model has good performance.

Section 10 presented the results of the 2002 Base Case modelling and the nine future scenarios. Annual average concentrations were calculated at specified receptor locations and to be plotted as pollution maps in a domain of 9.7km x 9.1km. NO_X concentrations were calculated for all the sources together and for groups of sources: the aircraft and other airport sources; road traffic sources; other background sources (Base Case only). Concentrations of NO_2 have been calculated for all the sources together for each scenario. NO_2 annual average concentrations have also been predicted at 2,900 receptors representing residential properties for the 2015SM, 2015MM and 2015MMRd scenarios. These results are reported in the PSDH population exposure studies.[4] Annual average contour plots of PM_{10} are presented for the Base Case.

In 2002 the annual average Limit Value for annual average NO_2 concentration ($40\mu g/m^3$) is predicted by the modelling to be exceeded on the airport, along the motorways and some main roads, along the main railway line and in areas of Harlington. In the future cases the areas of exceedence are reduced compared with 2002 and are confined mainly to the airport and along the motorways. This reduction is largely due to the reduction in NO_X emissions from road traffic. Rail emissions are predicted to decrease in 2010 and further in 2015 due to re-engining of high speed trains so the air quality impact of the railway emissions is predicted to decrease in future years. In all the scenarios background PM_{10} is the main contributor to total PM_{10} concentrations. The airport contribution to total PM_{10} concentrations is in all cases small.

In the 2030 mixed mode (2030MM) scenario there are no calculated exceedences of the Limit Value at the receptors considered. Note, however, that scenario 2030MM is included for comparative purposes. Mixed mode operation would be superseded by third runway operation from around 2020.

In the future scenarios modelled the predicted concentrations show the following features:

- ***Mixed Mode (2015MM):*** In the absence of any other changes the effect of mixed mode compared to segregated mode is to increase concentrations to the north-west of the airport (Longford) and to decrease concentrations to the south-west (Stanwell).

- ***Third Runway, MDL and MLD (2020R3, 2030R3):*** The hybrid results have been constructed assuming the airport operates with equal alternation between MDL and MLD modes of operation. The take-off emissions are the most significant ground level emissions and therefore in the MDL mode of operation higher concentrations are predicted to the north-east of the airport when 27C is used for take-offs than under MLD operation when 27C is used for landings.

- ***Easterly Preference (2015EP):*** Compared with the westerly preference scenario (2015SM), NO_x concentrations are predicted to increase at some receptors to the west of the airport, due to the increase in emissions on the 09L and 09R runways, and to decrease at receptors to the east of the airport. The greatest predicted increase in annual average NO_2 concentrations compared with 2015SM is an increase of 5% at LHR15 near the 09L runway and the greatest decrease is 5% at X11 near to 27R.

- ***No Cranford Agreement (2015NoC):*** For the "No Cranford Agreement" scenario the estimated annual average concentrations of NO_2 were 95%-113% of the corresponding "with Cranford Agreement" (2015SM) predicted concentrations. The largest increases in NO_2 concentrations are predicted at receptors to the north-west of the airport near to 09L and the greatest decreases in concentration are at receptors to the south-west of the airport near to 09R where there is decreased activity.

- ***Roads mitigation scenario (2015MMRd):*** Decreases in predicted NO_2 annual average concentration of up to $2\mu g/m^3$ were predicted with the largest decreases in concentration along the M4 and smaller decreases near to the airport around Harlington

The EU Limit Value for PM_{10} is $40\mu g/m^3$ as an annual average. In 2002 the highest predicted annual average concentration of PM_{10} is $28.63\mu g/m^3$ at receptor LHR10 that is beside the M25. In all future scenarios the predicted annual average PM_{10} concentration does not exceed $25\mu g/m^3$. Therefore, at the receptors considered in this modelling study there are no predicted exceedences of the annual average Limit Value for PM_{10}.

The EU is currently negotiating the introduction of a target value of $25\mu g/m^3$ of $PM_{2.5}$ as an annual average, to be achieved by 2010, whilst the same value has recently been adopted as an objective in the Air Quality Strategy[1] to be achieved by 2020. As $PM_{2.5}$ is a component of PM_{10} there are no predicted exceedences of $25\mu g/m^3$ by the annual mean $PM_{2.5}$ in the future scenarios.

12 Appendix: Determination of Aircraft Modelling Categories

12.1 Introduction

This section indicates that groups of aircraft have similar dispersion characteristics and then describes how as a consequence aircraft are assigned 'modelling categories' (MCATs). For calculating dispersion in ADMS-Airport each of the aircraft in a particular MCAT are assumed to have dispersion characteristics identical to the MCAT 'leader' and therefore identical normalised concentration distribution, where the concentration is normalised by the total mass of pollutant emitted for the stage of the landing and take-off cycle.

Engine exhaust data (jet velocity, mass flow, density, NO_X production rate and temperature) and stage data (duration, length, speed and altitude) were provided on a variety of aircraft representing a majority of the aircraft movements for a year. Initially these data were provided on the 2002 aircraft. Further information was then provided on the 2015 fleet, which included all of the aircraft in the 2002 fleet and a large number of additional aircraft, to account for new fleet not in operation in 2002. Further data were provided for the 2020 and 2030 fleets in turn, each of these took the previous fleet and added some new aircraft and removed other aircraft that would no longer be present in these years. For each aircraft data were provided covering each of the stages of movement for the aircraft and for several of these stages breaking it down into further sub stages. For the later stages of take-off and also for initial climb data were provided for a variety of different thrust percentages ranging from 75% to 100% in 5% intervals.

Initially investigations were carried out to determine if the choice of thrust made any difference to the normalised concentrations. Details of this investigation can be found in Section 12.2.

To determine the MCATs four stages of aircraft movement are used, these are outlined in Table 12.1. As it was found that the thrust used made little difference to the normalised concentration distributions for an individual aircraft, take-off and initial climb were modelled for a single thrust value (75%) when determining the MCATs.

Table 12.1: Stages and sub-stages of aircraft movement

Stage	**Sub stage**
Taxi	Taxi in/out option 1
Initial climb	Valt 1 (75% thrust)
Landing	Landing 1
	Landing 2
	Landing 3
	Landing 4
Take off	Break release
	Engine lag
	Initial roll
	Take off roll 1 (75% thrust)
	Take off roll 2 (75% thrust)
	Take off roll 3 (75% thrust)
	Wheels off (75% thrust)

For each stage the same MCATs are used so that for an individual stage there may be two or more MCATs which are very similar. The method used for creating the MCATs is as follows.

1. Model each of the stages for each aircraft using the raw data.
2. Plot normalised centreline plots for each stage.
3. Use these plots to decide upon initial MCATs
4. Plot the normalised total concentration and the absolute and percentage difference to the MCAT leader within each MCAT
5. Finalise MCATs

As mentioned above when determining the MCATs the concentrations have been normalised. This normalisation is done by dividing the concentrations by the total amount of material emitted for one complete stage. So for instance for the take-off calculations the concentrations will be normalised by the total amount of material emitted for one complete take-off of the appropriate aircraft.

Initial investigations were carried out with the 2002 aircraft data, details of the MCATs produced by these can be found in Section 12.2. Section 12.3 contains details of the 2015 aircraft fleet including covering the 2002 aircraft. The additional aircraft for the 2020 and 2030 fleet are covered in Sections 12.4 and 12.5 respectively.

12.2 Initial investigations

12.2.1 Thrust

The importance of the choice of thrust was investigated. This was investigated for take-off for an A320 and an A340. Runs were carried out at 75%, 80%, 90% and 100% thrust. These runs were carried out using the Heathrow 2002 meteorological conditions but with take-off only happening for met lines with a wind direction between 180^{o} and 360^{o}.

The normalised concentration and percentage difference plots for the A320 are shown in Figure 12.1 and for the A340 in Figure 12.2. We can see from these plots that there is only a small difference between the normalised concentrations for the different thrust levels.

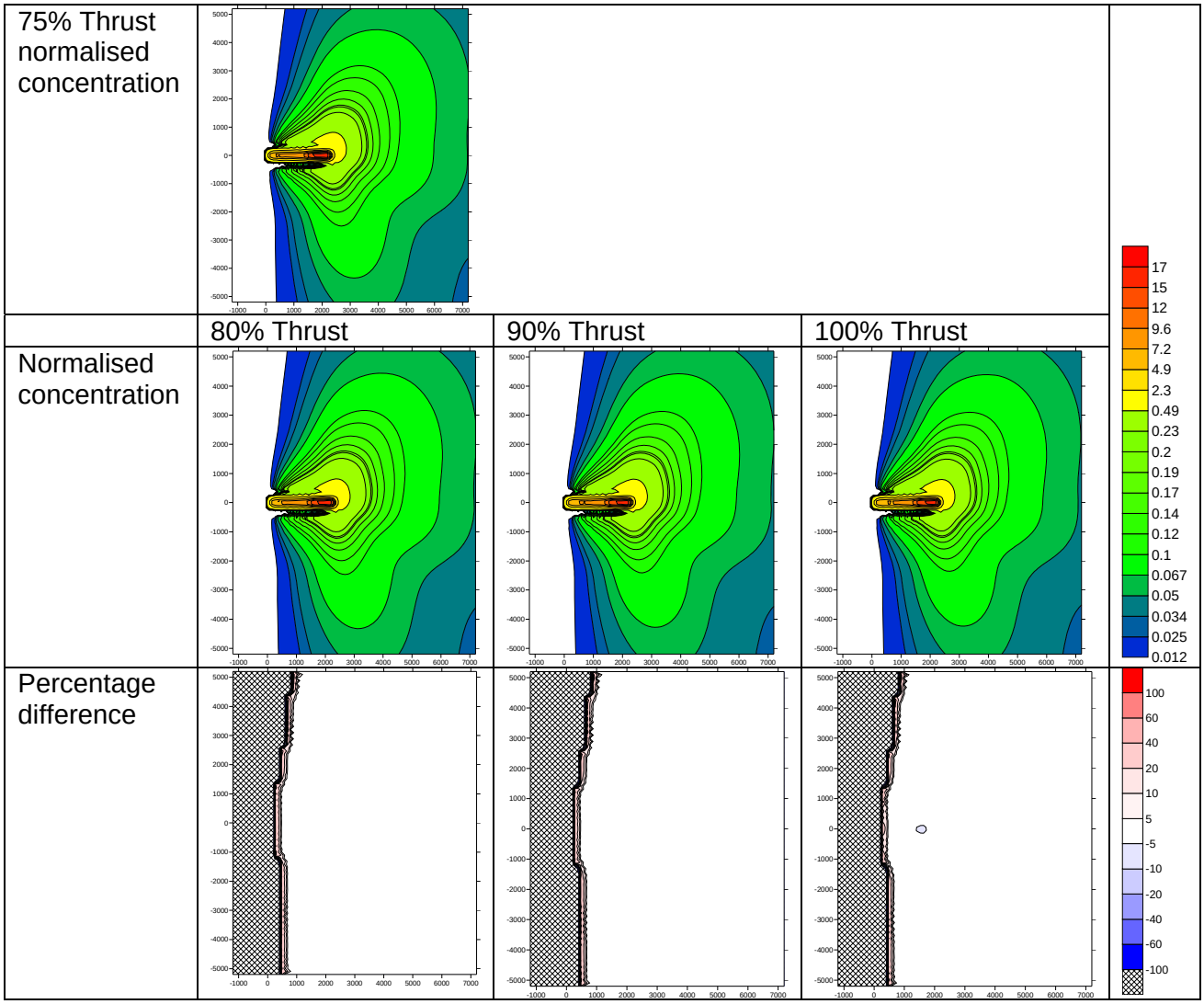

Figure 12.1. Normalised concentration and percentage difference plots for different Take-off thrusts for the A320

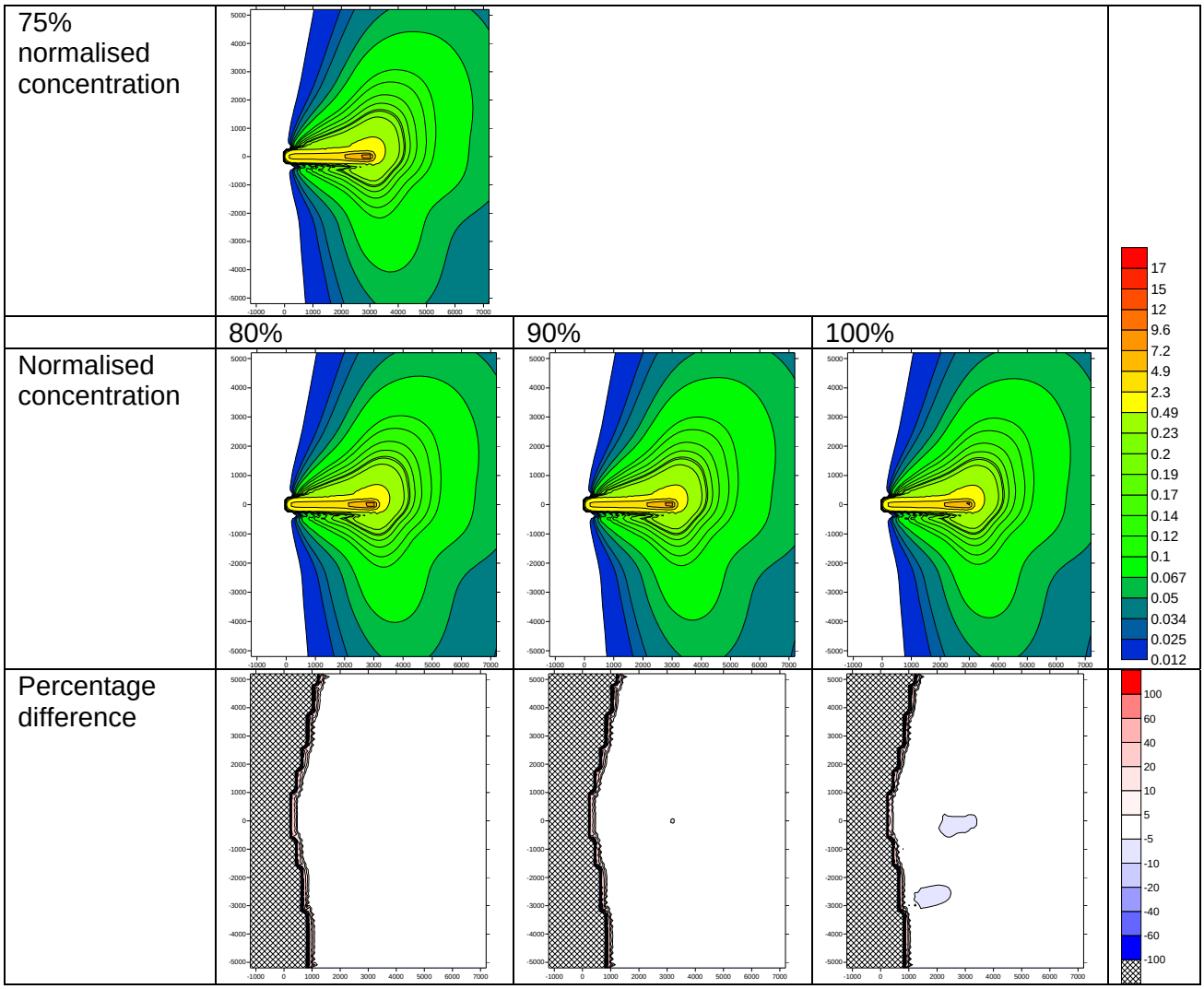

Figure 12.2. Normalised concentration and percentage difference plots for different Take-off thrusts for the A340

12.2.2 2002 MCATs

Initial investigations led to the following 2002 MCATs.

MCAT 1	A320-100/200 V2527-A5 B757-200 RB211-535E4
MCAT 2	A330-300 Trent 772 B767-300 RB211-524G/H
MCAT 3	A340-300 CFM56-5C4
MCAT 4	B737-400 CFM56-3C1
MCAT 5	B747-400 RB211-524G/H
MCAT 6	B777-200 Trent 892 B777-200 GE90-77B
MCAT 7	Concorde

Table 12.2 - Final MCATs, for the MCATs with multiple aircraft the lead aircraft has been underlined.

The data for the 2002 MCATs are covered by the 2015 fleet and so are presented as part of that. Note that 2002 has one additional MCAT, MCAT 7, which contains Concorde. No aircraft data was provided for Concorde and hence it was placed in its own MCAT.

12.2.3 2015 MCAT data

This chapter outlines the development of the 2015 MCATs. The 2002 fleet is included within this data.

The aircraft that have been examined in 2015, along with the designator used for them, are given in Table 12.3. The grammes of NOx emitted for one event of each mode each of these aircraft are given in Table 12.4.

Designator	Aircraft	Engine	UID
A320a	A320 family	V2527-A5	1|A003
A320b	A320 family	V2527-A5	1|A003
A330a	A330-300	Trent 772	3RR030/1
A330b	A330-300	Trent 772	3RR030
A330c	A330-300	Trent 772	3RR030/2
A340_300a	A340-300	CFM56-5C4	2CM015
A340_300b	A340-300	CFM56-5C4	2CM015/1
A340_300c	A340-300	CFM56-5C4	2CM015/2
A340_600a	A340-600	Trent 556	6RR041
A340_600b	A340-600	Trent 556	6RR041/1
A350_800	A350-800/B787-9 (250 l-haul)	T500 derivative	NE08/1
A350_900	A350-900/B787-10 (300 l-haul)	Trent 900/GP2700 growth	NE10/1
A380	A380	Trent 900/GP7200	NE01/1
B737_400	B737-400	CFM56-3C1	1CM007
B737_600a	B737-600/800	CFM56-7B24	3CM032
B737_600b	B737-600/800	CFM56-7B24	3CM032/1
B737_600c	B737-600/800	CFM56-7B24	3CM032/2
B747_400	B747-400	RB211-524G/H	4RR037
B747_800	B747-800	Genx – 2B67	NE02/1
B757_200	B757-200	RB211-535E4	5RR038
B767_300a	B767-300	RB211-524G/H	1RR011
B767_300b	B767-300	CF6-80C2B6F	2GE048
B777_200a	B777-200	GE90-77B	3GE059
B777_200b	B777-200	Trent 892	2RR027
B777_200c	B777-200	Trent 892	2RR027/1
B777_200d	B777-200	Trent 892	2RR027/2
B777_200e	B777-200/300	GE90-115B1	7G3099
B777_200f	B777-200/300	GE90-115B1	7G3099/1
B777_200g	B777-200/300	GE90-92B	3GE066
B777_200h	B777-200/300	GE90-92B	3GE066/1
B777_200i	B777-200/300	GE90-92B	3GE066/2
B787_3	B787-3	GENx	NE09/1
B787_8	B787-8	GENx	NE07/1

Table 12.3: The designations used for the 2015 aircraft.

Aircraft	Take-off NO_X (g)	Landing NO_X (g)	Initial Climb NO_X (g)	Taxi NO_X (g)
A320a	864	101	176	174
A320b	740	89	150	140
A330a	2,658	310	489	329
A330b	3,133	381	574	378
A330c	2,653	309	492	326
A340_300a	1,897	200	283	153
A340_300b	1,657	184	247	179
A340_300c	1,513	168	226	163
A340_600a	3,265	354	482	410
A340_600b	2,675	291	395	308
A350_800	2,567	238	497	303
A350_900	3,322	336	590	354
A380	3,747	387	492	365
B737_400	715	119	141	153
B737_600a	799	126	164	138
B737_600b	717	117	147	140
B737_600c	655	106	134	128
B747_400	2,855	405	392	311
B747_800	2,986	367	409	326
B757_200	1,168	170	232	228
B767_300a	4,368	300	799	358
B767_300b	2,205	353	390	281
B777_200a	3,209	484	681	440
B777_200b	4,210	456	907	461
B777_200c	3,943	432	845	430
B777_200d	3,600	394	772	391
B777_200e	5,427	729	1,122	568
B777_200f	4,647	581	964	470
B777_200g	4,856	643	1,039	518
B777_200h	4,178	520	896	490
B777_200i	3,732	460	801	427
B787_3	1,448	188	324	273
B787_8	2,063	241	440	314

Table 12.4: The grammes of NOx emitted for one event of each mode. Note that for taxi this event is a 2000m long taxi.

The NO_x concentrations were normalised by the NO_x emissions in Table 12.4. These normalised centreline concentrations for each the modes are plotted in Figures 12.3 to 12.6, with the final MCATs being listed in Table 12.5. Figures 12.7 to 12.63 then go through each MCAT showing the normalised concentration plots for each mode for the lead aircraft and then absolute and percentage difference plots for each of the other aircraft in that MCAT comparing them to the lead aircraft.

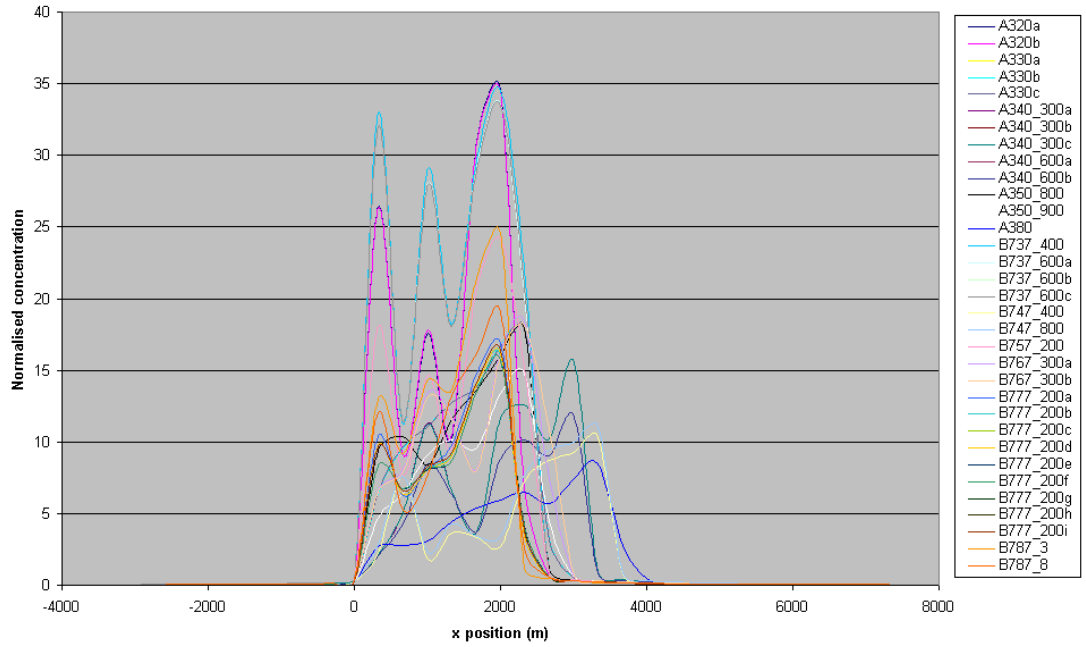

Figure 12.3: Normalised NO_x concentration plot for take off.

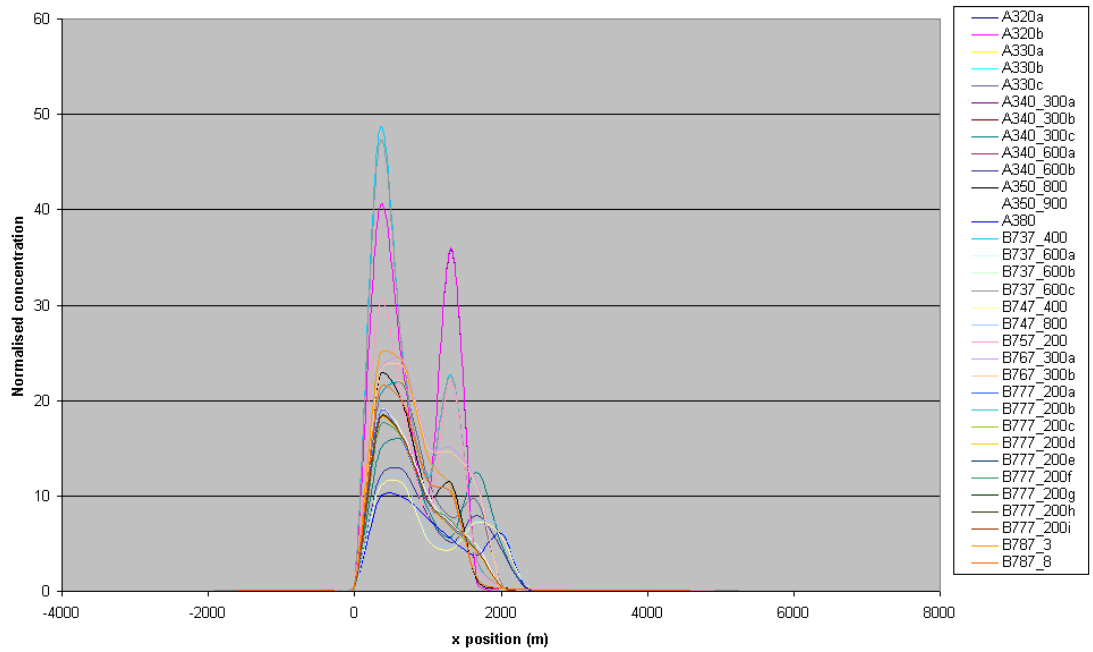

Figure 12.4: Normalised NO_x concentration plot for Landing

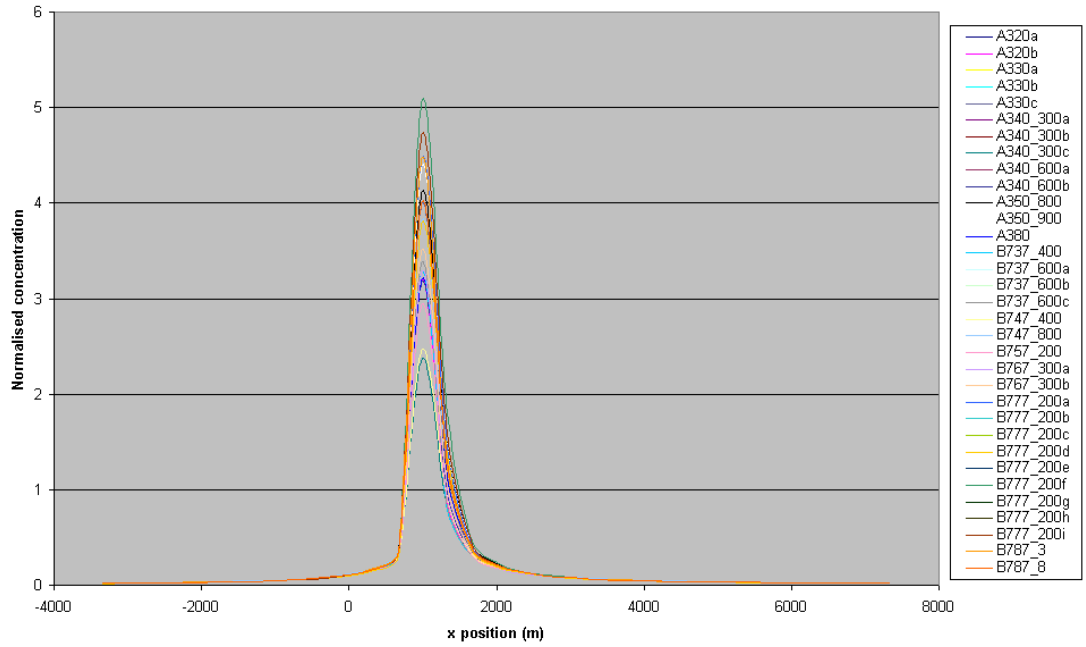

Figure 12.5: Normalised NO_x concentration plot for initial climb

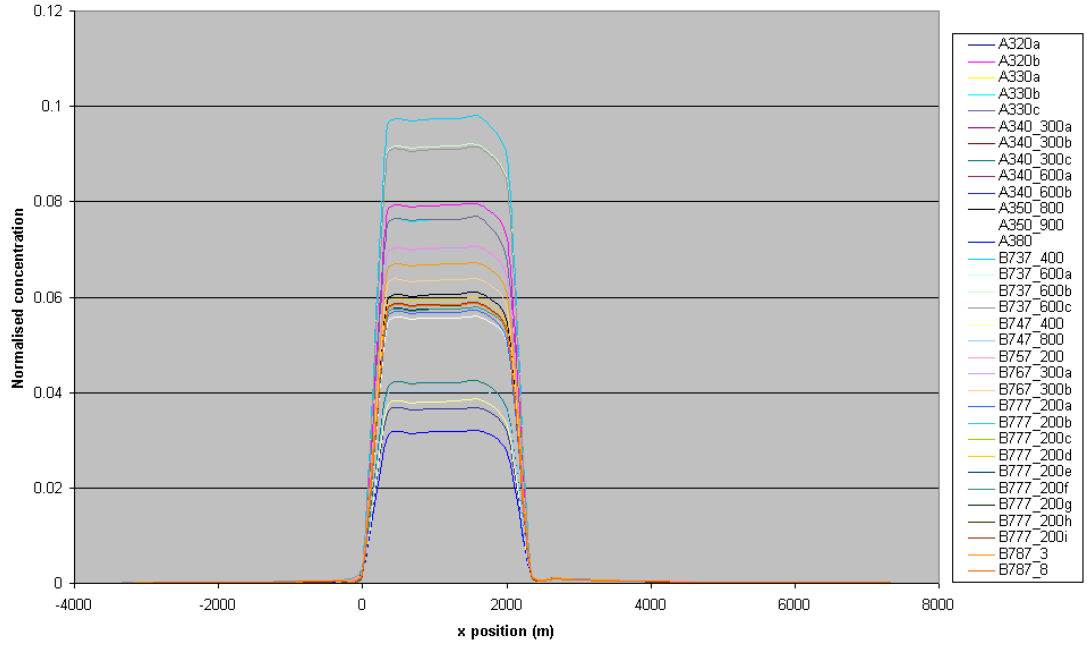

Figure 12.6: Normalised NO_x concentration plot for taxi.

MCAT	Lead aircraft	Other aircraft
1	A320 family V2527-A5	One more identical, B757-200 RB11-535E4
2	A330-300 Trent 772	Two more identical, B767-300 RB211-524G/H, B767-300 CF6-80C2B6F
3	A340-300 CFM56-5C4	Two more identical
4	B737-400 CFM56-3C1	Three identical B737-600/800 CFM56-7B24
5	B747-400 RB211-524G/H	B747-800 GENx-2B67, A380 Trent 900/GP7200
6	B777-200 Trent 892	Two more identical, B777-200 GE90-77B, two identical B777-200/300 GE90-115B1, three identical B777-200/300 GE90-92B
8	B787-3 GENx	B787-8 GENx
9	A340-600 Trent 556	One more identical
10	A350-800/B787-9 (250 L-haul) T500 derivative	A350-900/B787-10 (300 L-haul) Trent 900/GP7200 growth

Table 12.5: The final MCATs for 2015. The " identical" aircraft engines differ from the lead aircraft only in the emission rate of pollutants from the engine.

12.2.4 MCAT 1

A320a, A320b, B757_200

A320a

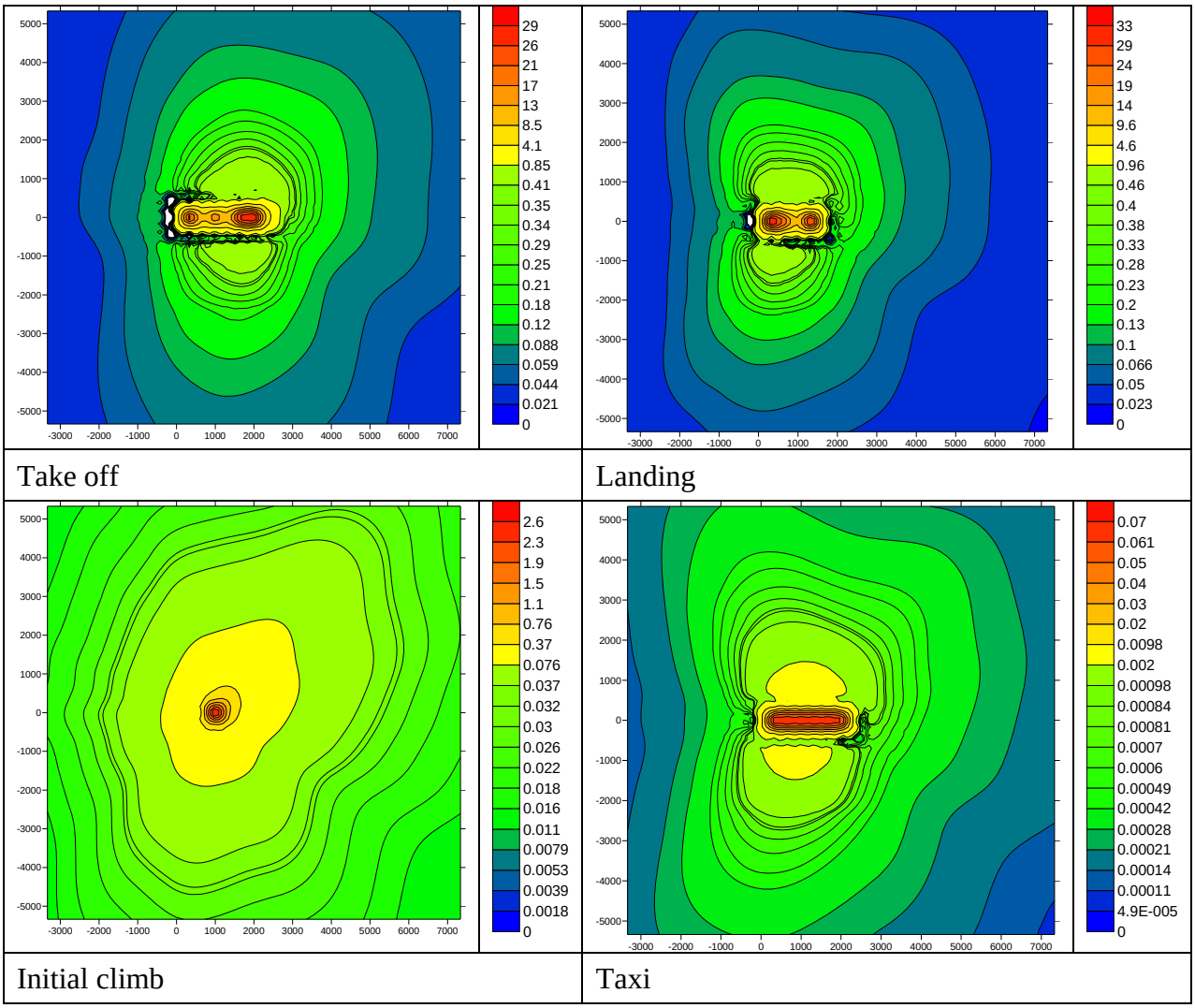

Figure 12.7: Normalised concentration plots for A320a the lead aircraft in MCAT 1.

A320b

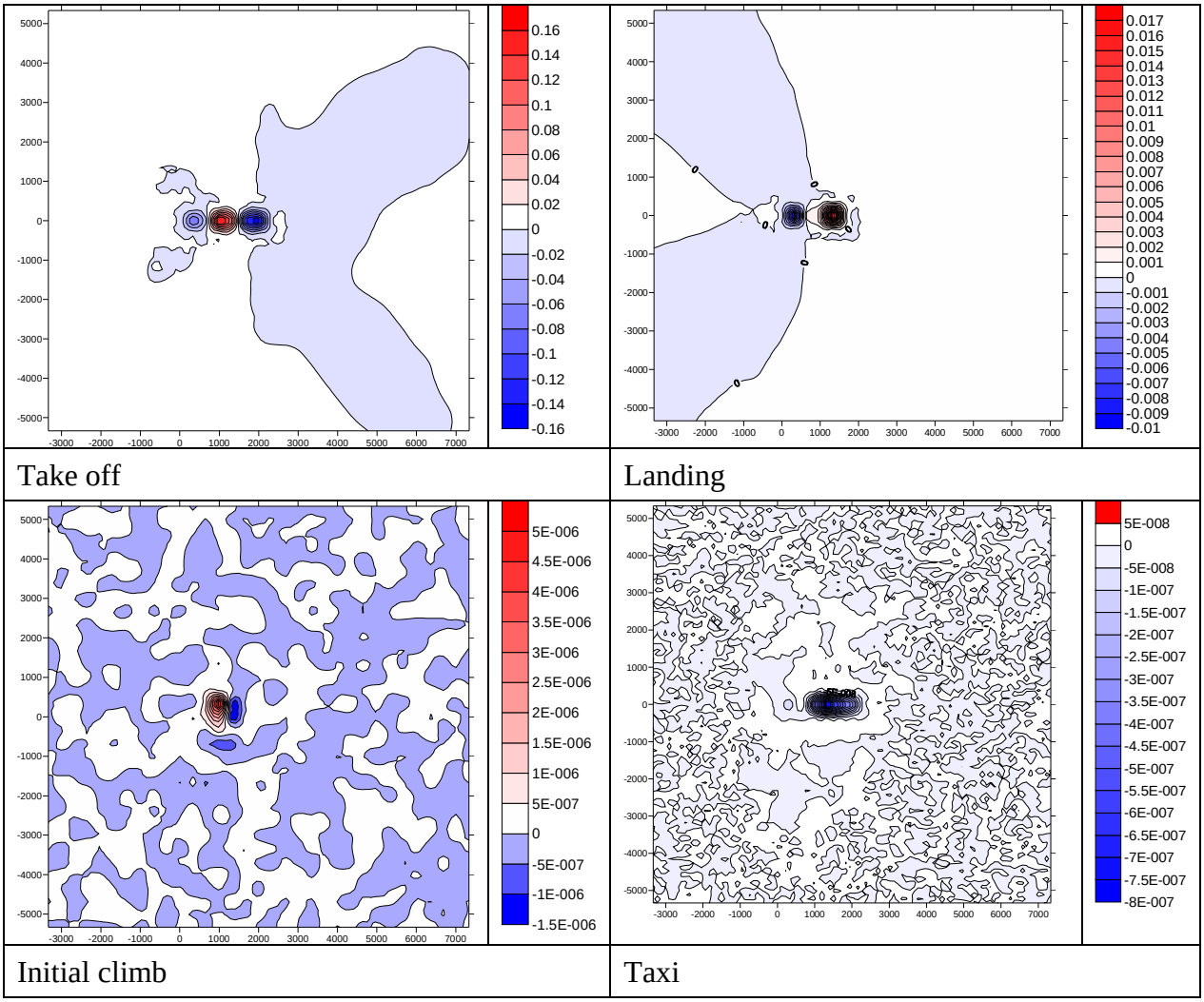

Figure 12.8: Absolute difference plots between A320b and MCAT 1 lead aircraft, A320a

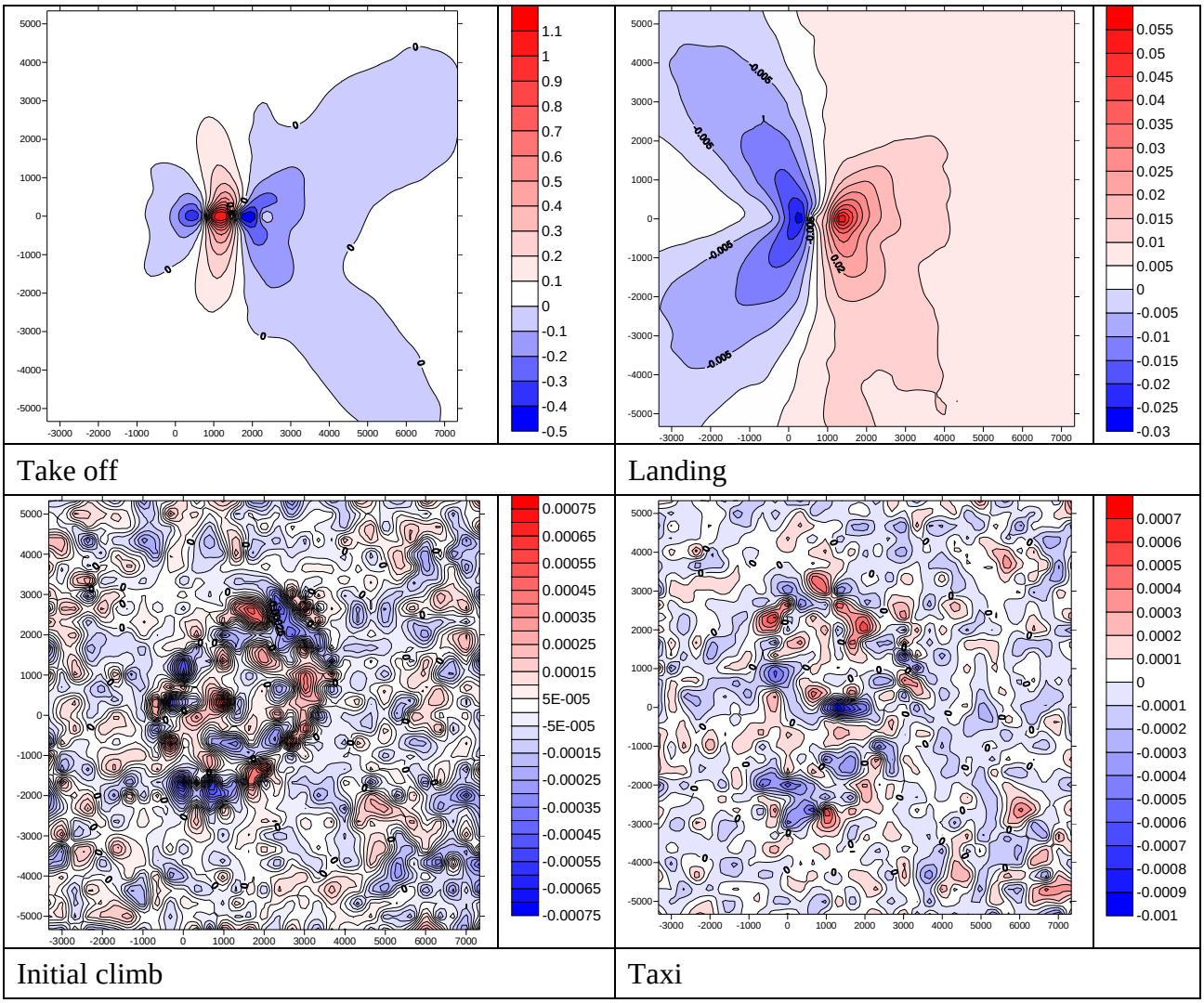

Figure 12.9: Percentage difference plots between A320b and MCAT 1 lead aircraft, A320a

B757_200

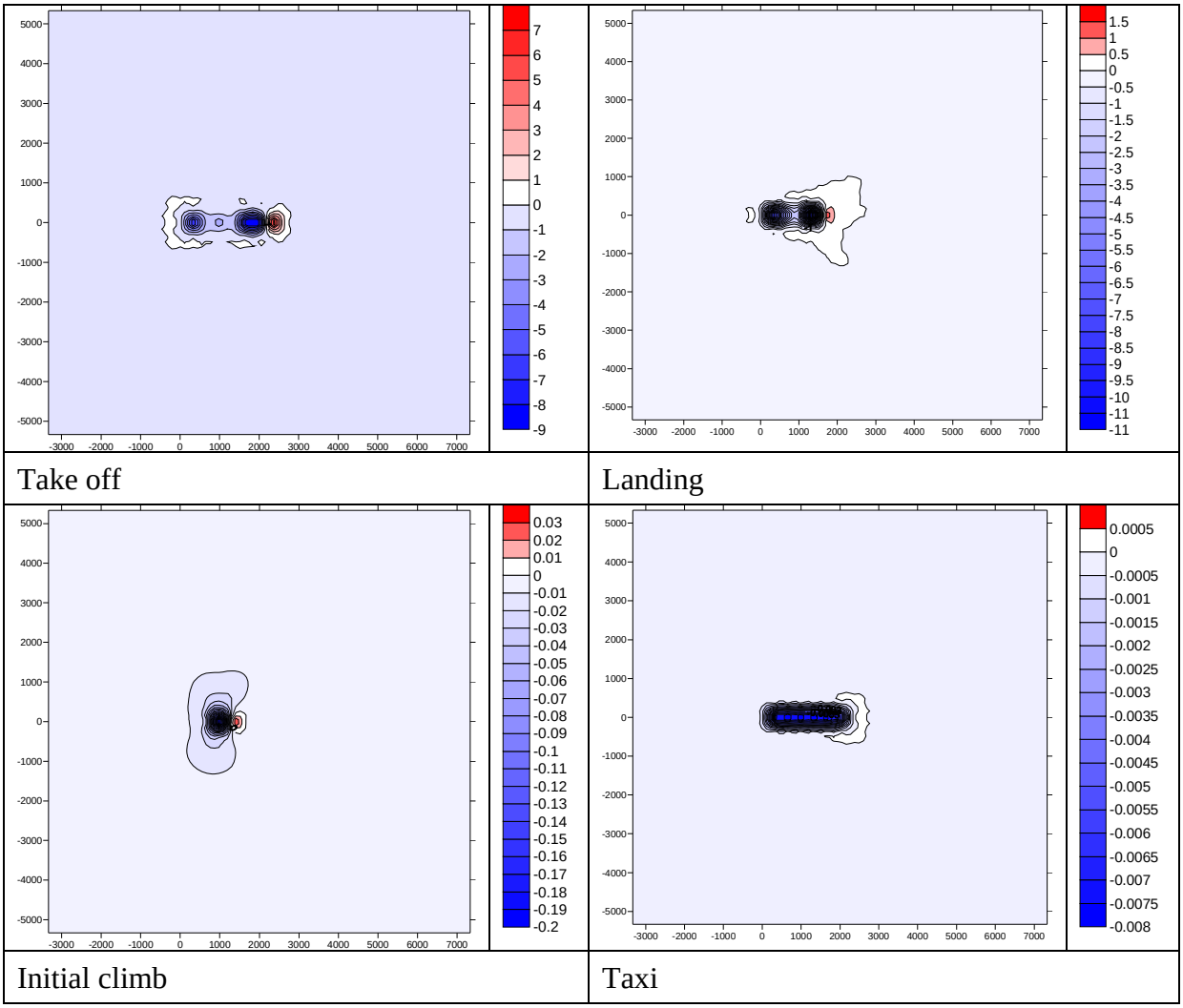

Figure 12.10: Absolute difference plots between B757_200 and MCAT 1 lead aircraft, A320a

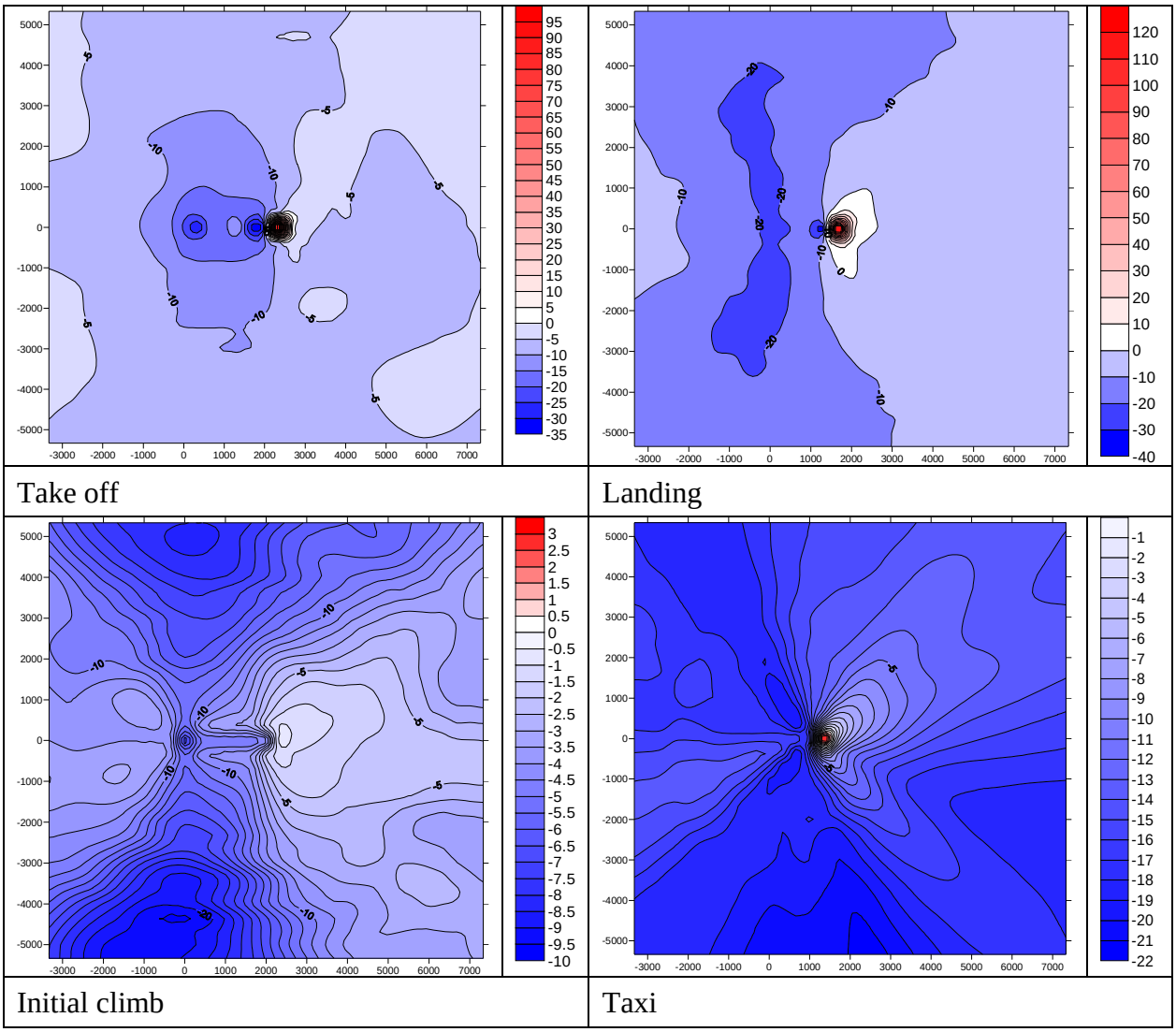

Figure 12.11: Percentage difference plots between B757_200 and MCAT 1 lead aircraft, A320a

12.2.5 MCAT 2

A330b, A330a, A330c, B767_300a, B767_300b

A330b

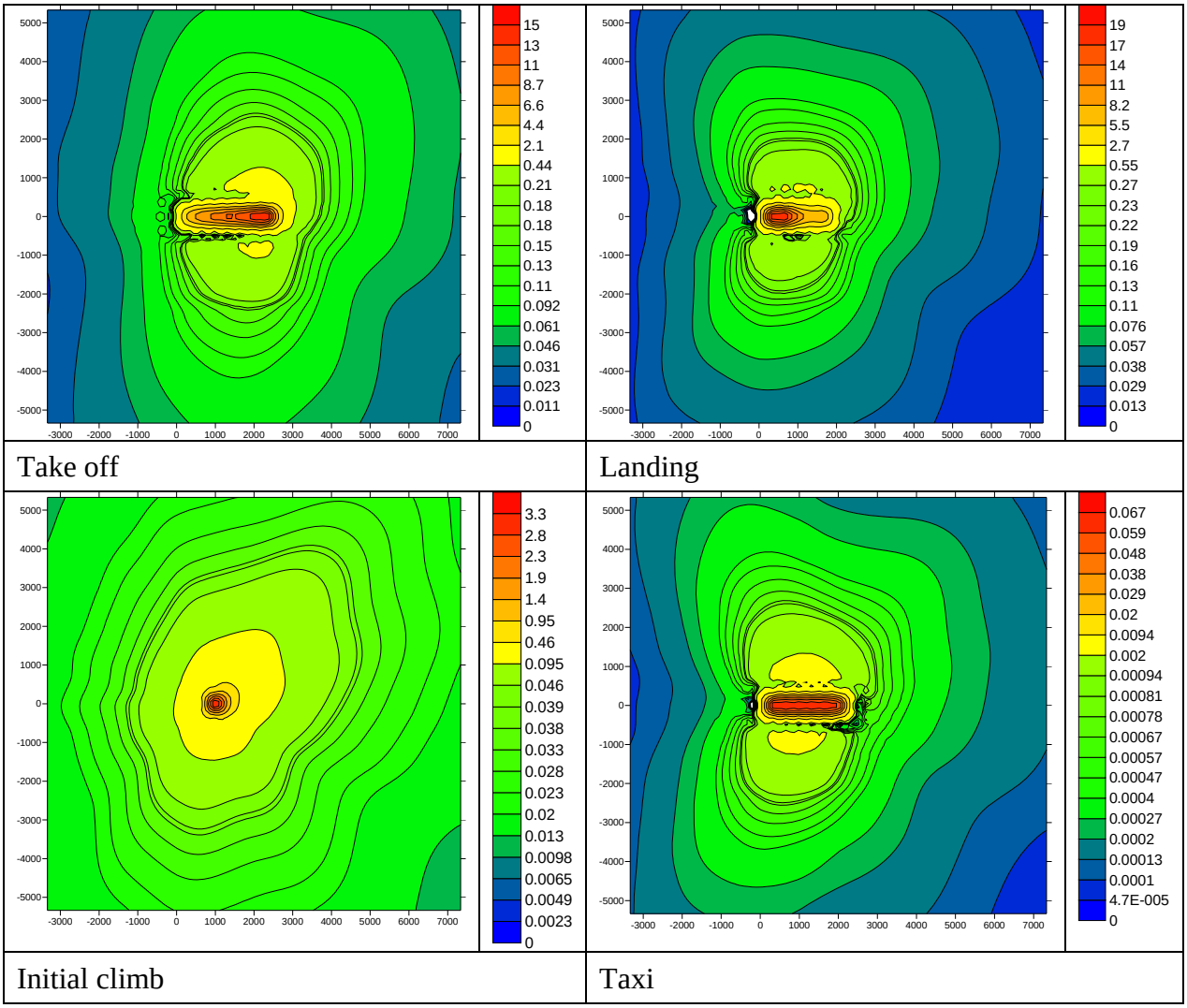

Figure 12.12: Normalised concentration plots for A330b the lead aircraft in MCAT 2

A330a

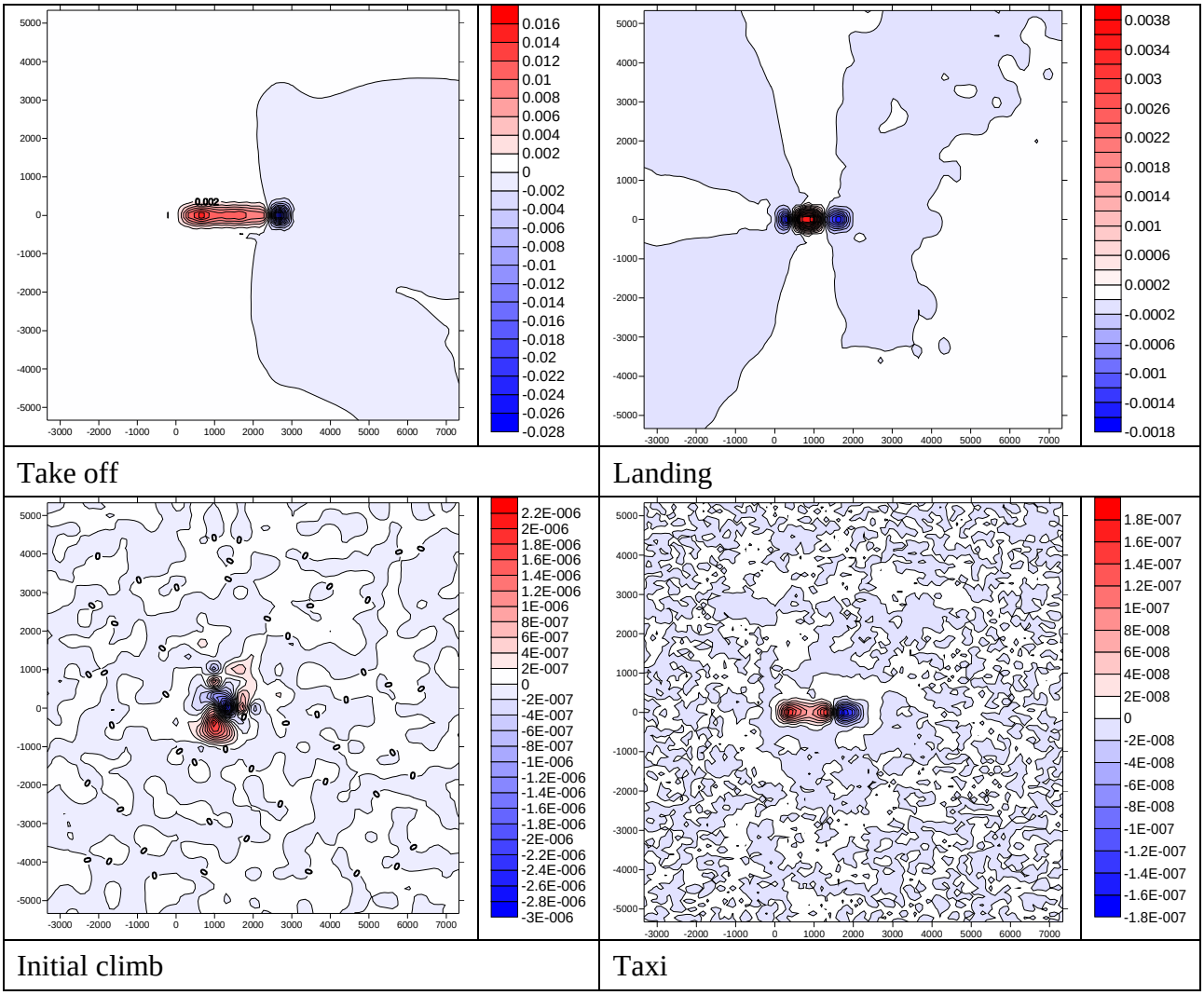

Figure 12.13: Absolute difference plots between A330a and MCAT 2 lead aircraft, A330b

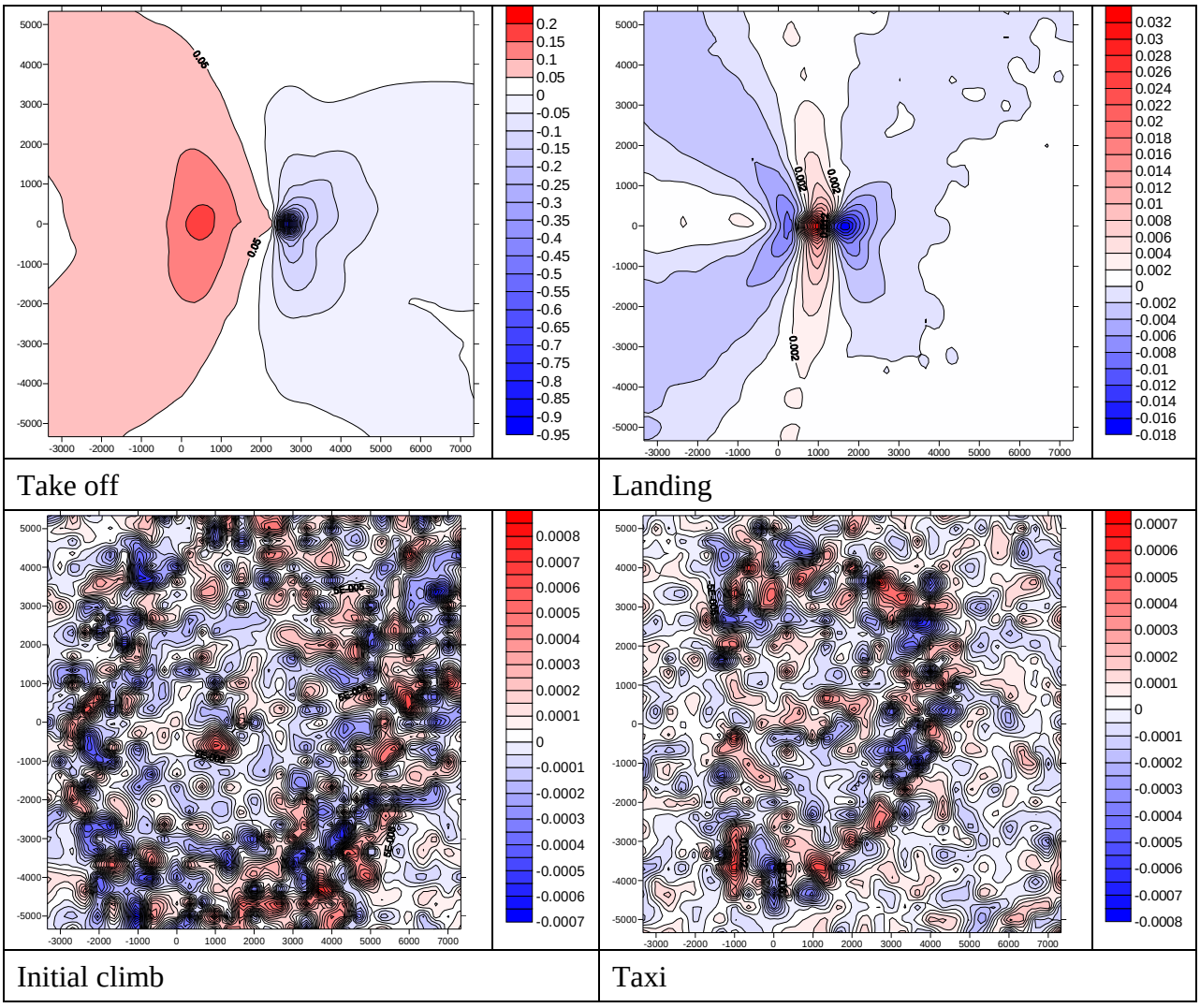

Figure 12.14: Percentage difference plots between A330a and MCAT 2 lead aircraft, A330b

A330c

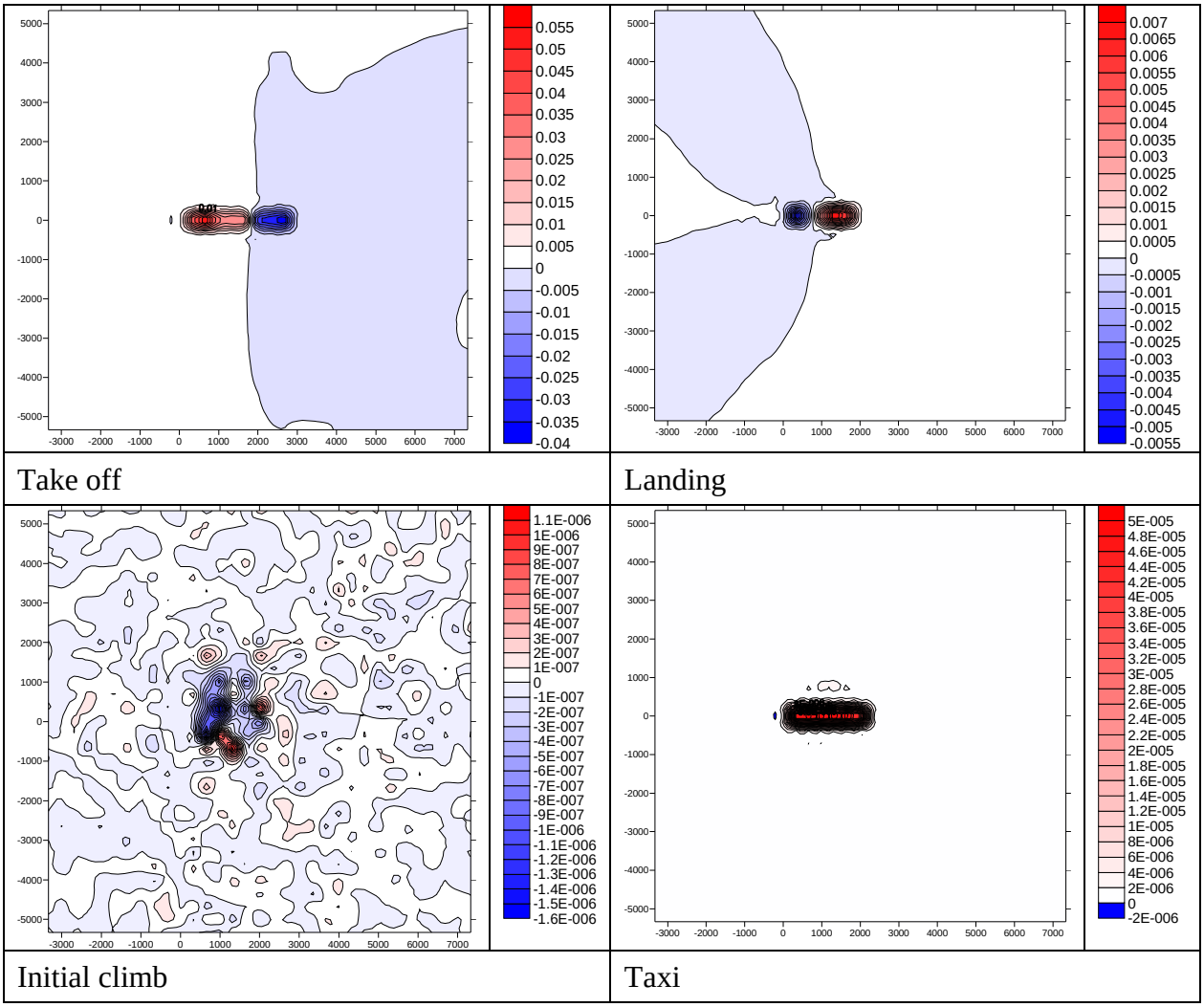

Figure 12.15: Absolute difference plots between A330c and MCAT 2 lead aircraft, A330b

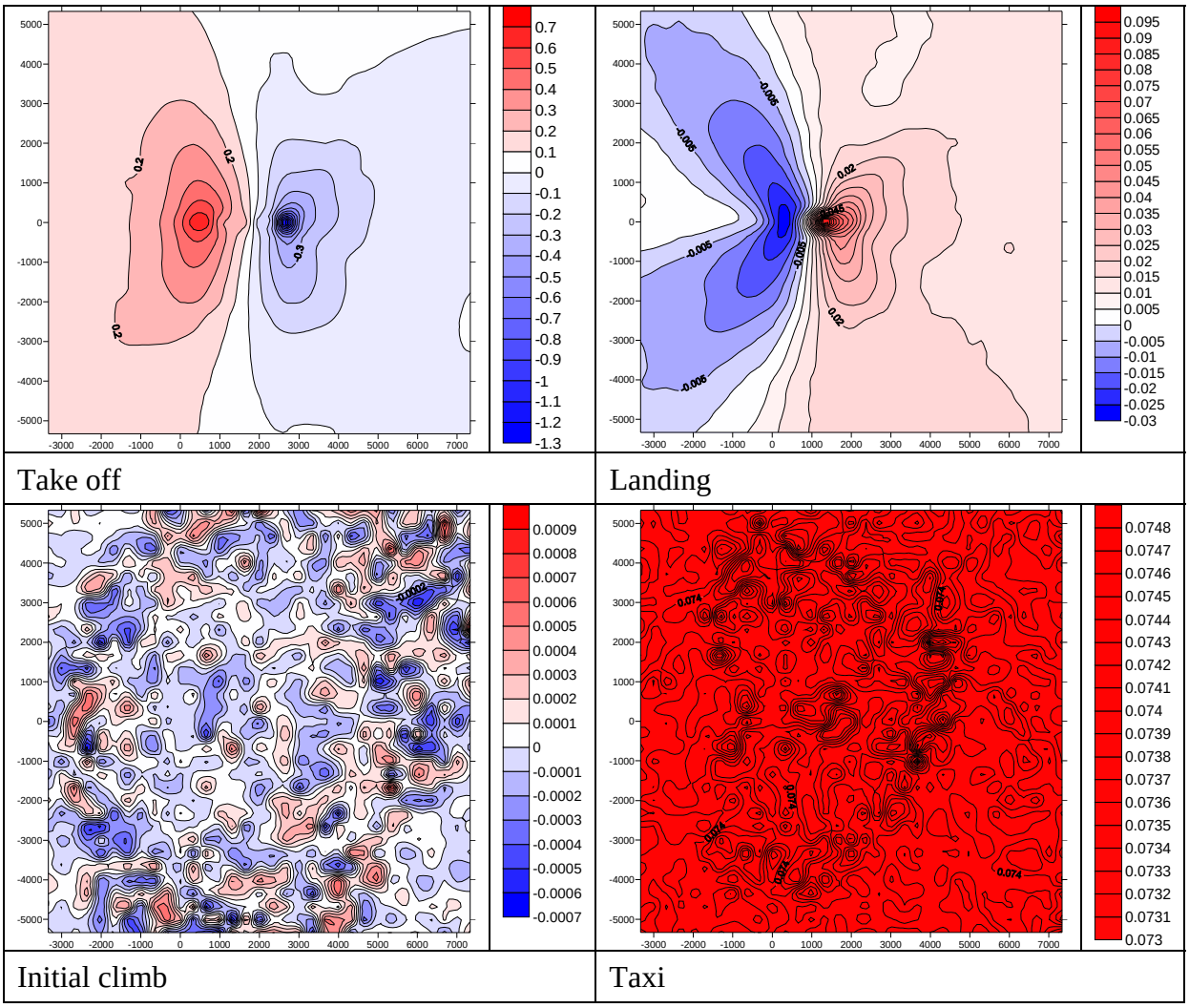

Figure 12.16: Percentage difference plots between A330c and MCAT 2 lead aircraft, A330b

B767_300a

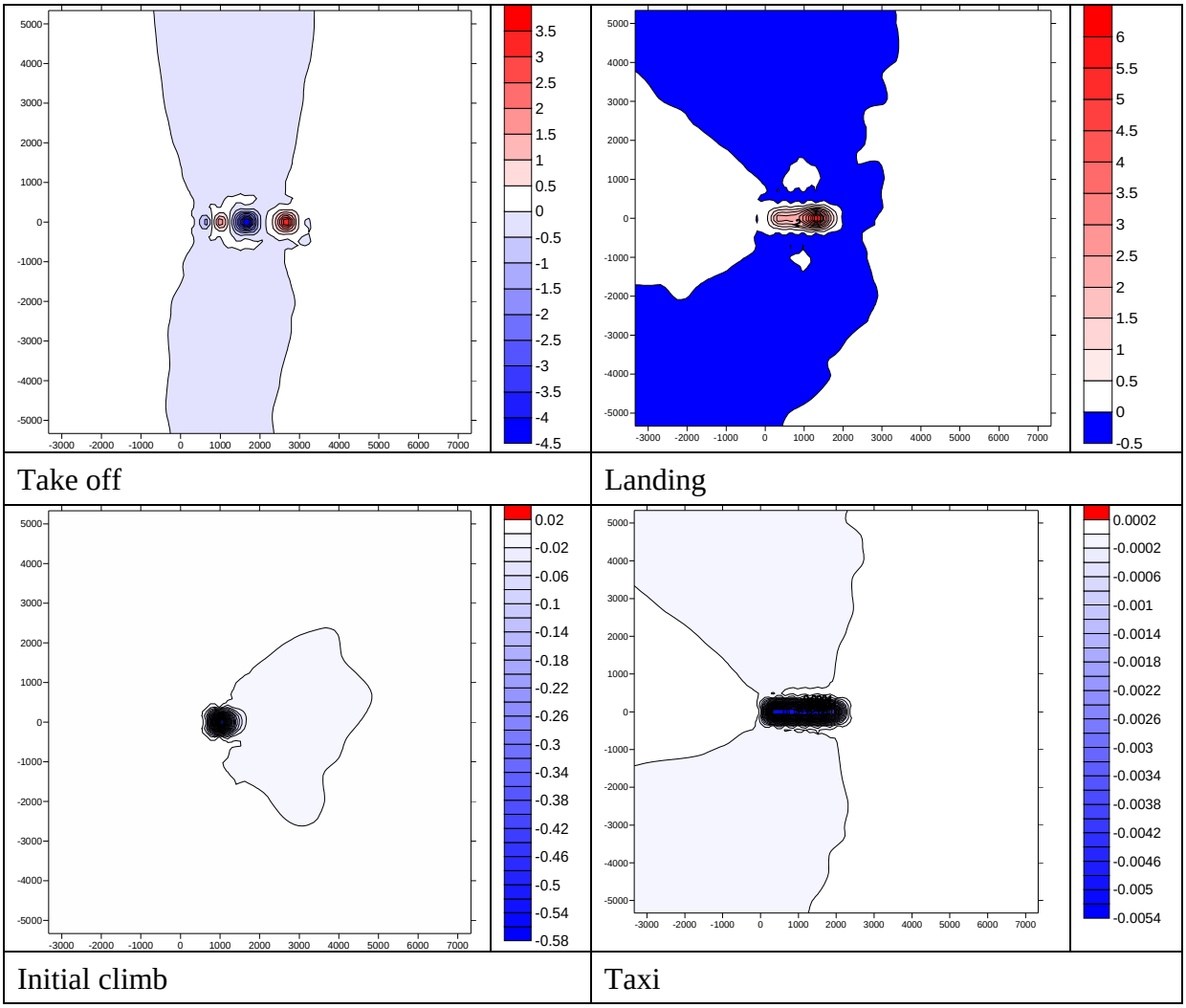

Figure 12.17: Absolute difference plots between B767_300a and MCAT 2 lead aircraft, A330b

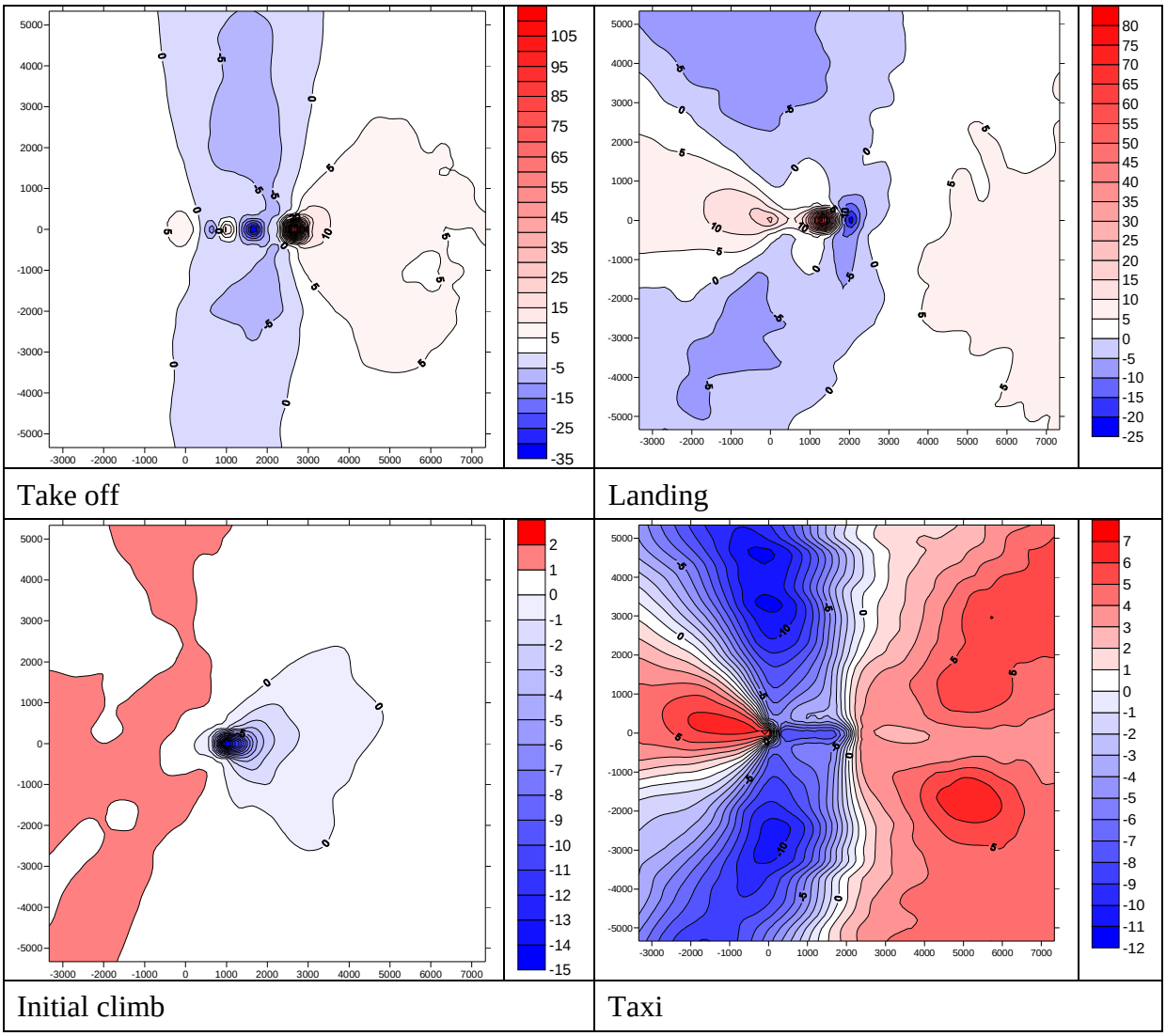

Figure 12.18: Percentage difference plots between B767_300a and MCAT 2 lead aircraft, A330b

B767_300b

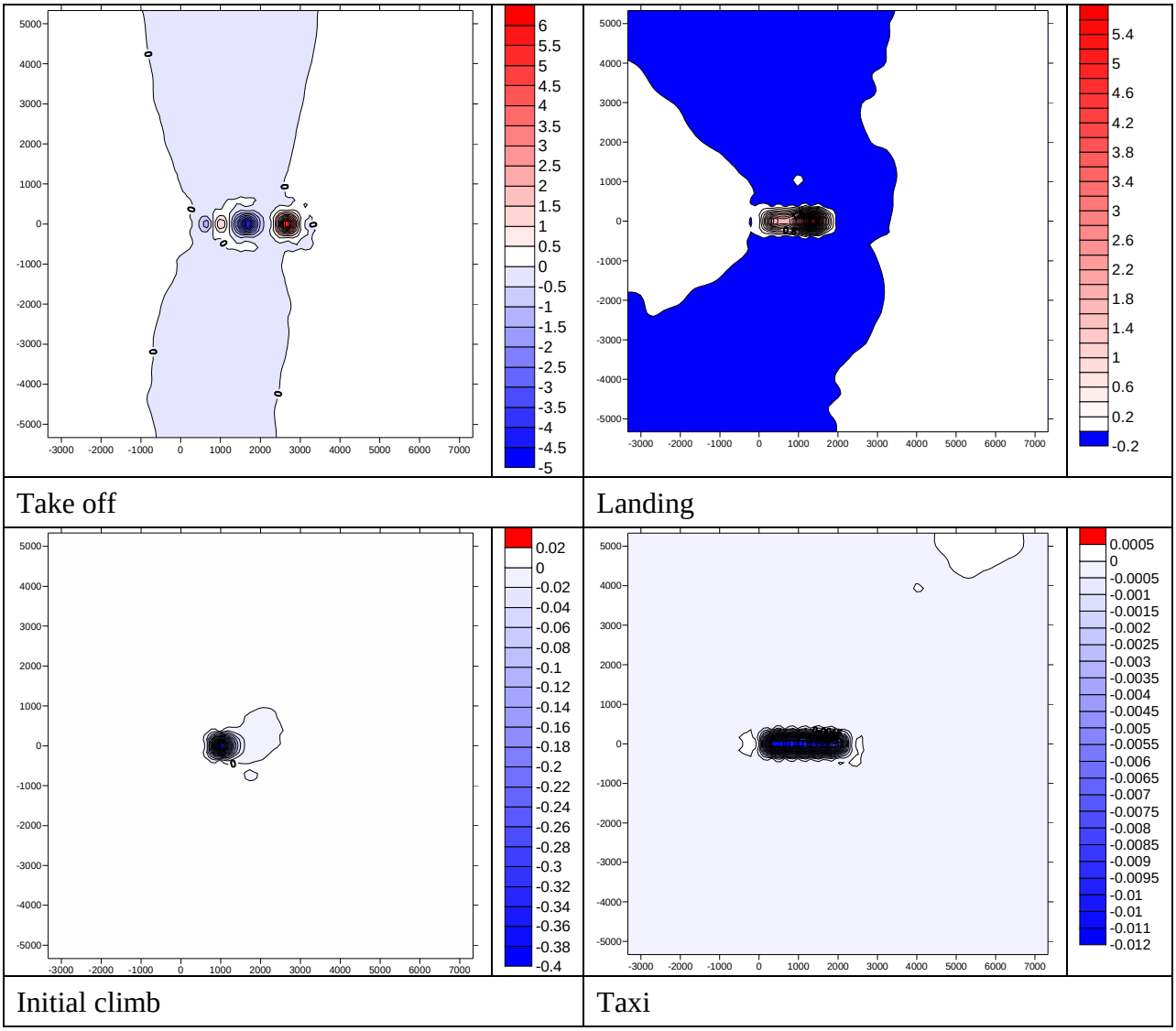

Figure 12.19:Absolute difference plots between B767_300b and MCAT 2 lead aircraft, A330b

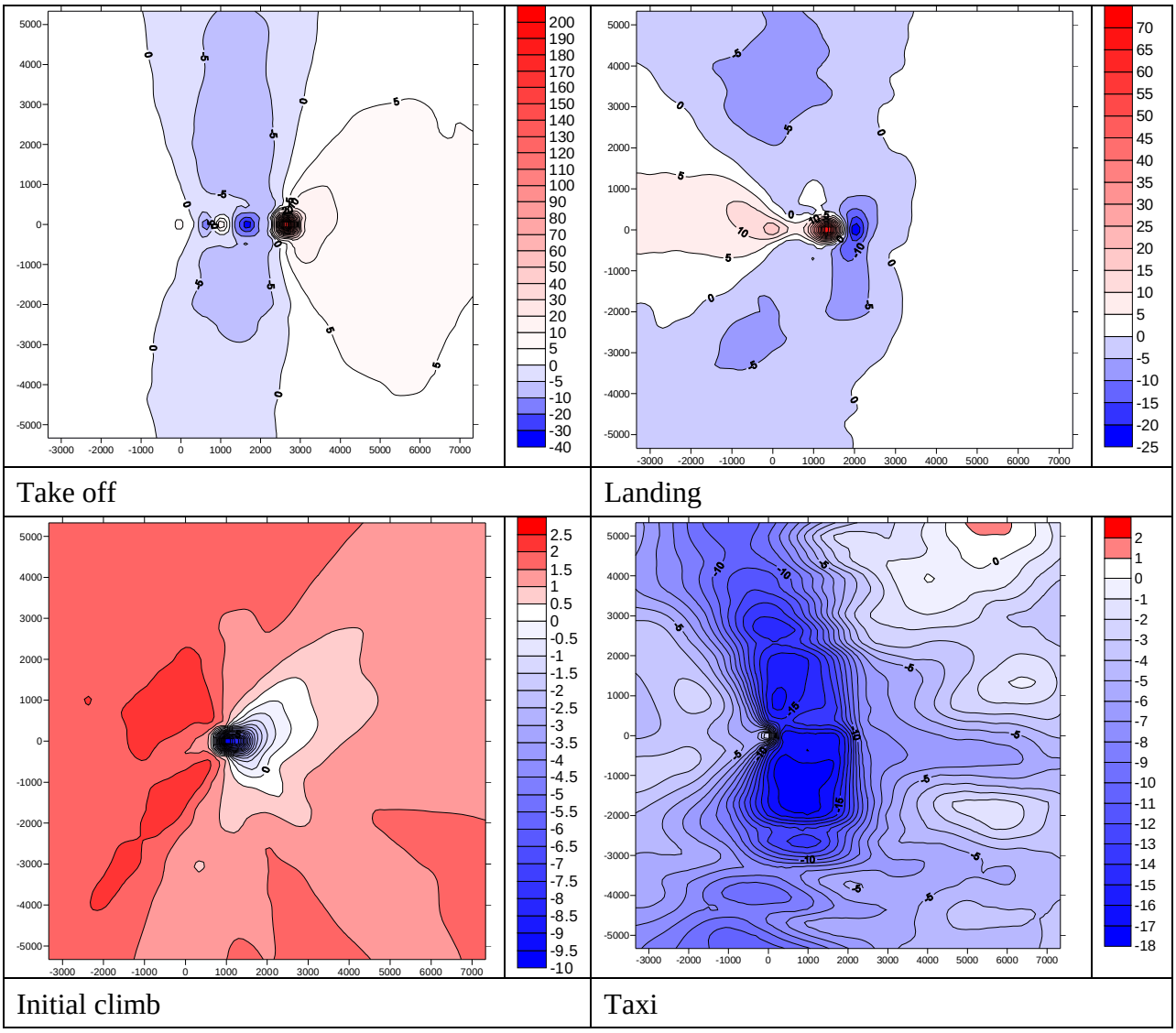

Figure 12.20: Percentage difference plots between B767_300b and MCAT 2 lead aircraft, A330b

12.2.6 MCAT 3

A340_300a, A340_300b, A340_300c

A340_300a

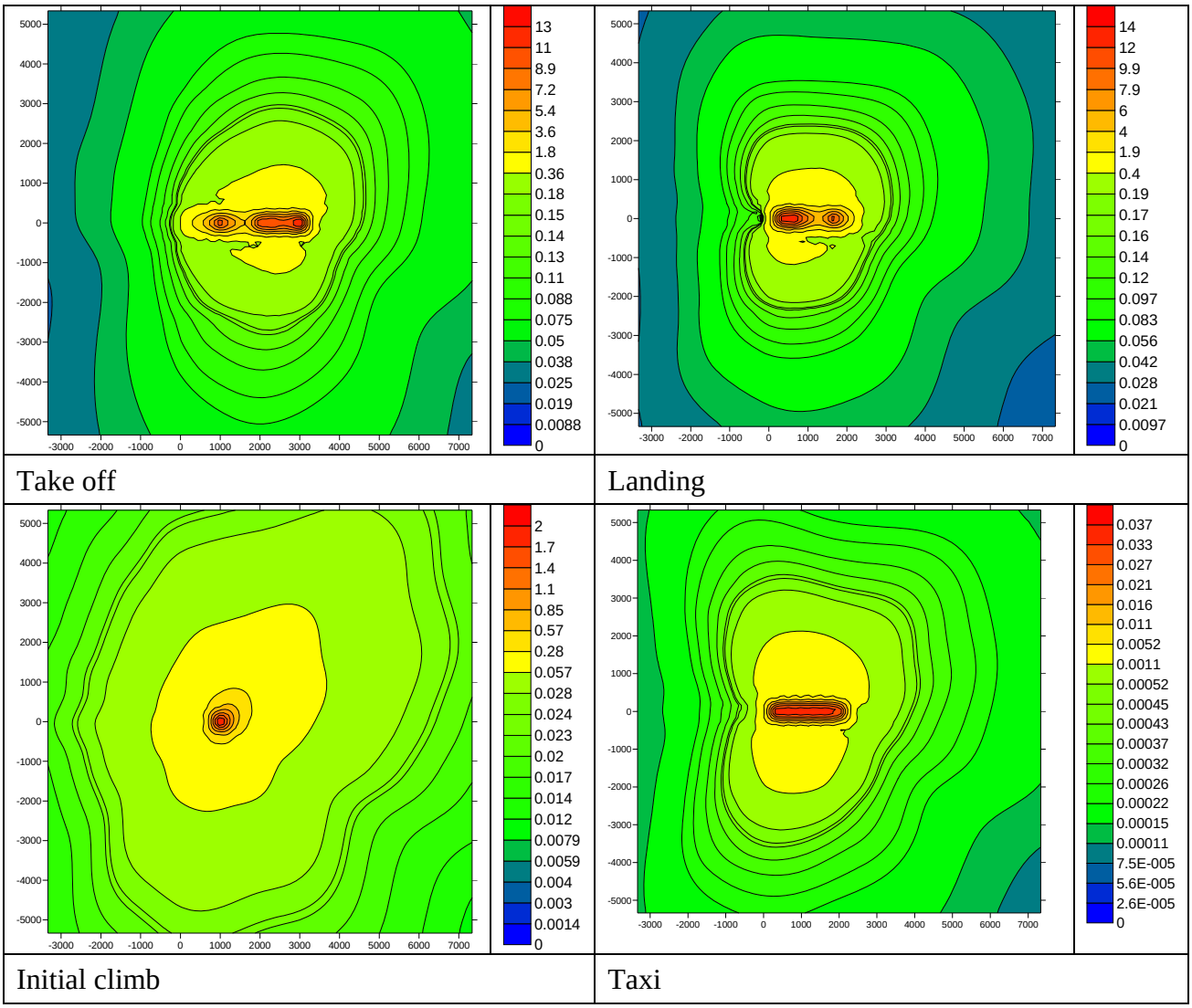

Figure 12.21: Normalised concentration plots for A340_300a the lead aircraft in MCAT 3

A340_300b

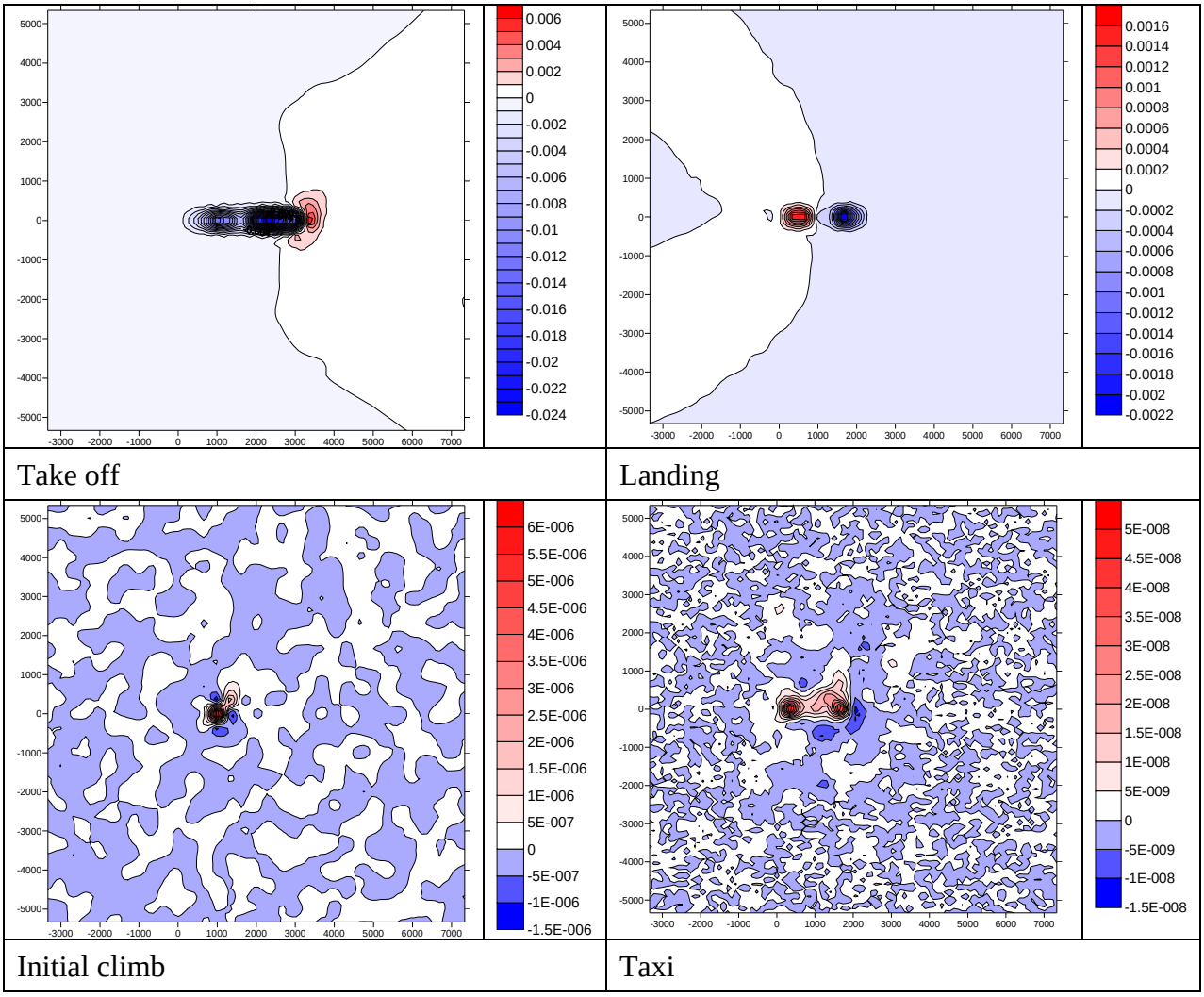

Figure 12.22: Absolute difference plots between A340_300b and MCAT 3 lead aircraft, A340_300a

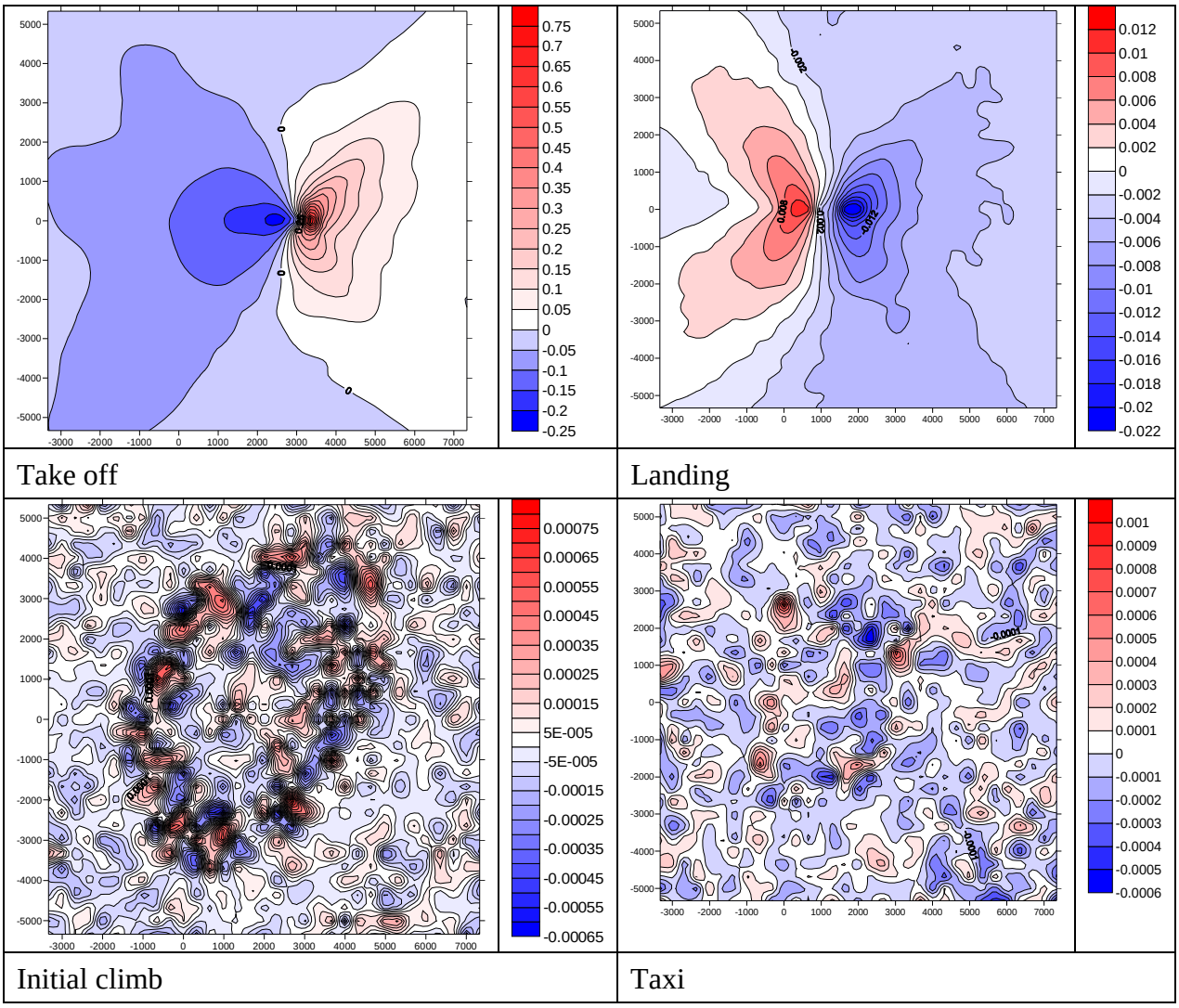

Figure 12.23: Percentage difference plots between A340_300b and MCAT 3 lead aircraft, A340_300a

A340_300c

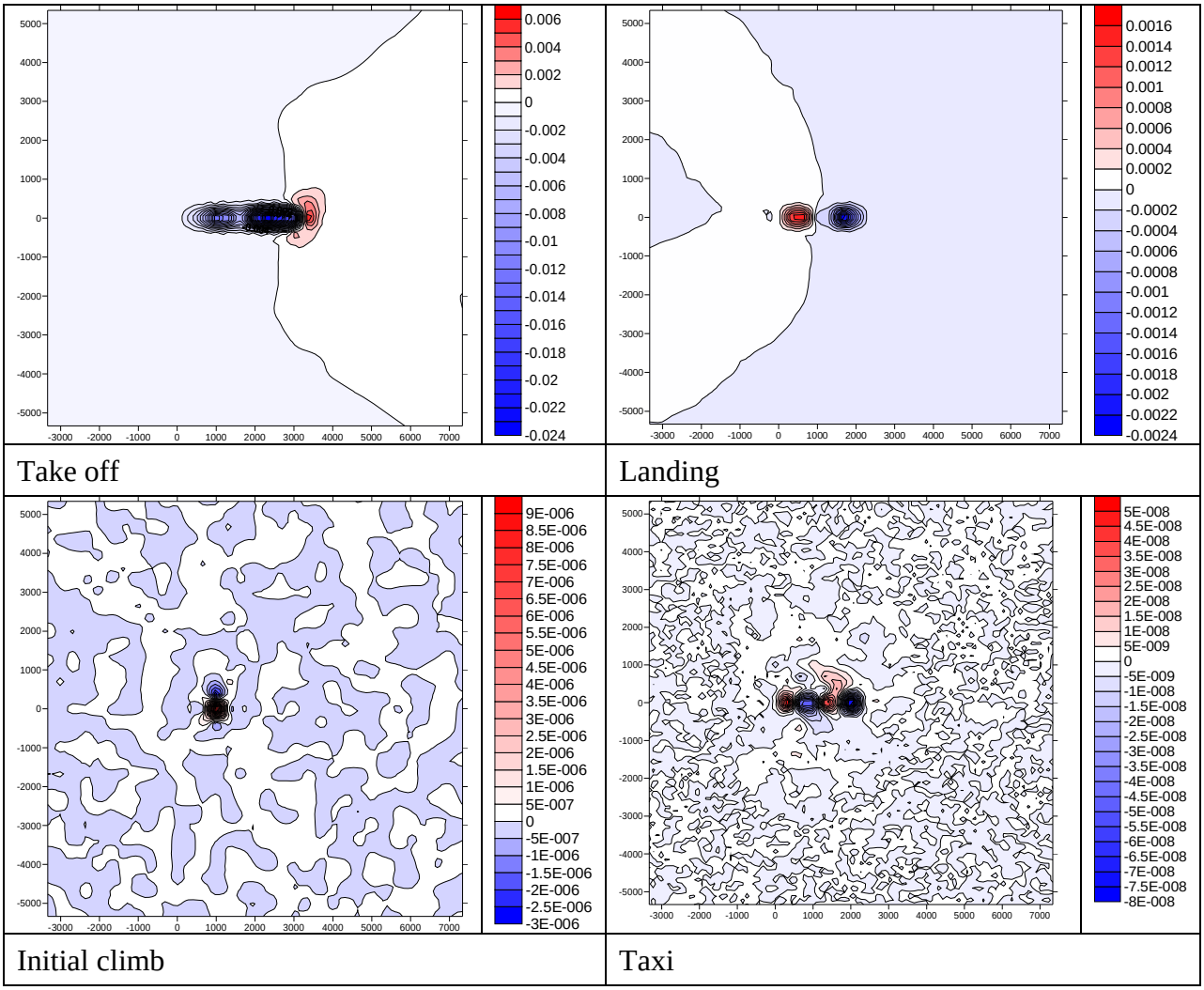

Figure 12.24: Absolute difference plots between A340_300c and MCAT 3 lead aircraft, A340_300a

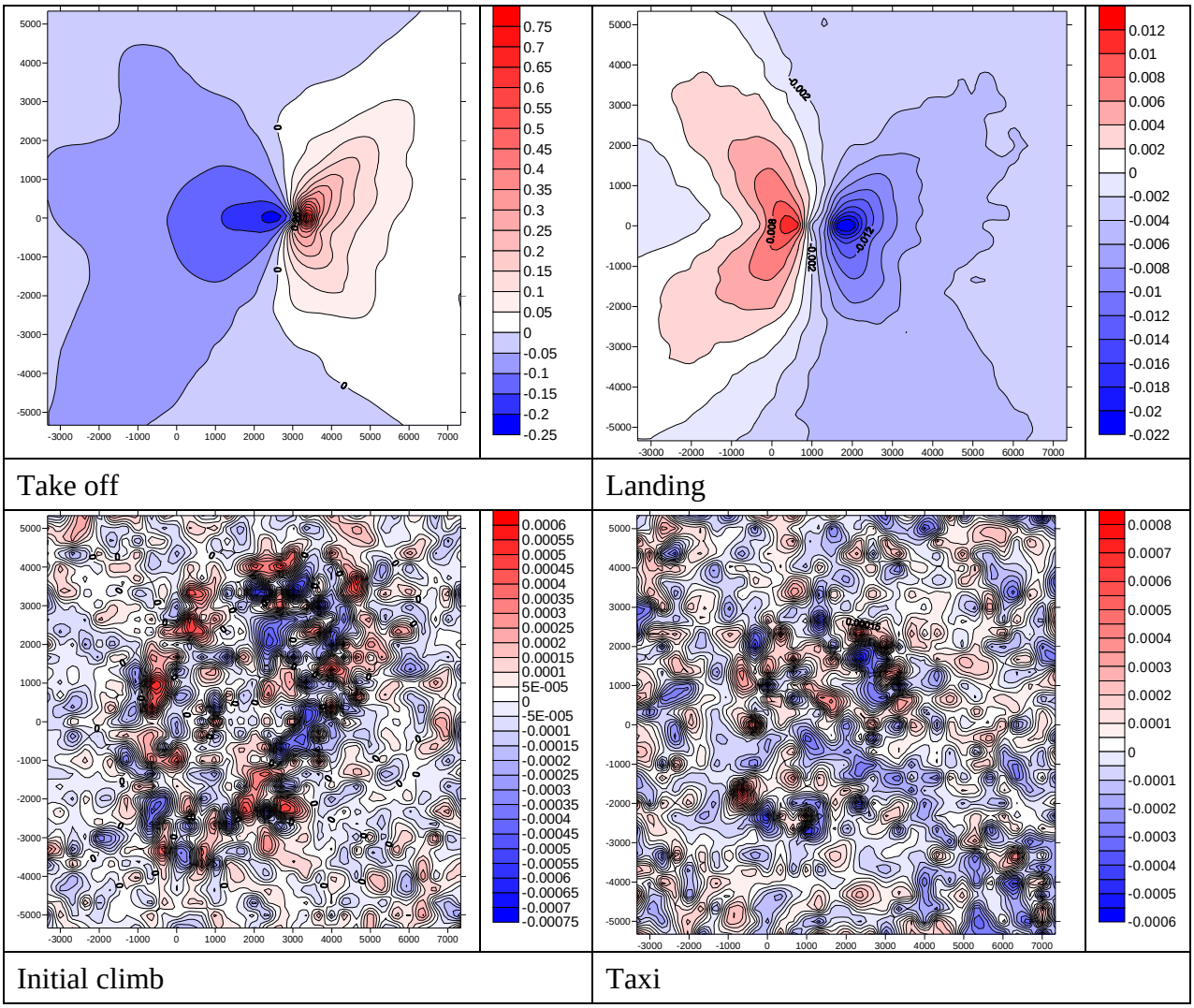

Figure 12.25: Percentage difference plots between A340_300c and MCAT 3 lead aircraft, A340_300a

12.2.7 MCAT 4

B737_400, B737_600a, B737_600b, B737_600c

B737_400

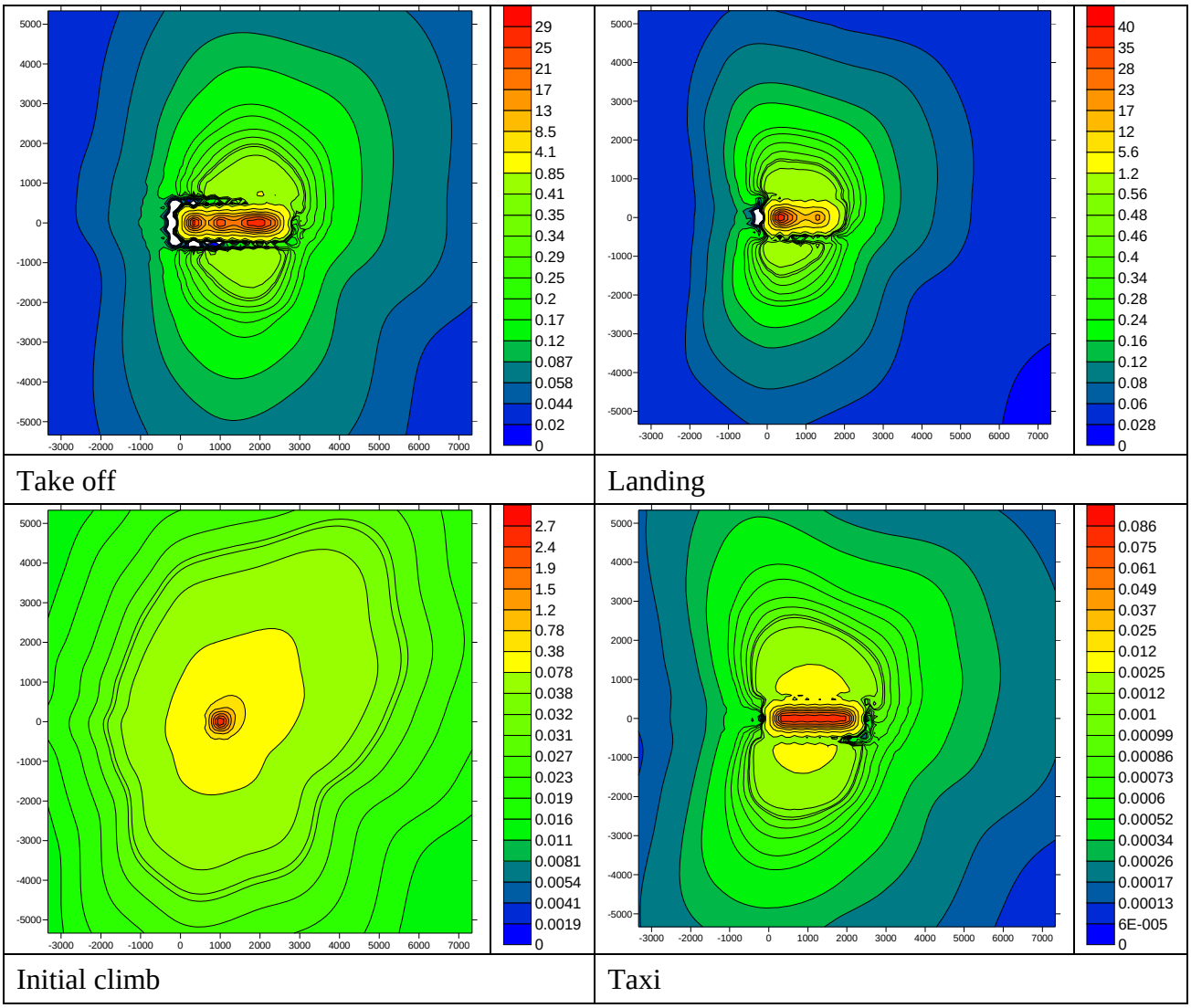

Figure 12.26: Normalised concentration plots for B737_400 the lead aircraft in MCAT 4

B737_600a

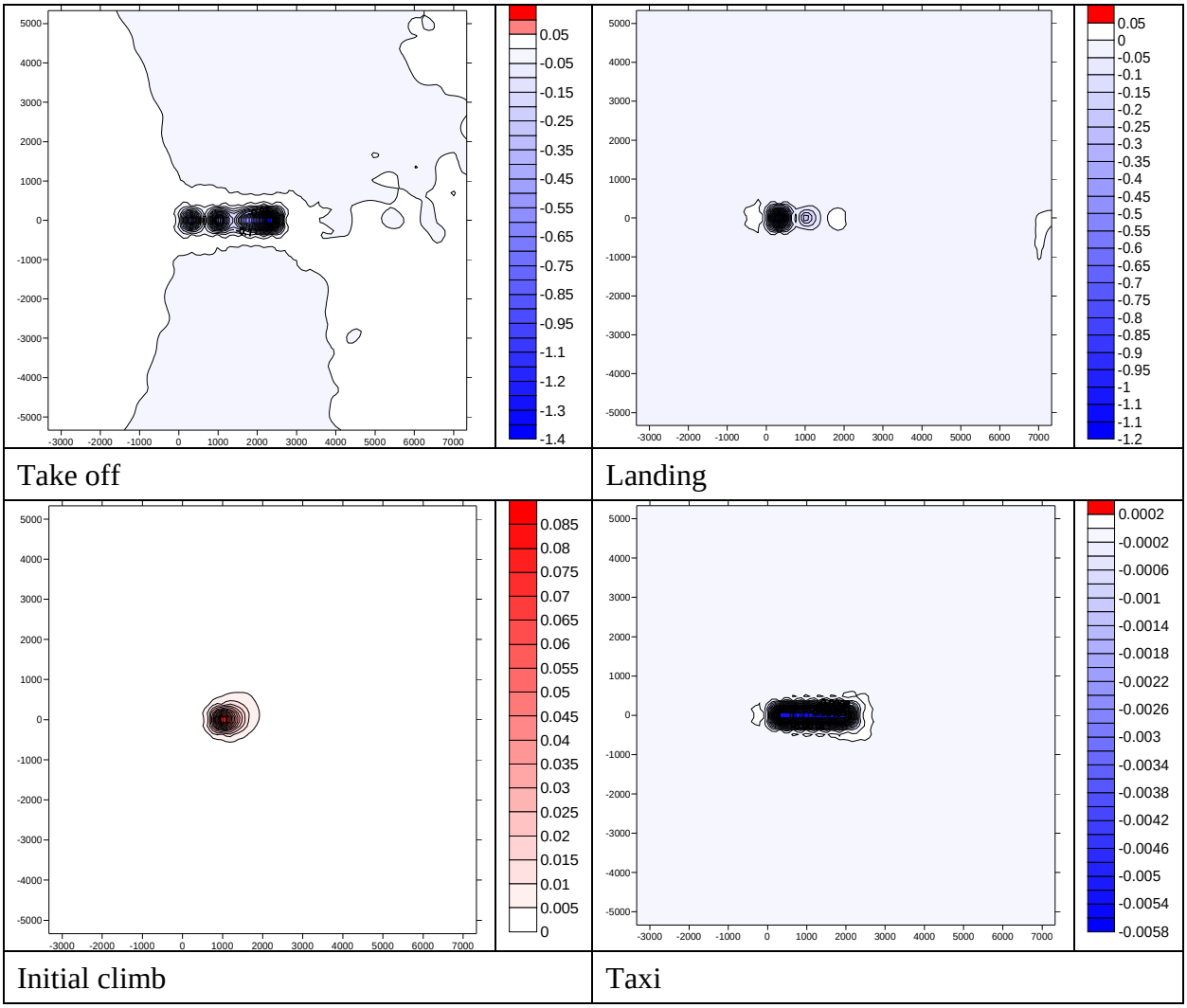

Figure 12.27: Absolute difference plots between B737_600a and MCAT 4 lead aircraft, B737_400

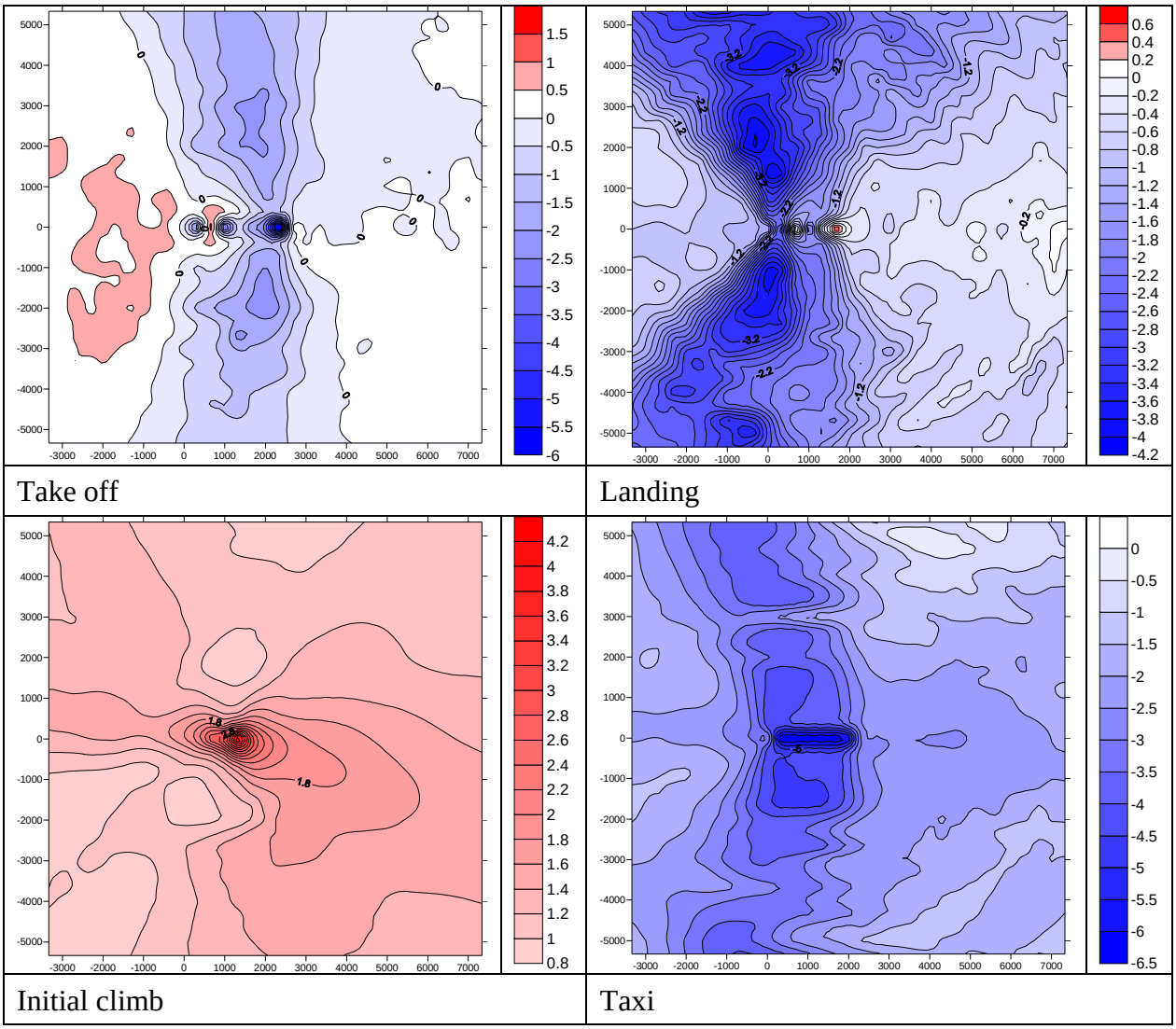

Figure 12.28: Percentage difference plots between B737_600a and MCAT 4 lead aircraft, B737_400

B737_600b

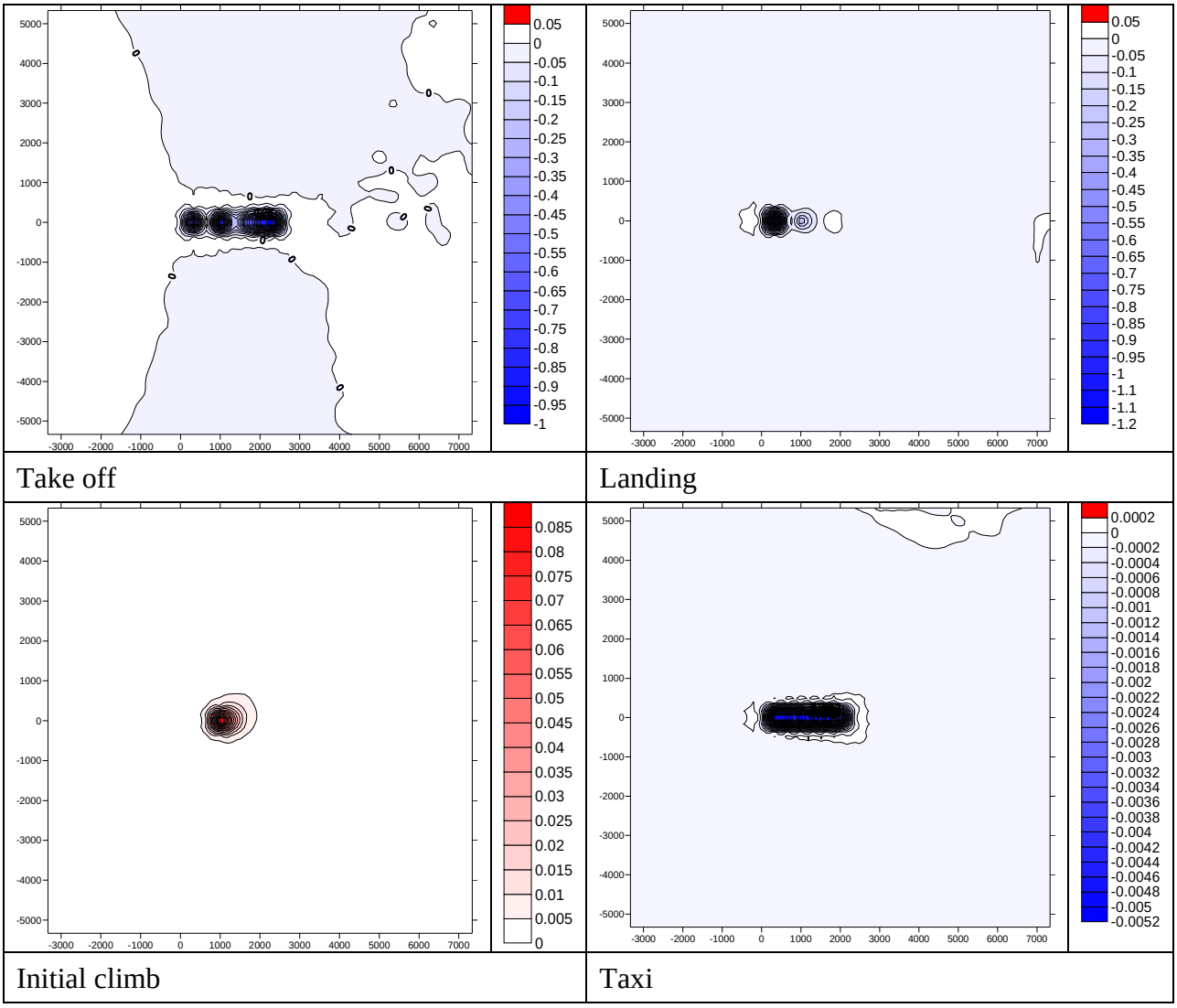

Figure 12.29: Absolute difference plots between B737_600b and MCAT 4 lead aircraft, B737_400

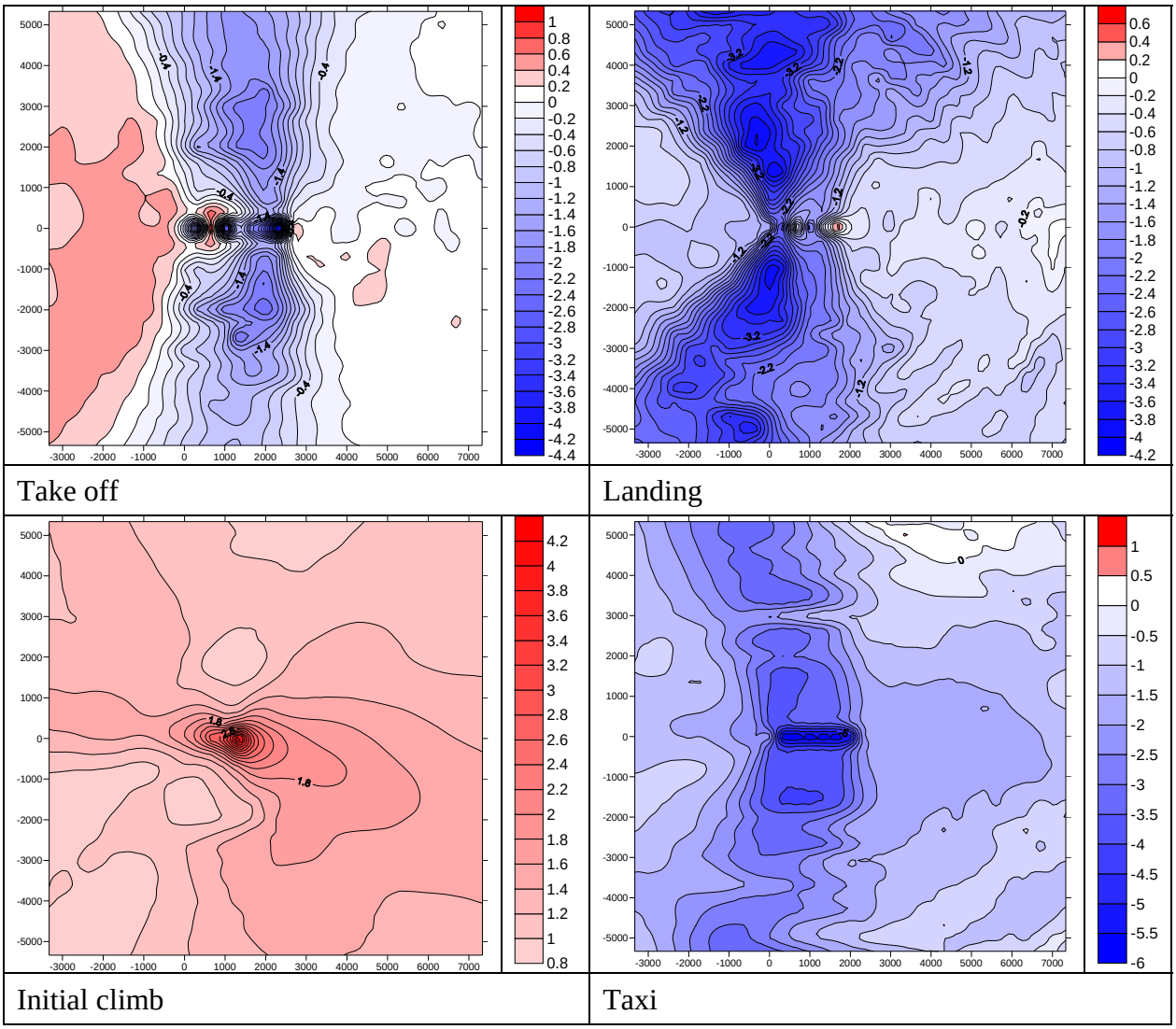

Figure 12.30: Percentage difference plots between B737_600b and MCAT 4 lead aircraft, B737_400

B737_600c

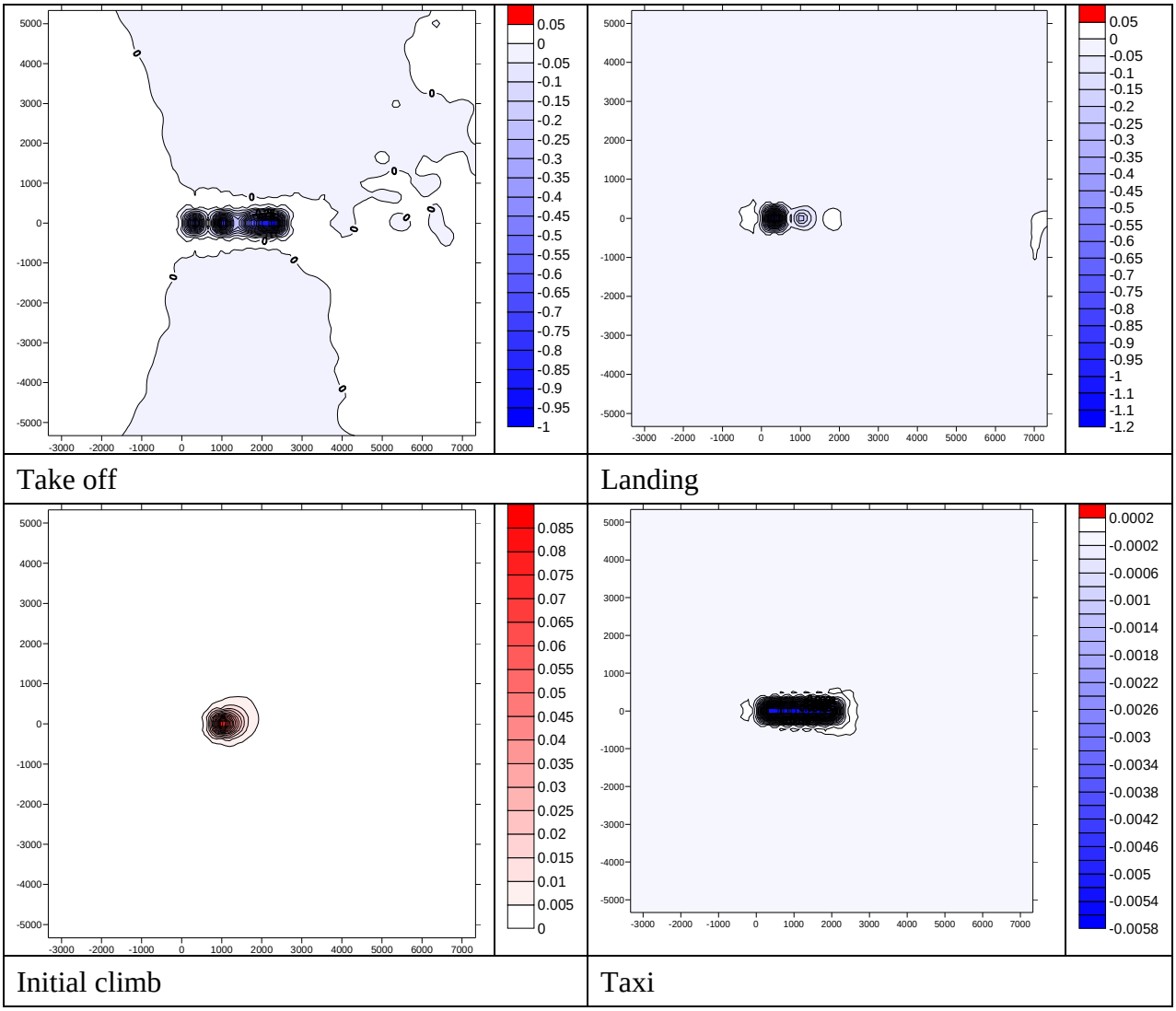

Figure 12.31: Absolute difference plots between B737_600c and MCAT 4 lead aircraft, B737_400

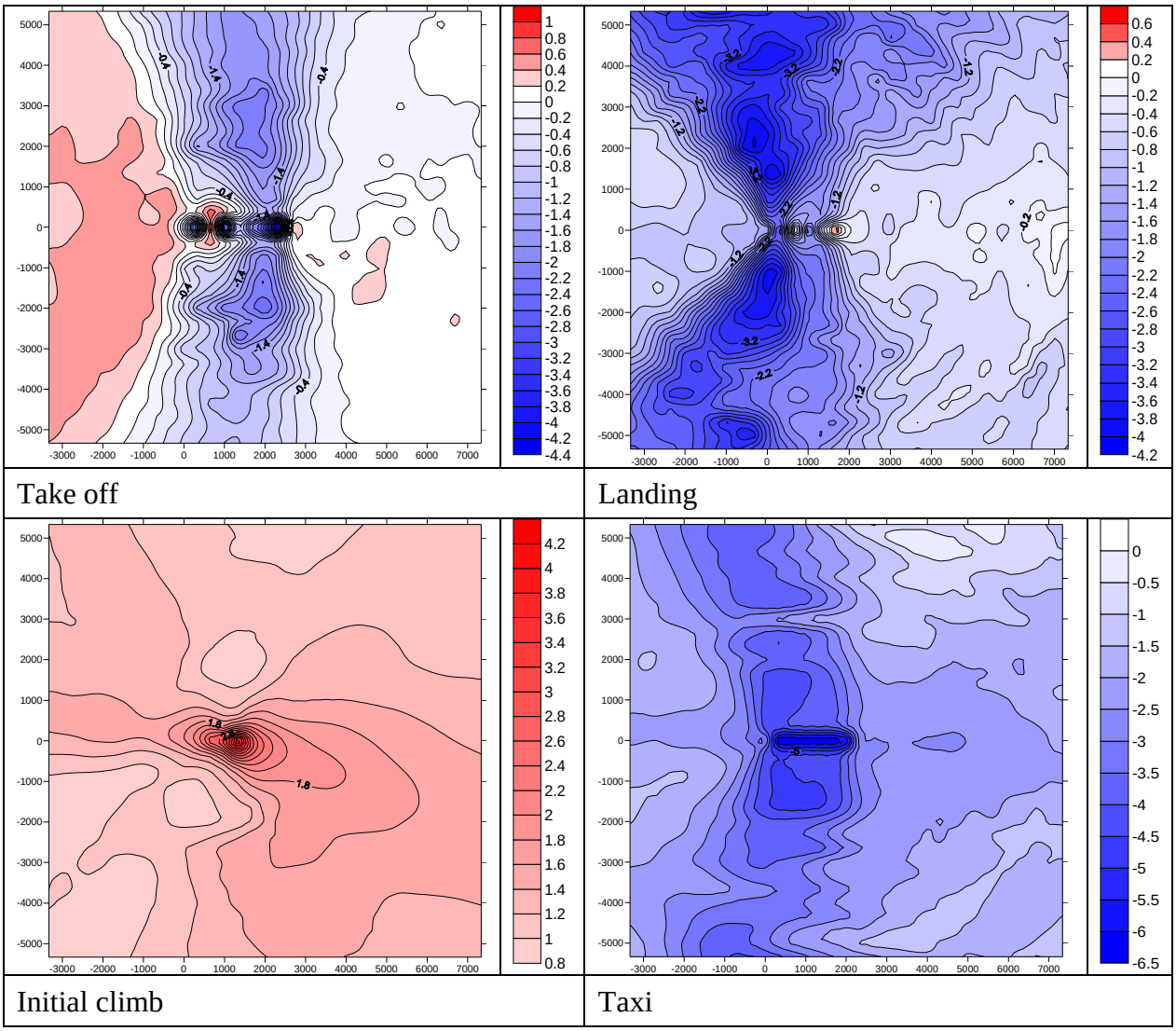

Figure 12.32: Percentage difference plots between B737_600c and MCAT 4 lead aircraft, B737_400

12.2.8 MCAT 5

B747_400, B747_800, A380

B747_400

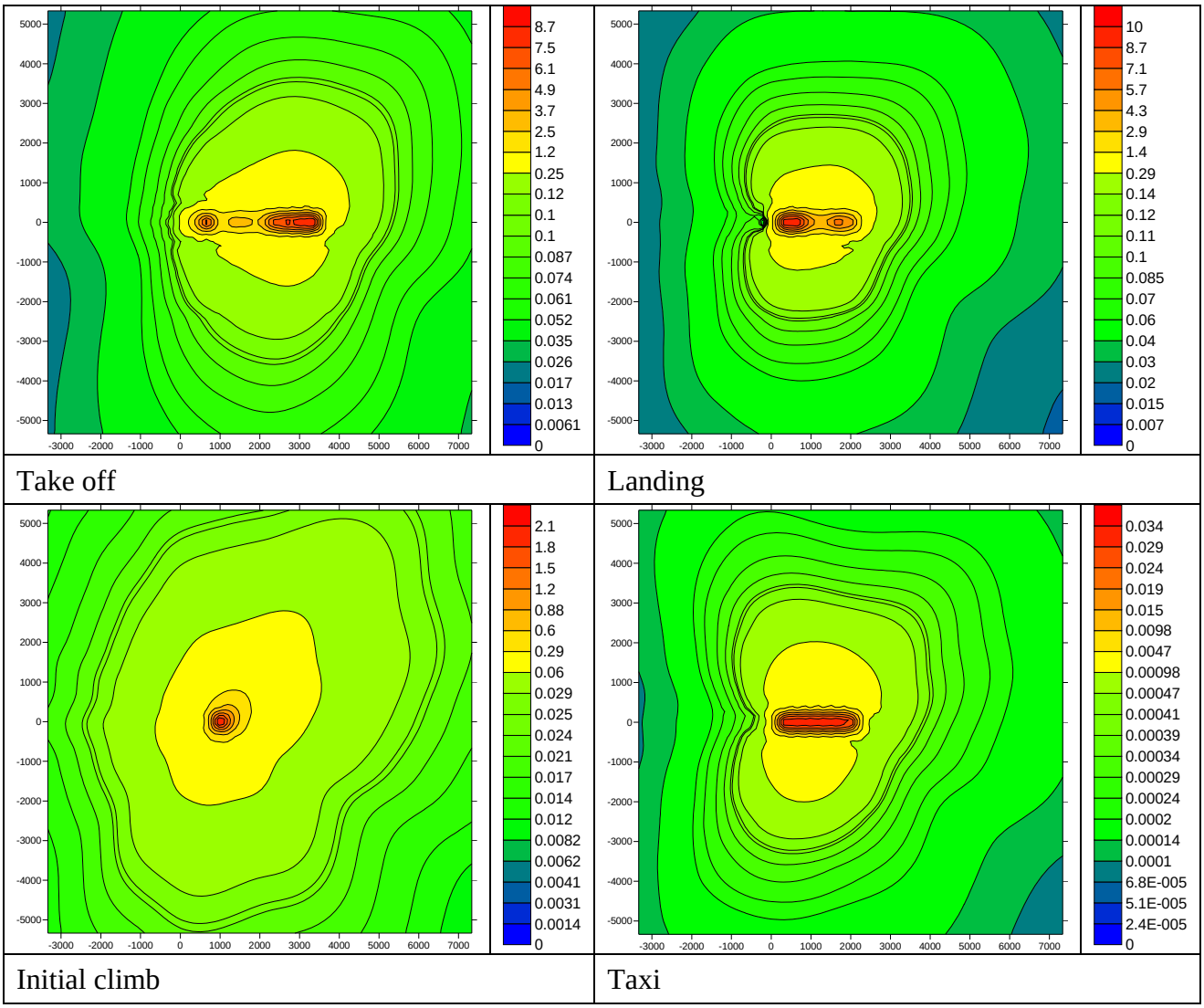

Figure 12.33: Normalised concentration plots for B747_400 the lead aircraft of MCAT 5

B747_800

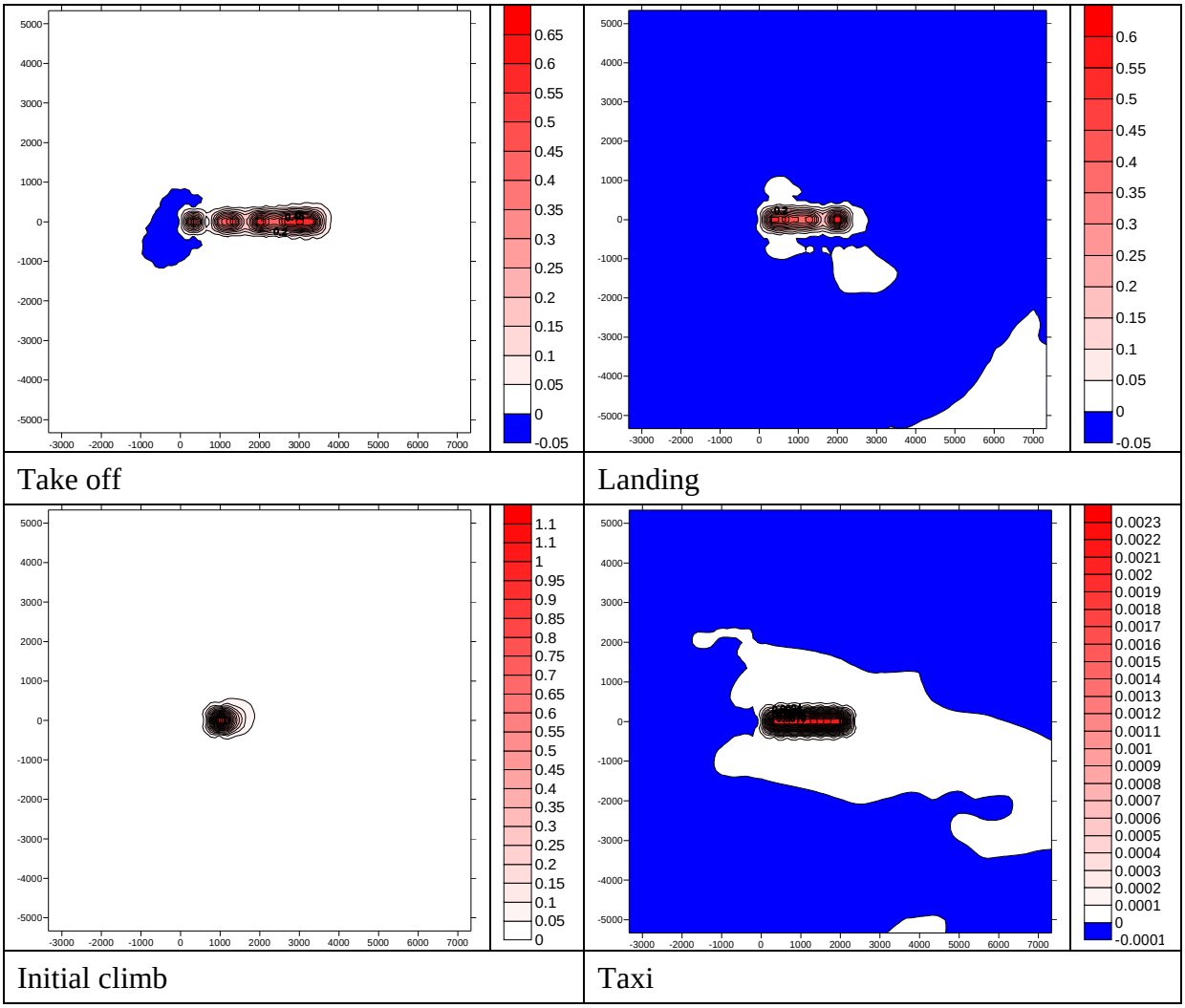

Figure 12.34: Absolute difference plots between B747_800 and MCAT 5 lead aircraft, B747_400

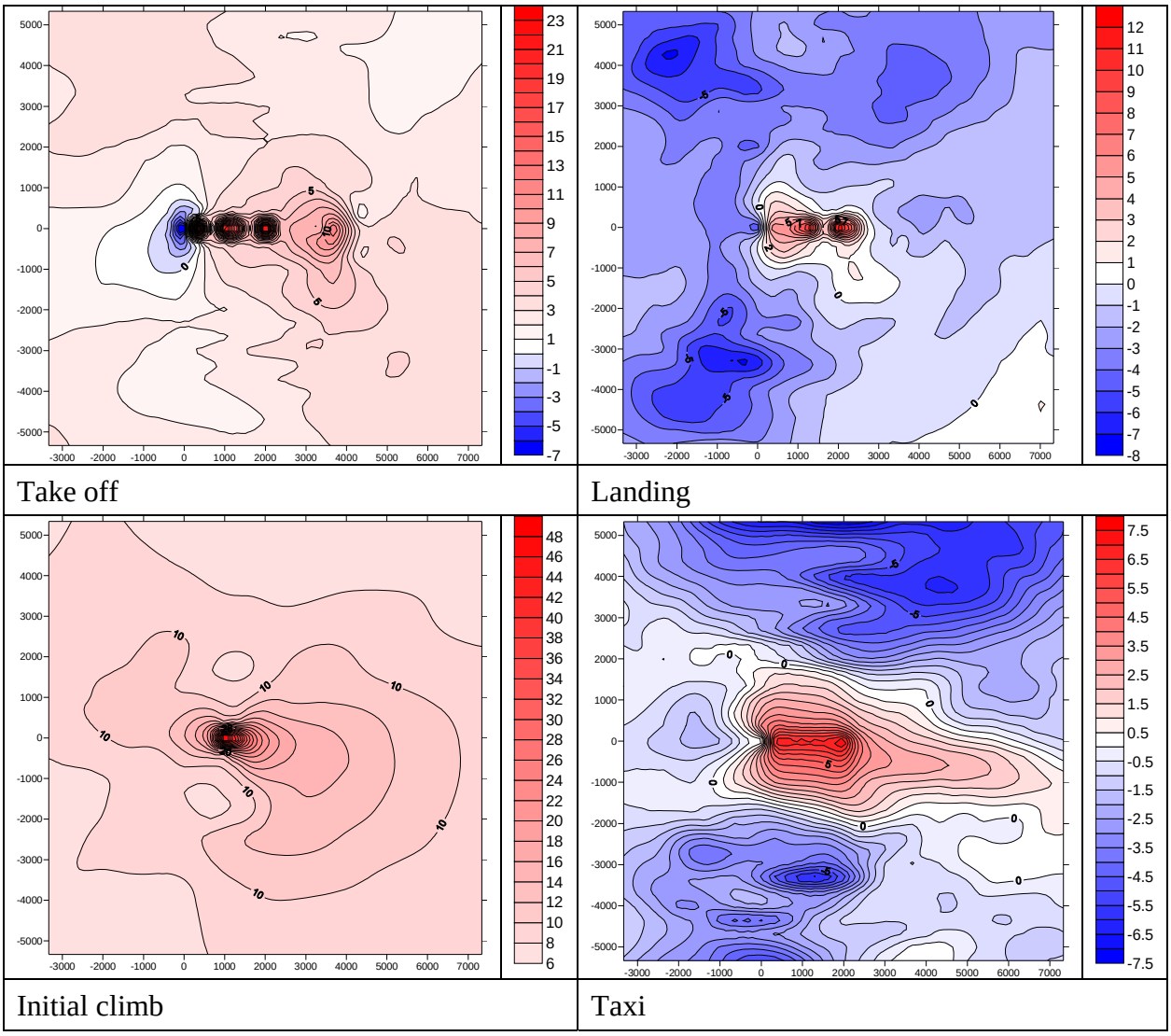

Figure 12.35: Percentage difference plots between B747_800 and MCAT 5 lead aircraft, B747_400

A380

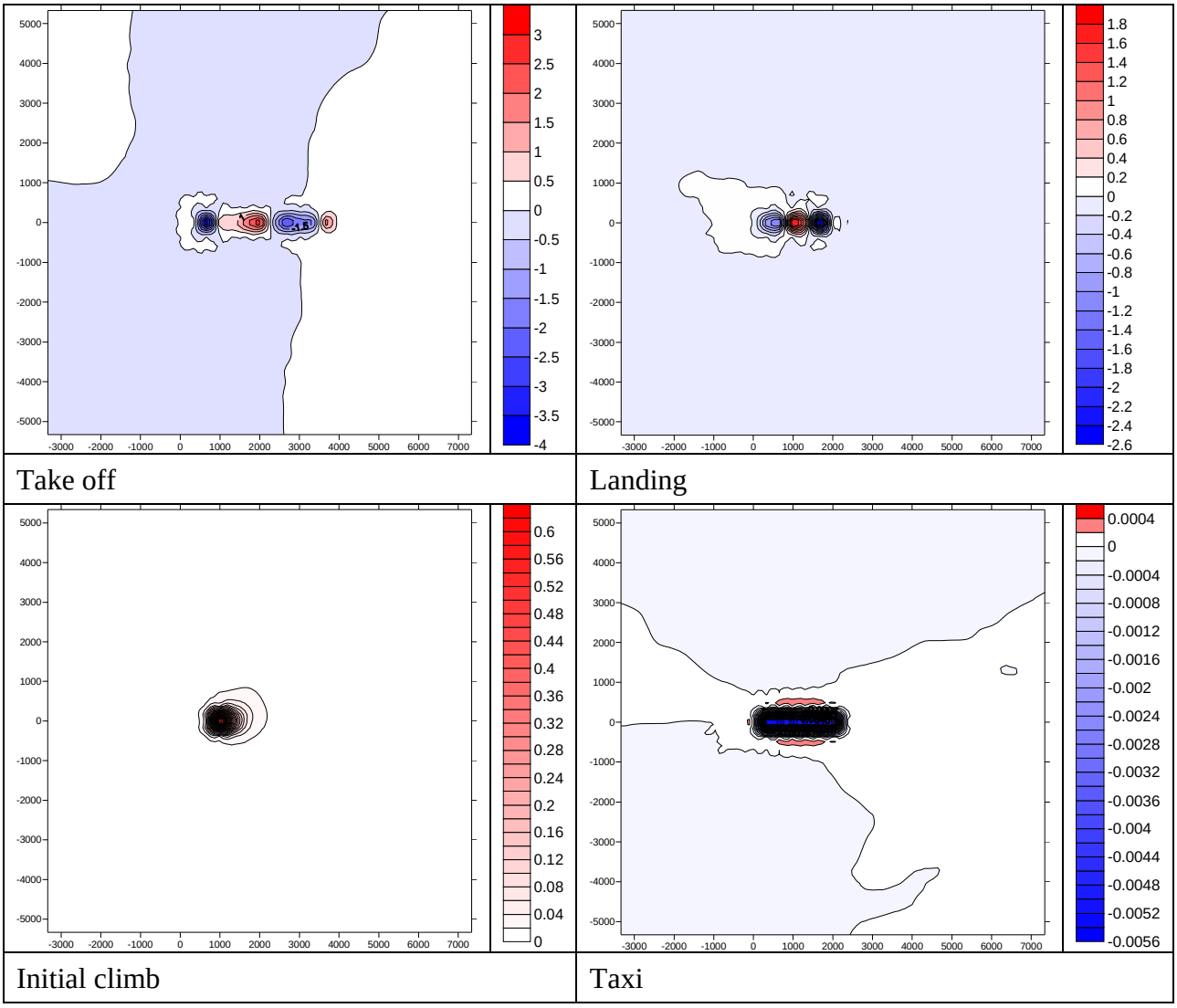

Figure 12.36: Absolute difference plots between A380 and MCAT 5 lead aircraft, B747_400

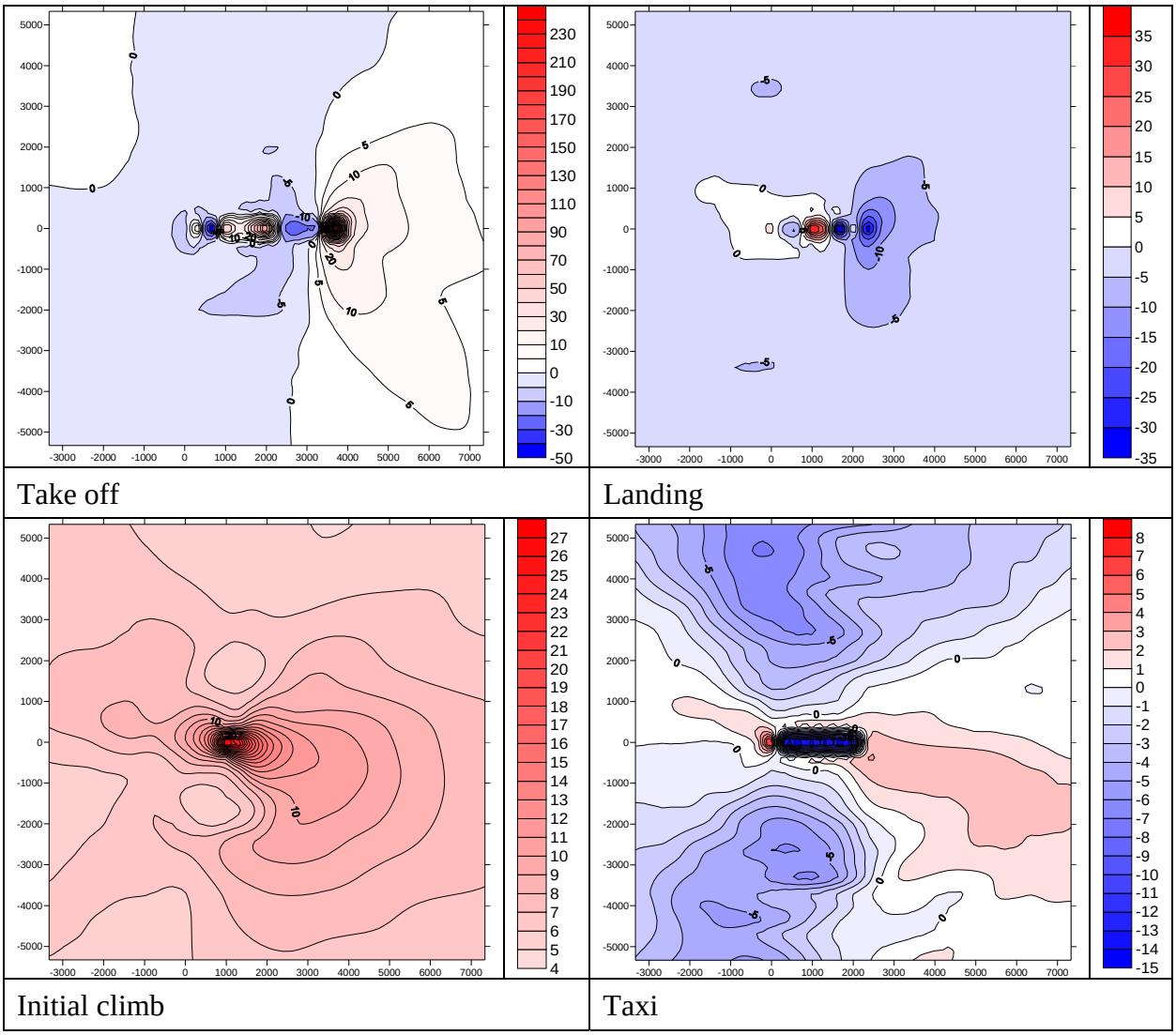

Figure 12.37: Percentage difference plots between A380 and MCAT 5 lead aircraft, B747_400

12.2.9 MCAT 6

B777_200b, B777_200a, B777_200c, B777_200d, B777_200e, B777_200f, B777_200g, B777_200h, B777_200i

B777_200b

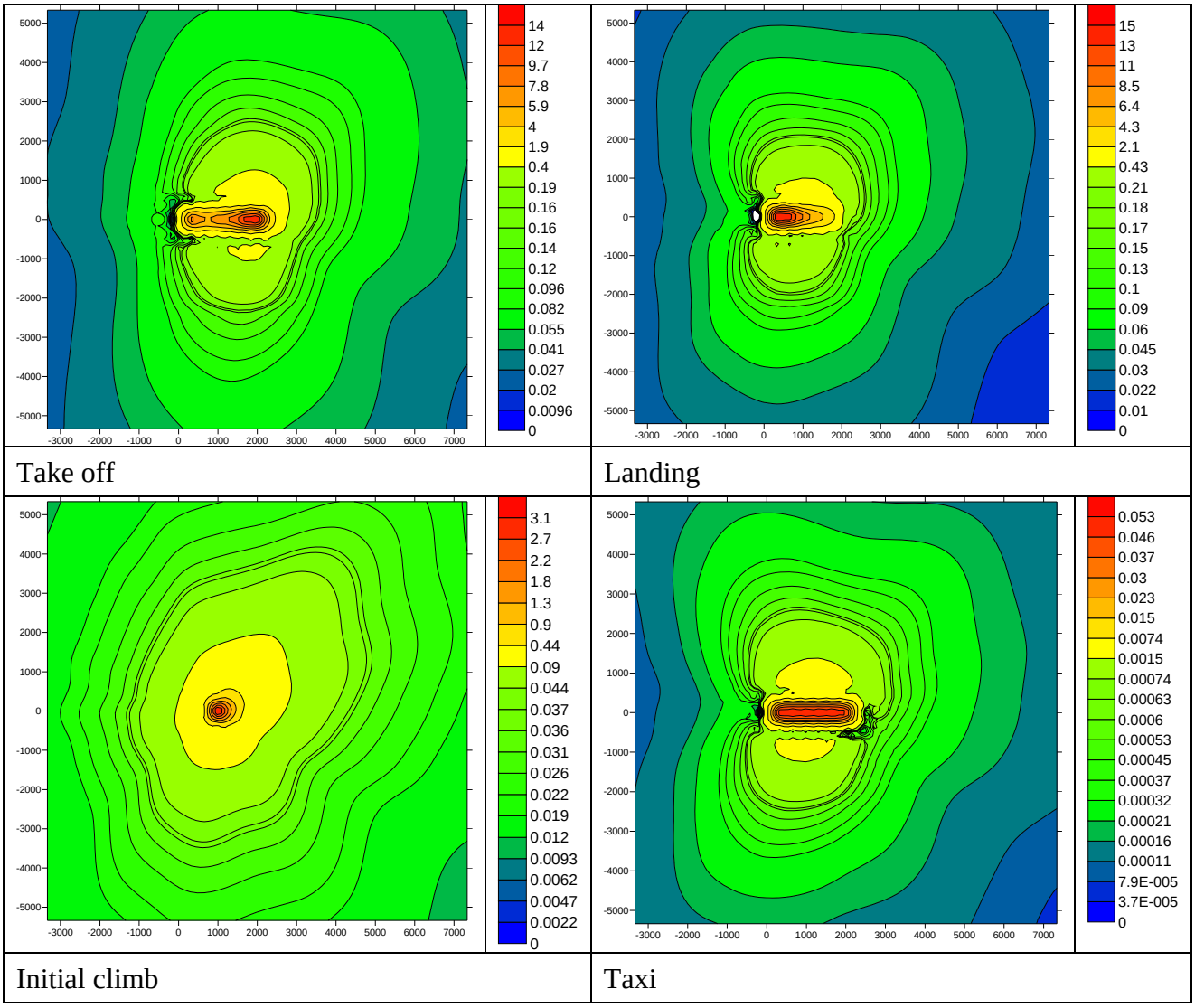

Figure 12.38: Normalised concentration plots for B777_200b the lead aircraft for MCAT 6

B777_200a

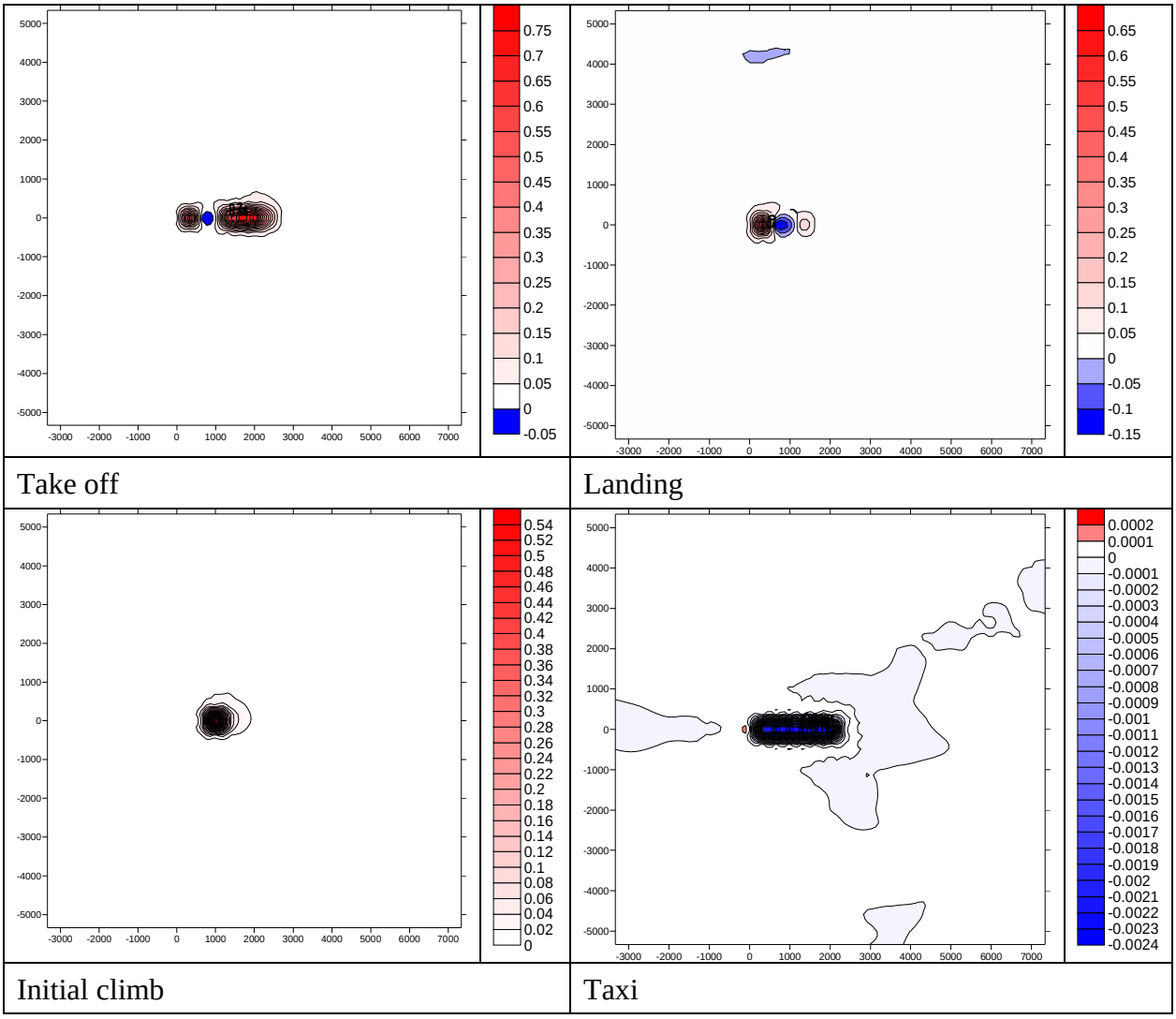

Figure 12.39: Absolute difference plots between B777_200a and MCAT 6 lead aircraft, B777_200b

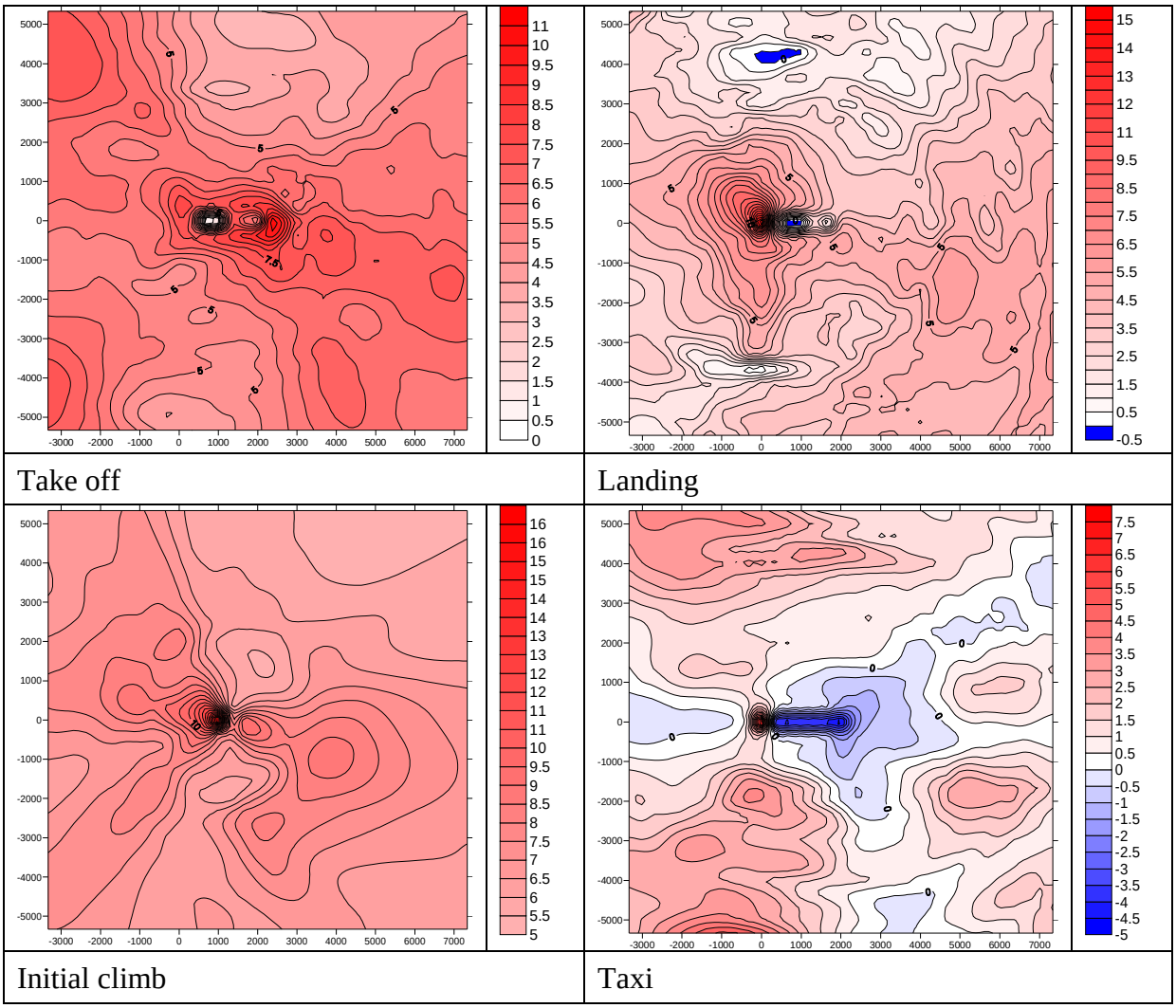

Figure 12.40: Percentage difference plots between B777_200a and MCAT 6 lead aircraft, B777_200b

B777_200c

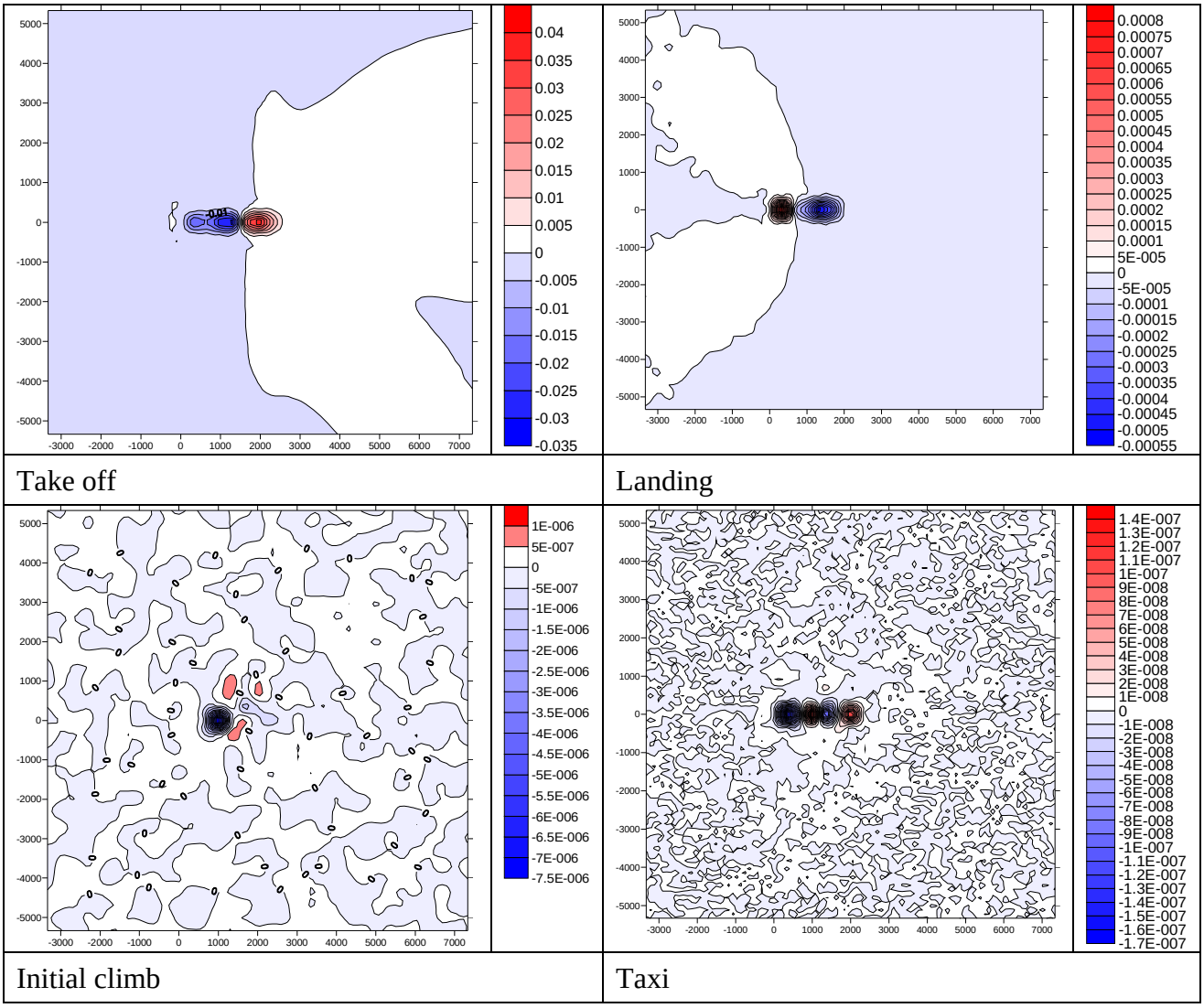

Figure 12.41: Absolute difference plots between B777_200c and MCAT 6 lead aircraft, B777_200b

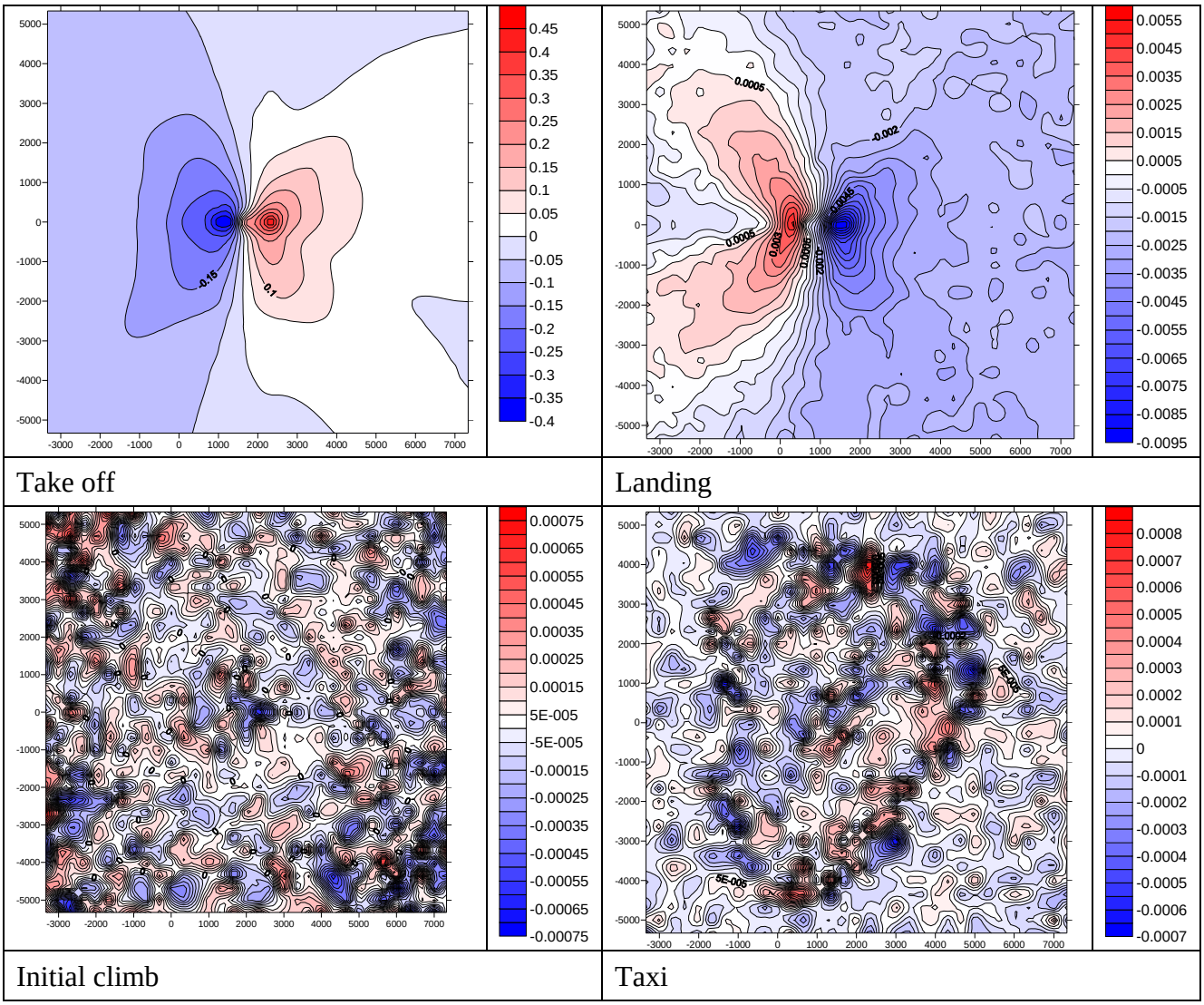

Figure 12.42: Percentage difference plots between B777_200c and MCAT 6 lead aircraft, B777_200b

B777_200d

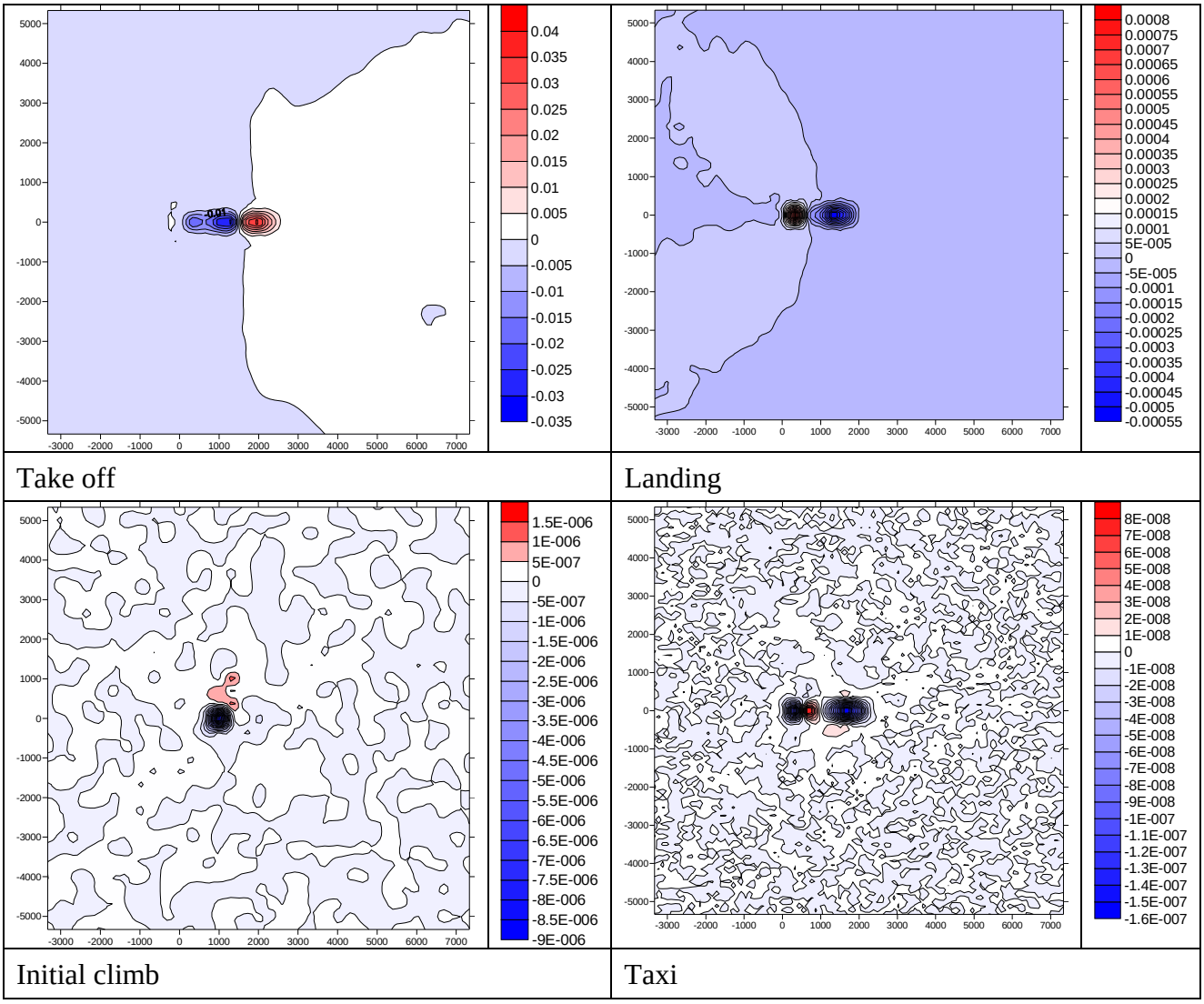

Figure 12.43: Absolute difference plots between B777_200d and MCAT 6 lead aircraft, B777_200b

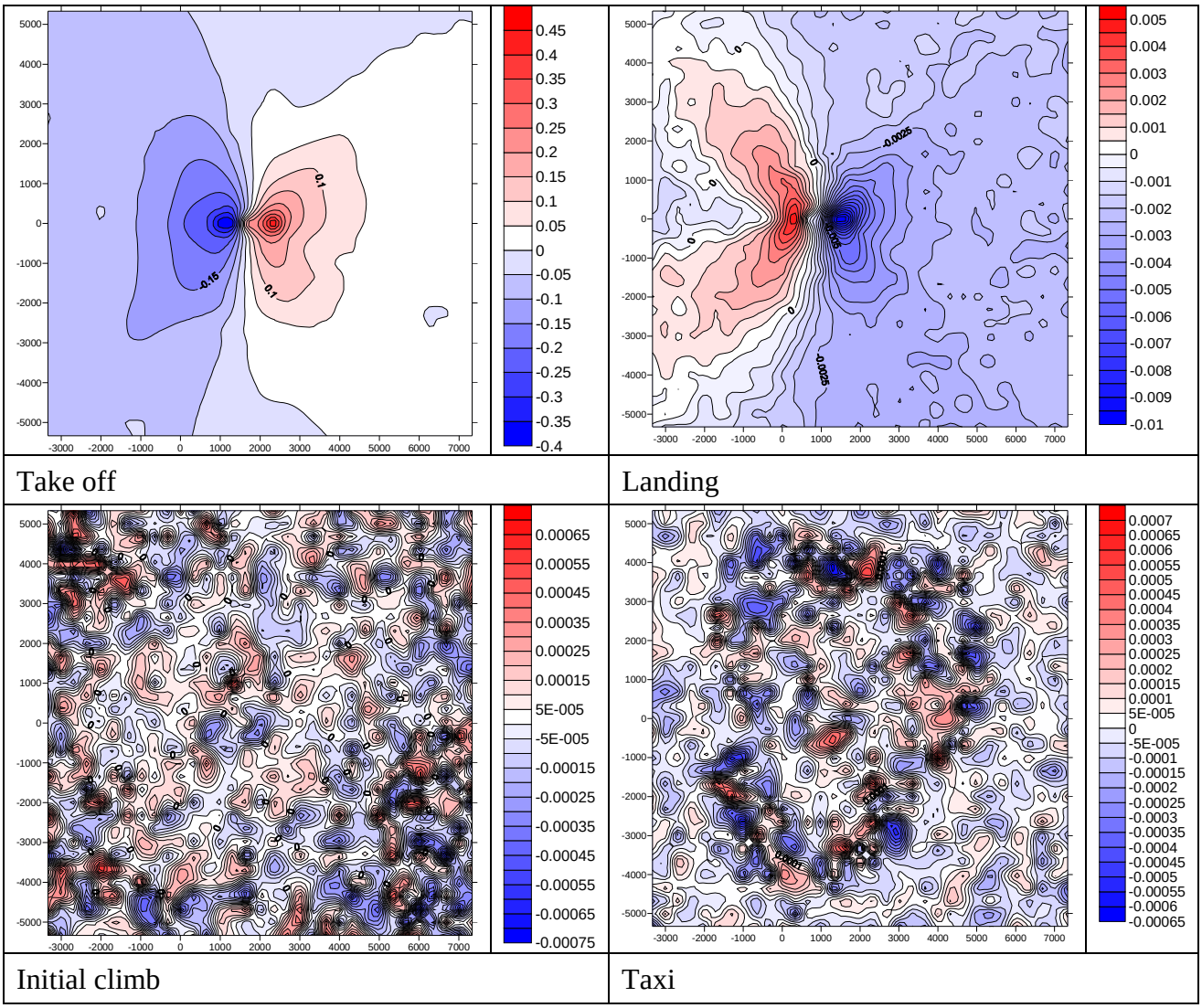

Figure 12.44: Percentage difference plots between B777_200d and MCAT 6 lead aircraft, B777_200b

B777_200e

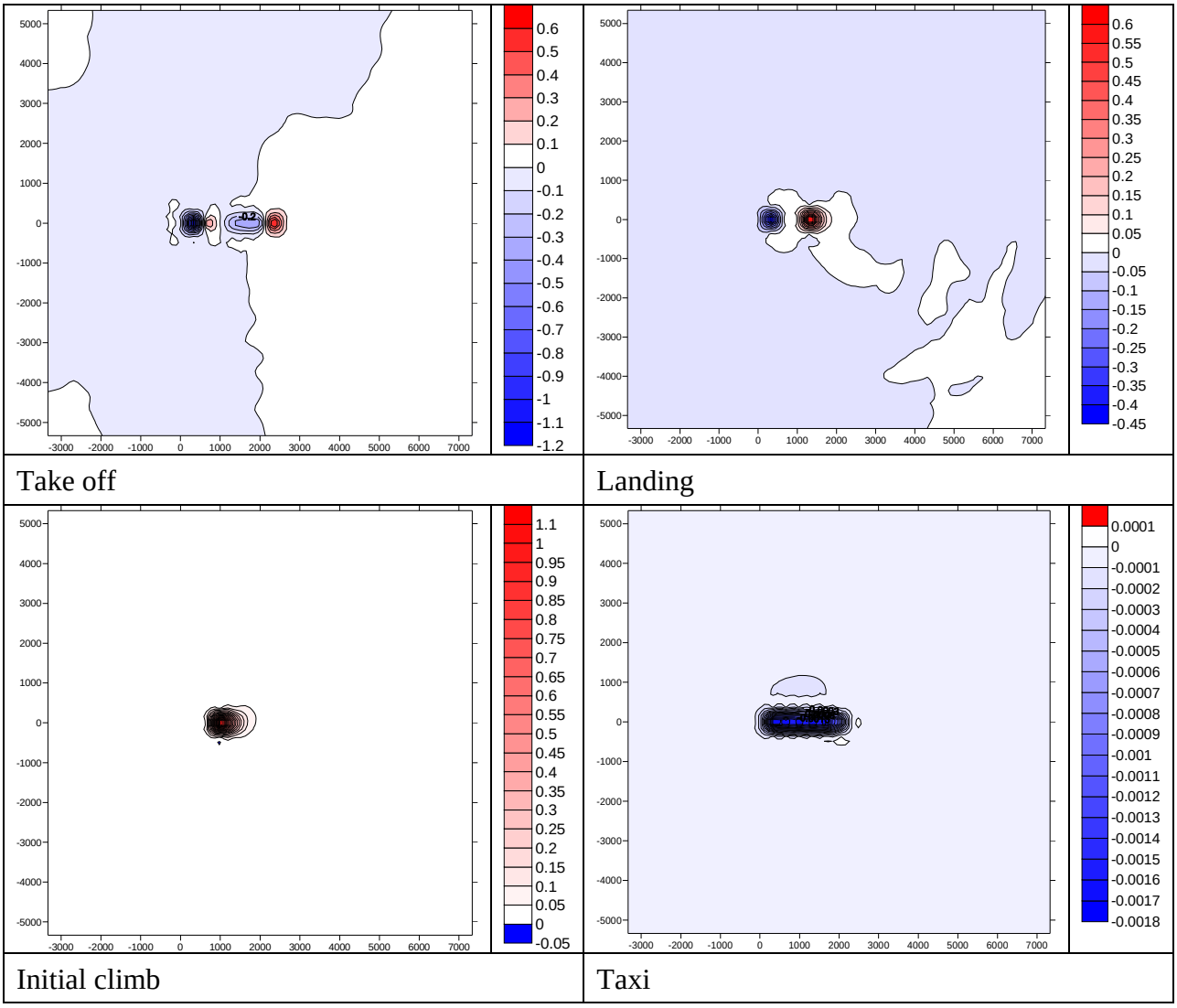

Figure 12.45: Absolute difference plots between B777_200e and MCAT 6 lead aircraft, B777_200b

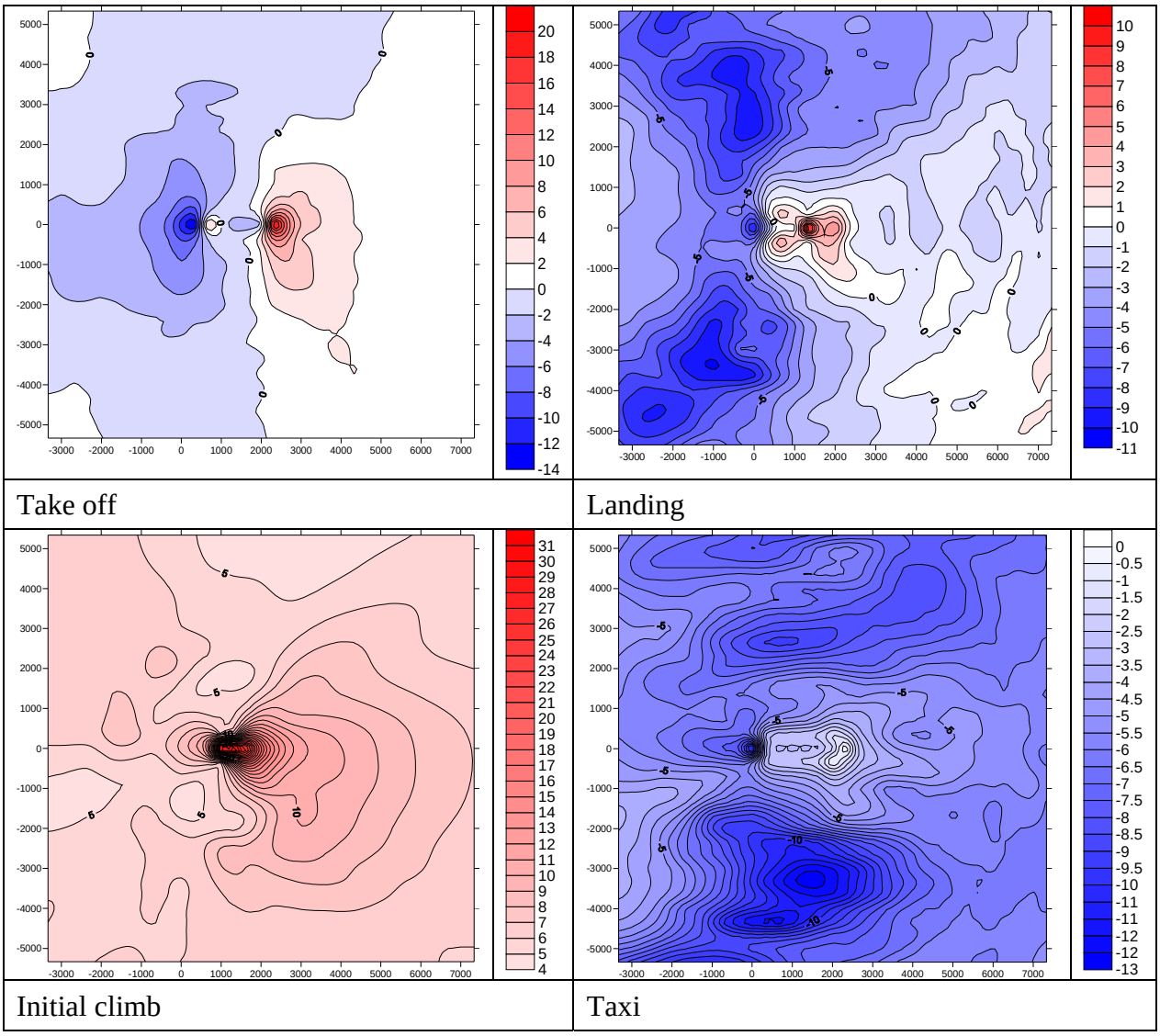

Figure 12.46: Percentage difference plots between B777_200e and MCAT 6 lead aircraft, B777_200b

B777_200f

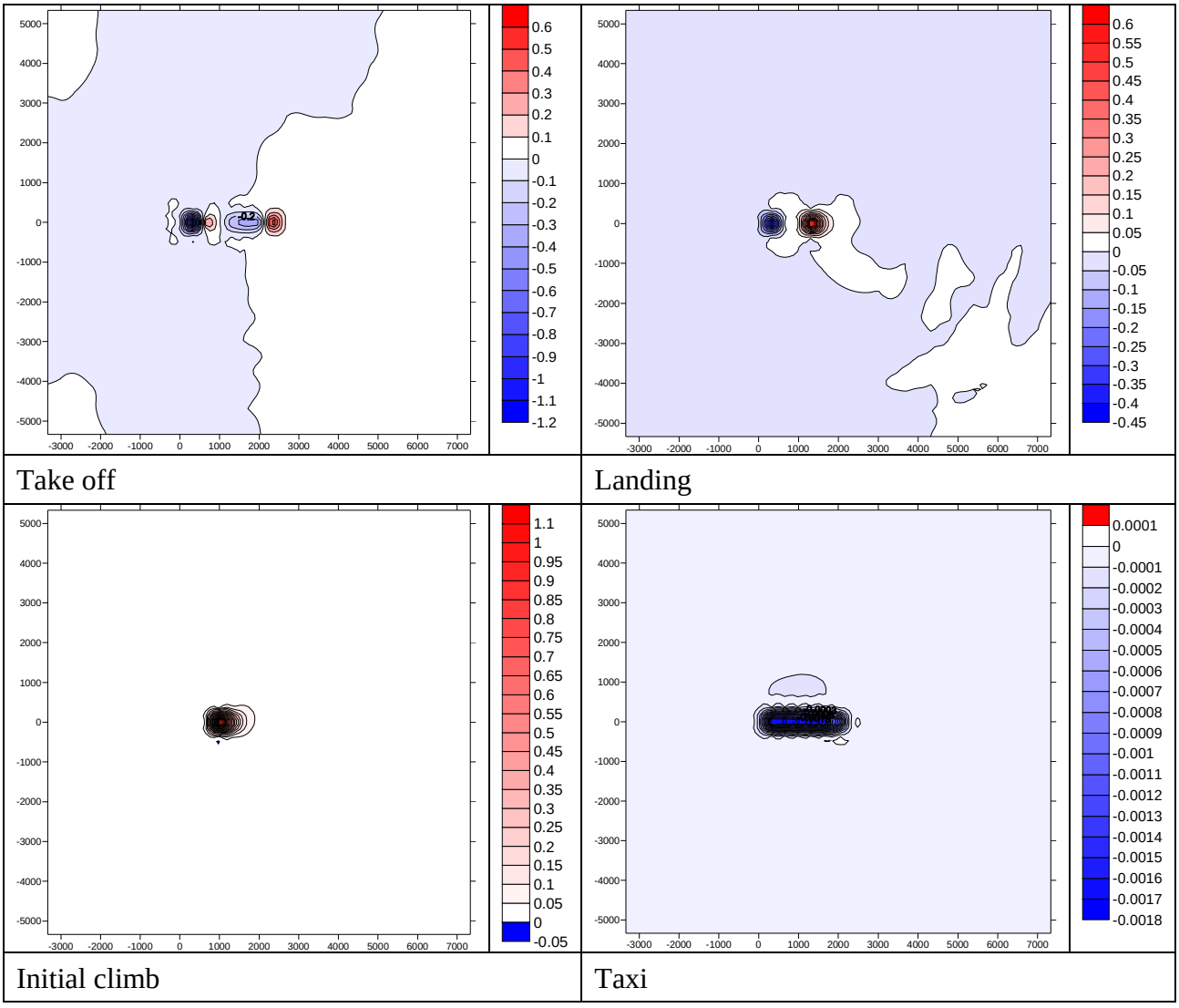

Figure 12.47: Absolute difference plots between B777_200f and MCAT 6 lead aircraft, B777_200b

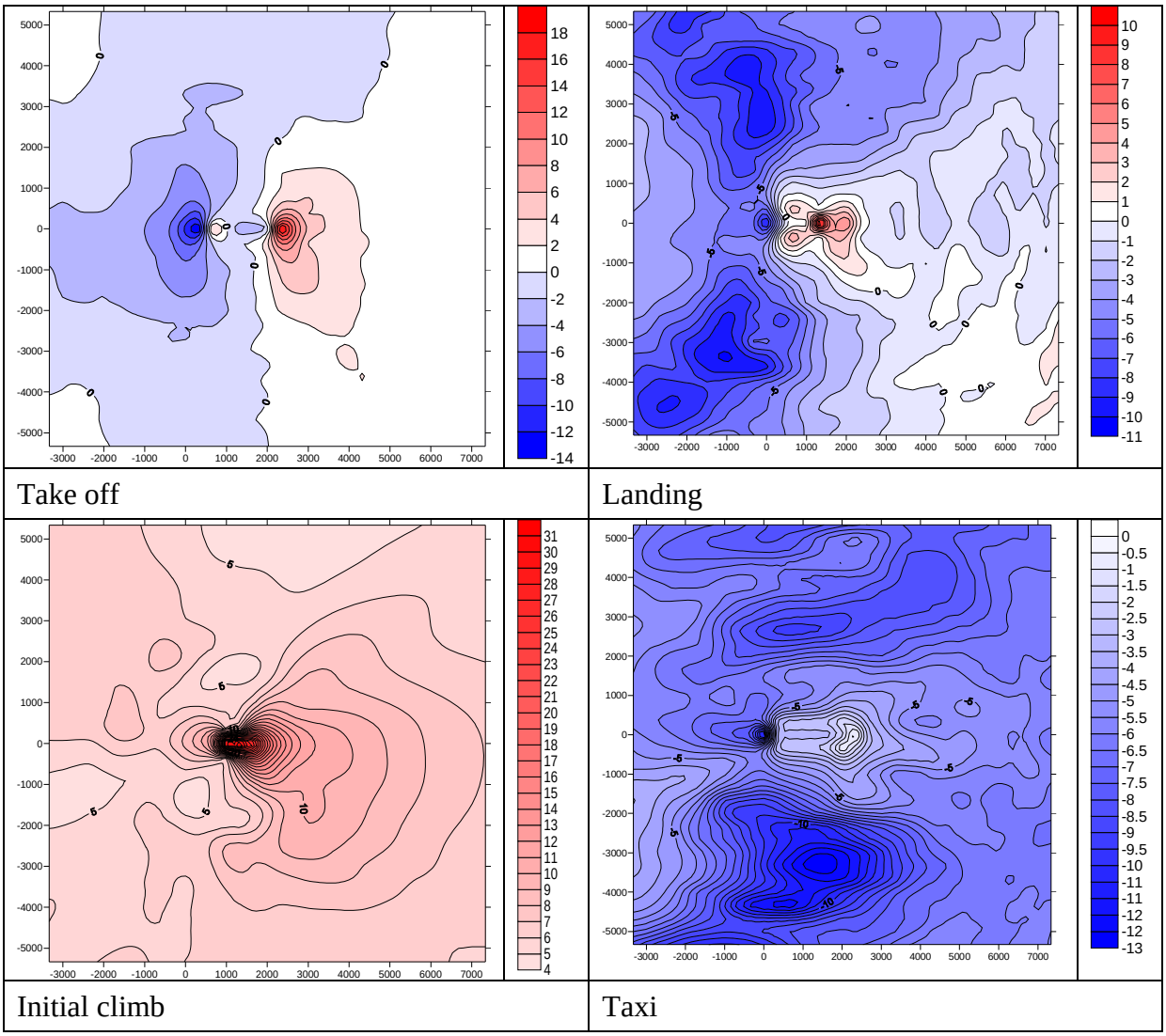

Figure 12.48: Percentage difference plots between B777_200f and MCAT 6 lead aircraft, B777_200b

B777_200g

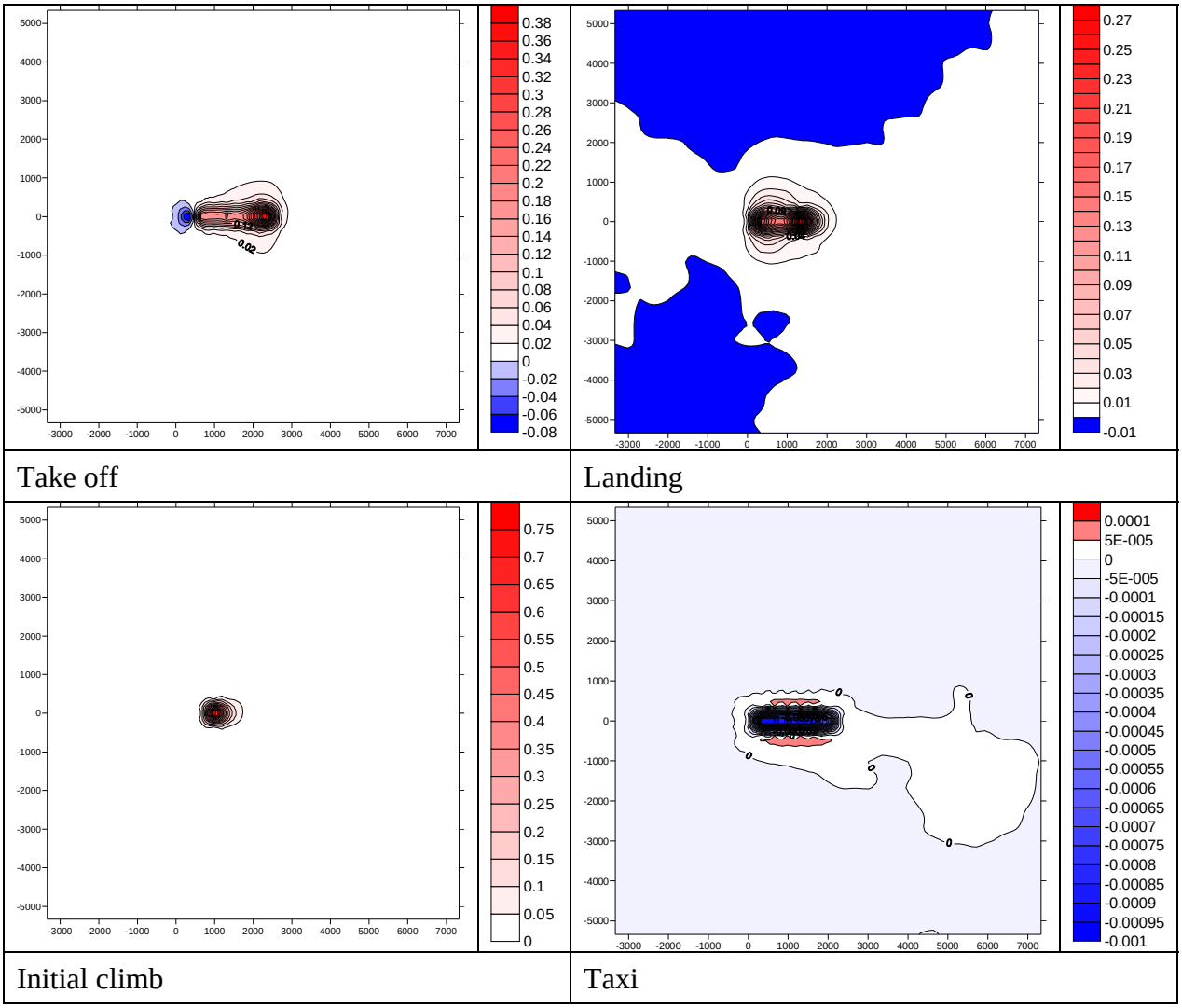

Figure 12.49: Absolute difference plots between B777_200g and MCAT 6 lead aircraft, B777_200b

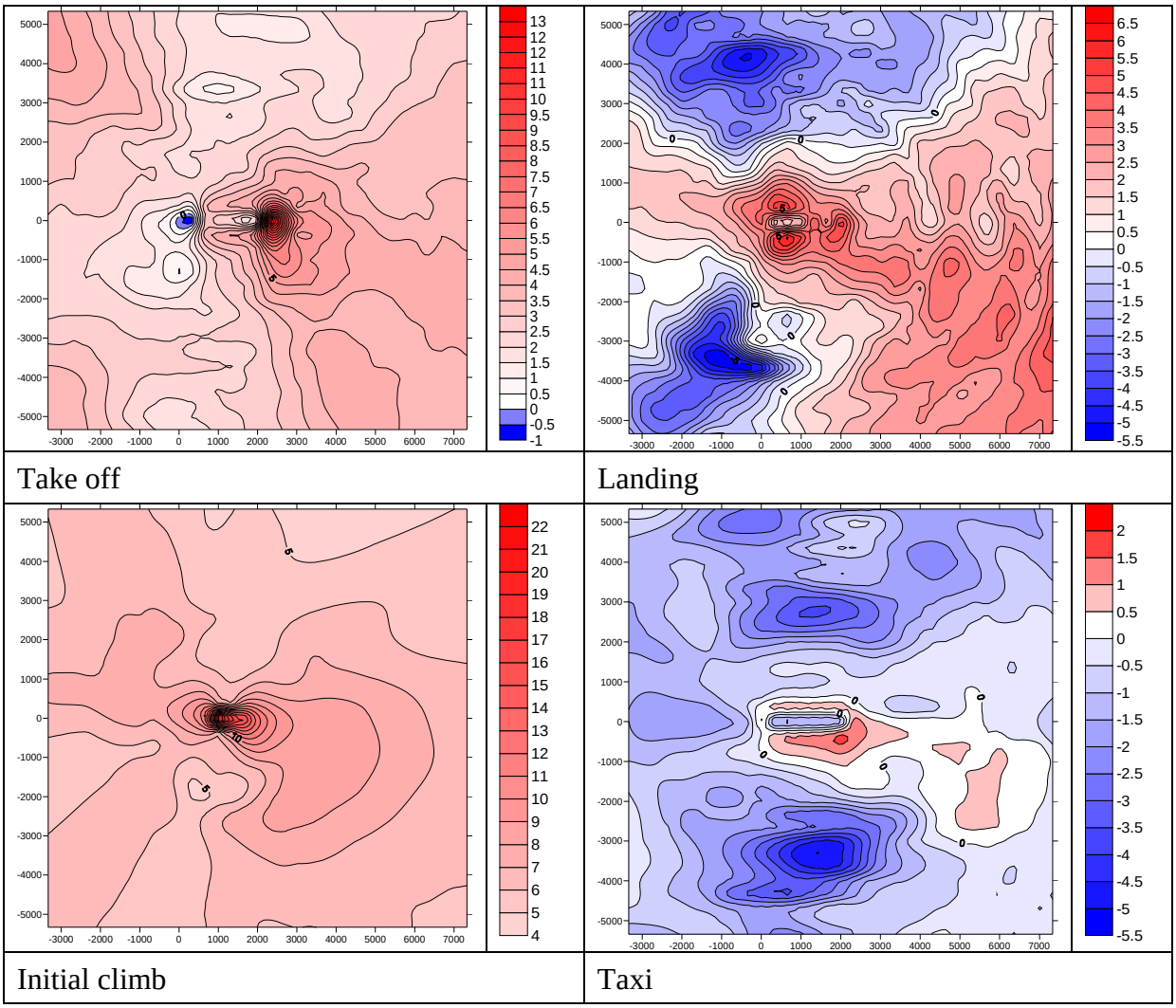

Figure 12.50: Percentage difference plots between B777_200g and MCAT 6 lead aircraft, B777_200b

B777_200h

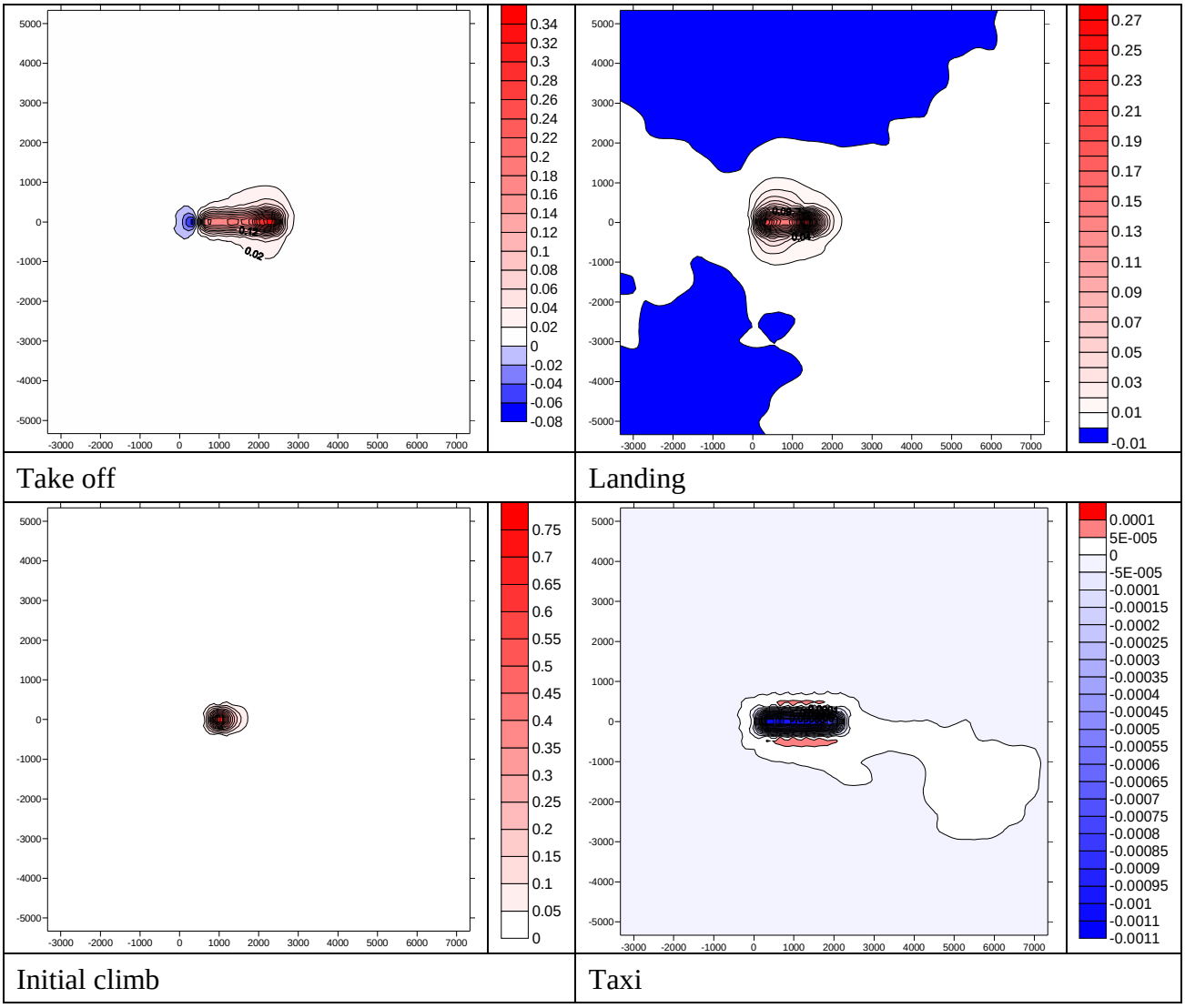

Figure 12.51: Absolute difference plots between B777_200h and MCAT 6 lead aircraft, B777_200b

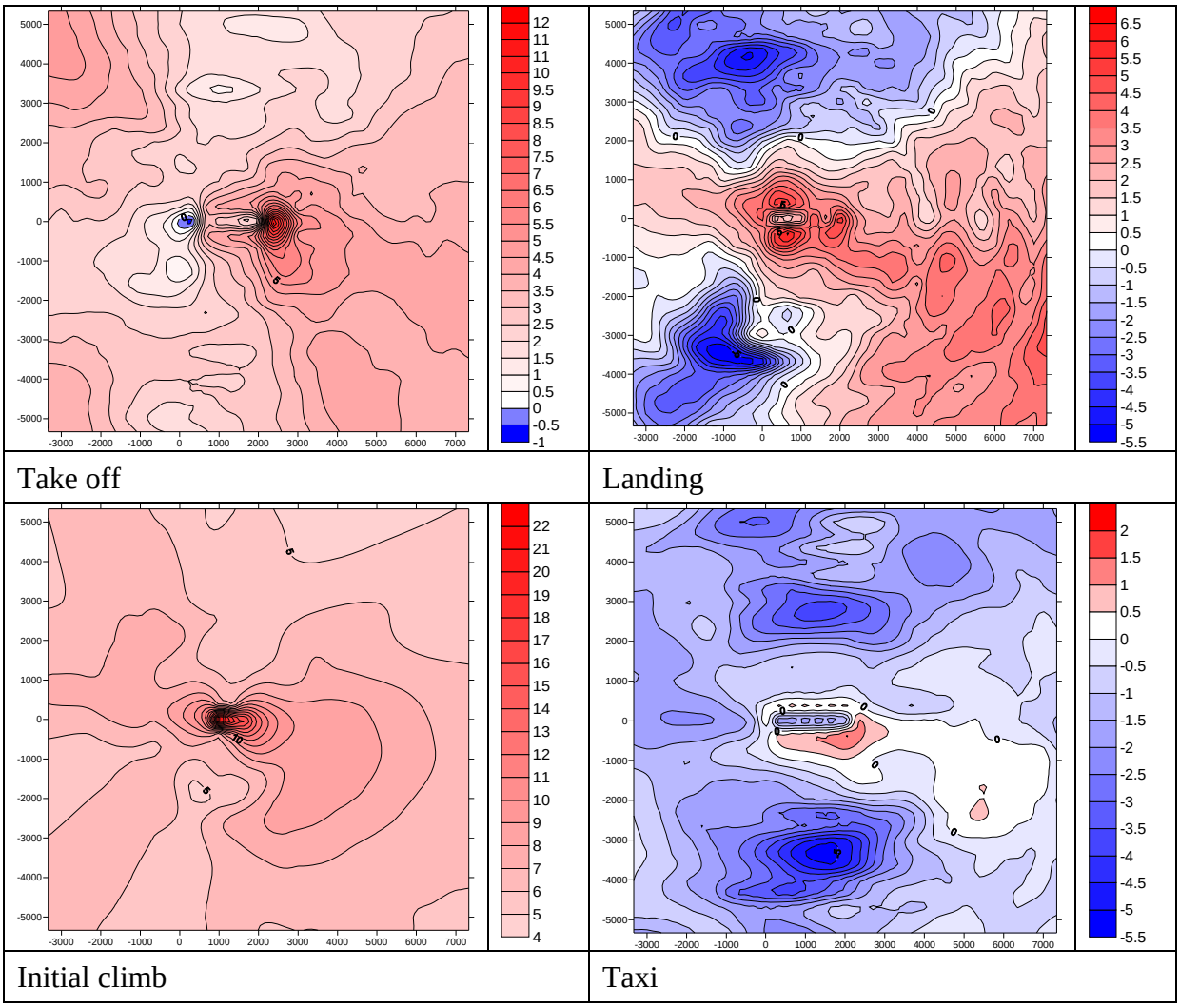

Figure 12.52: Percentage difference plots between B777_200h and MCAT 6 lead aircraft, B777_200b

B777_200i

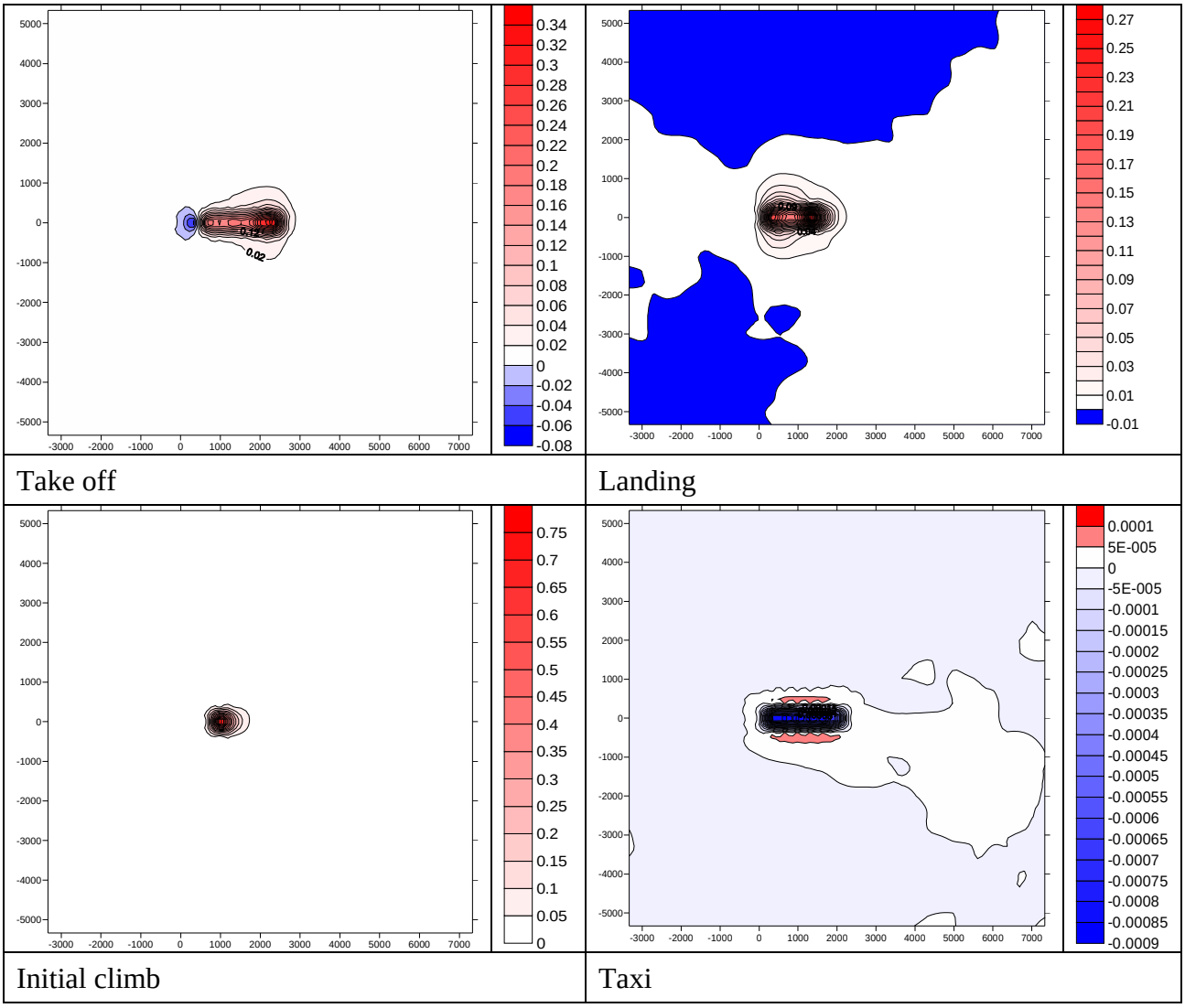

Figure 12.53: Absolute difference plots between B777_200i and MCAT 6 lead aircraft, B777_200b

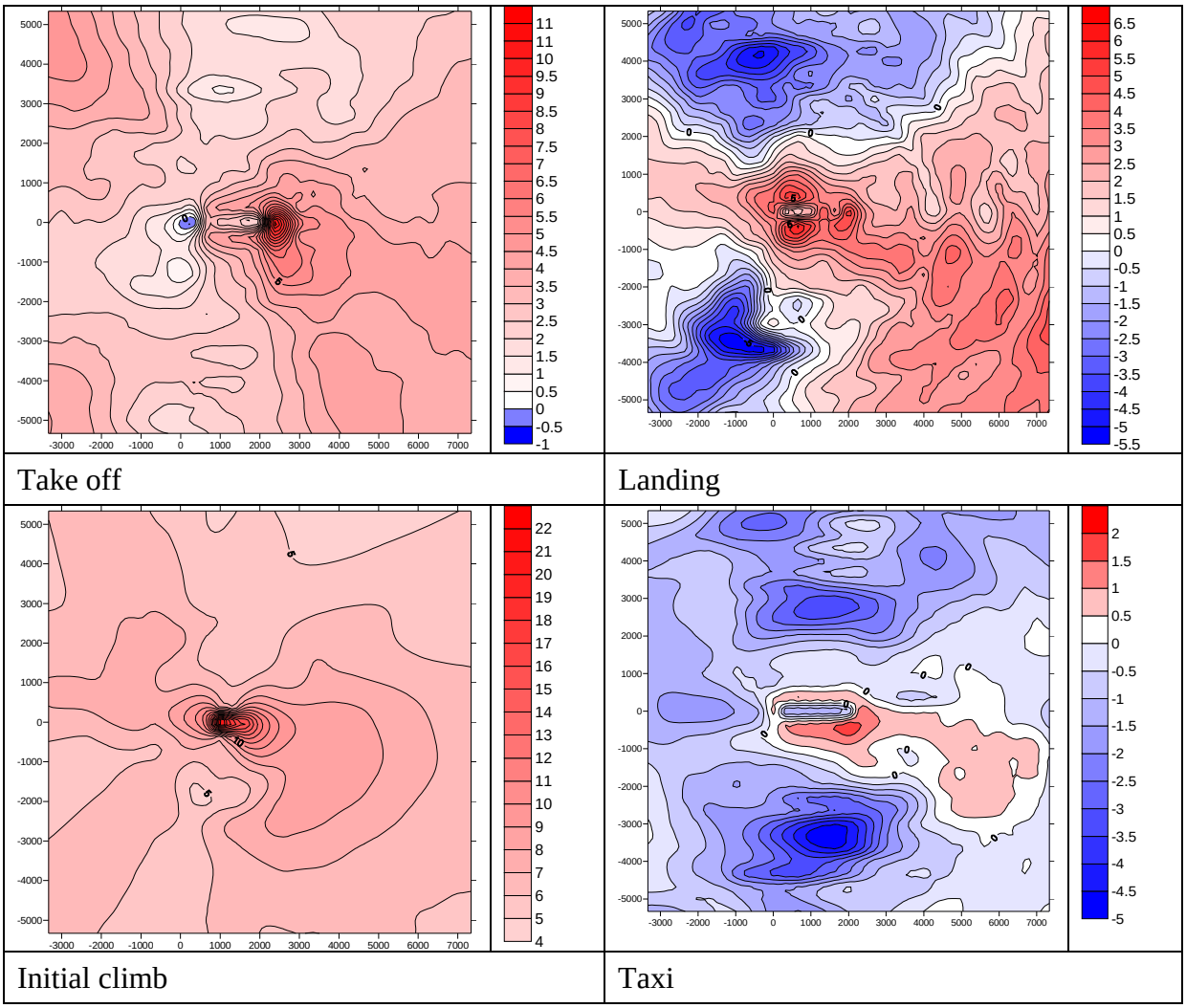

Figure 12.54: Percentage difference plots between B777_200i and MCAT 6 lead aircraft, B777_200b

12.2.10 MCAT 8

B787_3, B787_8

B787_3

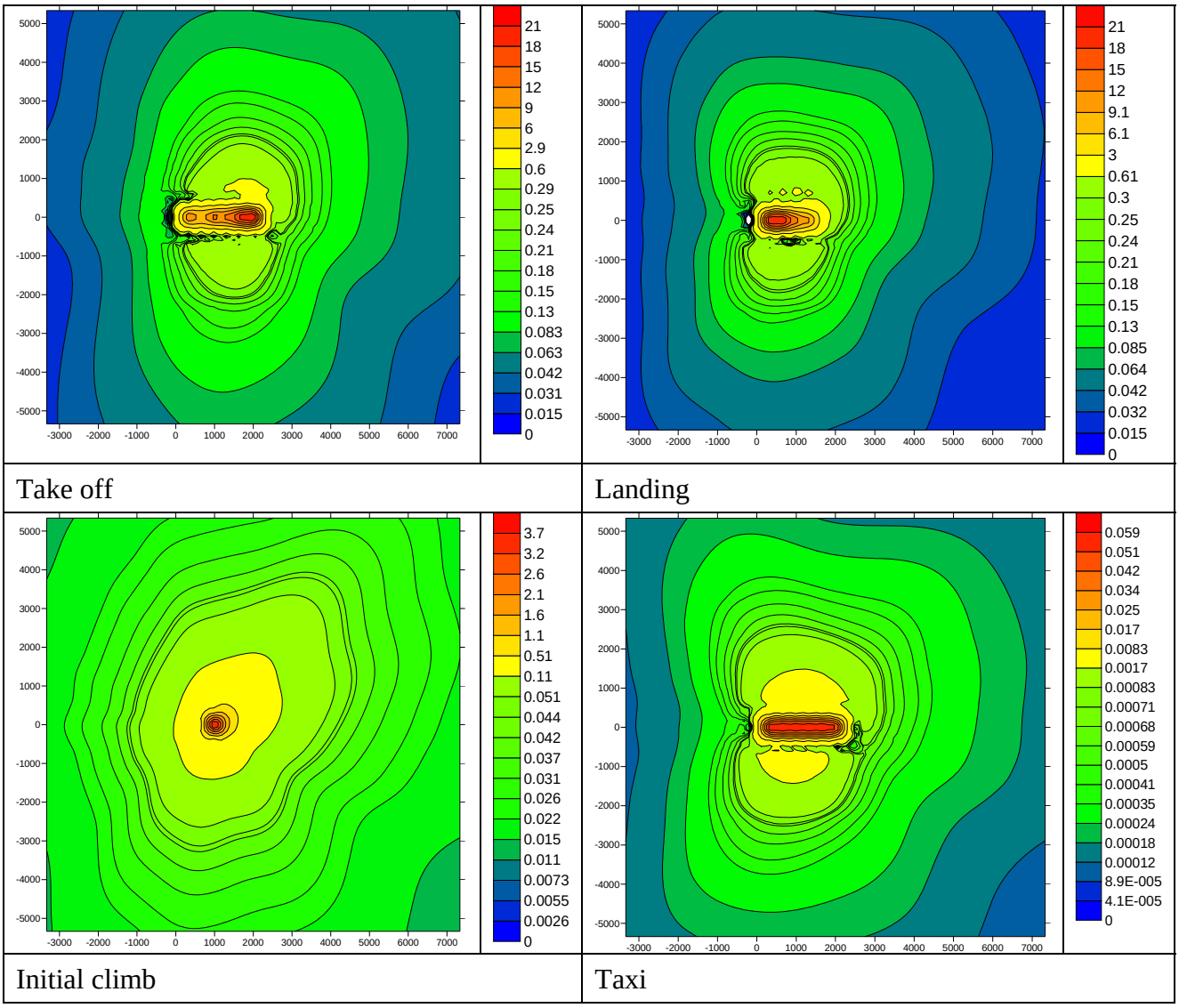

Figure 12.55: Normalised concentration plots for B787_3 the lead aircraft in MCAT 8

B787_8

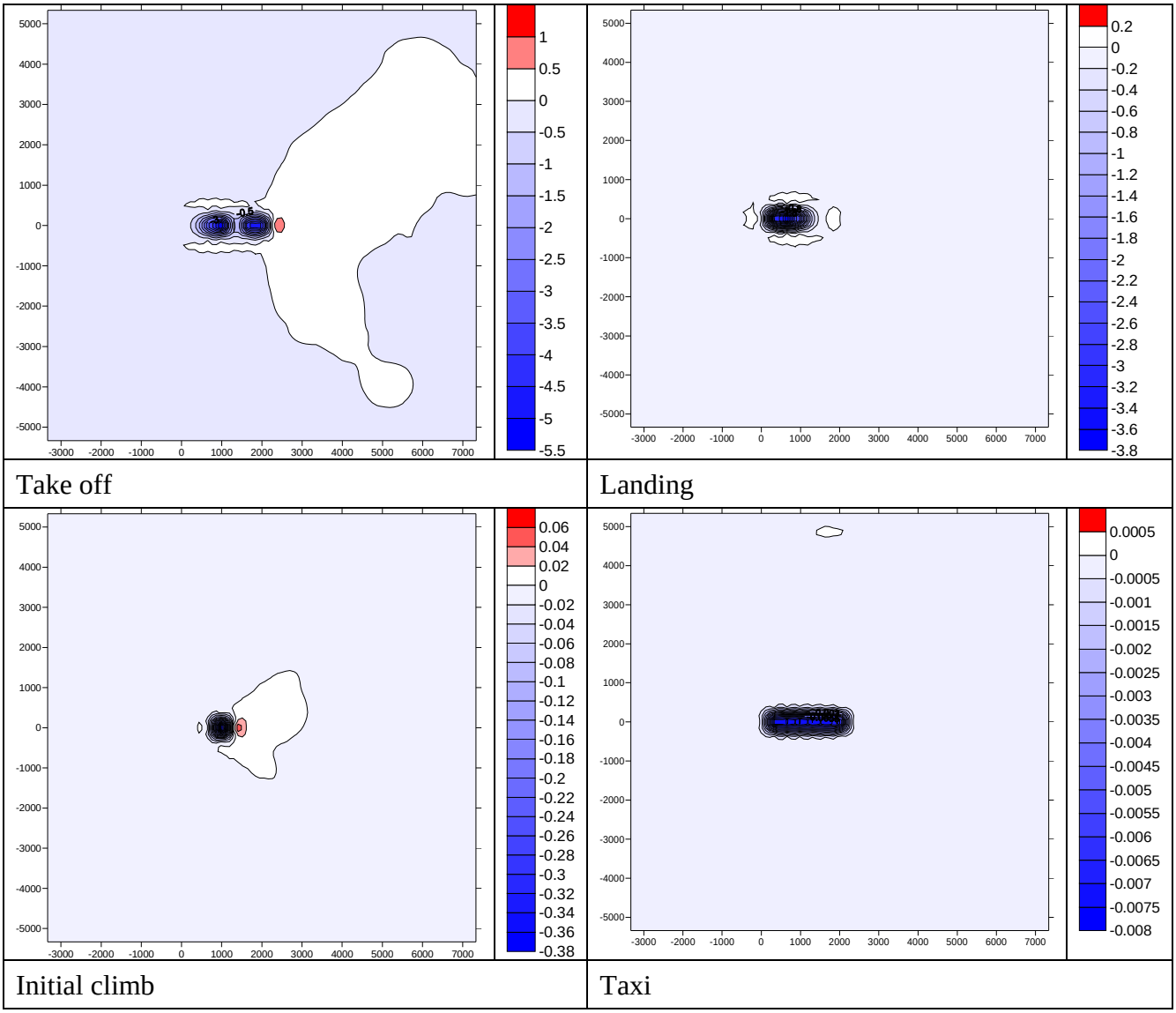

Figure 12.56: Absolute difference plots between B787_8 and MCAT 8 lead aircraft, B787_3

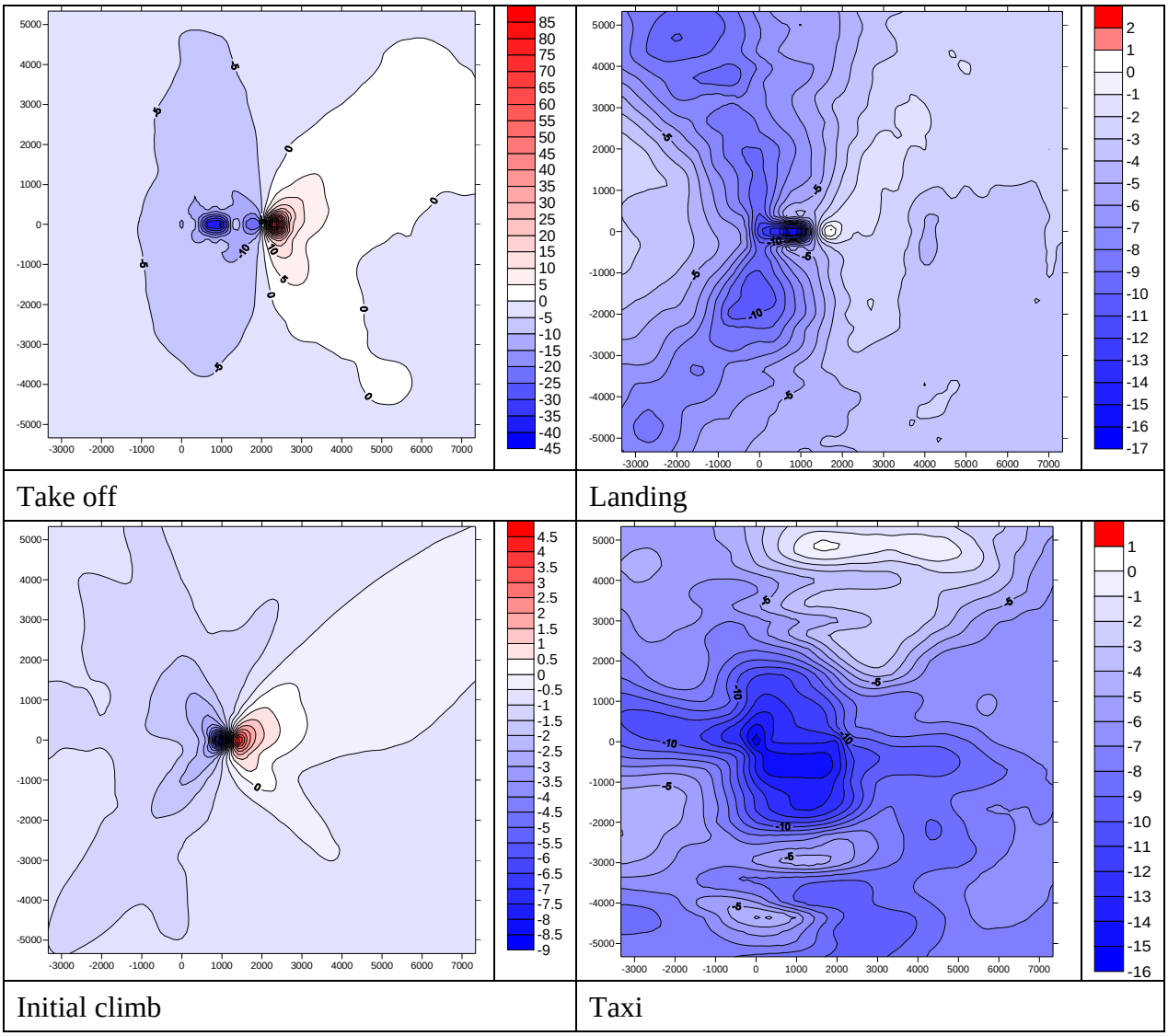

Figure 12.57: Percentage difference plots between B787_8 and MCAT 8 lead aircraft, B787_3

12.2.11 MCAT 9

A340_600a, A340_600b

A340_600a

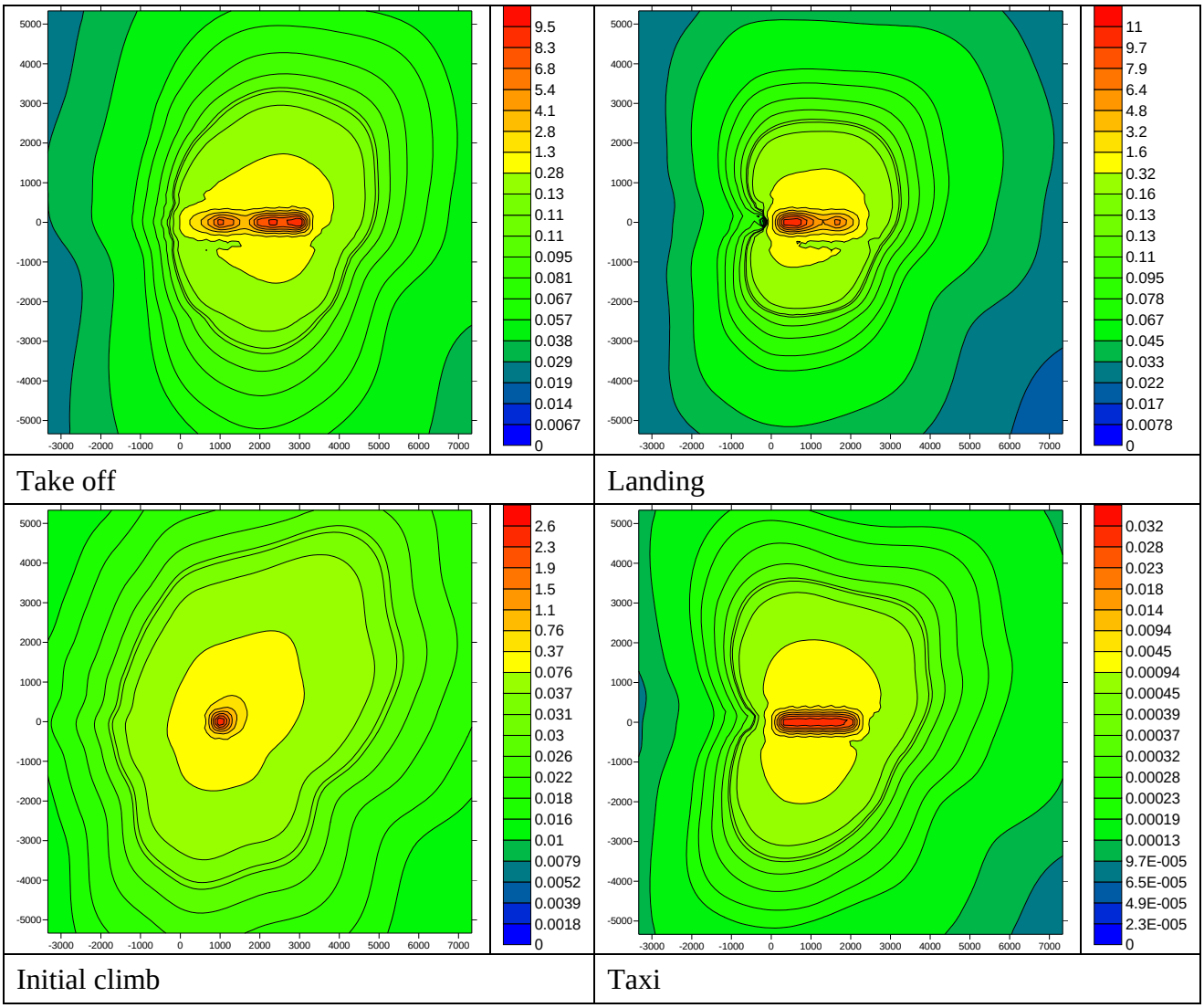

Figure 12.58: Normalised concentration plots for A340_600a the lead aircraft in MCAT 9

A340_600b

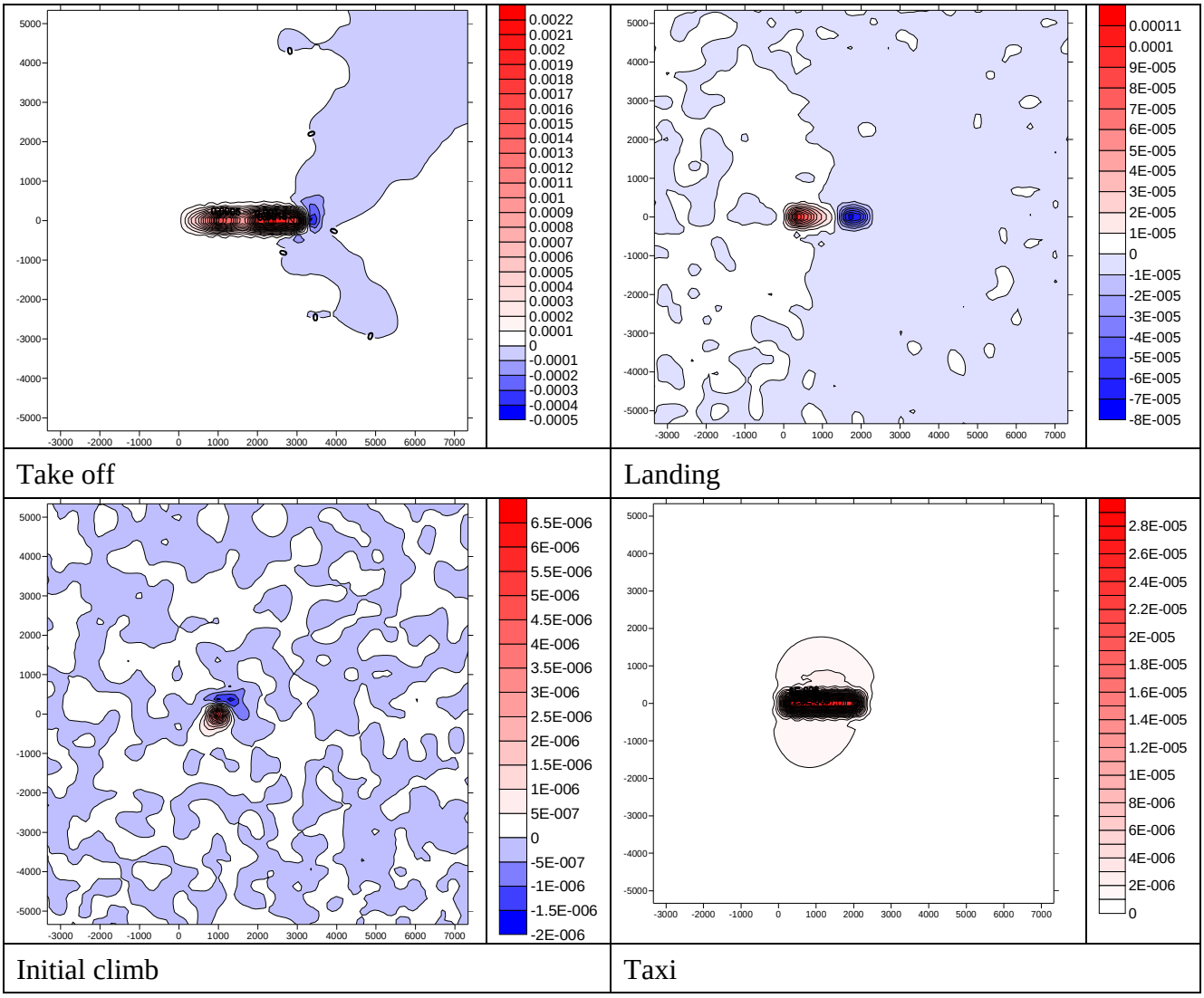

Figure 12.59: Absolute difference plots between A340_600b and MCAT 9 lead aircraft, A340_600a

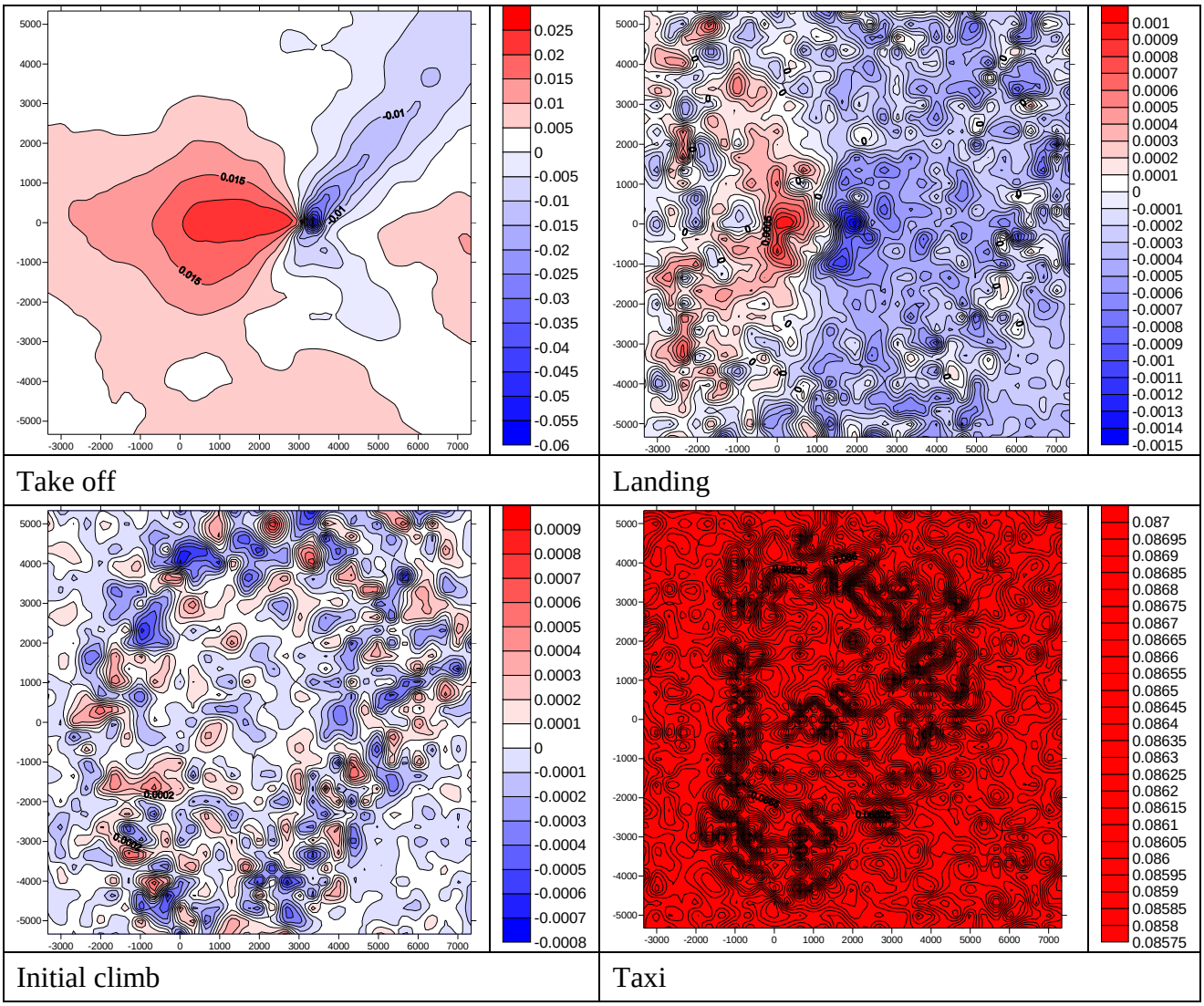

Figure 12.60: Percentage difference plots between A340_600b and MCAT 9 lead aircraft, A340_600a

12.2.12 MCAT 10

A350_800, A350_900

A350_800

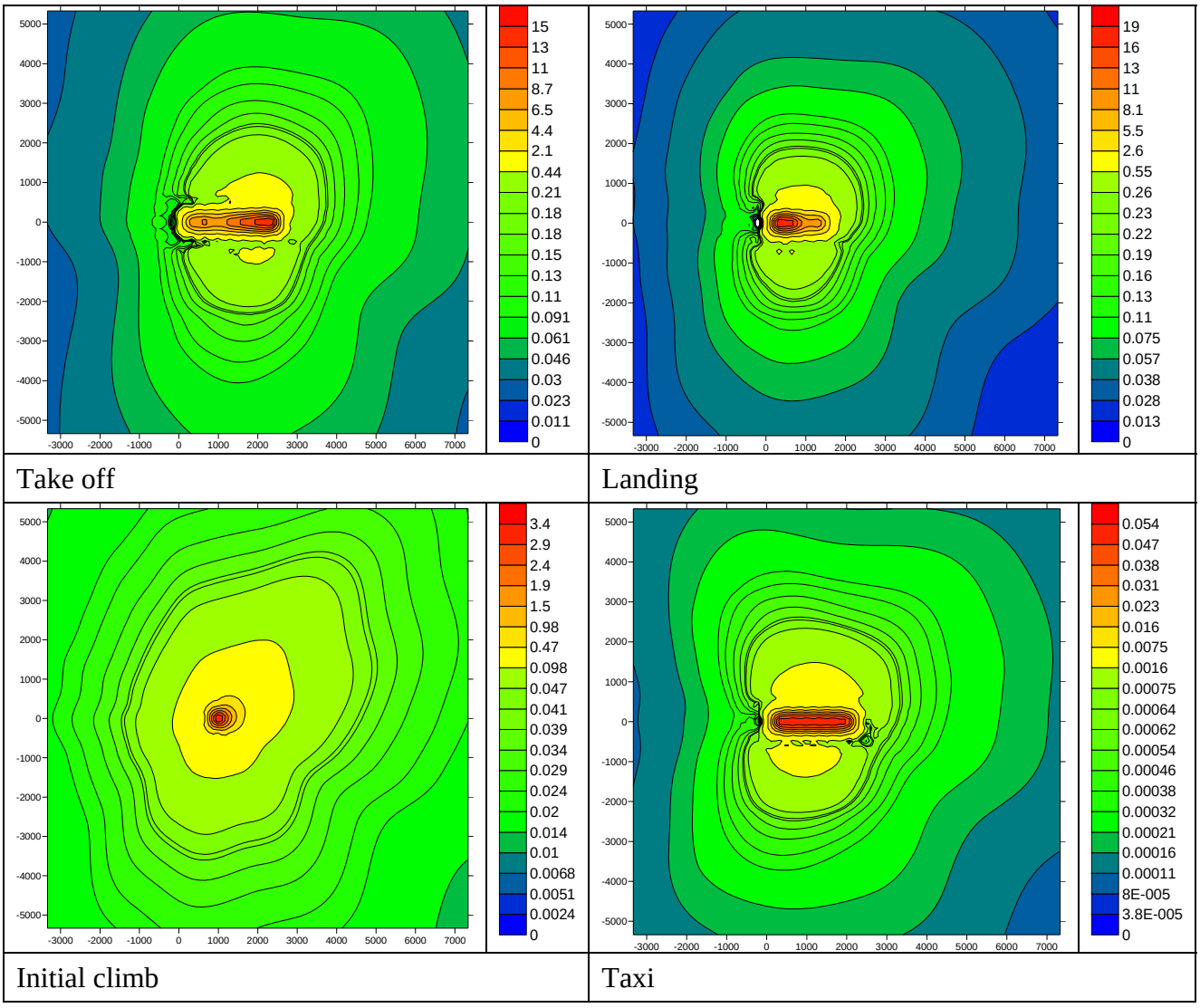

Figure 12.61: Normalised concentration plots for A350_800 the lead aircraft for MCAT 10

A350_900

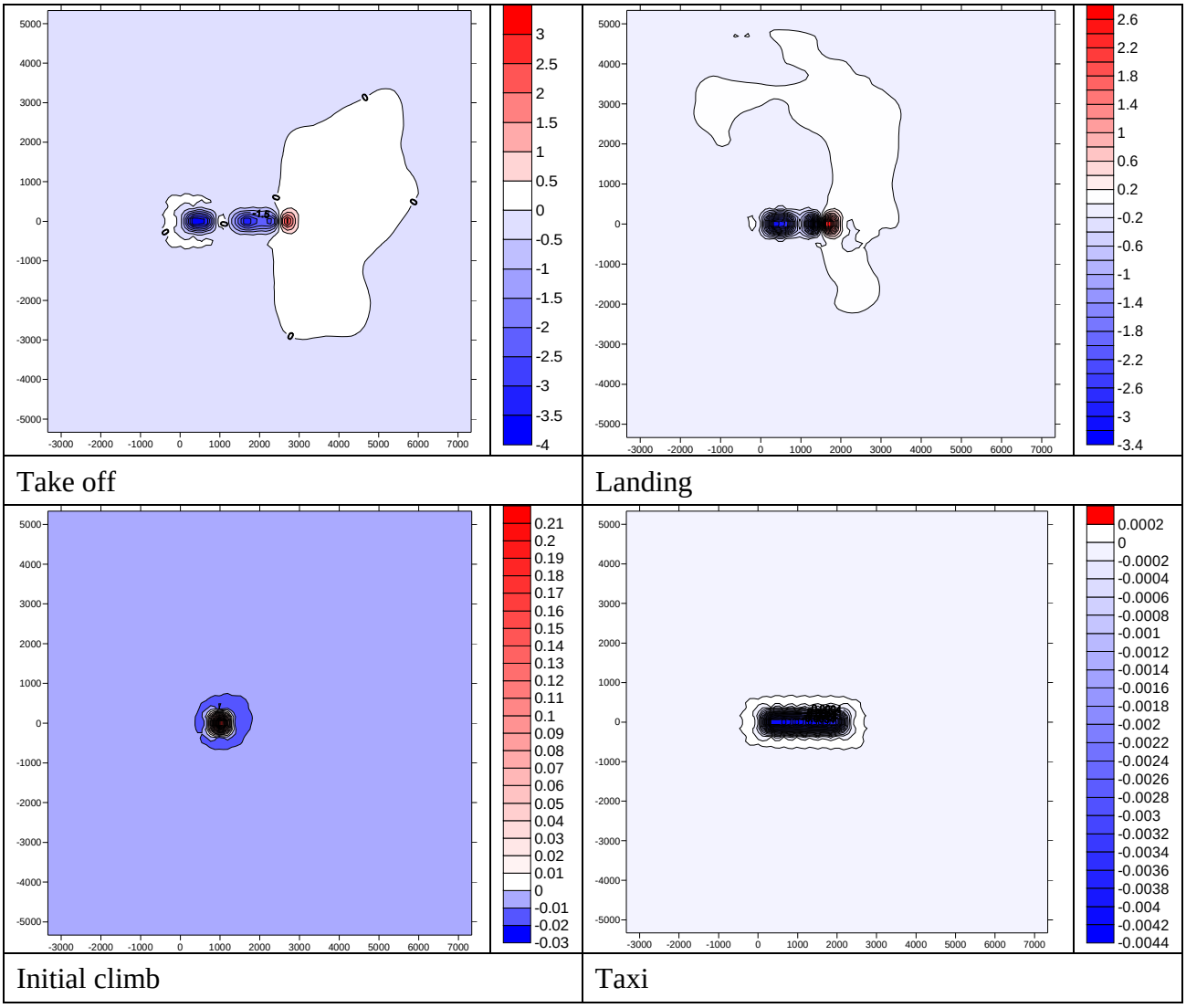

Figure 12.62: Absolute difference plots between A350_900 and MCAT 10 lead aircraft, A350_800

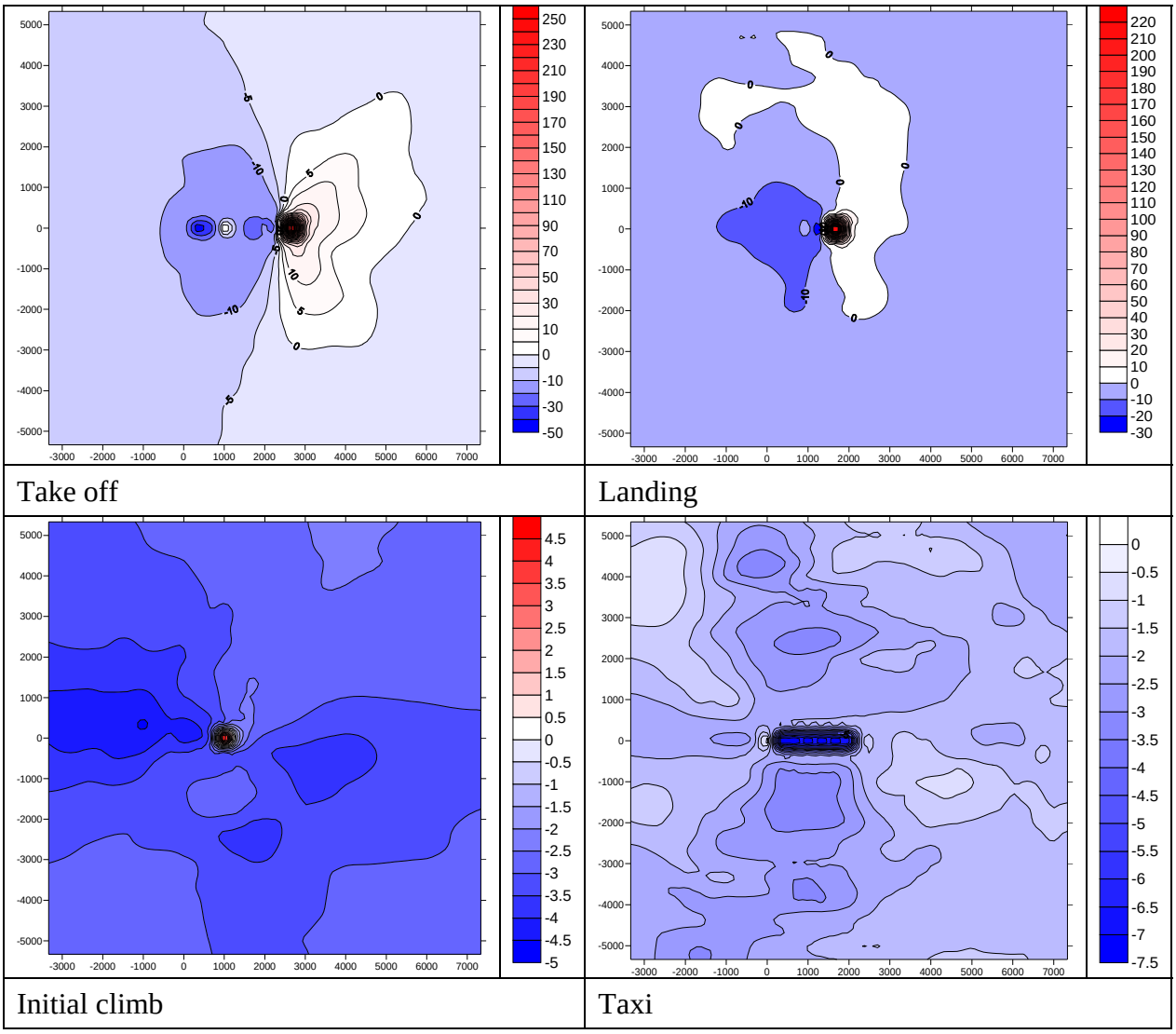

Figure 12.63: Percentage difference plots between A350_900 and MCAT 10 lead aircraft, A350_800

12.3 2020 MCAT data

This chapter outlines the development of the 2020 MCATs. Aircraft that were also present in 2015 have not been re-analysed. The new aircraft have been compared to the lead aircraft from the 2015 MCATs, this lead aircraft has been kept the same even in situations where that aircraft is no longer part of the fleet.

The aircraft that have been examined in 2020, along with the designator used for them, are given in Table 12.6. The total NOx emissions for each mode for each of the new aircraft are given in Table 12.7.

Designator	Aircraft	Engine	UID
A320a	A320 family	V2527-A5	1|A003
A320c*	A320 family	V2527-A5	1|A003
A330a	A330-300	Trent 772	3RR030/1
A330b	A330-300	Trent 772	3RR030
A330c	A330-300	Trent 772	3RR030/2
A340_600a	A340-600	Trent 556	6RR041
A340_600b	A340-600	Trent 556	6RR041/1
A350_800	A350-800/B787-9 (250 l-haul)	T500 derivative	NE08/1
A350_900	A350-900/B787-10 (300 l-haul)	Trent 900/GP2700 growth	NE10/1
A380	A380	Trent 900/GP7200	NE01/1
A380b*	A380	Trent 900/GP7200	NE01/2
B737_600a	B737-600/800	CFM56-7B24	3CM032
B737_600b	B737-600/800	CFM56-7B24	3CM032/1
B737_600c	B737-600/800	CFM56-7B24	3CM032/2
B737_800*	B737-800RE (220 s-haul)	Scaled Trent 500	NE06/1
B747_400	B747-400	RB211-524G/H	4RR037
B747_800	B747-800	Genx – 2B67	NE02/1
B747_800b*	B747-800	Genx – 2B67	NE02/2
B757_200	B757-200	RB211-535E4	5RR038
B777_200b	B777-200	Trent 892	2RR027
B777_200c	B777-200	Trent 892	2RR027/1
B777_200d	B777-200	Trent 892	2RR027/2
B777_200e	B777-200/300	GE90-115B1	7G3099
B777_200f	B777-200/300	GE90-115B1	7G3099/1
B777_200g	B777-200/300	GE90-92B	3GE066
B777_200h	B777-200/300	GE90-92B	3GE066/1
B777_200i	B777-200/300	GE90-92B	3GE066/2
B787_3	B787-3	GENx	NE09/1
B787_3b*	B787-3	GENx	NE09/2
B787_8	B787-8	GENx	NE07/1
B787_8b*	B787-8	GENx	NE07/2
N120s*	New 120 seater	CFM56-X	NE03AB/1
N150s*	New 150 seater	CFM65-X/V2500-X	NE04AB-1
N180s*	New 180 seater	CFM65-X/V2500-X	NE05AB-1

*Table 12.6: The aircraft in 2020 along with the designator used for them. The *s mark the aircraft which were not present in 2015.*

Aircraft	Take off	Landing	Initial climb	Taxi
A320c	754	90	158	141
A380b	3,447	356	453	336
B737_800	923	108	194	208
B747_800b	2,687	330	368	293
B787_3b	1,303	169	292	246
B787_8b	1,877	220	400	286
N120s	512	63	126	115
N150s	642	74	150	121
N180s	828	91	184	135

Table 12.7: The total NOx emissions for each mode for one event. Note for taxi this one event is a 2000m long taxi.

The normalised centreline concentration plots for the modes for each of the new aircraft along with the lead aircraft from the 2015 MCATs are shown in Figures 12.64 to12.67. With the final MCATS being listed in Table 12.8. Figures 12.68 to 12.85 then go through each MCAT showing the normalised concentration plots for each mode for the lead aircraft and then percentage difference plots for each of the new aircraft in that MCAT comparing them to the lead aircraft.

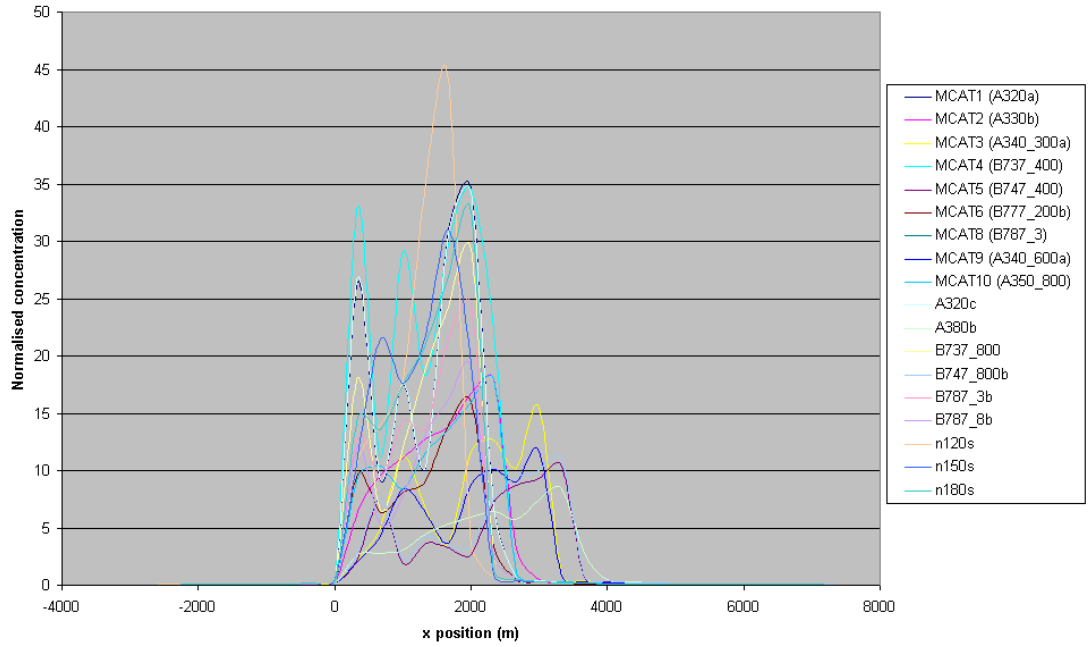

Figure 12.64: Normalised NO_x concentration plot for take off

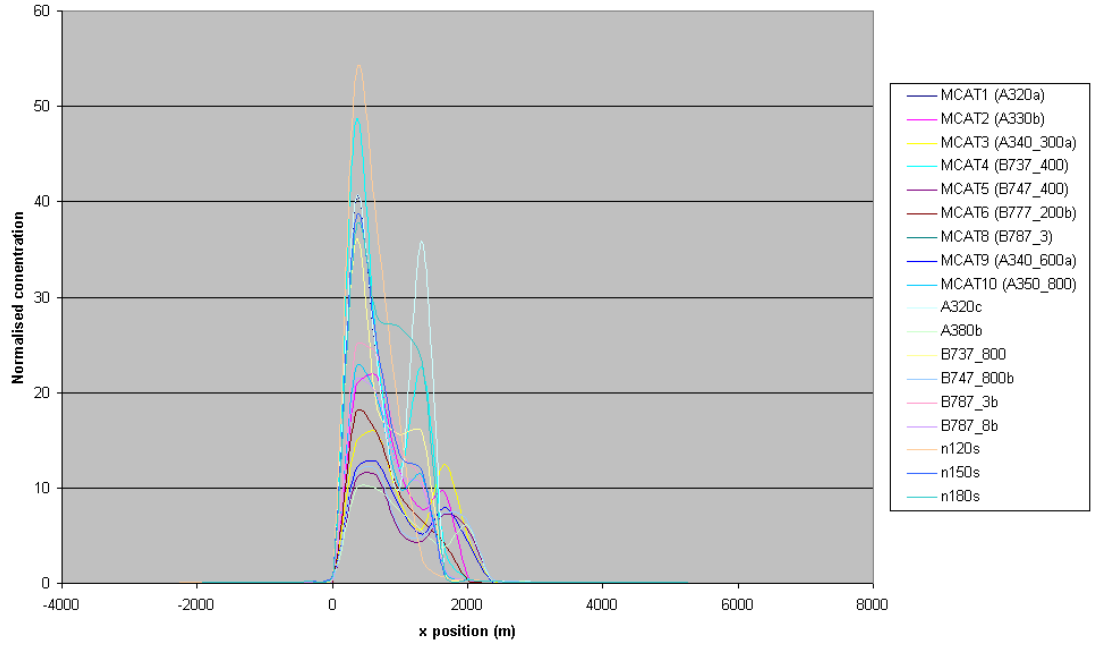

Figure 12.65: Normalised NO_x concentration plot for landing

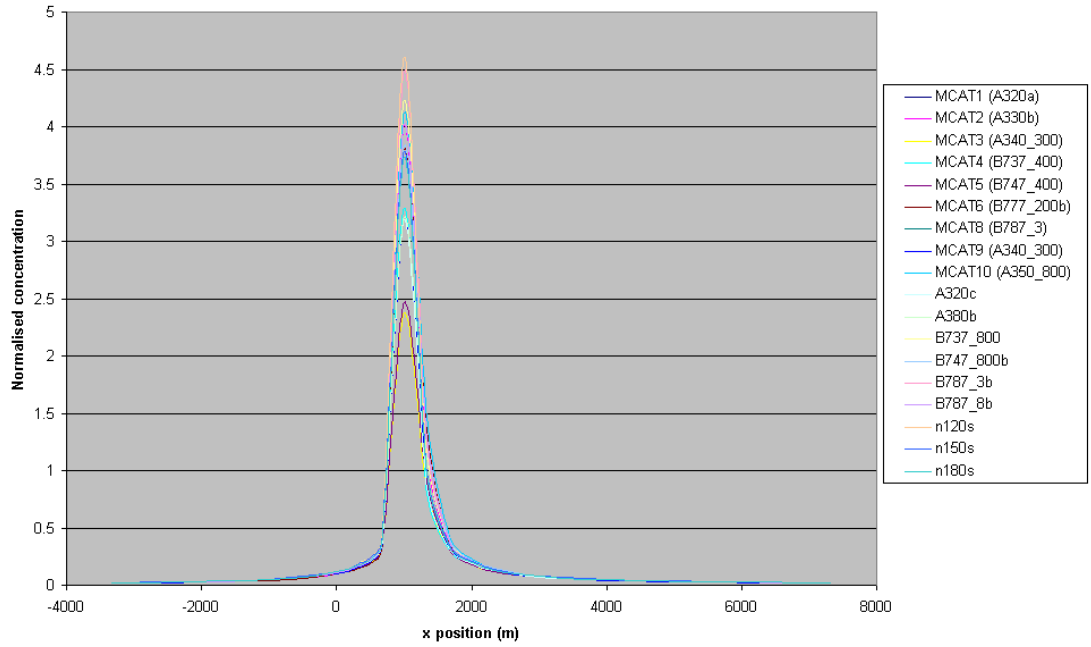

Figure 12.66: Normalised NO_x concentration plot for initial climb

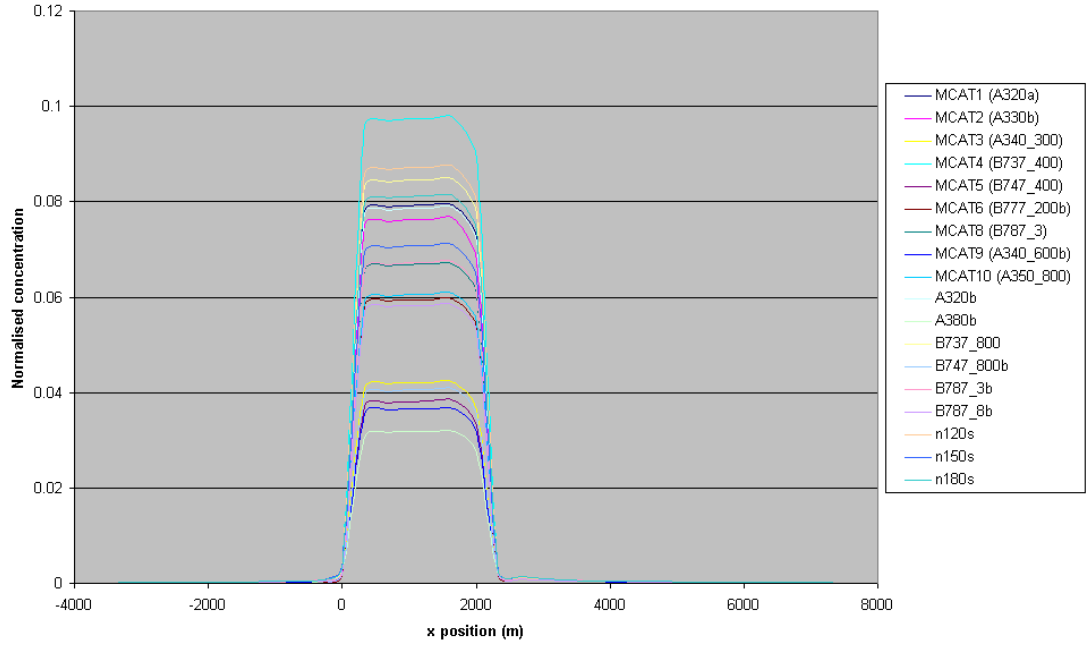

Figure 12.67: Normalised NO_x concentration plot for taxi.

MCAT	Lead aircraft	Other aircraft
1	A320 family V2527-A5	**One more identical**, B757-200 RB11-535E4
2	A330-300 Trent 772	Two more identical
3	A340-300 CFM56-5C4#	
4	B737-400 CFM56-3C1#	Three identical B737-600/800 CFM56-7B24
5	B747-400 RB211-524G/H	**Two identical** B747-800 GENx-2B67, **Two identical** A380 Trent 900/GP7200
6	B777-200 Trent 892	Two more identical, two identical B777-200/300 GE90-115B1, three identical B777-200/300 GE90-92B
8	B787-3 GENx	**One more identical**, **Two identical** B787-8 GENx
9	A340-600 Trent 556	One more identical
10	A350-800/B787-9 (250 L-haul) T500 derivative	A350-900/B787-10 (300 L-haul) Trent 900/GP7200 growth
11	**B737-800 RE (220 short haul) Scaled Trent 500**	
12	**New 120 seater CFM56-X**	
13	**New 150 seater CFM56-X/V2500-x**	
14	**New 180 seater CFM56-X/V2500**	

Table 12.8: The 2020 MCATs. The " identical" aircraft engines differ from the lead aircraft only in the emission rate of pollutants from the engine. Those aircraft marked with #'s are not present in the 2020 fleet but are left in as MCAT lead aircraft.

12.3.1 MCAT 1

A320a, A320c*, B757_200

A320a

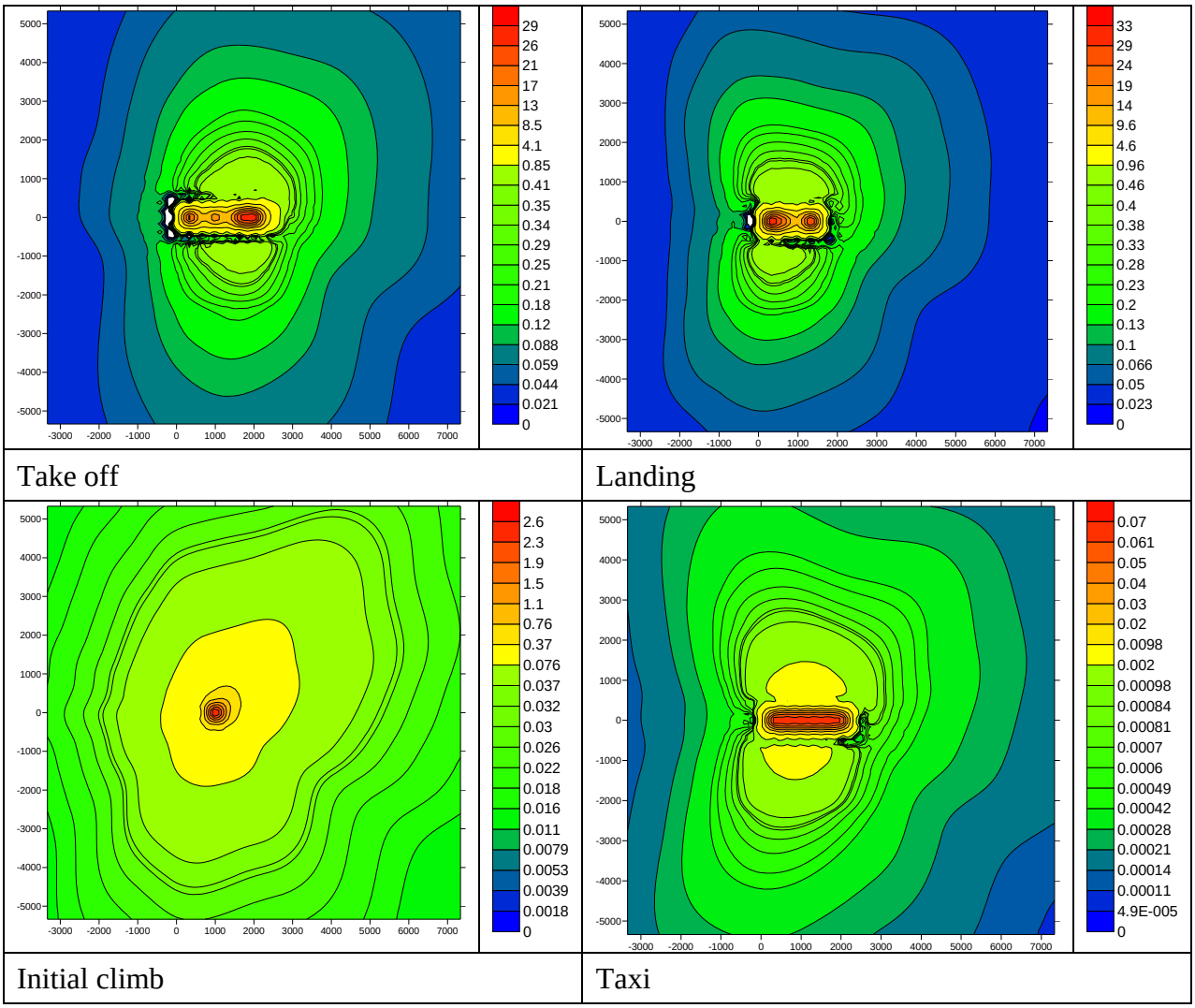

Figure 12.68: Normalised concentration plots for A320a the lead aircraft in MCAT 1.

A320c

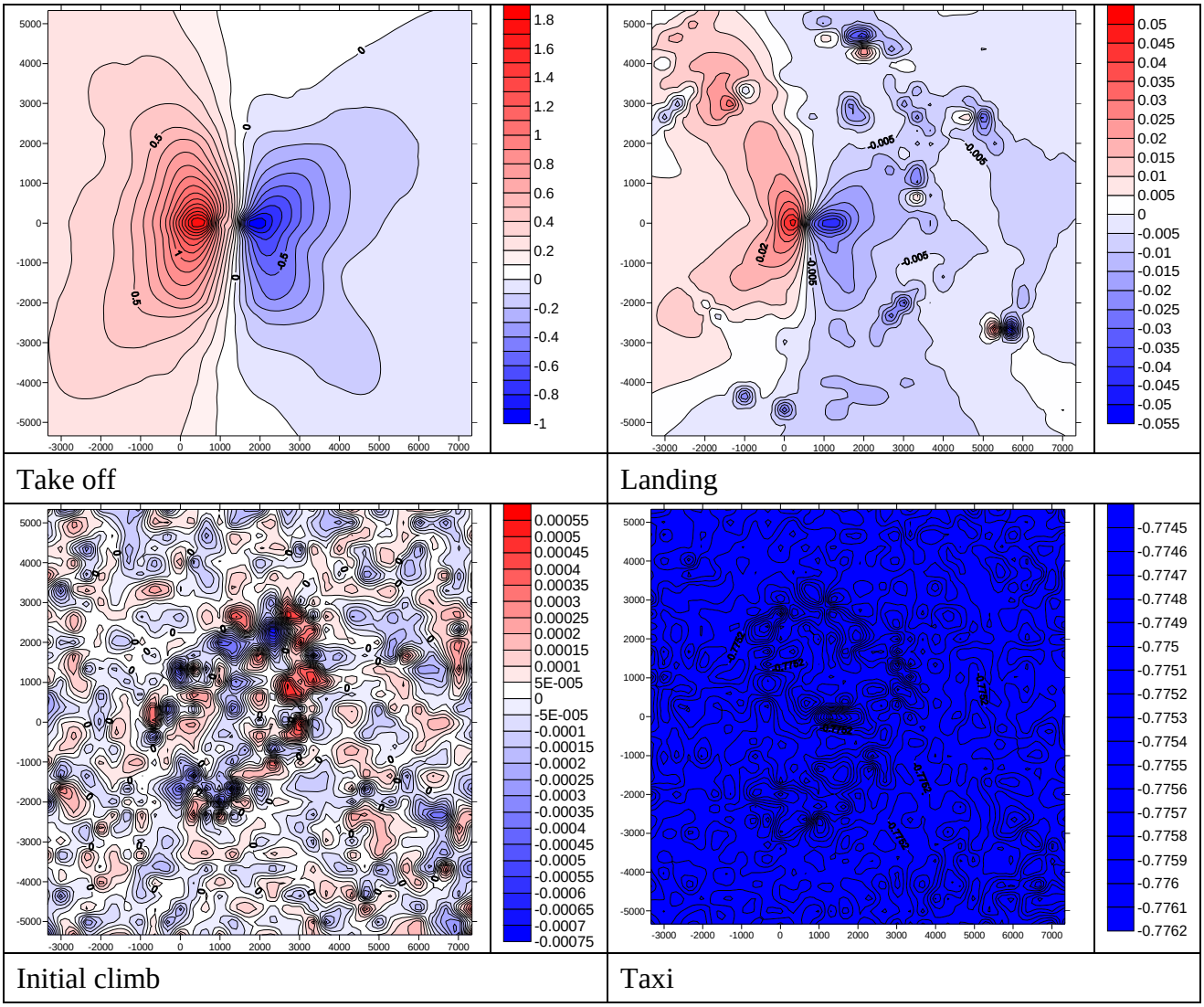

Figure 12.69: Percentage difference plots between A320c and MCAT 1 lead aircraft, A320a

12.3.2 MCAT 2

A330b, A330a, A330c

A330b

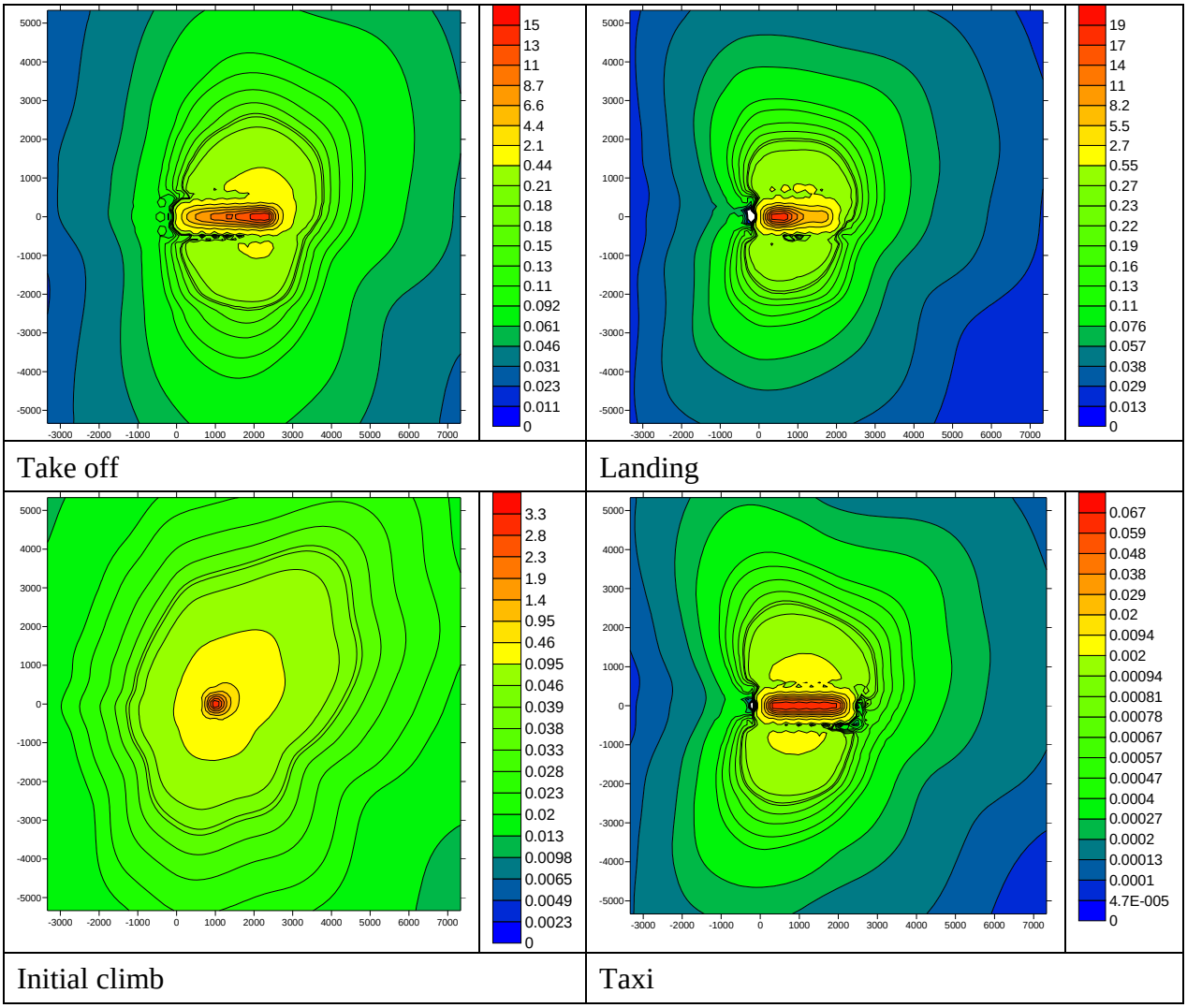

Figure 12.70: Normalised concentration plots for A330b the lead aircraft in MCAT 2

12.3.3 MCAT 3

A340_300a#

A340_300a

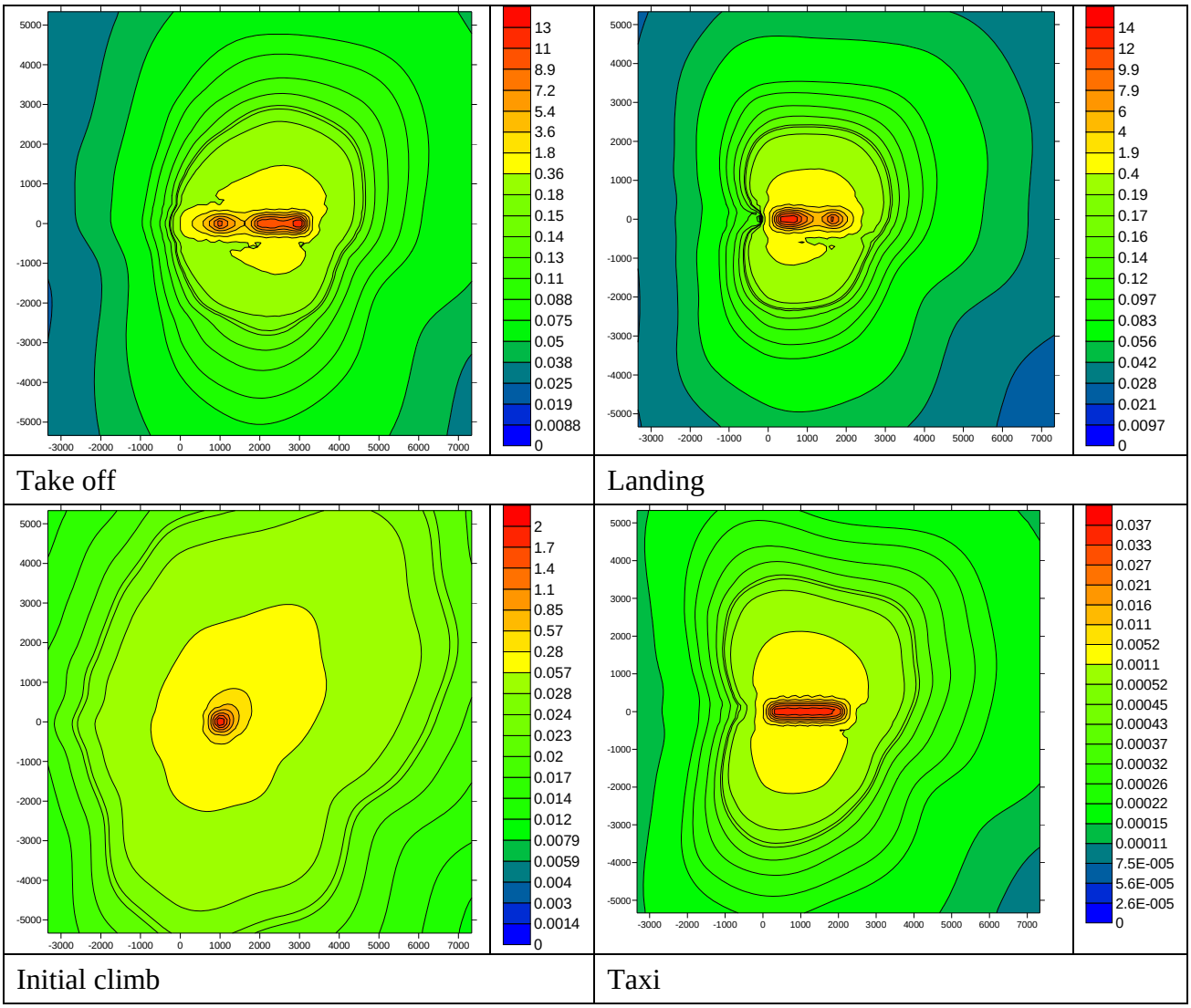

Figure 12.71: Normalised concentration plots for A340_300a the lead aircraft in MCAT 3

12.3.4 MCAT 4

B737_400[#]**,** B737_600a, B737_600b, B737_600c

B737_400

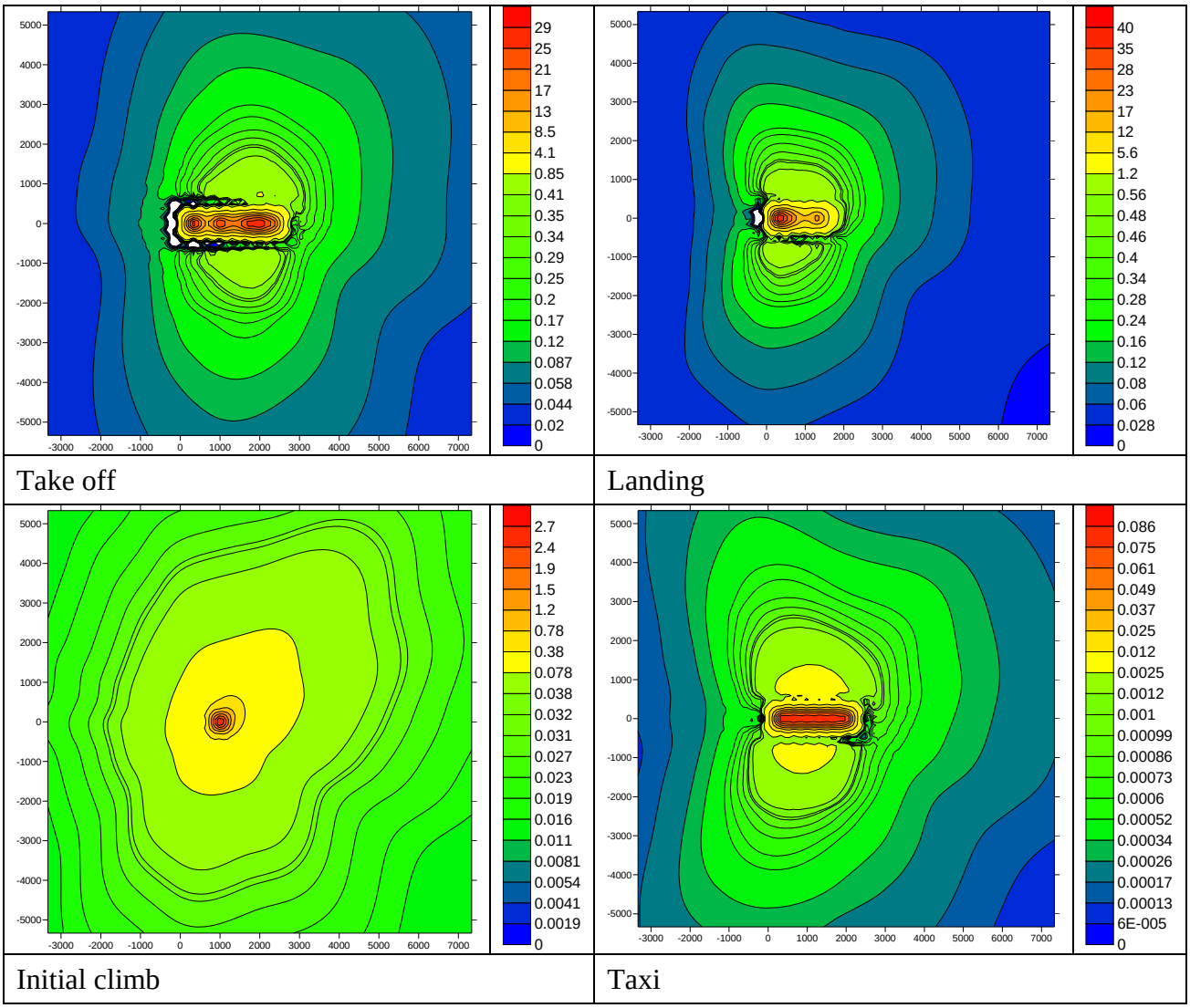

Figure 12.72: Normalised concentration plots for B737_400 the lead aircraft in MCAT 4

12.3.5 MCAT 5

B747_400, B747_800, B747_800b*, A380, A380b*

B747_400

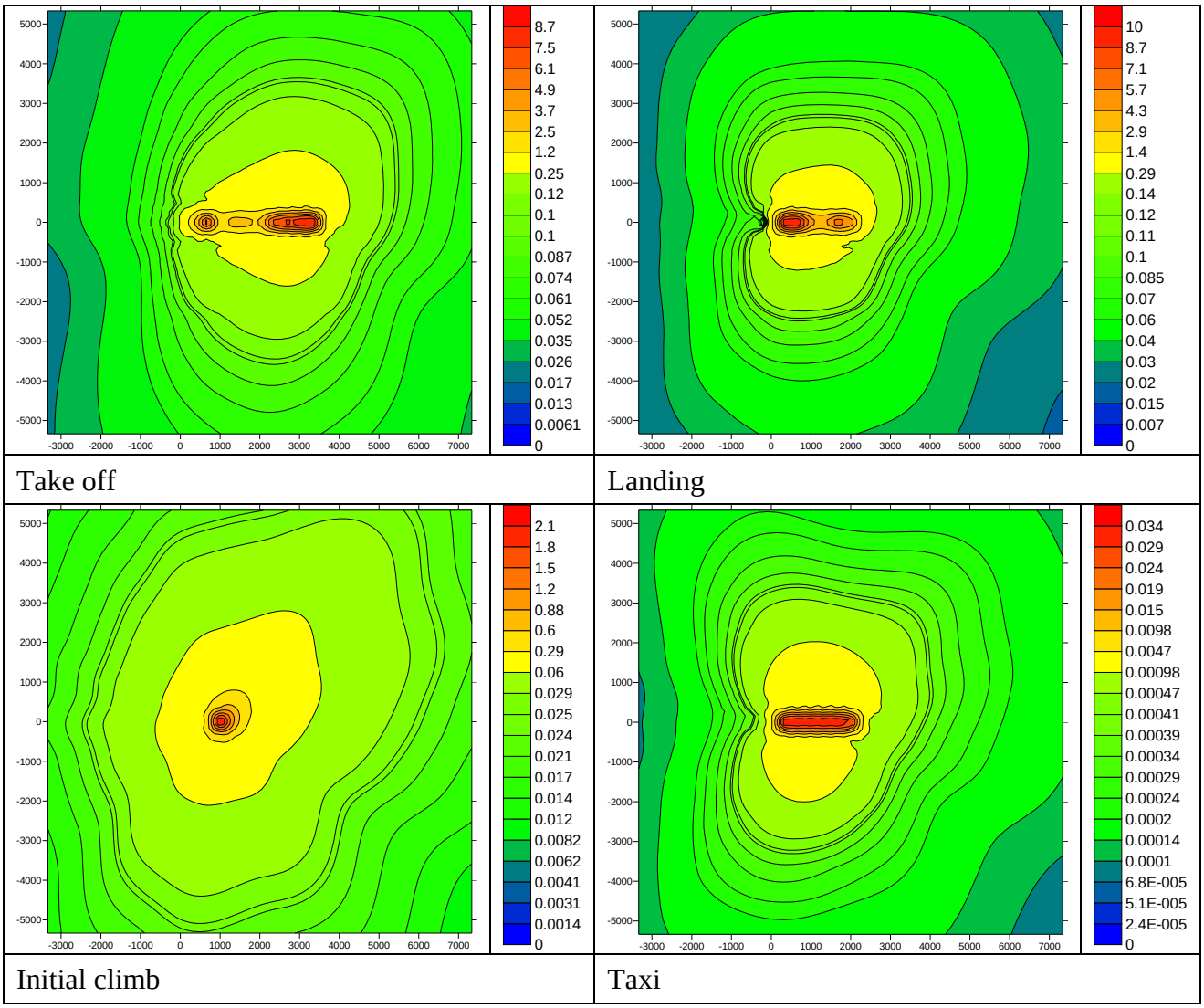

Figure 12.73: Normalised concentration plots for B747_400 the lead aircraft of MCAT 5

B747_800b

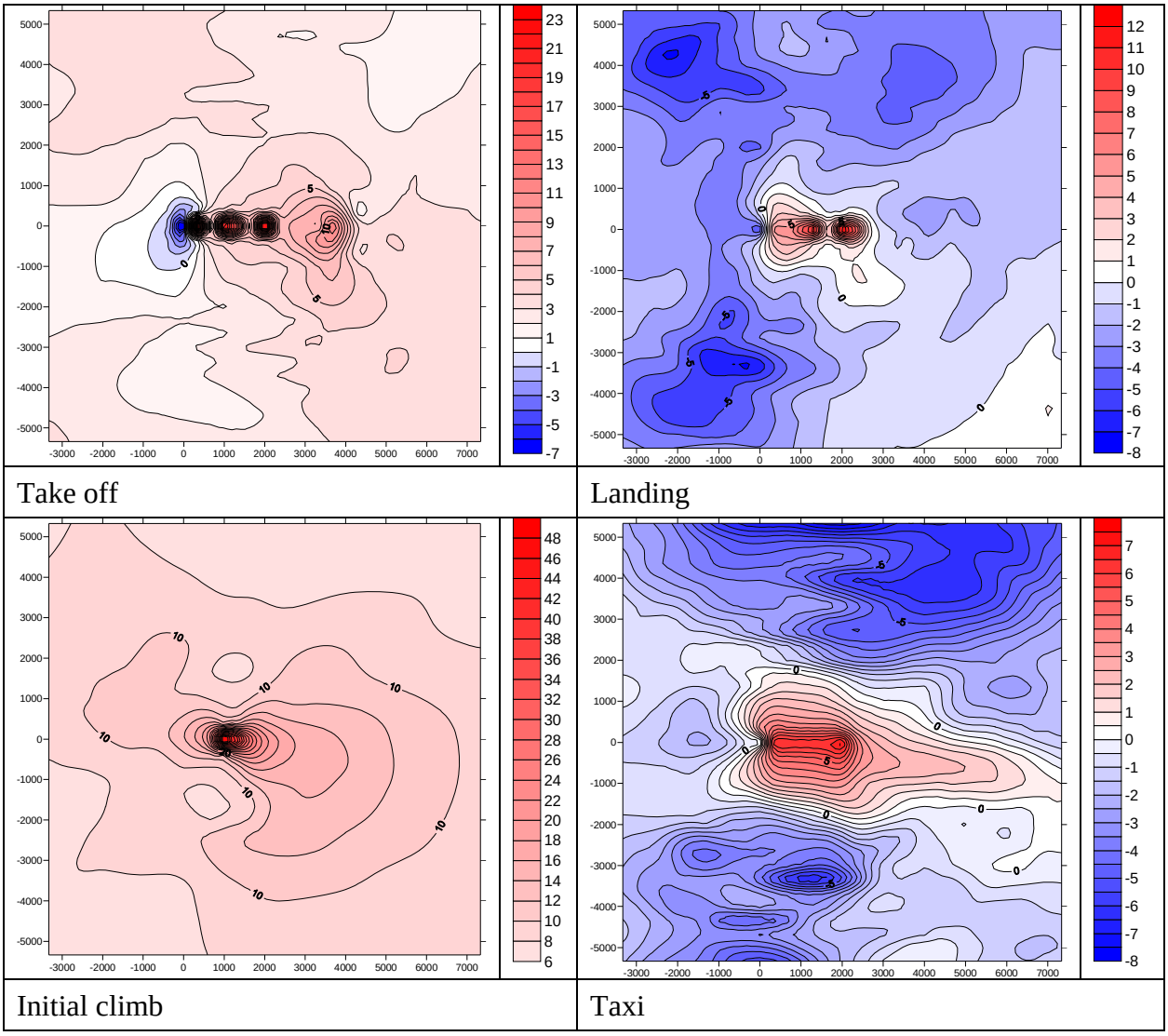

Figure 12.74: Percentage difference plots between B747_800b and MCAT 5 lead aircraft, B747_400

A380b

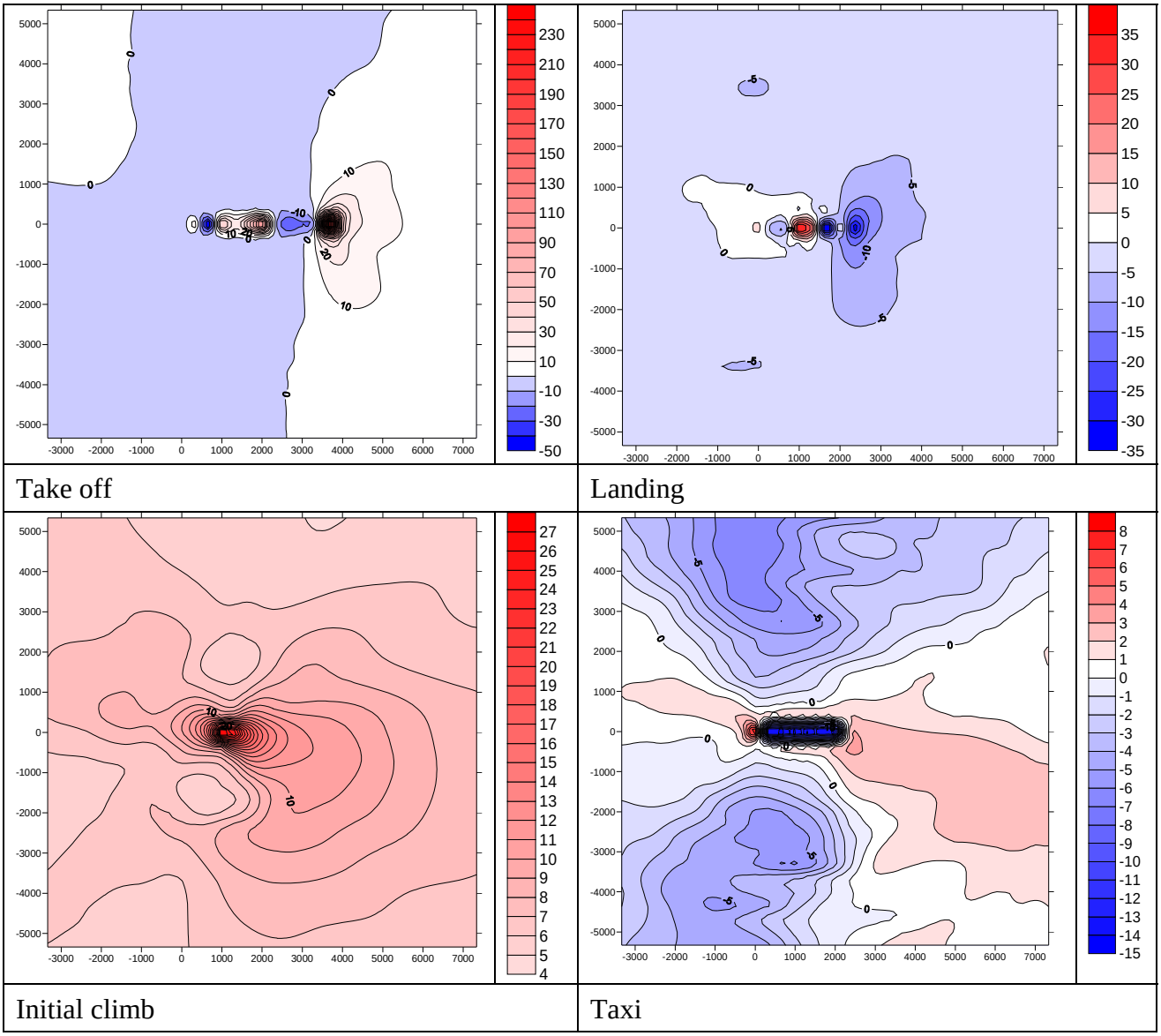

Figure 12.75: Percentage difference plots between A380b and MCAT 5 lead aircraft, B747_400

12.3.6 MCAT 6

B777_200b, B777_200c, B777_200d, B777_200e, B777_200f, B777_200g, B777_200h, B777_200i

B777_200b

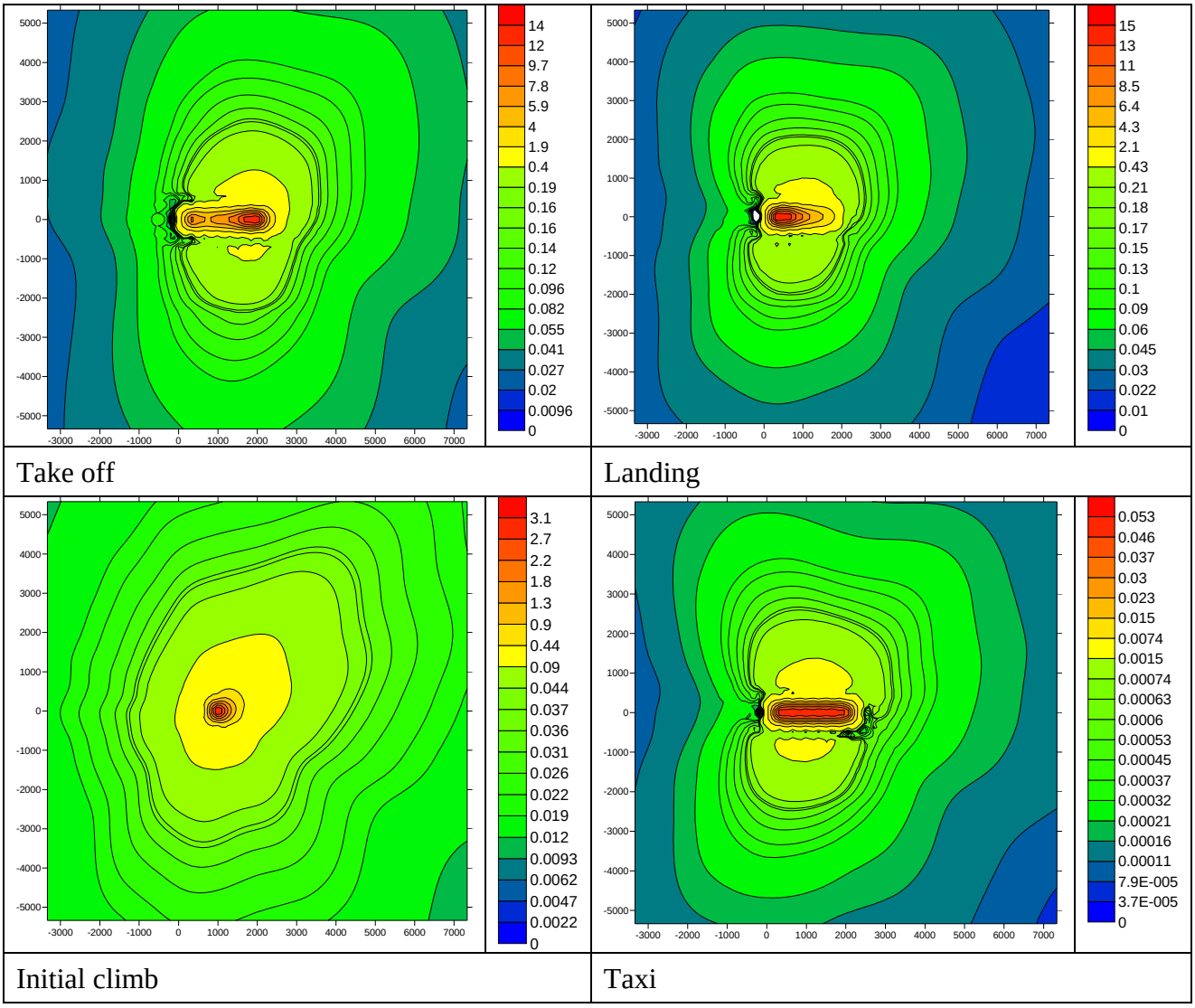

Figure 12.76: Normalised concentration plots for B777_200b the lead aircraft for MCAT 6

12.3.7 MCAT 8

B787_3, B787_3b*, B787_8, B787_8b*

B787_3

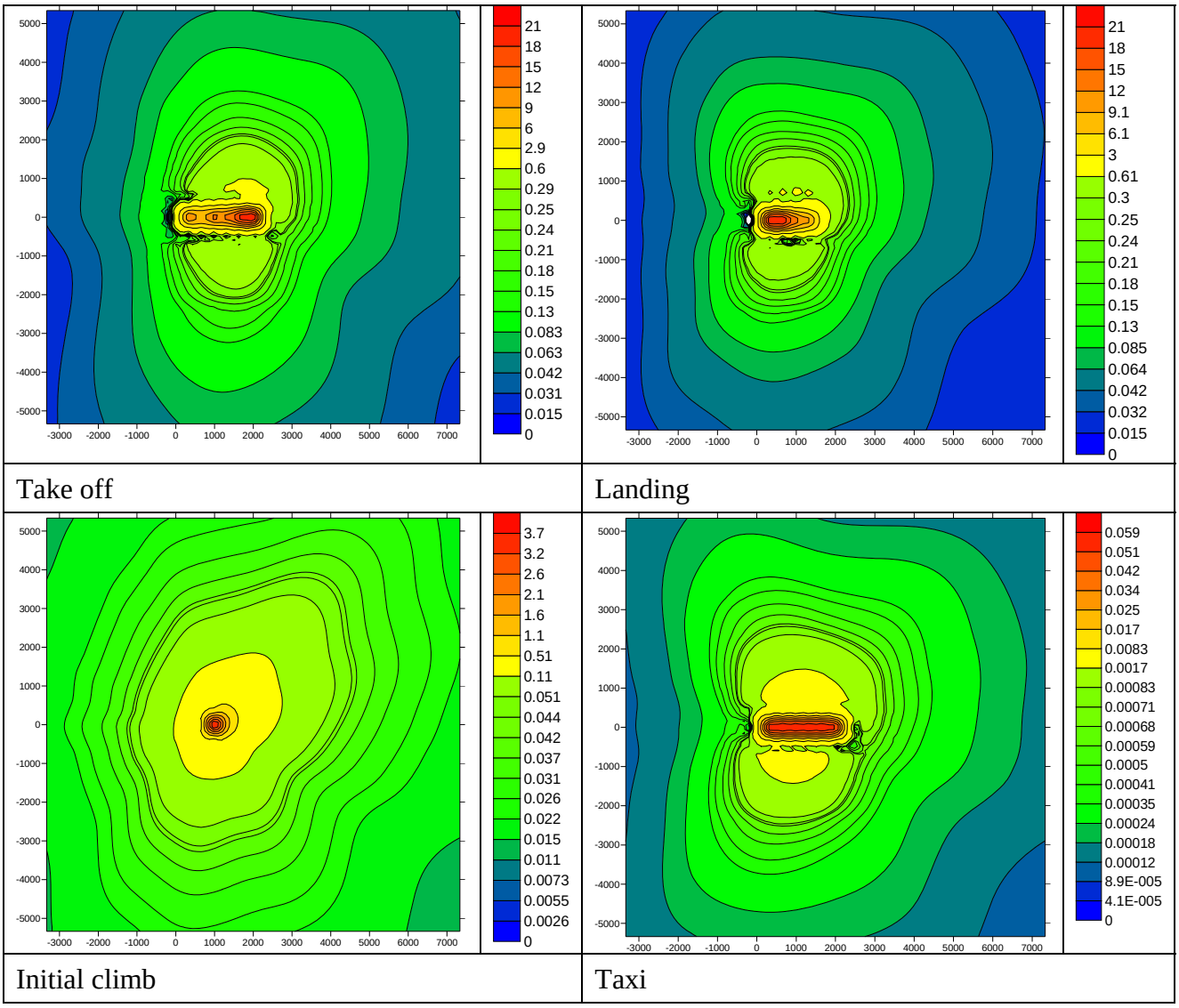

Figure 12.77: Normalised concentration plots for B787_3 the lead aircraft in MCAT 8

B787_3b

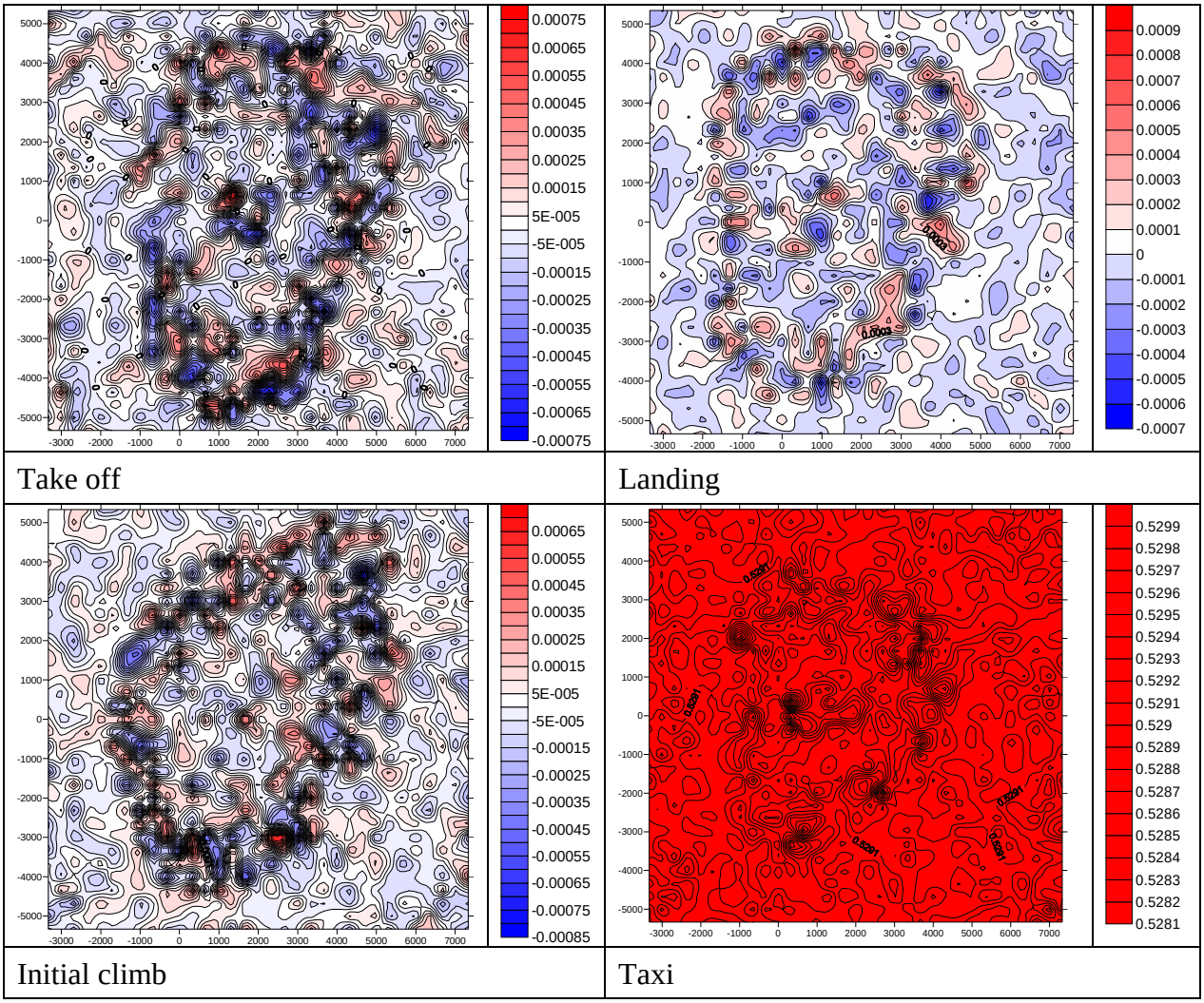

Figure 12.78: Percentage difference plots between B787_3b and MCAT 8 lead aircraft, B787_3

B787_8b

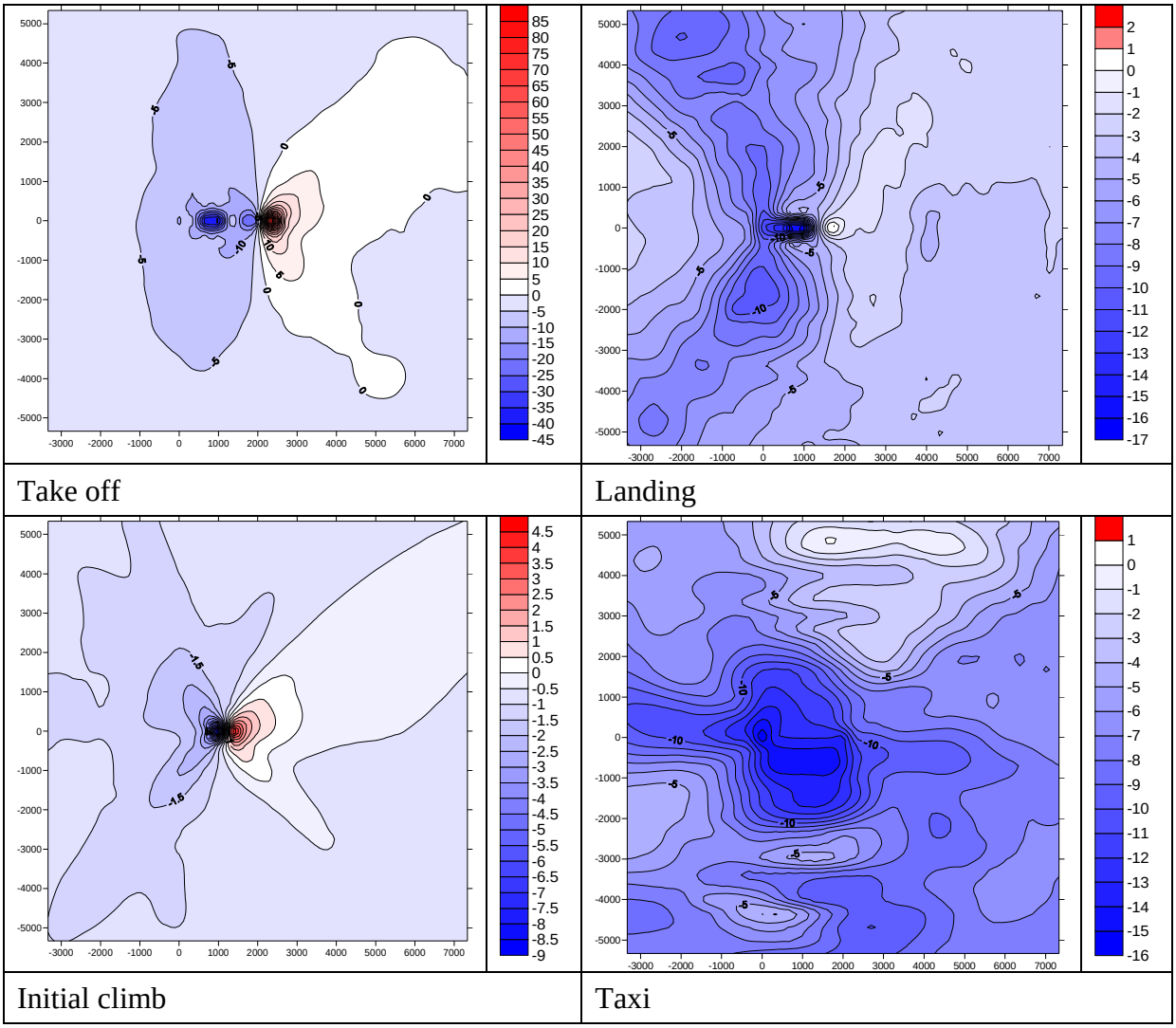

Figure 12.79: Percentage difference plots between B787_8b and MCAT 8 lead aircraft, B787_3

12.3.8 MCAT 9

A340_600a, A340_600b

A340_600a

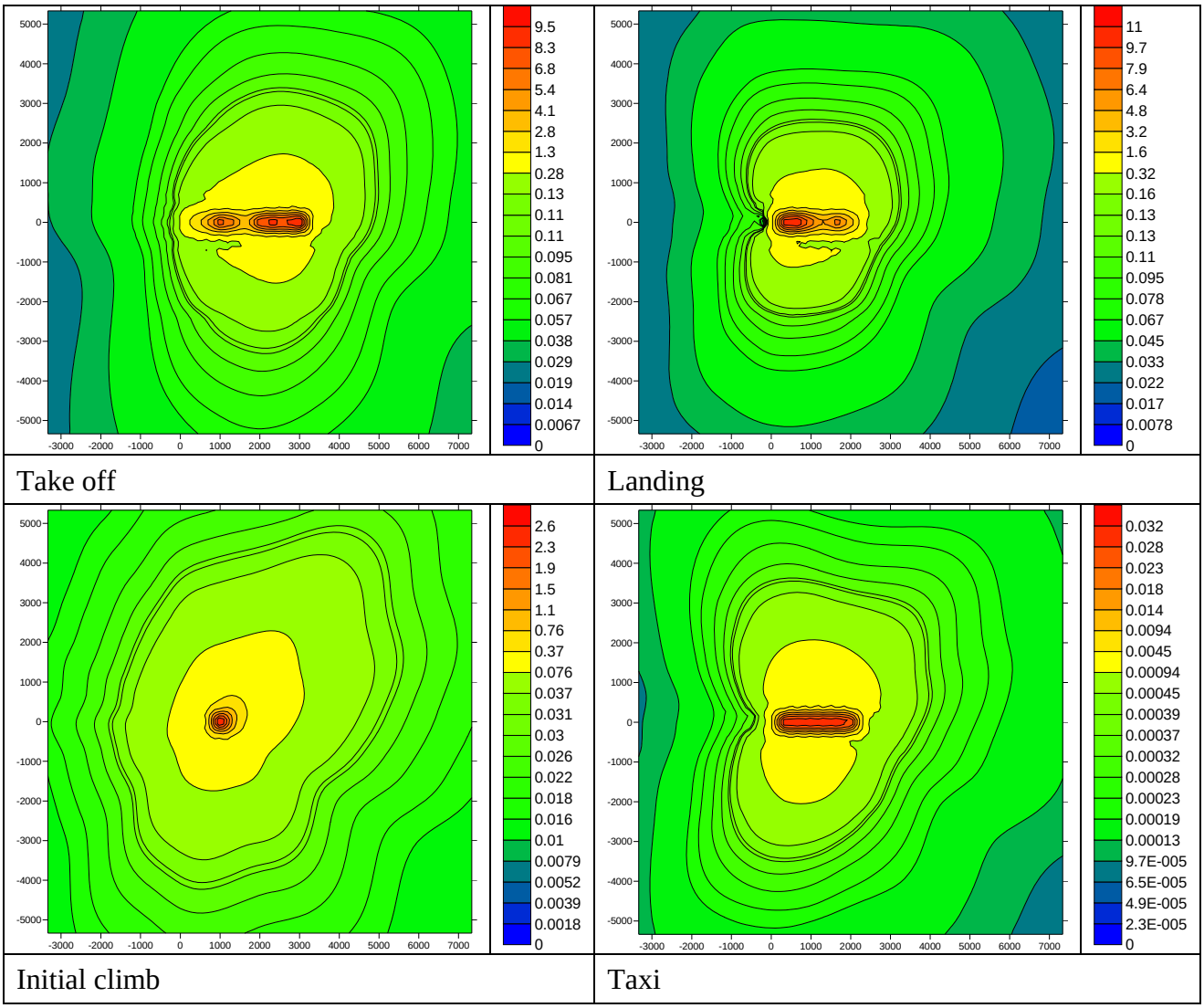

Figure 12.80: Normalised concentration plots for A340_600a the lead aircraft in MCAT 9

12.3.9 MCAT 10

A350_800, A350_900

A350_800

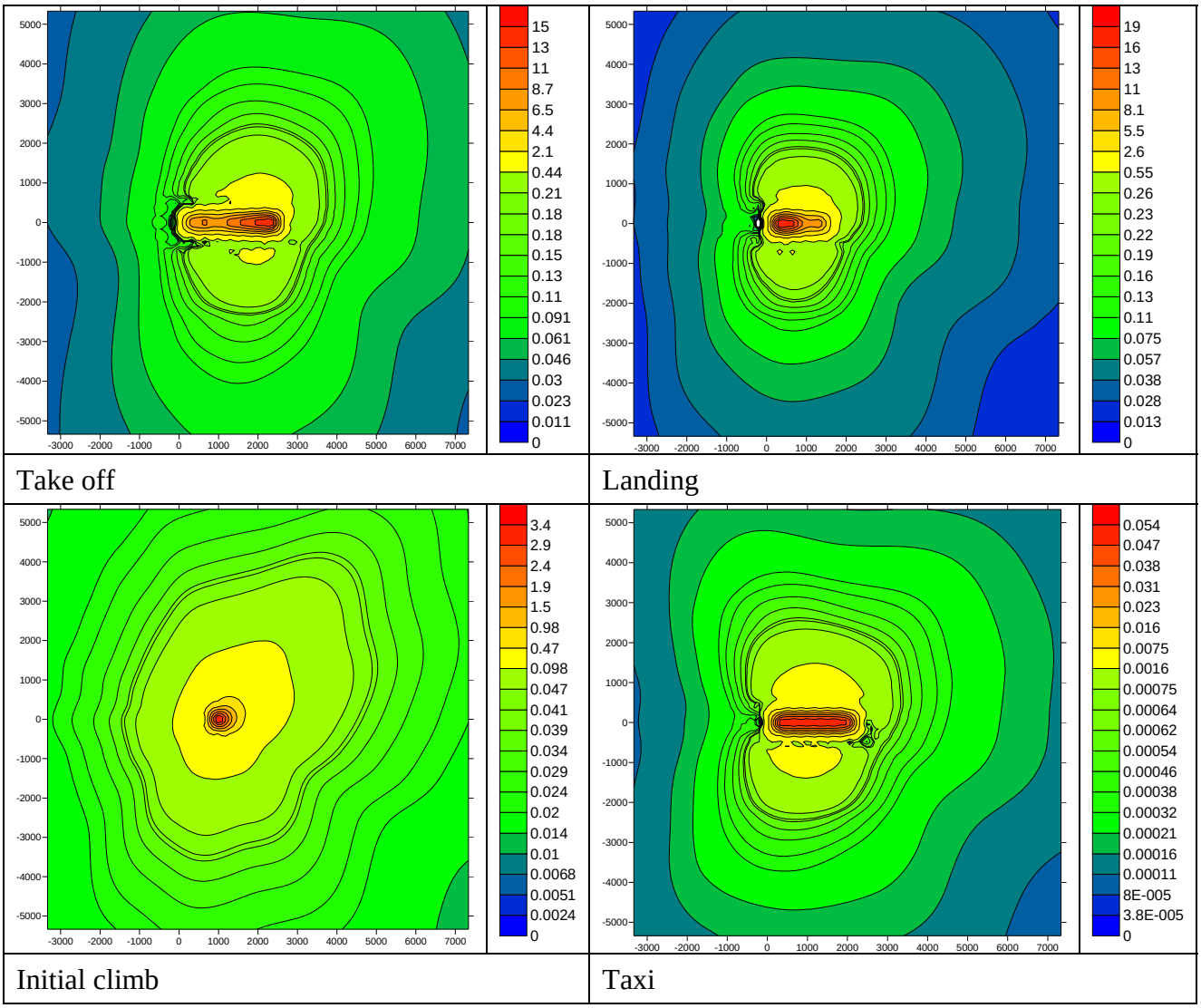

Figure 12.81: Normalised concentration plots for A350_800 the lead aircraft for MCAT 10

12.3.10 MCAT 11

B737_800

B737_800

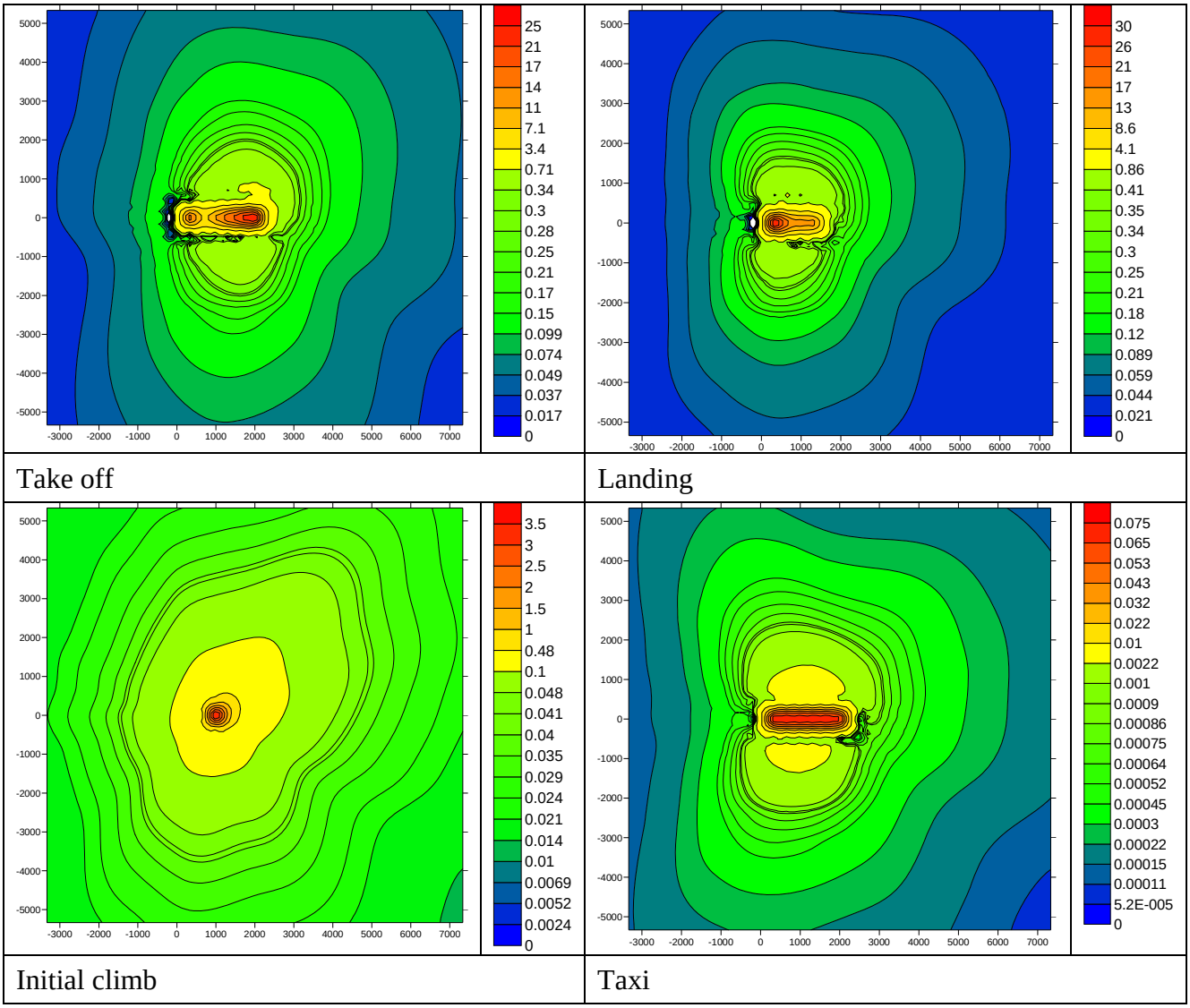

Figure 12.82: Normalised concentration plots for B737_800 the lead aircraft for MCAT 11

12.3.11 MCAT 12

N120s

N120s

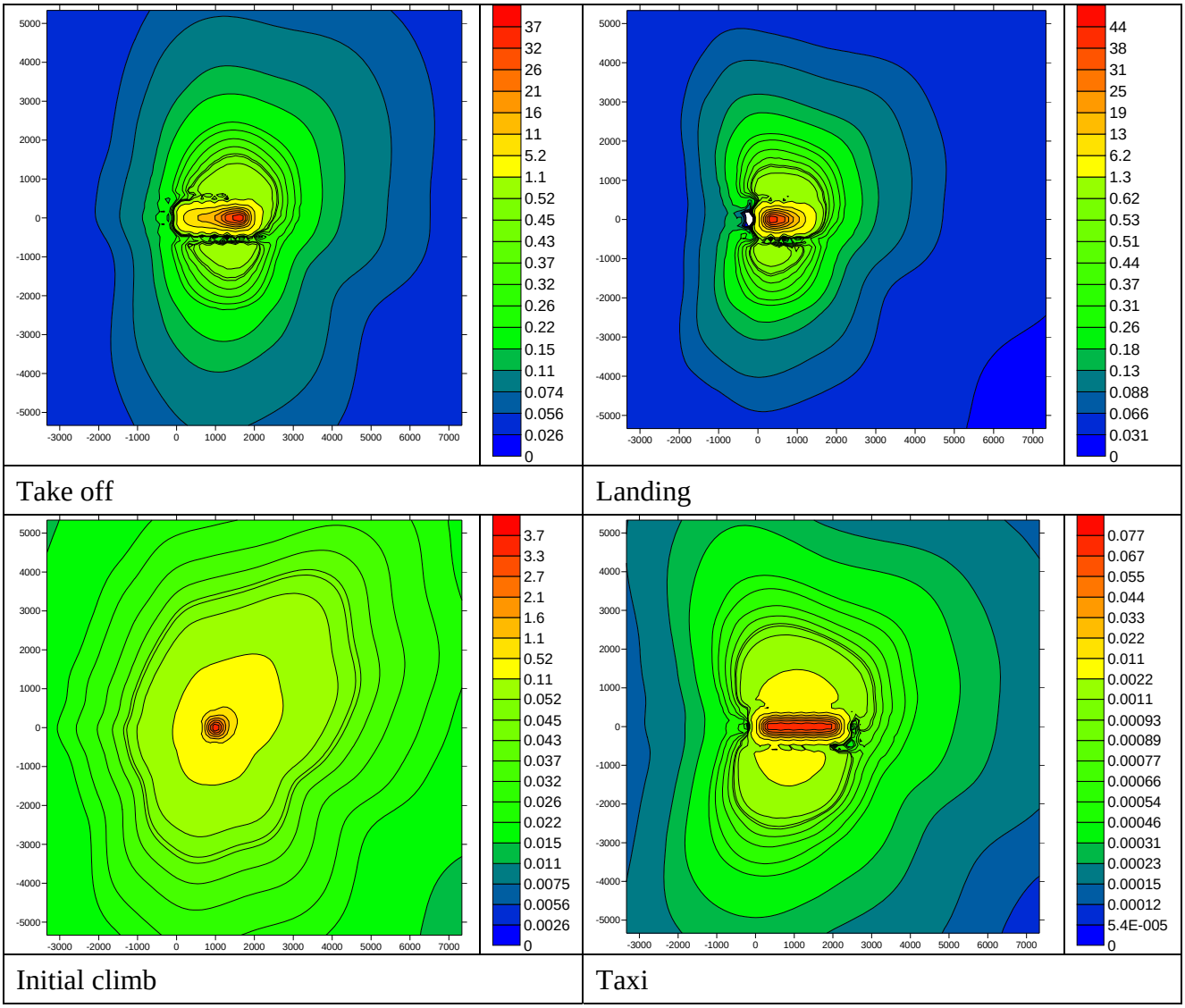

Figure 12.83: Normalised concentration plots for N120s the lead aircraft for MCAT 12

12.3.12 MCAT 13

N150s

N150s

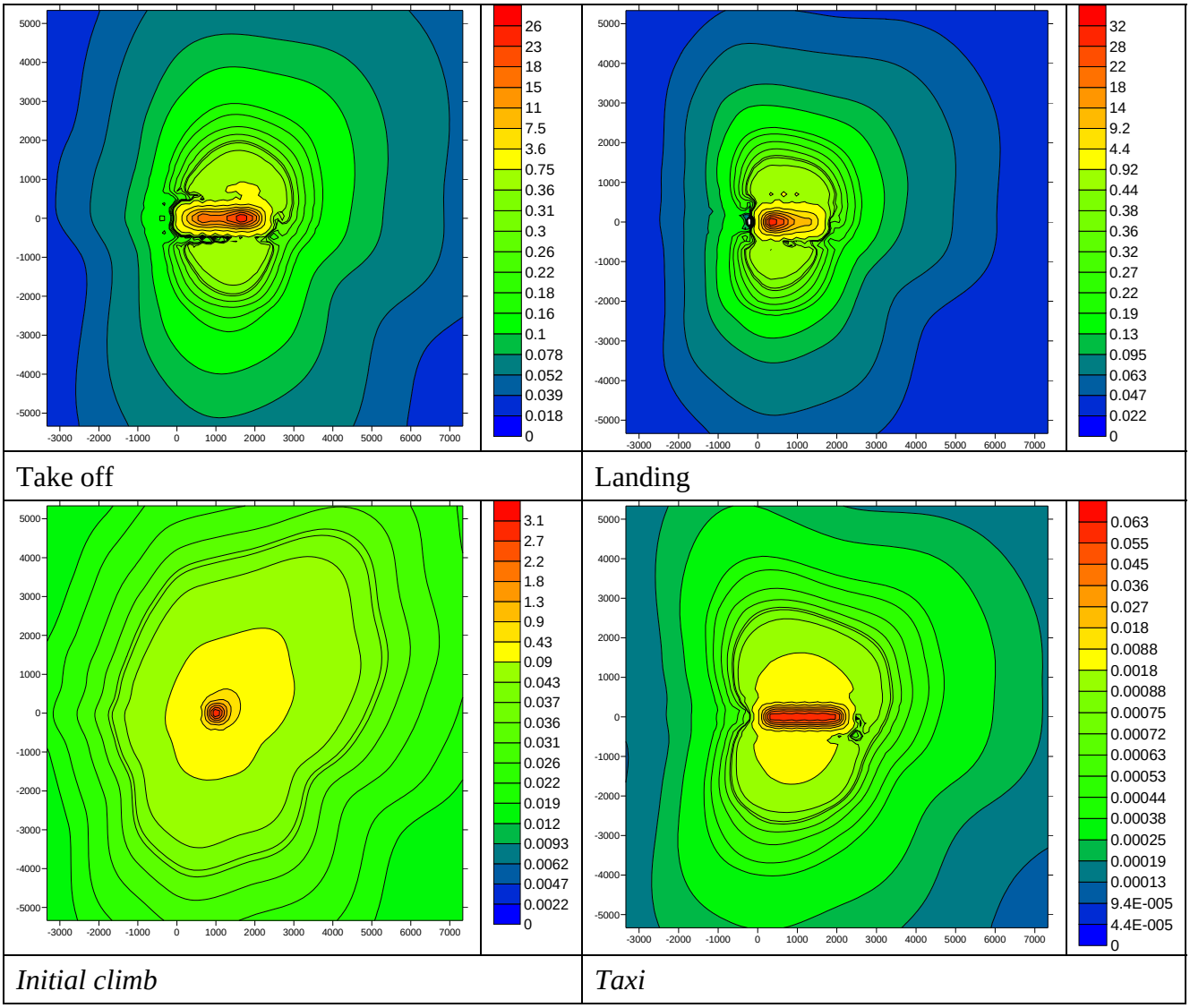

Figure 12.84: Normalised concentration plots for N150s the lead aircraft for MCAT 13

12.3.13 MCAT 14

N180s

N180s

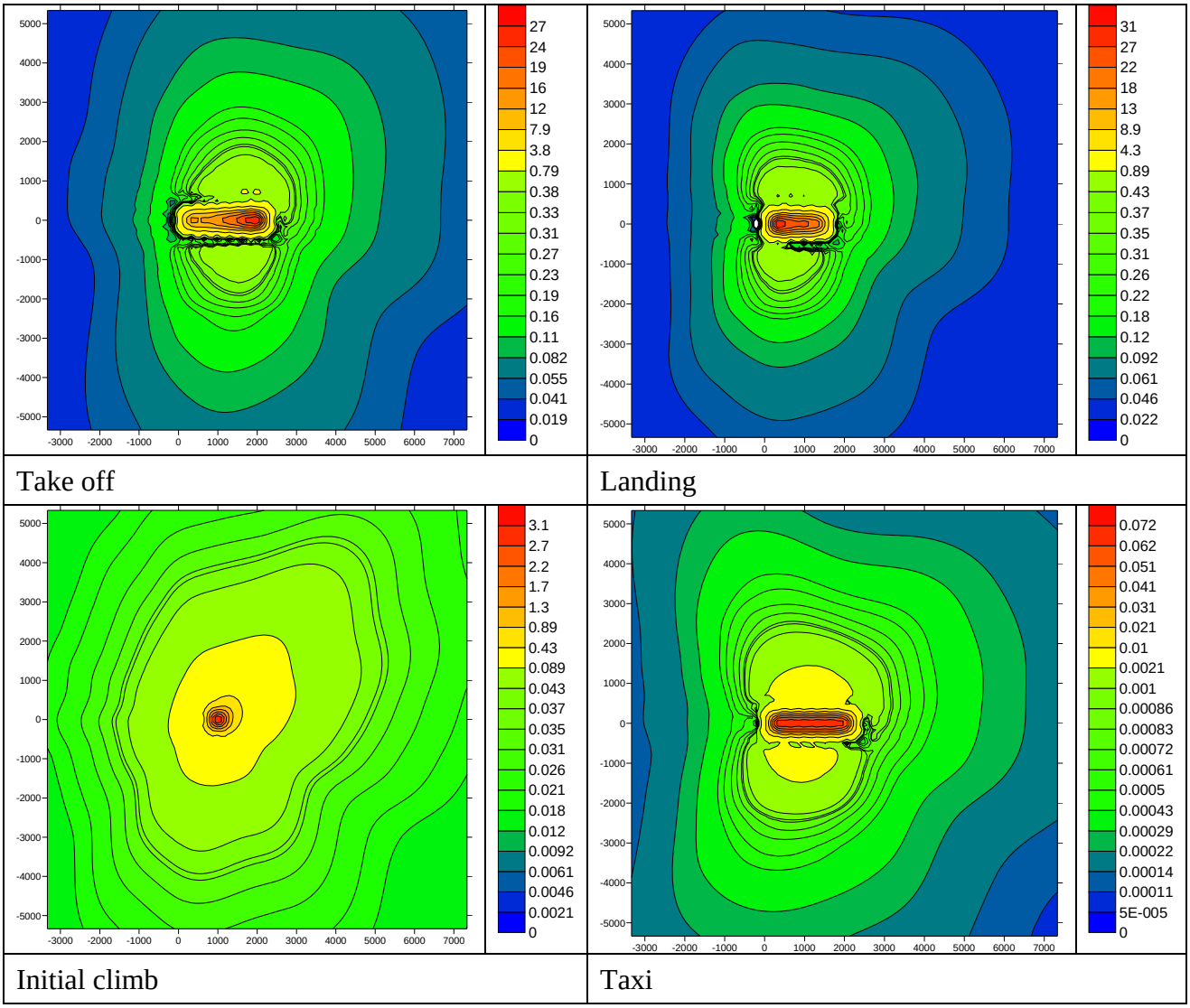

Figure 12.85: Normalised concentration plots for N180s the lead aircraft for MCAT 14

12.4 2030 MCAT data

This chapter outlines the development of the 2030 MCATs. Aircraft that were also present in 2020 or 2015 have not been re-analysed. The new aircraft have been compared to the lead aircraft from the 2015/2020 MCATs, this lead aircraft has been kept the same even in situations where that aircraft is no longer part of the fleet.

The aircraft that have been examined in 2030, along with the designator used for them, are given in Table 12.9. The total NOx emissions for each mode for each of the new aircraft are given in Table 12.10.

Designator	Aircraft	Engine	UID
A320a	A320 family	V2527-A5	1|A003
A320c	A320 family	V2527-A5	1|A003/1
A340_600a	A340-600	Trent 556	6RR041
A340_600b	A340-600	Trent 556	6RR041/1
A350_800	A350-800/B787-9 (250 l-haul)	T500 derivative	NE08/1
A350_800b*	A350-800/B787-9 (250 l-haul)	T500 derivative	NE08/2
A350_800c*	A350-800/B787-9 (250 l-haul)	T500 derivative	NE08/3
A350_900	A350-900/B787-10 (300 l-haul)	Trent 900/GP2700 growth	NE10/1
A350_900b*	A350-900/B787-10 (300 l-haul)	Trent 900/GP2700 growth	NE10/2
A350_900c*	A350-900/B787-10 (300 l-haul)	Trent 900/GP2700 growth	NE10/3
A380	A380	Trent 900/GP7200	NE01/1
A380b	A380	Trent 900/GP7200	NE01/2
A380c*	A380	Trent 900/GP7200	NE01/3
B737_800	B737-800RE (220 s-haul)	Scaled Trent 500	NE06/1
B737_800b*	B737-800RE (220 s-haul)	Scaled Trent 500	NE06/2
B747_800	B747-800	Genx – 2B67	NE02/1
B747_800b	B747-800	Genx – 2B67	NE02/2
B747_800c*	B747-800	Genx – 2B67	NE02/3
B777_200e	B777-200/300	GE90-115B1	7G3099
B777_200f	B777-200/300	GE90-115B1	7G3099/1
B777_200g	B777-200/300	GE90-92B	3GE066
B777_200h	B777-200/300	GE90-92B	3GE066/1
B777_200i	B777-200/300	GE90-92B	3GE066/2
B777_200j*	B777-200/300	GE90-115B1	7G3099/2
B787_3	B787-3	GENx	NE09/1
B787_3b	B787-3	GENx	NE09/2
B787_3c*	B787-3	GENx	NE09/3
B787_8	B787-8	GENx	NE07/1
B787_8b	B787-8	GENx	NE07/2
B787_8c*	B787-8	GENx	NE07/3
N120s	New 120 seater	CFM56-X	NE03AB/1
N120sb*	New 120 seater	CFM56-X	NE03AB/2
N150s	New 150 seater	CFM65-X/V2500-X	NE04AB/1
N150sb*	New 150 seater	CFM65-X/V2500-X	NE04AB/2
N180s	New 180 seater	CFM65-X/V2500-X	NE05AB/1
N180sb*	New 180 seater	CFM65-X/V2500-X	NE05AB/2
N450sa*	New 450 seater	GE09-130B	NE11/1
N450sb*	New 450 seater	GE09-130B	NE11/2

*Table 12.9: The aircraft considered for 2030 along with the designator used. The *s mark aircraft which were not present in 2020.*

Aircraft	Take off	Landing	Initial climb	Taxi
A350_800b	2,233	207	432	264
A350_800c	2,054	190	398	243
A350_900b	2,890	292	513	308
A350_900c	2,659	269	472	283
A380c	2,999	310	394	292
B737_800b	743	87	156	167
B747_800c	2,392	294	327	261
B777_200j	3,990	499	827	403
B787_3c	1,068	139	239	202
B787_8c	1,652	193	352	251
N120sb	416	54	102	86
N150sb	509	63	118	102
N180sb	663	74	147	115
N450sa	6,157	694	908	402
N450sb	5,972	674	881	390

Table 12.10: The total NOx emissions in grams for each mode for one event. Note for taxi this one event is a 2000m long taxi.

The normalised centreline concentration plots for the modes for each of the new aircraft along the lead aircraft from the 2020 MCATs are shown in Figures 12.86 to 12.89. With the final MCATs being listed in Table 12.11. Figures 12.90 to 12.117 then go through each MCAT showing the normalised concentration plots for each mode for the lead aircraft and then percentage difference plots for each of the new aircraft in that MCAT comparing them to the lead aircraft.

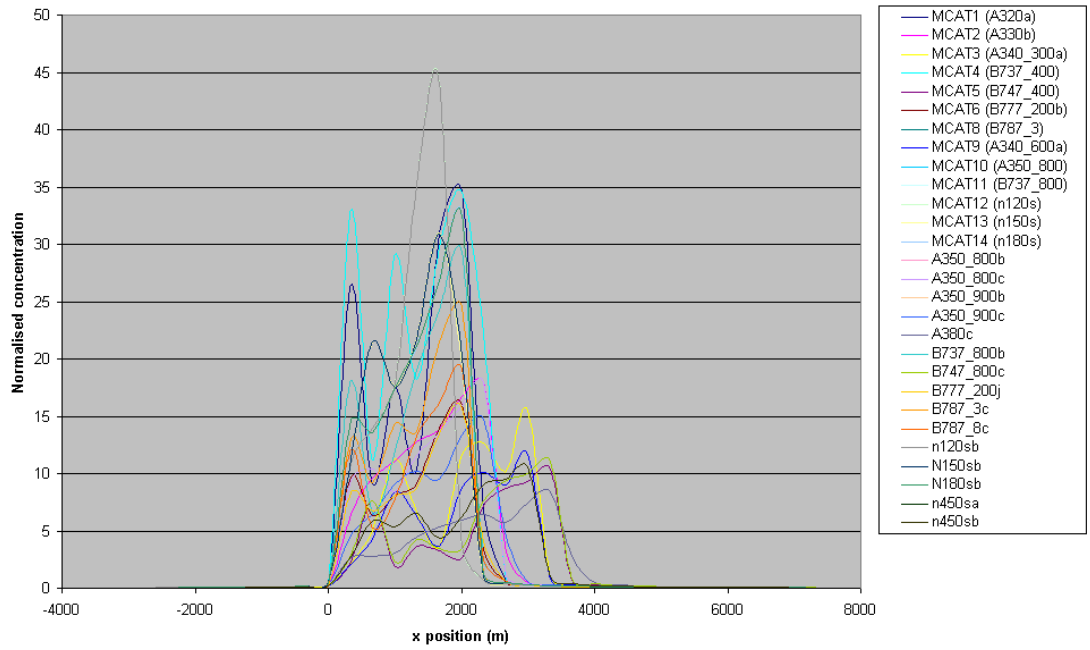

Figure 12.86: Normalised NO_x concentration plot for Take off

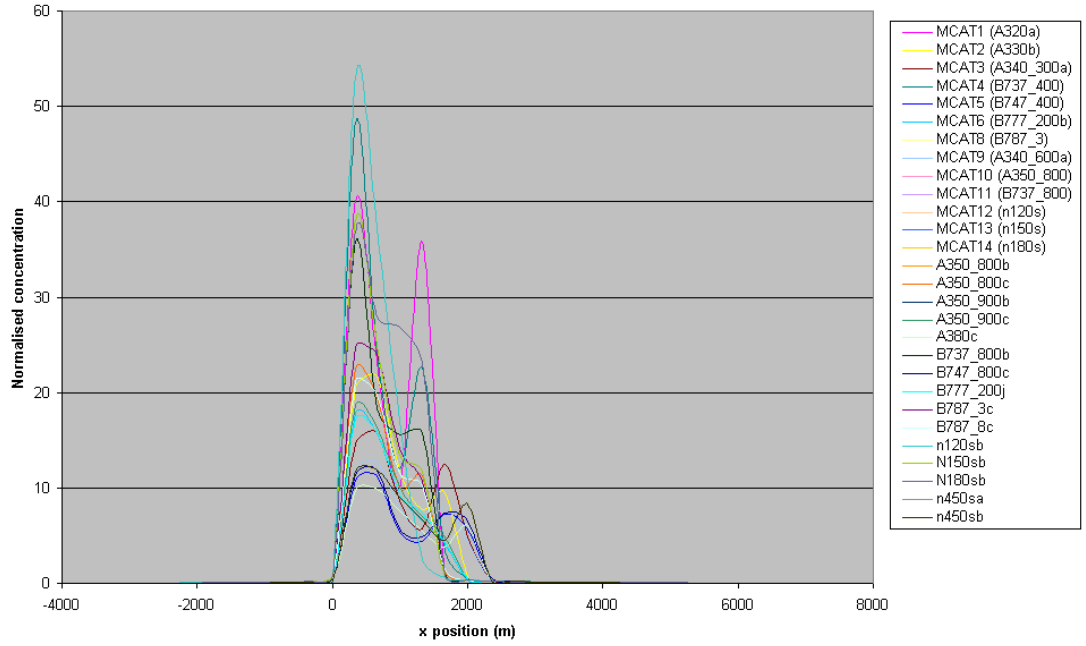

Figure 12.87: Normalised NO_x concentration plot for landing

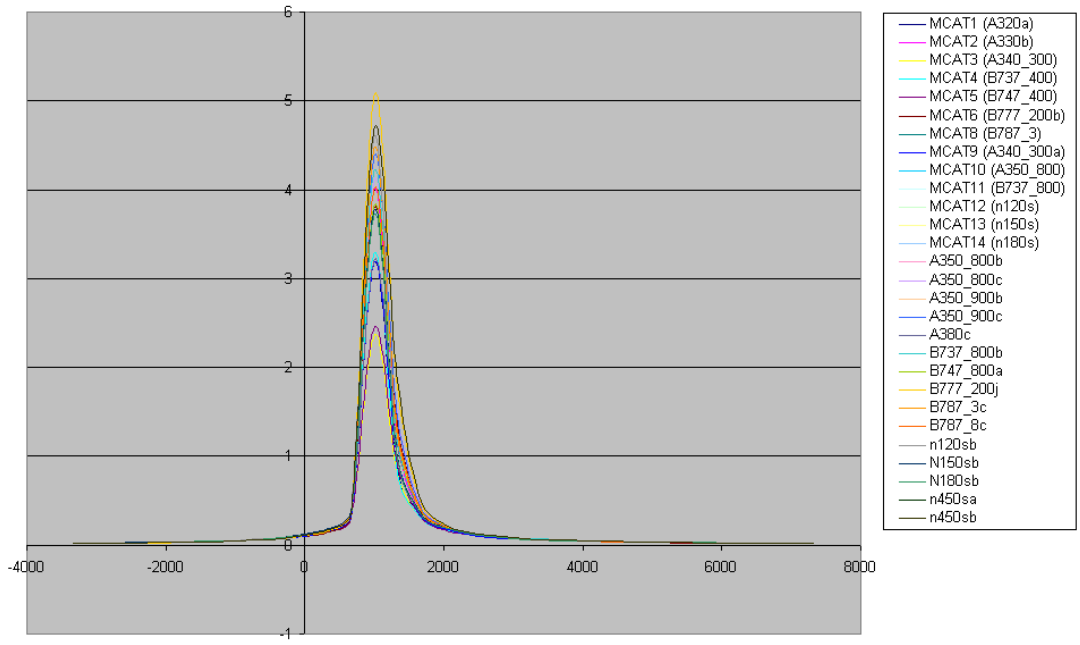

Figure 12.88: Normalised NO_x concentration plot for initial climb

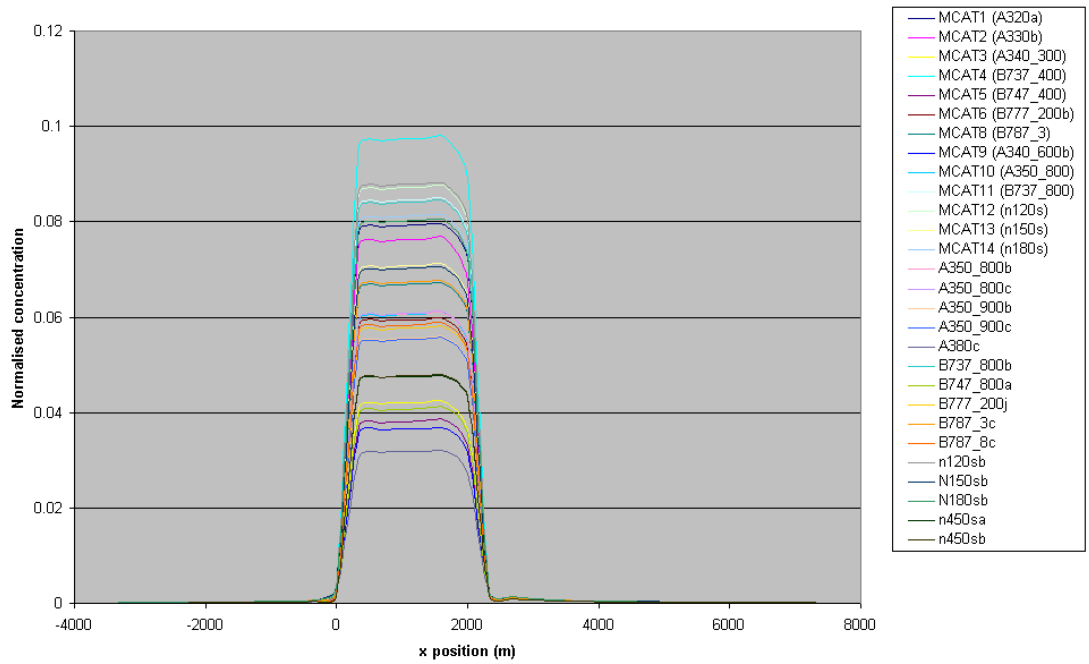

Figure 12.89: Normalised NO_x concentration plot for taxi

MCAT	Lead aircraft	Other aircraft
1	A320 family V2527-A5	One more identical
2	A330-300 Trent 772#	
3	A340-300 CFM56-5C4#	
4	B737-400 CFM56-3C1#	
5	B747-400 RB211-524G/H#	**Three** identical B747-800 GENx-2B67, **Three** identical A380 Trent 900/GP7200
6	B777-200 Trent 892#	**Three** identical B777-200/300 GE90-115B1, three identical B777-200/300 GE90-92B
8	B787-3 GENx	**Two** more identical, **Three** identical B787-8 GENx
9	A340-600 Trent 556	One more identical
10	A350-800/B787-9 (250 L-haul) T500 derivative	**Two more identical**, **Three identical** A350-900/B787-10 (300 L-haul) Trent 900/GP7200 growth
11	B737-800 RE (220 short haul) Scaled Trent 500	**One more identical**
12	New 120 seater CFM56-X	**One more identical**
13	New 150 seater CFM56-X/V2500-x	**One more identical**
14	New 180 seater CFM56-X/V2500	**One more identical**
15	**New 450 seater GE90-130B**	**One more identical**

Table 12.11: The final MCATs for 2030. The " identical" aircraft engines differ from the lead aircraft only in the emission rate of pollutants from the engine. A # represents an aircraft not present in 2030 but left in because it is the lead aircraft for an MCAT.

12.4.1 MCAT 1

A320a, A320c

A320a

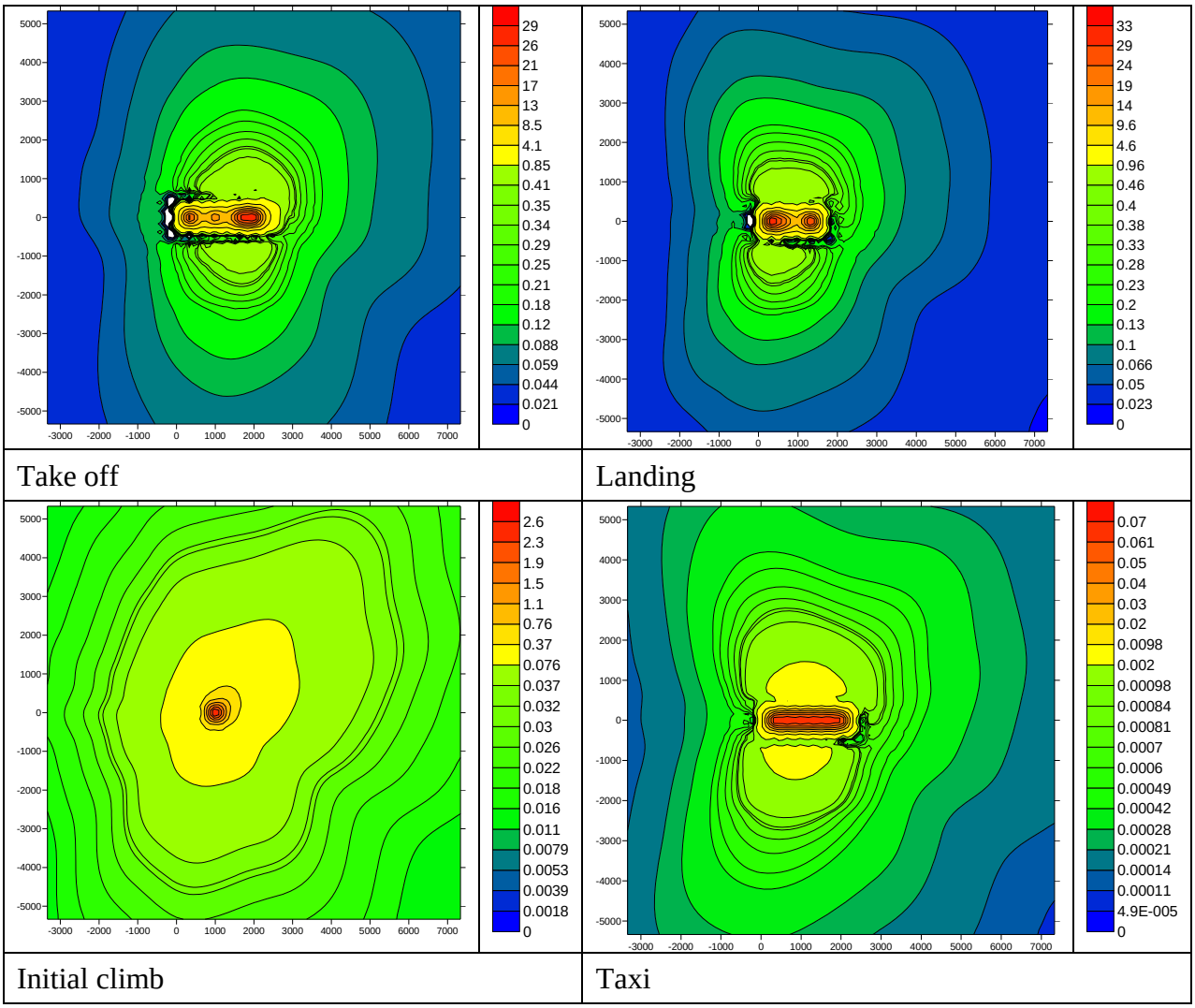

Figure 12.90: Normalised concentration plots for A320a the lead aircraft in MCAT 1.

12.4.2 MCAT 2

A330b#

A330b

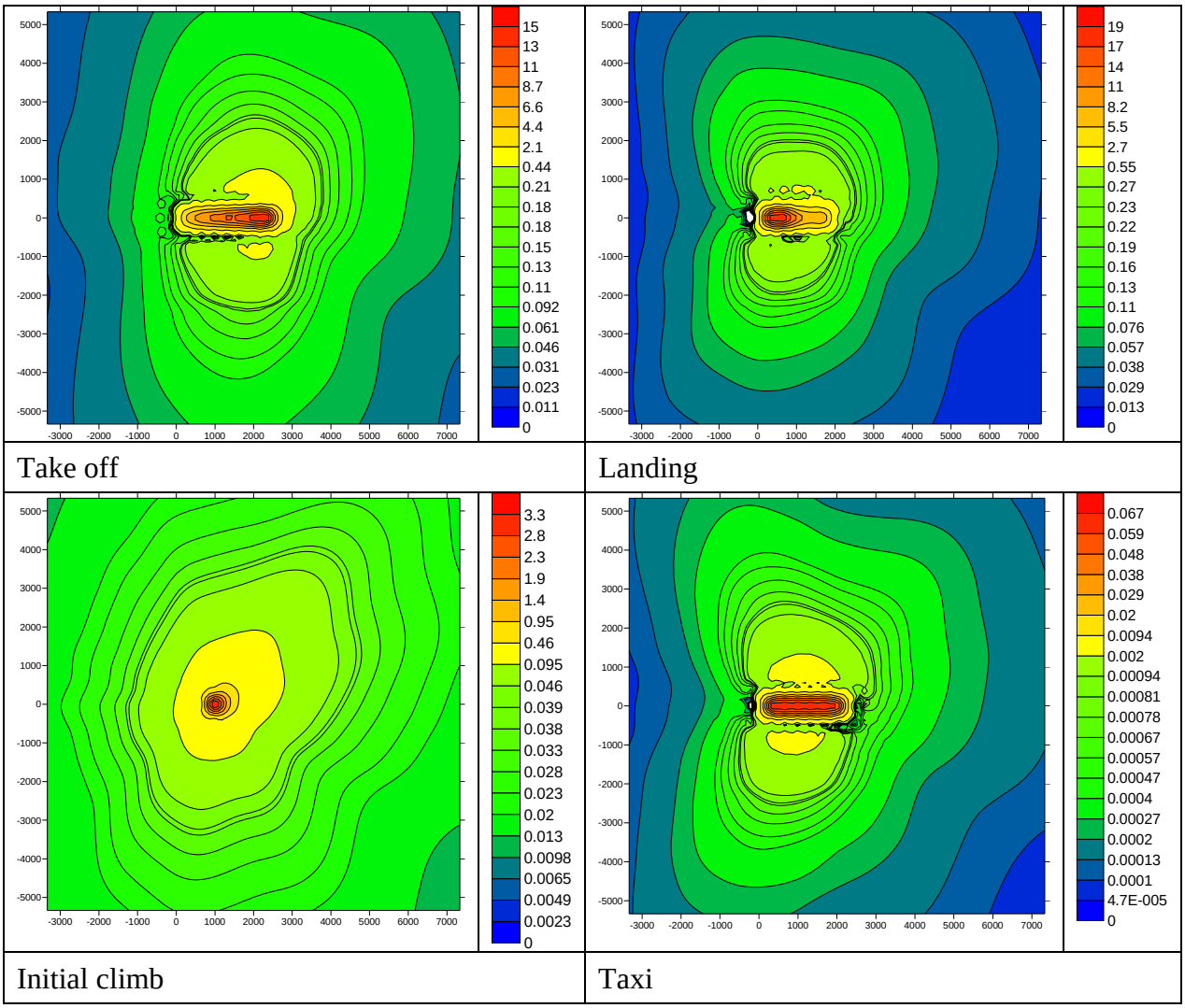

Figure 12.91: Normalised concentration plots for A330b the lead aircraft in MCAT 2

12.4.3 MCAT 3

A340_300a#

A340_300a

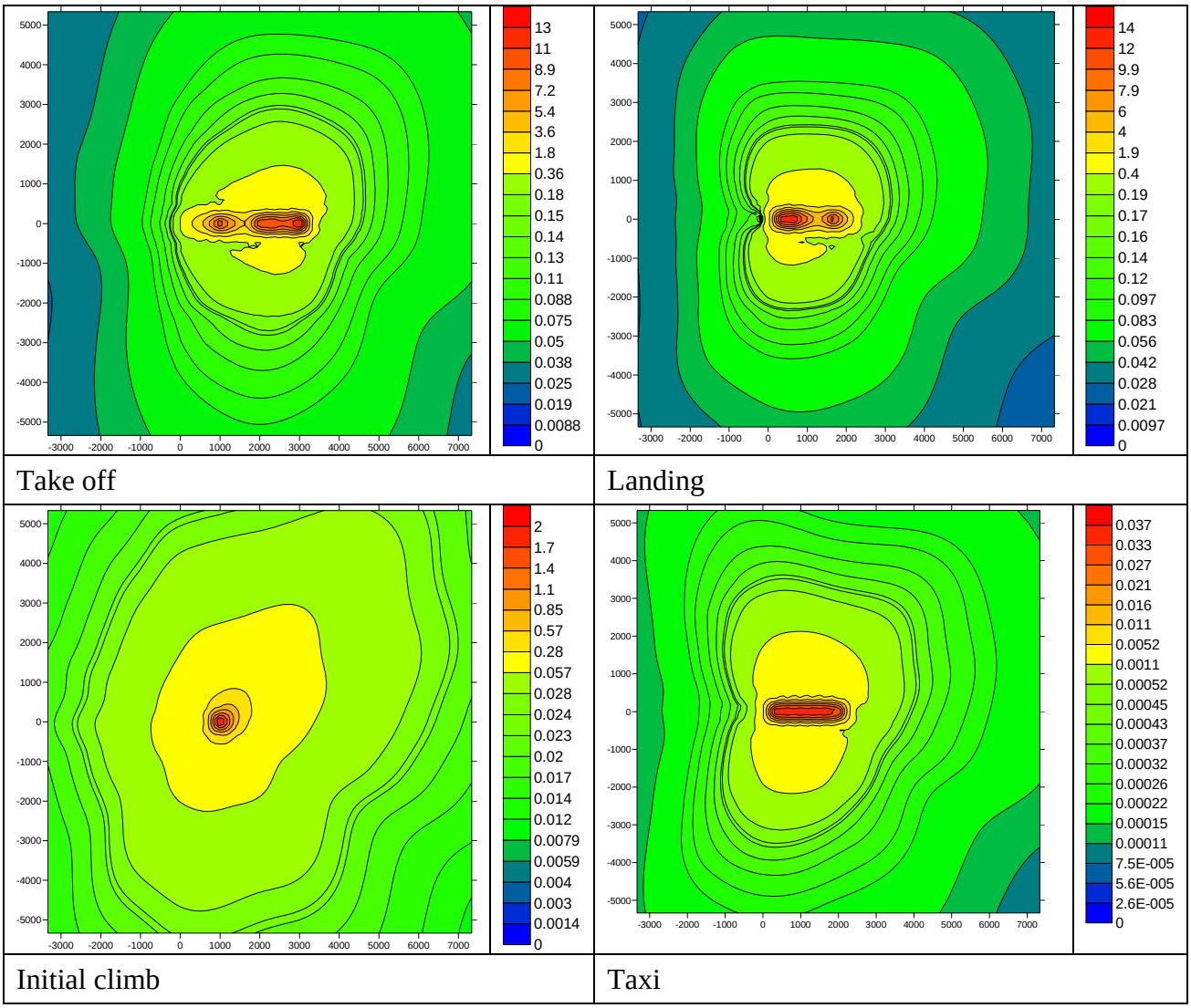

Figure 12.92: Normalised concentration plots for A340_300a the lead aircraft in MCAT 3

12.4.4 MCAT 4

B737_400#

B737_400

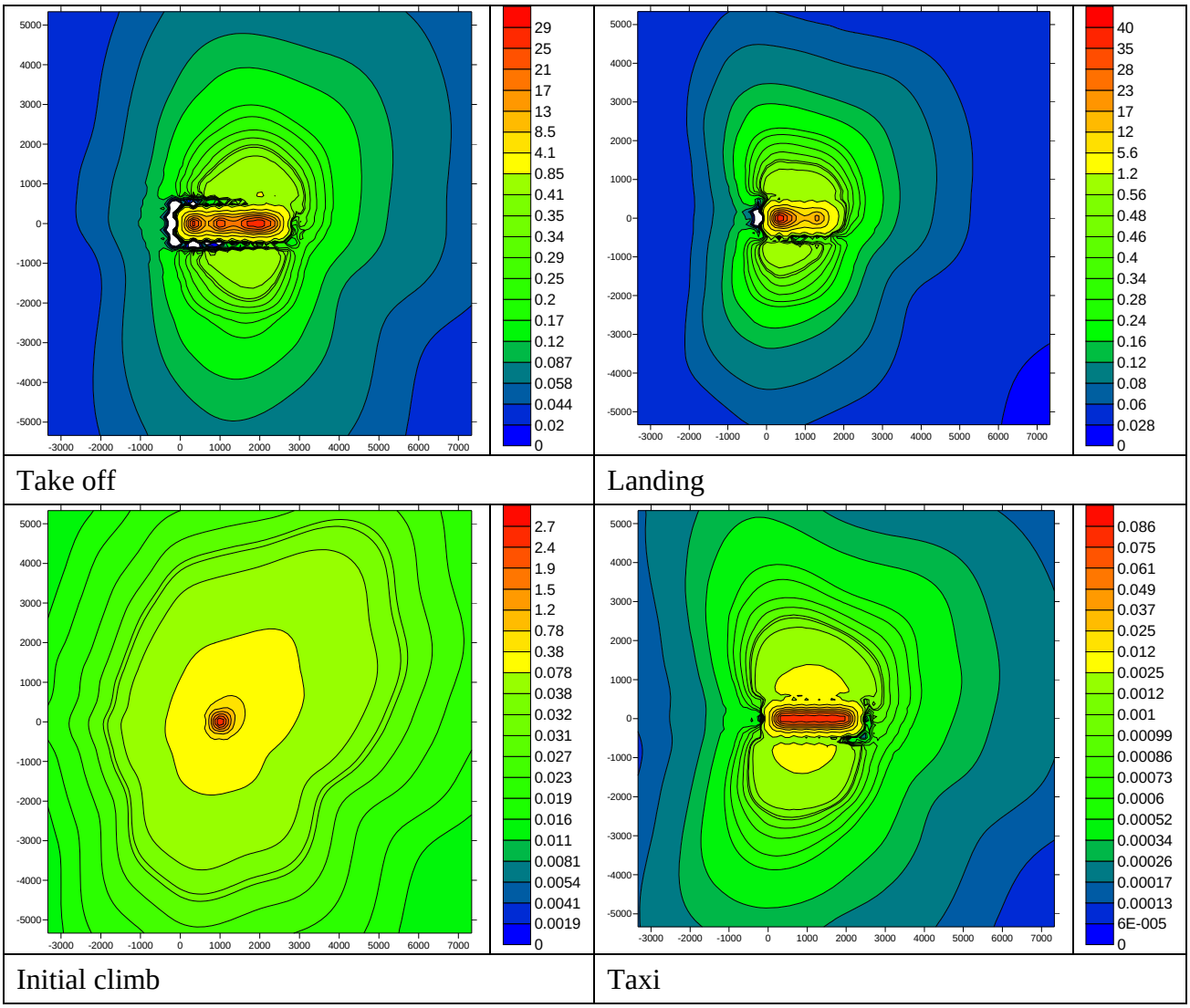

Figure 12.93: Normalised concentration plots for B737_400 the lead aircraft in MCAT 4

12.4.5 MCAT 5

B747_400[#]**,** B747_800, B747_800b, B747_800c* A380, A380b, A380c*

B747_400

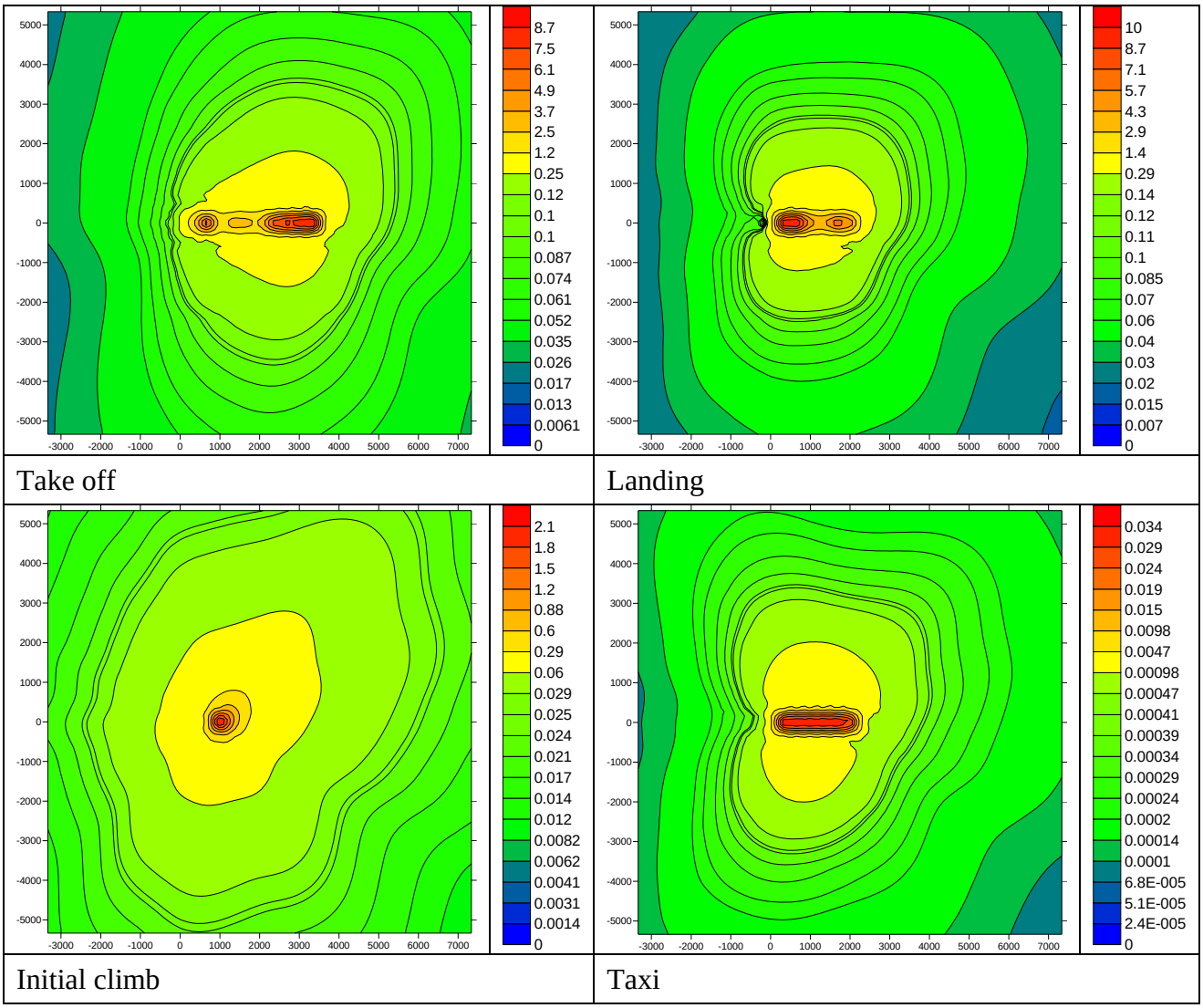

Figure 12.94: Normalised concentration plots for B747_400 the lead aircraft of MCAT 5

B747_800c

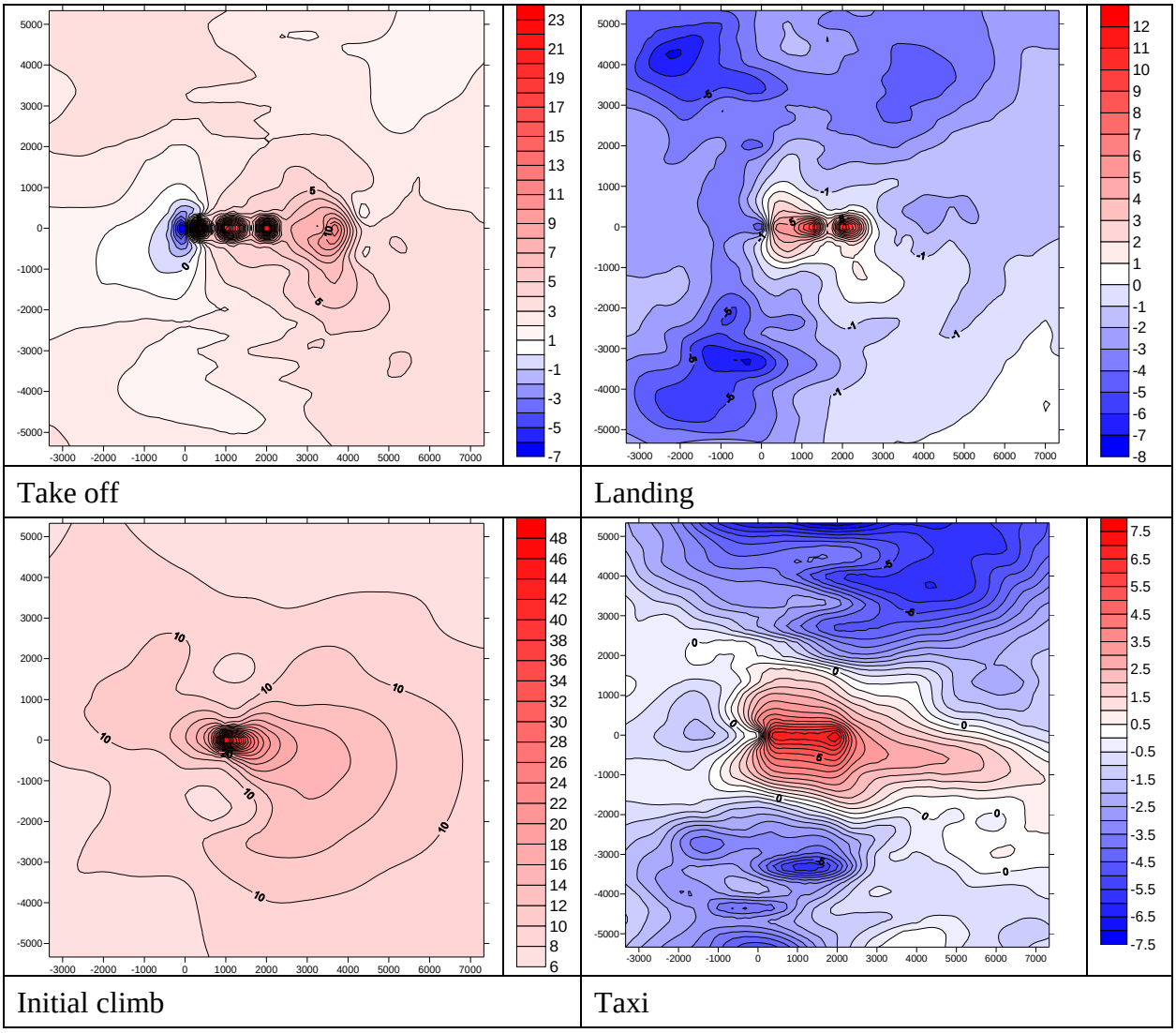

Figure 12.95: Percentage difference plots between B747_800c and MCAT 5 lead aircraft, B747_400

A380c

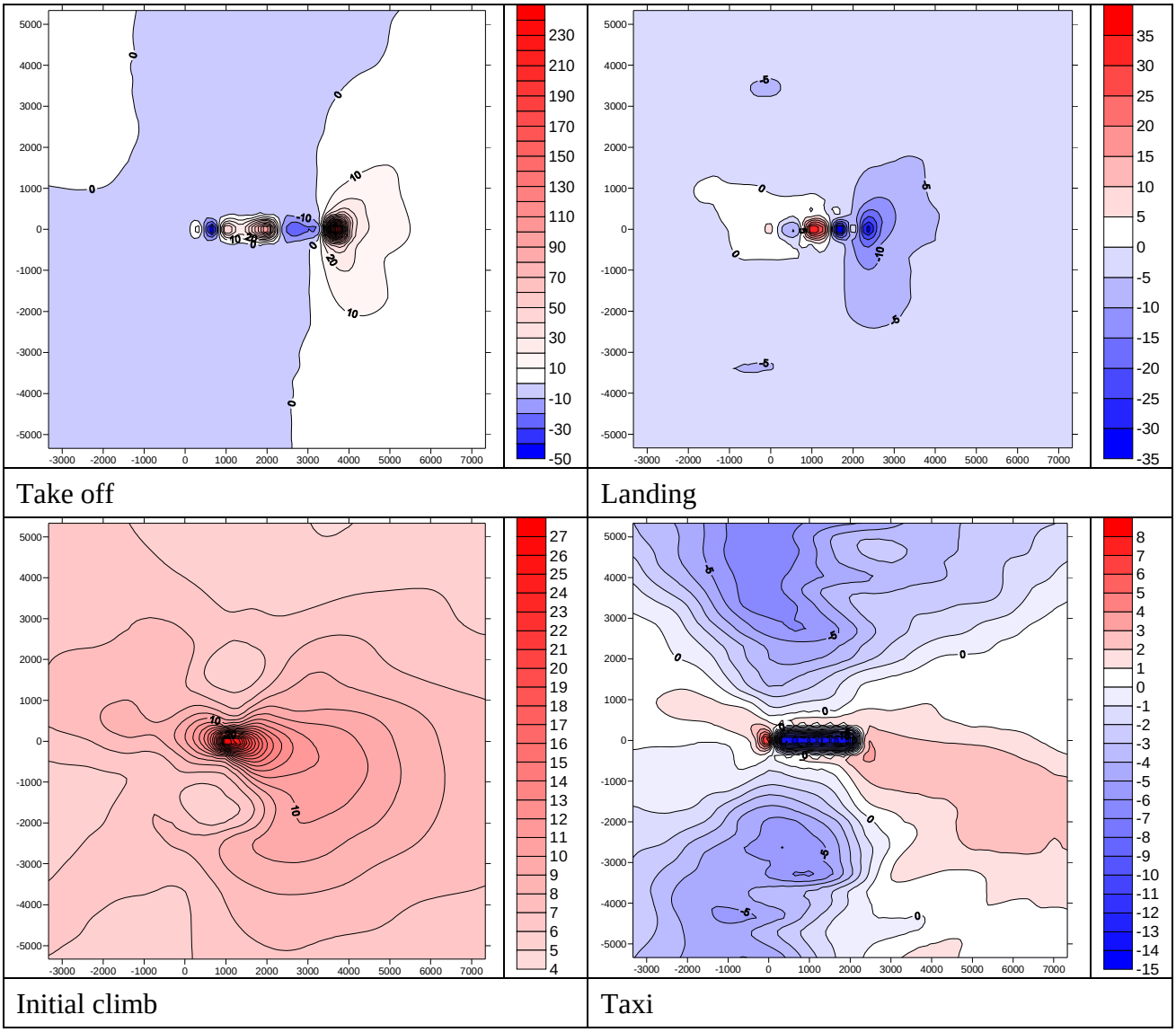

Figure 12.96: Percentage difference plots between A380c and MCAT 5 lead aircraft, B747_400

12.4.6 MCAT 6

B777_200b#, B777_200e, B777_200f, B777_200g, B777_200h, B777_200i, B777_200j*

B777_200b

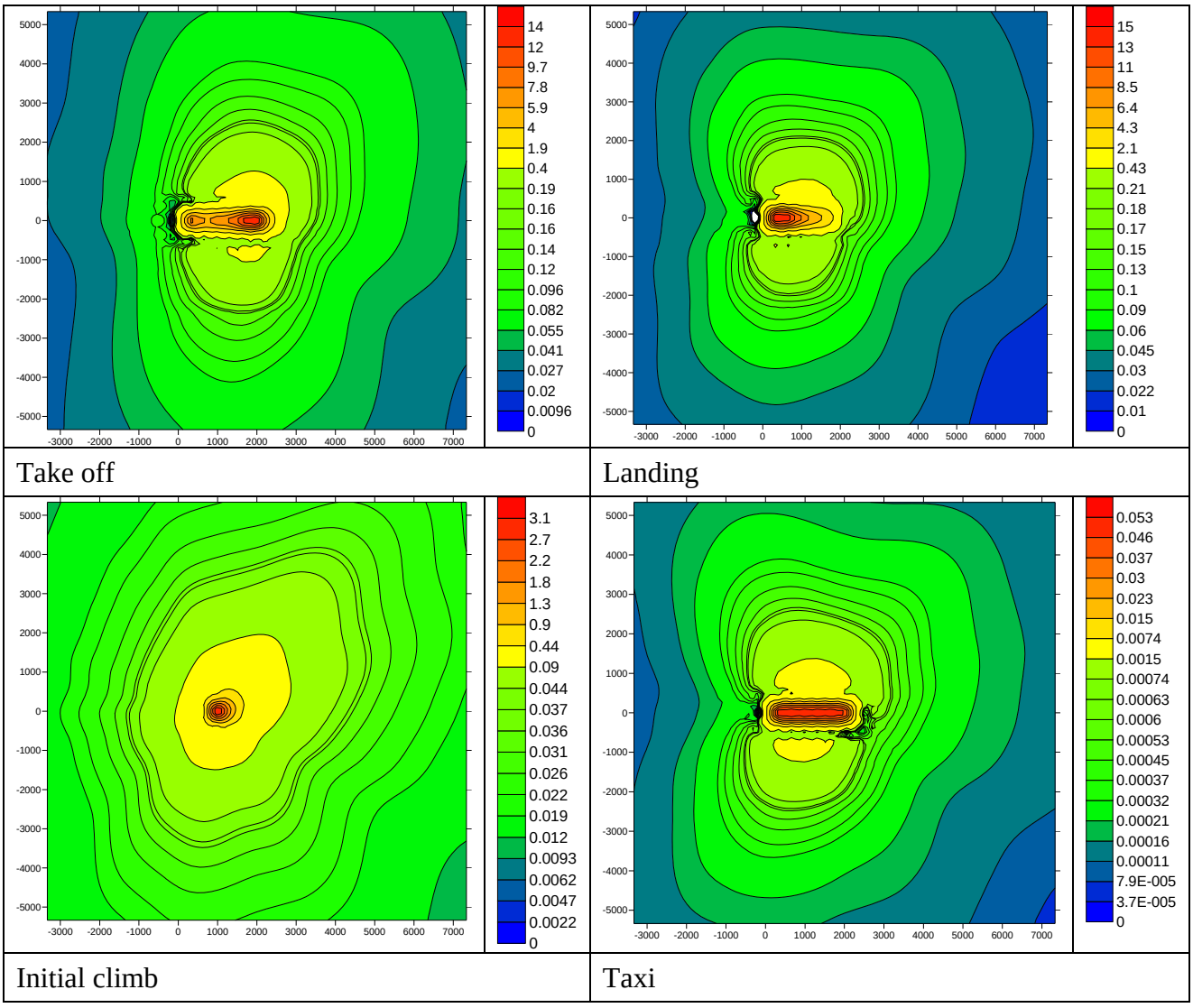

Figure 12.97: Normalised concentration plots for B777_200b the lead aircraft for MCAT 6

B777_200j

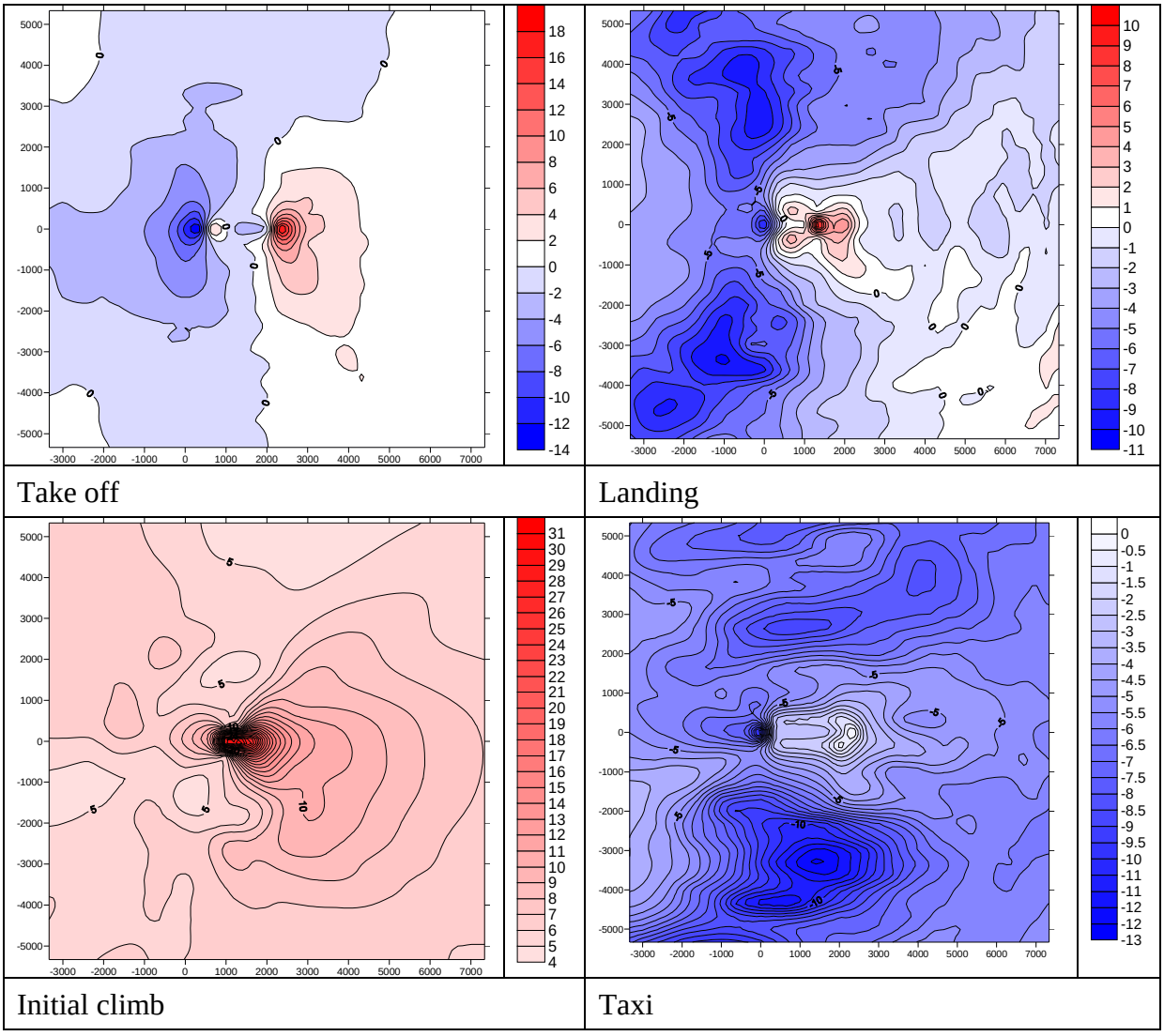

Figure 12.98: Percentage difference plots between B777_200j and MCAT 6 lead aircraft, B777_200b

12.4.7 MCAT 8

B787_3, B787_3b, B787_3c*, B787_8, B787_8b, B787_8c*

B787_3

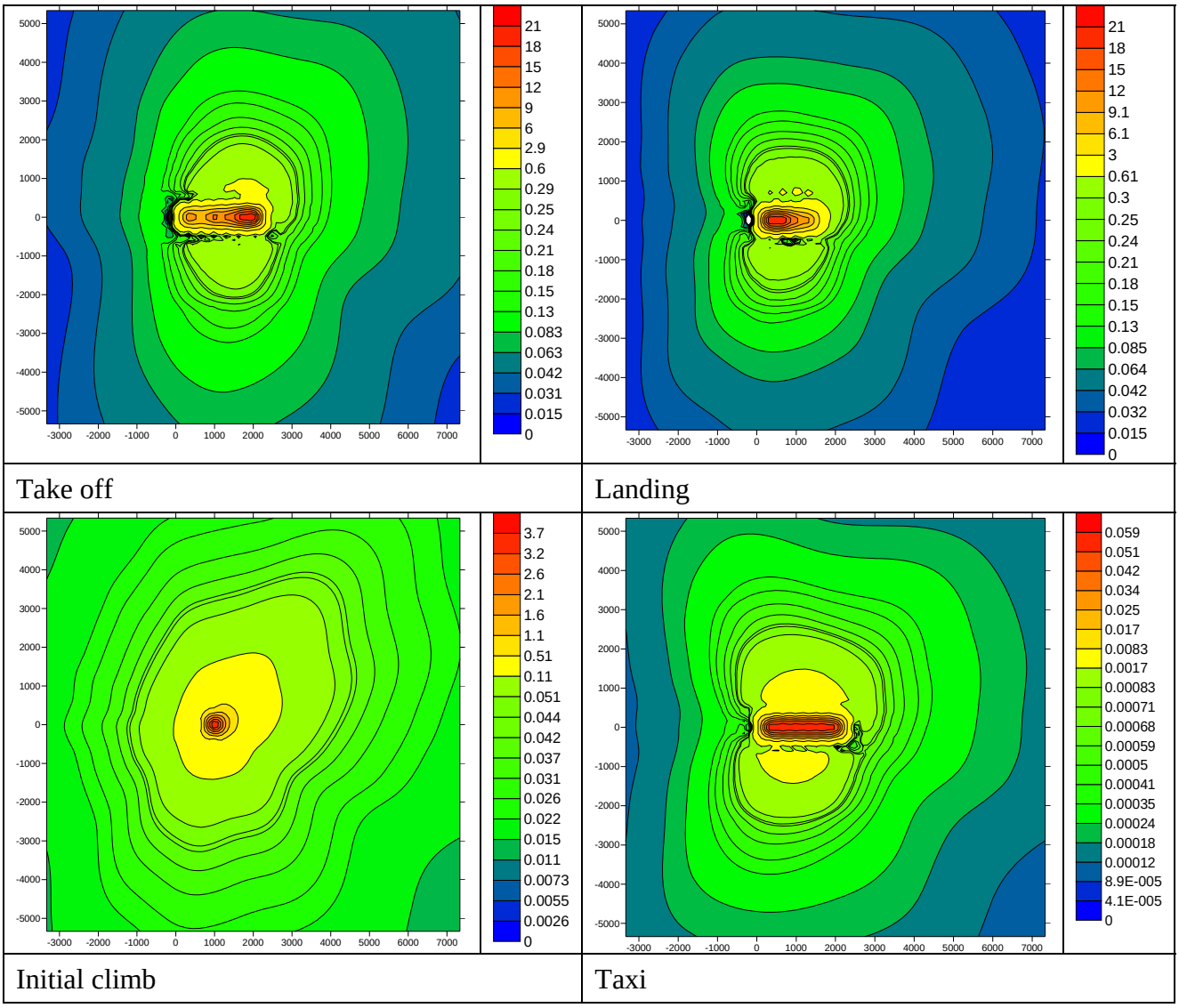

Figure 12.99: Normalised concentration plots for B787_3 the lead aircraft in MCAT 8

B787_3c

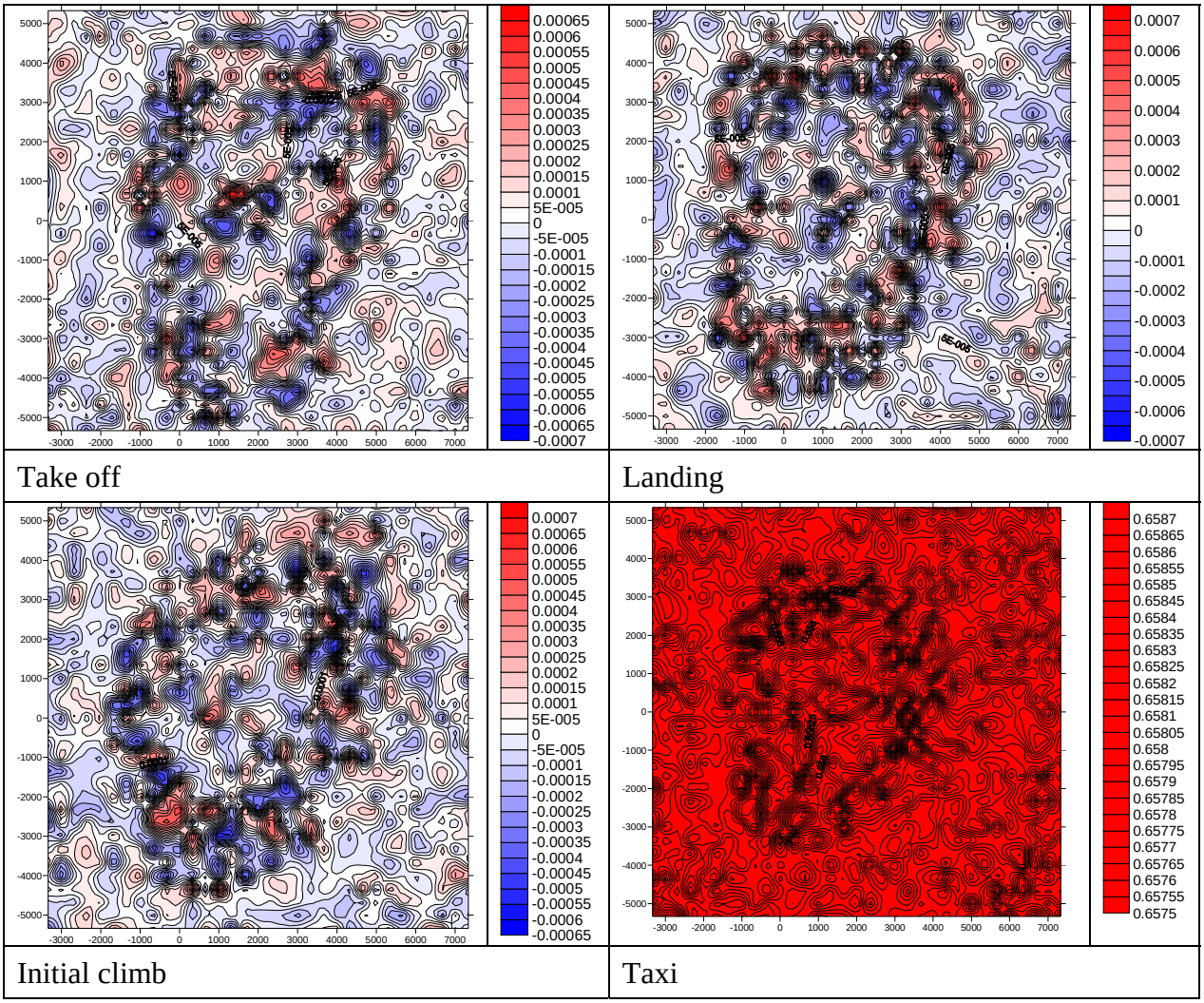

Figure 12.100: Percentage difference plots between B787_3c and MCAT 8 lead aircraft, B787_3

B787_8c

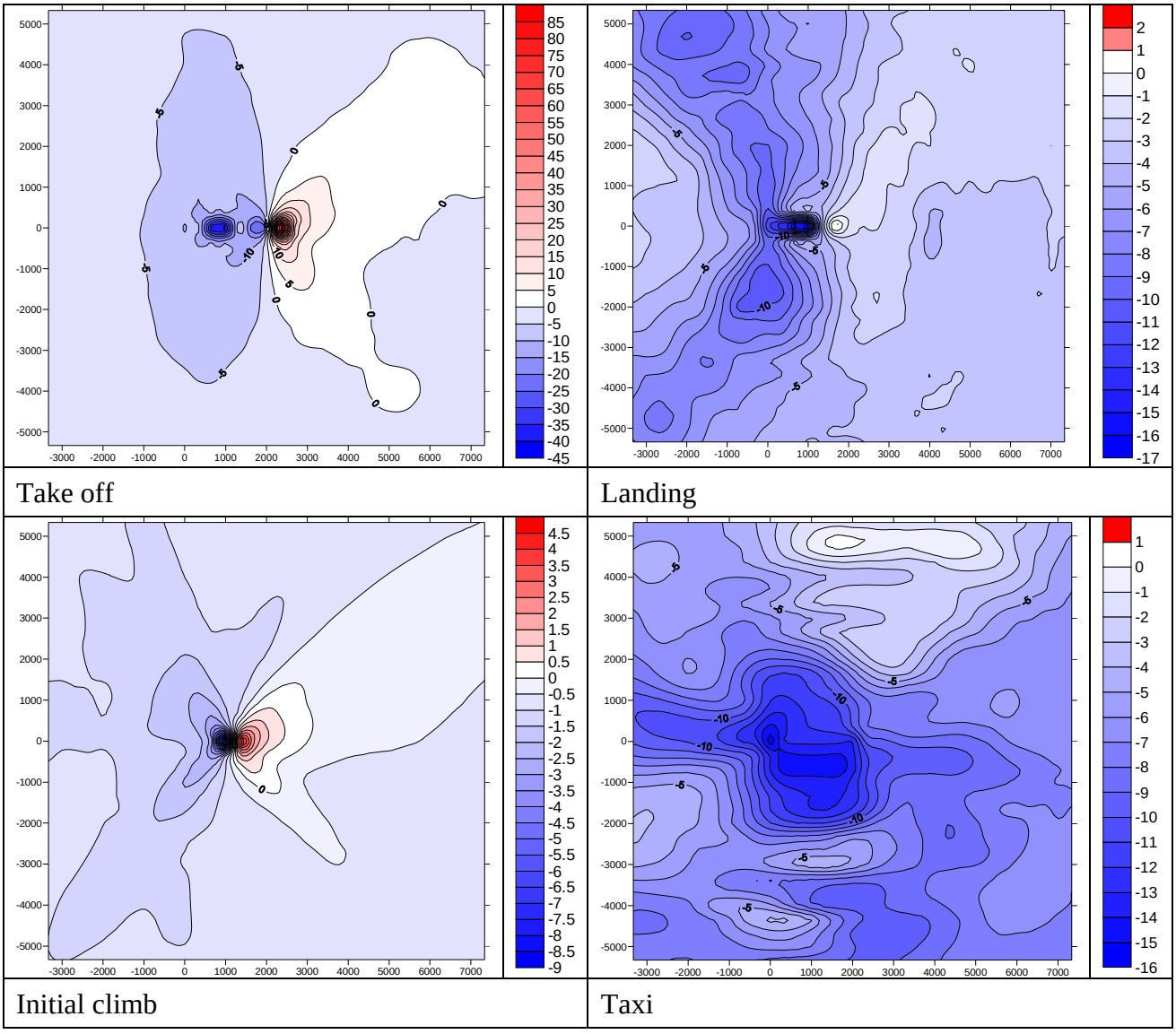

Figure 12.101: Percentage difference plots between B787_8c and MCAT 8 lead aircraft, B787_3

12.4.8 MCAT 9

A340_600a, A340_600b

A340_600a

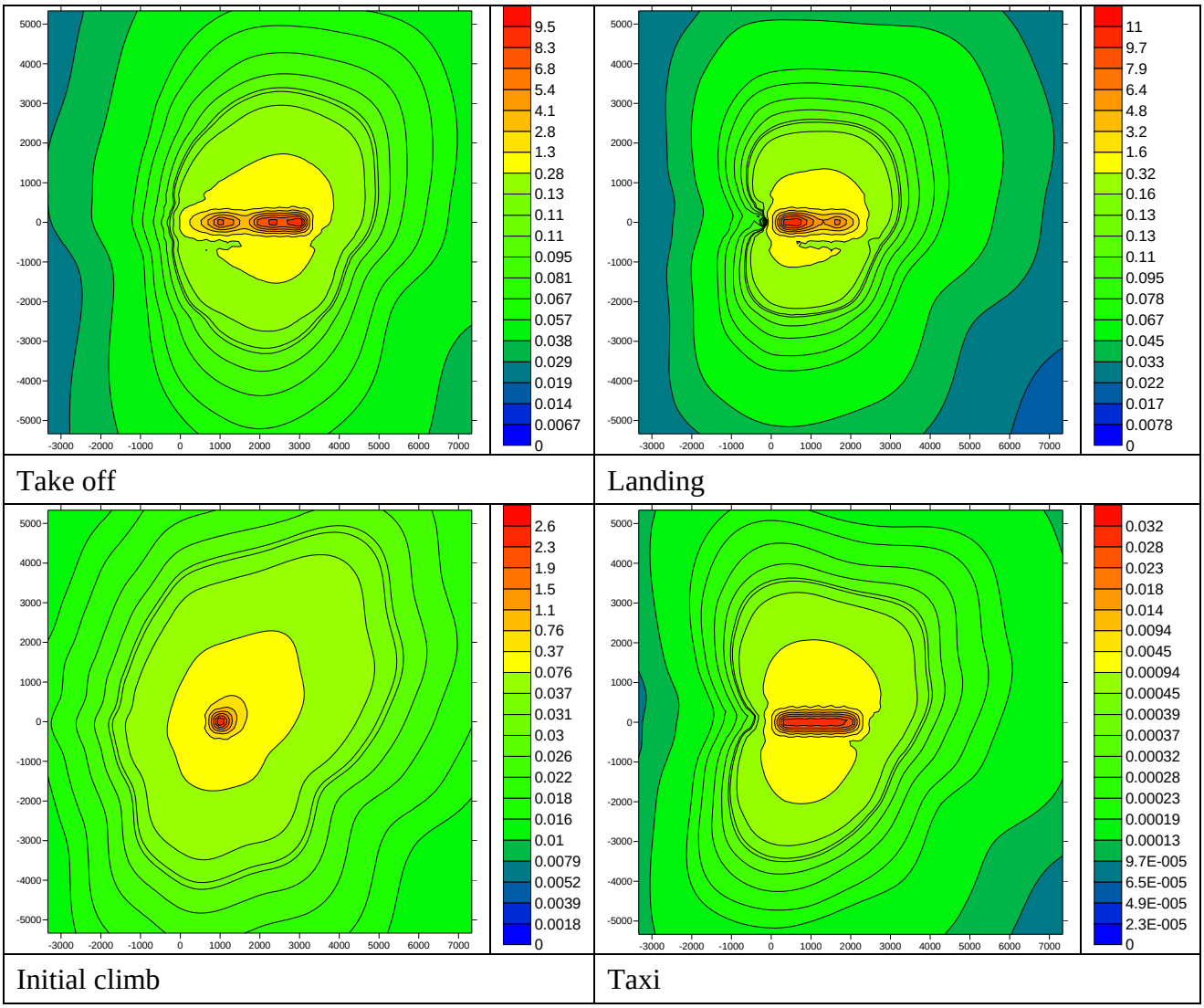

Figure 12.102: Normalised concentration plots for A340_600a the lead aircraft in MCAT 9

12.4.9 MCAT 10

A350_800, A350_800b*, A350_800c*, A350_900, A350_900b*, A350_900c*

A350_800

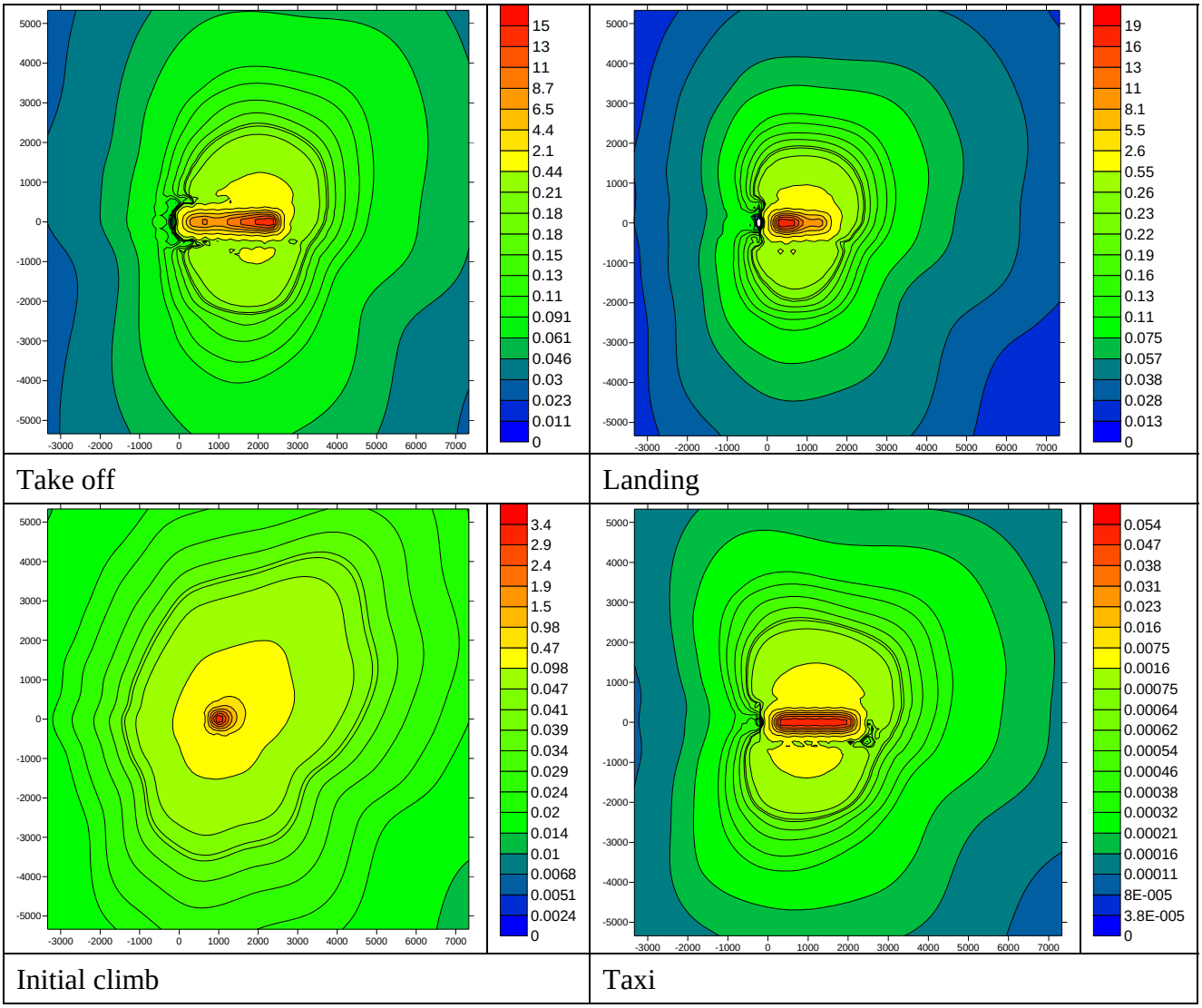

Figure 12.103: Normalised concentration plots for A350_800 the lead aircraft for MCAT 10

A350_800b

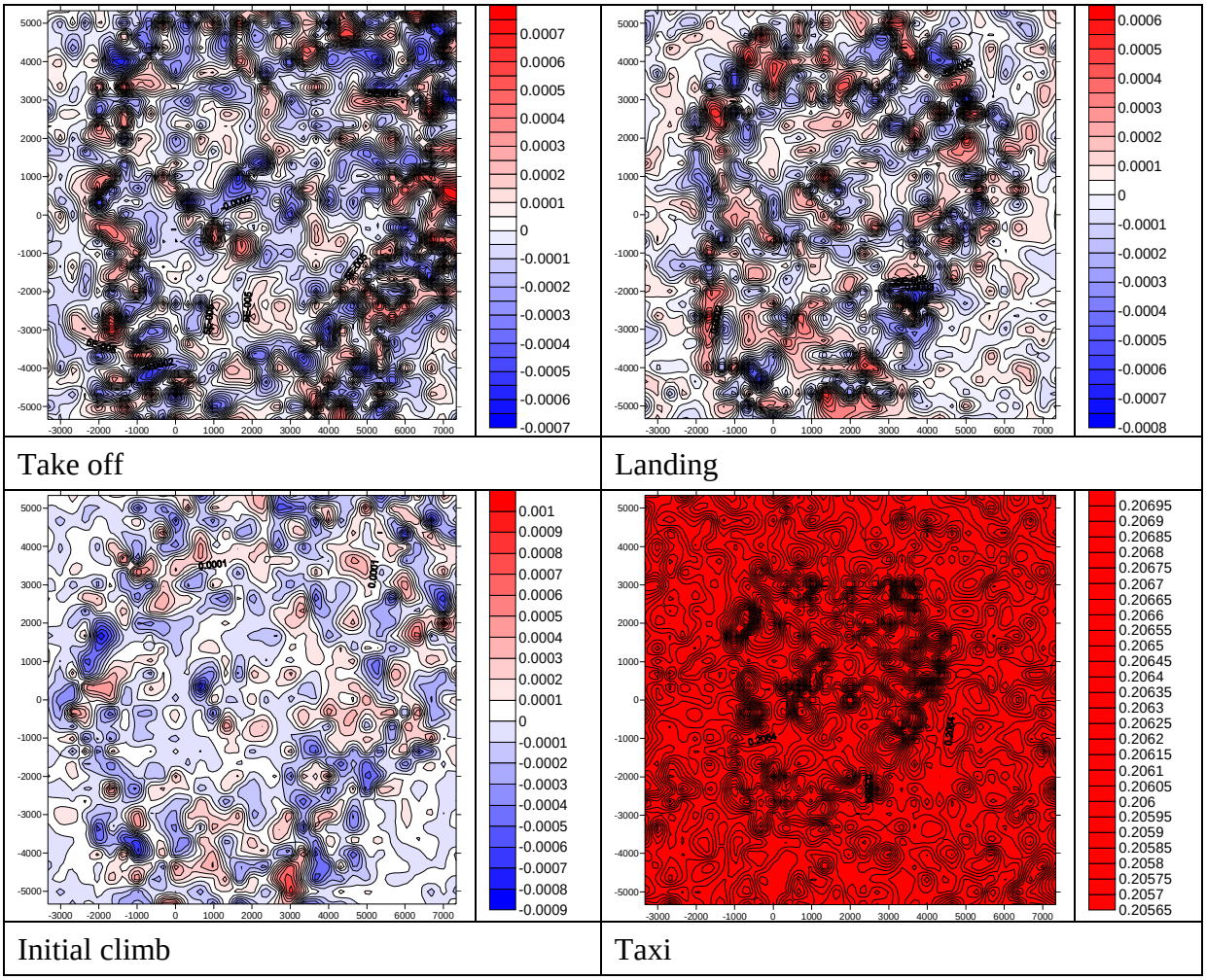

Figure 12.104: Percentage difference plots between A350_800b and MCAT 10 lead aircraft, A350_800

A350_800c

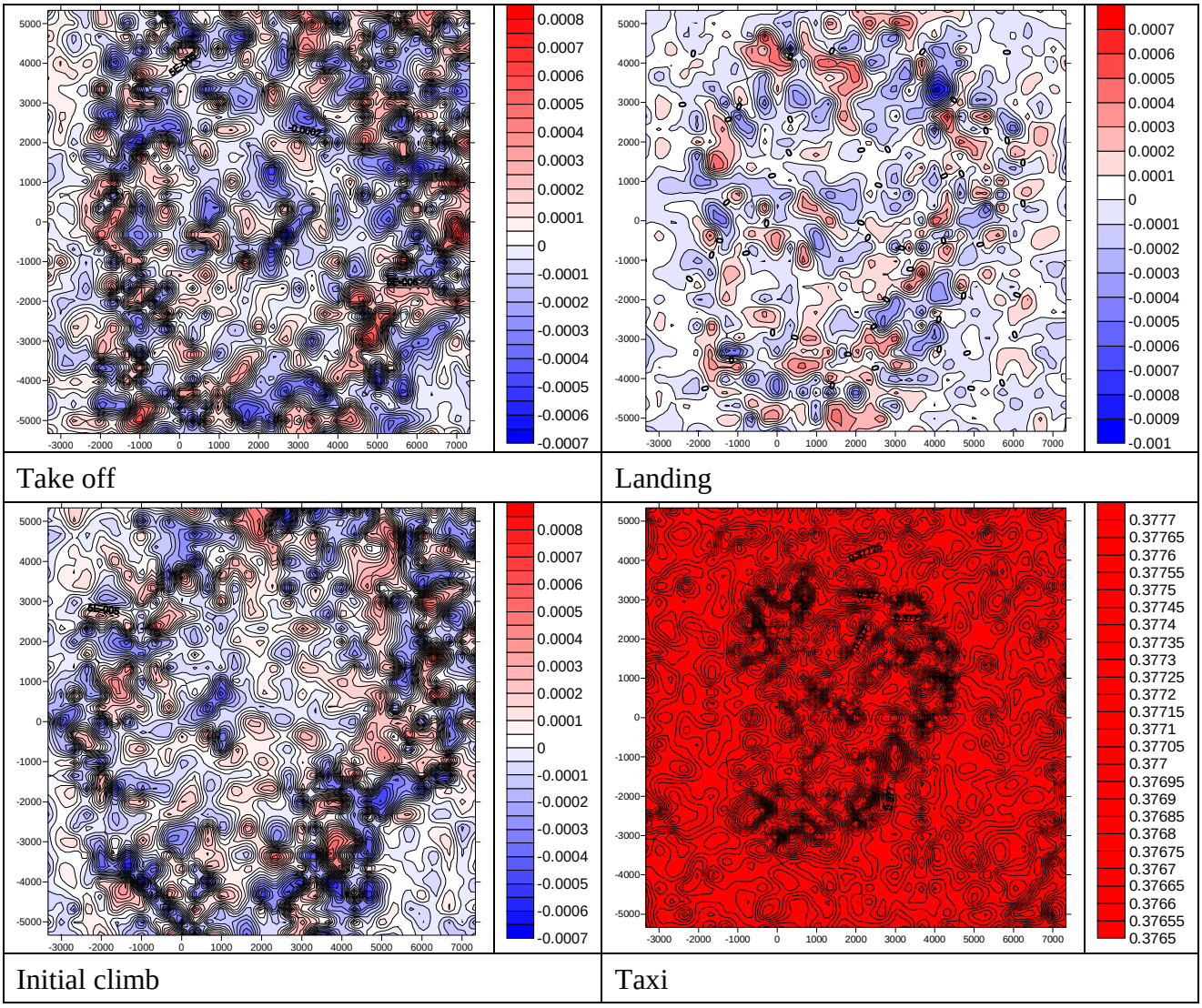

Figure 12.105: Percentage difference plots between A350_800c and MCAT 10 lead aircraft, A350_800

A350_900b

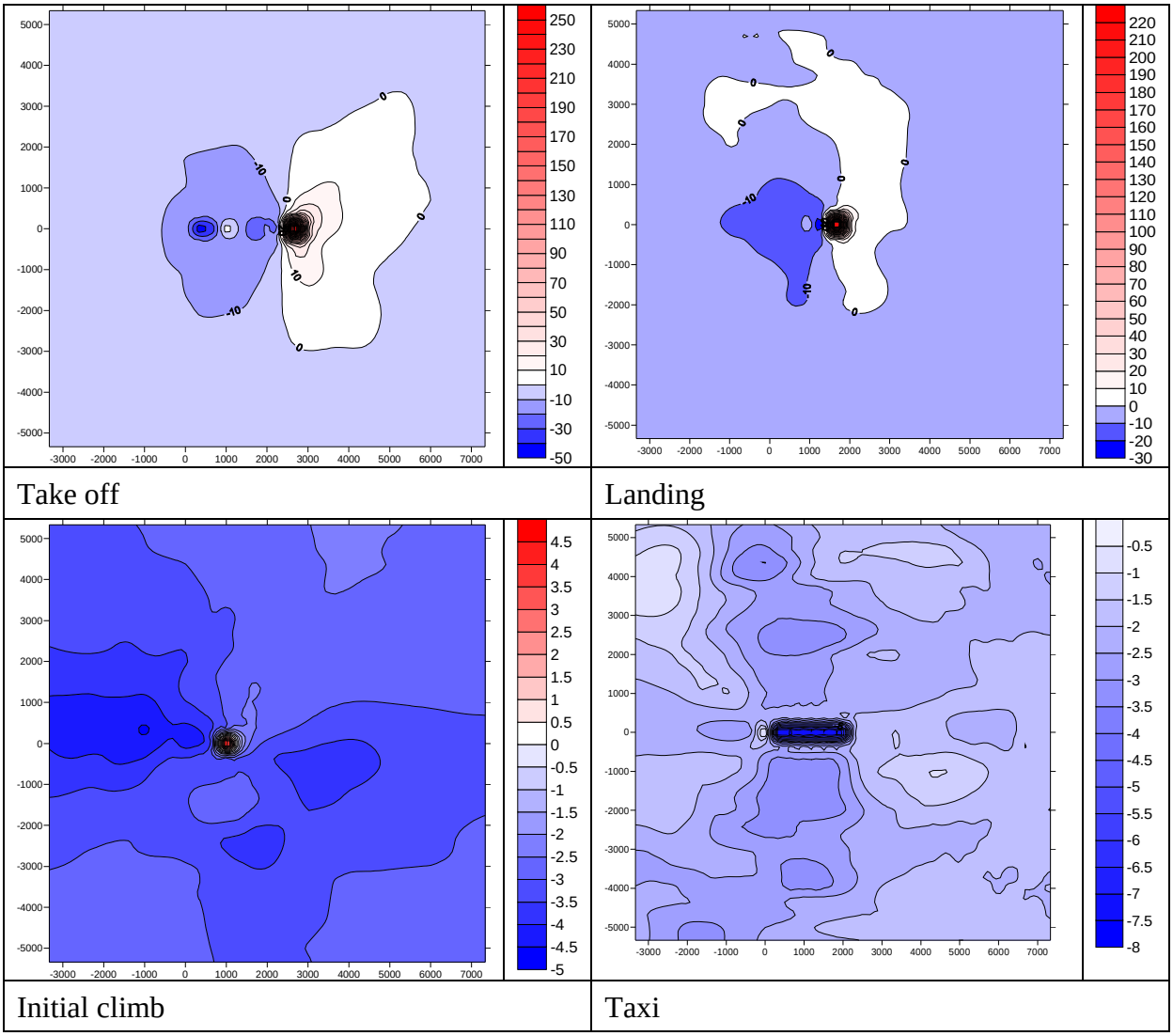

Figure 12.106: Percentage difference plots between A350_900b and MCAT 10 lead aircraft, A350_800

A350_900c

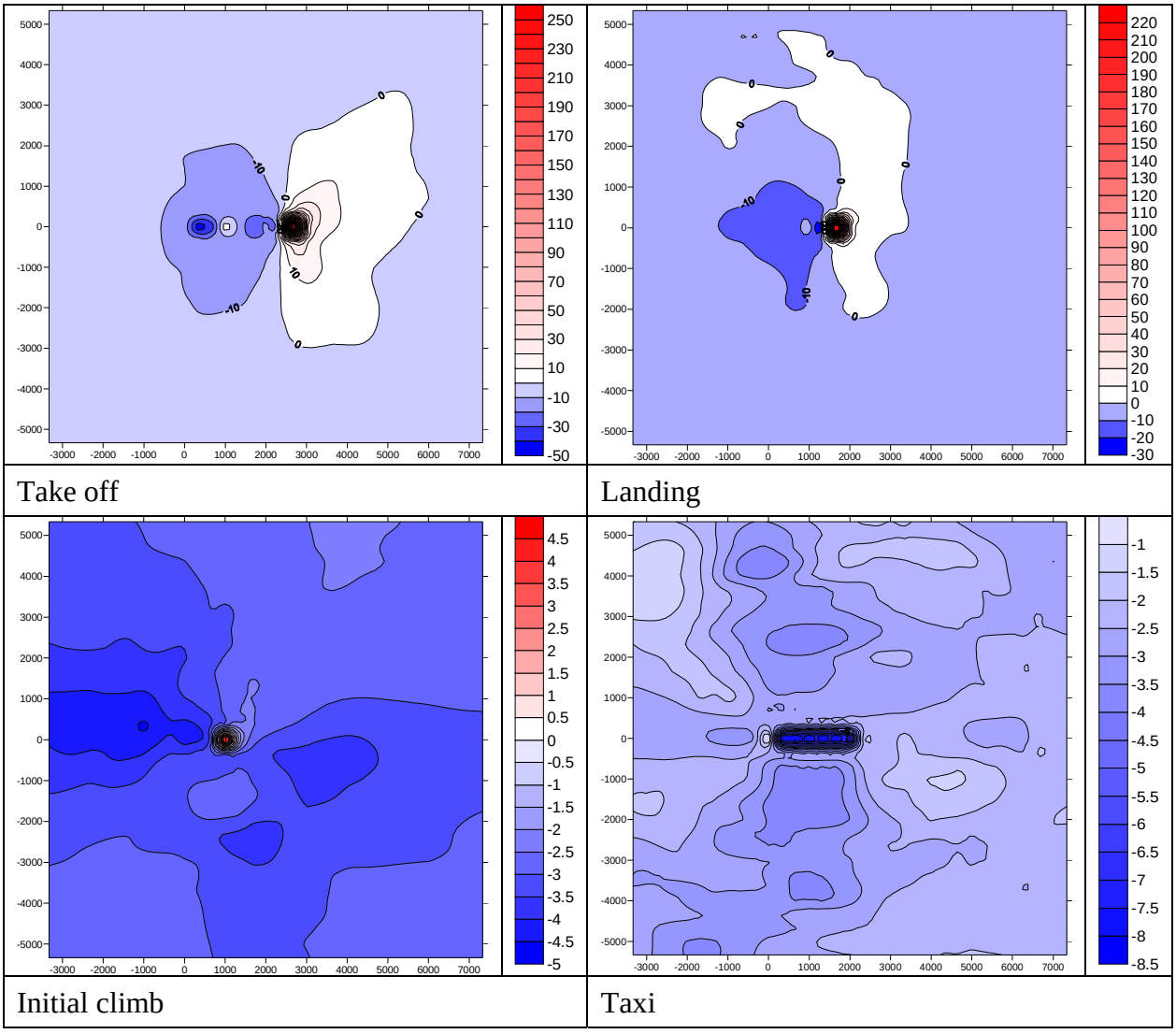

Figure 12.107: Percentage difference plots between A350_900c and MCAT 10 lead aircraft, A350_800

12.4.10 MCAT 11

B737_800, B737_800b

B737_800

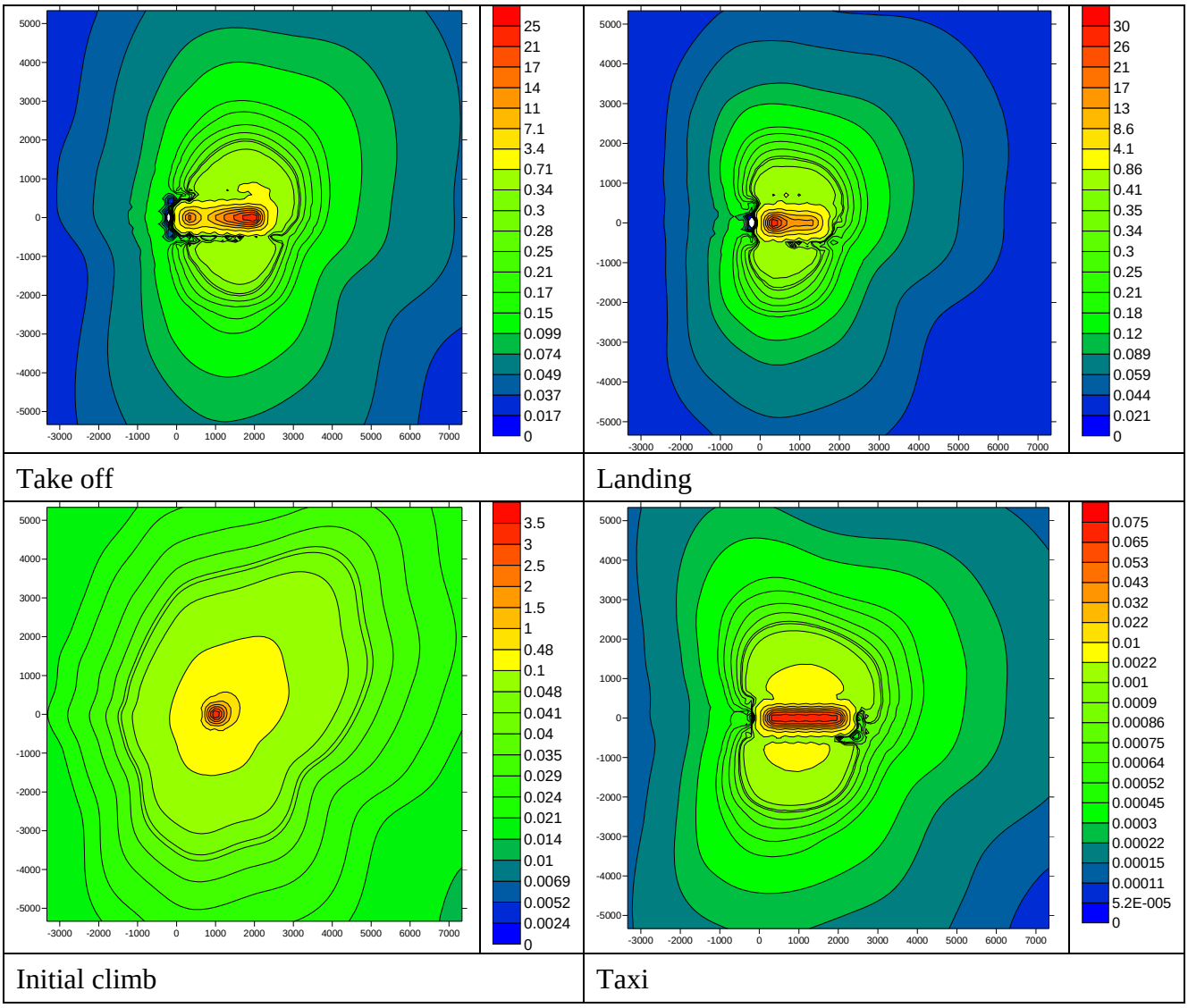

Figure 12.108: Normalised concentration plots for B737_800 the lead aircraft for MCAT 11

B737_800b

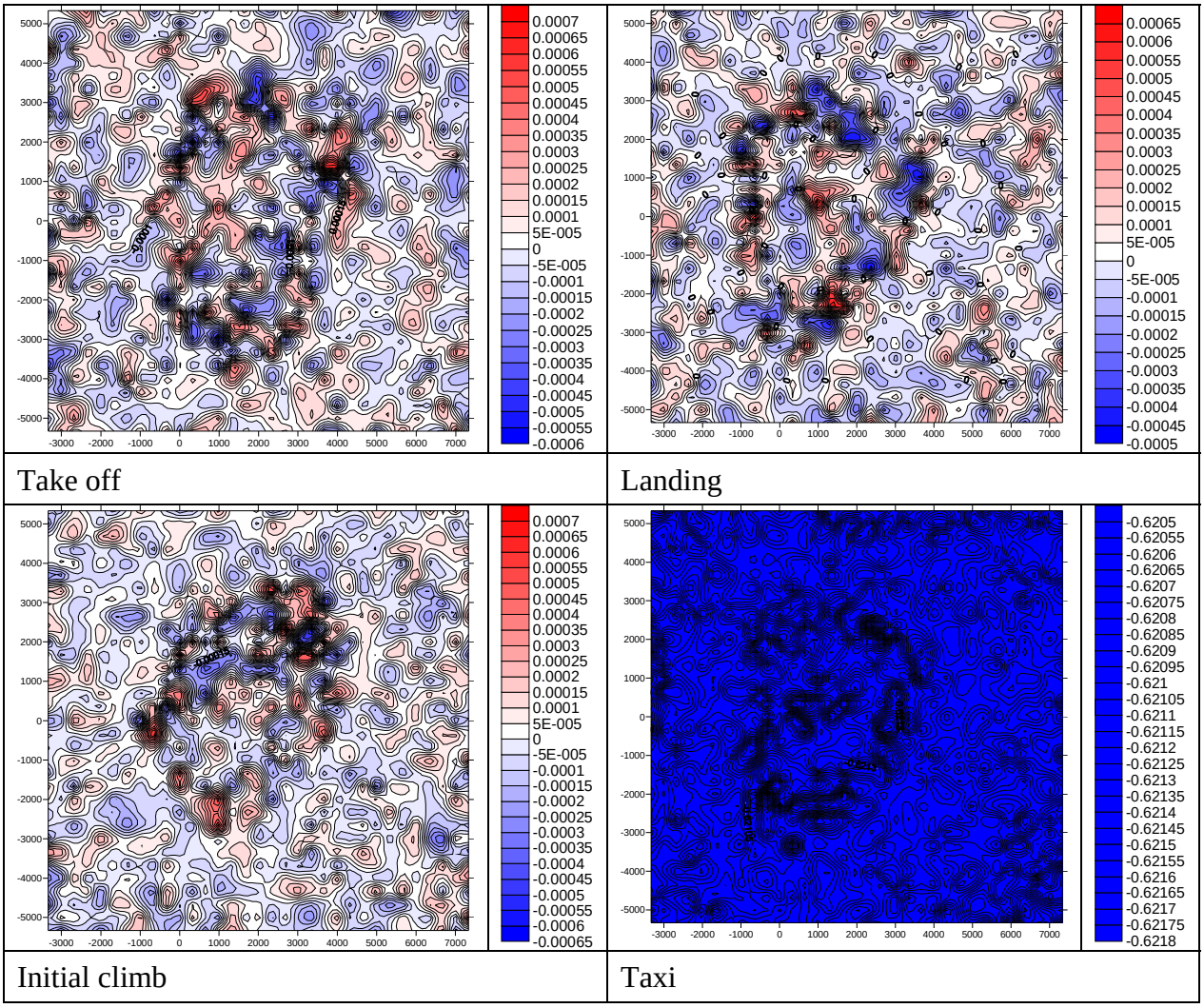

Figure 12.109: Percentage difference plots between B737_800b and MCAT 11 lead aircraft, B737_800

12.4.11 MCAT 12

N120s, N120sb

N120s

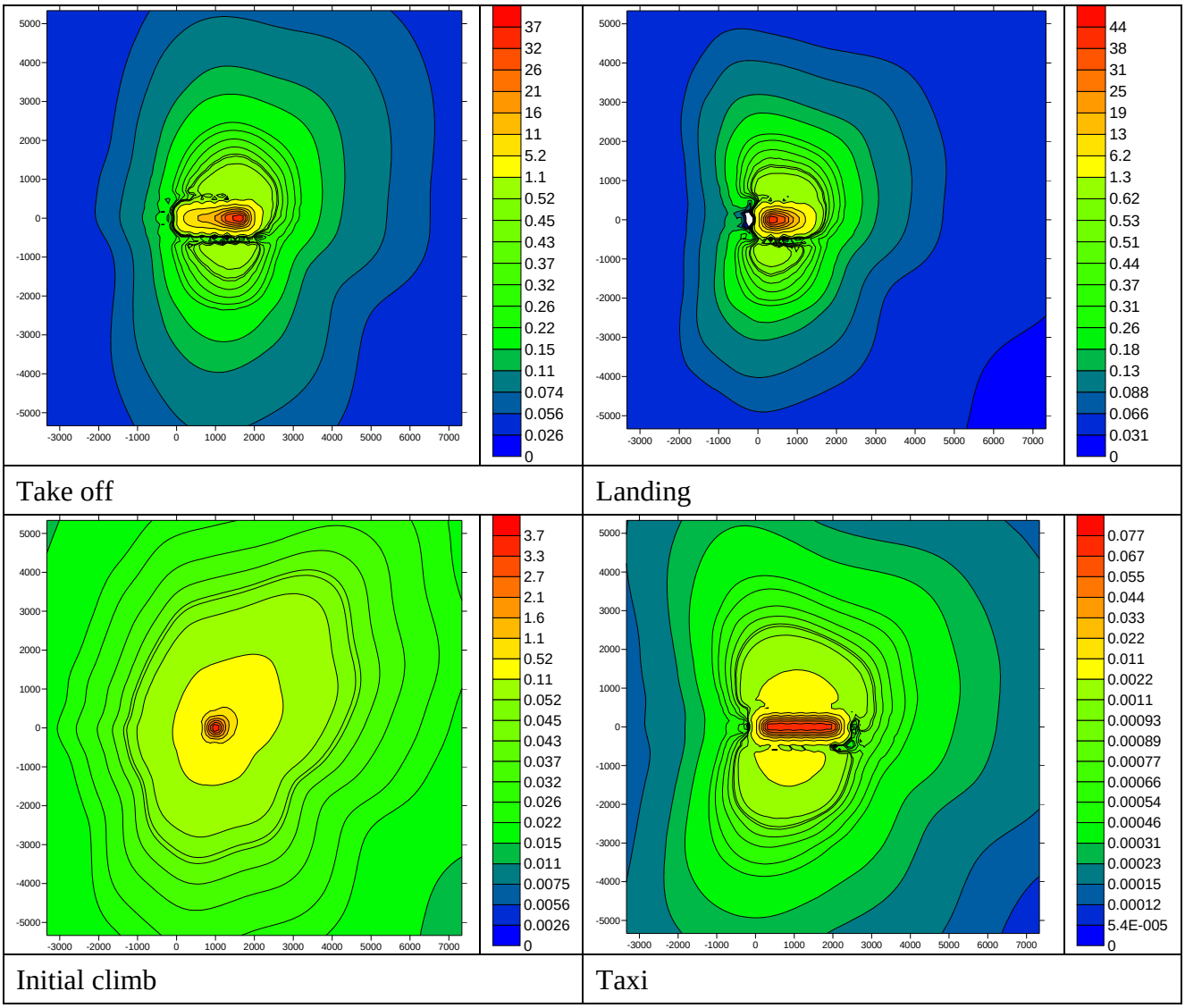

Figure 12.110: Normalised concentration plots for N120s the lead aircraft for MCAT 12

N120sb

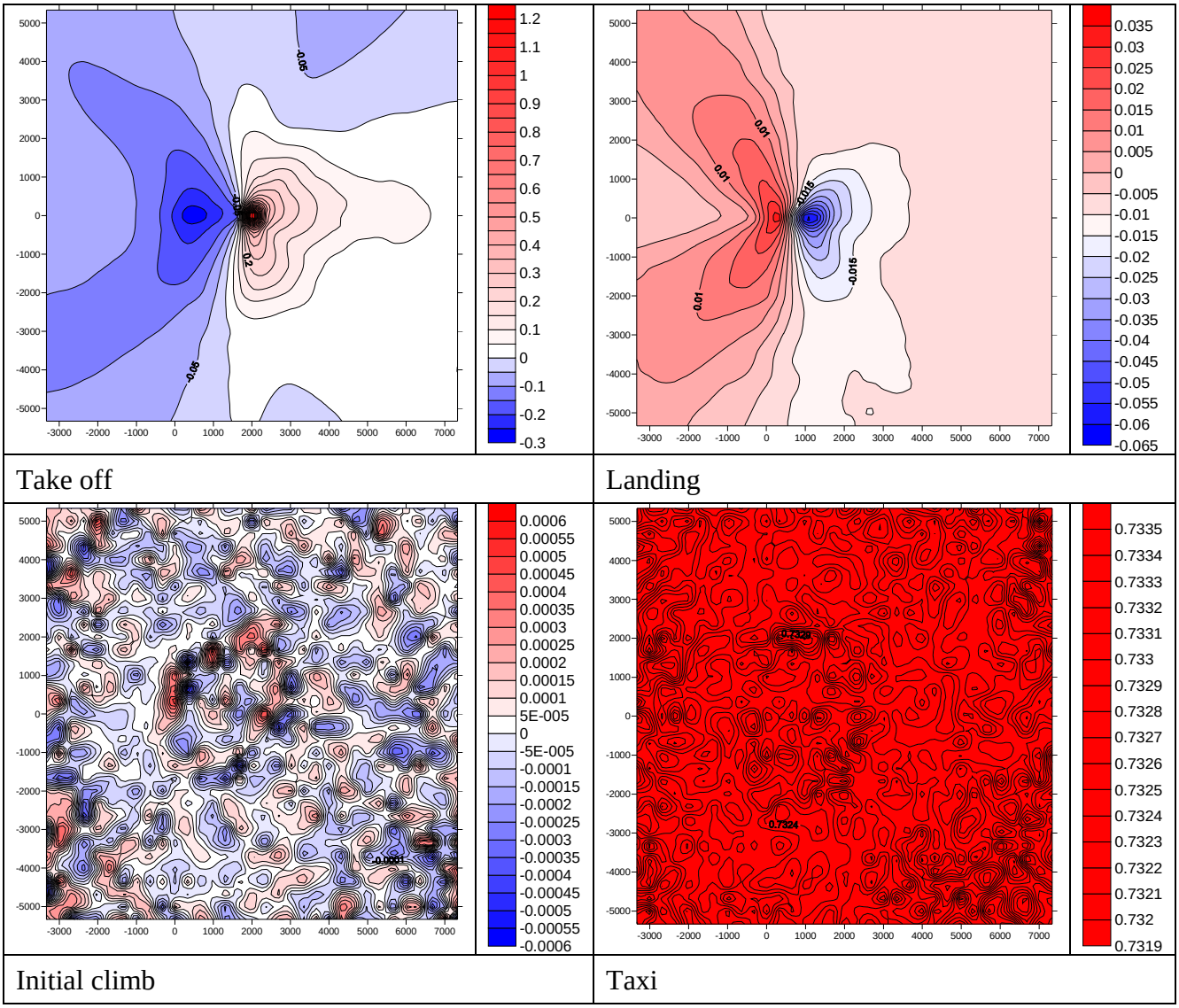

Figure 12.111: Percentage difference plots between N120sb and MCAT 12 lead aircraft, N120s

12.4.12 MCAT 13

N150s, N150sb

N150s

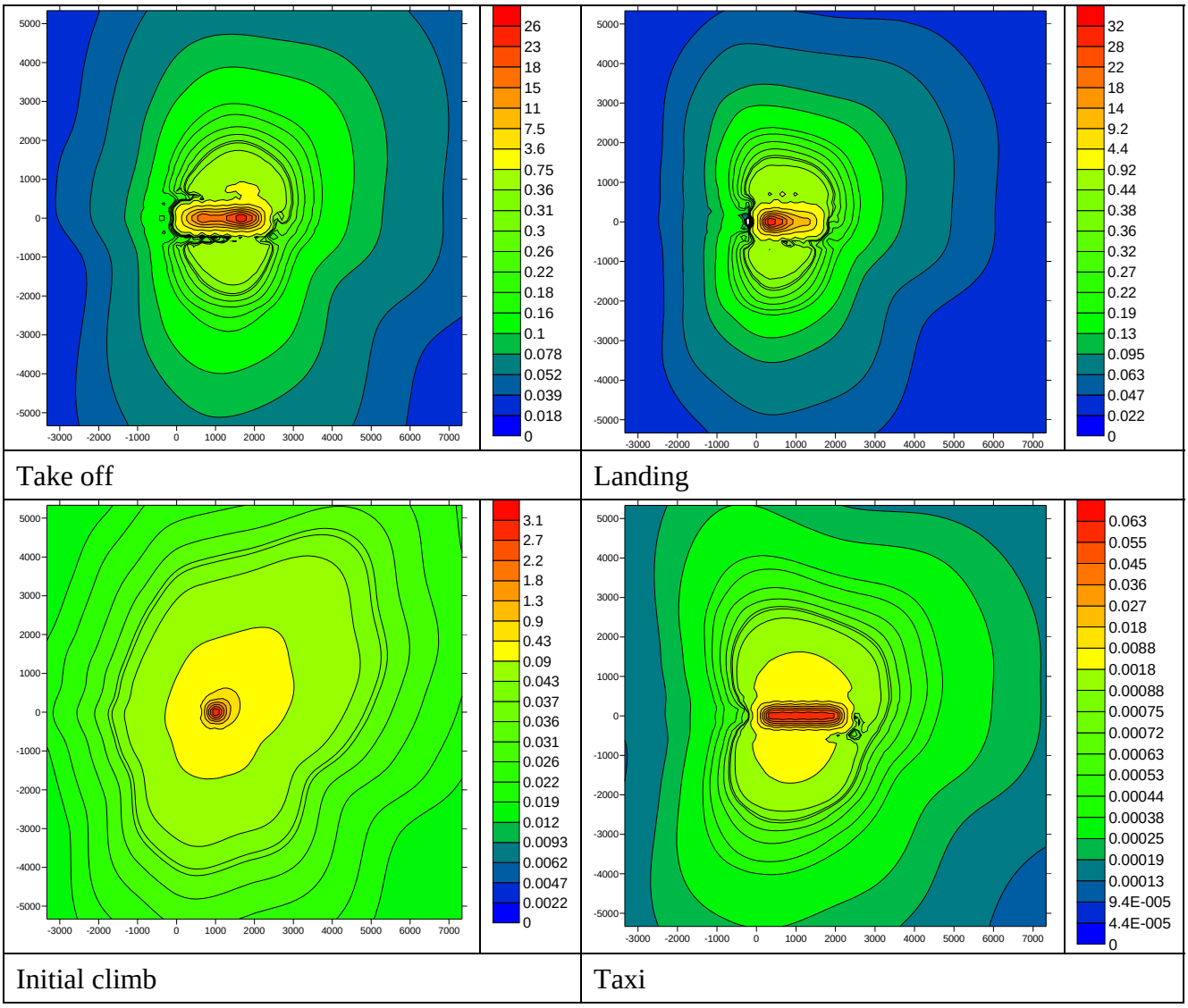

Figure 12.112: Normalised concentration plots for N150s the lead aircraft for MCAT 13

N150sb

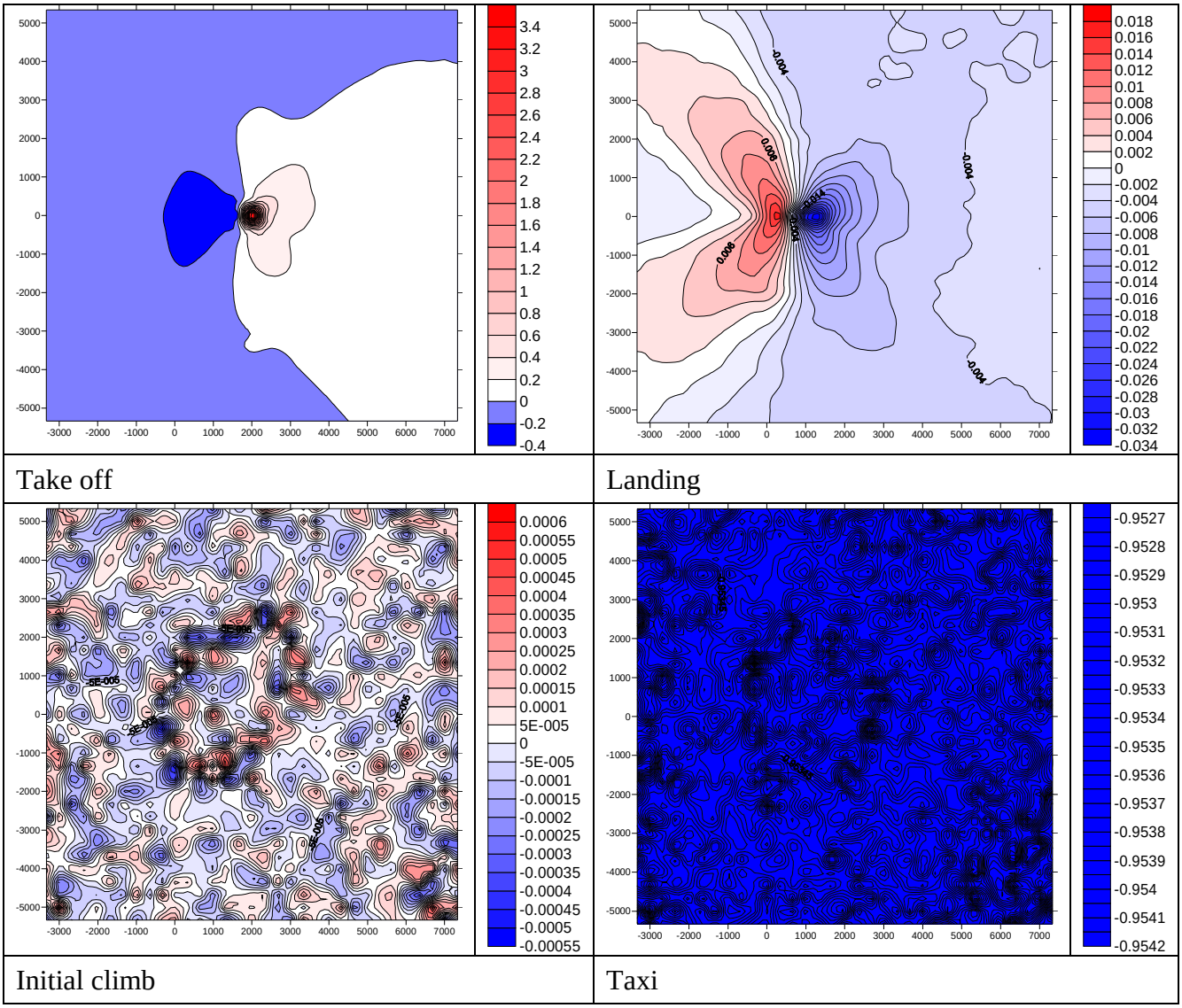

Figure 12.113: Percentage difference plots between N150sb and MCAT 13 lead aircraft, N150s

12.4.13 MCAT 14

N180s, N180sb

N180s

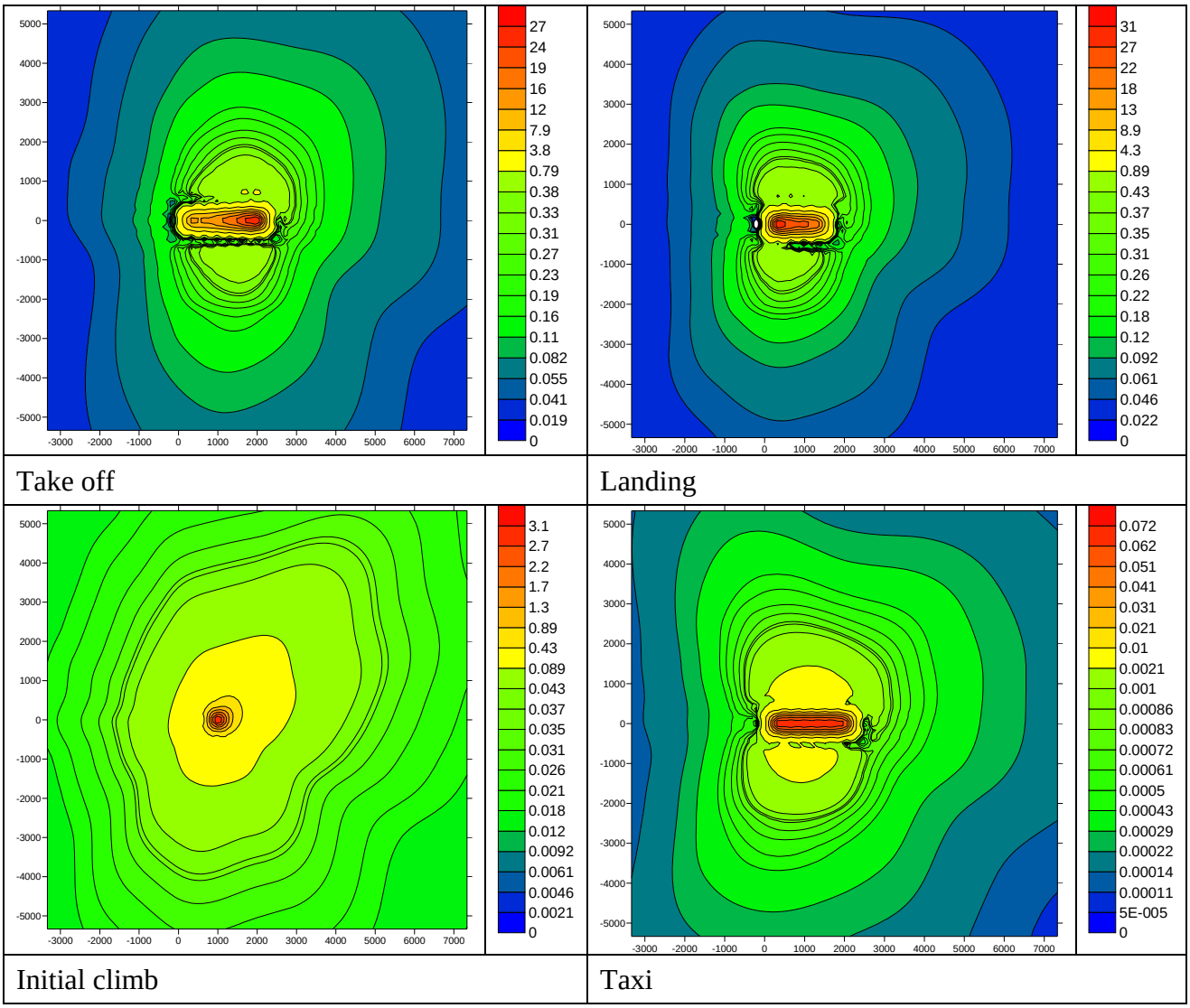

Figure 12.114: Normalised concentration plots for N180s the lead aircraft for MCAT 14

N180sb

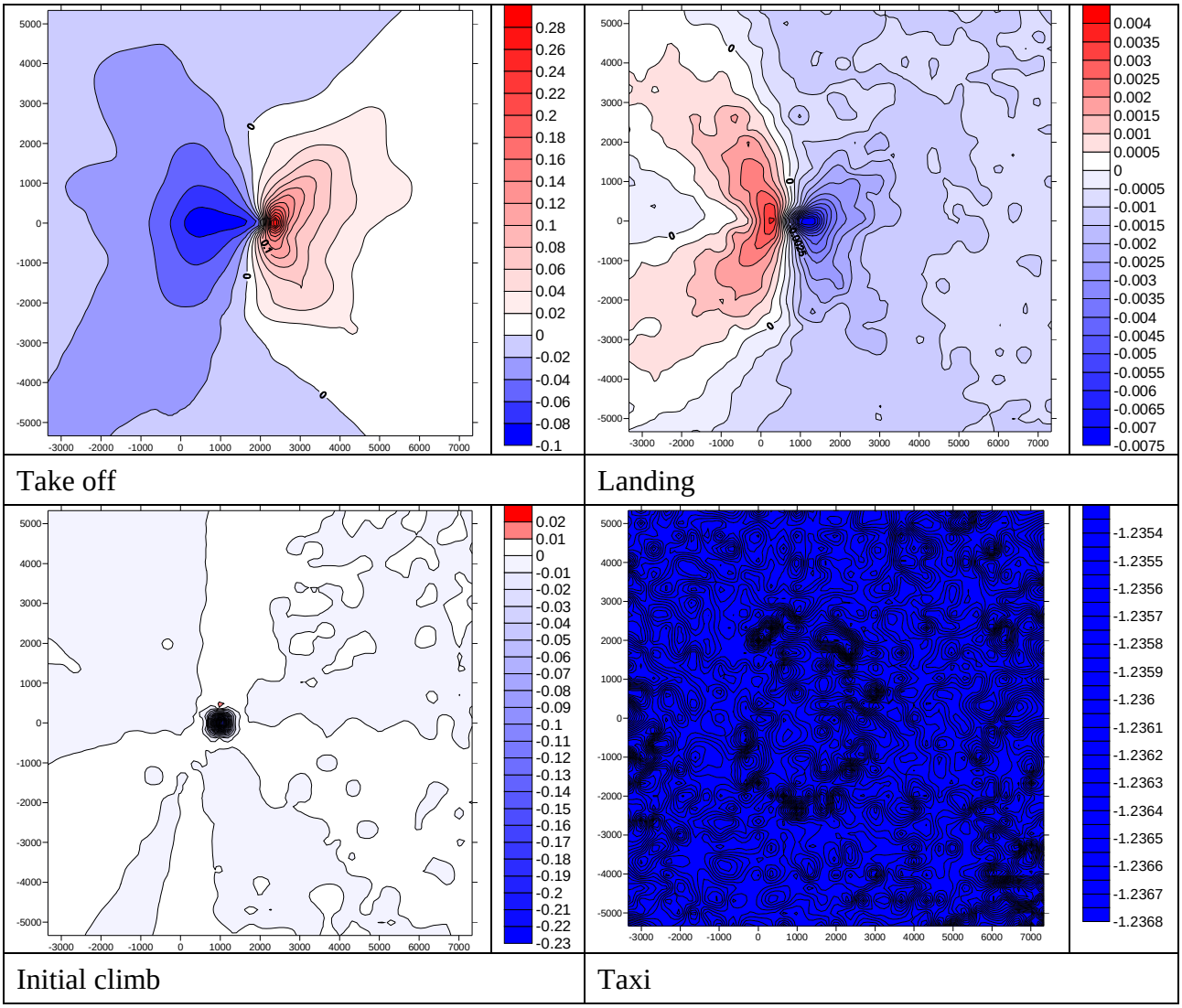

Figure 12.115: Percentage difference plots between N180sb and MCAT 14 lead aircraft, N180s

12.4.14 MCAT 15

N450sa, N450sb

N450sa

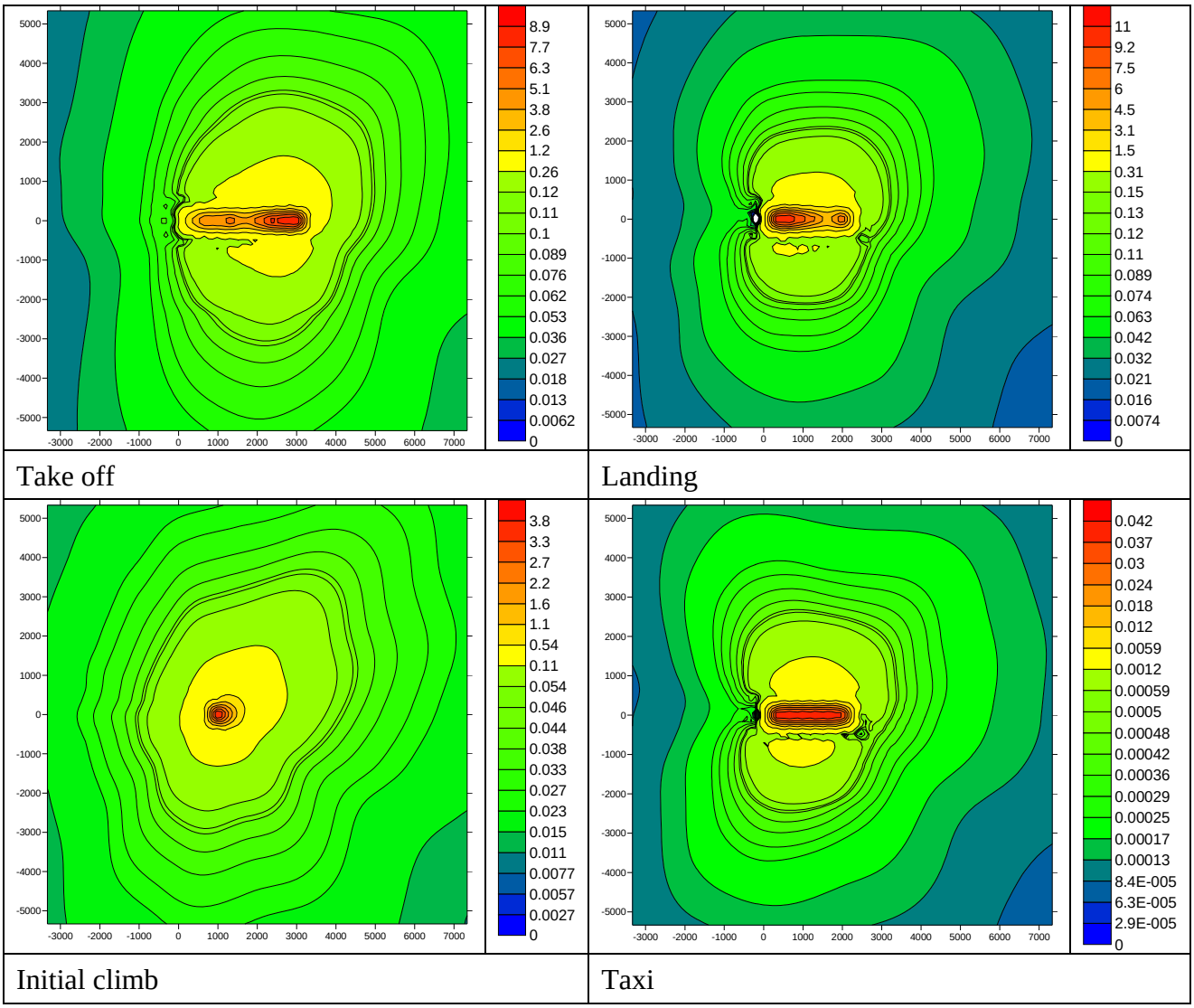

Figure 12.116: Normalised concentration plots for N450sa the lead aircraft for MCAT 15

N450sb

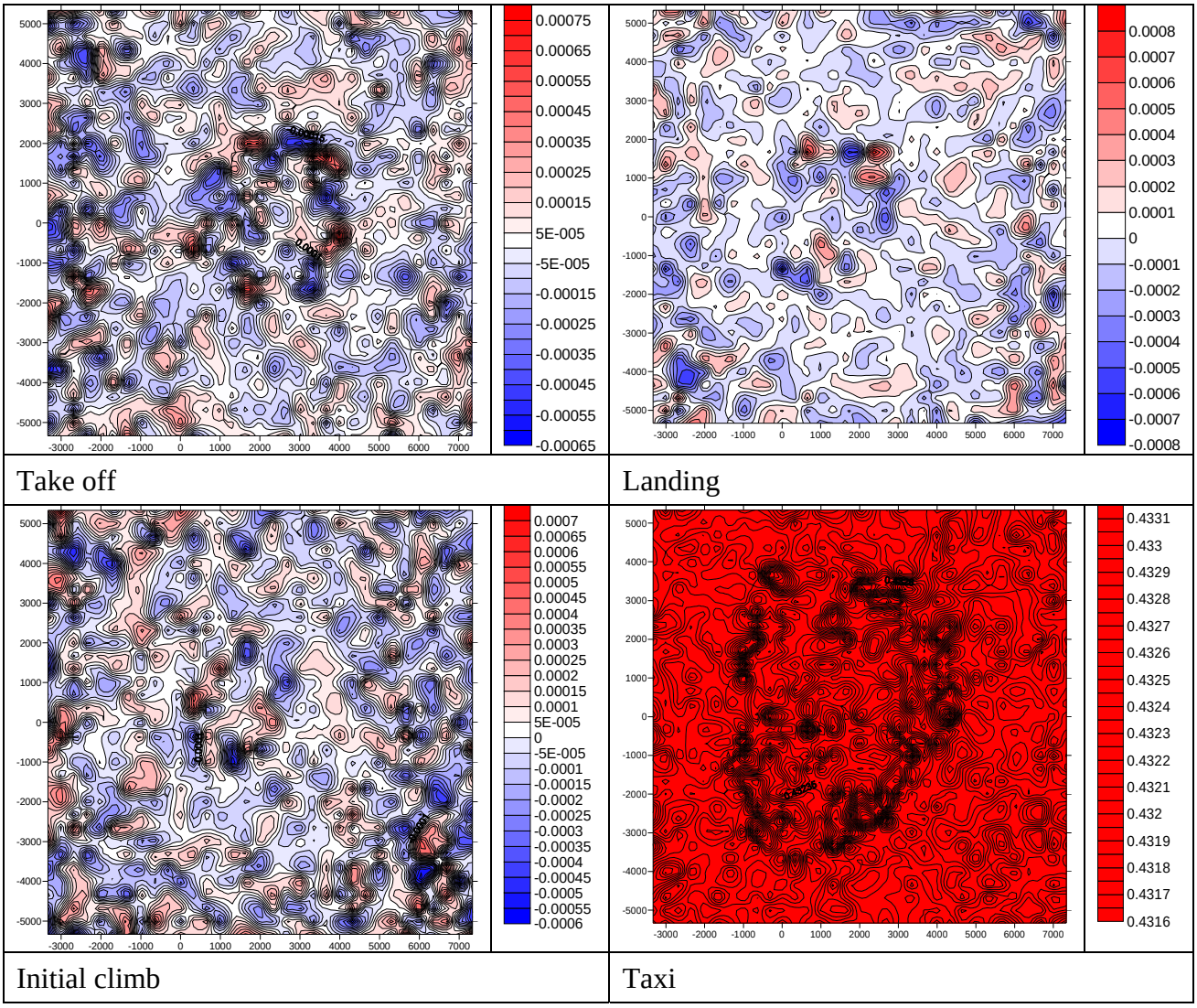

Figure 12.117: Percentage difference plots between N450sb and MCAT 15 lead aircraft, N450sa

12.5 Conclusions

12.5.1 Thrust

Modelling was carried out to determine the extent to which the thrust setting affects the annual average normalised concentrations for an aircraft. A take-off stage was modelled for a year of meteorological data with take-offs only occurring if the wind was from the west, the thrust settings used varied between 75% and 100%. Two different aircraft were considered, one with two engines and one with four engines. It was found that the normalised NOx concentration is quite insensitive to thrust for a given aircraft type in the range 75% to 100% thrust.

12.5.2 Modelling Categories - MCATs

Further modelling with ADMS-Airports was conducted to determine groupings of aircraft (MCATs) with similar normalised concentration signatures. This allowed the aircraft fleet to be modelled using the relatively small number of MCATs rather than all aircraft being modelled individually. Each aircraft was modelled for four different modes (take-off, initial climb, approach and taxiing) for a year of meteorological data. The annual average normalised concentrations produced by these modes were then compared between aircraft and similar aircraft grouped together in MCATs with a lead aircraft being assigned to each MCAT. The MCATs used in the modelling for 2002 are given in Table 12.2, for 2015 in Table 12.5, for 2020 in Table 12.8 and for 2030 in Table 12.11.

13 Appendix: Sensitivity comparisons of take-off effects by varying model parameters

13.1 Introduction

This section presents some calculations on the sensitivity of ADMS-Airport with respect to changing input parameters. These include changes to illustrate both the impact of possible adjustments to the model parameterisations and the effect of imprecision in the model input data. Concentrations of NO_x are calculated both as short term averages corresponding to a particular met condition and as long term averages. The study has arisen from discussions held by the modelling subgroup of PSDH on possible modifications to be made to ADMS-Airport in the light of the LIDAR (Light Detection and Ranging remote sensing technique) studies and other considerations regarding the effect of wake vortices and surface effects on jet plume dispersion. The scientific/technical actions were as follows:

1. Sensitivity tests of the relative effect of buoyancy prior to rotation - using the jet model, turn off buoyancy after the start of roll and rerun the model. Comparison of results to highlight effect on concentrations and the need or otherwise for further development work.

2. Sensitivity tests of take-off roll (TOR) effects by varying existing model parameters.

3. Produce a specification (if possible) for CFD testing using an existing CFD model to see what parameters most influence TOR effects - where to focus further efforts.

4. Clarify issues on the importance of effective diameter

5. Set out the approach to ground effect/wall jet.

6. Literature review of whether ground effects suppress plume rise.

7. Produce a specification for CFD testing of whether ground effects suppress plume rise. Output expected to be adjustments to lift-off parameters in ADMS-Airport.

8. Gather thoughts for possible substantive programme including measurements to nail down residual uncertainties.

9. Set out plan for conducting sensitivity analysis at receptor points once 2002/2015 inventories are available to guide subsequent work.

This section presents the results of the investigations into items 1 and 2.

The section is separated into three separate parts. The first part (Section 13.2) looks at the effect that the buoyancy of the release has on ground level concentrations for emissions during the take-off roll. This part has been conducted as it has been suggested that the effect of wake vortices produced in the later stages of take-off is to suppress the lift of the jet plume and that this may be parameterised by reducing the jet plume buoyancy.

The second part (Section 13.3) is an investigation into the impact of representing four-engined aircraft with a smaller number of representative sources, i.e. with two sources or one source. The need for this arises from the observation (e.g. LIDAR studies) that the jet exhausts may combine within a few wingspans of the aircraft, an effect most pronounced for jets from adjacent engines on one wing. Thus representing the sources with a reduced number of effective sources may

provide a more accurate representation of the effect of momentum and buoyancy on the jets as well as reducing model run time.

The third part (Sections 13.4-13.7) comprises of a series of sensitivity tests in which the exhaust temperature, engine velocity and engine diameter are varied by 50% to illustrate possible effects of uncertainty that may be present in the input parameters. The output concentrations are analysed to see how these uncertainties affect the concentration output plots.

Calculations on the effect on the sensitivity to thrust are not presented in this section. The reader is referred to Section 12 that describes the development of the MCATs (Aircraft Modelling Categories).

All the sections and tests use the same representative basic airport runway set-up. The runway is located at ground level (z=0) oriented (East-West). All the aircrafts take-off towards the west with 'wheels off' occurring at x=0. Because the different aircrafts have different take-off lengths the starting point varies for each plane.

Both short term single hour runs and long term annual average scenarios have been modelled. The long term scenarios use the 2002 Heathrow meteorological data. Since most take-offs occur into the wind only winds with a westerly component (wind direction from 180° to 360°) have been modelled. This corresponds to 59% of hours for the 2002 meteorological dataset.

13.2 Buoyancy effect

In this section the impact on pollutant concentrations of changes in jet plume buoyancy whilst maintaining constant momentum flux and thrust is modelled.

The momentum flux at the exhaust is given by

$$\dot{M}V = \frac{\pi d^2}{4} V^2 \rho$$

where $\dot{M}$ is the mass flow rate, d the effective diameter, V the jet velocity and ρ the exhaust density. It is assumed that $\rho \approx \frac{1}{T}$ where T is the exhaust temperature, then the original momentum flux equation becomes

$$\dot{M}V = \frac{\pi d^2}{4} V^2 \frac{1}{T}$$

Thus to keep the momentum flux constant and to reduce the buoyancy both the temperature and jet velocity must be reduced.

Short term and long term scenarios have been modelled to assess the impact that the reduction in buoyancy causes.

In the representation of the take-off roll in ADMS-Airport used to establish the MCATs the emissions of an aircraft along the runway are divided into seven sections, the first two representing the stationary phase when the thrust is initially 7% then increased to 19% thrust, the next stage is the start of the roll at 30% thrust, in the following three stages the maximum thrust is achieved and in the last stage wheels off occurs. The details of the seven stages for the A320 are shown in Table 13.1 and for the B747 in Table 13.2.

The following tests have been performed;

(a) All the engine exhausts at all stages of take-off are fully buoyant (the current model set-up)
(b) The engine exhausts are buoyant for the first five stages of the take-off roll only, for the other stages the temperature is ambient. This is to represent the possible impact of wake vortices in the later stages of the role.
(c) The engine exhausts are released at ambient temperature for all the stages of the take-off roll. This is for comparison purposes to show the impact of buoyancy in early stages of the take-off roll.

The ambient temperature is assumed to be 32°C for all the long term cases. This is because ADMS-Airport does not allow aircraft releases to be modelled at less than ambient temperature and so ambient has been set to the maximum temperature in the annual meteorological data file.

For the short term cases the temperature for an ambient release has been set to 15°C, the specified ambient temperature for that particular hour of data.

The results of the model calculations are shown in Figures 13.1-13.11. Note that in these calculations for convenience the concentrations do not take account of the frequency of flights and are not 'true' concentrations, however for comparative purposes they have been normalised by the concentration at the exit of one of the engines. Of relevance and interest is the spatial pattern of concentration and the difference in concentration between the cases not absolute value of concentration in any particular model run. For an A320 Figures 13.1-13.3 show for neutral conditions for three different wind flow directions short term ground level concentrations of air pollution, differences between concentration for the different cases and percentage differences in concentration between the different cases. Similar plots are presented for convective conditions (Figures 13.4-13.6) and stable conditions (Figures 13.7-13.9).

Long term average plots of concentration, absolute differences and percentage differences for the A320 are shown in Figure 13.10. As would be expected decreasing the buoyancy of the releases generally increases concentrations both for short term and for long term runs however the difference between case (b) (five stages buoyant) and case (a) all stages buoyant is small except close to the runway. 'Turning off' buoyancy for all stages causes significant impacts over a wider area. Long term average plots for the B747 are shown in Figure 13.11. The B747 shows the same trend as the A320 of having the largest changes in concentration closest to the runway for the first five stages buoyant case, although these changes are larger for the B747 than for the A320.

Take-off stage	A320			
	Speed (m/s)	Speed (m/s)		Emission (g)
	At beginning of stage	At end of stage	Length of stage (m)	NO_x
1	0	0	0	3.35
2	0	10	0	5.52
3	10	42.87	40	11.68
4	42.87	59.8	713	422.78
5	59.8	72.89	713	227.82
6	72.89	73.56	713	178.99
7	73.56	83.56	60	13.67
			Total emission	863.81

Table 13.1 *Stage data for the A320*

Take-off stage	B747			
	Speed (m/s)	Speed (m/s)		Emission (g)
	At beginning of stage	At end of stage	Length of stage (m)	NO_x
1	0	0	0	6.01
2	0	10	0	13.08
3	10	54.89	80	62.87
4	54.89	76.98	1076.67	1424.45
5	76.98	94.02	1076.66	734.94
6	94.02	95.16	1076.67	584.55
7	95.16	105.16	60.46	29.56
			Total emission	2855.44

Table 13.2 *Stage data for the B747*

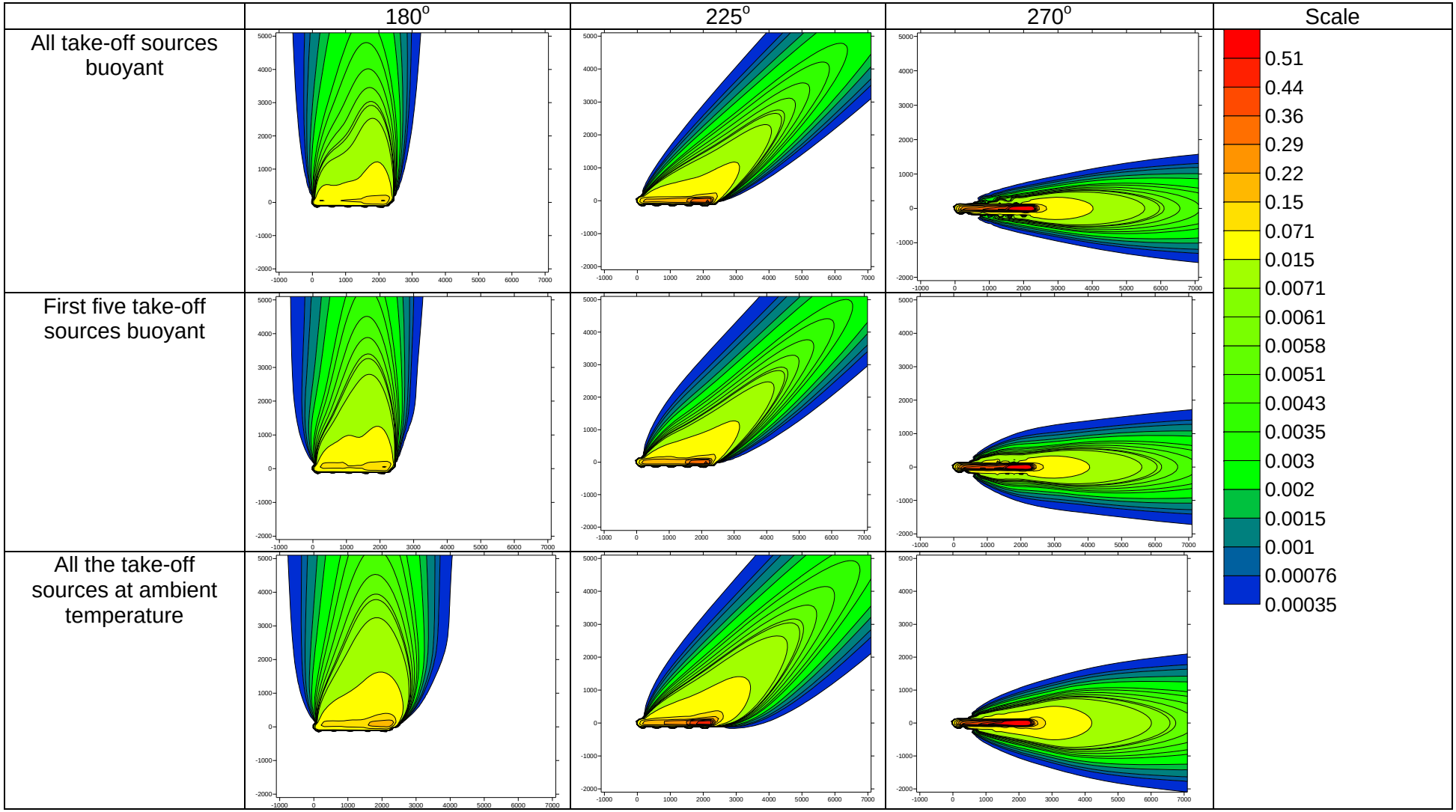

Figure 13.1 – A320 short term take off concentration plots for three different wind angles and buoyancy profiles. (Neutral meteorological condition)

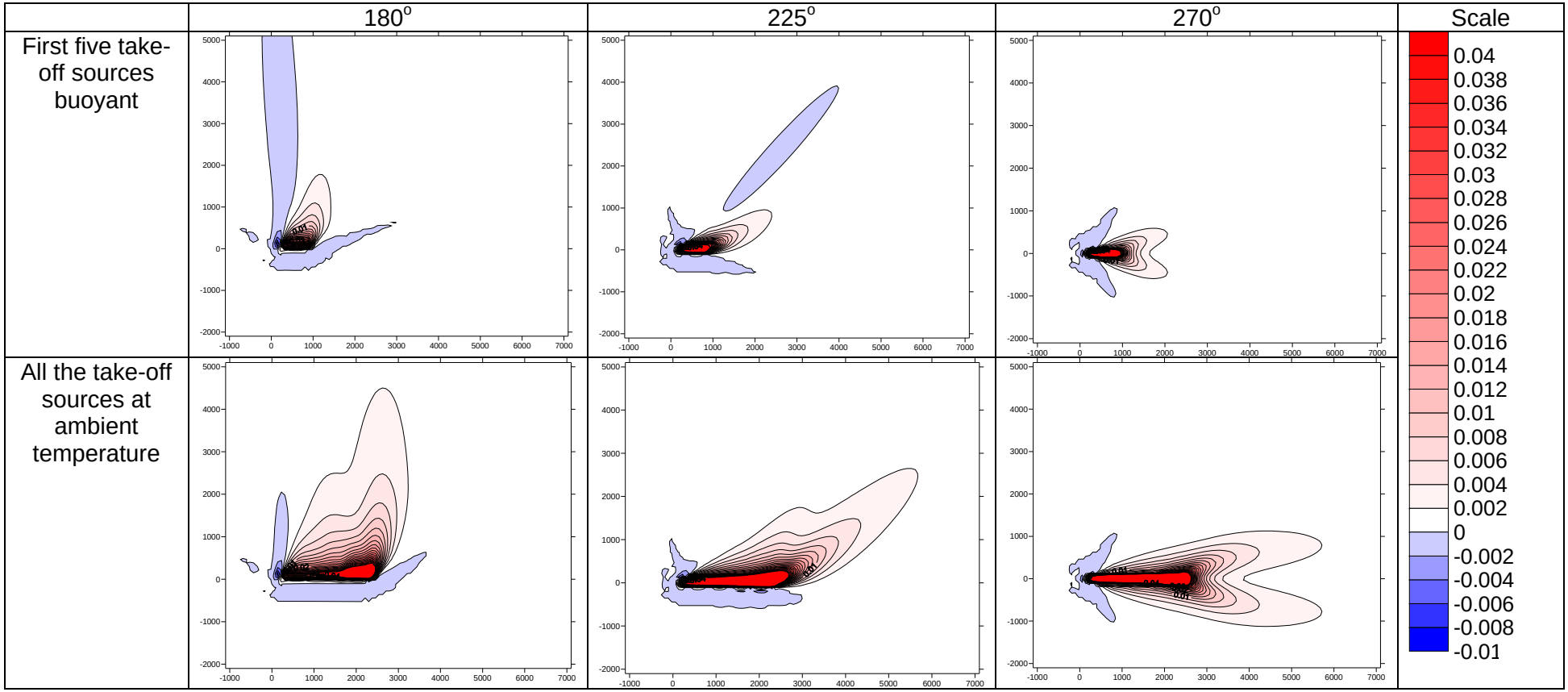

Figure 13.2 – A320 short term absolute difference plots. The 'All take-off sources buoyant' scenario in Figure 13. is taken as the base case. (Neutral meteorological condition)

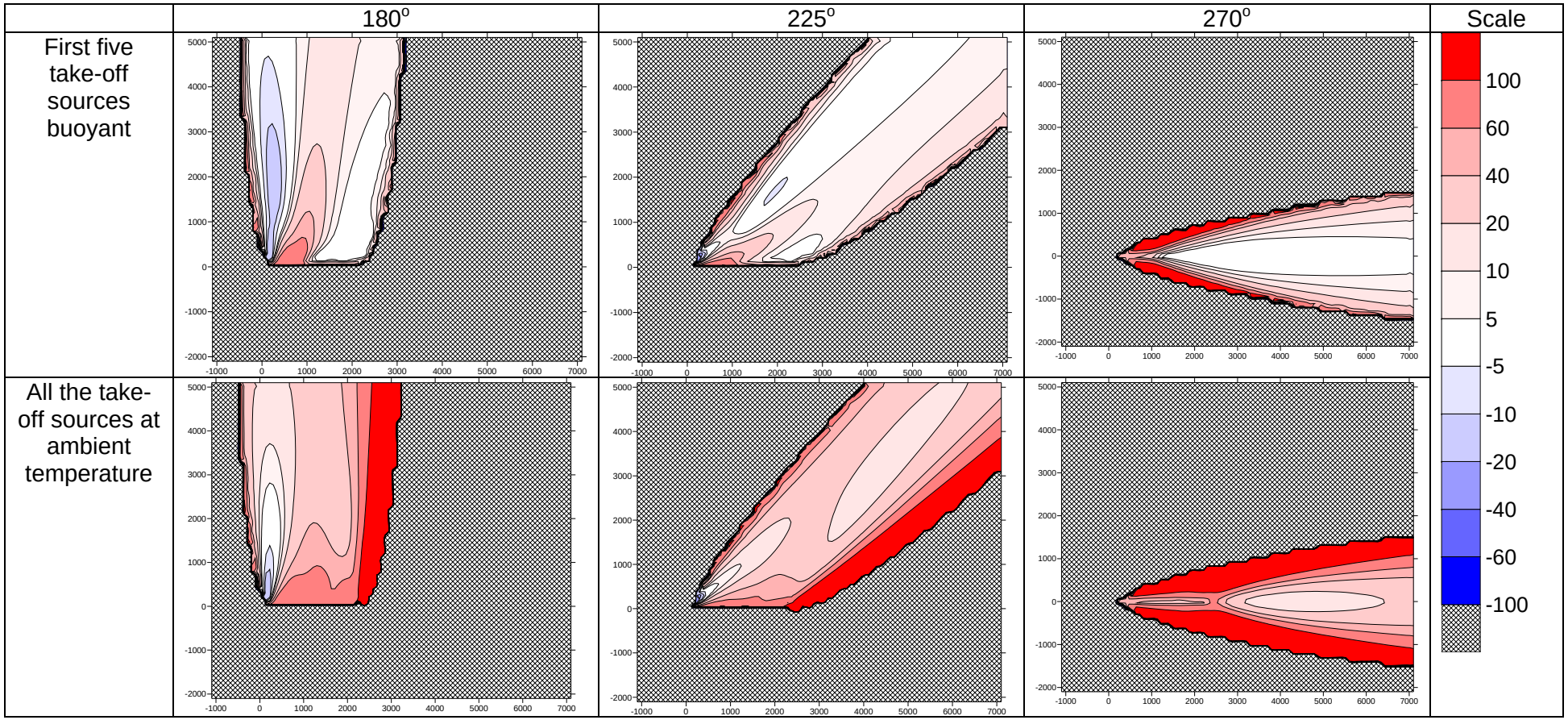

Figure 13.3 – A320 short term percentage difference plots. The 'All take-off sources buoyant' scenario in Figure 13. is taken as the base case. (Neutral meteorological condition)

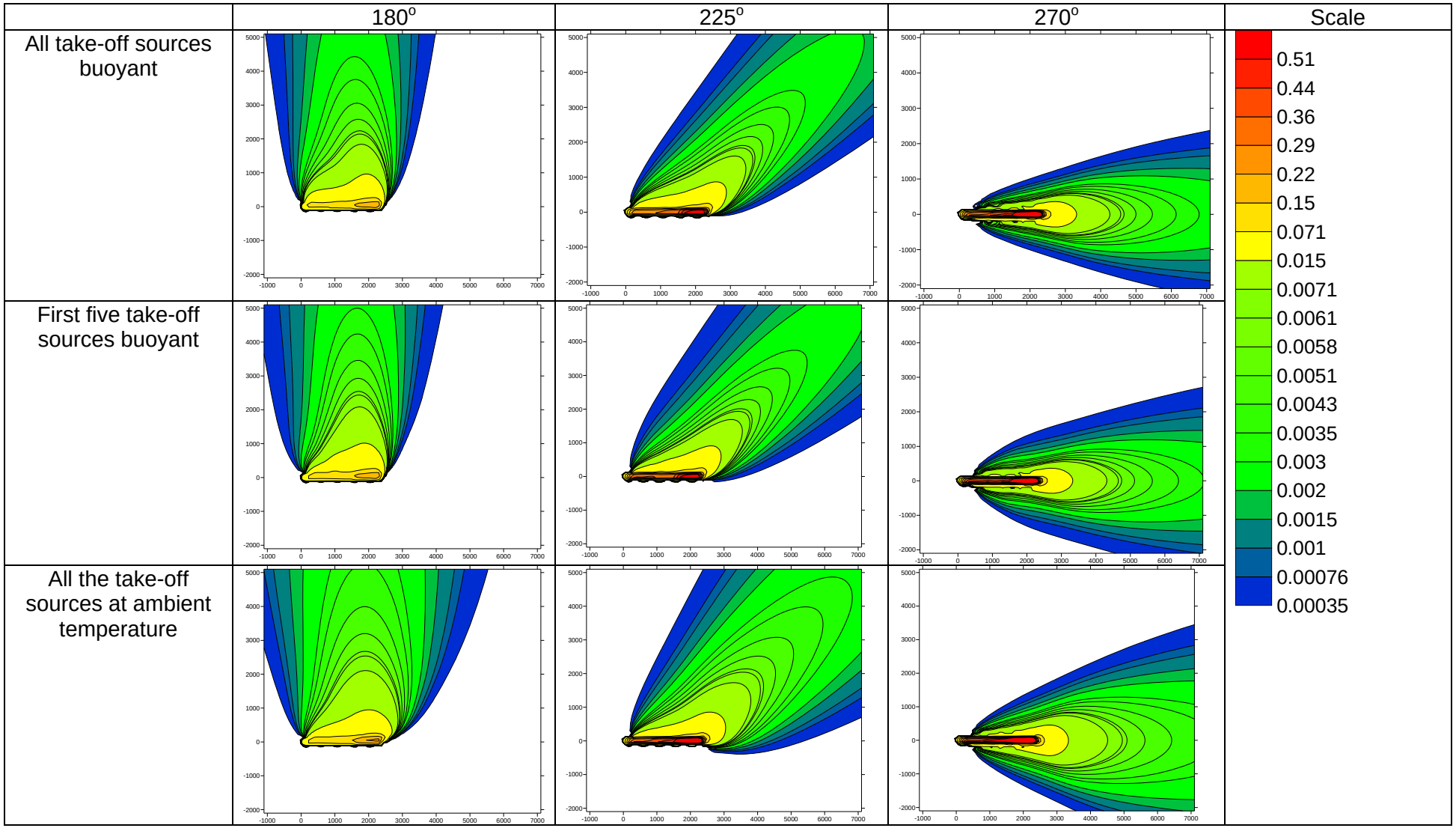

Figure 13.4 – A320 short term take off concentration plots for three different wind angles and buoyancy profiles. (Convective meteorological condition)

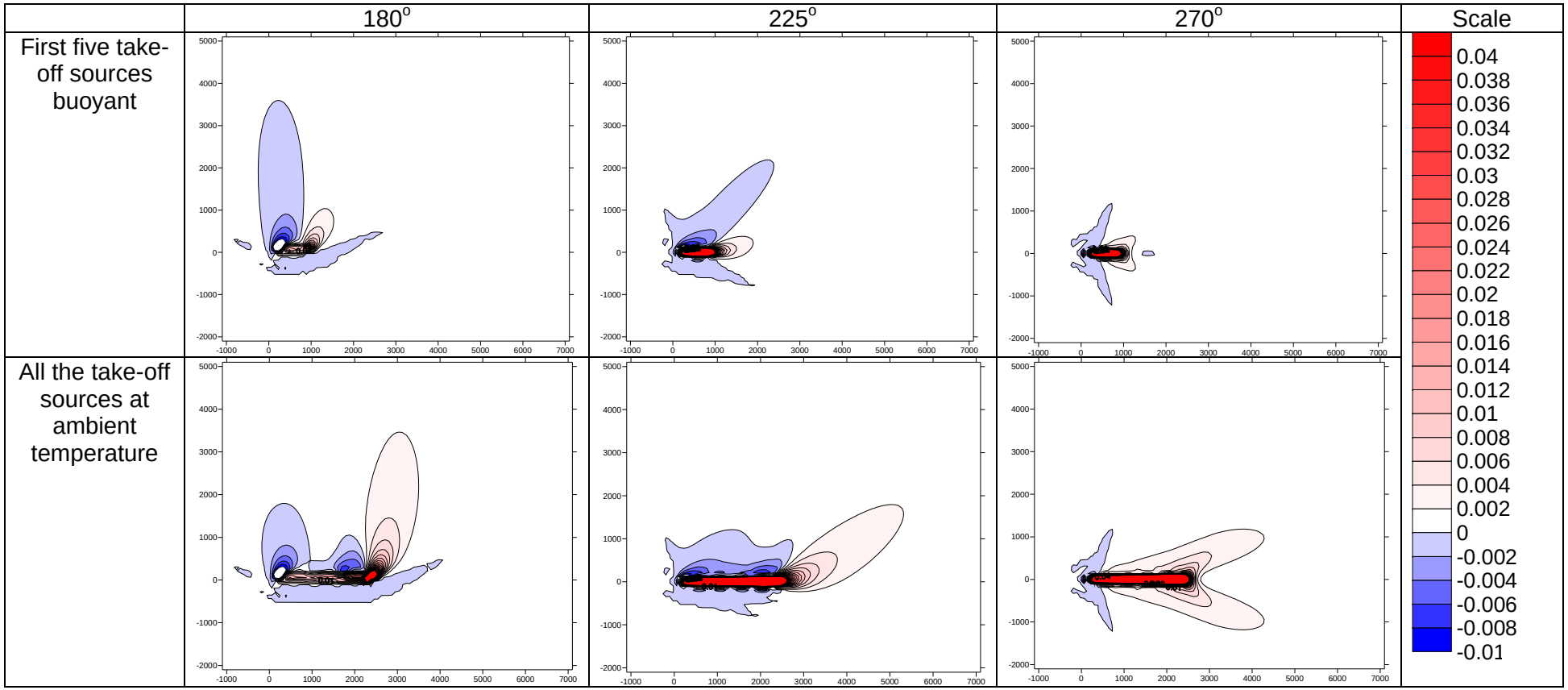

Figure 13.5 – A320 short term absolute difference plots. The 'All take-off sources buoyant' scenario in Figure 13. is taken as the base case. (Convective meteorological condition)

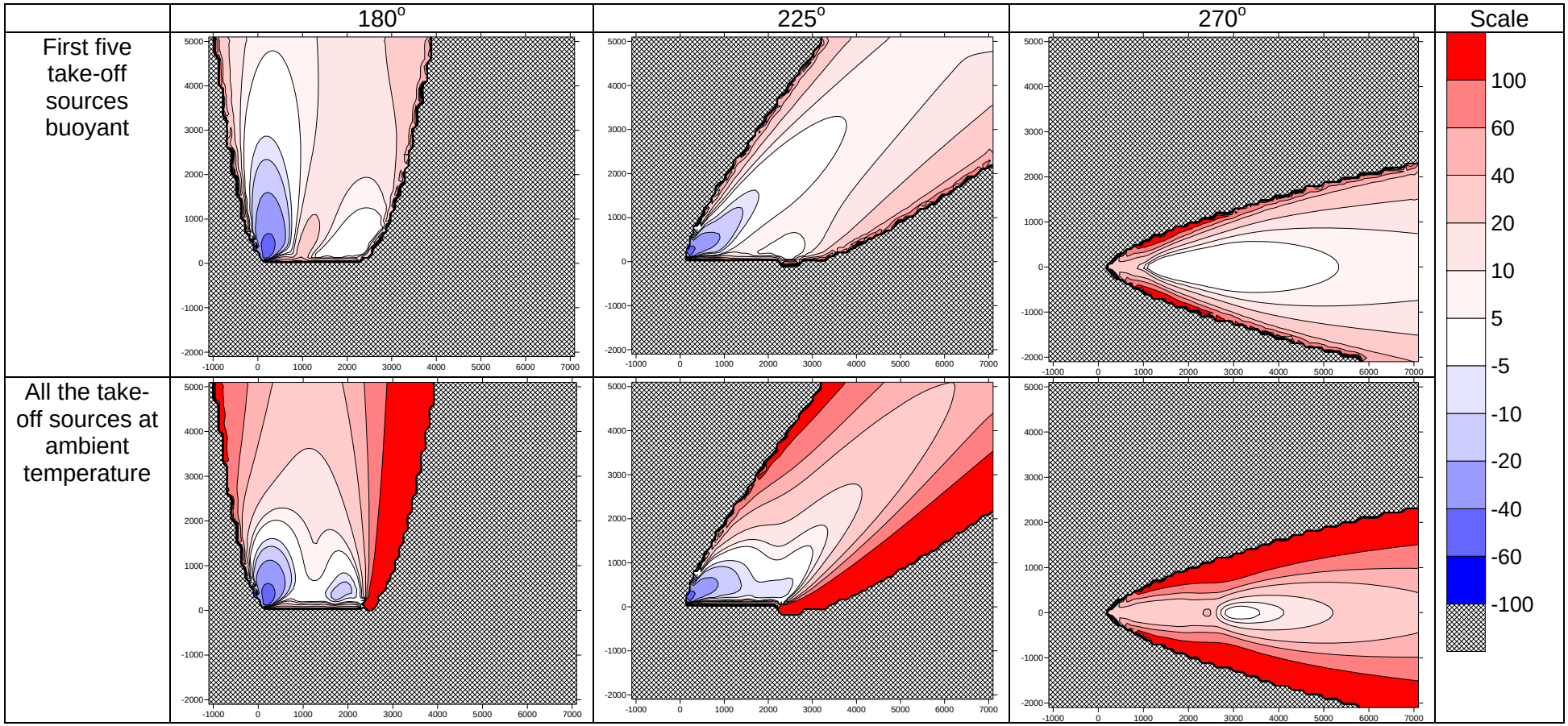

Figure 13.6 – A320 short term percentage difference plots. The 'All take-off sources buoyant' scenario in Figure 13. is taken as the base case. (Convective meteorological condition)

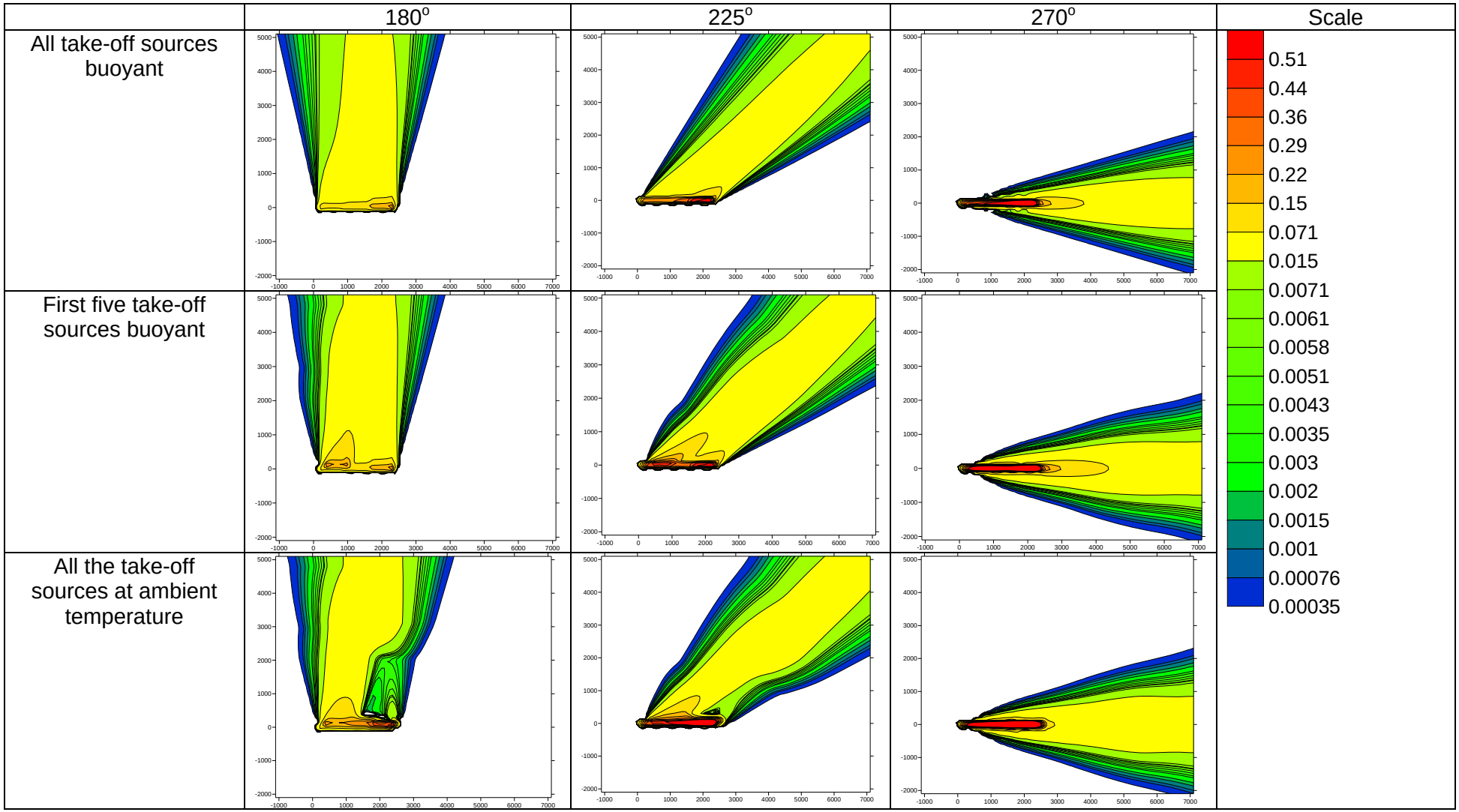

Figure 13.7 – A320 short term take off concentration plots for three different wind angles and buoyancy profiles. (Stable meteorological condition)

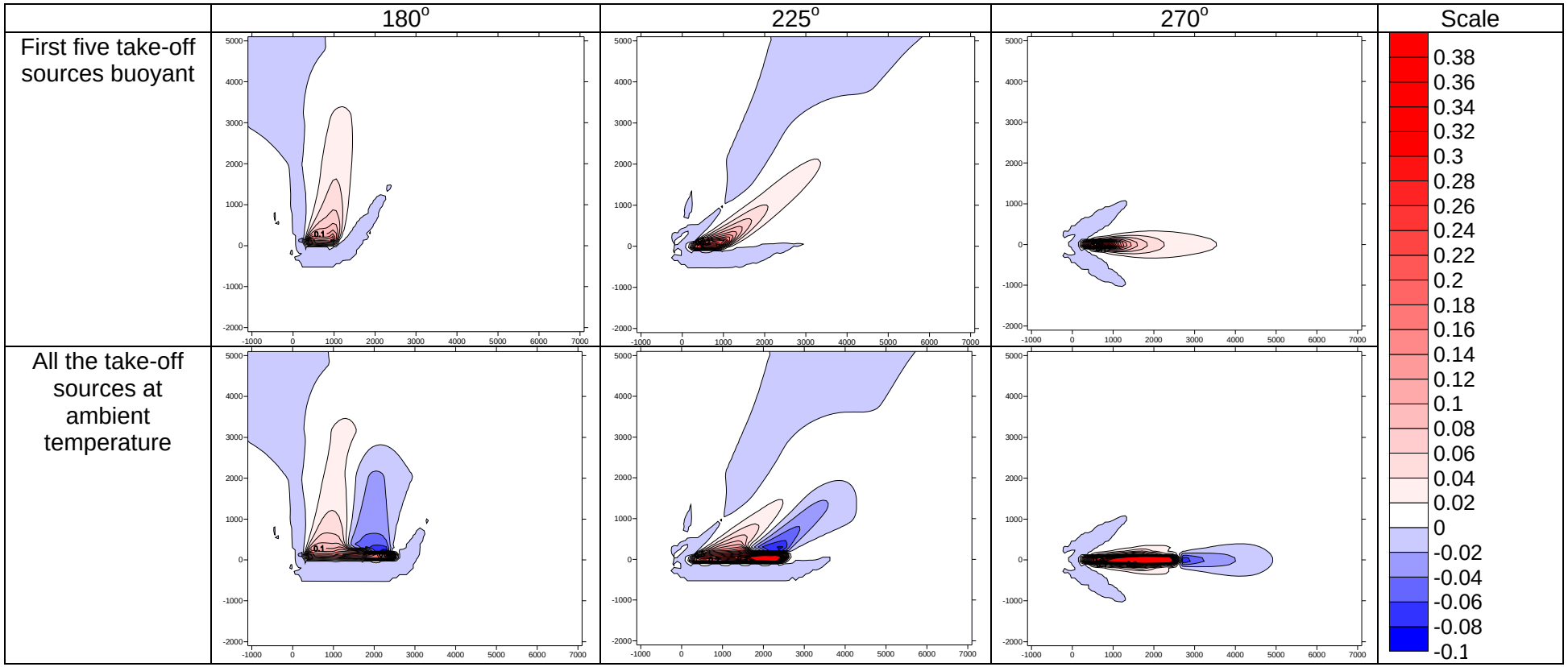

Figure 13.8 – A320 short term absolute difference plots. The 'All take-off sources buoyant' scenario in Figure 13. is taken as the base case. (Stable meteorological condition)

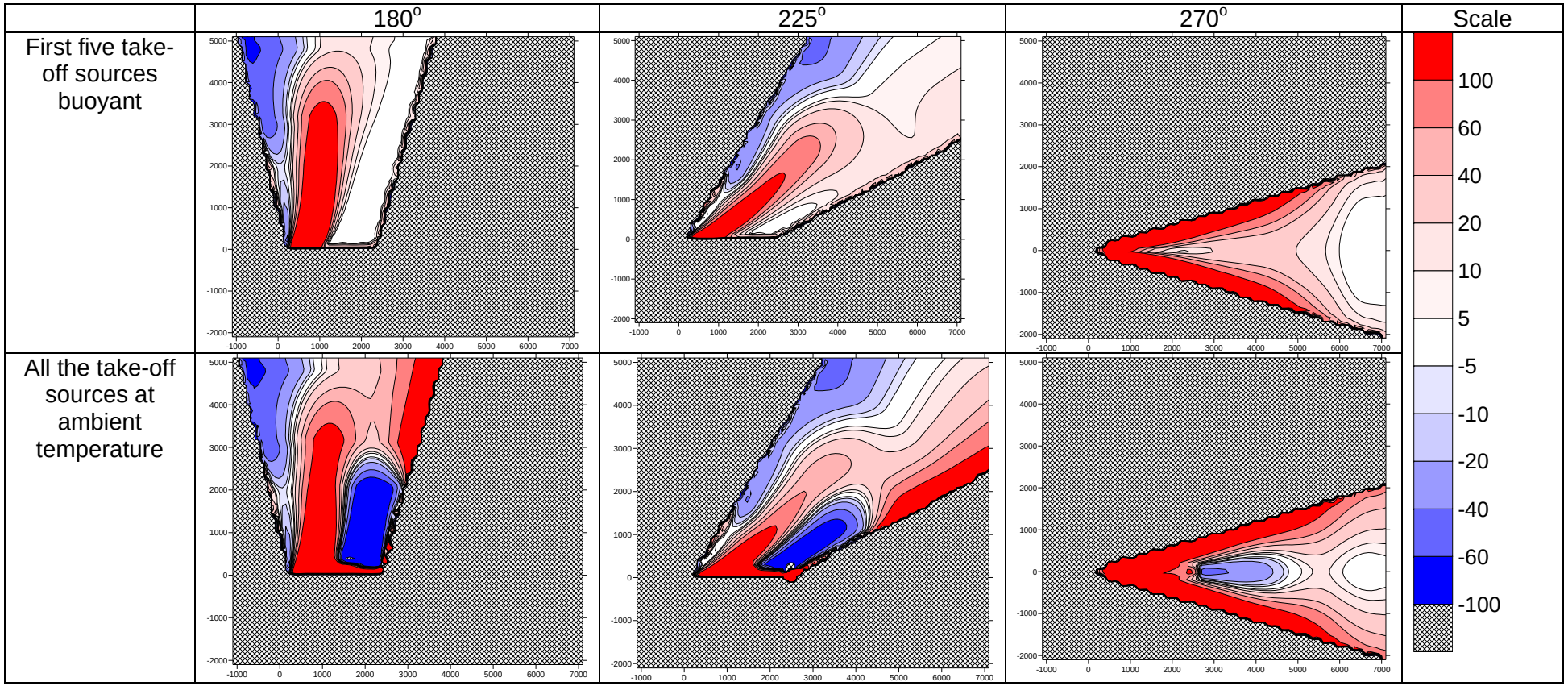

Figure 13.9 – A320 short term percentage difference plots. The 'All take-off sources buoyant' scenario in Figure 13. is taken as the base case. (Stable meteorological conditions)

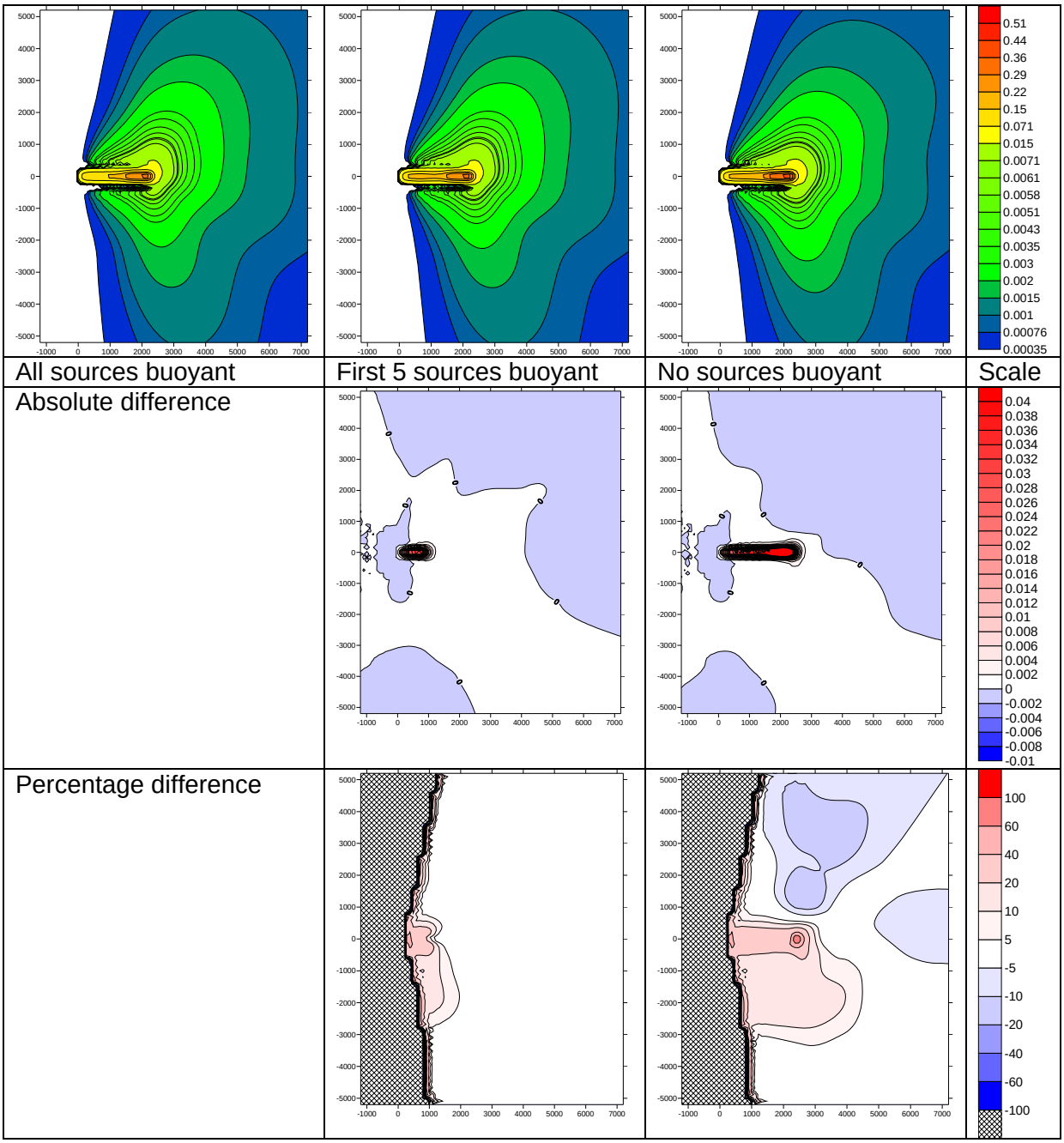

Figure 13.10 – A320 long term contour concentration and difference plots (middle row: absolute difference; bottom row: percentage difference). The difference plots use the 'All source buoyant' case as the base scenario.

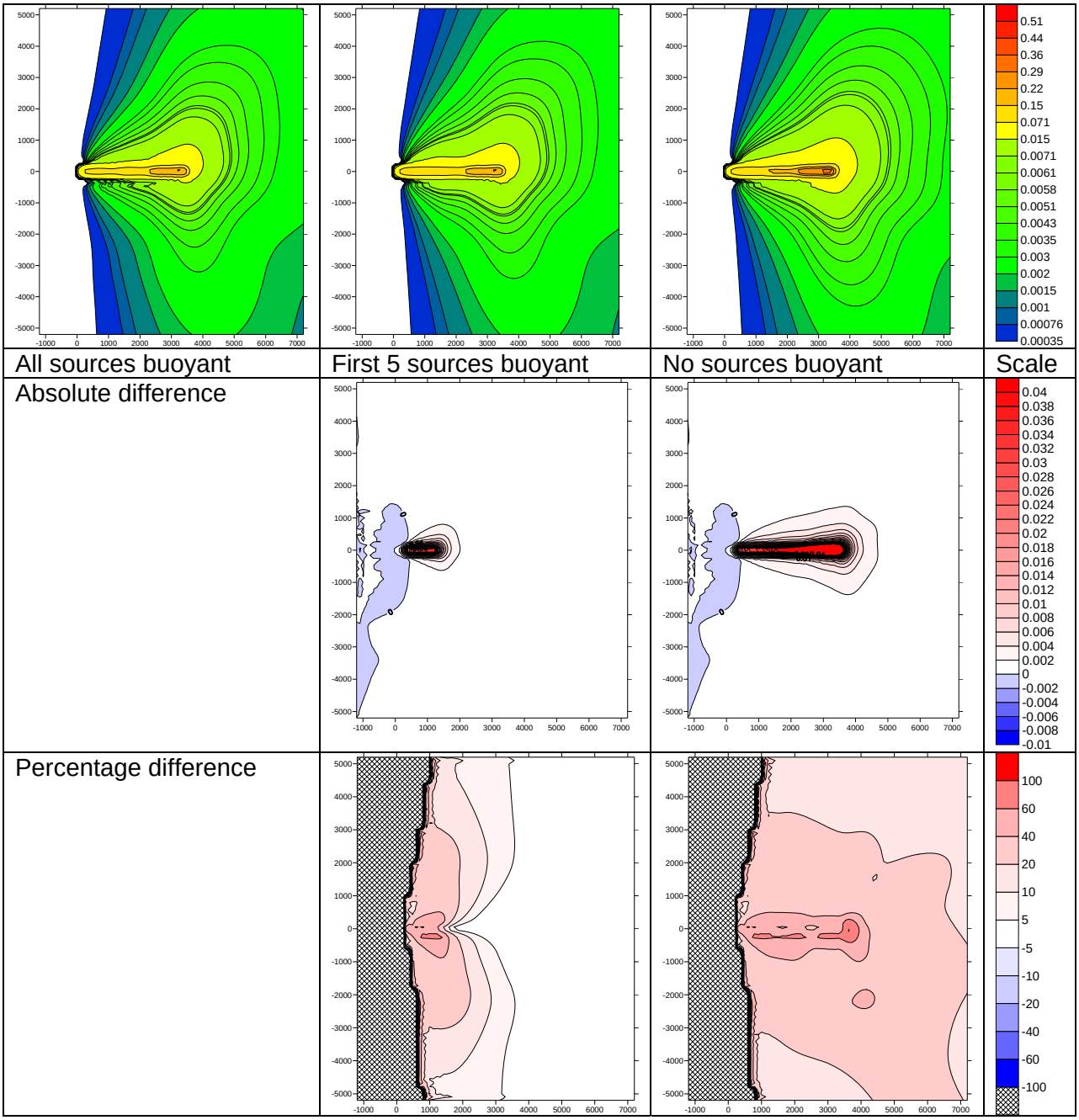

Figure 13.11 – B747 long term contour concentration and difference plots (middle row: absolute difference; bottom row: percentage difference). The difference plots use the 'All source buoyant' case as the base scenario.

13.3 Number of engines

Most of the aircraft studied have two engines, one on either wing. The A340 and B747 are the only exceptions within the 2002 Heathrow database with four engines, two engines on either wing.

The evidence of the LIDAR studies is that within a few wingspans the jet plumes from the different aircraft engines may combine, an effect most pronounced for adjacent engines on each wing of four engined aircraft. Thus the impact of the total buoyancy and momentum on four engined aircraft may best be represented in the model by combining the sources on each wing. In addition each engine increases the time taken to model a specific scenario.

For this study the A340 has been modelled, details of the stages for the A340 are shown in Table 13.3.

When combing engines both the position and diameter of the new engine need to be redefined. The position is taken as the average of the original two engines and the engine diameter is set to be equal to the sum of the two original engines, so the exhaust velocity is unchanged.

The A340 is firstly modelled using 2 engines, whereby the two engines on a wing have been combined to form a single engine, and is then simplified again to a single engine.

Figure 13.12 shows the long term average concentrations, absolute differences and percentage differences. Reducing the number of sources reduces concentrations significantly due to the increase in jet plume elevation.

Take-off stage	A340			
	Speed (m/s)	Speed (m/s)		Emission (g)
	At beginning of stage	At end of stage	Length of stage (m)	NO_x
1	0	0	0	2.95
2	0	10	0	6.85
3	10	47.02	80	33.94
4	47.02	65.74	973.33	944.76
5	65.74	80.2	973.33	496.02
6	80.2	81.28	973.33	390.98
7	81.28	91.28	60.46	21.84
			Total emission	1897.33

Table 13.3. *Stage data for the A340*

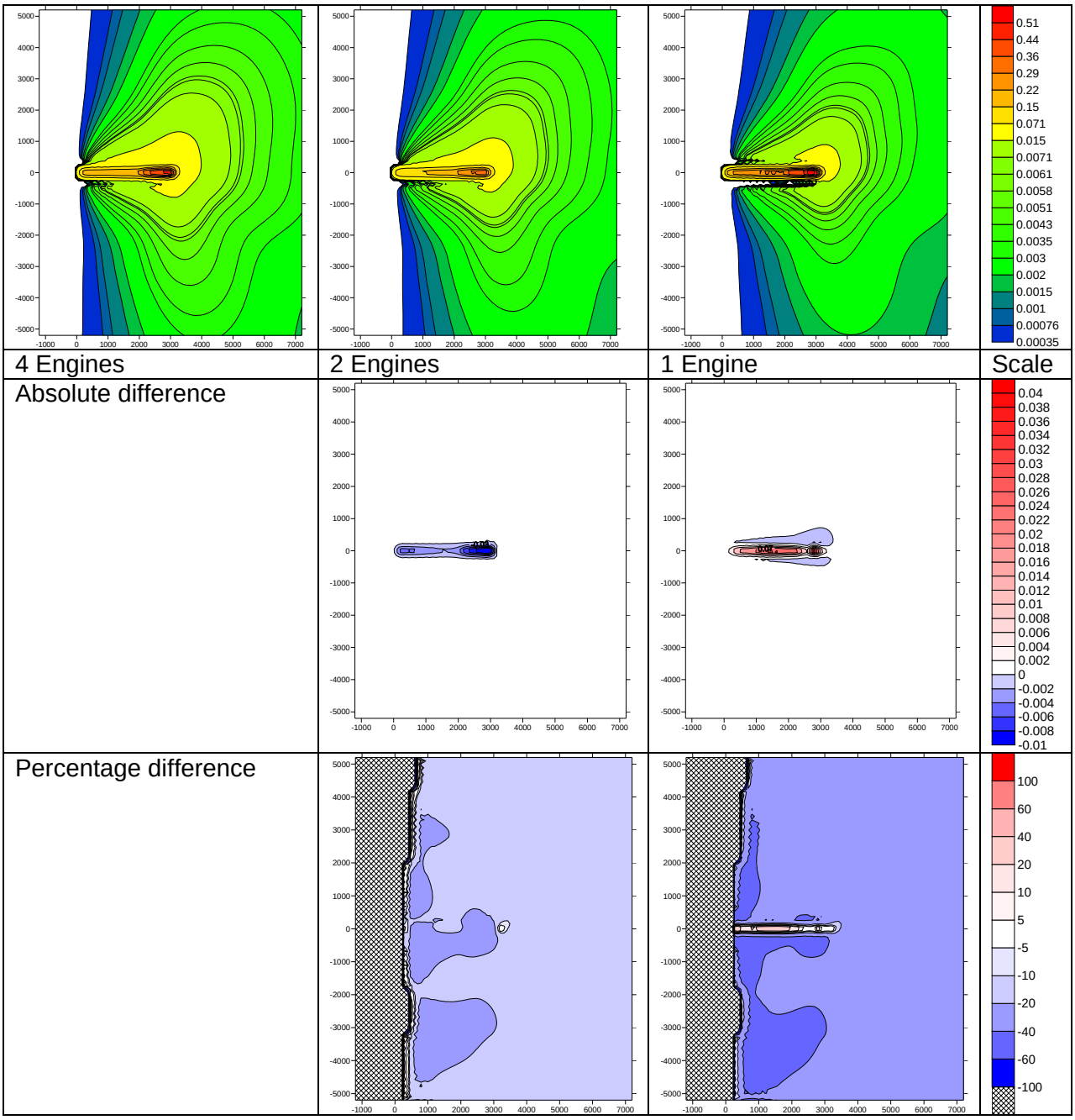

Figure 13.12 – A340 long term ground level concentration and difference plots (middle row: absolute difference; bottom row: percentage difference). Only wind directions from 180° to 360° have been modelled.

13.4 Parameter sensitivity

A number of sensitivity tests were performed to show how sensitive the model is to specification of the source input parameters. The scenarios modelled are physically unrealistic but show how a large error in the original input data will propagate into the output concentrations.

The input parameter files have been created by either increasing or decreasing the desired variable by 50%. Whereas in the buoyancy effect tests, two parameters (temperature and jet velocity) were changed to keep the mass flux constant, here we are assuming the input values have been incorrectly measured and therefore the other parameters have not been changed to compensate for the imagined 'error'.

The A320 has been modelled. Note that when increasing or decreasing the temperature it is the value in degrees Celsius that has been increased or decreased by 50% and not the value in Kelvin.

Impacts are presented for temperature (Figure 13.13), jet velocity (Figure 13.14), and effective diameter of engine exhaust (Figure 13.15).

13.5 Exhaust temperature

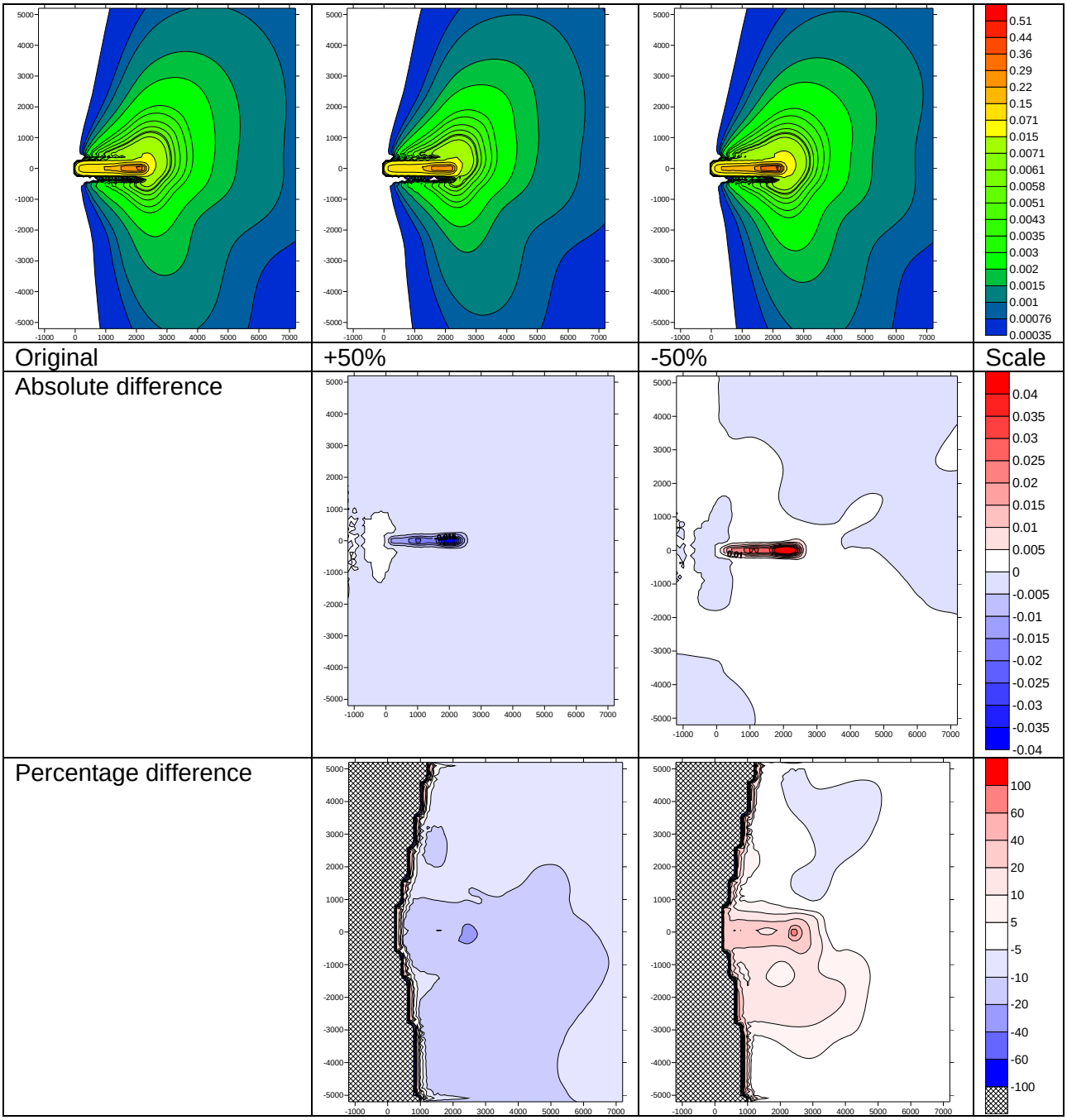

Figure 13.13 – A320 long term ground level concentration and difference plots for varying exhaust temperature. (Middle row: absolute difference; bottom row: percentage difference)

13.6 Jet velocity

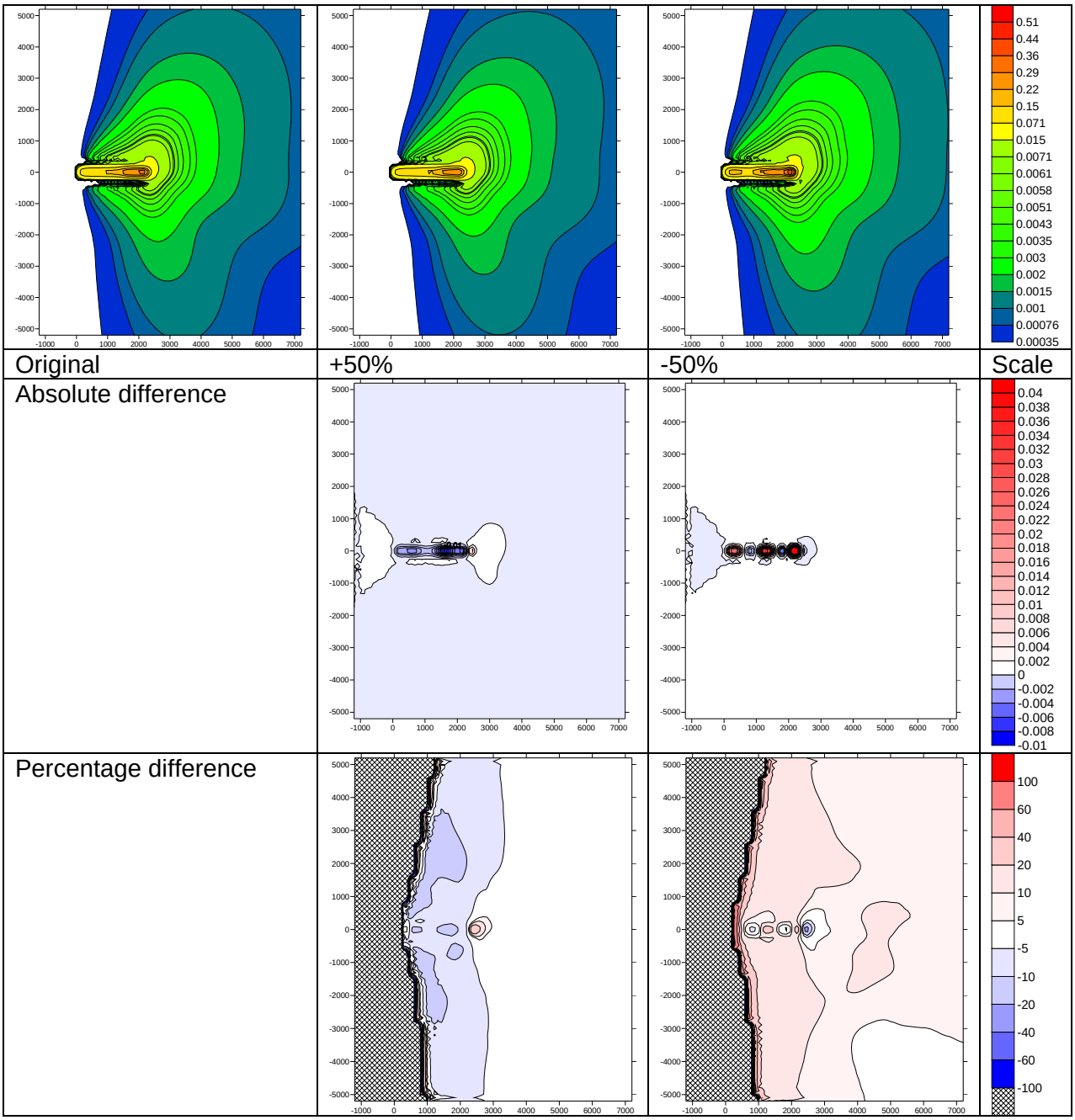

Figure 13.14 – A320 long term ground level concentration and difference plots for varying jet velocity. (Middle row: absolute difference; bottom row: percentage difference)

13.7 Engine diameter

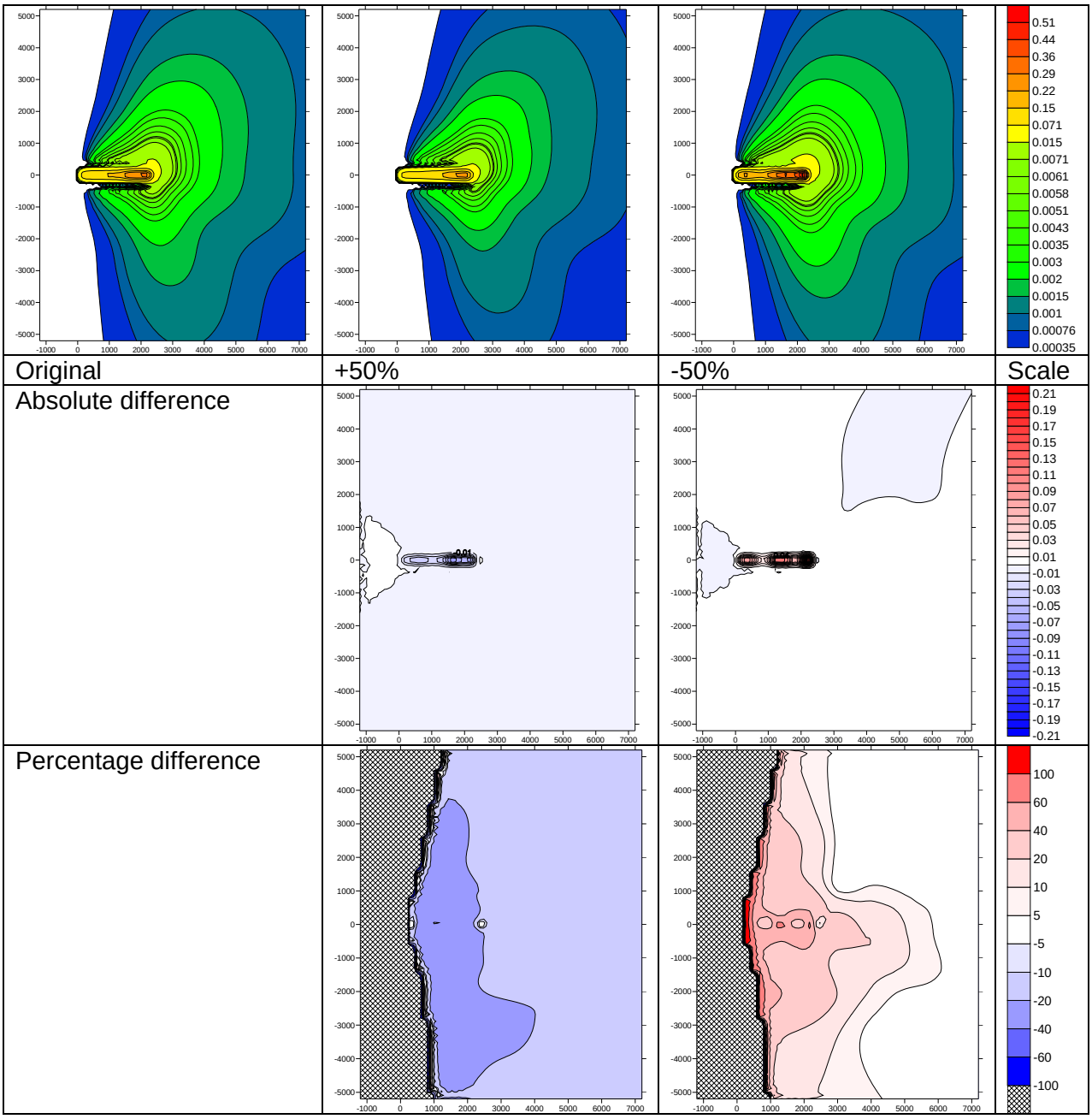

Figure 13.15 – A320 long term ground level concentration and difference plots for varying engine diameter. (Middle row: absolute difference; bottom row: percentage difference)

13.8 Conclusions and Recommendations

13.8.1 Suppression of jet plume rise by wake vortices

At the beginning of the take-off roll wake vortices are weak and have little if any impact on the engine exhaust jets whereas wake vortices are strong after rotation and can deflect the jets downwards or suppress their rise. There remains uncertainty as to whether the wake vortices significantly affect the jet plume rise in the latter stages of the take-off roll before rotation. However, modelling of the possible effect of suppression of jet plume rise by 'turning off' the buoyancy at different stages of the take-off roll has shown that effects are relatively small. A possible model modification is to suppress the buoyancy for the last two stages in the model representing the last one third of the take-off roll. By this relatively straightforward method the model would take account of wake vortex impacts in that part of the take-off roll where their effect may be relevant however the impact of this would be relatively small and has not been implemented in ADMS-Airport.

13.8.2 Number of jet sources

Representing four engine jets with two sources reduces surface concentrations as jet plume rise is increased. There is evidence (e.g. LIDAR study) that the jet plumes combine within a few wingspans of the aircraft. This change has been implemented in ADMS-Airport.

13.8.3 Thrust

Section 12, which describes the development of the MCATs (Aircraft Modelling Categories), discusses the effect of thrust. The normalised NO_x concentration is quite insensitive to thrust for a given aircraft type in the range 75% - 100% thrust.

13.8.4 Parameter Sensitivity

Section 13.5 shows the effect of varying exhaust temperature, jet velocity and engine diameter by +/- 50% to assess the impact of uncertainty in input data. The concentrations were least sensitive to the jet velocity.

13.9 Appendix A

The tables below show the factors used for the 'Buoyancy effects' section of the document.

Take-off stage	Jet velocity (m/s)	Exhaust temperature (°C)
1	66.10	57.46
2	114.26	66.46
3	148.07	69.41
4	239.16	76.26
5	242.68	76.10
6	245.44	75.80
7	245.63	75.84

Table 13.4 – Standard A320 take-off jet velocity and temperature values

Take-off stage	Jet velocity (m/s)	Exhaust temperature (°C)
1	66.10	57.46
2	114.26	66.46
3	148.07	69.41
4	239.16	76.26
5	242.68	76.10
6	223.04	15
7	223.20	15

Table 13.5 – Short term A320 take-off jet velocity and temperature values with the first five stages still buoyant

Take-off stage	Jet velocity (m/s)	Exhaust temperature (°C)
1	61.71	15
2	105.25	15
3	135.80	15
4	217.19	15
5	220.43	15
6	223.04	15
7	223.20	15

Table 13.6 – Short term A320 take-off jet velocity and temperature values with all the stages non-buoyant

Take-off stage	Jet velocity (m/s)	Exhaust temperature (°C)
1	66.10	57.46
2	114.26	66.46
3	148.07	69.41
4	239.16	76.26
5	242.68	76.10
6	229.52	32
7	229.68	32

Table 13.7 – Long term A320 take-off jet velocity and temperature values with the first five stages still buoyant

Take-off stage	Jet velocity (m/s)	Exhaust temperature (°C)
1	63.50	32
2	108.31	32
3	139.75	32
4	223.50	32
5	226.84	32
6	229.52	32
7	229.68	32

Table 13.8 – Long term A320 take-off jet velocity and temperature values with all the stages non-buoyant

Take-off stage	Jet velocity (m/s)	Exhaust temperature (°C)
1	91.16	54.11
2	152.21	63.11
3	197.97	70.07
4	323.58	89.50
5	327.48	89.52
6	330.95	89.38
7	331.45	89.54

Table 13.9 – Standard B747 take-off jet velocity and temperature values

Take-off stage	Jet velocity (m/s)	Exhaust temperature (°C)
1	91.16	54.11
2	152.21	63.11
3	197.97	70.07
4	323.58	89.50
5	327.48	89.52
6	303.63	32
7	304.02	32

Table 13.10 – Long term B747 take-off jet velocity and temperature values with the first five stages still buoyant

Take-off stage	Jet velocity (m/s)	Exhaust temperature (°C)
1	88.03	32
2	145.00	32
3	186.67	32
4	296.82	32
5	300.39	32
6	303.63	32
7	304.02	32

Table 13.11 – Long term B747 take-off jet velocity and temperature values with all the stages non-buoyant

Take-off stage	Jet velocity (m/s)	Exhaust temperature (°C)
1	80.40	53.96
2	134.62	61.57
3	174.78	66.25
4	284.75	79.42
5	288.58	79.32
6	292.39	79.20
7	292.48	79.23

Table 13.12 – Standard A340 take-off jet velocity and temperature values

Number of engines location and diameter

	Engine 1			Engine 2			Engine 3			Engine 4			Diameter (m)
	X(m)	Y(m)	Z(m)	X(m)	Y(m)	Z(m)	X(m)	Y(m)	Z(m)	X(m)	Y(m)	Z(m)	
4 engines	-21.4	9.1	2.5	-21.4	-9.1	2.5	-27.5	19.6	2.9	-27.5	-19.6	2.9	1.393
2 engines	-24. 5	14.4	2.7	-24.5	-14.4	2.7							1.971
1 engine	-24. 5	0.0	2.7										2.787

Table 13.13 – A340 engine locations and diameters

CERC